Institutional Repository - Research Portal
Dépôt Institutionnel - Portail de la Recherche
researchportal.unamur.be
University of Namur

THESIS / THÈSE

DOCTOR OF SCIENCES

Boratriptycenes
Development and Reactivity of Non-Planar Boranes

OSI, Arnaud

Award date:
2023

Awarding institution:
University of Namur

Link to publication

General rights
Copyright and moral rights for the publications made accessible in the public portal are retained by the authors and/or other copyright owners and it is a condition of accessing publications that users recognise and abide by the legal requirements associated with these rights.

- Users may download and print one copy of any publication from the public portal for the purpose of private study or research.
- You may not further distribute the material or use it for any profit-making activity or commercial gain
- You may freely distribute the URL identifying the publication in the public portal ?

Take down policy
If you believe that this document breaches copyright please contact us providing details, and we will remove access to the work immediately and investigate your claim.

Download date: 17. Jul. 2025

University of Namur

Faculty of Sciences

Chemistry Department

Boratriptycenes: Development and Reactivity of Non-Planar Boranes

by

Arnaud Osi

Promotor: Prof. Dr. Guillaume Berionni

Jury Members:

Prof. Dr. Johan Wouters	University of Namur
Prof. Dr. Steve Lanners	University of Namur
Prof. Dr. Didier Bourissou	University Toulouse III – Paul Sabatier
Prof. Dr. Holger Braunschweig	University of Würzburg

A Thesis Submitted in Partial Fulfilment of the Requirements for the Degree of Doctor of Philosophy

Cover design: © Presses universitaires de Namur

© Presses universitaires de Namur & Arnaud Osi, 2023
Rue Grandgagnage 19
B – 5000 Namur (Belgium)
pun@unamur.be - www.pun.be

Registration of copyright: D/2023/1881/10
ISBN: 978-2-39029-172-5
Printed in Belgium.

Abstract

Mentioned for the first time more than 50 years ago as a theoretical curiosity for its predicted exceptional Lewis acidity, the parent 9-boratriptycene was *in-situ* generated and trapped under the form of bench stable Lewis adducts, providing glimpse of its reactivity. Extensive investigations of its electronic properties revealed that the Lewis acidity of this non-planar borane is governed by two major factors: *i)* the pre-pyramidalization of the boron atom which reduces the reorganization energy of the Lewis acid upon coordination with a Lewis base and *ii)* the absence of p_z–π-conjugation between the boron atom and the aromatic rings of the triptycene scaffold preventing electron donation from the aromatic π-system into the boron p_z-orbital. The 9-boratriptycene showed a high propensity to undergo protodeborylation leading to the decomposition of the compound. The introduction of a sulfonium bridgehead allowed to increase the stability towards protodeborylation as well as the Lewis acidity, approaching the one of silylium ions. Synthesis of bench stable "ate"-complexes with weakly coordinating anions and hydride- and fluoride-bridged dimers shed light on the steric protection of the boron σ^*-orbital provided by the triptycene scaffold. This revealed the impossibility to perform S_N2 type reactions at the boron center, conferring a remarkable stability to even the weakest "ate"-complexes or Lewis adducts and allowing the synthesis of borylated equivalents of protonated sulfuric, triflic and triflimidic acids. The propensity of this 9-sulfonium-10-boratriptycene to perform Csp^2–H borylation reactions was the highlighted. The reaction conditions were extensively optimized and a wide array of electron rich to electron depleted arenes could be successfully borylated. A mechanistic investigation was performed revealing that the donor-free Lewis acid is only a transient species which is found in solution under several complexed formed with the solvent or a counter-anion. The impact of the pre-pyramidalization of the boron atom was then demonstrated by synthesizing the selenenium derivatives and comparing it with the sulfonium derivative.

Preface

I joined the lab of Prof. G. Berionni as one of the three first Master students, with Damien Mahaut and Xavier Antognini Silva, as the lab was at the very beginning. Three topics were available as Master thesis research topics and I choose to work on the 9-boratriptycene. At that stage, this molecule was only theoretical and I started the synthesis with synthetic pathways envisioned by Prof. Berionni. After countless attempts and synthetic pathway modifications, an alkyl-boron-ate complex of the 9-boratriptycene could be obtained at the end of the Master thesis.

Boosted by the work and the results obtained during my Master thesis, I decided to write a project with Prof. G. Berionni and Dr. A. Chardon. I presented and defended this project for the obtention of a FRIA grant to continue a PhD on this topic. The initial goal of the project was to use the Lewis acidity of 9-boratriptycene derivatives to perform C–F bond abstractions and functionalizations. This was rapidly set aside to devote attention on the unique reactivity of these species.

Chapter II concerns the 9-boratriptycene and presents the first results obtained during my PhD thesis in keeping with my Master thesis. Chapter III presents the first results obtained in line with the initial project. The synthesis of the 9-sulfonium-10-boratriptycene is reported with insights of its exceptional reactivity. Chapter IV is an account of Csp^2–H borylation reactions firstly observed in Chapter III, with the extensive optimization and development presented in Chapter IV. A mechanistic investigation has been performed which allowed a better understanding of the whole reactivity of the 9-sulfonium-10-boratriptycene and, by extension, the 9-and 10-boratriptycenes family. Chapter IV also presents the unexpectedly complex functionalization of the C–B bonds from the borylated arenes. Only few examples of regioselective mono-deuterations could be reported. Chapter V can be considered as a direct application of the ability of the 9-sulfonium-10-boratriptycene to form stable “ate”-complexes and Lewis adducts with weakly

coordinating anions. Borylated equivalents of protonated sulfuric, triflic and sulfuric acids are presented in this chapter. The fluoride ion affinities of these species have been evaluated revealing strong Lewis acidities approaching tris(pentafluorophenyl)borane. Chapter VI is the last chapter presenting experimental results and concerns the synthesis of the 9-selenenium-10-boratriptycene. This work was initially dedicated to Prof. A. Krief and has been published in a special issue of the Synthesis review in his honor. However, the substitution of a sulfur atom by a selenium atom in the bridgehead position of a boratriptycene allowed to experimentally demonstrate the impact of the pyramidalization of the boron atom alone on the Lewis acidity of the corresponding boratriptycene. Chapter II, V and VI are transcripts of scientific articles published (Chapter II and VI) and under review (Chapter V) during this PhD thesis. Chapter III is partially a transcript of the article dedicated to the 9-sulfonium-10-boratriptycene with the addition of numerous attempts to isolate the donor-free Lewis acid. Chapter IV is the biggest chapter and present unpublished results concerning Csp^2–H borylation reactions with the 9-sulfonium-10-boratritpycene and subsequent functionalization of the C–B bonds. Chapter I presents a general introduction, each chapter beginning with a more specific introduction concerning the work presented in the concerned chapter and Chapter VII is a general conclusion and presents some perspective that I consider of interest to pursue this work on 9- and 10-boratriptycenes.

Acknowledgements

Je voudrais, dans un premier temps, remercier mon promoteur, Prof. Guillaume Berionni qui m'a accueilli dans son laboratoire en tant qu'étudiant en master et qui m'a donné l'opportunité d'embrayer sur une thèse de doctorat dans la continuité de mon sujet de master. Je voudrais le remercier de m'avoir laissé la liberté de choisir et d'écrire moi-même mon sujet de thèse en fonction des axes de recherches qui m'intéressaient. Une des choses les plus importantes pour moi durant ces année de master et de doctorat a été l'immense liberté qui m'a été laissée d'essayer et d'explorer absolument tout ce dont j'avais envie au sujet des boratriptycenes. Je pense que cette liberté m'a permis de rester motivé tout au long de la thèse. Merci pour la confiance et la liberté que tu m'as accordée.

Je voudrais ensuite remercier mon mentor, Dr. Aurélien Chardon, qui au fur-et-à-mesure est devenu un ami. Je voudrais le remercier pour ses connaissances qui semblaient illimitées et qu'il m'a transmises tout aux long des presque cinq années passées au labo ensemble. Merci pour tout le temps passé à me faire répéter pour le FRIA, pour le temps passé sur l'écriture et la correction des publis (une en particulier 😉), pour tous ces bons moments de rigolade au labo, ces bons moments de picole aussi (particulièrement durant le confinement) mais par-dessus tout, merci d'avoir supporté ma mauvaise humeur et mes coups de gueule à certains moments. Je n'aurais certainement pas eu tous ces résultats et ces publis, et ne serait peut-être pas en train d'écrire ces remerciements si tu n'avais pas été là chef !

Un énorme merci est également à adresser à Dr. Nikolay Tumanov pour nous avoir permis d'obtenir toutes ces structures moléculaires par diffractions de rayons X. C'est certains que toutes les publis réalisée n'auraient pas été possibles sans ses talents. Je serai toujours émerveillé par son habilité à trouver des cristaux là ou la plupart des gens n'auraient même pas essayé de regarder l'échantillon.

Merci également à Dr. Luca Fusaro pour son aide et sa très grande expertise concernant la RMN. Merci d'avoir été toujours présent et disponible pour discuter des différents problèmes que nous avons rencontrés ainsi que pour les solutions que tu as pu trouver pour nous aider. Ca a été un vrai plaisir de collaborer et de discuter avec toi et ca m'a permis d'appendre beaucoup de choses.

Concernant la préparation à la thèse, je voudrais remercier le professeur Alain Krief pour toutes ces heures passées à nous faire présenter, répéter et répondre à des questions toutes plus tordues les unes que les autres. Merci de nous avoir accordé autant de temps pour nous préparer pour cette épreuve du FRIA.

Je voudrais remercier mon comparse de bac, master, FRIA et doctorat, Damien Mahaut. La préparation au FRIA et toute la thèse n'auraient clairement pas été la même sans toutes ces discussions, ces fous rires, ces ragotages et surtout toutes ces parties de FIFA 07/09. On aura quand même bien poncé les jeux ! Merci également pour cette, bien sympathique, semaine de congrès à Barcelone. Ça aura été un vrai plaisir de partager tous ces moments avec toi l'ami !

Je voudrais également remercier plus généralement tous les membres du RCO, Nicolas Niessen, Antoine Willems, et plus récemment Dr. Kajetan Bijouard (merci d'avoir relu le gros chapitre de ma thèse 😊 au passage), Sayandip Chakraborty et Marion Mathot pour tous ces bons moments de rigolade pendant et en dehors des heures de labo et pour toutes ces parties de fléchettes qui s'éternisent parfois un peu à chaque temps de midi.

Merci à ma maman et mon papa pour ce qui est peut-être le plus important, m'avoir donné l'opportunité d'arriver jusqu'ici en me faisant confiance, en m'offrant toute cette liberté et en me laissant un maximum d'autonomie pendant toutes mes années d'études. Merci d'avoir cru en moi et de m'avoir soutenu du début à la fin et particulièrement dans les moments plus difficiles où j'ai été particulièrement à cran.

Merci à Marine pour avoir été présente pendant presque toutes ces années à l'université. Tu es probablement la personne qui a vécu le plus près les périodes les plus difficiles, particulièrement la préparation au FRIA durant laquelle j'étais particulièrement tendu, et qui m'a supporté durant toutes ces périodes.

List of Abbreviations

A	Electron acceptor
AN	Acceptor Number
BCF	tris(pentafluorophenyl)borane
CCSD	Coupled cluster singles and doubles
D	Electron donor
DABCO	1,4-diazabicyclo[2,2,2]octane
DFT	Density functional theory
DIPEA	Diisopropylethylamine
DTBMP	2,6-Di*ter*butyl-4-methyl-pyridine
e	Elemental charge
EIE	Equilibrium isotope effect
FF	Friedel-Crafts
FIA	Fluoride ion affinity
FLP	Frustrated Lewis pair
GB	Gutmann-Beckett
GEI	Global electrophilicity index
GIAO	Gauge independant atomic orbital
HIA	Hydride ion affinity
HIE	Hydrogen isotope exchange
HOMO	Highest occupied molecular orbital
ITC	Isothermal titration calorimetry
KIE	Kinetic isotope effect
LUMO	Lowest unoccupied molecular orbital
MIDA	*N*-Methylimidodiacetic
MTBD	7-Methyl-1,5,7-triazabicyclo(4.4.0)dec-5-ene
NBO	Natural bond orbital
NFSI	*N*-Fluorobenzenesulfonimide
NHC	*N*-heterocyclic carbene
NMP	*N*-Methylpyrrolidine
NMR	Nuclear magnetic resonance
RE	Reorganization energy
SET	Single electron transfer
SIMes	1,3-bis(2,4,6-trimethylphenyl)-2-imidazolidinylidene
TMA	*N*,*N*,3,5-tetramethylaniline
TMPH	Tetramethylpiperidine
TMS	Trimethylsilyl
VT	Variable temperature
WCA	Weakly coordinating anions

Table of content

Chapter I : General Introduction 5
I.1. Lewis acid-base theory 7
I.2. Lewis acids in organic chemistry 8
I.3. Boron Lewis acids 10
I.3.1 Applications in the chemistry of frustrated Lewis pairs (FLP) 12
I.3.2 Increasing the Lewis acidity of boranes 15
I.4. Reorganization energy 19
I.5. Quantification of the Lewis acidity 23
I.5.1 Gutmann-Beckett and Childs methods 24
I.5.2 IR spectroscopy using AcOEt and MeCN as probes 25
I.5.3 Fluoride ion affinity and hydride ion affinity 25
I.5.4 Global electrophilicity index 27
I.5.5 General comments of different Lewis acidity scales 28
I.5.6 Ofial Lewis acidity scale 29
I.6. Non-planar boranes and triarylboranes 31
I.7. Objectives 35
I.8. References 37
Chapter II : Controlled Generation of 9-Boratriptycene by Lewis Adduct Dissociation: Accessing a Non-Planar Triarylborane 43
II.1. Introduction 47
II.2. Preliminary results 48
II.3. Generation of 9-boratriptycene and trapping with Lewis bases 49
II.4. Evaluation of the Lewis acidity of 9-boratriptycene. 53
II.5. Quantum chemical investigations 54
II.6. Conclusion 58
II.7. References 59
Chapter III : Taming the Lewis Superacidity of Non-Planar Boranes: C–H Bond Activation and Non-Classical Binding Modes at Boron 65
III.1. Introduction 69
III.2. Synthesis of precursors and non-classical bonding at 9-sulfonium-10-boratriptycene. 70
III.2.1 Synthesis of 9-sulfonium-10-boratriptycene precursors 70

III.2.2 Hydride abstraction from 10-hydrido-9-sulfonium-10-boratriptycene-ate complex 71
III.2.3 Fluoride abstraction from 10-fluoride-9-sulfonium-10-boratriptycene-ate complex 74
III.3. Evaluation of the Lewis acidity 75
III.4. Brief aspect on borylation and functionalization of Csp^2–H bonds 76
III.5. Demonstration of borylation of Csp^3–H bonds and abstraction of Csp^3-Si and Csp^3–Csp^3 bonds. 78
III.6. Synthesis of 9-sulfonium-10-boratriptycene stabilized molecular oxide bis-anion. 80
III.7. Complements on attempted isolation of the donor-free 9-sulonium-10-boratriptycene. 81
III.7.1 Attempted protodeborylation with 2,6-dibromopyridinium 81
III.7.2 Modified conditions of hydride abstraction 85
III.8. Conclusion 95
III.9. References 96
Chapter IV : Csp^2-H Borylation and Functionalization of Arenes 101
IV.1. Introduction 103
IV.1.1 Brief introduction of transition metal catalyzed Csp^2–H borylation 103
IV.1.2 Transition-metal-free Csp^2–H borylation 105
IV.1.3 Summary and comparison of intermolecular electrophilic Csp^2-H borylation methods 113
IV.1.4 Regioselective mono- and perdeuteration of arenes 117
IV.2. Preliminary Results 121
IV.3. Optimization 124
IV.4. Substrate scope 143
IV.5. Mechanistic investigations 147
IV.5.1 Experimental investigations 147
IV.5.2 Quantum chemical investigation 162
IV.6. Aromatic Csp^2-B functionalization 165
IV.6.1 *Ipso*-Csp^2–B halogenation 166
IV.6.2 Suzuki-Miyaura cross coupling 174
IV.6.3 *Ipso*-Csp^2-B deuteration 175
IV.7. Conclusion 179
IV.8. Reference 182

Chapter V : From Proton to Boron: The Lewis Analogs of Protonated Brønsted Super Acids189
V.1. Introduction.....193
V.2. Synthesis of mono-, bis- and tris-borylated sulfate.....194
V.3. Synthesis of bis-borylated triflimidate.....197
V.4. Synthesis of bis-borylated trilfate.....200
V.5. Quantum chemical investigations.....201
V.6. Conclusion.....202
V.7. References.....203
Chapter VI : A Selenenium-Bridged 10-Boratriptycene Lewis Acid.....207
VI.1. Introduction.....211
VI.2. Synthesis of precursors and and generation of the 9-selenenium-10-boratriptycene.. 213
VI.3. Evaluation of the 9-selenenium-10-boratriptycene Lewis acidity. 216
VI.4. Conclusion.....219
VI.5. References.....220
Chapter VII : General Conclusions and Perspectives.....225
VII.1. Conclusion 227
VII.2. Perspectives.....236
VII.3. References.....241

Chapter I

General Introduction

I.1. Lewis acid-base theory

Over a century ago, G. N. Lewis expressed the theory of Lewis acids and Lewis bases constituting a major breakthrough for describing the behavior of chemical species.[1] A Lewis acid is defined as a chemical species able to accept a pair of electrons while a Lewis base is a chemical species able to donate an electron pair. The association of a Lewis acid and base leads to the quenching of their respective properties and to the formation of a so-called donor-acceptor complex or Lewis adduct.[2,3] Addition of a stronger acid or base to an adduct can lead to the formation of a new donor-acceptor complex and, therefore to the release of the weakest acid or base, respectively (**Figure I.1**).

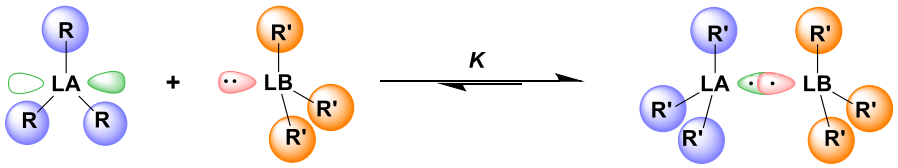


Figure I.1 : Lewis acid and base reactivity.

The concept of Lewis acids and bases as expressed by G. N. Lewis has been modified and completed over the years and in the 1950s, R. S. Mulliken added quantum mechanics in this theory[4][5]. Mulliken defined electron donors (D) and acceptors (A) as species such as, during the interaction between D and A, a transfer of negative charge from D to A takes place.[3] The introduction of quantum mechanics allowed to state if an electron pair is fully or partially donated upon association of Lewis acids and bases and, more importantly, removed the oversimplified single point description of Lewis acid-base interaction. Indeed, as initially stated by Lewis, the acidic or basic character of a species was centered on a single atom while with Mulliken's theory, donor-acceptor interactions are considered between molecules as whole entities. He also diversified the types of donors and acceptors considering the orbitals involved in donor-acceptor interactions,

introducing π- and σ-donors in addition to lone pairs as donors as well as π- and σ-acceptors in addition to empty orbital as acceptors.

In 1978, the improvements introduced by Mulliken were completed by Jensen, expressing the Lewis-Mulliken-Jensen acid-base definition[6]. Jensen explained donor-acceptor interactions in terms of HOMO and LUMO overlap and defined a Lewis acid as a species that employs a double unoccupied orbital in initiating a reaction and a Lewis base as a species that employs a double occupied orbital in initiating a reaction. He also formulated nine types of donor-acceptor interactions based on bonding and symmetry properties of the orbitals involved in the interactions (**Table I.1**).[3] However, considering the most common Lewis acid-base interactions, only $n \rightarrow n^*$ donor-acceptor interactions are taken into account in the following work.

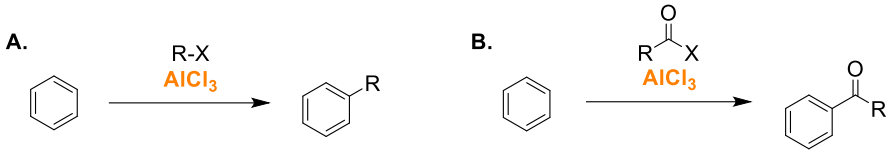
Table I.1 : Jensen's classification of donor-acceptor interactions.

Donor \ Acceptor	n^*	σ^*	π^*
n	$n \rightarrow n*$	$n \rightarrow \sigma^*$	$n \rightarrow \pi^*$
σ	$\sigma \rightarrow n^*$	$\sigma \rightarrow \sigma^*$	$\sigma \rightarrow \pi^*$
π	$\pi \rightarrow n^*$	$\pi \rightarrow \sigma^*$	$\pi \rightarrow \pi^*$

I.2. Lewis acids in organic chemistry

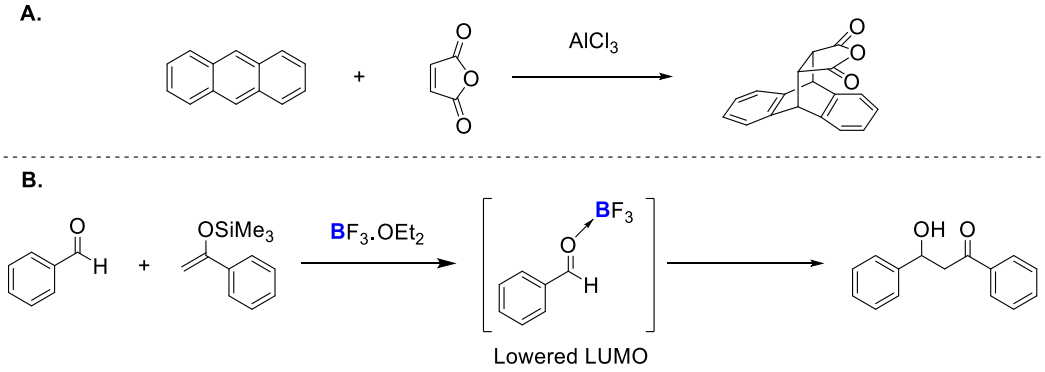
Developed in 1877 by C. Friedel and J. Crafts, the Friedel-Crafts alkylation and acylation reactions are among the first and very famous examples of Lewis acid-mediated reactions (**Scheme I.1**) .[7,8] These reactions allow the synthesis of alkyl- and acyl- substituted aromatic compounds from simple aromatics such as benzene and haloalkanes or acyl halides respectively, in presence of a strong Lewis acid, such as aluminum trichloride ($AlCl_3$). Since

1877, a wide variety of these reactions have been developed and their scope widely extended.



Scheme I.1 : Friedel-Crafts reactions **A.** alkylation and **B.** acylation

However, uses and applications of Lewis acids remained sparse until 1950s with the discovery of olefin polymerization by K. Ziegler and the application of Lewis acids in this field.[9,10] In the same period, applications of Lewis acids started to spread as catalysts for classical reactions such as Diels-Alder, with the report of Yates and Eaton that $AlCl_3$ can speed up Diels-Alder reactions, or aldol reactions (**Scheme I.2**).[11] Such species interact with functional groups behaving as Lewis bases, increasing their reactivity by lowering the LUMO of the molecule.[12,13]



Scheme I.2 : Example of Lewis acid catalysed **A.** Diels-Alder reaction and **B.** aldol reaction.

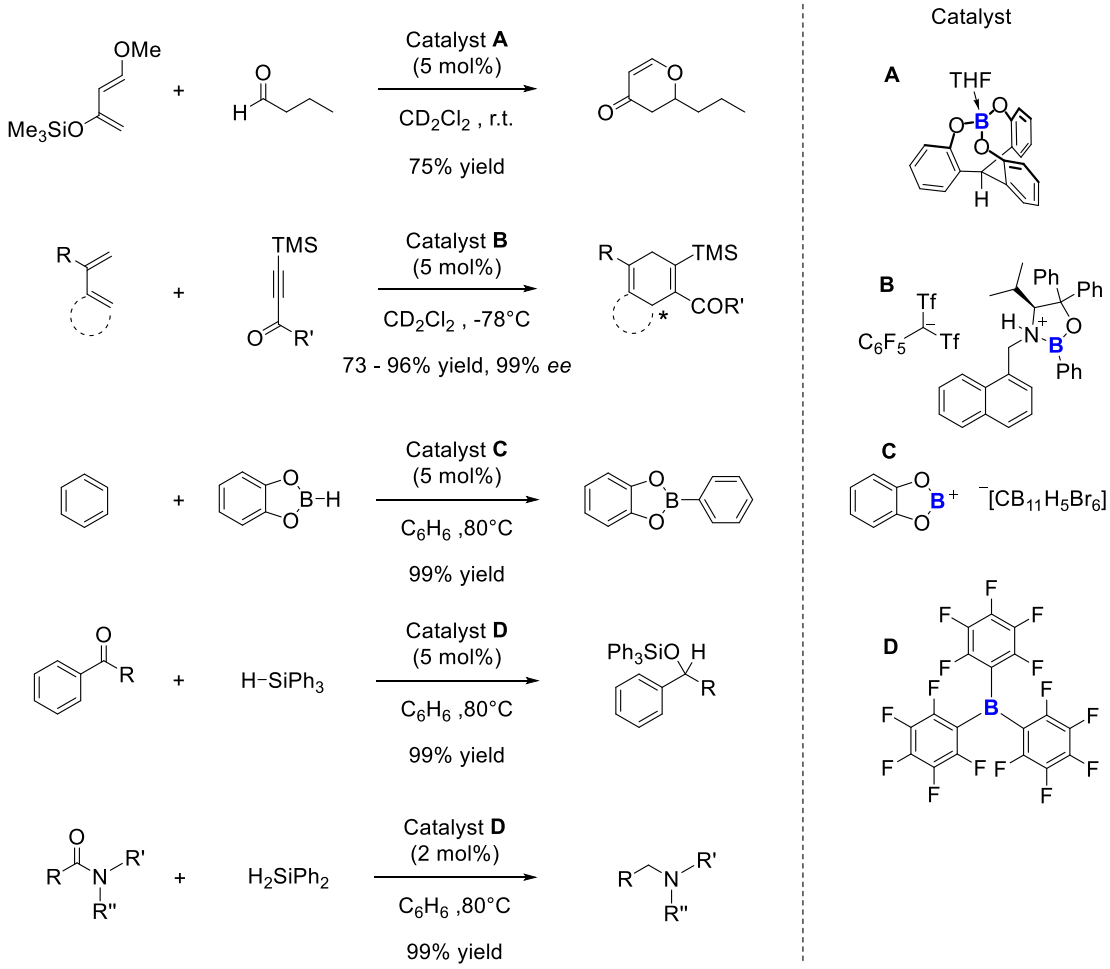
Originally mostly restricted to cationic species or simple metal halides, the library of Lewis acids is now ranging from organometallic complexes to main-group compounds among many others.[12,13] In a first approach, most of these species exhibited a similar reactivity, however, since the 1970s extensive attention is devoted to the development of Lewis acids with finely tuned properties. Compounds are designed to exhibit increased selectivity

for specific functional groups and their substituents are modulated to either increase or decrease the strength of the acid to make them more versatile.[14] Lewis acids can also be combined with Brønsted acids leading to drastically increased Brønsted acidity, as in the case of fluoroantimonic acid ($HF{\cdot}SbF_5$) resulting from the combination of hydrofluoric acid (HF) and antimony (V) pentafluoride (SbF_5) forming one of the strongest Brønsted acids.[15] Among all chemical elements, boron has found extensive applications in the design of Lewis acids starting from borane (BH_3) and halogenated derivatives (BX_3) to highly functionalized derivatives.

I.3. Boron Lewis acids

Boron Lewis acids are among the most widely used Lewis acids and find applications in a wide variety of domains from physics to chemistry and materials science.[16,17] Boron (III) compounds represent the archetypal Lewis acids due to the vacant p_z-orbital on the boron which therefore does not satisfy the octet rule, making them particularly reactive towards functional groups containing heteroatoms with lone-pairs such as nitrogen, oxygen or halogens. The reactivity of these species can easily be tuned by varying the substituents on the boron atom. For example, switching halogen with fluorinated aryl substituents leads to similar Lewis acidic properties but highly enhanced stability towards moisture.[18] Surprisingly, despite boron Lewis acid-mediated deoxygenation of alcohols being known since the 1970's, applications of boron Lewis acids in catalysis remained sparse since 1996 with the pioneering work of Piers and co-workers.[19,20] There are five major categories of boron compounds in which the boron atom exhibits Lewis acidic properties : boric, boronic and borinic acids and their corresponding esters, boranes and cationic boron species. Although several cage-shaped borate esters, developed by Yasuda and co-workers, have been used as catalysts for Diels-Alder reactions, their applications as Lewis acids remain

limited.[21,22] Boronic and borinic acids and esters have found broad applications as catalysts in a wide variety of organic reactions as Lewis acids or Lewis acid assisted Bronsted acid, especially in enantioselective catalysis.[12] A very famous example of cationic boron species are Corey's oxazaborolidinium cations which have been widely applied in asymmetric Diels-Alder reactions and Michael additions.[23] Borenium cations have also been extensively studied by Ingleson and co-workers and Vedejs and co-workers and showed potent activity in C–H borylation reactions (**Scheme I.3**).[24,25]



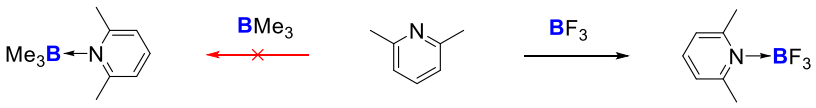
Scheme I.3 : Examples of catalytic applications of various boron Lewis acids.

A major class of boron Lewis acids are boranes which encompass a wide variety of species exhibiting a wide variety of reactivities from trihaloboranes to trialkylboranes and triarylboranes. Such compounds are useful tools in

organic synthesis for performing classical reactions such as cleavage of ethers, hydroboration and halide abstraction reactions for example.[20] However, triarylboranes have been gaining an increasing importance and interest with the extensive work of Piers and co-workers and Stephan and co-workers who shed light on fluoroaryl boranes and especially on tris(pentafluorophenyl)borane (BCF).[19,26] Indeed, Stephan and co-workers demonstrated in 2006 that the combination of strong and bulky Lewis acids, such as BCF, and bases do not form a Lewis adduct but can react in a cooperative pathway to heterolytically split dihydrogen.[26] This type of reactivity of a combination of Lewis acids and bases has been called frustrated Lewis pairs (FLP) and has been extensively studied since 2006 leading to the development of a wide variety of new Lewis acids and especially boron Lewis acids.

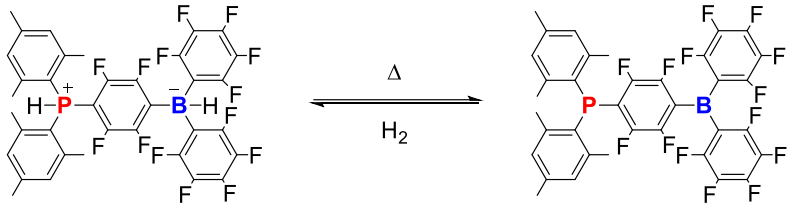
I.3.1 Applications in the chemistry of frustrated Lewis pairs (FLP)

As previously presented, combining Lewis acids and bases leads to the formation of Lewis adducts and results in the quenching their respective Lewis acidic or basic properties. However, in 1942, Brown and co-workers discovered that mixing lutidine with trifluoroborane (BF_3) led to the formation of a Lewis adduct while no Lewis adduct was observed with trimethylborane (BMe_3).[27] Trimethylborane being bulkier and less acidic than BF_3, does not react with sterically hindered Lewis bases such as 2,6-lutidine (**Scheme I.4**). This stands for the first example of a so-called frustrated Lewis pair, even though no application had been found at that stage.



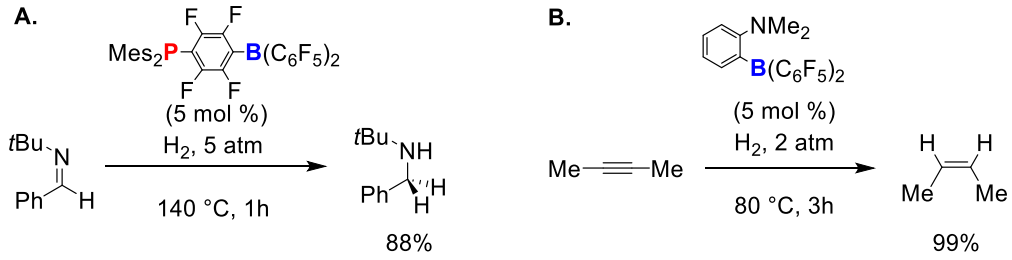
Scheme I.4 : Reaction of 2,6-lutidine with BMe_3 and BF_3.

More than sixty years after the observation of Brown and co-workers, Stephan and co-workers demonstrated that a combination of strong and sterically hindered Lewis acids and bases do not form Lewis adducts but can react in a cooperative pathway to heterolytically split molecular dihydrogen (**Scheme I.5**). This reaction can be seen as a Lewis acid assisted deprotonation, the Lewis acid interacting with molecular hydrogen and lowering its pK_a from 35 to around 5, allowing the deprotonation by the Lewis base.[26] Similar results have been obtained by Erker and co-workers with other FLP systems.[28–30]



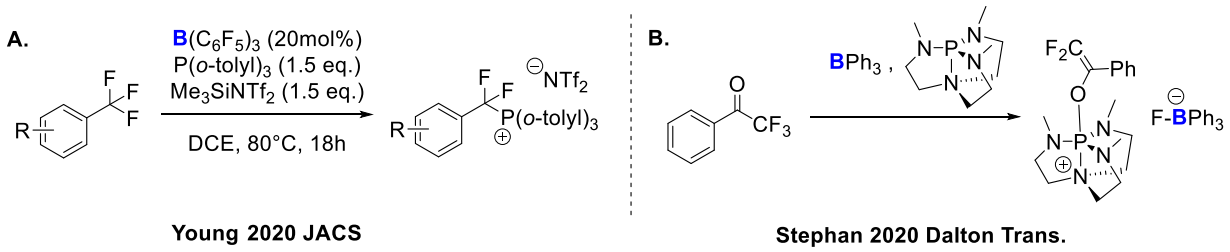
Scheme I.5 : Reversible splitting of molecular hydrogen by a FLP system

Only one year after the first FLP mediated activation of molecular hydrogen, Stephan and co-workers reported the first examples of catalytic hydrogenation reactions of imines using hydrogen and similar metal-free FLP systems (**Scheme I.6, A**).[31] Nowadays, hydrogenation reactions using FLP systems as catalyst have been widely employed for the reduction of imines, ketones, alkenes or alkynes (**Scheme I.6, B**).[32–36]



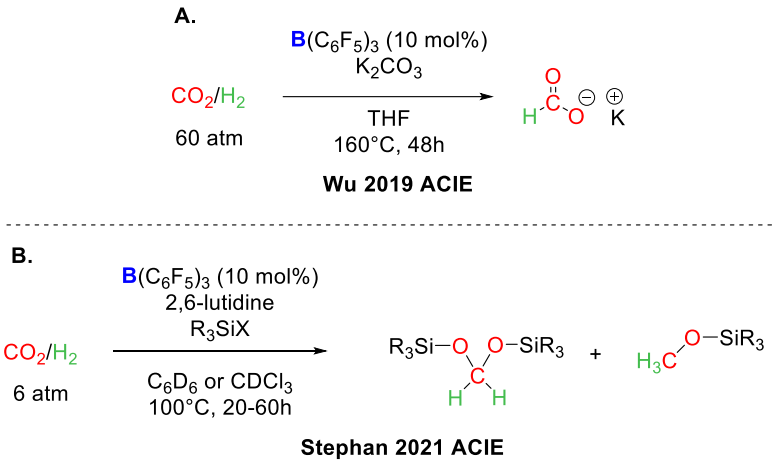
Scheme I.6 : Hydrogenation reactions using FLPs: **A.** reduction of imines and **B.** partial hydrogenation of alkynes.

Since its discovery in 2006, the field of frustrated Lewis pairs has widened, finding applications in a wide variety of important chemical transformations. Recently challenging C–F functionalizations were reported by Young and co-workers using a combination of $B(C_6F_5)_3$ and tris(*o*-tolyl)phosphine for the selective C–F monofunctionalization of trifluoromethyl substituted aromatic compounds (**Scheme I.7, A**). Selective C–F functionalizations of trifluoromethyl acetophenone were also reported by Stephan and co-workers using combination of a strong Verkade base and triphenylborane (**Scheme I.7, B**).[37,38]



Scheme I.7 : Selective C–F monofunctionalization of trifluoromethyl substituents: **A.** trifluoromehtyl substituted aromatic rings and **B.** trifluoromethyl acetophenone.

In 2019, Wu and co-workers achieved a long-standing challenge in FLP chemistry by reporting a transition-metal-free reduction of CO_2 into formate, catalyzed by $B(C_6F_5)_3$ (**Scheme I.8, A**).[39] Two years later, Stephan and co-workers reported an extended methodology of an FLP catalyzed reduction of CO_2 in presence of silylhalides. With a fine selection of the silylhalide, they were able to control the reduction reaction to selectively form silylated acetal or methanoate (**Scheme I.8, B**).[40]



Scheme I.8 : FLP mediated reduction of CO_2 in **A.** formate and **B.** acetal and methanoate.

As a consequence of the striking development of FLP chemistry, increasing attention was devoted to the development of ever-stronger Lewis acids, attempting to surpass the Lewis acidity of tris(pentafluorophenyl)borane (BCF).

I.3.2 Increasing the Lewis acidity of boranes.

The Lewis acidity of boron compounds strongly depends on the substituents linked to the boron center. The steric and electronic properties of the substituents directly impact the boron p_z-orbital and therefore the Lewis acidic properties of the resulting compound.[38,41] In a first approach it is important to look at classical boron compounds such as trialkylboranes. They are generally considered as relatively strong Lewis acids, especially BH_3 which has a similar Lewis acidity as BF_3. However trialkylboranes are extremely reactive and pyrophoric species and are rarely used only for their Lewis acidic properties, BH_3 and stabilized derivatives are used as hydride donors and triethylborane can be used in rocket fuels due to its propensity to form free-radicals in presence of oxygen.[42,43] Furthermore, modifications of the alkyl chains have a limited impact on the acidity of the boron center except upon addition of fluorine substituents. Indeed, tris(trifluoromethyl)borane ($B(CF_3)_3$) is one of the strongest boron Lewis

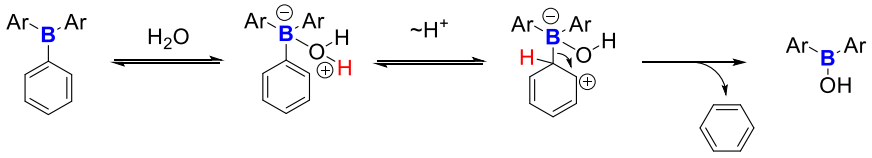
acids and has never been isolated under its free trivalent form.[44,45] A second type of classical boron Lewis acids are tris(halogenated)boranes. These exhibit a high Lewis acidity and evaluating this property along the series of halogens reveals singular features. The Lewis acidity increases in the following order: $BF_3 < BCl_3 < BBr_3 < BI_3$, which is counter-intuitive since fluorine is the most electron withdrawing substituent and iodine the least one.[41] Several theories tried to explain this phenomenon, each bringing interesting explanations. However, the most common explanation states that, due to better overlap between boron $2p_z$- and fluorine 2p-orbitals, efficient electron donation from fluorine to boron takes place, increasing electron density on the boron atom and leading to a reduced Lewis acidity. Going down the series of halogens, the size of halogens p-orbitals increases (from 2p for fluorine to 5p for iodine) reducing the overlap with the boron $2p_z$-orbital (**Figure I.2**). Considering tris(halogenated)boranes, the electron donation from the halogen to the boron overtakes the electron withdrawing effect of halogens. Despite their strong Lewis acidic properties, boron trihalides are extremely sensitive towards ambient conditions, leading to immediate formation of boric acid and the corresponding hydrogen halide. Furthermore, switching from one halogen to another only modulates the Lewis acidity without modifying its stability or propensity to quickly hydrolyze in presence of moisture.[46,47]



Figure I.2 : Electron retrodonation from halogen p-orbitals into boron p_z-orbital.

In order to increase the Lewis acidity of boron compounds as well as modify their steric and electronic properties, triarylborane derivatives are seemingly the best candidates. Even though triphenyl- and triethylborane are similar

in terms of Lewis acidity, triphenylborane is much more stable towards ambient conditions and far less reactive with oxygen.[48] Addition of electron-withdrawing substituents such as fluorine on the aromatic rings leads to considerable increase of Lewis acidity, making $B(C_6F_5)_3$ one of the strongest boron Lewis acids.[41,48] A similar consequence is observed with pentachlorophenyl substituents. Beyond the increase of Lewis acidity, electron-withdrawing substituents on the aromatic rings lead to increased stability towards protodeborylation which occurs in presence of acidic protons and leads to decomposition of the triarylborane.[16] Such reactions generally occur in presence of water, the Lewis acid forming a complex with water, strongly decreasing its pK_a which protonates the aromatic ring linked to the boron atom via S_EAr, followed by the breaking of the C–B bond and subsequent formation of the corresponding borinic acid (**Scheme I.9**). Electron-withdrawing substituents on aromatic rings decrease the reactivity in S_EAr.[49,50]



Scheme I.9 : Mechanism of the protodeborylation of triarylboranes.

Electron-withdrawing substituents on the aromatic rings increase the Lewis acidity, however, considering $B(C_6F_5)_3$, further increasing the number of electron-withdrawing substituents is challenging. In 2017, Mitzel and co-workers synthesized the tris(perfluorotoly)borane which is a slightly stronger Lewis acid than $B(C_6F_5)_3$.[51]

Another strategy, developed by Piers and co-workers, consists in designing an anti-aromatic moiety containing a trivalent boron atom. They showed that combining electron-withdrawing substituents and anti-aromaticity leads to a further increased Lewis acidity (**Figure I.3**). The major drawback of this

system is the decreased stability. It has been shown that treatment of perfluorinated pentarylborole with molecular dihydrogen leads to the heterolytic rupture of dihydrogen and the rupture of the conjugation in the borole system through a C–B bond cleavage, highlighting the extreme reactivity as well as the instability of the borole moiety (**Scheme I.10**).[52–54]

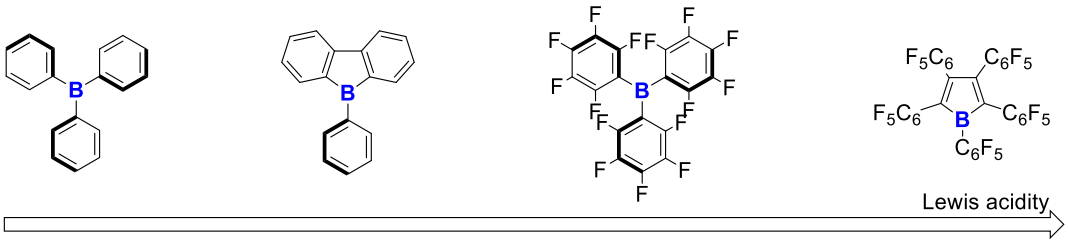
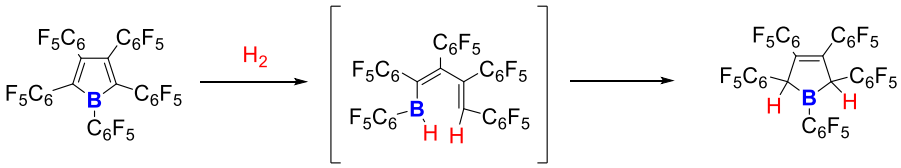
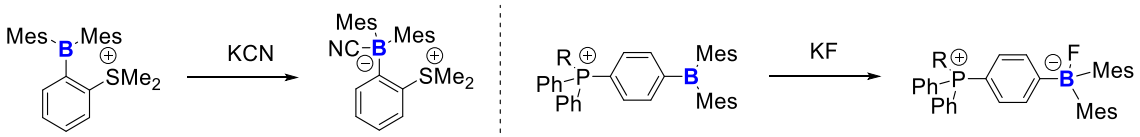


Figure I.3 : Evolution of the Lewis acidity with the introduction of anti-aromaticity and electron-withdrawing substituents.



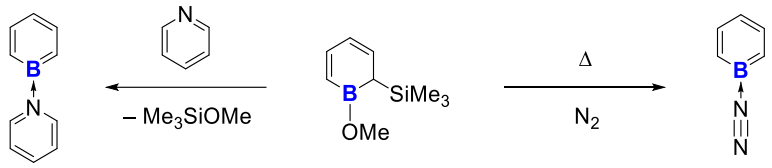
Scheme I.10 : Heterolytic splitting of hydrogen with perfluorninated pentaphenylborole.

Another strategy for increasing the Lewis acidity of triarylboranes is the introduction of cationic substituents on the aromatic rings. This strategy has been extensively used by Gabbaï and co-workers for the design of anion sensors, introducing phosphonium and sulfonium substituents on the aromatic rings (**Scheme I.11**). Such cationic substituents have similar impact on the Lewis acidity as trifluoromethyl substituents.[55,56]



Scheme I.11 : Cationic substituted triarylboranes as anion censors.

A last strategy available to increase the Lewis acidity of trivalent boron compounds is to constrain the boron atom into an aromatic structure. This strategy is relatively limited and only few examples have been reported, e. g. borabenzene and boraanthracene.[57,58] Borabenzene is by far the most extensively studied even though it has never been isolated or observed under a donor-free form. Borabenzene is synthesized as Lewis adduct with pyridine or triphenylphosphine (**Scheme I.12**). Attempts to generate the donor-free form are reported by flash thermolysis. However, it was reported that under N_2 atmosphere, the generated borabenzene forms a Lewis adduct with molecular nitrogen while under Ar atmosphere, the generated Lewis acid reacts with the wall of the apparatus.[59,60]



Scheme I.12 : Generation of borabenzene and formation of Lewis adducts with molecular nitrogen and pyridine.

I.4. Reorganization energy

It has been postulated by Drago and co-workers and later by Frenking and co-workers that the difference between BF_3 and BCl_3 in terms of Lewis acidity did not come from the donation of halogen substituents but from the reorganization energy of the substituents.[47,61,62] The reorganization energy is the energy required to undergo geometrical modifications, from a trigonal planar structure in the free Lewis acid to a tetrahedral one in the Lewis adduct. In the trivalent form, the Lewis acid has a trigonal planar geometry, upon complexation with a Lewis base, the geometry changes to a tetrahedral geometry implying a reorganization of the substituents which is energetically demanding. Therefore, the higher the reorganization energy is, the weaker the Lewis acid will be. It has been postulated that due to the longer B–Cl than B–F bonds, the reorganization energy is smaller in the case of BCl_3 than

BF_3 implying that BCl_3 is a stronger Lewis acid than BF_3. Comparing various group 13 Lewis acid derivatives, the Lewis acidity decreases in the following order Al>Ga>In>B, showing that boron Lewis acids are the weakest of the series.[63–65] Recently Timoshkin and co-workers studied the dissociation energy of group 13 element trispentafluorophenyl complexes with diethyl ether and showed that $B(C_6F_5)_3 \cdot OEt_2$ is the complex with the weakest binding enthalpy in the series. In terms of Lewis acidity, the difference between $Al(C_6F_5)_3$ and $B(C_6F_5)_3$ is mainly due to the reorganization energy.[66] In 2012, Timoshkin and co-workers studied with quantum chemical calculations the dissociation energy of several group 13 elements complexes with ammonia. For most of the examined compounds, similar reactivity trends were observed and Al Lewis acids were generally stronger than B ones. However, for some specific structures where the heteroatom is constrained in a pyramidal shape rather than in a trigonal planar geometry, these trends were inverted. Due to the pyramidal geometry, the reorganization required to form a Lewis adduct is reduced and therefore, the Lewis acidity is increased. The pyramidal shape has a stronger impact on boron derivatives than any other group 13 elements, leading to stronger boron Lewis acids than other group 13 derivatives.[67] They postulated that boron Lewis acids are intrinsically stronger than aluminum derivatives but, due to stronger reorganization energy, their Lewis acidity is much more reduced than that of aluminum derivatives. Whereas preorganization of the Lewis acid in a pyramidal shape restores the intrinsic Lewis acidity of the boron by reducing the reorganization energy (**Figure I.4**).

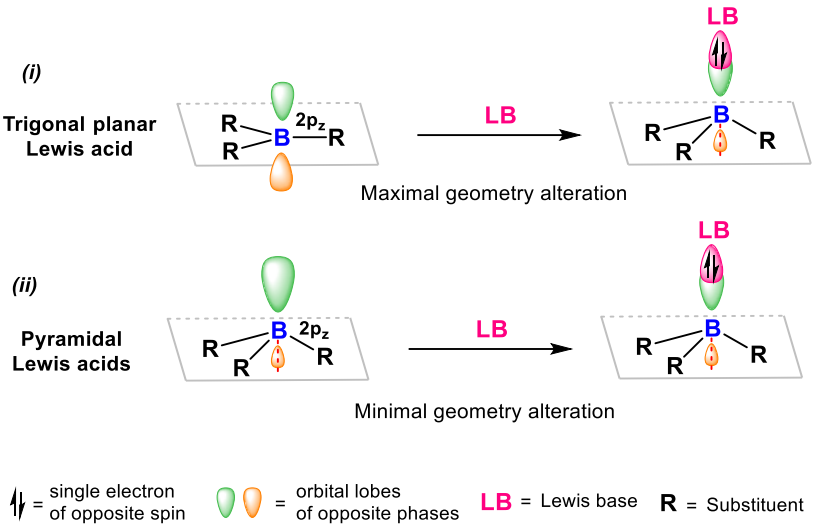


Figure I.4 : Comparison of the reorganization energy between trigonal planar and pyramidal Lewis acids upon coordination with a Lewis base.

This concept of constraining a Lewis acid in a defined geometry for modifying its Lewis acidic properties has been used by Yamaguchi and co-workers. Indeed, while it was demonstrated using quantum chemical analysis that constraining a trivalent boron atom into a pyramidal geometry led to drastically increased Lewis acidity, Yamaguchi and co-workers demonstrated that constraining a trivalent boron atom into a planar architecture led to a decreased Lewis acidity. In this case, the rigid structure reduces the propensity of the system to reach a tetrahedral geometry upon coordination with a Lewis base. While designing a planarized triarylborane in order to maximize the π–p_z-conjugation, they observed that this planarized structure confers an increased stability to the system compared to other triarylboranes as well as a reduced propensity to bind even strong Lewis bases such as DABCO (**Figure I.5**). However, the system remains Lewis acidic enough to bind the fluoride ion, even though this binding was shown to be reversible in presence of a stronger Lewis acid such as $BF_3{\cdot}OEt_2$.[68,69]

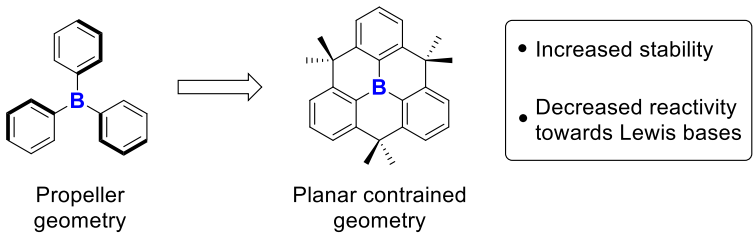


Figure I.5 : Yamaguchi's planarized boranes

It is important to note that the idea of constraining a Lewis acidic center into a defined geometry for altering the reorganization energy upon coordination with a Lewis base is not a theoretical concept. Even though it has not been described using these terms, the concept of strain-release Lewis acidity, mentioned for the first time by Denmark and co-workers in 1990, perfectly fits the concept of reorganization energy.[70] Strain release Lewis acidity has been most widely explored with silanes but can be extended to other main group heteroatoms.[71,72] It has been noted that performing Mukaiyama aldol reactions, the reaction rate can be drastically increased using cyclic silyl group instead of acyclic silyl groups (**Figure I.6, A**).[73] This increased reactivity was attributed to the increased Lewis acidity of the silicon center embedded in a cyclic moiety such as a cyclobutyl ring. It has been demonstrated that embedding the silicon atom into a cyclobutyl ring decreases the angle between the substituents, constraining the silicon atom to adopt a geometry closer to its pentavalent form (trigonal bypiramidal geometry) (**Figure I.6, B**).[74] Therefore, the reorganization of the substituents required to reach the complexed form is reduced and the Lewis acidity of the silicon species is increased, similarly to what has been computed by Timoshkin and co-workers with group 13 species.

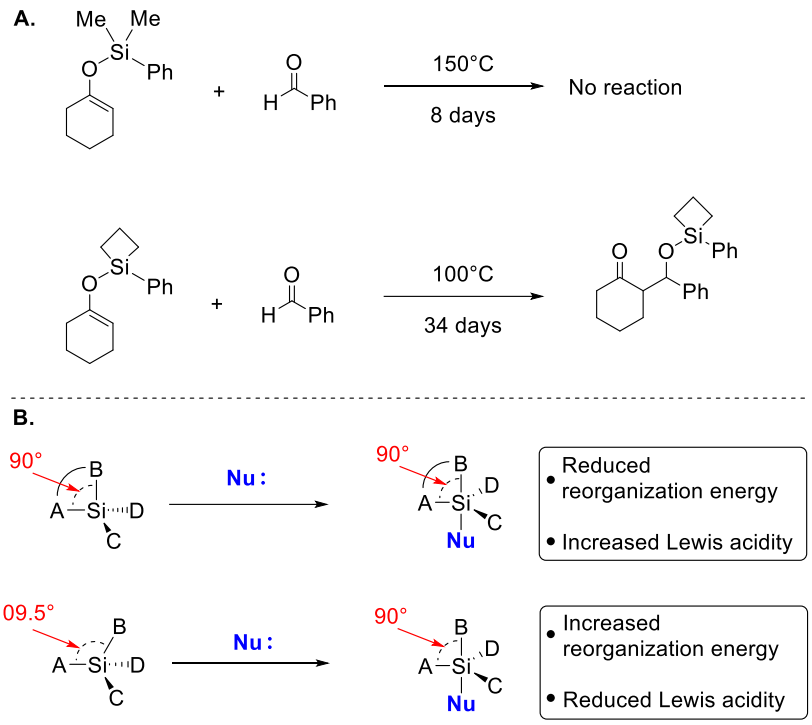


Figure I.6 : **A.** Observation and **B.** rationalization of the strain-release Lewis acidity.

I.5. Quantification of the Lewis acidity

In the context of the development of ever stronger Lewis acids, quantification of the Lewis acidity appears as a relevant method to classify and rank these species. Whereas the Brønsted acidity scale is based on the ability of a chemical species to release a proton (H^+), it is important to define a Lewis acidity scale. However, defining a universal Lewis acidity scale revealed to be illusive due to the dependency to the reference Lewis base used.[75–79] As H^+ is a very small entity, steric effects can be neglected since almost no steric hindrance is generally associated with the Brønsted acidity.[48] Considering Lewis acids, the situation is completely different since steric effects between the Lewis acid and base can not be neglected and will be modified with the acid or base considered, therefore affecting the Lewis acidity value.

I.5.1 Gutmann-Beckett and Childs methods

One of the oldest method to evaluate the Lewis acidity is the Gutmann-Beckett Lewis acidity scale which has been developed by Gutmann and co-workers in 1975 and improved by Beckett and co-workers in 1996.[80–82] This scale is based on ^{31}P NMR spectroscopic measurements and uses triethylphosphine oxide as the reference Lewis base. Upon coordination of a Lewis acid with the oxygen of $OPEt_3$, its ^{31}P NMR signal is deshielded. The chemical shift recorded can then be put in the following equation: $AN = 2.21 \times (\delta_{sample} - 41.0)$ where AN is the acceptor number and gives the position of the Lewis acid on the scale, the higher the AN the higher the Lewis acidity. This scale is based on two references, the lowest point is the chemical shift of $OPEt_3$ in hexane (δ = 41.0 ppm, AN 0) and the highest point is the chemical shift of $OPEt_3$ in $SbCl_5$ as solvent (δ = 86.1 ppm, AN 100) (**Figure I.7, A**). A second commonly used scale is the Childs Lewis acidity scale and is based on ^{1}H NMR spectroscopy.[83] This scale is based on the ^{1}H NMR chemical shift of crotonaldehyde H^3. The lowest point is the chemical shift of the proton H^3 in $CDCl_3$ or CD_2Cl_2 (δ = 6.98 ppm) and the highest point is the chemical shift of the proton H^3 in presence of boron tribromide (BBr_3) in the same solvents (δ = 8.47 ppm) (**Figure I.7, B**). Althoug those two methods are powerful tools to evaluate the Lewis acidity, they often provide opposite results for the same Lewis acid due to variable interactions of the Lewis acid with the Lewis base.[41]

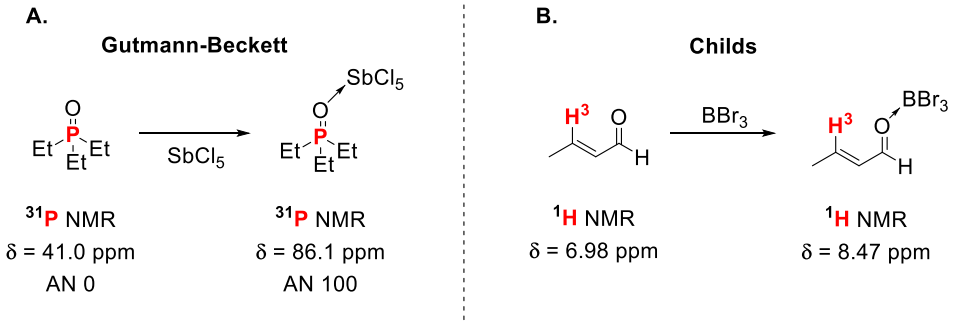


Figure I.7 : **A.** Gutmann-Beckett and **B.** Childs Lewis acidity scales.

I.5.2 IR spectroscopy using AcOEt and MeCN as probes

Other spectroscopic techniques can be used to evaluate the Lewis acidity, such as IR spectroscopy using ethyl acetate or acetonitrile as probes. Those two methods are less common than Gutmann-Beckett or Childs methods, however they can provide additional informations especially if opposite results are obtained with the two NMR based methods. These IR spectroscopy methods are based on the stretching frequency of the C=O and C≡N bonds respectively. Upon coordination of the probe with a Lewis acid, the stretching frequency is shifted, bathochromic shift in the case of AcOEt and hypsochromic shift in the case of MeCN (**Figure I.8**).[84–86] The obtained value for a specific Lewis acid can then be compared with other ones, however, this is not a proper Lewis acidity scale since there is no reference point as for Gutmann-Beckett or Childs scales, only qualitative analysis are possible.

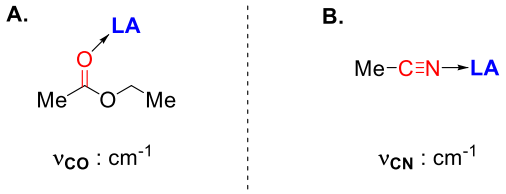


Figure I.8 : IR spectroscopy evaluation of the Lewis acidity using **A.** AcOEt and **B.** MeCN as probes.

I.5.3 Fluoride ion affinity and hydride ion affinity

The most commonly used method to evaluate the Lewis acidity as well as the most developed is the fluoride ion affinity (FIA) scale. Based on the energy difference between the free Lewis acid and the free fluoride ion on one side and the complex on the other side, this scale provides a precise evaluation of the Lewis acidity.[48,87] Evaluations of FIA values are mainly achieved using quantum chemical calculations which are relatively easy and

accurate but can also be achieved experimentally by isothermal titration calorimetry (ITC) or UV-visible spectroscopy.

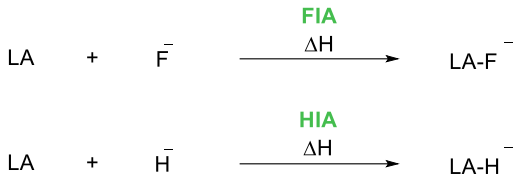


Figure I.9 : Fluoride and hydride ion affinities.

Evaluation of FIAs via quantum chemical calculations is a relatively easy process since only three energies must be evaluated separately: the free Lewis acid, the free fluoride ion and the "ate"-complex. However, an accurate evaluation of the free fluoride ion energy is relatively difficult, and the obtained value can drastically change with the method used. Therefore, to avoid eventual fluctuations, it has been proposed to use a system of three chemical equations corresponding to three reactions. The first reaction is the reference which contains three anchor points that must only be computed once, containing the free fluoride ion. The energy of these three anchor points is evaluated with a very high level of theory (such as CCSD) providing an accurate reference. The second reaction is an isodesmic reaction containing the Lewis acid to evaluate and the reference, which avoids considering the free fluoride ion in the equation. Finally, the third equation is the subtraction of the second and first reactions which gives the FIA (**Figure I.10**). The anchor points can be chosen arbitrarily and the most commonly used have been proposed by Krossing and co-workers which also defined a Lewis superacid as a Lewis acid with a FIA exceeding the one of SbF_5.[88]

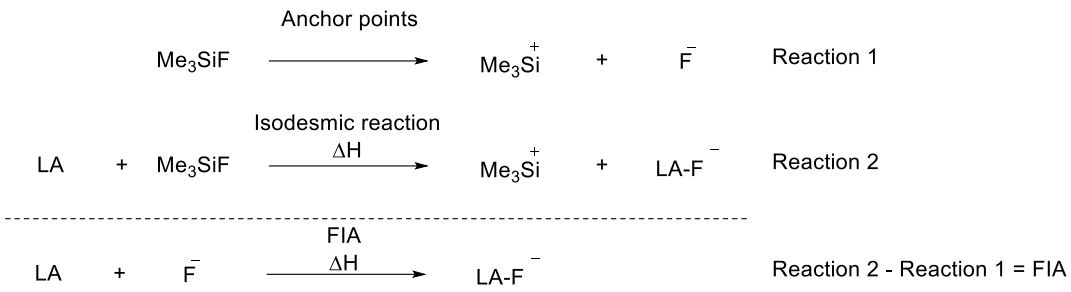


Figure I.10 : Fluoride ion affinity and calculation details.

Similarly to the FIA, the hydride ion affinity (HIA) was introduced and is complementary to the FIA despite a so far more limited database even though the extensive work of Greb and co-workers contributed to develop this database.[89–92] The HIA scale is more generally used to evaluate the Lewis acidity of carbocations or "soft" Lewis acids in general.[93]

I.5.4 Global electrophilicity index

In 2018, Stephan and co-workers suggested to use the global electrophilicity index (GEI, ω) as a metric for Lewis acidity.[94] This parameter was introduced by Parr and co-workers in 1999 and relies on the chemical hardness (η) and the electronegativity (χ) of the atom and, by extension, the molecule considered.[95]

$$\omega = \frac{\chi^2}{2\eta}$$

The GEIs of series of fluoroaryl boranes and other main group Lewis acids were computed and a good to excellent correlation with their FIA was demonstrated. This method can serve as a predictive tool to evaluate the Lewis acidity of new species while requiring less intensive quantum chemical calculations than the FIA. However, it is important to note that, as this method does not take into account the Lewis acid-base association, some effects emerging only upon binding can be missed such as the reorganization energy of the Lewis acid and base.[93]

I.5.5 General comments of different Lewis acidity scales

According to Greb and co-workers, three distinct classes of Lewis acidity have to be distinguished, each relying on a Lewis acidity scale and evaluation method.[93] The first class is the global Lewis acidity (gLA) which corresponds to the thermodynamics of an adduct formation (ΔH and ΔG), obeying the IUPAC definition of Lewis acidity. This type of Lewis acidity is illustrated by the fluoride ion affinity (FIA), hydride ion affinity (HIA) or the ammonia affinity. The data generally comes from quantum chemical calculations even though this Lewis acidity can be evaluated by experimental techniques.

The second class of Lewis acidity is the effective Lewis acidity (eLA) which corresponds to the induced changes of physiochemical properties of a Lewis base used as probe upon binding of the Lewis acid. This consists in the archetypal Lewis acidity evaluated experimentally by NMR spectroscopy (via Guttman-Beckett or Childs methods) and/or IR spectroscopy (upon coordination with ethylacetate or acetonitrile). The third and last class is the intrinsic Lewis acidity (iLA) which reflects the properties of the uncoordinated Lewis acid. In this case, the Lewis acidity is based on the LUMO energy, global electrophilicity index, electron affinity or even NMR chemical shift of the free Lewis acid (**Figure I.11**).

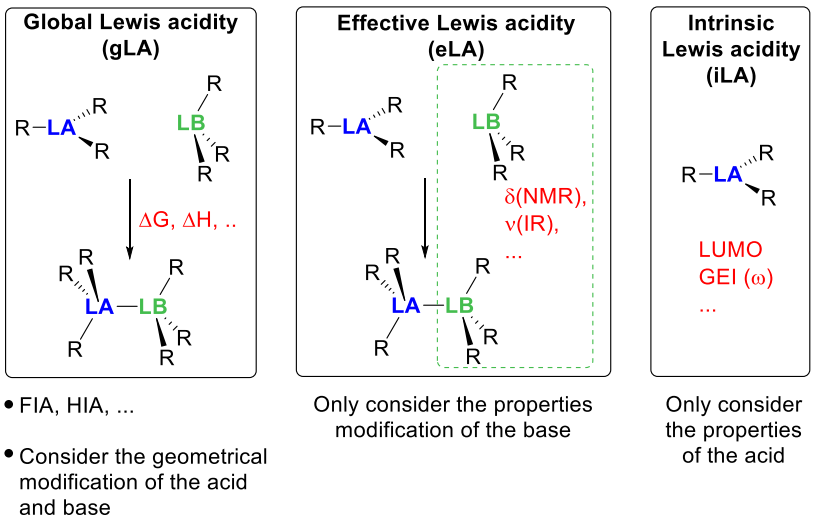


Figure I.11 : Illustration of the different classes of Lewis acidity scaling methods

By comparing the Guttman-Beckett values of more than a hundred Lewis acids with their FIA, Greb and co-workers concluded that eLA and gLA must be seen as two distinct properties of a Lewis acid. More importantly, they highlighted that eLA does not reflect the deformation energy of the acid and base upon formation of the Lewis adduct while this parameter is taken into account in the gLA. This can lead to absurd observations while comparing the acceptor numbers of structurally different Lewis acids. It is then suggested that GB measurements can only be used for conclusive assessments of gLA if structurally similar compounds with an identical central element are compared.

I.5.6 Ofial Lewis acidity scale

Very recently, Ofial and co-workers published a new quantitative Lewis acidity/basicity scale based on equilibrium constants between acids and bases.[96] They started with the observation that a single Lewis base as reference is not accurate enough to compare Lewis acids, especially boranes, of widely differing Lewis acidities. Using a single Lewis base as reference will provide accurate equilibrium constant values in a specific range of Lewis

acidity and lead to important variation to the linearity with very weak or very strong Lewis acids. Following this observation, they decided to use several reference Lewis bases of variable strengths and build a floating Lewis acidity scale where each set of data determined with a Lewis base overlaps the set of data determined with another one. Strong Lewis bases were combined with weak Lewis acids and inversely. This method allows to establish Lewis acidity/basicity scales that both cover 15 orders of magnitude and correlate the equilibrium constant of a Lewis acid-base reaction with Lewis acidity and basicity values, which can be found in databases, only by the following equation: $\lg K_B = LA_B + LB_B$ (in dichloromethane at 20°C) where K_B is the equilibrium constant, LA_B a Lewis acidity parameter specific for a certain triarylborane with reference being the triphenylborane with $LA_B = 0$ and LB_B a parameter referring to a specific Lewis base (**Figure I.12**). They also showed that their Lewis acidity scale correlates with the FIA value of most of the considered boranes, deviations appearing only with very sterically hindered systems.

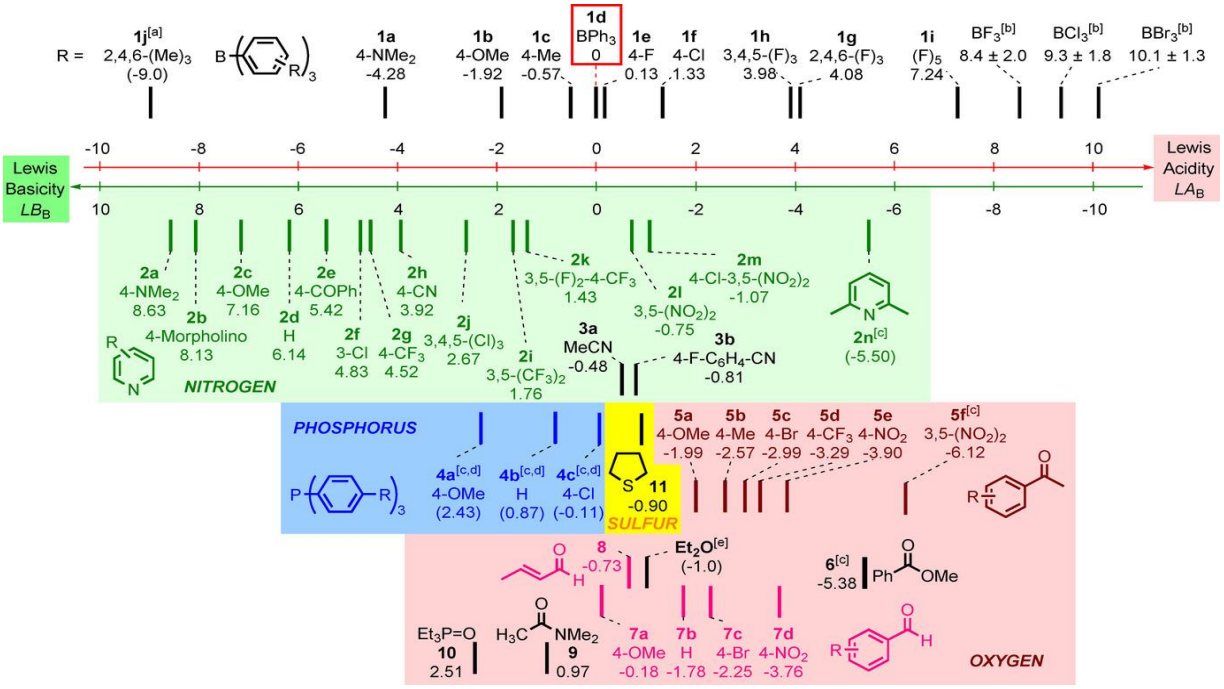


Figure I.12 : Experimental Lewis acidity and basicity scales for boranes and N-, O-, S- and P-centered Lewis bases. Right image adapted with permission from R. J. Mayer, N. Hampel, A. R. Ofial, *Chem. Eur. J.*, **2021**, 27, 4070.

I.6. Non-planar boranes and triarylboranes

As presented before, constraining a tricoordinated boron atom in a pyramidal shape allows to recover the intrinsic Lewis acidity of the boron and therefore increases it by lowering the reorganization energy. However, this strategy remains relatively unexplored and only a few examples of pyramidalized trivalent boron compounds have been synthesized so far. Nevertheless, extensive quantum chemical calculations have been performed to evaluate the properties of such systems. The first non-planar trialkylborane synthesized is 1-boraadmantane, firstly reported by Mikhailov and co-workers in 1974.[97] This highly pyrophoric compound is liquid at room temperature and the structure has been determined only using a derivative with an extra methyl substituent by Mitzel and co-workers in 2012.[98] The structure revealed a relatively small but clear pyramidalization of the boron atom with an average C–B–C angle of 116°. Compared to triethylborane, 1-boraadamantane turned out to be more Lewis acidic, showing that pyramidalization of the boron atom increases the Lewis acidity. However, 1-boraadmantane has never been used for its Lewis acidic properties but rather in complexes for biological applications (**Figure I.13**).[99–101]

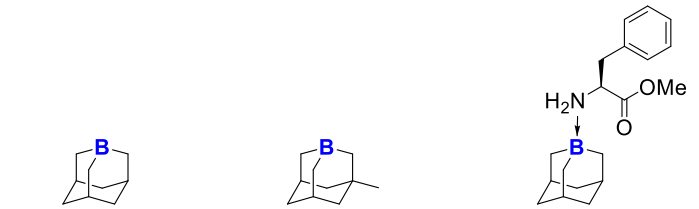


Figure I.13 : 1-Boraadamantane, 3-methyl-1-boraadamantane and example of biologically active derivative.

Trisusbtituted non-planar borates have also been developed incorporating the boron atom in a cage-shaped structure and linked to three oxygen or nitrogen atoms. Such species show relatively high affinities for small anions such as fluoride and have been used in the development of anion carriers in batteries with non-aqueous solvents.[102] Cage-shaped non-planar triarylborate derivatives have been synthesized by Yasuda and co-workers exhibiting a small pyramidalization of the boron atom.[21,103] However, such triarylborates exhibit high Lewis acidity due to their geometry, precluding electron donation from the oxygen p-orbitals into the boron p_z-ortbital. In these structures, the three aromatic rings are anchored on a central atom at the bridgehead position of the cage-shaped structure, the boron atom being at the second bridgehead position. Modification of the anchor carbon atom by heteroatoms such as N, Si or Ge leads to the modification of the Lewis acidic properties via proposed transannular p_z-σ^* interaction (**Figure I.14**).[104] Applications of these triarylborates have been developed in catalysis, especially for Diels-Alder reactions.

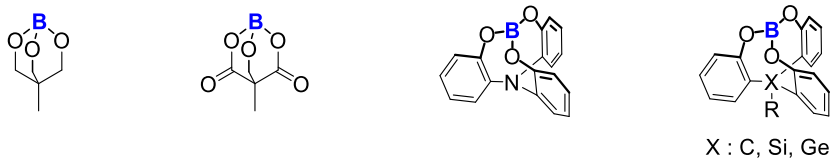
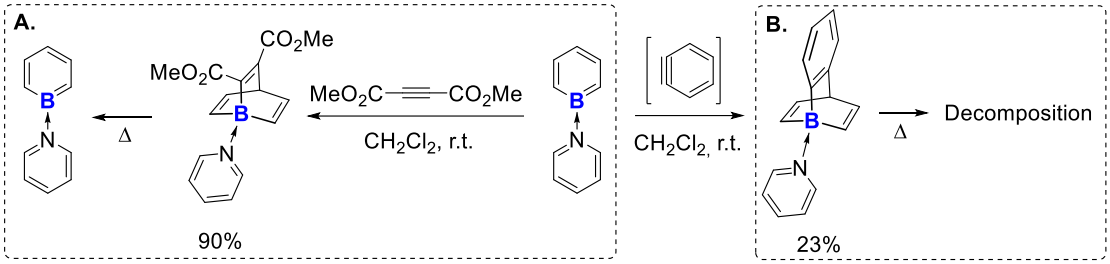


Figure I.14 : Examples of non-planar trialkyl- and triarylborates.

Attempts have been made by Piers and co-workers in 2009 to synthesize non-planar alkenyl- and arylboranes by performing [4+2] cycloaddition with the borabenzene-pyridine adduct and electrophilic alkynes or benzyne.[105] This led to the formation of pyridine-1-borabarrelene derivatives (**Scheme I.13, A**) and the pyridine-1-borabenzobarrelene Lewis adduct (**Scheme I.13, B**) respectively. However, attempts to generate the free non-planar boron Lewis acids were unsuccessful and DSC/TGA analysis showed that, in the case of pyridine-1-borabenzobarrelene, dissociation of pyridine started

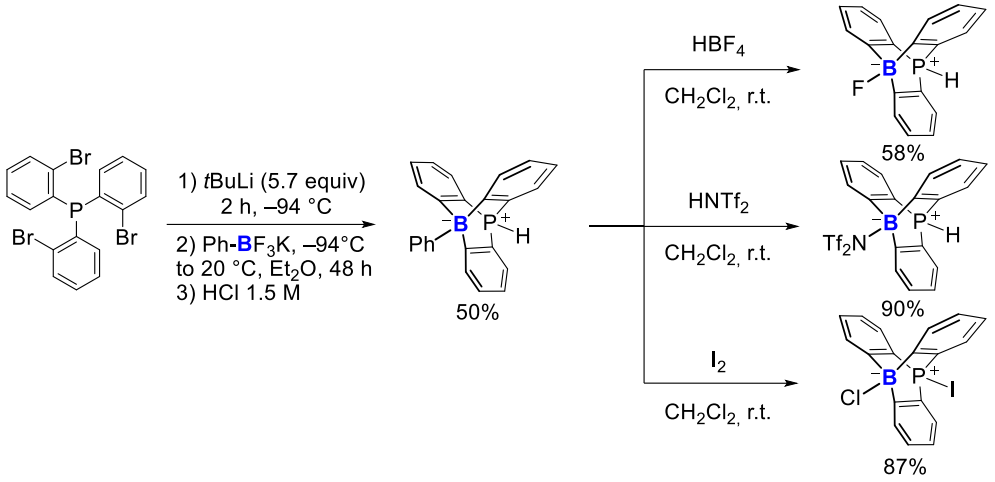
at a high temperature (222°C) followed by the decomposition while in the case of pyridine-1-borabarrelene, retro-Diels-Alder occurred at 216°C instead of releasing pyridine.



Scheme I.13 : Synthesis of **A.** pyridine-1-borabarrelene and **B.** pyridine-1-borabenzobarrelene.

A decade after the work of Piers and co-workers about 1-borabenzobarrelene, Berionni and co-workers published the synthesis of another triarylborane derivatives, 9-phosphonium-10-boratriptycene which has never been observed in its trivalent form.[106] Due to the extreme Lewis acidity, even weakly coordinating anions (WCA) react with the Lewis acid forming boron-ate complexes. Generation of the donor-free Lewis acid was attempted using 10-phenyl-9-phosphonium-10-boratriptycene-ate complex as precursor in presence of strong electrophiles. Treatment of the precursor with tetrafluoroboric acid (HBF_4) led to the formation the 10-fluoro-9-phosphonium-10-boratriptycene-ate complex, the generated Lewis acid instantly abstracting a fluoride ion from the BF_4 anion. A similar result was obtained upon treatment with triflimidic acid, leading to the immediate coordination of the triflimidate ion. Halogens were also attempted as electrophiles to generate the donor-free acid showing singular reactivity in presence of halogenated solvents such as CH_2Cl_2. Treatment of the 10-phenyl-9-phosphonium-10-boratriptycene-ate complex with iodine in dichloromethane did not produce the iodide boron-ate complex but the chloride boron-ate complex, suggesting the formation of a Lewis adduct with the solvent followed by S_N2 with the iodide ion (**Scheme I.14**). Even though 9-phosphonium-10-boratritpycene has never been observed as the donor-

free Lewis acid, this non-planar Lewis acid is one of the strongest ever reported, according to its FIA (-845 kJ.mol^{-1}).



Scheme I.14 : Synthesis of 10-phenyl-9-phosphonium-10-boratriptycene-ate complex and reaction with electrophiles.

Even though very few non-planar boron Lewis acids have been synthesized, extensive quantum chemical calculations have been performed to evaluate the properties of these particular species. Recently, Phukan and co-workers studied the potential application of non-planar trialkylboranes and borates as acceptor molecules in unsupported transition-metal-boron complexes.[107] Transition metals are generally stabilized by coordinating electron-donating ligands, however they can also act as Lewis bases and coordinate Lewis acids via "metal-to-ligand" dative bonding. Such coordinations of Lewis acids with transition-metals are predicted to be unstable which can come from the large reorganization energy of planar boranes required to form these unsupported transition-metal-boron complexes. Phukan and co-workers showed that pyramidalized boron Lewis acids could form stable complexes by reducing the reorganization energy.[107]

Potential applications of non-planar boron Lewis acids were also highlighted by Timoshkin and co-workers and Gilbert and co-workers in the field of frustrated Lewis pair chemistry for the trapping or the spontaneous splitting of hydrogen or nitrous oxide (**Figure I.15**).[108,109]

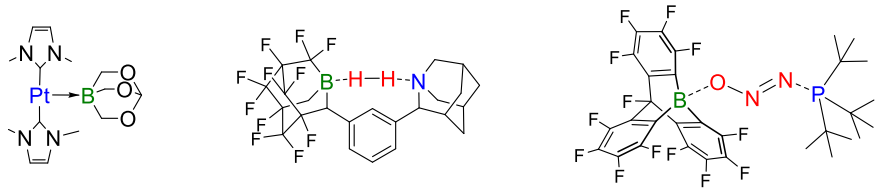


Figure I.15 : Theoretical applications of non-planar boron Lewis acids.

I.7. Objectives

With 9-phosphonium-10-boratriptycene already reported, the first objective of the thesis was to synthesize the parent 9-boratriptycene. A similar strategy as for the phosphonium derivative will be attempted, consisting in synthesizing a "ate"-complex precursor and generating the Lewis acid via protodeborylation reaction. Once the Lewis acid generated, its Lewis acidity and reactivity will be evaluated.

Other boratriptycene derivatives will be synthesized, presenting other heteroatoms in bridgehead position. One of the most relevant derivative being the 9-sulfonium-10-boratriptycene since its Lewis acidity was predicted to be higher than the parent one and even than the phosphonium derivative. Attention will be devoted to generating the Lewis acid and to isolate it under a donor-free form. A major objective will be to obtain a single crystal X-ray diffraction analysis of the donor-free Lewis acid.

Another relevant derivative would be the 9-selenenium-10-boratriptycene. Since selenium shows a similar electronegativity as sulfur with an increased covalent radius, it will be possible to isolate the impact of the pyramidalization of the boron atom on the Lewis acidity.

Considering the considerable predicted Lewis acidity and FIA of the 9-sulfonium-10-boratriptycene, its reactivity in the field of C–F bond abstraction will be evaluated. The most relevant perspective would be to perform Csp^2–F bond abstraction and functionalization mediated by our Lewis acid. Evaluation of the reactivity of 9-sulfonium-10-boratriptycene and derivatives in the field of C–H borylation will also be considered.

Following these objectives, the following chapter deals with the synthesis of precursors and the generation of 9-boratriptycene.

I.8. References

[1] J. B. Van Doren, *J. Chem. Educ.* **1967**, *44*, A82.
[2] K. Ishihara, *Boron Reagents in Synthesis, Chapter 2*, ACS Symposium Series, Washington, **2016**.
[3] S. E. Denmark, G. L. Beutner, *Angew. Chem. Int. Ed.* **2016**, 47, 1560–1638.
[4] R. S. Mulliken, *J. Am. Chem. Soc.* **1952**, *74*, 811–824.
[5] R. S. Mulliken, *J. Phys. Chem.* **1952**, *56*, 801–822.
[6] W. B. Jensen, *Chem. Rev.* **1978**, *78*, 1–22.
[7] C. Friedel, J. M. Crafts, *Compt. Rend.* **1877**, *84*, 1392–1450.
[8] C. C. Price, *The Alkylation of Aromatic Compounds by the Friedel-Crafts Method*, John Wiley & Sons, Inc., **1946**.
[9] K. Ziegler, E. Holzkamp, H. Breil, H. Martin, *Angew. Chem.* **1955**, *67*, 426–426.
[10] G. Natta, *J. Polym. Sci. Part A Polym. Chem.* **1996**, *34*, 321–332.
[11] P. Yates, P. Eaton, *J. Am. Chem. Soc.* **1960**, *82*, 4436–4437.
[12] H. Yamamoto, *Lewis Acids in Organic Synthesis*, John Wiley & Sons, Inc., **2000**.
[13] H. Yamamoto, *Lewis Acid Reagents: A Practical Approach*, Oxford University Press, New York, **1999**.
[14] L. E. Overman, D. Schinzer, *Selectivities in Lewis Acid Promoted Reactions*, Springer, **1989**.
[15] G. A. Olah, G. K. Surya Prakash, R. Molnr, J. Sommer, *Superacid Chemistry*, John Wiley & Sons, Inc.,**2009**.
[16] W. E. Piers, *Adv. Organomet. Chem.* **2005**, *52*, 1–76.
[17] A. Wakamiya, S. Yamaguchi, *Bull. Chem. Soc. Jpn.* **2015**, *88*, 1357–1377.
[18] W. E. Piers, T. Chivers, *Chem. Soc. Rev.* **1997**, *26*, 345.
[19] D. J. Parks, W. E. Piers, *J. Am. Chem. Soc.* **1996**, *118*, 9440–9441.
[20] H. Fang, M. Oestreich, *Chem. Sci.* **2020**, *11*, 12604–12615.
[21] M. Yasuda, S. Yoshioka, H. Nakajima, K. Chiba, A. Baba, *Org. Lett.* **2008**, *10*, 929–932.
[22] A. Konishi, K. Nakaoka, H. Nakajima, K. Chiba, A. Baba, M. Yasuda, *Chem. Eur. J.* **2017**, *23*, 5219–5223.
[23] E. Dimitrijević, M. S. Taylor, *ACS Catal.* **2013**, *3*, 945–962.
[24] V. Bagutski, A. Del Grosso, J. A. Carrillo, I. A. Cade, M. D. Helm, J. R. Lawson, P. J. Singleton, S. A. Solomon, T. Marcelli, M. J. Ingleson, *J. Am. Chem. Soc.* **2013**, *135*, 474–487.
[25] J. R. Lawson, R. L. Melen, *Inorg. Chem.* **2017**, *56*, 8627–8643.
[26] G. C. Welch, R. R. S. Juan, J. D. Masuda, D. W. Stephan, *Science* **2006**, *314*, 1124–1126.
[27] H. C. Brown, H. I. Schlesinger, S. Z. Cardon, *J. Am. Chem. Soc.* **1942**, *64*, 325–329.
[28] P. Spies, G. Erker, G. Kehr, K. Bergander, R. Fröhlich, S. Grimme, D.

W. Stephan, *Chem. Commun.* **2007**, *2*, 5072–5074.
[29] G. C. Welch, D. W. Stephan, *J. Am. Chem. Soc.* **2007**, *129*, 1880–1881.
[30] D. W. Stephan, G. Erker, *Angew. Chem. Int. Ed.* **2015**, *54*, 6400–6441.
[31] P. A. Chase, G. C. Welch, T. Jurca, D. W. Stephan, *Angew. Chem. Int. Ed.* **2007**, *46*, 8050–8053.
[32] L. Greb, P. Oña-Burgos, B. Schirmer, S. Grimme, D. W. Stephan, J. Paradies, *Angew. Chem. Int. Ed.* **2012**, *51*, 10164–10168.
[33] K. Chernichenko, Á. Madarász, I. Pápai, M. Nieger, M. Leskelä, T. Repo, *Nat. Chem.* **2013**, *5*, 718–723.
[34] A. Marek, M. H. F. Pedersen, *Tetrahedron* **2015**, *71*, 917–921.
[35] É. Rochette, M. A. Courtemanche, F. G. Fontaine, *Chem. Eur. J.* **2017**, *23*, 3567–3571.
[36] M. A. Légaré, M. A. Courtemanche, É. Rochette, F. G. Fontaine, *Science* **2015**, *349*, 513–516.
[37] D. Mandal, R. Gupta, A. K. Jaiswal, R. D. Young, *J. Am. Chem. Soc.* **2020**, *142*, 2572–2578.
[38] A. I. Briceno-Strocchia, T. C. Johnstone, D. W. Stephan, *Dalt. Trans.* **2020**, *49*, 1319–1324.
[39] T. Zhao, X. Hu, Y. Wu, Z. Zhang, *Angew. Chem. Int. Ed.* **2019**, *58*, 722–726.
[40] T. Wang, M. Xu, A. R. Jupp, Z. Qu, S. Grimme, D. W. Stephan, *Angew. Chem. Int. Ed.* **2021**, *60*, 25771–25775.
[41] I. B. Sivaev, V. I. Bregadze, *Coord. Chem. Rev.* **2014**, *270–271*, 75–88.
[42] A. Gutowska, L. Li, Y. Shin, C. M. Wang, X. S. Li, J. C. Linehan, R. S. Smith, B. D. Kay, B. Schmid, W. Shaw, et al., *Angew. Chem. Int. Ed.* **2005**, *44*, 3578–3582.
[43] A. Young, *The Saturn V F-1 Engine*, Springer New York, New York, NY, **2008**.
[44] M. Finze, E. Bernhardt, A. Terheiden, M. Berkei, H. Willner, D. Christen, H. Oberhammer, F. Aubke, *J. Am. Chem. Soc.* **2002**, *124*, 15385–15398.
[45] D. J. Brauer, H. Bürger, F. Dörrenbach, B. Krumm, G. Pawelke, W. Weuter, *J. Organomet. Chem.* **1990**, *385*, 161–172.
[46] G. Frenking, S. Fau, C. M. Marchand, H. Grützmacher, *J. Am. Chem. Soc.* **1997**, *119*, 6648–6655.
[47] F. Bessac, G. Frenking, *Inorg. Chem.* **2003**, *42*, 7990–7994.
[48] L. Greb, *Chem. Eur. J.* **2018**, *24*, 17881–17896.
[49] P. A. Cox, A. G. Leach, A. D. Campbell, G. C. Lloyd-Jones, *J. Am. Chem. Soc.* **2016**, *138*, 9145–9157.
[50] P. A. Cox, M. Reid, A. G. Leach, A. D. Campbell, E. J. King, G. C. Lloyd-Jones, *J. Am. Chem. Soc.* **2017**, *139*, 13156–13165.

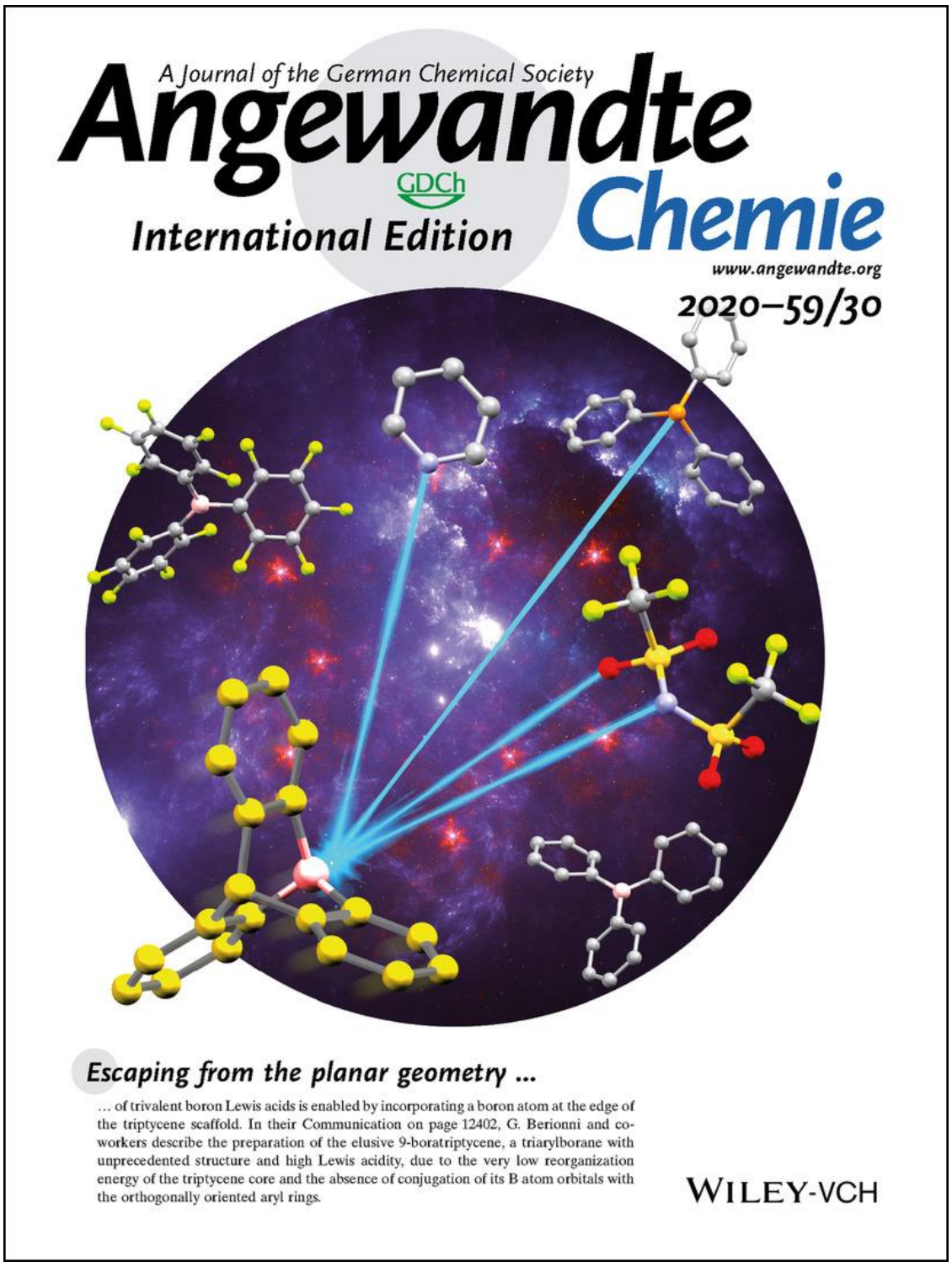
[51] L. A. Körte, J. Schwabedissen, M. Soffner, S. Blomeyer, C. G. Reuter, Y. V. Vishnevskiy, B. Neumann, H. G. Stammler, N. W. Mitzel, *Angew. Chem. Int. Ed.* **2017**, *56*, 8578–8582.
[52] P. A. Chase, W. E. Piers, B. O. Patrick, *J. Am. Chem. Soc.* **2000**, *122*, 12911–12912.
[53] P. A. Chase, P. E. Romero, W. E. Piers, M. Parvez, B. O. Patrick, *Can. J. Chem.* **2005**, *83*, 2098–2105.
[54] C. Fan, L. G. Mercier, W. E. Piers, H. M. Tuononen, M. Parvez, *J. Am. Chem. Soc.* **2010**, *132*, 9604–9606.
[55] Y. Kim, H. Zhao, F. P. Gabbai, *Angew. Chem. Int. Ed.* **2009**, *48*, 4957–4960.
[56] G. Park, F. P. Gabbaï, *Angew. Chem. Int. Ed.* **2020**, *59*, 5298–5302.
[57] R. Boese, N. Finke, J. Henkelmann, G. Maier, P. Paetzold, H. P. Reisenauer, G. Schmid, *Chem. Ber.* **1985**, *118*, 1644–1654.
[58] T. K. Wood, W. E. Piers, B. A. Keay, M. Parvez, *Angew. Chem. Int. Ed.* **2009**, *48*, 4009–4012.
[59] G. Maier, H. P. Reisenauer, J. Henkelmann, C. Kliche, *Angew. Chemie Int. Ed. English* **1988**, *27*, 295–296.
[60] J. Cioslowski, P. J. Hay, *J. Am. Chem. Soc.* **1990**, *112*, 1707–1710.
[61] R. S. Drago, B. B. Wayland, *J. Am. Chem. Soc.* **1965**, *87*, 3571–3577.
[62] D. G. Brown, R. S. Drago, T. F. Bolles, *J. Am. Chem. Soc.* **1968**, *90*, 5706–5712.
[63] A. Y. Timoshkin, G. Frenking, *Organometallics* **2008**, *27*, 371–380.
[64] A. Y. Timoshkin, E. I. Davydova, T. N. Sevastianova, A. V. Suvorov, H. F. Schaefer, *Int. J. Quantum Chem.* **2002**, *88*, 436–440.
[65] E. I. Davydova, T. N. Sevastianova, A. Y. Timoshkin, *Coord. Chem. Rev.* **2015**, *297–298*, 91–126.
[66] I. V. Kazakov, A. S. Lisovenko, N. A. Shcherbina, I. V. Kornyakov, N. Y. Gugin, Y. V. Kondrat'ev, A. M. Chernysheva, A. S. Zavgorodnii, A. Y. Timoshkin, *Eur. J. Inorg. Chem.* **2020**, *2020*, 4442–4449.
[67] L. A. Mück, A. Y. Timoshkin, G. Frenking, *Inorg. Chem.* **2012**, *51*, 640–646.
[68] Z. Zhou, A. Wakamiya, T. Kushida, S. Yamaguchi, *J. Am. Chem. Soc.* **2012**, *134*, 4529–4532.
[69] T. Kushida, C. Camacho, A. Shuto, S. Irle, M. Muramatsu, T. Katayama, S. Ito, Y. Nagasawa, H. Miyasaka, E. Sakuda, et al., *Chem. Sci.* **2014**, *5*, 1296–1304.
[70] S. E. Denmark, R. T. Jacobs, G. Dai-Ho, S. Wilson, *Organometallics* **1990**, *9*, 3015–3019.
[71] W. Zhao, P. K. Yan, A. T. Radosevich, *J. Am. Chem. Soc.* **2015**, *137*, 616–619.
[72] E. Rytter, J. A. Støvneng, J. L. Eilertsen, M. Ystenes, *Organometallics* **2001**, *20*, 4466–4468.

[73] A. G. Myers, S. E. Kephart, H. Chen, *J. Am. Chem. Soc.* **1992**, *114*, 7922–7923.
[74] X. Zhang, K. N. Houk, J. L. Leighton, *Angew. Chem. Int. Ed.* **2005**, *44*, 938–941.
[75] R. S. Drago, B. B. Wayl, *J. Am. Chem. Soc.* **1965**, *87*, 3571–3577.
[76] G. C. Vogel, R. S. Drago, *J. Chem. Educ.* **1996**, *73*, 701.
[77] R. S. Drago, *Coord. Interact.* **2006**, 73–139.
[78] D. P. N. Satchell, R. S. Satchell, *Chem. Rev.* **1969**, *69*, 251–278.
[79] D. P. N. Satchell, R. S. Satchell, *Q. Rev. Chem. Soc.* **1971**, *25*, 171–199.
[80] U. Mayer, V. Gutmann, W. Gerger, *Monatsh. Chem.* **1975**, *106*, 1235–1257.
[81] M. A. Beckett, G. C. Strickland, J. R. Holland, K. Sukumar Varma, *Polymer* **1996**, *37*, 4629–4631.
[82] A. Zheng, S. Bin Liu, F. Deng, *Chem. Rev.* **2017**, *117*, 12475–12531.
[83] R. F. Childs, D. L. Mulholland, A. Nixon, *Can. J. Chem.* **1982**, *60*, 801–808.
[84] I. R. Beattie, T. Gilson, *J. Chem. Soc.* **1964**, 2292.
[85] K. F. Purcell, R. S. Drago, *J. Am. Chem. Soc.* **1966**, *88*, 919–924.
[86] D. G. Brown, R. S. Drago, T. F. Bolles, *J. Am. Chem. Soc.* **1968**, *90*, 5706–5712.
[87] M. O'Keeffe, *J. Am. Chem. Soc.* **1986**, *108*, 4341–4343.
[88] H. Böhrer, N. Trapp, D. Himmel, M. Schleep, I. Krossing, *Dalt. Trans.* **2015**, *44*, 7489–7499.
[89] S. K. Shin, J. L. Beauchamp, *J. Am. Chem. Soc.* **1989**, *111*, 900–906.
[90] Z. M. Heiden, A. P. Lathem, *Organometallics* **2015**, *34*, 1818–1827.
[91] S. Ilic, A. Alherz, C. B. Musgrave, K. D. Glusac, *Chem. Soc. Rev.* **2018**, *47*, 2809–2836.
[92] P. Erdmann, L. Greb, *ChemPhysChem* **2021**, *22*, 935–943.
[93] P. Erdmann, L. Greb, *Angew. Chem. Int. Ed.* **2022**, *61*, e202114550.
[94] A. R. Jupp, T. C. Johnstone, D. W. Stephan, *Inorg. Chem.* **2018**, *57*, 14764–14771.
[95] R. G. Parr, L. V. Szentpály, S. Liu, *J. Am. Chem. Soc.* **1999**, *121*, 1922–1924.
[96] R. J. Mayer, N. Hampel, A. R. Ofial, *Chem. Eur. J.* **2021**, *27*, 4070–4080.
[97] B. M. Mikhailov, *Pure Appl. Chem.* **1974**, *39*, 505–523.
[98] Y. V. Vishnevskiy, M. A. Abaev, A. N. Rykov, M. E. Gurskii, P. A. Belyakov, S. Y. Erdyakov, Y. N. Bubnov, N. W. Mitzel, *Chem. Eur. J.* **2012**, *18*, 10585–10594.
[99] P. Kaszynski, S. Pakhomov, M. E. Gurskii, S. Y. Erdyakov, Z. A. Starikova, K. A. Lyssenko, M. Y. Antipin, V. G. Young, Y. N. Bubnov, *J. Org. Chem.* **2009**, *74*, 1709–1720.
[100] S. Y. Erdyakov, A. V. Ignatenko, T. V. Potapova, K. A. Lyssenko, M. E.

Gurskll, Y. N. Bubnov, *Org. Lett.* **2009**, *11*, 2872–2875.
[101] C. E. Wagner, M. L. Mohler, G. S. Kang, D. D. Miller, E. E. Geisert, Y. A. Chang, E. B. Fleischer, K. J. Shea, *J. Med. Chem.* **2003**, *46*, 2823–2833.
[102] D. Shanmukaraj, S. Grugeon, G. Gachot, S. Lauelle, D. Mathlron, J. M. Tarascon, M. Armand, *J. Am. Chem. Soc.* **2010**, *132*, 3055–3062.
[103] M. Yasuda, S. Yoshioka, S. Yamasaki, T. Somyo, K. Chiba, A. Baba, *Org. Lett.* **2006**, *8*, 761–764.
[104] A. Konishi, K. Nakaoka, H. Nakajima, K. Chiba, A. Baba, M. Yasuda, *Chem. Eur. J.* **2017**, *23*, 5219–5223.
[105] T. K. Wood, W. E. Piers, B. A. Keay, M. Parvez, *Org. Lett.* **2006**, *8*, 2875–2878.
[106] A. Ben Saida, A. Chardon, A. Osi, N. Tumanov, J. Wouters, A. I. Adjieufack, B. Champagne, G. Berionni, *Angew. Chem. Int. Ed.* **2019**, *58*, 16889–16893.
[107] B. Borthakur, S. Das, A. K. Phukan, *Chem. Commun.* **2018**, *54*, 4975–4978.
[108] M. El-Hamdi, M. Solà, J. Poater, A. Y. Timoshkin, *J. Comput. Chem.* **2016**, *37*, 1355–1362.
[109] T. M. Gilbert, *Dalt. Trans.* **2012**, *41*, 9046.

Chapter II

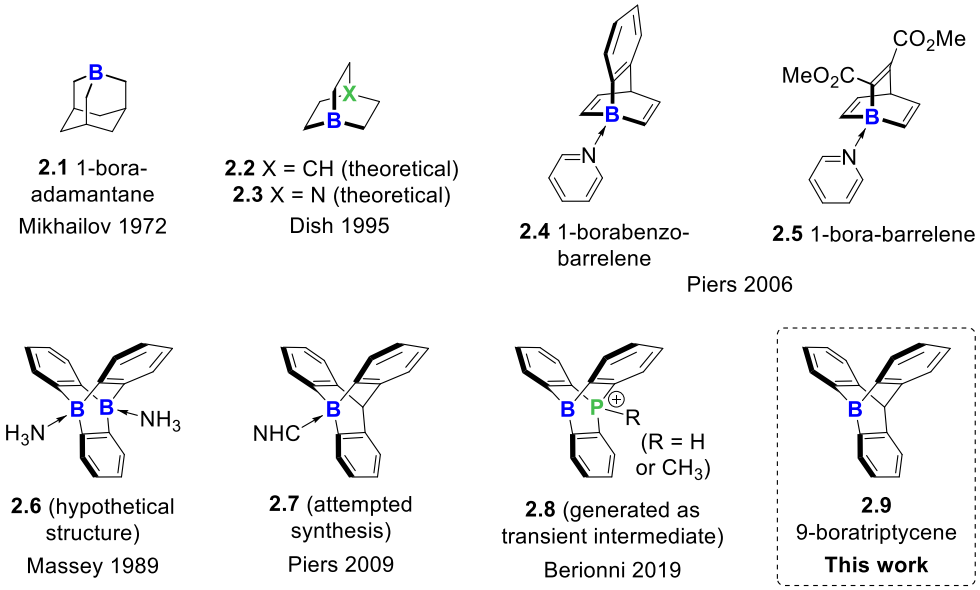
Controlled Generation of 9-Boratriptycene by Lewis Adduct Dissociation: Accessing a Non-Planar Triarylborane



A. Chardon, A. Osi, D. Mahaut, T.-H. Doan, N. Tumanov, J. Wouters, L. Fusaro, B. Champagne, G. Berionni, *Angew. Chem. Int. Ed.* **2020**, *59*, 12402

II.1. Introduction

Boron Lewis acids are archetypal trigonal planar Lewis acids with numerous applications in materials sciences and catalysis.[1–3] Numerous stereo and electronic factors affect the boron Lewis acidity such as the lone pair donation to the boron vacant orbital in boronates[4–6] and haloboranes[7–9], the steric shielding of the substituents, the extent of conjugation with contiguous aromatic π-systems[10–14], and the reorganization energy upon coordination with a Lewis base.[15–18] Preventing structural reorganization by coercing boron Lewis acids in a rigid and fully planar geometry with linkers and tethers between the boron substituents was recently shown to be a powerful strategy to design new π-conjugated materials with high robustness and stability.[14] In contrast, embedding a tricoordinate boron atom in cage-shaped or pyramidal scaffolds, thus forcing the boron environment to adopt an unconventional pyramidal geometry, strikingly enhances its Lewis acidity as in 1-boraadamantane (**2.1**) (**Scheme II.15**).[15,18–21]



2.1 1-bora-adamantane
Mikhailov 1972

2.2 X = CH (theoretical)
2.3 X = N (theoretical)
Dish 1995

2.4 1-borabenzo-barrelene

2.5 1-bora-barrelene

Piers 2006

2.6 (hypothetical structure)
Massey 1989

2.7 (attempted synthesis)
Piers 2009

2.8 (generated as transient intermediate)
Berionni 2019

2.9
9-boratriptycene
This work

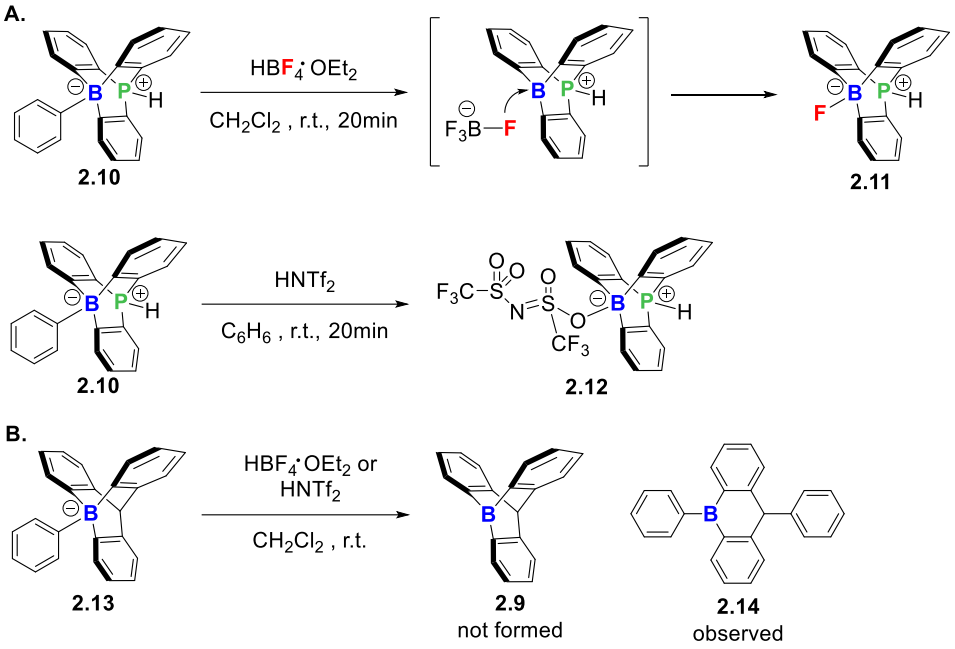
Scheme II.15 : Known and theoretical pyramidal Lewis acids (**2.1**-**2.9**).

The out of plane distortion of the boron atom is smaller in **2.1** and in the borabicyclo-[2.2.2]octane derivatives (**2.2**-**2.3**)[22,23] than in the Lewis base free bora-barrelene derivatives (**2.4**-**2.5**) (**Scheme II.15**). However, the Lewis base-free borabarrelene and benzo-borabarrelene Lewis acids have not been obtained under their trivalent form because of the high dissociation energies of the attached pyridine (or phosphine) Lewis bases.[24] Non-planar triarylboranes belonging to the triptycene family such as the 9,10-bis-boratriptycene (**2.6**) first mentioned by Massey in 1989,[25] and the NHC-protected 9-boratriptycene (**2.7**) nearly reached by Piers in 2009[26] are not experimentally known, and the synthesis of the parent 9-boratriptycene (**2.9**) remained an open challenge in the past three decades (**Scheme II.15**).

Recent quantum chemical investigations showed that owing to its unique tricyclic polyaromatic iptycene core, 9-boratriptycene (**2.9**) may potentially be applied for developing new cryptands[27], frustrated Lewis pairs[28,29] and donor-acceptor complexes of noble gases[30], hence being a key boron Lewis acid for unlocking many applications in catalysis and materials chemistry.

II.2. Preliminary results

In an effort to access 9-boratriptycene derivatives, we recently developed a method to generate the strongly pyramidalized 9-phosphonium-10-boratriptycene (**2.8**) as a transient Lewis acid with exceptionally high Lewis acidity (**Scheme II.16, A**).[31] Though the protodeboronation of **2.10** proceeded selectively at the exocyclic C–B bond (**Scheme II.16, B**), disappointingly, the protodeboronation of the 9-phenyl-boratriptycene ate-complex (**2.13**) lacking the phosphonium bridge occurred at an intracyclic C–B bond, thus preventing the formation of the 9-boratriptycene (**2.9**) (**Scheme II.16, B**).[31]



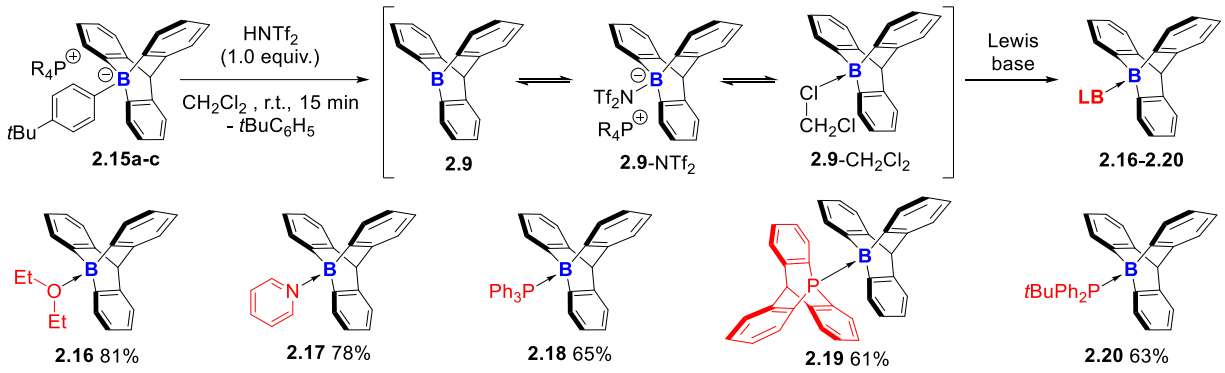
Scheme II.16 : **A.** Generation of 9-phosphonium-10-boratriptycene (**2.8**), **B.** Unsuccessful attempts to generate 9-boratriptycene (**2.9**) and formation of borane (**2.14**).[31]

II.3. Generation of 9-boratriptycene and trapping with Lewis bases

We now designed a synthetic route for producing **2.9** in solution and trapped it with a series of O-, N- and P-centred Lewis bases. Characterization of these Lewis adducts by X-ray diffraction, NMR, IR and UV-Vis spectroscopy revealed that **2.9** exhibits a higher Lewis acidity than all non-planar boranes known so far. Quantum chemical calculations showed that the absence of π-donation from the triptycene aryl rings to the orthogonal p_z boron vacant orbital is a key factor, in addition to the strain that avoids the planar geometry, conferring to **2.9** its very high Lewis acidity. For producing 9-boratriptycene **2.9**, we reasoned that replacing the phenyl ring in **2.13** by a more electron-rich[32] –C_6H_4*t*Bu ring as in the boron ate-complexes **2.15a-c** (See SI for synthesis of **2.15a-c**) should favour a selective exocyclic C–B bond protodeboronation (**Scheme II.17**) and avoid a competing

protodeboronation leading to the cleavage of a C–B bond part of the triptycene skeleton.

When treating **2.15a** with one equivalent of $HNTf_2$ in CD_2Cl_2, the colourless solution turned to deep yellow and ^1H NMR spectroscopy indicated the spontaneous consumption of **2.15a** and the formation of *t*BuC_6H_5. The ^{11}B NMR spectra showed a broad signal at 60 ppm, consistent with a three coordinated boron[33] but downshifted from the predicted value of 92 ppm (GIAO-DFT at the B3LYP/6-311+G(2d,p)//M06-2X/6-311G(d) level of theory), suggesting a reversible coordination of **2.9** with Tf_2N^- (**Scheme II.17** and SI). We next performed the addition of selected Lewis bases to **2.9**, and observed the fast vanishing of the ^{11}B NMR signal at 60 ppm and the formation of the Lewis adducts **2.16**-**2.20**, which have been isolated in good yields after flash chromatography (**Scheme II.17**).



Scheme II.17 : Generation of 9-boratriptycene (**2.9**) in equilibrium with triflimidate anion in solution and CH_2Cl_2 and formation of its Lewis adducts (**2.16**-**2.20**) (See SI). R_4P^+ = $MePh_3P^+$, *n*Bu_4P^+ or Ph_4P^+, respectively in **2.15a-c**.

The molecular structures of **2.16**-**2.19** in the solid state were determined by single-crystal X-ray diffraction analysis (**Figure II.16, Figure II.17**). The B–N distance in **2.17** (1.594(2) Å) is shorter than in the pyridine-$B(C_6F_5)_3$ Lewis adduct (1.614(2) Å)[34] and similar to that in the pyridine Lewis adduct **2.4** (1.584(2) Å)[24], one of the shortest B–N bond lengths reported with a neutral boron Lewis acid. Steric repulsions between the

boratriptycene peri-hydrogen atoms and the pyridine moiety caused its deviation by a tilt angle β of 15° from the triptycene central B···C axis (**Figure II.16, C, D**). The pyramidalization angle α in **2.17** (23.8°) is higher than in the pyridine Lewis adduct of $B(C_6F_5)_3$ (22.2°)[35] and comparable to that in the borabarrelene **2.5** (24.5°).[24] The pyramidalization angle α is defined as the angle between the B–X (X = C, N, O, P) bond and the plane spanned by the *ipso*-carbon atoms of the triptycene benzene rings. The 9-boratriptycene–PPh_3 Lewis adduct **2.18** featured one of the shortest B–P bonds (1.976(4) Å) reported so far for Ar_3B–PAr_3 Lewis adducts. For minimizing steric repulsions, the 9-boratriptycenyl aryl rings and the phosphine phenyl groups adopted a staggered conformation with CPBC torsion angles of 44° in the solid state (**Figure II.17**).

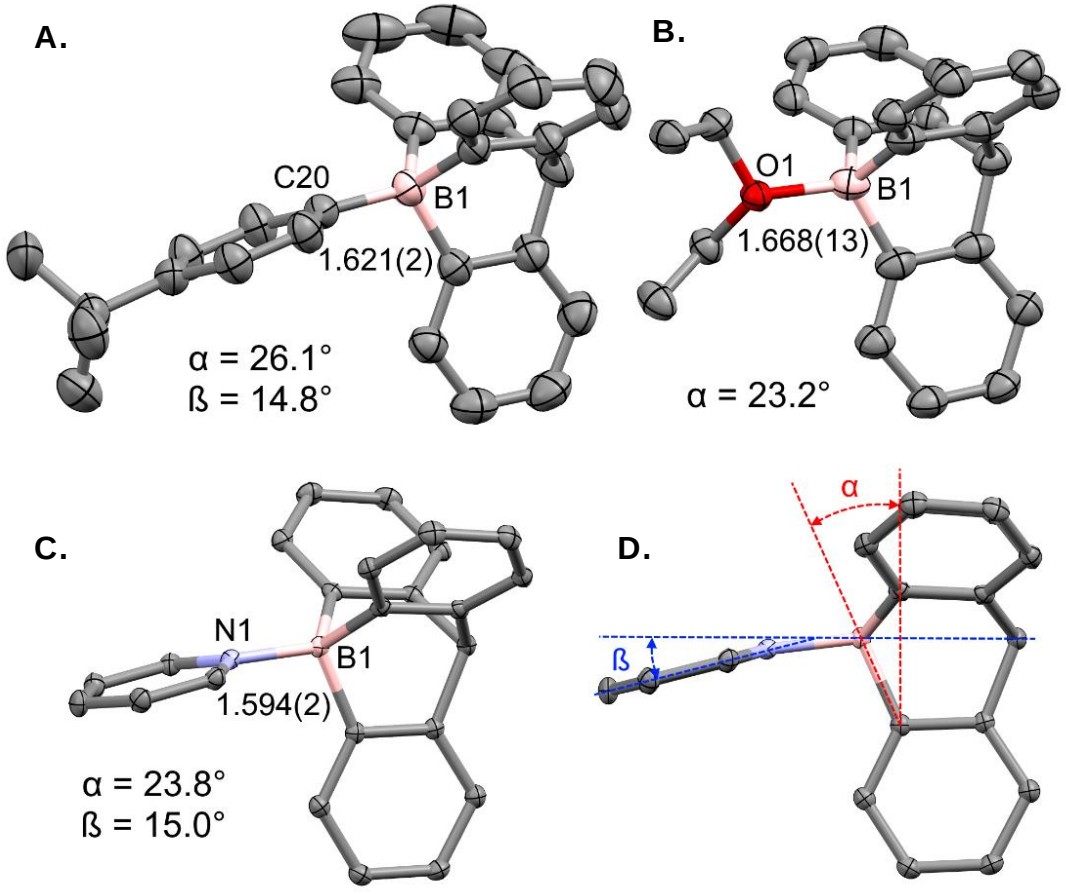


Figure II.16 : Molecular structures: **A.** of **2.15a** with the Ph_4P^+ counter ion omitted; **B.** of the Lewis adduct of 9-boratriptycene with Et_2O (**2.16**); **C.** of 9-boratriptycene with pyridine (**2.17**);

D. side view of **2.17** showing the out of plane twisting of pyridine (tilt angle β) and the pyramidalisation of the boron atom (defined as pyramidalisation angle α). Here and further structures in Figure 2 are shown in thermal ellipsoids representation with 50% probability level. H-atoms and solvate molecules are omitted for clarity, bond lengths in Å.

The Lewis adduct **2.19** of 9-phosphatriptycene[36] with 9-boratriptycene is a unique P/B isostructural analogue of the highly congested 9,9'-bistriptycene[37,38] where the rotation around the Csp^3–Csp^3 bond (1.558(3) Å) connecting the two triptycenes is locked (rotation barrier > 225 kJ mol^{-1}). In the case of **2.20**, the *t*Bu- substituent precluded rotation around the P–B bond on the NMR time scale, as evidenced by ^1H, NOESY, TOCSY and VT-NMR spectroscopy measurements up to 75 °C (see the SI).

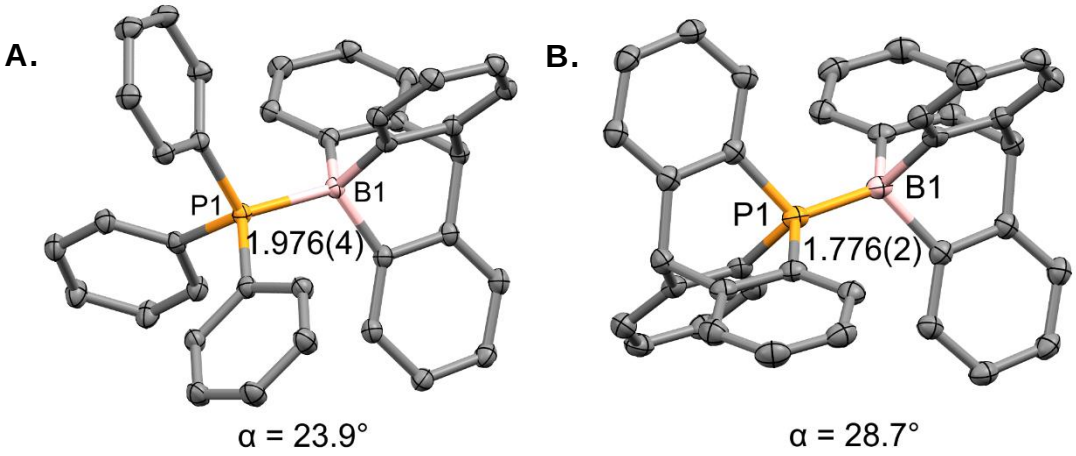
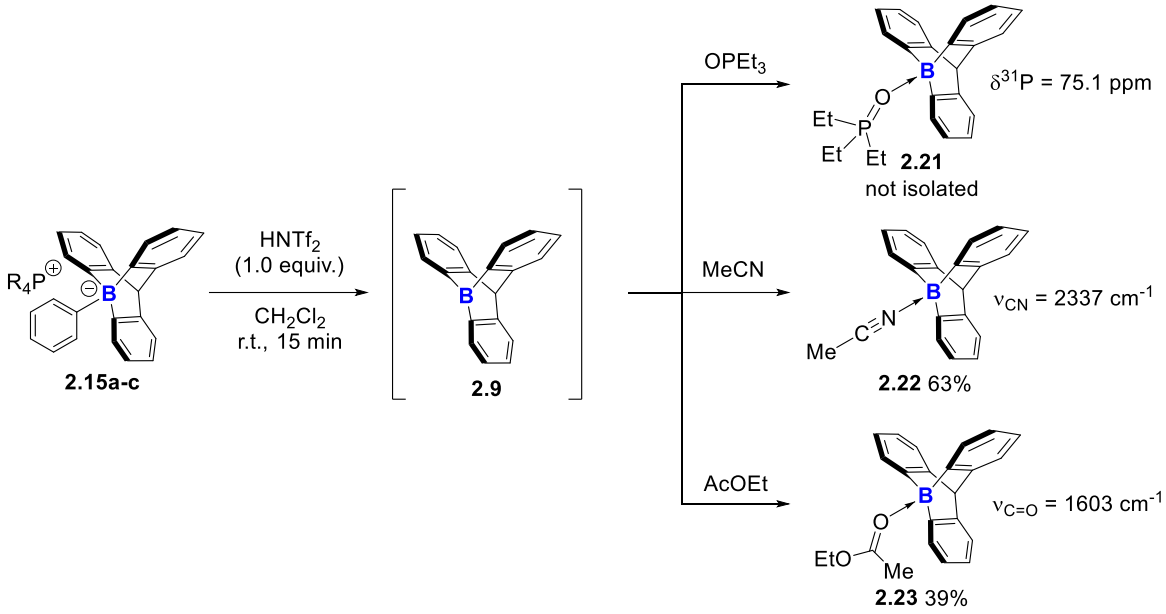


Figure II.17 : Molecular structure of the Lewis adducts **A. 2.18** and; **B. 2.19**. H-atoms and solvate molecules are omitted for clarity, bond lengths in Å.

The thermal stabilities of the 9-boratriptycene Lewis adducts **2.16** and **2.17** were next analysed by DSC/TGA analysis (see the SI). The Lewis adduct **2.16** undergoes a mass loss beginning at 175 °C with a 20.6% weight loss consistent with the Et_2O dissociation (calc. 22.0%). For the Lewis adduct **2.17**, only a single stage decomposition process is observed (180-250°C).

II.4. Evaluation of the Lewis acidity of 9-boratriptycene.

The Lewis acidity of **2.9** was quantified by IR and NMR spectroscopy investigations of its Lewis adducts with $OP(Et)_3$, CH_3CN and EtOAc (**Scheme II.18, Figure II.18**).



Scheme II.18 : Synthesis of the $OPEt_3$, CH_3CN and EtOAc Lewis adducts of **2.9**.

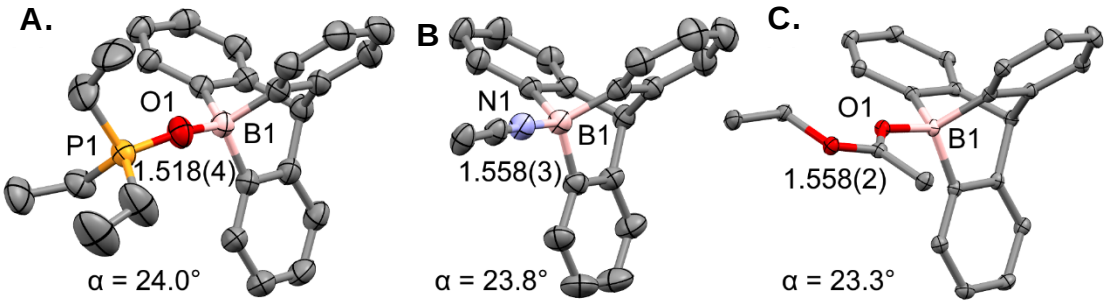


Figure II.18 : Molecular structures of the Lewis adducts **2.21**-**2.23**. Structures are shown in thermal ellipsoids representation with 30% probability level.

According to the Gutmann-Becket scale[39–42], the $\delta^{31}P$ chemical shift of 75 ppm in **2.21** indicated that 9-boratriptycene (**2.9)** has a smaller acceptor number (AN = 76) and is apparently a weaker Lewis acid than $B(C_6F_5)_3$ (AN = 80)[4] for the $OPEt_3$ Lewis base. In contrast, IR spectroscopy showed that

the CN stretching vibration (2337 cm^{-1}) of **2.22** is similar than in Greb's bis(perchlorocatacholato)silane (2335 cm^{-1})[43] and blue shifted by 88 cm^{-1} with respect to free CH_3CN.[44] The $\nu_{C=O}$ stretching vibration of EtOAc in **2.23** (1603 cm^{-1})[45] and in $B(C_6F_5)_3$ (1648 cm^{-1})[31] also indicated that **2.9** is a stronger Lewis acid than $B(C_6F_5)_3$.

II.5. Quantum chemical investigations

Quantum chemical calculations were thus undertaken by Damien Mahaut to evaluate the reorganization energy (RE) of **2.9** and of other boron Lewis acids upon complexation with H^-, F^-, NH_3, PPh_3 and pyridine (**Table II.1**). With NH_3 a RE of 45 kJ mol^{-1} is calculated for **2.9**, nearly identical to that of **2.1** and **2.24** (**Table II.1**) and consistent with the data of Timoshkin.[15] The RE of **2.9** increases up to 55 and 58 kJ mol^{-1} upon coordination with PPh_3 and pyridine, respectively, again similar to that of **2.1** and **2.24**. The REs of **2.9** are 14 to 87 kJ mol^{-1} lower than those of BPh_3 **2.25**, showing that structural REs account for up to 50% of their Lewis acidity difference in terms of Lewis bases affinities (**Table II.1**).

In line with the calculated NH_3, PPh_3, HIA and FIA affinities, the global electrophilicity index (GEI) predicts that **2.9** (1.20) is more electrophilic than **2.1** (0.88) and **2.24** (1.02). However, as GEIs are *per se* global quantities based on ground-state properties of Lewis acids (HOMO and LUMO energy levels) in their initial geometries, reorganization energies are not considered, and GEI values erroneously indicated that BPh_3 (**2.25)** and $B(C_6F_5)_3$ (**2.26**) are stronger Lewis acids than **2.9** (**Table II.1**), in contradiction with experimental spectroscopic data and calculated Lewis bases affinities. In contrast, the local electrophilicity index ω_B of the B atom reflected correctly the Lewis acidity trends for all boranes. Competition experiments showed that **2.9** is a weaker Lewis acid than $B(C_6F_5)_3$ (**2.26)**

for the small and anionic Lewis bases H^- and F^- but is stronger than **2.26** for neutral Lewis bases from NH_3 to PPh_3, in agreement with the computed values (see the SI).

Table II.1 Pyramidalisation of the boron atom α, reorganisation energies (REs) and Lewis bases affinities ($-\Delta H^0$)[46] of selected boron Lewis acids with anionic and neutral Lewis bases as well as global (GEI) and local (ω_B) electrophilicity index of the B atom of the Lewis acids.[47–52]

Boron Lewis acids		REs with Lewis bases (kJ mol^{-1})					Lewis bases affinities (kJ mol^{-1}) and global and local electrophilicities (eV)						
	α^a	H^-	F^-	NH_3	PPh_3	C_6H_5N	HIA^b	FIA^b	NH_3	PPh_3	C_6H_5N	GEI	ω_B
triethylborane (BEt_3)	0.90	125	118	72	81	86	292	285	92	38	86	0.97	-0.67
1-boraadamantane **2.1**	11.0	101	91	48	54	59	326	282	74	85	116	0.88	-0.57
1-borabarrelene **2.24**	15.4	95	87	45	50	52	412	395	172	164	176	1.02	-1.23
9-boratriptycene **2.9**	15.5	92	87	45	55	58	496	476	206	194	200	1.20	-1.50
BPh_3 **2.25**	0	130	174	74	69	113	352	333	88	72	79	1.53	-0.65
$B(C_6F_5)_3$ **2.26**	0	144	132	97	82	121	516	466	159	133	144	2.79	-1.23

[a] α= pyramidalization angle in degrees, [b] HIA= hydride ion affinity, FIA = fluorine anion affinity. Pseudo-isodesmic reactions have been used, with the HIA of $SiMe_3H$ and the FIA of $SiMe_3F$ as the anchor point evaluated at the reference G3 level[6,46]

Due to the strained nature of **2.9**, the pπ-orbitals of the triptycene aryl rings and the formally vacant $2p_z$ orbital of the boron atom are nearly orthogonal to each other, precluding any stabilizing overlap or π-electron delocalization. This is clearly visualized when comparing the HOMO-5 and LUMO orbitals of BPh_3 (**2.25**) and 9-boratriptycene (**2.9**) (**Figure II.19**). In **2.9** the LUMO is principally located on the $2p_z$ boron orbital (**Figure II.19, A, B**) whereas it is distributed over the whole pπ-carbon orbital of its phenyl substituents in BPh_3 (**2.25**) (**Figure II.19, C**), indicating a high contribution of the

pπ-orbitals to the LUMO. The HOMO-5 of **2.25** shows an entire distribution and an overall orbital overlap over the B atom and aromatic π-system (**Figure II.19, D.**), which is not the case in **2.9**.

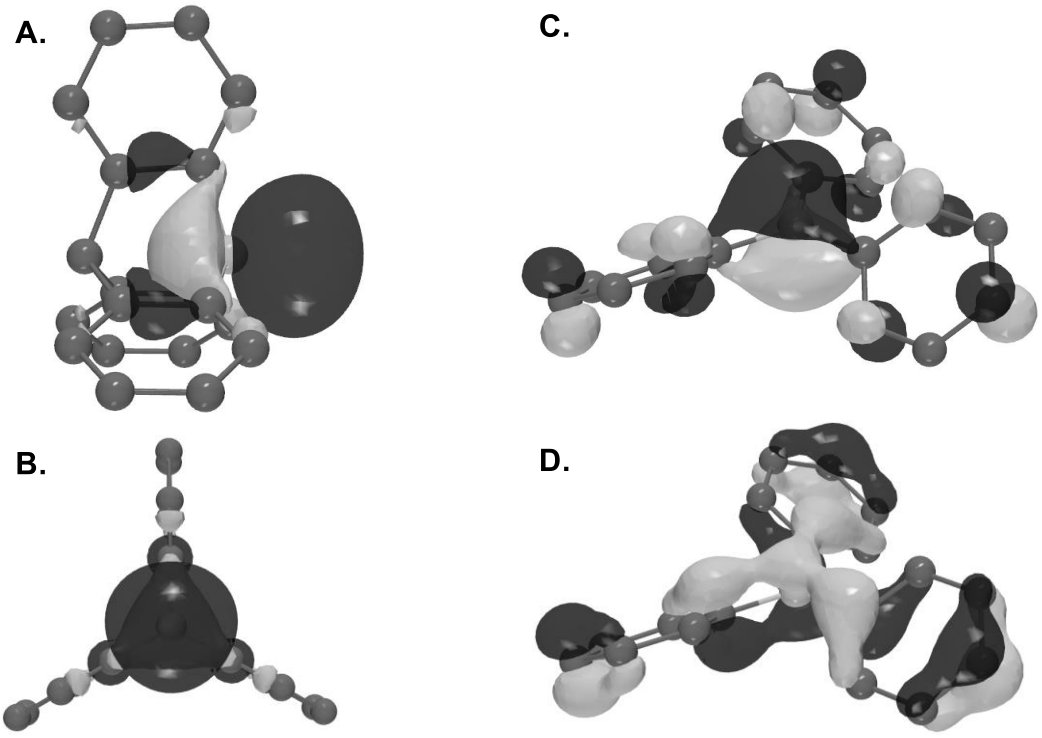
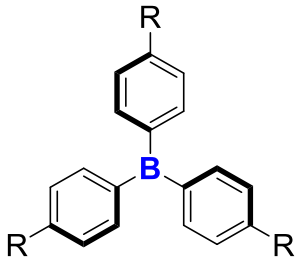
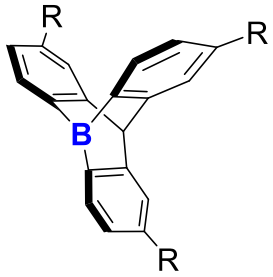


Figure II.19 : **A.** Plot of the LUMO (-0.64 eV) of 9-boratriptycene (**2.9**); **B.** side view of the LUMO of **2.9**; **C.** plot of the LUMO (-1.12 eV) of triphenylborane (**2.25**); **D.** plot of the HOMO-5 (-8.71 eV) of **2.25**. All were derived after M06-2X/6-311G(d) geometry optimization (isosurface value of 0.045 a.u).[46]

Calculations of natural bond orbital (NBO) and of natural charges on the boron atom confirmed the low contribution of the π-system to the formally empty orbital of the boron in **2.9** (**Table II.2**).

Table II.2 : Electron occupancy at the formally vacant p empty orbital of the boron atom (in electrons) and natural charge of boron. Calculations at the M06-2X/6-311G(d) level of theory using the Gaussian NBO 3.1 program.[53]

								
Number of -NMe_2 groups	0	1	2	3	0	1	2	3
Occupancy of B p_z-orbital	0.22	0.24	0.25	0.26	0.08	0.08	0.08	0.08
B natural charge	0.92	0.89	0.88	0.86	1.00	1.00	1.00	1.00

Indeed, the electron occupancy of the $2p_z$ boron orbital of triphenyl boranes increases linearly from 0.22 to 0.26 e^- when adding up to three electron-donating $-NMe_2$ groups at the *para* positions. In contrast, the electron occupancy of the $2p_z$ boron orbital of 9-boratriptycenes is very low (0.08 e^-) and independent on the number of $-NMe_2$ substituents (**Scheme 5, right**). Natural charge of the substituted boratriptycenes B atom is equal to +1 and is strictly independent of their $-NMe_2$ substitution pattern, unambiguously demonstrating the absence of orbital overlap between the π-system and the boron atom due to the geometrical (and symmetry) constraints of the triptycene core.

II.6. Conclusion

In summary, 9-boratriptycene is a non-conjugated triarylborane, with no electron delocalization between its aryl rings and the boron $2p_z$-orbital. Due to its pyramidal boron atom, its strained triptycene scaffold with large spaces between the aryl rings, and its low energy of reorganisation during coordination with a Lewis base, 9-boratriptycene, though not having any fluorine substituents, can exhibit a higher Lewis acidity than $B(C_6F_5)_3$ especially for neutral and large Lewis bases. The unprecedent reactivity and stereo and electronic properties of boratriptycenes are particularly appealing for the conception of strongly acidic boron Lewis acids. Work is ongoing in our laboratories for functionalizing the triptycene core with bulky substituents for the design of new sterically hindered and unsymmetrically substituted boron-chirogenic Lewis acids.

With the parent 9-boratriptycene synthesized and its reactivity in the present chapter, the following chapter deals with the synthesis and reactivity of a sulfonium derivative, 9-sulfonium-10-boratriptycene, which is predicted to be a stronger Lewis acid than the parent 9-boratriptycene.

II.7. References

[1] W. E. Piers, *Adv. Organomet. Chem.* **2005**, *52*, 1–76.

[2] W. E. Piers, T. Chivers, *Chem. Soc. Rev.* **1997**, *26*, 345–354

[3] A. Wakamiya, S. Yamaguchi, *Bull. Chem. Soc. Jpn.* **2015**, *88*, 1357–1377.

[4] I. B. Sivaev, V. I. Bregadze, *Coord. Chem. Rev.* **2014**, *270–271*, 75–88.

[5] L. A. Körte, J. Schwabedissen, M. Soffner, S. Blomeyer, C. G. Reuter, Y. V. Vishnevskiy, B. Neumann, H. G. Stammler, N. W. Mitzel, *Angew. Chem. Int. Ed.* **2017**, *56*, 8578–8582.

[6] L. Greb, *Chem. Eur. J.* **2018**, *24*, 17881–17896.

[7] G. Frenking, S. Fau, C. M. Marchand, H. Grützmacher, *J. Am. Chem. Soc.* **1997**, *119*, 6648–6655.

[8] F. Bessac, G. Frenking, *Inorg. Chem.* **2003**, *42*, 7990–7994.

[9] B. D. Rowsell, R. J. Gillespie, G. L. Heard, *Inorg. Chem.* **1999**, *38*, 4659–4662.

[10] C. R. Wade, A. E. J. Broomsgrove, S. Aldridge, F. P. Gabbaï, *Chem. Rev.* **2010**, *110*, 3958–3984.

[11] F. Jäkle, *Chem. Rev.* **2010**, *110*, 3985–4022.

[12] A. Lorbach, A. Hübner, M. Wagner, *Dalton Trans.* **2012**, *41*, 6048–6063.

[13] L. Ji, S. Griesbeck, T. B. Marder, *Chem. Sci.* **2017**, *8*, 846–863.

[14] M. Hirai, N. Tanaka, M. Sakai, S. Yamaguchi, *Chem. Rev.* **2019**, *119*, 8291–8331.

[15] L. A. Mück, A. Y. Timoshkin, G. Frenking, *Inorg. Chem.* **2012**, *51*, 640–646.

[16] E. I. Davydova, T. N. Sevastianova, A. Y. Timoshkin, *Coord. Chem. Rev.* **2015**, *297–298*, 91–126.

[17] G. Bouhadir, D. Bourissou, *Chem. Soc. Rev.* **2004**, *33*, 210–217.

[18] A. Konishi, K. Nakaoka, H. Nakajima, K. Chiba, A. Baba, M. Yasuda, *Chem. Eur. J.* **2017**, *23*, 5219–5223.

[19] B. M. Mikhailov, *Pure Appl. Chem.* **1974**, *39*, 505–523.

[20] S. Y. Erdyakov, A. V. Ignatenko, T. V. Potapova, K. A. Lyssenko, M. E. Gurskll, Y. N. Bubnov, *Org. Lett.* **2009**, *11*, 2872–2875.

[21] Y. V. Vishnevskiy, M. A. Abaev, A. N. Rykov, M. E. Gurskii, P. A. Belyakov, S. Y. Erdyakov, Y. N. Bubnov, N. W. Mitzel, *Chem. Eur. J.* **2012**, *18*, 10585–10594.

[22] J. M. Schulman, R. L. Disch, *J. Mol. Struct.* **1995**, *338*, 109–115.

[23] A. Gregory, M. Paddon-Row, L. Radom, W. Stohrer, *Aust. J. Chem.* **1977**, *30*, 473–485.

[24] T. K. Wood, W. E. Piers, B. A. Keay, M. Parvez, *Org. Lett.* **2006**, *8*, 2875–2878.

[25] N. A. A. Al-Jabar, J. B. Jones, D. S. Brown, A. H. Colligan, A. G. Massey, J. M. Miller, J. W. Nye, *Appl. Organomet. Chem.* **1989**, *3*, 459–468.

[26] T. K. Wood, Boron-Containing Aromatic Compounds: Synhtesis, Characterization and Reactivity, University of Calgary, **2009**.

[27] A. Y. Timoshkin, K. Morokuma, *Phys. Chem. Chem. Phys.* **2012**, *14*, 14911–14916.

[28] T. M. Gilbert, *Dalton Trans.* **2012**, *41*, 9046–9055.

[29] D. W. Stephan, G. Erker, *Angew. Chem. Int. Ed.* **2015**, *54*, 6400–6441.

[30] L. A. Mück, A. Y. Timoshkin, M. Von Hopffgarten, G. Frenking, *J. Am. Chem. Soc.* **2009**, *131*, 3942–3949.

[31] A. Ben Saida, A. Chardon, A. Osi, N. Tumanov, J. Wouters, A. I. Adjieufack, B. Champagne, G. Berionni, *Angew. Chem. Int. Ed.* **2019**, *58*, 16889–16893.

[32] C. Hansch, A. Leo, R. W. Taft, *Chem. Rev.* **1991**, *91*, 165–195.

[33] S. Hermanek, *Chem. Rev.* **1992**, *92*, 325–362.

[34] K. Tanifuji, S. Tajima, Y. Ohki, K. Tatsumi, *Inorg. Chem.* **2016**, *55*, 4512–4518.

[35] P. Kaszynski, S. Pakhomov, M. E. Gurskii, S. Y. Erdyakov, Z. A. Starikova, K. A. Lyssenko, M. Y. Antipin, V. G. Young, Y. N. Bubnov, *J. Org. Chem.* **2009**, *74*, 1709–1720.

[36] L. Hu, D. Mahaut, N. Tumanov, J. Wouters, R. Robiette, G. Berionni, *J. Org. Chem.* **2019**, *84*, 11268–11274.

[37] M. H. P. Ardebili, D. A. Dougherty, K. Mislow, L. H. Schwartz, J. G. White, *J. Am. Chem. Soc.* **1978**, *100*, 7994–7997.

[38] L. H. Schwartz, C. Koukotas, C.-S. Yu, *J. Am. Chem. Soc.* **1977**, *99*, 7710–7711.

[39] U. Mayer, V. Gutmann, W. Gerger, *Monatsh. Chem.* **1975**, *106*, 1235–1257.

[40] V. Gutmann, *Coord. Chem. Rev.* **1976**, *18*, 225–255.

[41] M. A. Beckett, G. C. Strickland, J. R. Holland, K. Sukumar Varma, *Polymer* **1996**, *37*, 4629–4631.

[42] M. A. Beckett, D. S. Brassington, S. J. Coles, M. B. Hursthouse, *Inorg. Chem. Commun.* **2000**, *3*, 530–533.

[43] R. Maskey, M. Schädler, C. Legler, L. Greb, *Angew. Chem. Int. Ed.* **2018**, *57*, 1717–1720.

[44] M. F. Lappert, *J. Chem. Soc.* **1962**, 542–548.

[45] D. G. Brown, R. S. Drago, T. F. Bolles, *J. Am. Chem. Soc.* **1968**, *90*, 5706–5712.

[46] H. Böhrer, N. Trapp, D. Himmel, M. Schleep, I. Krossing, *Dalton Trans.* **2015**, *44*, 7489–7499.

[47] A. R. Jupp, T. C. Johnstone, D. W. Stephan, *Dalton Trans.* **2018**, *47*, 7029–7035.

[48] A. R. Jupp, T. C. Johnstone, D. W. Stephan, *Inorg. Chem.* **2018**, *57*, 14764–14771.

[49] R. G. Parr, L. v. Szentpály, S. Liu, *J. Am. Chem. Soc.* **1999**, *121*, 1922–1924.

[50] W. Yang, W. J. Mortier, *J. Am. Chem. Soc.* **1986**, *108*, 5708–5711.

[51] P. Pérez, A. Aizman, R. Contreras, *J. Phys. Chem. A* **2002**, *106*, 3964–3966.

[52] P. K. Chattaraj, D. R. Roy, *Chem. Rev.* **2007**, *107*, PR46–PR74.

[53] F. Glendening, A. D., Reed, A. E., Carpenter, J. E., Weinhold, **2003**, NBO Vesrion 3.1. Gaussian Inc. Pittsburgh.

Chapter III

Taming the Lewis Superacidity of Non-Planar Boranes: C–H Bond Activation and Non-Classical Binding Modes at Boron

Check for updates

C–H Activation Hot Paper

How to cite: *Angew. Chem. Int. Ed.* **2022**, *61*, e202112342
International Edition: doi.org/10.1002/anie.202112342
German Edition: doi.org/10.1002/ange.202112342

Taming the Lewis Superacidity of Non-Planar Boranes: C–H Bond Activation and Non-Classical Binding Modes at Boron

Arnaud Osi, Damien Mahaut, Nikolay Tumanov, Luca Fusaro, Johan Wouters, Benoît Champagne, Aurélien Chardon, and Guillaume Berionni**

Abstract: *The rational design of a geometrically constrained boron Lewis superacid featuring exceptional structure and reactivity is disclosed. It enabled the formation of non-classical electron deficient B–H–B type of bonding, which was supported by spectroscopic and structural parameters as well as computational studies. Taming the pyramidal Lewis acid electrophilicity through weak coordinating anion dissociation enabled a series of highly challenging chemical transformations, such as Csp^2–H and Csp^3–H activation under a frustrated Lewis pair regime and the cleavage of Csp^3–Si bonds. The demonstration of such rich chemical behaviour and flexibility on a single molecular compound makes it a unique mediator of chemical transformations generally restricted to transition metals.*

Lewis acids are defined as electron-pair accepting species.[1] Among all these species are boranes, the boron analogs of carbenium ions, which are compounds with a neutral tricoordinated boron atom.[2] Although their popularization was spurred by the discovery of frustrated Lewis pairs (FLPs) in 2006,[3] trivalent boron species have been recognized for decades as prototypical Lewis acids and have found, to date, numerous applications far outside this topic.[4] It is only recently that highly electron-deficient pyramidal boranes were predicted to enable the activation of small molecules and the formation of donor-acceptor complexes of noble gases,[5] and to facilitate new mode of bonding owing to their unusual non-planar structures and to the unsymmetrical distribution of the empty orbital around their boron atom.[6] Although these seminal theoretical studies revealed the promising chemical reactivity such species, the chemistry of non-VSEPR Lewis acids remains largely unexplored.[7] For instance, the parent 9-boratriptycene has been reported to be highly unstable in the condensed phase and could only be observed as Lewis adduct even with very weak Lewis bases and with weakly coordinating anions.[8] Therefore, their uses in the activation of strong covalent bonds and applications in synthesis remained unexplored up to date. Here we describe the rational design of a non-planar boron Lewis superacid based on the following guidelines (Figure 1A): i) the orthogonal arrangement between the triptycene aryl rings π-orbitals and the formally pz empty orbital of the boron atom will prevent π-backdonation at boron; ii) the high pre-pyramidalization of the boron atom in **1** is minimizing the structural reorganization energy during a bond activation process, iii) the strong withdrawing ability of the sulfonium linker is providing high Lewis acidity at boron and preventing fast protodeboronation. The impressive Lewis acidity of the boron atom in the unique pyramidal yet trivalent boron Lewis superacid **1** led to the formation of non-classical hydride and fluoride complexes, of a unique encapsulated molecular oxide dianion through water activation and was found to serve as a highly polyvalent platform for the activation of strong Csp^2–H and Csp^3–H bonds through the formation of tetra-aryl-borates complexes. The super-electrophilic cleavage of Csp^3–Si bonds is also reported.

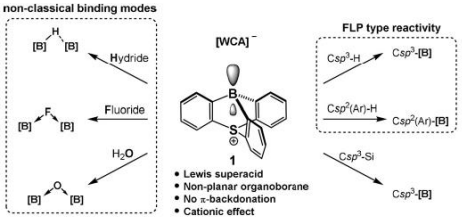


Figure 1. Overview of the binding modes involving the boron Lewis superacid **1** (left) and of its chemical behavior in challenging chemical transformations (right). WCA = weakly coordinating anion.

The 10-mesityl-9-sulfonium-10-boratriptycene **3**, obtained by a formal cycloaddition of benzyne on the B/S dipole **2** was treated with the Brønsted superacid $HCTf_3$ to induce the B–C bond cleavage affording complex **4** (Figure 2A). Due to the non-coordinating nature of the triflide counteranion, this type of coordination was previously unknown in the case of boron Lewis acids. In the solid state S1, S2, C1, and S3 are in trigonal planar arrangement (sum of bond angles = 360°) with a C–S3 bond length of [1.682(4) Å] which is shorter than that of single bond,[9] confirming the π-character of the C=S3 bond (Figure 2D). Complex **4** is stable both in the solid state and in solution, and despite having a high dissociation enthalpy (ΔH_0 = 199 kJ mol-1) the B–O bond dissociation was triggered by raising the temperature to 80 °C and led to the formation of borohydride **5** in the presence of *N*,*N*-dimethyl-

[*] A. Osi, D. Mahaut, Dr. N. Tumanov, Dr. L. Fusaro, Prof. Dr. J. Wouters, Prof. Dr. B. Champagne, Dr. A. Chardon, Prof. Dr. G. Berionni
Chemistry Department—Namur Institute of Structured Matter—University of Namur
61 rue de Bruxelles, 5000 Namur (Belgium)
E-mail: aurelien.chardon@unamur.be
guillaume.berionni@unamur.be
Supporting information and the ORCID identification number(s) for the author(s) of this article can be found under: https://doi.org/10.1002/anie.202112342.

© 2021 Wiley-VCH GmbH

15213773, 2022, 7, Downloaded from https://onlinelibrary.wiley.com/doi/10.1002/anie.202112342 by Universite De Namur (Cnamur), Wiley Online Library on [13/01/2023]. See the Terms and Conditions (https://onlinelibrary.wiley.com/terms-and-conditions) on Wiley Online Library for rules of use; OA articles are governed by the applicable Creative Commons License

III.1. Introduction

Lewis acids are defined as electron-pair accepting species.[1] Among all these species are boranes, the boron analogs of carbenium ions, which are compounds with a neutral tricoordinated boron atom.[2–4] Although their popularization was spurred by the discovery of frustrated Lewis pairs (FLPs) in 2006,[5,6] trivalent boron species are recognized since decades as prototypical Lewis acids and have found, to date, numerous applications far outside this topic.[7–10] It's only recently that highly electron-deficient pyramidal boranes were predicted to enable the activation of small molecules and the formation of donor-acceptor complexes of noble gases,[11–16] and to facilitate new mode of bonding owing to their unusual non-planar structures and to the unsymmetrical distribution of the empty orbital around their boron atom.[17,18] Although these seminal theoretical studies revealed the promising chemical reactivity of such species, the chemistry of non-VSEPR Lewis acids remains largely unexplored.[19–24] For instance, the parent 9-boratriptycene has been reported to be highly unstable in the condensed phase and could only be observed as Lewis adduct even with very weak Lewis bases and with weakly coordinating anions.[25] Therefore, their uses in the activation of strong covalent bonds and applications in synthesis remained unexplored up to date. Here we describe the rational design of a non-planar boron Lewis superacid based on the following guidelines (**Figure III.20**): *(i)* the orthogonal arrangement between the triptycene aryl rings π-orbitals and the formally p_z empty orbital of the boron atom will prevent π-backdonation at boron; *(ii)* the high pre-pyramidalization of the boron atom in **3.1** is minimizing the structural reorganization energy during the formation of complexes, *(iii)* the strong withdrawing ability of the sulfonium linker is providing high Lewis acidity at boron and preventing fast protodeboronation. The impressive Lewis acidity of the boron atom in the unique pyramidal yet trivalent boron Lewis superacid **3.1** led to the

formation of non-classical hydride and fluoride complexes, of a unique encapsulated molecular oxide dianion through complexation with water and was found to serve as a highly polyvalent platform for the borylation of strong Csp^2–H, which will be extensively discussed in the following chapter, and Csp^3–H bonds through the formation of tetra-aryl-borates complexes. The super-electrophilic cleavage of Csp^3–Si bonds is also reported.

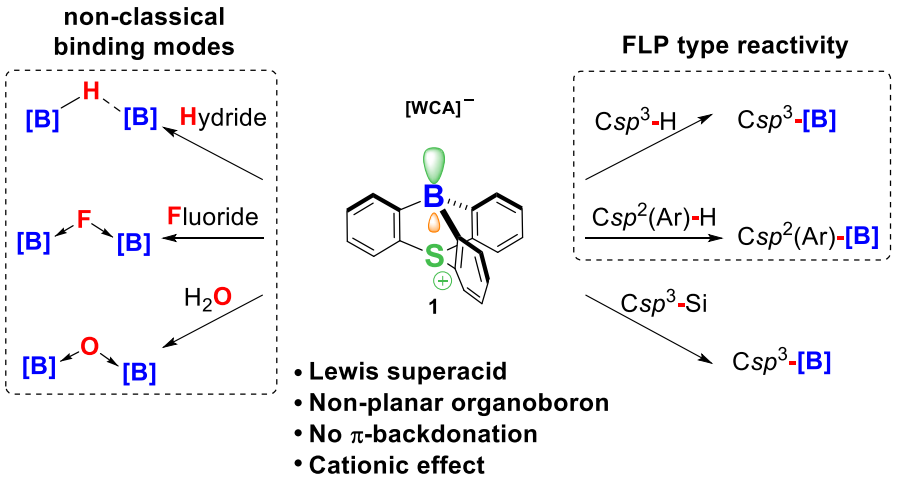


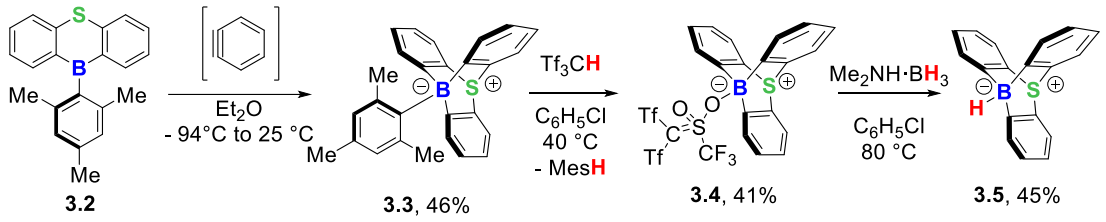
Figure III.20 : Overview of the binding modes involving the boron Lewis superacid **1** (left) and of its chemical behavior in challenging chemical transformations (right). WCA = weakly coordinating anion.

III.2. Synthesis of precursors and non-classical bonding at 9-sulfonium-10-boratriptycene

III.2.1 Synthesis of 9-sulfonium-10-boratriptycene precursors

The 10-mesityl-9-sulfonium-10-boratriptycene-ate complex **3.3**, obtained by a formal cycloaddition of benzyne on the B/S dipole **3.2** was treated with the Brønsted superacid $HCTf_3$ to induce the B–C bond cleavage affording the complex **3.4** (**Scheme III.19**). Due to the non-coordinating nature of the triflide couteranion, this type of coordination was previously unknown in the case of boron Lewis acids. In the solid state S1, S2, C1 and S3 are in trigonal

planar arrangement (sum of bond angles = 360 °) with a C–S3 bond length of [1.682(4) Å] which is shorter than that of single bond,[26] confirming the π-character of the C=S3 bond. Complex **3.4** is stable both in the solid state and in solution, and despite having a high dissociation enthalpy (ΔH^0 = 199 kJ.mol^{-1}) the B–O bond dissociation was triggered by raising the temperature to 80 °C and led to the formation of borohydride **3.6** in the presence of *N,N*-dimethyl-amine-borane as hydride donor (**Scheme III.19** and structure of **3.6** in the solid state in the SI Figure SIII.18). Triarylborohydride **3.5** exhibited an impressive chemical stability, being unreactive upon treatment with a HCl solution for a week or by treatment with $HNTf_2$ (triflimidic acid) (Figures SIII.4-SIII.6 in the Supporting information). This feature is consistent with the value of the hydride ion affinity (HIA) of **3.1** (880 kJ.mol^{-1}), which is higher than those of silylium ions (Mes_3Si^+: 577 kJ.mol^{-1}) and of the analogous phosphonium bridged 10-boratriptycene (871 kJ.mol^{-1}).[19,27]

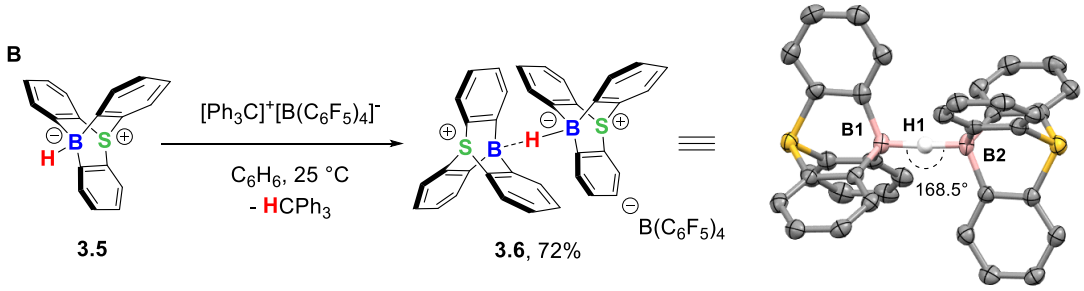


Scheme III.19 : Formal 1,4-cycloaddition to form the 9-sulfonium-10-boratriptycene ate-complex **3.3**, subsequent protodeboronation to form the triflide-complex **3.4** and hydride transfer to form the hydridoborate **3.5**.

III.2.2 Hydride abstraction from 10-hydrido-9-sulfonium-10-boratriptycene-ate complex

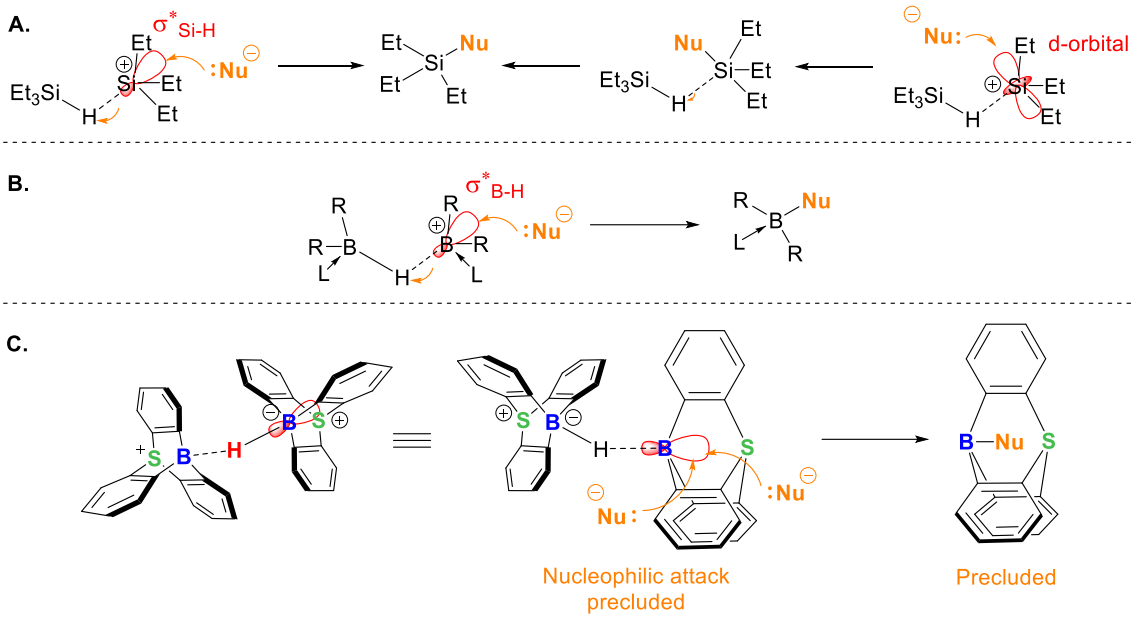
Next, the Bartlet-Condon-Schneider protocol was submitted to borohydride **3.5** (**Scheme III.20**).[28,29] According to ^{11}B NMR spectroscopy, borohydride **3.5** was totally consumed and a new signal appeared at δ = 8.8 ppm, indicating the formation a new species with a decreased coordination number

at boron. The chemical shift is however not that expected for **3.1** which has a predicted value of 82 ppm obtained by GIAO-DFT at the B3LYP/6-311+G(2d,p)//M06-2X/6-311G(d) level of theory. Crystallization in benzene showed evidence for the structure of **3.6** (**Scheme III.20**). The structure in the solid state is nearly a centrosymmetric dimer, featuring two units of 9-sulfonium-10-boratriptycene linked together with a 3c/2e BHB bond, similar to that previously observed for carbenium,[30] borenium and silylium cations.[31–33] Both boron atoms are tetracoordinated, and the pyramidalization in **3.6** [0.560 Å], defined as the distance between the boron atom and the plane spanned by the *ipso*-carbon atoms of the three triptycene benzene rings is between those of borohydride **3.5** [0.663 Å] and that computed for **3.1** [0.384 Å]. The BHB unit is quasi linear with a B1–H–B2 angle of [168.5°], both B–H bond lengths are equivalents [1.293(4) Å] and significantly longer than those of borohydride **3.5** [1.150(3) Å] which correspond to an elongation of 13%. It is worth noting that the presence of the bridged hydrogen atom in **3.6** was confirmed by T1-filtered $^{1}H\{^{11}B\}$ NMR analysis at 55 °C, however variable-temperature (VT) NMR analysis from -30 °C to 55 °C showed no evidence for the splitting of the ^{11}B NMR chemical shift of **3.6** (Figures SIII.1 and SIII.2 in the Supporting Information).



Scheme III.20 : Synthesis of **3.6** via hydride redistribution reaction and molecular structure. H-atoms (except the boron-bound hydrogen) and counter anion are omitted for clarity; thermal ellipsoids are represented with a 50% probability level.

Then, the bonding nature in **3.6** was probed by quantum chemical calculations. Natural bond orbital (NBO) analysis gave similar partials charges for both boron atoms (0.54e, e = elemental charge) and negative charge for H1 (-0.12e). The Lewis structure depicted in the NBO analysis displays a hypovalent three-center B–H–B bond (electron occupancy of 1.98). The percentage of valence hybrids composition of the NBO expressed from the natural population shows that the main contribution is from the hydrogen (55.8% w.r.t. 22.1% for each boron atoms). Thus, experimental and theoretical data suggest a symmetrical 3c2e bonding situation in **3.6**, resulting from a mechanistic scenario implying the transient formation of **3.1** via a hydride transfer which reacts with a remaining B–H σ-bond of borohydride **3.5**. However, the aforementioned HIA of **3.2** (880 kJ.mol-1) is comparable to that of Ph_3C^+ (885 kJ.mol^{-1})[34] reflecting that the hydride abstraction from **3.5** is not strongly thermodynamically favored, but the formation of the 3c2e bond is highly exothermic (ΔH^0_{ass} = -169 kJ.mol^{-1}) and serves as an extra driving force. Compound **3.6** showed a surprising high stability, and due to the electronic inaccessibility of the B–H bond implied in the 3c2e unit, no additional hydride abstraction is observed with an excess of $[Ph_3C]^+[B(C_6F_5)_4]^-$, and the protonation of the B–H bond was not observed with $HNTf_2$ (Figures SIII.9-SIII.10 in the SI). Moreover, due to the steric protection of the B–H σ*–orbital in combination with the high stability of the BHB bond, even a strong Lewis base such as 1,3-bis(2,4,6-trimethylphenyl)-2-imidazolidinylidene (SIMes) is not strong enough to replace one B–H unit (**Scheme III.21**, Figure SIII.7-SIII.8 in the SI).

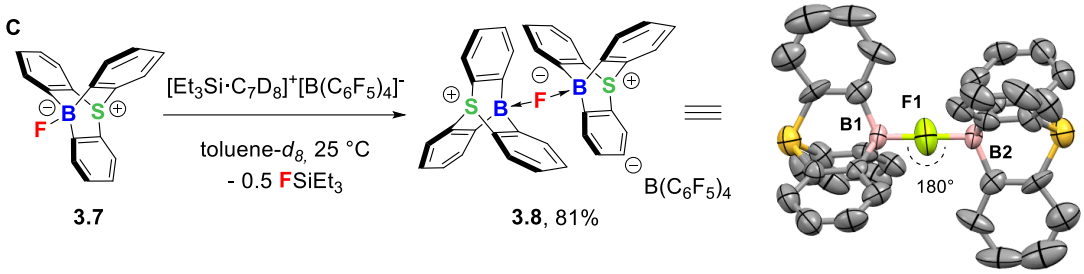


Scheme III.21 : Nucleophilic attack at hydride-bridged **A.** silylium, **B.** borenium and **C.** 9-sulfonium-10-boratriptycene (**3.1**).

III.2.3 Fluoride abstraction from 10-fluoride-9-sulfonium-10-boratriptycene-ate complex

Given the isoelectronic relationship and orthogonal reactivity between carbenium and silylium cations,[35,36] we next reasoned that a donor-free form of **3.1** could be accessible via a fluoride ion transfer reaction starting from the 10-fluoro-9-sulfonium-10-boratriptycene-ate complex. Thus, fluoroborate **3.7** was added to a solution of $[Et_3Si{\cdot}C_7D_8]^+[B(C_6F_5)_4]^-$ and ^{19}F NMR analysis showed the total consumption of **3.8** as well as a new signal at δ = -250 ppm, suggesting the formation of a new B–F bonded species. A single crystal X-ray structure analysis confirmed the structure of **3.8** as a sum of two units of 9-sulfonium-10-boratriptycene linked by a fluoride bridge and showed notable differences from those of reported fluoride bridged organoborons (**Scheme III.22**).[37] The BFB unit is in a unique linear arrangement with a B1–F–B2 angle of [180°], the similar B–F bond lengths of [1.506(13) Å] and [1.532(13) Å] indicated a symmetrical B–F–B bonding

and are shorter than those observed by Piers in the formally cationic $[R_3B–F–BR_3]^+[NTf_2]^-$ complex,[38] the latter having B–F bond lengths of [1.576(5)Å] and [1.566(5) Å] and a bent BFB unit with an angle of 131.7(3)°.



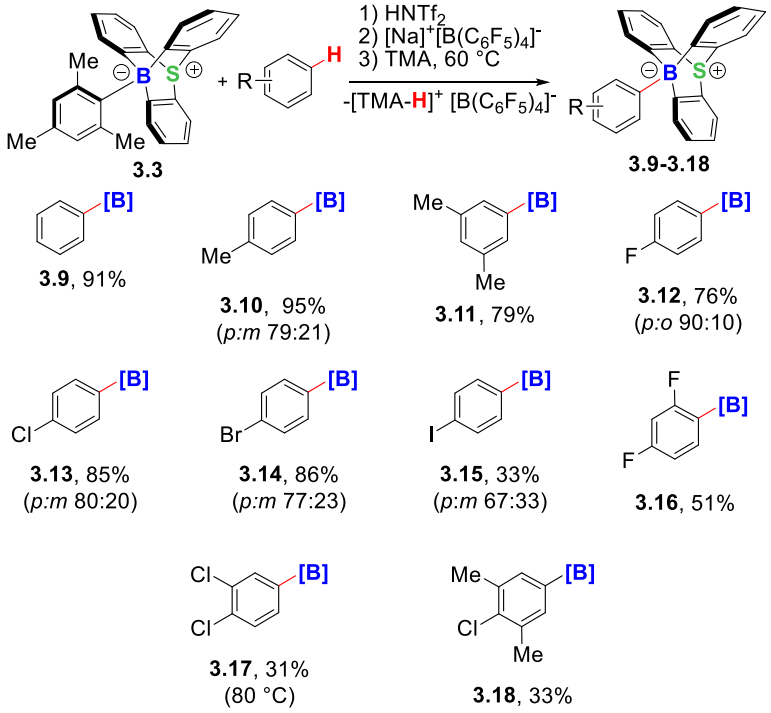
Scheme III.22 : Silylium cation mediated fluoride abstraction from **3.7** to form the fluoride bridged ate-complex **3.8** and molecular structure. H-atoms and counter anion are omitted for clarity; thermal ellipsoids are represented with a 50% probability level.

III.3. Evaluation of the Lewis acidity

Recognizing that **3.1** should possess a highly electron-deficient boron center, several Lewis acidity tests were undertaken. Protodeboronation of **3.3** with $HNTf_2$ in a presence of Et_3PO provided the Gutmann-Becket Lewis adduct $Et_3PO{\cdot}$**3.1** as evidenced by a broad singlet in the ^{31}P NMR spectrum at δ = 81.2 ppm (Figure SIII.11 in the SI).[39–41] Additional experimental Lewis acidity determinations based on infrared spectroscopy confirmed the high Lewis acidity of **1** (see the SI). Next, its fluoride ion affinity (FIA) was evaluated. The gas phase isodesmic FIA of **3.1** (854 kJ.mol^{-1}) is exceeding by far that of $B(C_6F_5)_3$ (466 kJ.mol^{-1}) and 9-boratriptycene (476 kJ.mol^{-1})[25] and is comparable or higher to that of main group cationic Lewis acids such as $[tolyl{\cdot}Si(CH_3)_3]^+$ (842 kJ.mol^{-1}), $[Ge(CH_3)_3]^+$ (875 kJ.mol^{-1}), $[Ga(Me_2)]^+$ (853 kJ.mol^{-1}) and 9-phopshonium-10-boratriptycene (845 kJ.mol^{-1}).[19,42]

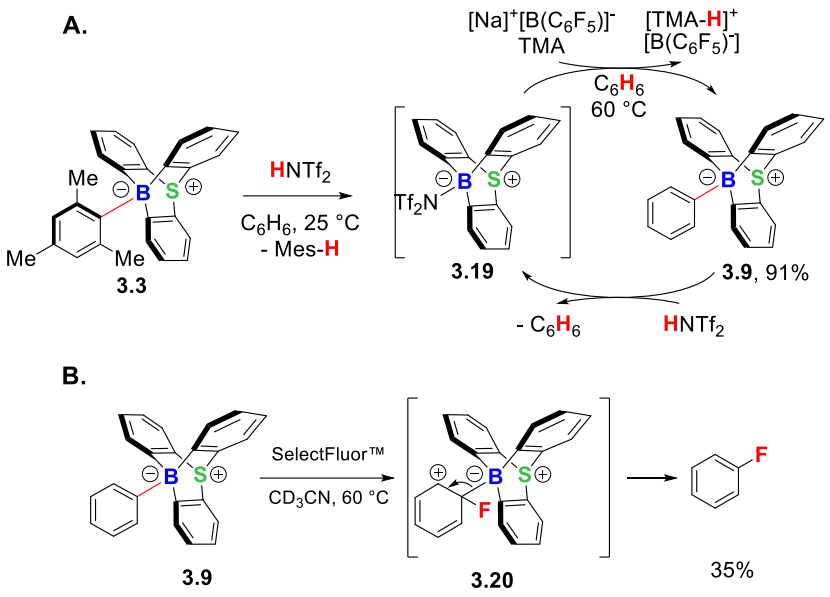
III.4. Brief aspect on borylation and functionalization of Csp^2–H bonds

These findings prompted us to investigate the reactivity of **3.1**. The metal-free Csp^2–H bond borylation of a plethora of substrates by haloboranes and boreniums cations has been reported,[43,44] but apart from very rare exceptions,[45,46] is restricted to activated arenes. After 16h at 60 °C, 9-sulfonium-10-boratriptycene-ate-complexes **3.9** (91% yield), **3.10** (95% yield), **3.11** (79% yield) and **3.12** (76%) have been isolated from solutions of pre-generated **3.1** in C_6H_6, C_6H_5Me, *m*-$C_6H_4Me_2$ and C_6H_5F in a presence of 3,5-*N*,*N*-tetramethylaniline (TMA) (**Scheme III.23**). Even poorly reactive arenes such as C_6H_5Cl (85%), C_6H_5Br (86%) and C_6H_5I (33%) were also converted to the aryl ate-complexes **3.12**-**3.15**, demonstrating the exceptional electrophilicity of **3.2**. The process is not limited to mono-substituted arenes but can also be employed on bis and trisubstituted derivatives, leading to the formation of ate complexes **3.16**-**3.18** in moderate to good yields (31-51%) with complete regioselectivity. Competitive C–H borylation of a mixture of C_6H_5Cl and *p*-xylene afforded exclusively the ate-complex **3.13** (76% yield) with no traces of *p*-xylene Csp^2–H borylation being detected, illustrating that the C–H borylation process is highly sensitive to steric hindrance and react preferentially with the less reactive but less hindered arene (see the SI for details, Figure SIII.13).



Scheme III.23 : Csp^2–H borylaion of unactivated arenes.

More importantly, protodeboronation of **3.9** by $HNTf_2$ led to the formation of benzene and regenerated triflimidate-complex **3.19** (**Scheme III.24, A** and Figures SIII.14-SIII.16 in the SI). This closed synthetic loop consisting in successive C–H borylation/ protodeboration starting and ending with **3.19** is a proof of concept that a catalytic cycle is in principle possible. Despite some breakthrough,[47] the transition metal-free functionalization of Csp^2–H bonds of arenes remains very challenging, and their direct conversion to fluoroarenes has never been achieved. Since arylborates are orders of magnitude more nucleophilic than unactivated arenes,[48] it was expected that **3.9** react with SelectFluor® to give fluorobenzene.[49] This process starts with an exocyclic-*ipso*-fluorination forming the Wheland intermediate **3.20**, which rearomatizes via C–B bond cleavage (**Scheme III.24, B**).



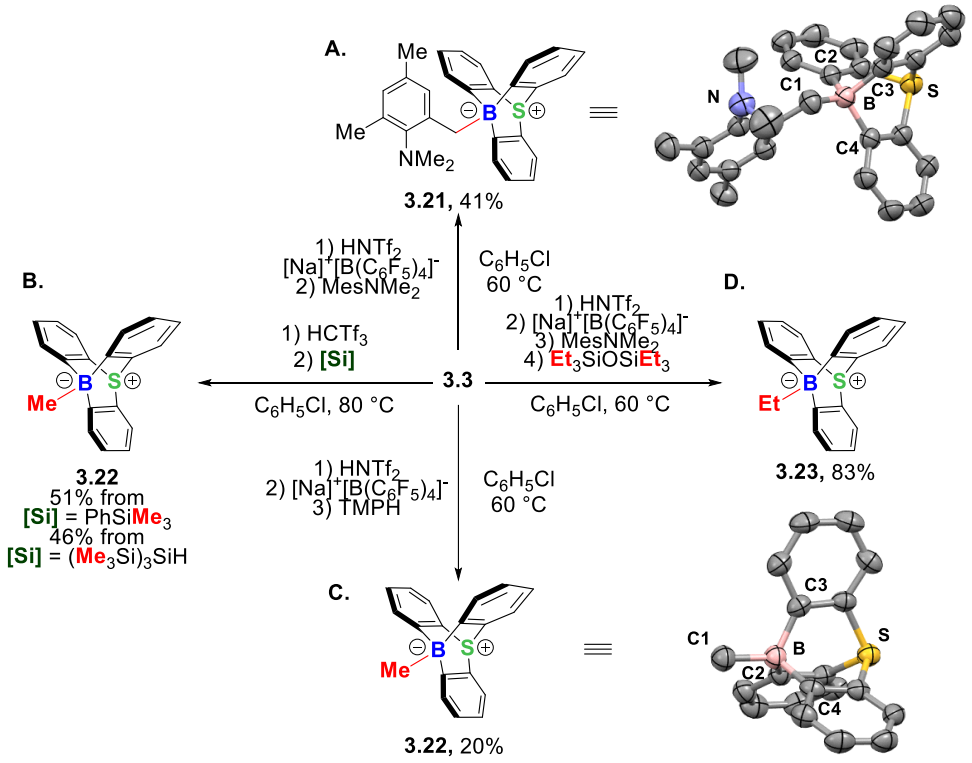
Scheme III.24 : **A.** Cycle of C–H activation of benzene and protodeboronation of **3.9** to produce **3.19** and **B.** Ipso deborono fluorination of **3.9** to yield fluorobenzene.

Although remaining a stoichiometric procedure, the demonstration of this C–H functionalization sequence is a first step towards the establishment of a transition-metal-free catalytic C–H bond functionalization process of unactivated arenes by using frustrated Lewis pairs.

III.5. Demonstration of borylation of Csp^3–H bonds and abstraction of Csp^3-Si and Csp^3–Csp^3 bonds.

We finally reasoned that **3.2** has the potential to borylate stronger C–H bonds. Despite intense efforts,[50,51] the transition-metal-free Csp^3–H bond borylation remains a holy grail, and there are still speculations on the fact that FLPs could perform such type of transformations.[52] Protodeboronation of **3.3** with $HNTf_2$ followed by the addition of $[Na]^+[B(C_6F_5)_4]^-$ and 2-dimethylamino-mesitylene afforded ate-complex **3.21** in 41% yield (**Scheme III.25, A**). When repeating the Csp^2–H borylation procedure with Ph–$SiMe_3$ instead of C_6H_6, neither the Csp^2–H borylation nor the classical *ipso*-Friedel-Crafts reactions occurred, and only the methyl ate-complex

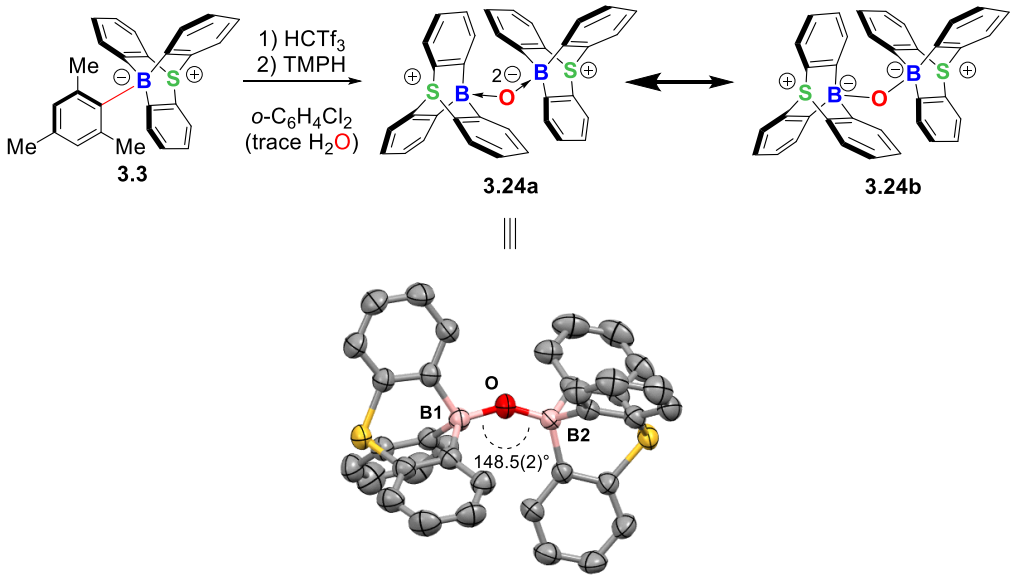
3.22 was formed via a selective cleavage of a Csp^3–Si bond (**Scheme III.25, B**). Although similar Csp^3–Si bond cleavage have been reported with carborane acid,[53,54] this type of selectivity is striking, given that kind of Brønsted super-acid usually trigger *ipso*-directed protodesilylation.[55] Surprisingly, reaction of **3.1** with $(Me_3Si)_3SiH$ resulted in the selective cleavage of the Csp^3–Si bond and not of the weaker - but less accessible Si–H bond, affording **3.22** in 46% yield. Reaction of hexaethyldisiloxane with **3.1** produced the ate-complex **3.23** in 83% yield (**Scheme III.25, D.**). While main-group Lewis acids are inert towards Csp^3–Csp^3 bond, a solution of **3.19** in *m*-difluorobenzene turned yellow upon addition of $[Na]^+[B(C_6F_5)_4]^-$ and tetramethylpiperidine (TMPH). Boron ate-complex **3.22** was then isolated with 20% yield and its molecular structure reveals a formal methyl-anion abstraction from TMPH (**Scheme III.25, C** and SI for details).



Scheme III.25 : Reactivity of 9-sulfonium-10-boratriptycene toward Csp^3–H, Si–Csp^3 and Csp^3–Csp^3 bonds. Molecular structures of compounds **3.21**-**3.22** Selected bond lengths in Å; (19) B–C1 1.609(3); B–C2 1.643(3); B–C3 1.653(4); B–C4 1.637(3). (20): B–C1 1.618(4). H-atoms are omitted for clarity; thermal ellipsoids are represented with a 50% probability level.

III.6. Synthesis of 9-sulfonium-10-boratriptycene stabilized molecular oxide bis-anion.

Protodeboronation of **3.3** by $HCTf_3$ in *o*-$C_6H_5Cl_2$ and subsequent addition of wet TMPH showed no evidence for a C–H borylation process and the unique diborate **3.24a** with two 9-sulfonium-10-boratriptycene units connected through an oxygen atom was isolated in 26% yield (**Scheme III.26**).



Scheme III.26 : Formation of the molecular oxide bis-anion (**3.24**) and its molecular structure derived from X-ray structure analysis. H-atoms are omitted for clarity; thermal ellipsoids are represented with a 50% probability level.

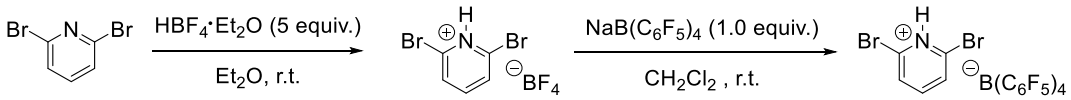
A reasonable mechanistic scenario accounting for the formation of **3.24a** is the initial coordination of adventitious water to **3.2** followed by deprotonation by TMPH,[56] corresponding to a twofold Lewis acid assisted O–H deprotonation of water. In the solid state, the two halves of the molecule are not significantly different with a pyramidalization of [0.711 Å] and [0.702 Å] for B1 and B2 respectively, and a B1–O1–B2 angle of [148.5(2)°] (**Scheme III.26**). The B1–O1 [1.411(4) Å] and B2–O1 [1.408(8) Å] bond lengths are equivalents when considering experimental uncertainty and are between those of coordinative [1.597(2) Å] and covalent

[1.311(2) Å] B–O single bonds.[57] Inspection of the NBO (See the Supporting information for details) indicates that the bonding situation between the boron atoms and the oxygen atom in **3.24a** comes from donor-acceptor O–B interactions rather than conventional σ-bonding. Therefore, the B–O σ-bonded form **3.24b** featuring two negatively charged boron atoms is a far weaker resonance contribution than the donor-acceptor form **3.24a**, which shows a unique dianionic oxygen atom coordinated by two boron atoms (**Scheme III.26**).

III.7. Complements on attempted isolation of the donor-free 9-sulonium-10-boratriptycene.

III.7.1 Attempted protodeborylation with 2,6-dibromopyridinium

Considering that even triflide anion forms a relatively stable "ate"-complex **3.4** with the 9-sulfonium-10-boratriptycene (**3.1**), we reasoned that performing the protodeborylation with a strong and hindered Brønsted acid could prevent the formation of a Lewis adduct or "ate"-complex. With a predicted pK_a of -3.6 and a considerable steric hindrance surrounding the nitrogen atom, 2,6-dibromopyridinium was selected and its tetrafluoroborate (**3.25**) and tetrakis(pentafluorophenyl)borate (**3.26**) salts were synthesized according to modified literature procedure (**Scheme III.27**).[58]

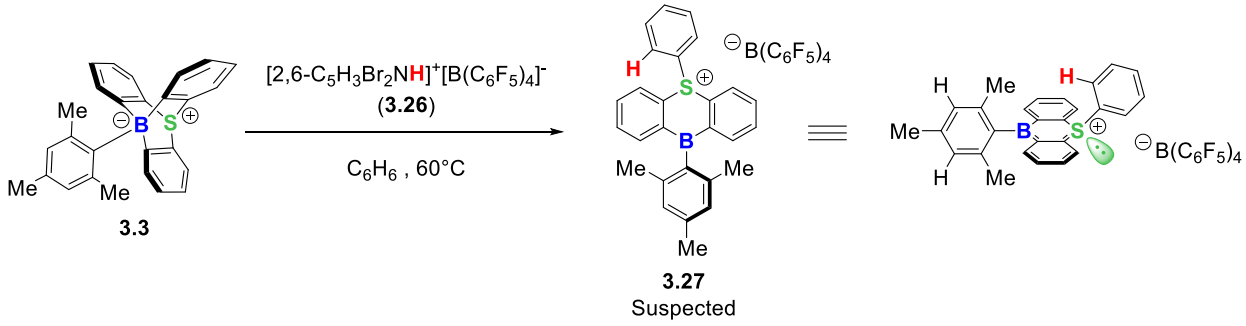


3.25 72% **3.26** 81%

Scheme III.27 : Synthesis of 2,6-dibromopyridinium tetrakis(pentafluorophenyl)borate (**3.26**).

Surprisingly, the protodeborylation turned out to be much slower than in previous cases. After 72h, the crude was submitted to NMR analysis revealing the relatively clean formation of a single product with a ^{1}H NMR

signature that did not match with 9-sulfonium-10-boratriptycene derivatives while the ^{11}B NMR spectrum still suggested the formation of a trivalent boron species (**Scheme III.28**, **Figure III.22**). A closer analysis to the crude ^{1}H NMR spectrum suggests that the protodeborylation reaction occurred at one of the phenyl rings *ipso*-position rather than at the mesityl substituent. Indeed, the formed borane would be similar to 10-mesityl-10***H***-9-thia-10-boraanthracene (**3.2**) with the two faces of the anthracene moiety being chemically different (**Figure III.21**). While in 10-mesityl-10***H***-9-thia-10-boraanthracene (**3.2**), the mesityl substituent presents two signals for the methyl substituents and a single signal for the two aromatic protons, in our unknown product, the two protons in the aromatic region of the mesityl substituent are unequivalent as well as the three methyl substituents. Unfortunately, due to relative instability towards ambient conditions, this borane (**3.27**) could not be isolated from the crude mixture. The observed signal at δ = 71.5 in ^{11}B NMR is surprisingly deshielded for a triarylborane which generally present a signal around δ = 60 ppm (58 ppm for $B(C_6F_5)_3$) (**Figure III.22**). However, a value of δ = 71.5 ppm is in the range of the phosphonium and sulfonium boranes reported by Gabbaï and co-workers.[59–62]



Scheme III.28 : Protodeborylation of 10-mesityl-9-sulfonium-10-boratriptycene-ate complex (**3.3**) with 2,6-dibromopyridinium tetrakis(pentafluorophenyl)borate (**3.26**).

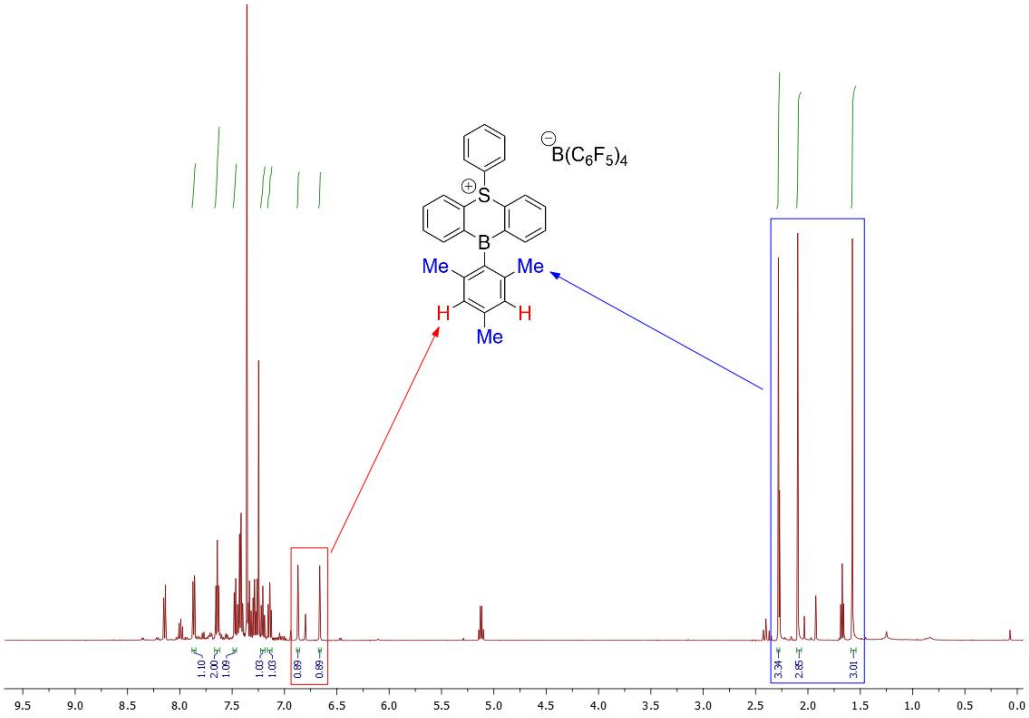


Figure III.21 : Crude ^{1}H NMR of protodeborylation of 10-mesityl-9-sulfonium-10-boratriptycene-ate complex (**3.3**) with 2,6-dibromopyridinium tetrakis(pentafluorophenyl)borate (**3.26**).

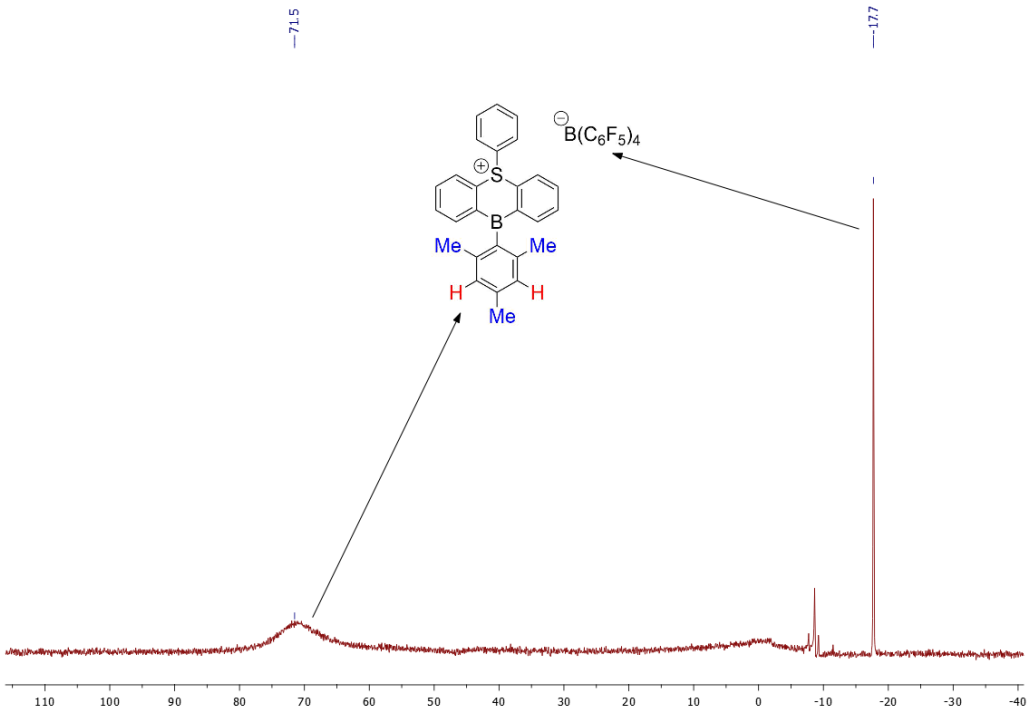
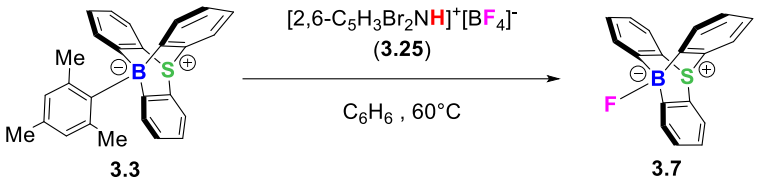


Figure III.22 : Crude ^{11}B NMR of protodeborylation of 10-mesityl-9-sulfonium-10-boratriptycene-ate complex (**3.3**) with 2,6-dibromopyridinium tetrakis(pentafluorophenyl)borate (**3.26**).

The observed opposite selectivity compared to all the previously performed protodeborylation reactions led us to the hypothesis that the steric hindrance around the pyridinium acidic center might lead to the protonation of a phenyl ring instead of the mesityl substituent. A second hypothesis could be that, in absence of sufficiently coordinating Lewis base, the 9-sulfonium-10-boratriptycene (**3.1**) could not be generated, leading to opening of the triptycene scaffold to form the corresponding triarylborane, being the most thermodynamically stable species. This second hypothesis was supported by performing the same reaction with 2,6-dibromopyridinium tetrafluoroborate (**3.25**) (**Scheme III.29**). The reaction was stirred and warmed only for 1h before analysis resulting in incomplete reaction. However, the single reaction product formed was 10-fluoro-9-sulfonium-10-boratriptycene (**3.7**), unambiguously identified by ^{19}F NMR spectroscopy with appearance of a characteristic signal at δ = -236.1 ppm (**Figure III.23**).



Scheme III.29 : Protodeborylation of 10-mesityl-9-sulfonium-10-boratriptycene-ate complex (**3.3**) with 2,6-dibromopyridinium tetrafluoroborate (**3.7**).

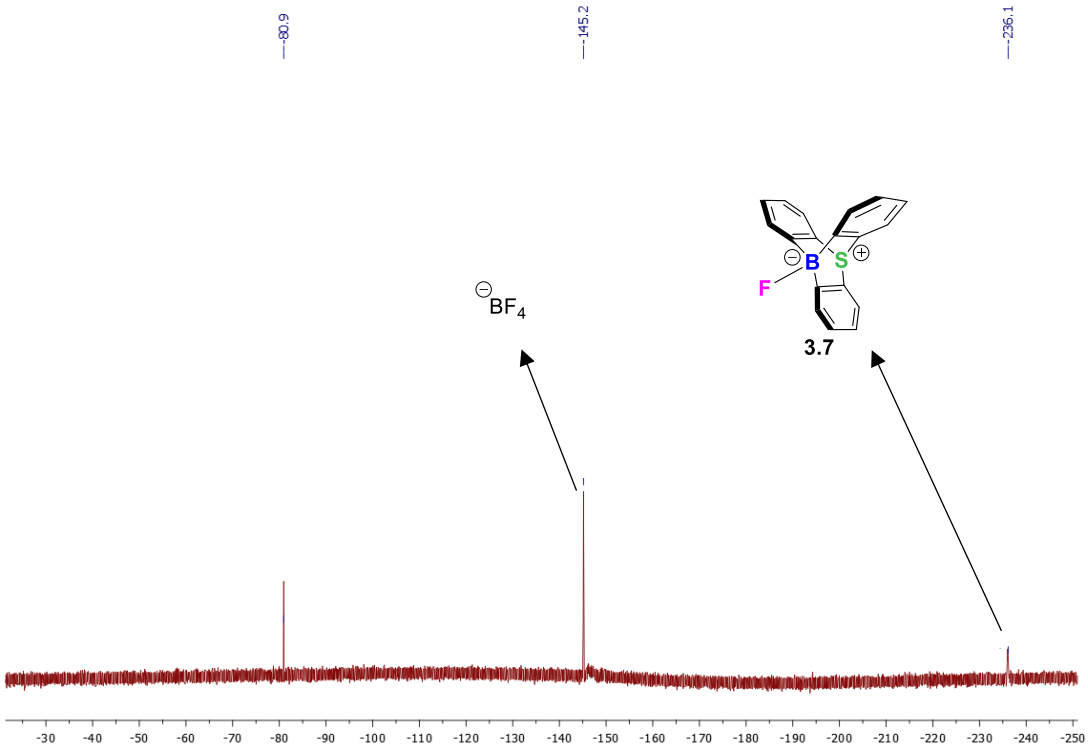


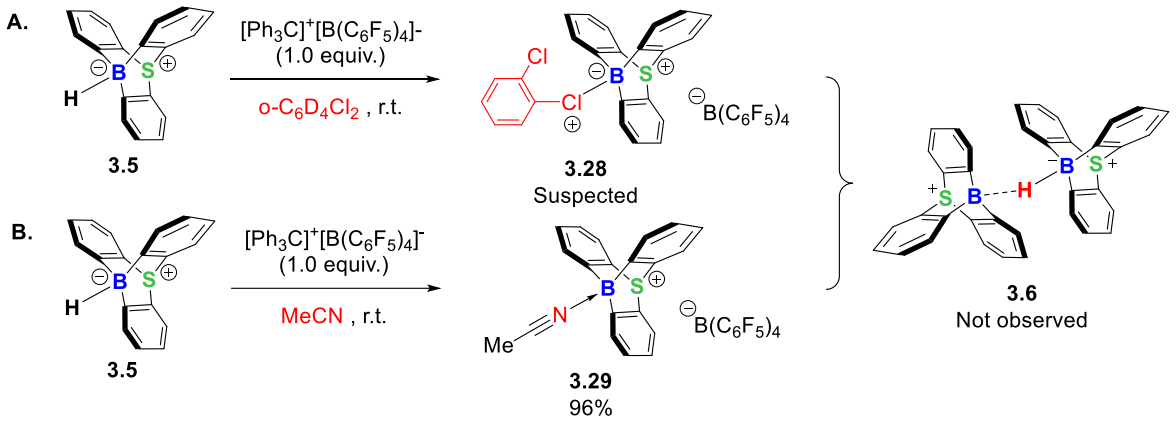
Figure III.23 : Crude ^{19}F NMR of protodeborylation of 10-mesityl-9-sulfonium-10-boratriptycene-ate complex (**3.1**) with 2,6-dibromopyridinium tetrafluoroborate (**3.26**).

The formation 10-fluoride-9-sulfonium-10-boratriptycene-ate complex (**3.7**) performing the protodeborylation with 2,6-dibromopyridinium tetrafluoroborate (**3.26**) refutes the first hypothesis and shows that the steric hindrance around the pyridinium Brønsted acidic center does not preclude the protonation of the mesityl ring.

III.7.2 Modified conditions of hydride abstraction

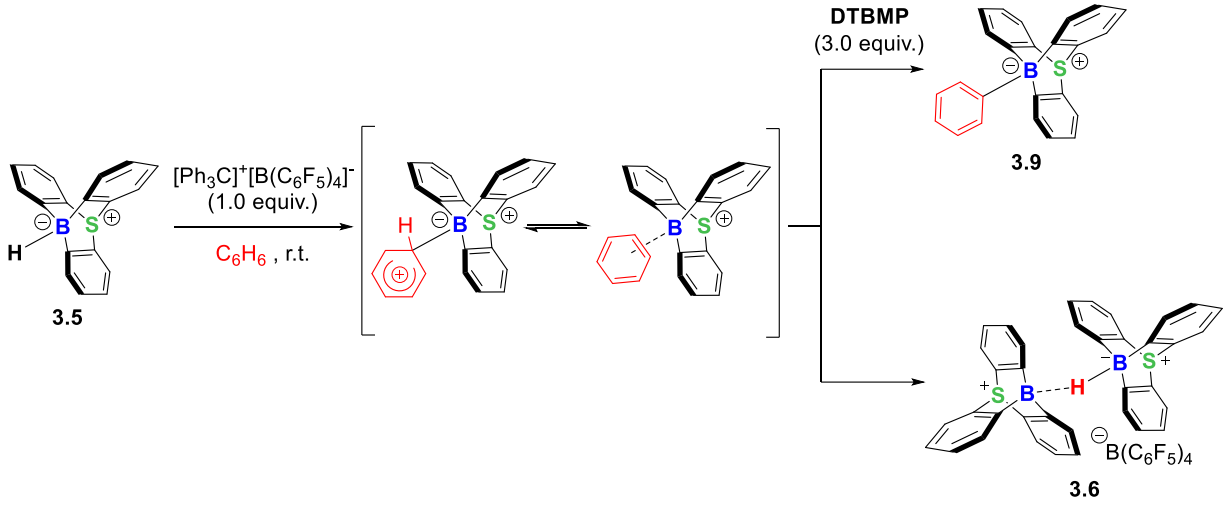
As already mentioned in **section III.2.2**, treating the hydride-ate complex **3.5** with $[Ph_3C]^+[B(C_6F_5)_4]^+$ in benzene or toluene led to the formation a remarkably stable hydride-bridged dimer **3.6** (**Scheme III.20**, **Scheme III.21**). Interestingly, performing this boron-to-carbon hydride transfer in *o*-dichlorobenzene instead of toluene or benzene led to the formation of a totally different product. All ^1H and heteronuclear NMR analysis suggested the formation of borylated 2-chlorophenyl-chloronium ion (**3.28**) (**Scheme**

III.30, A).[33,36,63,64] Unfortunately, despite many attempts, crystals suitable for X-ray diffraction analysis could not be obtained to confirm the formation of this product. Nevertheless, performing the reaction in acetonitrile as solvent led to clean and complete formation of 10-acetonitrile-9-sulfonium-10-boratriptycene-Lewis adduct (**3.29**) (**Scheme III.30, B**). This confirms that, in presence of sufficiently σ-donating solvent, the formation of the corresponding Lewis adduct is reached instead of the hydride-bridged dimer (**3.6**).

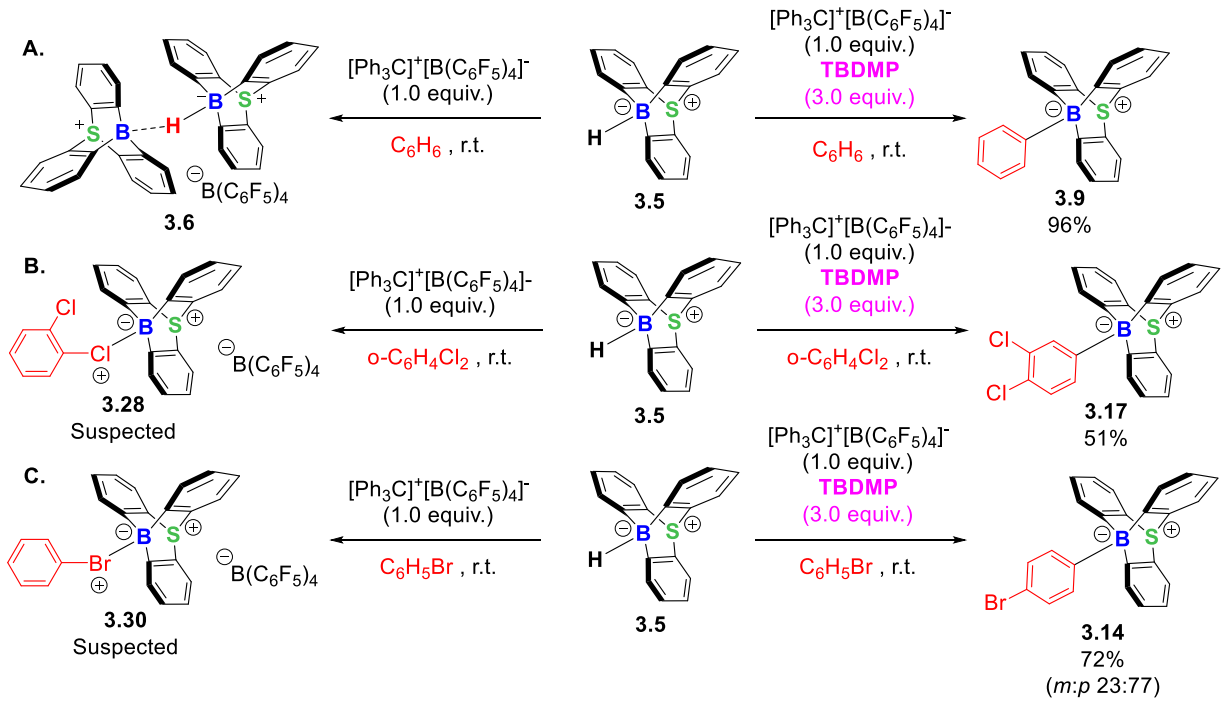


Scheme III.30 : Hydride abstraction from 10-hydrido-9-sulfonium-10-boratriptycene-ate complex (**3.5**) with tritylium ion in **A.** *o*-dichlorobenzene and **B.** acetonitrile.

More importantly, while performing this hydride abstraction in benzene or toluene led to the formation of the hydride-bridged dimer (**3.6**), modifying the reaction conditions by adding a Brønsted base led to clean and complete Csp^2–H borylation of the solvent within seconds (**Scheme III.31**). This suggests that the immediate product formed after hydride abstraction is a π- or σ-complex with benzene[65,66] which, in absence of Brønsted base, reacts with the starting borohydride **3.5** to form dimer **3.6** while, in presence of Brønsted base, is deprotonated to form a phenyl- (**3.9**) or tolyl-ate (**3.10**) complex. Similar reactivity is observed even with deactivated arenes such as *o*-dichlorobenzene or bromobenzene, the reaction being completed within seconds (**Scheme III.32**).

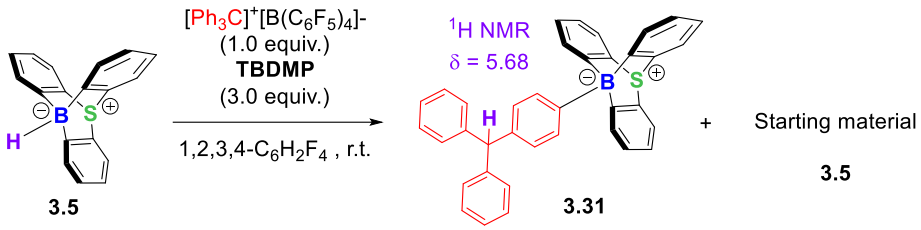


Scheme III.31 : Proposed mechanism of formation of 10-phenyl-9-sulfonium-10-boratriptycene-ate complex (**3.9**) and tetraki(pentafluorophenyl)borate 10,10'-hydronium-bis(9-sulfonium-10-boratriptycene) (**3.6**) from 10-hydrido-9-sulfonium-10-boratriptycen-ate complex (**3.5**) via hydride abstraction.



Scheme III.32 : Dual reactivity of 9-sulfonium-10-boratriptycene **3.1** generated by hydride abstraction in presence or absence of Brønsted base in **A.** benzene, **B.** *o*-dichlorobenzene, **C.** bromobenzene.

Against all odds, performing the reaction in weakly nucleophilic solvents such as tri- or tetrafluorinated benzene in presence of Lewis base did not lead to the formation of the hydride-bridged dimer **3.6** but to a very slow borylation of triphenylmethane itself formed by boron-to-carbon hydride transfer, allowing the generation of 9-sulfonium-10-boratriptycene **3.1** (**Scheme III.33, Figure III.24**). However, this product **3.31** is obtained in very small amount, the major product being unconverted starting material. This apparently slow reaction combined with the absence of hydride-bridged dimer **3.6** formation and the presence of remaining starting material was and remains very surprising and, so far, no real explanation has been found.



Scheme III.33 : Observed borylation of triphenylmethane resulting from hydride abstraction from 10-hydrido-9-sulfonium-10-boratriptycene-ate complex (**3.5**) in strongly deactivated solvent and in presence of Brønsted base.

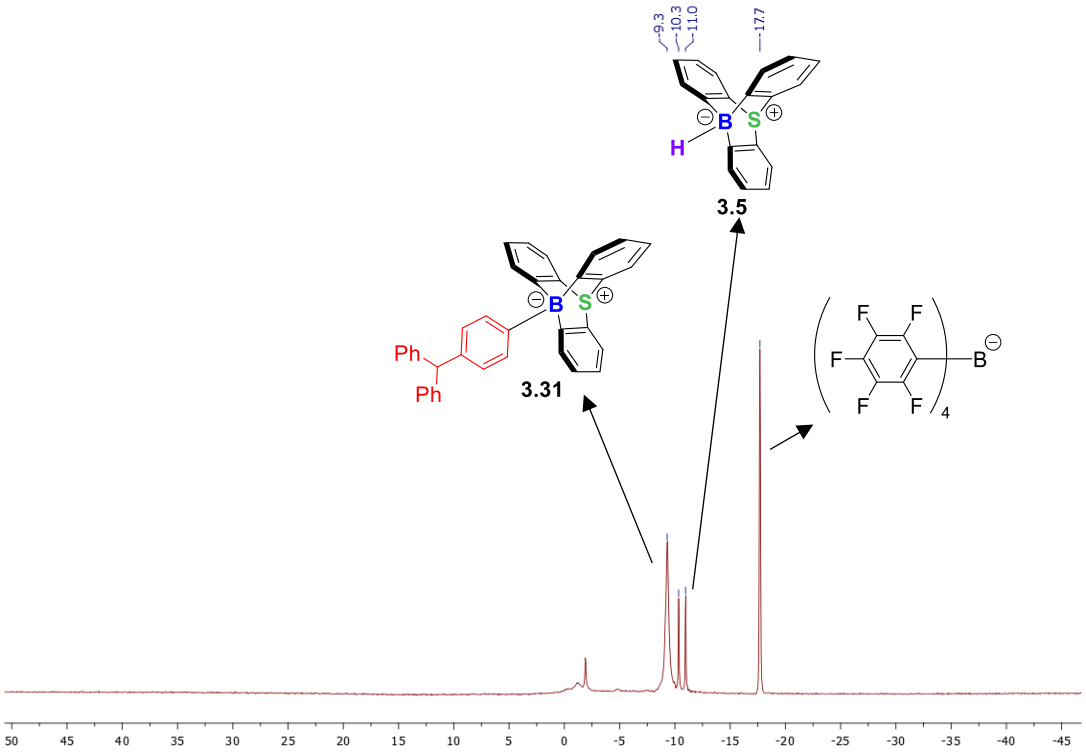
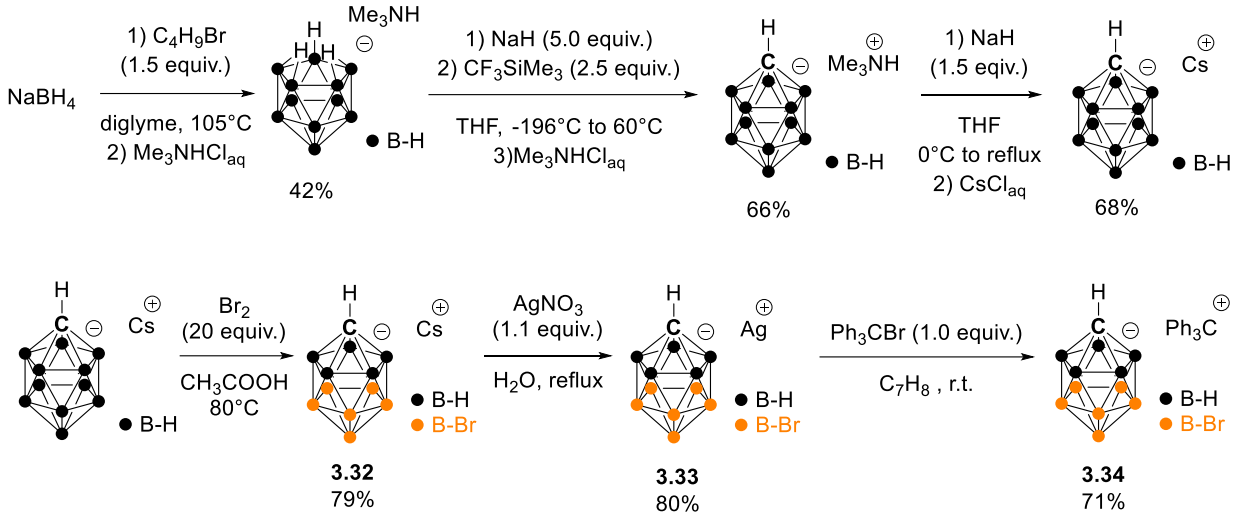


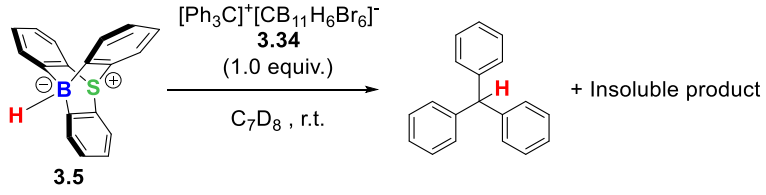
Figure III.24 : Crude ^{11}B NMR showing the borylation of triphenylmethane resulting from hydride abstraction from 10-hydrido-9-sulfonium-10-boratriptycene-ate complex (**3.5**) in strongly deactivated solvent and in presence of Brønsted base.

Considering that a boron-to-carbon hydride transfer does not necessarily lead to the formation of the hydride-bridged dimer as dead end, it was envisioned that switching from tritylium tetrakis(pentafluorophenyl)borate to a tritylium carborate derivative might allow the formation of a carborate-ate complex. Indeed, as the isolation of the donor-free 9-sulfonium-10-boratriptycene seems to be illusive, the final goal would be to synthesize a carborate-ate complex as the closest analog of the free Lewis acid. As halogenated carbadodecaborates are not commercially available, these must be synthesized in the lab from $NaBH_4$, cesium carbadodecaborate and decaborane being far too expensive to be purchased in our lab. Tritylium 7,8,9,10,11,12-hexabromo-carbadodecaborate (**3.34**) was then chosen as most easily accessible halogenated carbadodecaborate derivative and synthesized according to several literature procedures from $NaBH_4$ (**Scheme III.34**).[67–69]



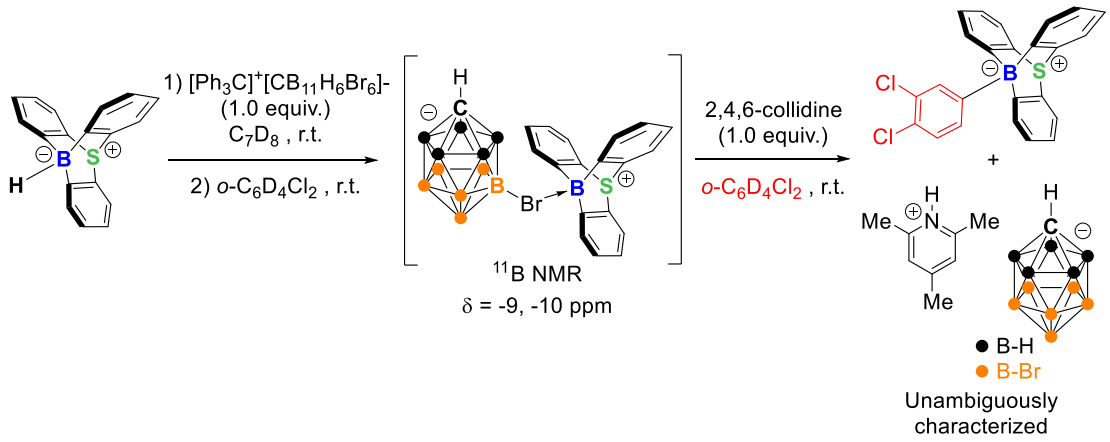
Scheme III.34 : Synthesis of tritylium 7,8,9,10,11,12-hexabromo-carbadodecaborate (**3.34**) from sodium borohydride.

With tritylium 7,8,9,10,11,12-hexabromo-carbadodecaborate (**3.34**) in hands, boron-to-carbon hydride transfer was performed in similar conditions as previously described. While with the $B(C_6F_5)_4$ anion the reaction cleanly provided the hydride-bridged dimer (**3.6**) in toluene, with the $CB_{11}H_6Br_6$ anion, a dense insoluble precipitate immediately formed and the only product detected in the crude ^1H NMR was triphenylmethane originating from the hydride abstraction (**Scheme III.35**). It was initially suspected that the precipitate was also the hydride-bridged dimer, this product being already poorly soluble in toluene with $B(C_6F_5)_4$ as counteranion.



Scheme III.35 : Hydride abstraction from 10-hydrido-9-sulfonium-10-boratriptycene-ate complex (**3.5**) with tritylium 7,8,9,10,11,12-hexabromo-carbadodecaborate (**3.34**) in toluene-d_8.

In order to identify this product, the reaction was performed again in the same conditions, the solid was filtered and washed with toluene prior to be solubilized in *o*-$C_6D_4Cl_2$. This time, ^{1}H and ^{11}B NMR analysis suggested a different product which did not correspond to the previously suggested 10-(2-chlorophenyl)chloronium-9-sulfonium-10-boratriptycene (**3.28**). The ^{11}B NMR particularly draw our attention since two signals were observed at δ = -9.0 and -10.1 ppm along with a broad signal at δ = -21.1 ppm (**Figure III.25, Figure III.26**). This signal did not match with the signature of 7,8,9,10,11,12-hexabromo-carbadodecaborate ion which would show a singlet at δ = -10.9 ppm and a doublet at δ = -21.2 ppm (**Scheme III.36**).[69] This ^{11}B NMR signature may suggest a "ate"-complex formed between the 7,8,9,10,11,12-hexabromo-carbadodecaborate ion and the 9-sulfonium-10-boratriptycene (**3.35**). A very similar ^{11}B NMR spectrum is reported by Oestreich and co-workers for their $[t\text{Bu}_2\text{HSi}]^+[\text{CB}_{11}\text{H}_6\text{Br}_6]$.[53,55,70–72] Further addition of one equivalent of collidine in the NMR tube led to drastic modifications of the NMR spectras, with appearance of protonated collidine in ^{1}H NMR and a signal corresponding to previously observed 10-aryl-9-sulfonium-10-boratriptycene-ate complex at -9.2 ppm along with the expected signal of 7,8,9,10,11,12-hexabromo-carbadodecaborate ion (**Scheme III.36, Figure III.27, Figure III.28, Figure III.29**).



Scheme III.36 : Hydride abstraction from 10-hydrido-9-sulfonium-10-boratriptycene-ate complex (**3.5**) with tritylium 7,8,9,10,11,12-hexabromo-carbadodecaborate (**3.34**) performed in toluene-d_8 and analyzed in *o*-$C_6D_4Cl_2$ followed by addition of 2,4,6-collidine.

These simple experiments strongly suggested that hydride abstraction from 10-hydrido-9-sulfonium-10-boratriptycene-ate complex (**3.5**) with tritylium 7,8,9,10,11,12-hexabromo-carbadodecaborate (**3.34**) in toluene led to the formation of the desired 10-(7,8,9,10,11,12-hexabromo-carbadodecaborate)-9-sulfonium-10-boratriptycene-ate complex (**3.35**) which in presence of a Brønsted base is able to undergo the borylation of *o*-$C_6D_4Cl_2$ present as solvent. Unfortunately, several attempts to obtain crystals of this carbadodecaborate-ate complex suitable for X-ray diffraction analysis failed. Crystals suitable for X-ray diffraction analysis were obtained several times but always revealed a decomposition of the expected product with an opening of the triptycene scaffold. The formation of this degraded product is not in agreement with the reactivity and the NMR data observed previously which suggested that the product suspected as the "ate"-complex **3.35** is not sable in solution more than few hours and decomposes during the crystallization. Similar results were obtained starting from mesityl-boron-ate complex **3.3** using benzenium instead of tritylium 7,8,9,10,11,12-hexabromo-carbadodecaborate (**3.35**). However, the methodology is much less convenient since it requires to additional steps to synthesize benzenium

7,8,9,10,11,12-hexabromo-carbadodecaborate, which can't be stored indefinitely even in glovebox.

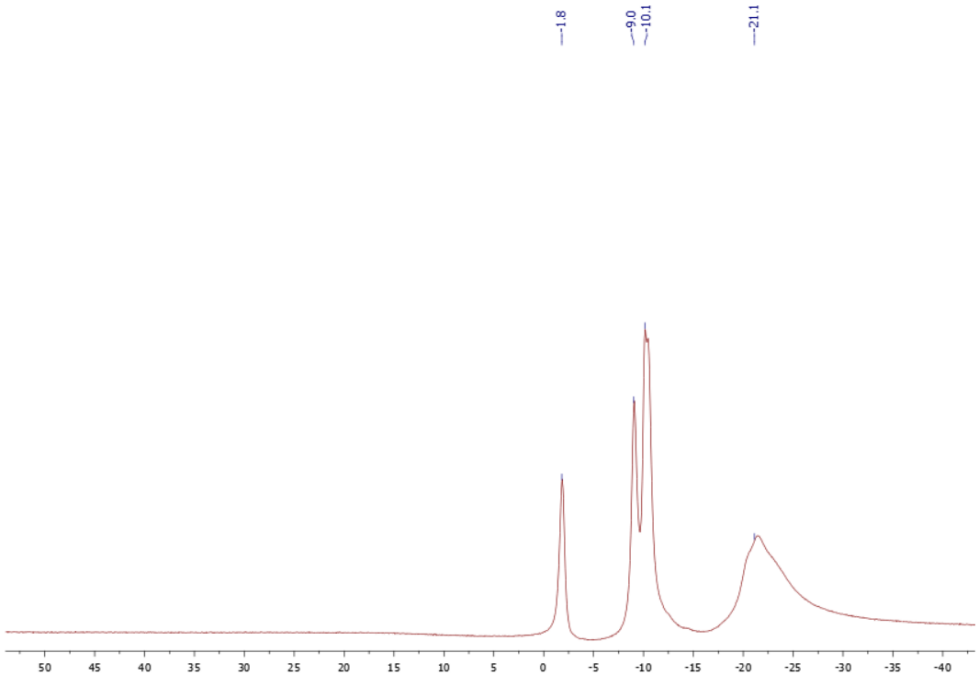


Figure III.25 : Crude ^{11}B NMR of hydride abstraction from **3.5** with **3.24** performed in toluene-d_8 and analyzed in *o*-$C_6D_4Cl_2$ before addition of 2,4,6-collidine.

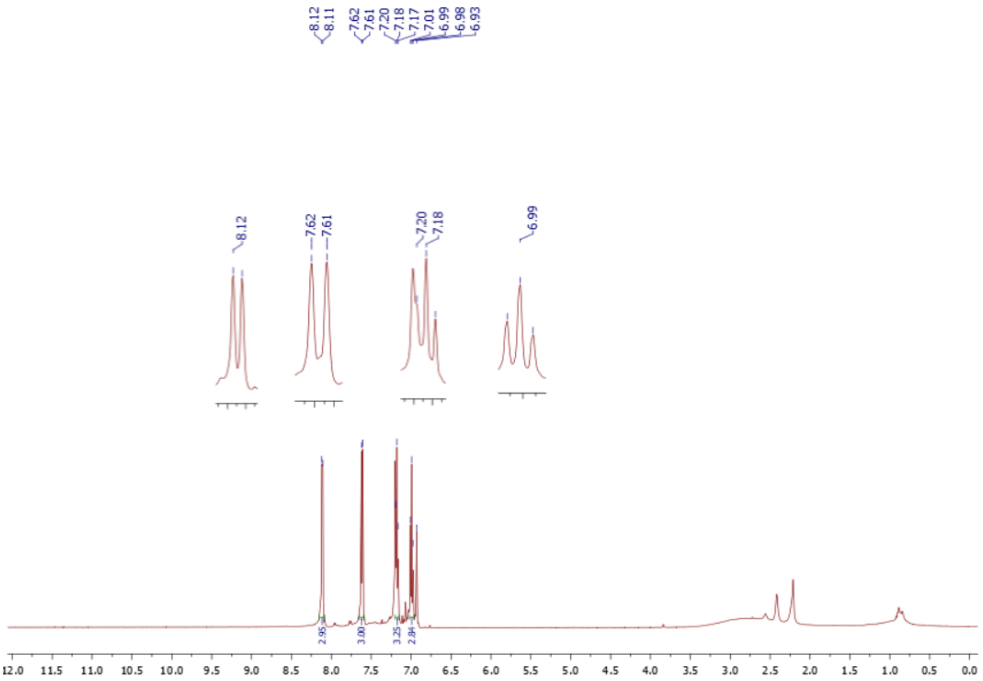


Figure III.26 : Crude ^{1}H NMR of Hydride abstraction from **3.5** with **3.24** performed in toluene-d_8 and analyzed in *o*-$C_6D_4Cl_2$ before addition of 2,4,6-collidine.

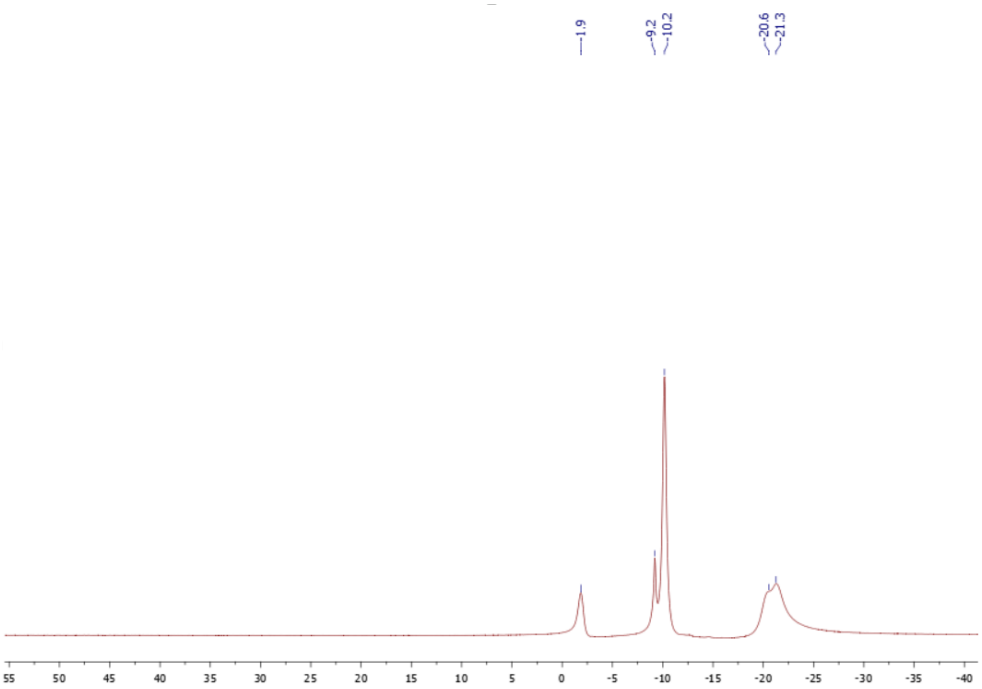


Figure III.27 : Crude ^{11}B NMR of hydride abstraction from 10-hydrido-9-sulfonium-10-boratriptycene-ate complex (**3.5**) with tritylium 7,8,9,10,11,12-hexabromo-carbadodecaborate (**3.24**) performed in toluene-d_8 and analyzed in *o*-$C_6D_4Cl_2$ after addition of 2,4,6-collidine.

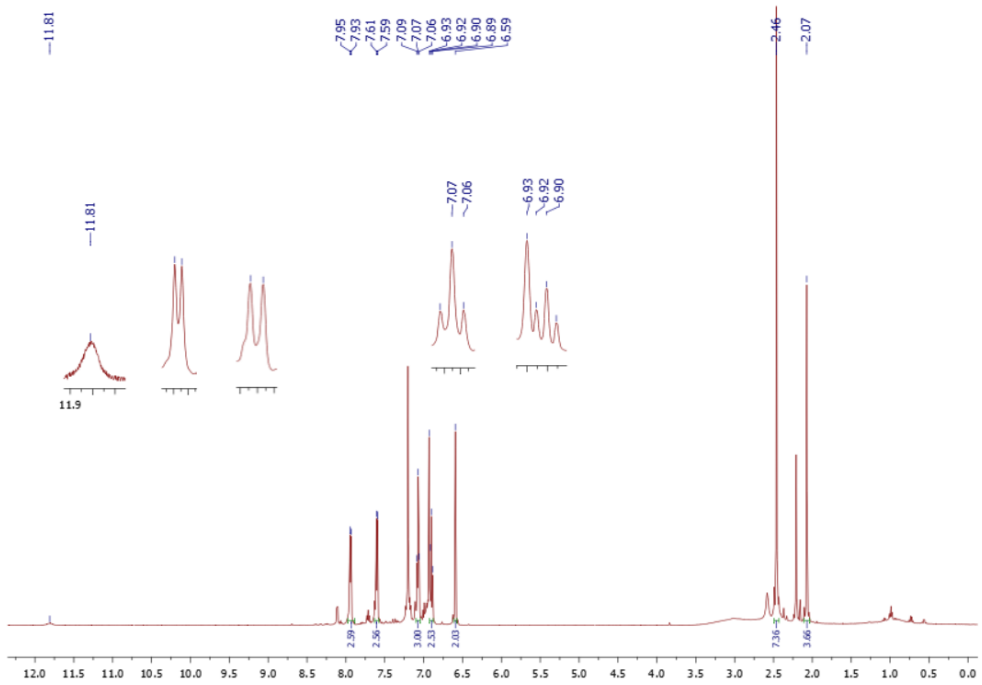


Figure III.28 : Crude ^1H NMR of hydride abstraction from **3.5** with **3.24** performed in toluene-d_8 and analyzed in *o*-$C_6D_4Cl_2$ after addition of 2,4,6-collidine.

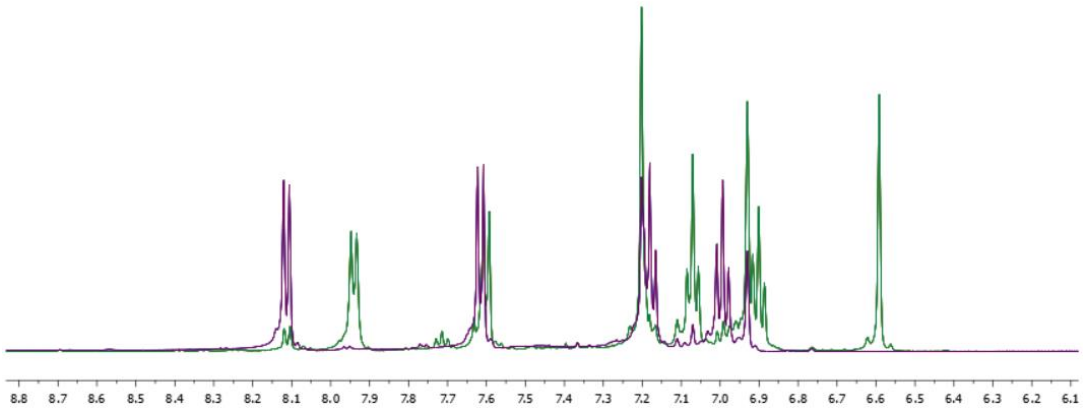


Figure III.29 : Superposed crude ^{1}H NMR of hydride abstraction from **3.5** with **3.24** performed in toluene-d_8 and analyzed in *o*-$C_6D_4Cl_2$ before (purple curve) and after (green curve) addition of 2,4,6-collidine.

III.8. Conclusion

In essence, the molecular design and chemical reactivity presented here outline a blueprint for the rational development of new electron deficient species and will allow a better understanding of the principles that governs the chemical behavior of p-block Lewis acids. Although not previously computationally predicted, the potential of pyramidal organoboron Lewis superacids to activate inert C–H bonds is another demonstration that main group Lewis acids and especially FLPs derived from them can mimics the chemical behavior of transition metals. Our efforts are now devoted towards the borylation of non-activated hydrocarbons and on the exploitation of superelectrophiles mediated C–H activation processes for transition-metal-free catalytic C–H functionalization reactions.

A brief demonstration was done in this chapter of the ability of 9-sulfonium-10-boratriptycene to Csp^2–H bonds, the subsequent chapter presents a detailed investigation of Csp^2–H borylation using 9-sulfonium-10-boratriptycene.

III.9. References

[1] G. N. Lewis, *Valence and the Structure of Atoms and Molecules in The Chemical Catalog Company*, Book Department, New York, **1923**.
[2] W. E. Piers, *Adv. Organomet. Chem.* **2005**, *52*, 1–76.
[3] W. E. Piers, T. Chivers, *Chem. Soc. Rev.* **1997**, *26*, 345–354.
[4] J. L. Carden, A. Dasgupta, R. L. Melen, *Chem. Soc. Rev.* **2020**, *49*, 1706–1725.
[5] D. W. Stephan, G. Erker, *Angew. Chem. Int. Ed.* **2010**, *49*, 46–76.
[6] G. C. Welch, R. R. S. Juan, J. D. Masuda, D. W. Stephan, *Science* **2006**, *314*, 1124–1126.
[7] M. A. Légaré, C. Pranckevicius, H. Braunschweig, *Chem. Rev.* **2019**, *119*, 8231–8261.
[8] F. Jäkle, *Chem. Rev.* **2010**, *110*, 3985–4022.
[9] A. Lorbach, A. Hübner, M. Wagner, *Dalt. Trans.* **2012**, *41*, 6048–6063.
[10] M. Li, J. S. Fossey, T. D. James, *Boron: Sensing, Synthesis and Supramolecular Self-assembly*, RSC, Cambridge, **2015**.
[11] L. A. Mück, A. Y. Timoshkin, G. Frenking, *Inorg. Chem.* **2012**, *51*, 640–646.
[12] E. I. Davydova, T. N. Sevastianova, A. Y. Timoshkin, *Coord. Chem. Rev.* **2015**, *297–298*, 91–126.
[13] A. Y. Timoshkin, K. Morokuma, *Phys. Chem. Chem. Phys.* **2012**, *14*, 14911.
[14] L. A. Mück, A. Y. Timoshkin, M. Von Hopffgarten, G. Frenking, *J. Am. Chem. Soc.* **2009**, *131*, 3942–3949.
[15] J. M. Oliva-Enrich, I. Alkorta, J. Elguero, *Molecules* **2020**, *25*, 1042.
[16] D. Mahaut, A. Chardon, L. Mineur, G. Berionni, B. Champagne, *ChemPhysChem* **2021**, *22*, 1958–1966.
[17] G. Bouhadir, D. Bourissou, *Chem. Soc. Rev.* **2004**, *33*, 210–217.
[18] A. Chardon, A. Osi, D. Mahaut, A. Ben Saida, G. Berionni, *Synlett* **2020**, *31*, 1639–1648.
[19] A. Ben Saida, A. Chardon, A. Osi, N. Tumanov, J. Wouters, A. I. Adjieufack, B. Champagne, G. Berionni, *Angew. Chem. Int. Ed.* **2019**, *58*, 16889–16893.
[20] Y. V. Vishnevskiy, M. A. Abaev, A. N. Rykov, M. E. Gurskii, P. A. Belyakov, S. Y. Erdyakov, Y. N. Bubnov, N. W. Mitzel, *Chem. Eur. J.* **2012**, *18*, 10585–10594.
[21] F. Ebner, H. Wadepohl, L. Greb, *J. Am. Chem. Soc.* **2019**, *141*, 18009–18012.
[22] F. Ebner, L. Greb, *Chem* **2021**, *7*, 2151–2159.
[23] M. B. Kindervater, K. M. Marczenko, U. Werner-Zwanziger, S. S. Chitnis, *Angew. Chem. Int. Ed.* **2019**, *58*, 7850–7855.
[24] K. M. Marczenko, J. A. Zurakowski, M. B. Kindervater, S. Jee, T. Hynes, N. Roberts, S. Park, U. Werner-Zwanziger, M. Lumsden, D. N. Langelaan, S. S. Chitnis, *Chem. Eur. J.* **2019**, *25*, 16414–16424.

[25] A. Chardon, A. Osi, D. Mahaut, T. H. Doan, N. Tumanov, J. Wouters, L. Fusaro, B. Champagne, G. Berionni, *Angew. Chem. Int. Ed.* **2020**, *59*, 12402–12406.
[26] N. Trinajstić, *Tetrahedron Lett.* **1968**, *9*, 1529–1532.
[27] H. Großekappenberg, M. Reißmann, M. Schmidtmann, T. Müller, *Organometallics* **2015**, *34*, 4952–4958.
[28] I. M. Riddlestone, A. Kraft, J. Schaefer, I. Krossing, *Angew. Chem. Int. Ed.* **2018**, *57*, 13982–14024.
[29] J. Y. Corey, *J. Am. Chem. Soc.* **1975**, *97*, 3237–3238.
[30] H. Kawai, T. Takeda, K. Fujiwara, T. Suzuki, *J. Am. Chem. Soc.* **2005**, *127*, 12172–12173.
[31] B. Inés, M. Patil, J. Carreras, R. Goddard, W. Thiel, M. Alcarazo, *Angew. Chem. Int. Ed.* **2011**, *50*, 8400–8403.
[32] Q. Wu, A. Roy, G. Wang, E. Irran, H. F. T. Klare, M. Oestreich, *Angew. Chem. Int. Ed.* **2020**, *59*, 10523–10526.
[33] T. Müller, *Angew. Chem. Int. Ed.* **2001**, *40*, 3033–3036.
[34] D. G. Gusev, O. V. Ozerov, *Chem. Eur. J.* **2011**, *17*, 634–640.
[35] V. Y. Lee, *Russ. Chem. Rev.* **2019**, *88*, 351–369.
[36] H. F. T. Klare, L. Albers, L. Süsse, S. Keess, T. Müller, M. Oestreich, *Chem. Rev.* **2021**, *121*, 5889–5985.
[37] C. R. Wade, A. E. J. Broomsgrove, S. Aldridge, F. P. Gabbaï, *Chem. Rev.* **2010**, *110*, 3958–3984.
[38] C. Bonnier, W. E. Piers, A. A. S. Ali, A. Thompson, M. Parvez, *Organometallics* **2009**, *28*, 4845–4851.
[39] U. Mayer, V. Gutmann, W. Gerger, *Monatsh. Chem.* **1975**, *106*, 1235–1257.
[40] M. A. Beckett, G. C. Strickland, J. R. Holland, K. Sukumar Varma, *Polymer* **1996**, *37*, 4629–4631.
[41] I. B. Sivaev, V. I. Bregadze, *Coord. Chem. Rev.* **2014**, *270–271*, 75–88.
[42] L. Greb, *Chem. Eur. J.* **2018**, *24*, 17881–17896.
[43] S. A. Iqbal, J. Pahl, K. Yuan, M. J. Ingleson, *Chem. Soc. Rev.* **2020**, *49*, 4564–4591.
[44] A. Ros, R. Fernández, J. M. Lassaletta, *Chem. Soc. Rev.* **2014**, *43*, 3229–3243.
[45] V. Bagutski, A. Del Grosso, J. A. Carrillo, I. A. Cade, M. D. Helm, J. R. Lawson, P. J. Singleton, S. A. Solomon, T. Marcelli, M. J. Ingleson, *J. Am. Chem. Soc.* **2013**, *135*, 474–487.
[46] A. Del Grosso, J. Ayuso Carrillo, M. J. Ingleson, *Chem. Commun.* **2015**, *51*, 2878–2881.
[47] M. A. Légaré, M. A. Courtemanche, É. Rochette, F. G. Fontaine, *Science* **2015**, *349*, 513–516.
[48] G. Berionni, B. Maji, P. Knochel, H. Mayr, *Chem. Sci.* **2012**, *3*, 878–882.

[49] T. Shamma, H. Buchholz, G. K. S. Prakash, G. A. Olah, *Isr. J. Chem.* **1999**, *39*, 207–210.
[50] É. Rochette, M. A. Courtemanche, F. G. Fontaine, *Chem. Eur. J.* **2017**, *23*, 3567–3571.
[51] G. Q. Chen, G. Kehr, C. G. Daniliuc, M. Bursch, S. Grimme, G. Erker, *Chem. Eur. J.* **2017**, *23*, 4723–4729.
[52] Y. Ma, S.-J. Lou, Z. Hou, *Chem. Soc. Rev.* **2021**, *50*, 1945–1967.
[53] Q. Wu, Z. W. Qu, L. Omann, E. Irran, H. F. T. Klare, M. Oestreich, *Angew. Chem. Int. Ed.* **2018**, *57*, 9176–9179.
[54] K. Matsuoka, N. Komami, M. Kojima, T. Mita, K. Suzuki, S. Maeda, T. Yoshino, S. Matsunaga, *J. Am. Chem. Soc.* **2021**, *143*, 103–108.
[55] Q. Wu, E. Irran, R. Müller, M. Kaupp, H. F. T. Klare, M. Oestreich, *Science* **2019**, *365*, 168–172.
[56] A. Di Saverio, F. Focante, I. Camurati, L. Resconi, T. Beringhelli, G. D'Alfonso, D. Donghi, D. Maggioni, P. Mercandelli, A. Sironi, *Inorg. Chem.* **2005**, *44*, 5030–5041.
[57] D. Neculai, H. W. Roesky, A. M. Neculai, J. Magull, B. Walfort, D. Stalke, *Angew. Chem. Int. Ed.* **2002**, *41*, 4294–4296.
[58] R. Guo, X. Qi, H. Xiang, P. Geaneotes, R. Wang, P. Liu, Y. M. Wang, *Angew. Chem. Int. Ed.* **2020**, *59*, 16651–16660.
[59] H. Zhao, Y. Kim, G. Park, F. P. Gabbai, *Tetrahedron* **2019**, *75*, 1123–1129.
[60] C. W. Chiu, Y. Kim, P. F. Gabbaï, *J. Am. Chem. Soc.* **2009**, *131*, 60–61.
[61] Y. Kim, F. P. Gabbaï, *J. Am. Chem. Soc.* **2009**, *131*, 3363–3369.
[62] M. H. Lee, T. Agou, J. Kobayashi, T. Kawashima, F. P. Gabbaï, *Chem. Commun.* **2007**, 1133–1135.
[63] A. Schäfer, W. Saak, D. Haase, T. Müller, *Angew. Chem. Int. Ed.* **2012**, *51*, 2981–2984.
[64] S. J. Connelly, W. Kaminsky, D. M. Heinekey, *Organometallics* **2013**, *32*, 7478–7481.
[65] G. A. Olah, G. A. Olah, **1970**, *4*, 240–248.
[66] B. Galabov, D. Nalbantova, P. V. R. Schleyer, H. F. Schaefer, *Acc. Chem. Res.* **2016**, *49*, 1191–1199.
[67] G. B. Dunks, K. Barker, E. Hedaya, C. Hefner, K. Palmer-Ordonez, P. Remec, *Inorg. Chem.* **1981**, *20*, 1692–1697.
[68] L. Toom, A. Kütt, I. Leito, *Dalton Trans.* **2019**, *48*, 7499–7502.
[69] C. A. Reed, *Acc. Chem. Res.* **2010**, *43*, 121–128.
[70] C. A. Reed, Z. Xie, R. Bau, A. Benesi, *Science* **1993**, *262*, 402–404.
[71] Z. Xie, J. Manning, R. W. Reed, R. Mathur, P. D. W. Boyd, A. Benesi, C. A. Reed, *J. Am. Chem. Soc.* **1996**, *118*, 2922–2928.
[72] S. P. Hoffmann, T. Kato, F. S. Tham, C. A. Reed, *Chem. Commun.* **2006**, 767–769.

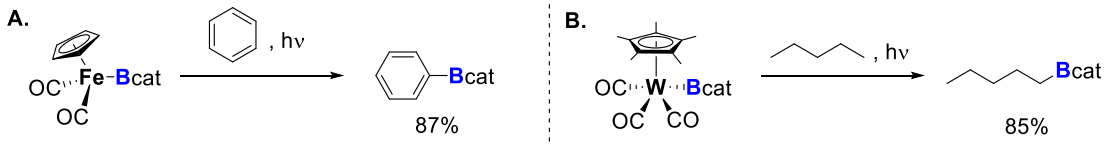
Chapter IV

Csp^2-H Borylation and Functionalization of Arenes

IV.1. Introduction

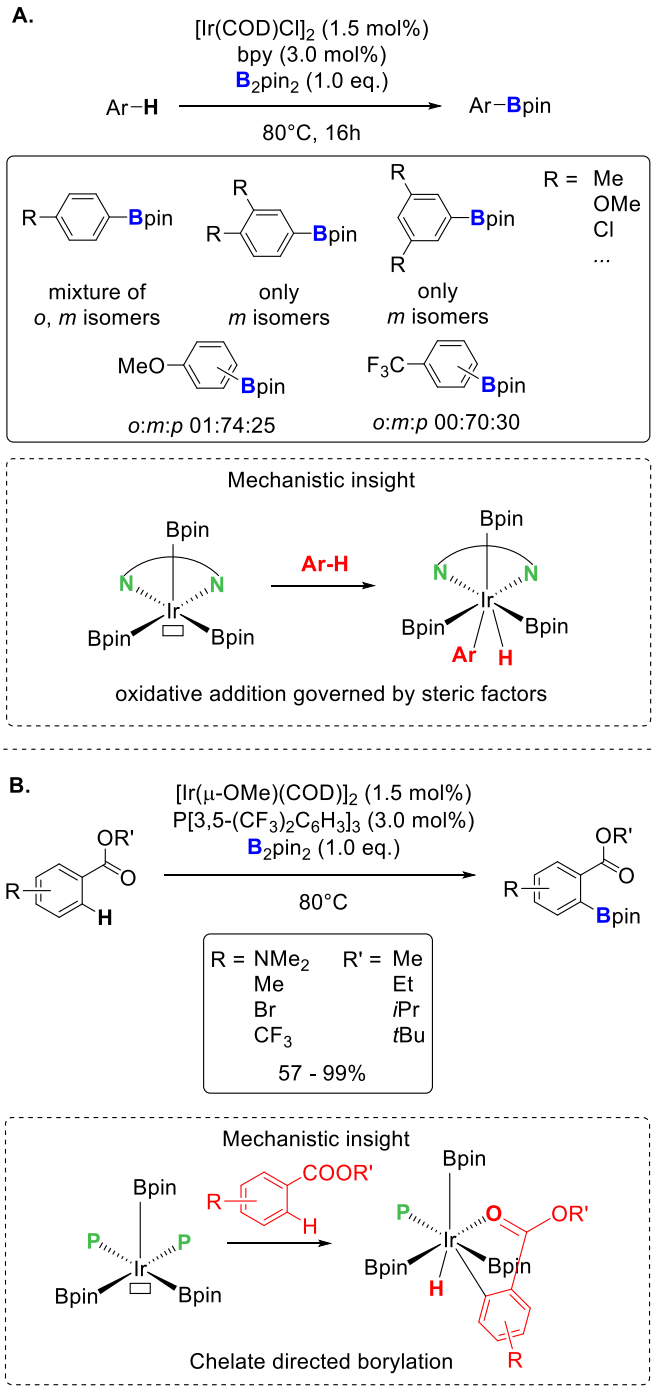
IV.1.1 Brief introduction of transition metal catalyzed Csp^2–H borylation

Since the emergence of transition metals, demonstration of their interest for the construction of C–O, C–N, C–S or C–C bonds has been extensively done, especially in the past decades.[1–3] These transformations often require prefunctionalized reagents such as organohalides and organoboron species.[2] The ever-growing importance of the Suzuki-Miyaura cross-coupling reaction for the synthesis of value added products such as pharmaceuticals is directly inducing an increasing need for organoboron building blocks along with ever more straightforward synthetic methods.[4] Even though extremely powerful, transition-metals mediated transformations such as Suzuki-Miyaura coupling generally require expensive prefunctionalized starting materials or several additional synthetic steps for introducing C–X and C–B bonds.[3] Attention was then devoted to C–H functionalization which rapidly evolved as a major tool in modern synthetic chemistry since it allows a better atom-economy and requires less synthetic steps to reach functionalized value-added products.[5,6] One of the most efficient and well-investigated reaction in this field is the C–H borylation. In 1995, Hartwig and co-workers reported the first Csp^2–H borylation of alkenes and arenes with transition-metal-boryl complexes and two years later, they reported the first selective C–H borylation of alkanes with similar transition-metal complexes, both methods requiring a stoichiometric amount of the metal complex (**Scheme IV.37**).[7,8]



Scheme IV.37 : First examples of transition-metal catalyzed borylation of **A.** arene and **B.** alkane.

While the first transition metal catalyzed Csp^2- and Csp^3-H borylation were reported using essentially rhodium and iridium catalysts,[9–11] focus was then directed on Ir catalysis, especially for Csp^2–H borylation, since these reaction produce higher yields in reduced reaction time, especially with electron-deficient substrates, and under milder conditions than with Rh catalysts.[5,11] Over the years, Ir catalyzed Csp^2–H borylation of arenes has been extensively developed and optimized with the use of a wide variety of ligands.[5] A significant feature of these transition-metal catalyzed borylations is that the selectivity is mostly governed by steric factors generally leading to a mixture of *meta* and *para* borylated products (**Scheme IV.38, A**). Highly regioselective Csp^2–H borylations could be achieved *via* introduction of directing groups but still remain challenging (**Scheme IV.38, B**).[5,6,12,13]

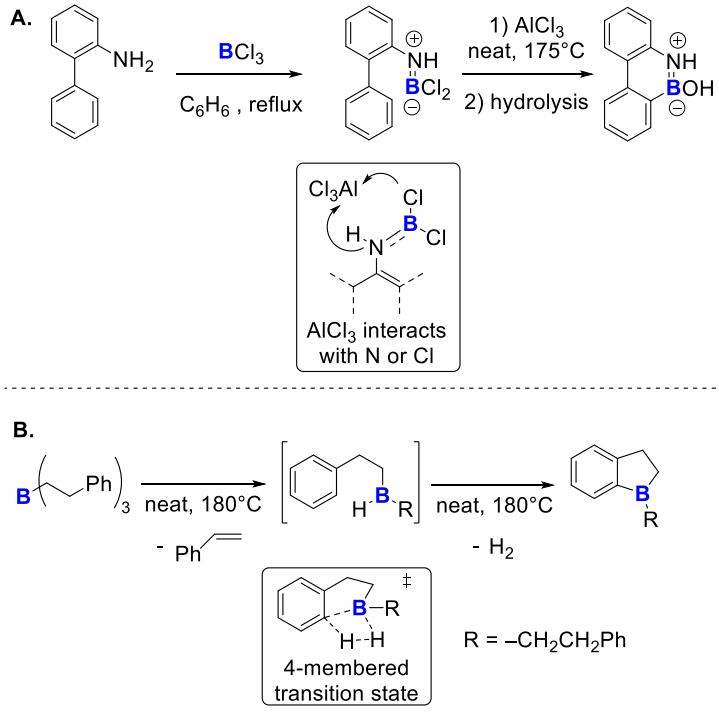


Scheme IV.38 : Selected examples of **A.** undirected and **B.** directed Ir catalyzed C–H borylation of arenes.

IV.1.2 Transition-metal-free Csp^2–H borylation

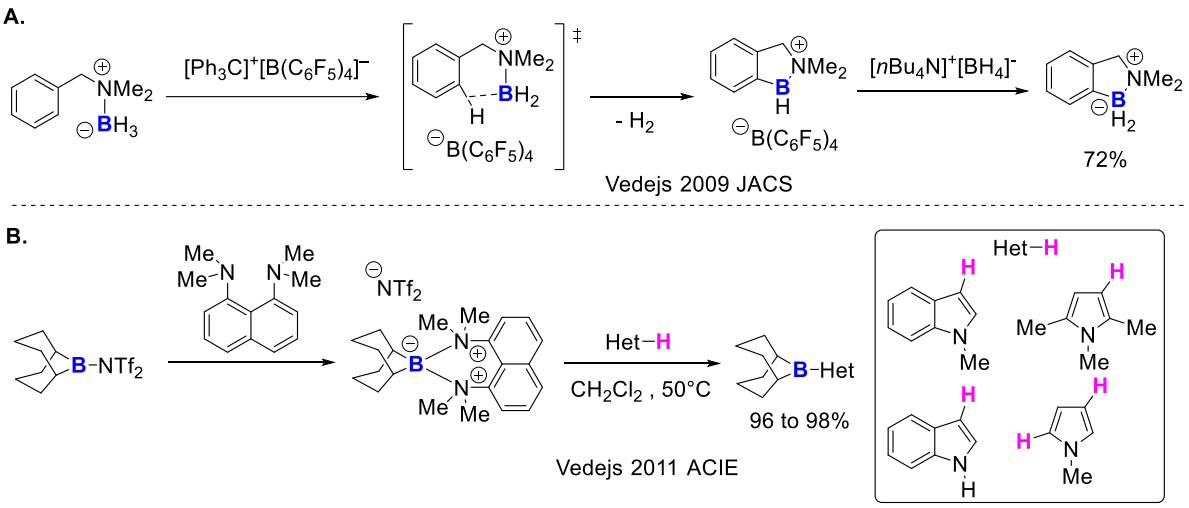
Interestingly, transition-metal-free Csp^2–H borylation have been reported almost 40 years before the first transition-metal catalyzed equivalents.

In 1958, Dewar and co-workers reported the synthesis of 9-aza-10-boraphenanthrene by reaction of BCl_3 and 2-aminobiphenyl in presence of $AlCl_3$ under harsh conditions (**Scheme IV.39, A**).[14] In the following years, similar results were reported by Dewar and co-workers and Muetterties and co-workers.[15–18] In such electrophilic borylations, the active species was postulated to be derived from $AlCl_3$ which interact with either –Cl or –N in the amido borane and the selectivity is mostly controlled by steric effects and by the coordination of the boron electrophile with the $–NH_2$ moiety. In the same period, intramolecular Csp^2–H borylations were reported by Hurd then by Köster and co-workers using borane and organoborane at elevated temperature. In this case, the reaction is driven by the release of molecular hydrogen or an alkane and a mechanism proceeding *via* σ-bond metathesis through a four-membered transition state was proposed (**Scheme IV.39, B**).[19]



Scheme IV.39 : First examples of intramolecular electrophilic Csp^2–H borylation using **A.** BCl_3 and **B.** alkyl borane as electrophilic boron source.

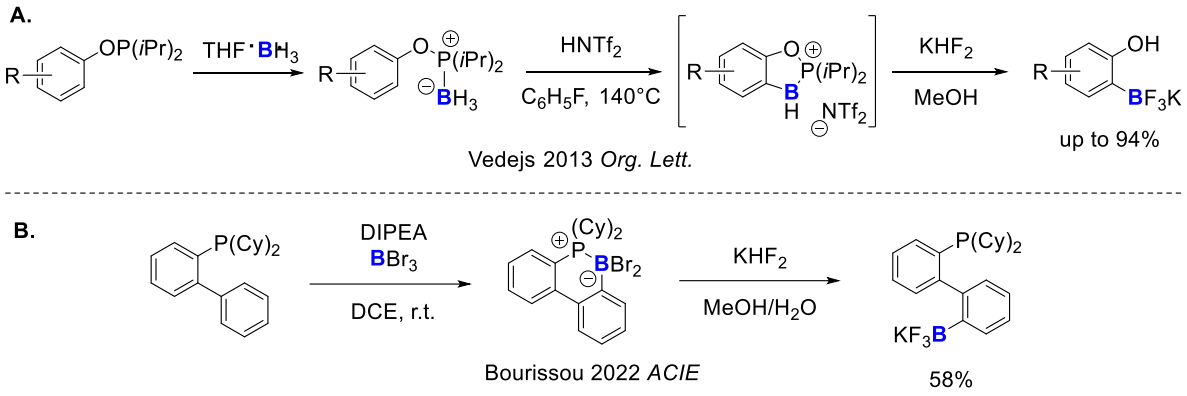
After pioneering work of Dewar, Muetterties and Köster such borylation methods were only sporadically used until late 2000's and only few improvements were proposed. The use of BBr_3 and later BI_3 was proposed since they outperform BCl_3 in terms of isolated yields and do not necessarily require $AlCl_3$.[20–22] During the last 20 years, the extensive work of Vedejs and co-workers on borenium ions and more generally on cationic boron species led to the development of new borylation methods with highly electrophilic boron species (**Scheme IV.40, A**).[23,24] Initially, reported Csp^2–H borylations remained intramolecular but rapidly intermolecular borylations were developed, allowing a variety of electron rich arenes as substrates (**Scheme IV.40, B**).[25,26]



Scheme IV.40 : Selected examples of aromatic Csp^2–H borylation reported by Vedejs and co-workers with **A.** borenium and **B.** boronium ions.

Few years later, Vedejs and co-workers reported an *ortho*-directed C–H borylation of phenol derivatives using removable phosphorus directing group (**Scheme IV.41, A**). This strategy consists in the prefunctionalization of phenols into diisopropylphosphinites followed by coordination of BH_3 to the phosphorous atom and formation of the corresponding borenium by treatment with $HNTf_2$ which then performs the *ortho*-borylation. Once the desired product formed, treatment with KHF_2 affords the corresponding

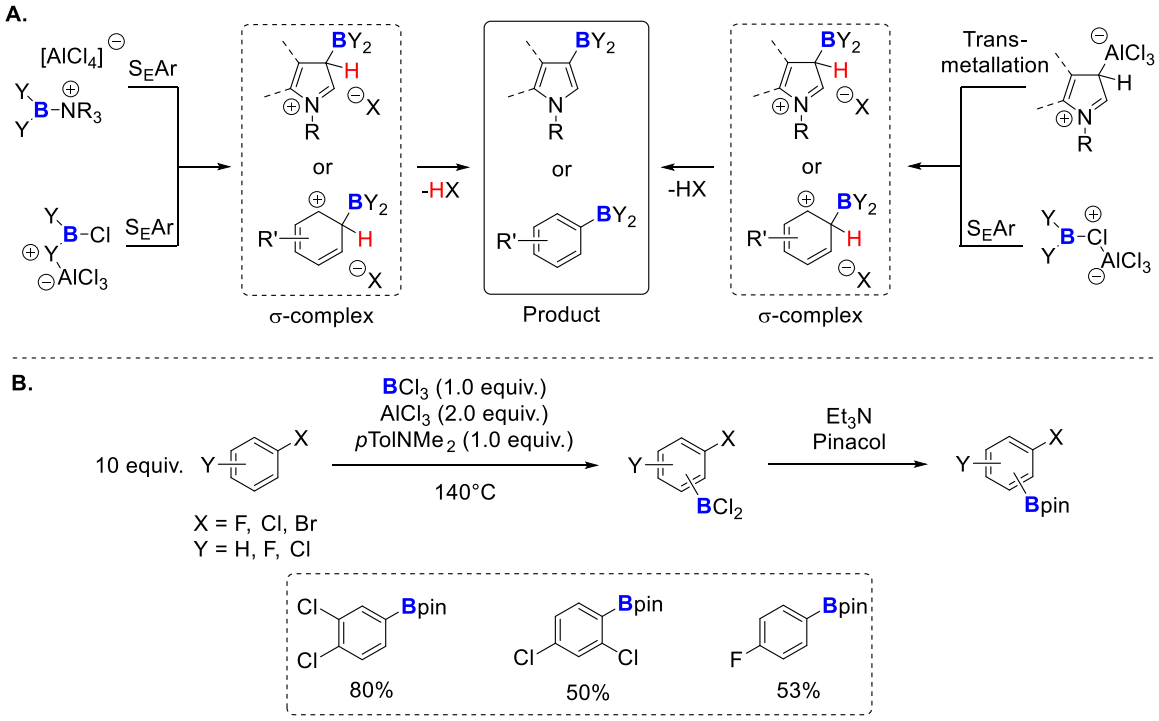
phenol trifluoroborate salt.[27] This strategy of P-directed *ortho*-borylation of arenes was extensively used in transition-metal catalyzed borylations but, very recently, Shi and co-workers and Bourissou and co-workers reported a transition-metal free version using BBr_3 and an hindered Brønsted base (DIPEA) as proton scavenger (**Scheme IV.41, B**).[28,29]



Scheme IV.41 : Reported synthesis of potassium aryl trifluoroborates using Csp^2–H borylation.

Concomitantly with the work of Vedejs and co-workers, intermolecular borylations of arenes were extensively developed by Ingleson and co-workers in parallel of their work on borenium ions. They started by attempting the synthesis and isolation of superelectrophilic catechol borinium and were able to perform the catalytic borylation of benzene.[30] Later on, they described the synthesis of aryl pinacol boronates by borylation of electron rich arenes which were used for further functionalization, *via* Suzuki-Miyaura cross coupling reaction for example.[31] In 2013, they reported the synthesis of a large scope of aryl boronate species *via* amine-mediated electrophilic borylation as well as a full mechanistic investigation.[32] This revealed that the electrophilic borylation of arenes can proceed *via* different mechanisms, regarding the electrophilic boron species implied as well as the aromatic substrate. Even though the multiple proposed mechanisms remained relatively similar and proceed *via* a S_EAr pathway, the electrophilic boron species can vary regarding the reaction conditions.

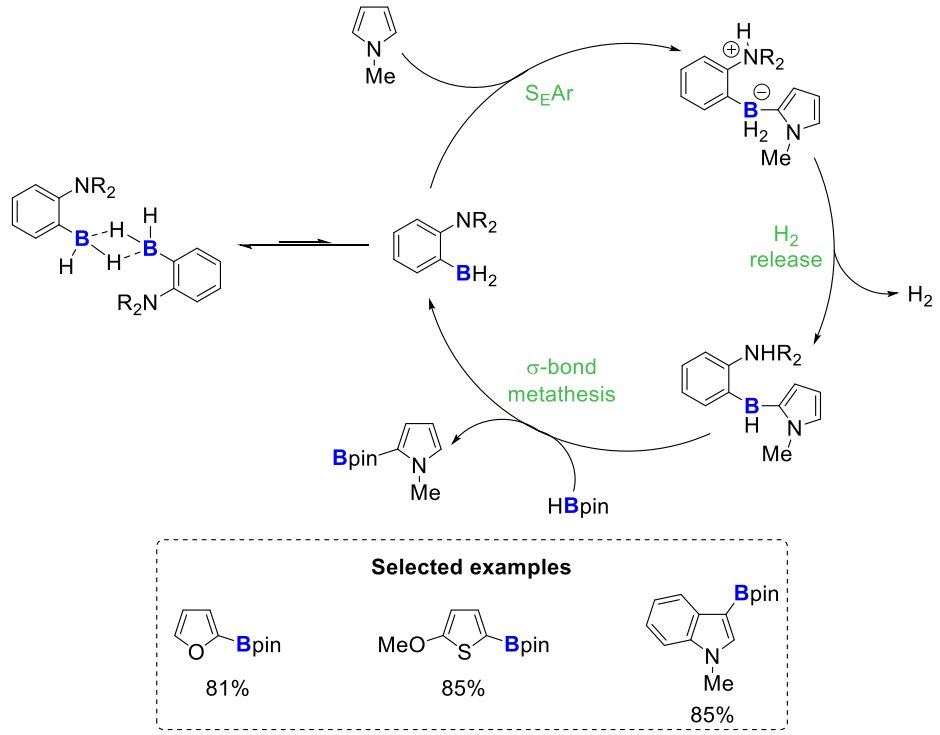
The starting boron electrophile, the additive, the coordinating character of the base or the counter-anion can impact the reactivity and the formation of the electrophilic boron species implied in the borylation sequence (**Scheme IV.42, A**).



Scheme IV.42 : **A.** Proposed mechanisms and electrophilic boron species depending on the boron starting materials and arene considered. **B.** Selected example of borylation of haloarenes.

In 2015, Ingleson and co-workers reported the borylation of weakly nucleophilic haloarenes such as 1,2-dichlorobenzene using a similar method as reported precedently (**Scheme IV.42, B**).[33] Such haloarenes are generally considered as ideal unreactive solvents for superelectrophilic boron or silicon species. Two years later, Oestreich and co-workers reported the borylation of electron rich arenes using pinacol borane and $B(C_6F_5)_3$ as hydride abstractor to form the borenium/boronium reactive species.[34] In 2015, Fontaine and co-workers reported a metal-free catalytic borylation method of heteroarenes using an intramolecular frustrated Lewis pair (FLP) (**Scheme IV.43**).[35] This system allows the synthesis of pinacol esters from

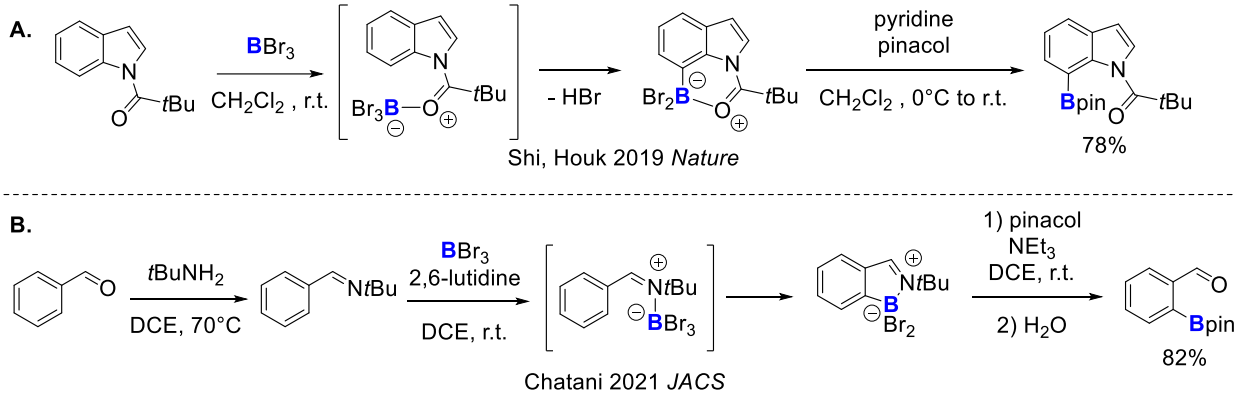
pyrrole, indole, furane and thiophene derivatives with good to excellent yields under relatively mild conditions using commercially available starting materials and a readily available catalyst. The first step of the catalytic cycle is an electrophilic borylation occurring through a S_EAr pathway, followed by elimination of molecular hydrogen and σ-bond metathesis with pinacolborane regenerating the catalyst and forming the aryl pinacol ester.



Scheme IV.43 : Proposed mechanism for Fontaine's FLP catalyzed Csp^2–H borylation and selected examples.

Recently, Shi, Houk and co-workers reported a regioselective metal-free directed Csp^2–H borylation of arenes and heteroarenes (**Scheme IV.44, A**).[36] Analogously to what has been done with transition-metals for improving the selectivity, they used a directing group, in this case a pivaloyl moiety, to selectively direct the C7- or *ortho*-borylation. This convenient one-pot borylation proceeds at room temperature and allows a straightforward synthesis of aryl pinacol boronates using only readily and commercially available starting materials while providing exclusively one

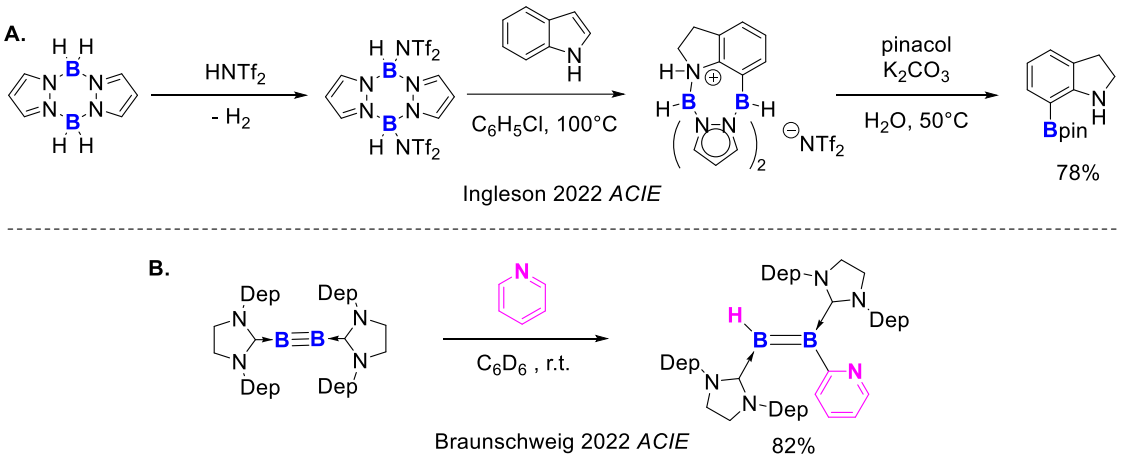
regioisomer. At the exact same time, Ingleson and co-workers reported a similar strategy for *ortho*-borylation of aniline and C7-borylation of indoles with BBr_3.[37] In 2021, Chatani and co-workers reported the regioselective synthesis of benzaldehyde pinacol boronates *via* electrophilic borylation using a transient imine as directing group (**Scheme IV.44, B**).[38,39] Starting from benzaldehyde derivatives, this methodology consists in transforming the aldehyde group into an imine which can *ortho*-direct the borylation using BBr_3. After quenching in presence of pinacol and hydrolysis, the desired *ortho*-borylated benzaldehyde derivatives can be obtained.



Scheme IV.44 : Recent regioselective Csp^2-H borylation using *in-situ* generated borenium ions from BBr_3.

In 2022, Ingleson and co-workers reported an innovative way to direct the C7-borylation of indoles using pyrazabole derivatives (**Scheme IV.45, A**).[40] Protonation of the pyrazabole leads to elimination of molecular hydrogen generating a pyrazabole bis-triflimidate which binds the indole nitrogen atom. This directs the C7-borylation by the second boron atom. The hydrolysis in presence of pinacol leads to the formation of C7-borylated indolines. During the reaction, the indole is reduced into indoline. The same year, Braunschweig and co-workers reported another metal-free borylation method of *N*-heterocycles, this time using B–B multiple bonds (**Scheme IV.45, B**).[41] The propensity of NHC- and CAAC-stabilized diboryne to

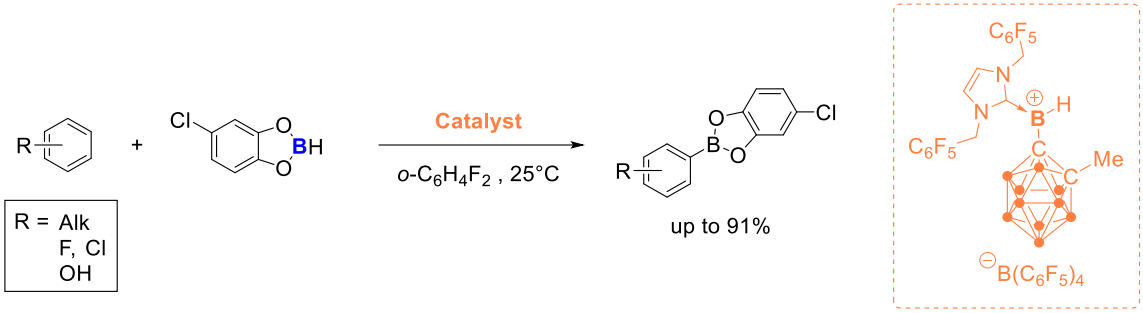
borylate heterocycles such as pyridine and quinolines was investigated and a full DFT investigation of the mechanism was provided.



Scheme IV.45 : Recent examples of Csp^2-H borylation using **A.** pyrazabole derivatives and **B.** diboryne.

Also very recently, end of 2022, Wang and co-workers reported the electrophilic borylation or arenes using an carborane-substituted borenium catalyst and a catechol borane derivative (**Scheme IV.46**).[42] This system allows the borylation of a wide variety of activated and unactivated arenes with good to excellent yields. Although the use of the terms "activated" or "unactivated" have no definitive meaning, they refer to the reactivity of the arene substrates in aromatic electrophilic substitutions. The term "unactivated" refers to substrate that have a nucleophilicity comparable to benzene or being alkyl substituted benzene species while "activated" refers to (hetero)aromatic substrates bearing strong electron donor substituents such as methoxy- or dimethylamino- groups, strongly increasing the nucleophilicity. On the other hand, "deactivated" refers to arene substrates bearing electron-withdrawing substituents such as halogens or nitro-groups, decreasing the nucleophilicity of the substrate. Interestingly, their system also allows the borylation of phenol derivatives without prior introduction of protecting group on the Lewis basic oxygen, even though a large excess of catechol borane is required and acts as a protecting group.

The regioselectivities are similar to the one reported previously by Ingleson and co-workers.[32]

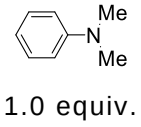
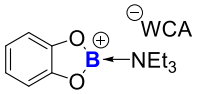
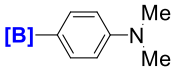
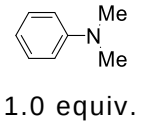
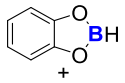
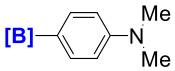
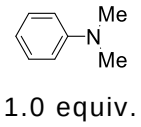
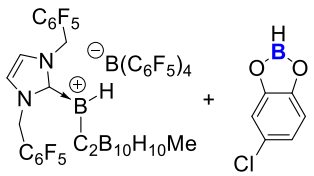
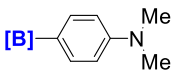


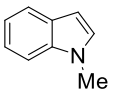
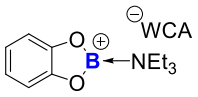
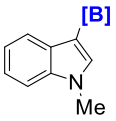
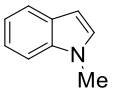
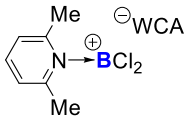
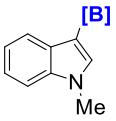
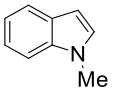
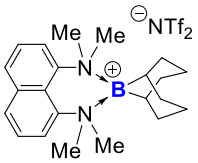
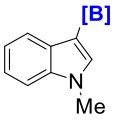
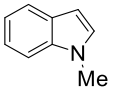
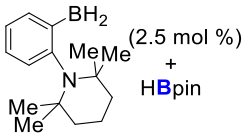
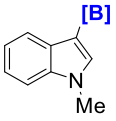
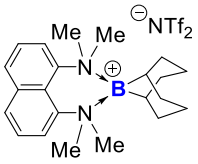
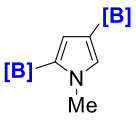
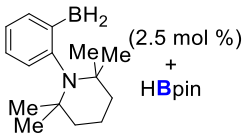
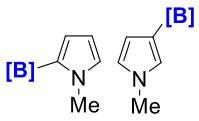
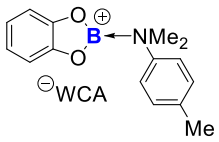
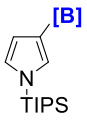
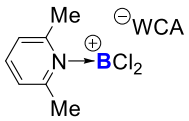
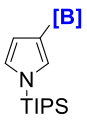
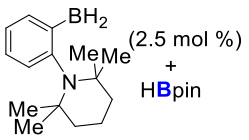
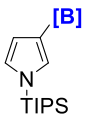
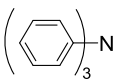
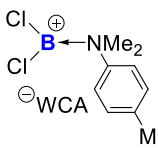
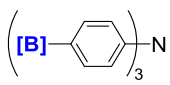
Scheme IV.46 : Recent carborane-substituted borenium ion catalyzed Csp^2-H borylation.

IV.1.3 Summary and comparison of intermolecular electrophilic Csp^2-H borylation methods

To summarize the different borylation methods presented in the precedent section, it might be of interest to compare the methods in terms of substrates, regioselectivity, reaction time and temperature, yield, and amount of substrate. Such a comparison presents a great interest especially for intermolecular and non-directed methods.

Table IV.3 : Comparison of intermolecular electrophilic borylation methodologies for activated (hetero)arenes.

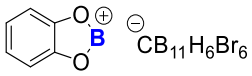
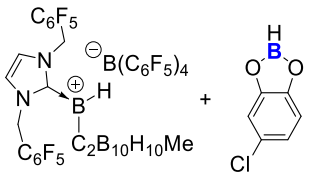
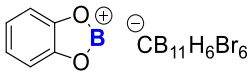
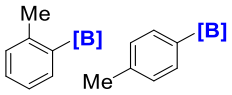
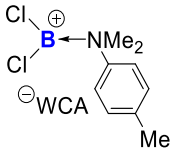
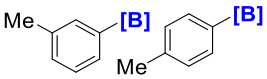
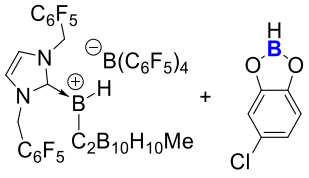
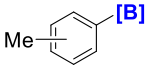
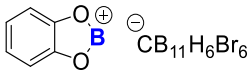
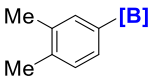
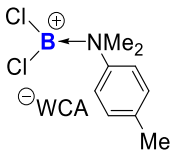
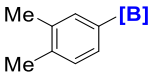
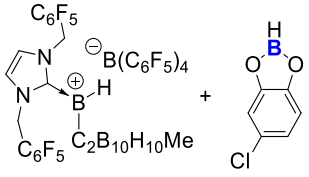
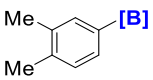
	Substrate	Reagent	Product	Time (h)	Temp (°C)	Yield (%)
1	 1.0 equiv.			1	20	85[32]
2	 1.0 equiv.			48	120	83[34]
3	 1.0 equiv.			24	25	65[42]

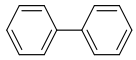
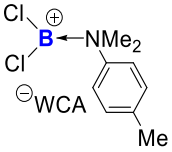
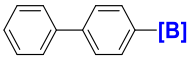
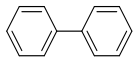
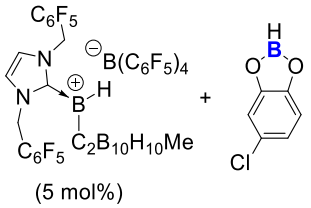
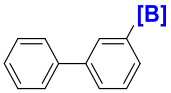
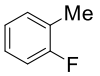
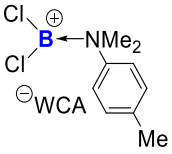
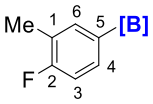
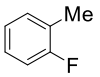
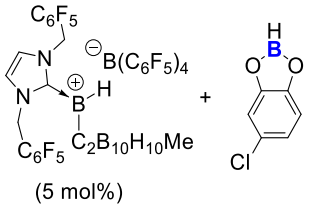
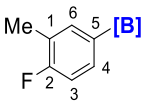
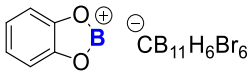
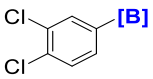
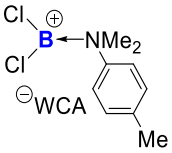
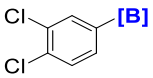
4	 1.0 equiv.			4	20	93[32]
5	 1.0 equiv.			14	20	83[32]
6	 1.0 equiv.			1.5	50	96[26]
7	 1.0 equiv.			16	80	85[35]
8	 1.0 equiv.			3.5	50	97[26]
9	 1.0 equiv.		 93 : 7	16	80	93[35]
10	 1.0 equiv.			1	20	95[32]
11	 1.0 equiv.			14	20	53[32]
12	 1.0 equiv.			16	80	98[35]
13	 0.33 equiv.			22	120	74[32]

At first sight, it is interesting to note that most of the reported methods allow the borylation of electron-rich arenes such as anilines and heteroarenes with good yields and under relatively mild conditions (**Table IV.3**). Except for the method described by Oestreich and co-workers (**Table IV.3**, entry **2**) which requires 120°C and the method described by Fontaine and co-workers (**Table IV.3**, entries **7**, **9** and **12**), requiring 80°C, the other methods can be performed at room temperature or under mild heating. The selectivity is similar for all the methods presented with complete or almost complete regioselectivity.

Considering unactivated arenes, it is important to note that only three methods afford effective borylation while only two methods allow the borylation of strongly deactivated haloarenes such as 1,2-dichlorobenzene (**Table IV.4**, entries **13**, **14**). Except for the method reported by Wang and co-workers (**Table IV.4**, entries **2**, **5**, **8**, **10**, **12**) which is not applicable for strongly deactivated arenes, high temperatures above 100°C are required. It is also important to note that the regioselectivity is also reduced compared to what was observed with activated arenes. In most cases at least two regioisomers are obtained (**Table IV.4**, entries **3**, **4**, **11**) and sometimes even three regioisomers (**Table IV.4**, entries **5**, **6**, **12**). These methods, even though being relatively effective, still suffer from regioselectivity issues especially with mono-substituted substrates. Elevated temperatures are generally required for unactivated substrates, except for Wang's method but requires a sophisticated catalyst while Ingleson's methods allow the use of commercially available reagents.

Table IV.4 : Comparison of intermolecular electrophilic borylation methodologies for unactivated and deactivated arenes.

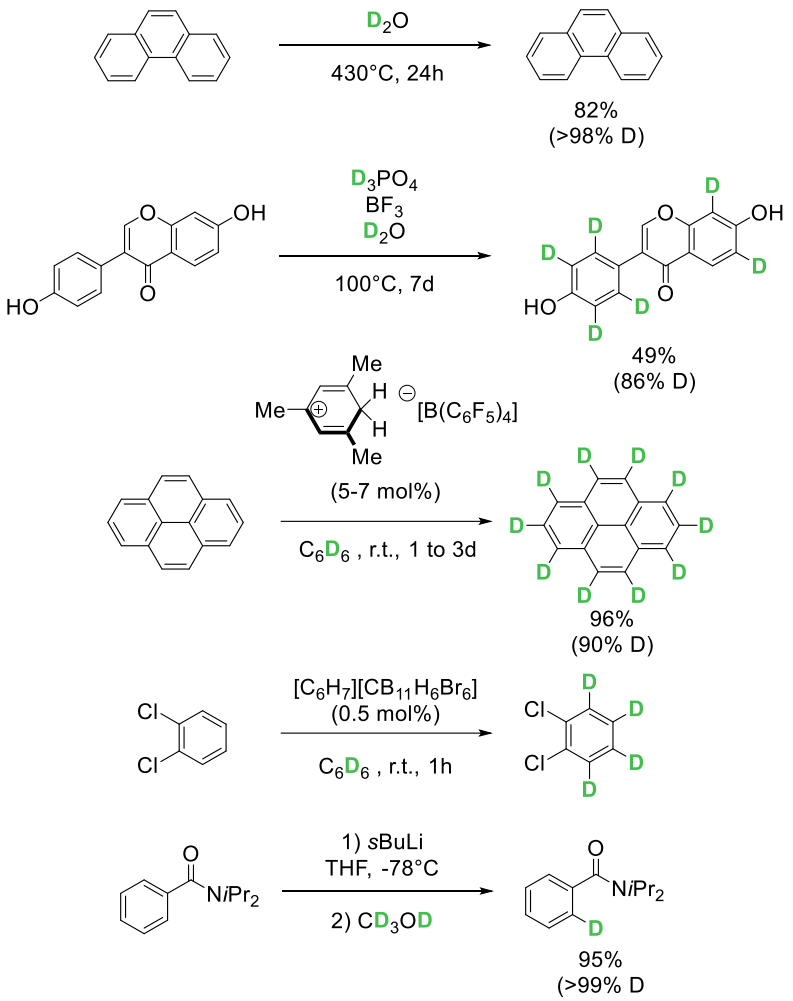
	Substrate	Reagent	Product	Time (h)	Temp (°C)	Yield (%)
1	 Solvent			15	80	86[30]
2	 1.0 equiv.	 (5 mol%)		24	25	83[42]
3	 Solvent		 55 : 45	24	25	65[30]
4	 1.0 equiv.		 16 : 84	21	110	75[32]
5	 1.0 equiv.	 (5 mol%)	 *o*:*m*:*p* 04:51:45	24	25	87[42]
6	 Solvent		 Several regioisomers	10	140	92[30]
7	 1.0 equiv.			36	120	67[32]
8	 1.0 equiv.	 (5 mol%)		24	25	91[42]

9	 1.0 equiv.			36	120	54[32]
10	 1.0 equiv.	 (5 mol%)	 *m*:*p* 71:29	24	25	77[42]
11	 10 equiv.		 4-:5- 17:83	1	140	75[33]
12	 1.0 equiv.	 (5 mol%)	 3-:4-:5- 6:29:65	24	25	74[42]
13	 Solvent			10	140	99[30]
14	 10 equiv.			24	140	80[33]

IV.1.4 Regioselective mono- and perdeuteration of arenes

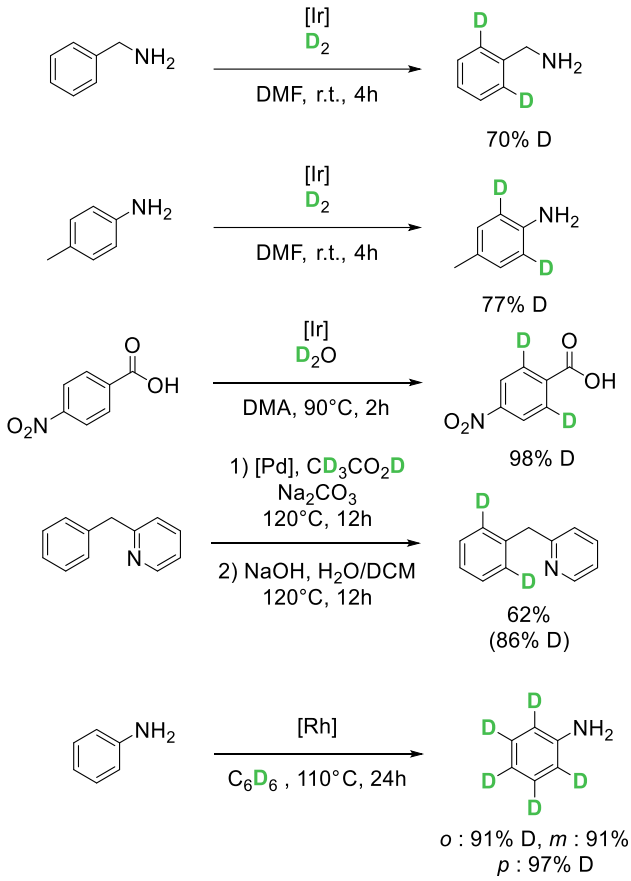
Deuterium-labeled compounds are of high interest in life sciences or physical organic chemistry since they serve as probes for mechanistic investigations.[43–45] Even though several methods have been reported, allowing the regioselective monodeuteration or even perdeuteration of arenes, the development of new and additional methods allowing the synthesis of deuterium labeled species is an ever-growing research field.[46] The oldest method used for the deuteration and particularly the

perdeuteration of aromatic substrates is the pH-dependent hydrogen isotope exchange (HIE). This strategy generally consists in submitting the substrate to an intensive thermal treatment in a deuterated solvent. Addition of an acid or base may be required to perform the exchange. This method is generally limited to simple substrates which can withstand relatively harsh conditions (**Scheme IV.47**).[43,45,47]



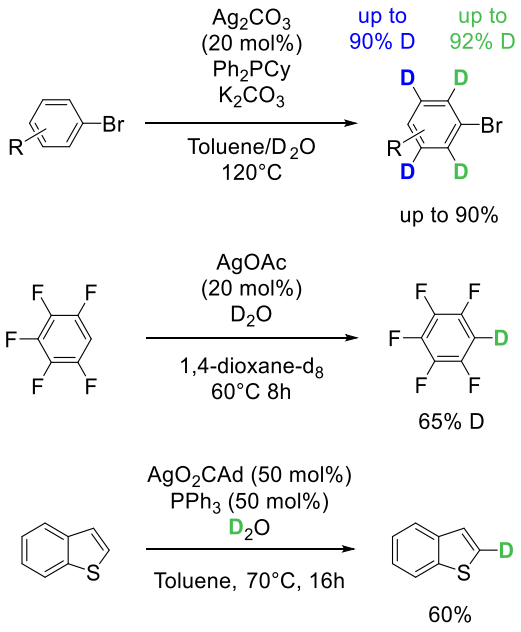
Scheme IV.47 : Selected examples of mono-, poly- and perdeuterations of aromatic substrates using pH-dependent hydrogen isotope exchange.

More recently, transition-metal-catalyzed H/D exchanges have been developed using a wide variety of transition metals. This generally requires the use of directing groups and is mostly reported to introduce a deuterium atom in *ortho*-position of the directing group however, several methods have been developed for performing perdeuterations (**Scheme IV.48**).[48]



Scheme IV.48 : Selected examples of transition-metal-catalyzed site selective and perdeuteration of aromatic substrates.

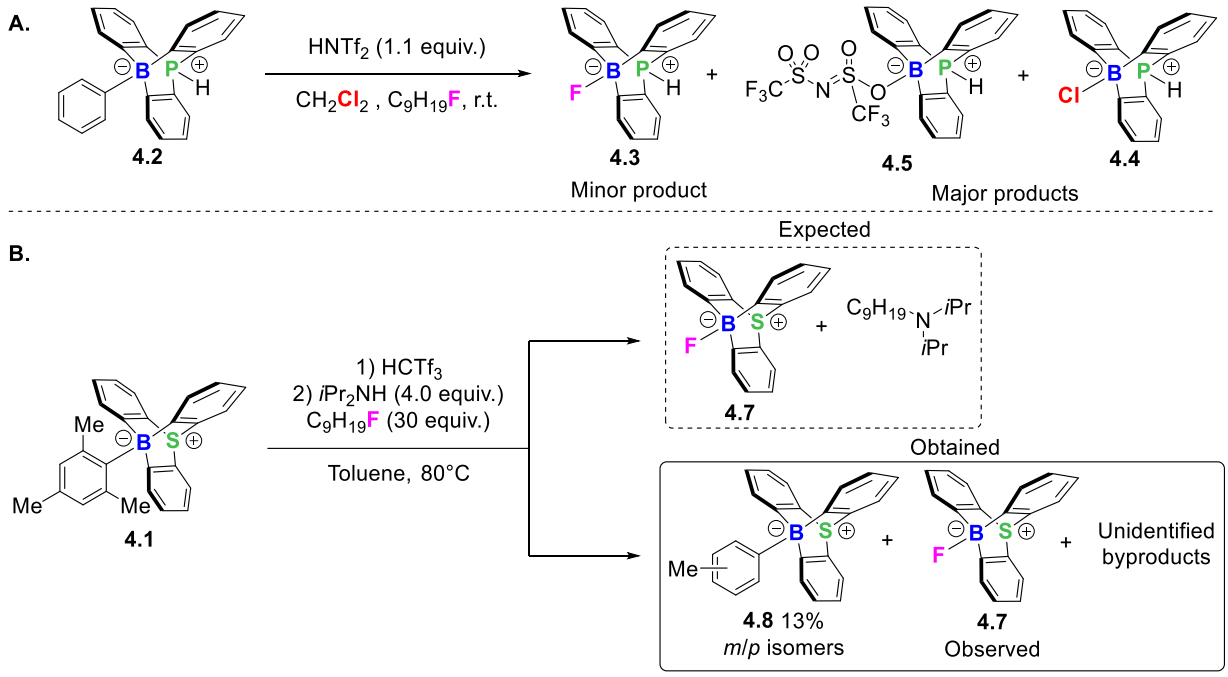
In the past decade, Ag(I)-catalysis as emerged as a powerful tool for either site selective or perdeuterations essentially of electron depleted haloarenes which remain challenging substrates to tackle (**Scheme IV.49**).[49–52]



Scheme IV.49 : Selected examples of Ag(I) catalyzed site selective deuteration of aromatic substrates.

IV.2. Preliminary Results

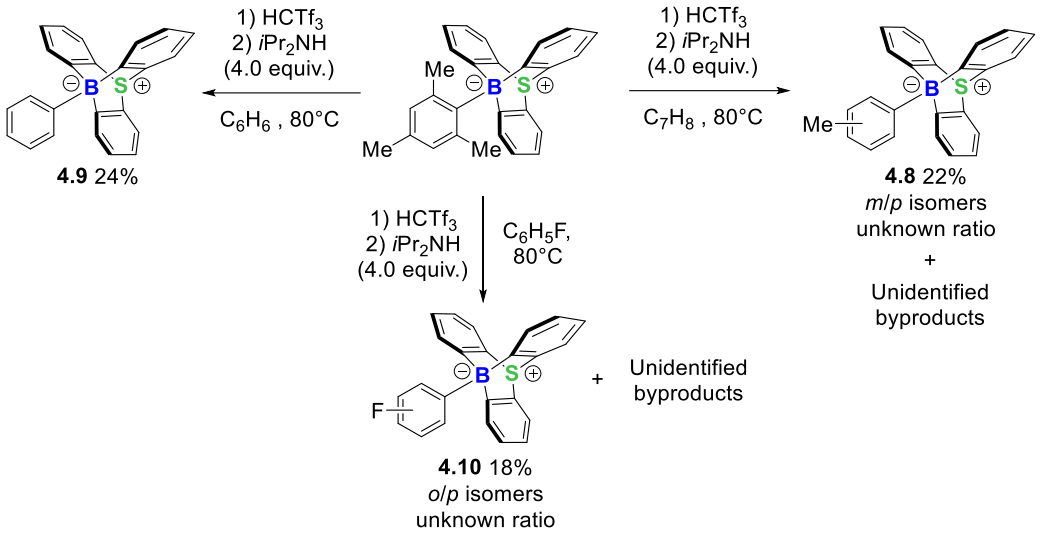
Once the synthesis of the 9-sulfonium-10-boratriptycene precursor **4.1** was achieved, despite all attempts to isolate the donor-free Lewis acid did fail, it was considered to use the previously observed reactivity of the *in-situ* generated Lewis acid. Inspired by the work of Siegel and co-workers and Nelson and co-workers[53–55], the initial goal was to take advantage of the exceptionally high Lewis acidity and FIA of the 9-sulfonium-10-boratriptycene to perform Csp^3–F and Csp^2–F bond abstractions and functionalizations. As a starting point, it was decided to begin with adapting a preliminary observation from a parallel project. It was already observed with the 9-phosphonium-10-boratriptycene that the *in-situ* generation of the Lewis acid, from the phenyl-ate complex precursor **4.2**, in presence of 1-fluorononane led to the formation of the 10-fluoro-9-phosphonium-10-boratriptycene-ate complex **4.3**. This product could only result from the abstraction of a fluoride ion from 1-fluorononane. However, as the reaction was performed in CH_2Cl_2, the major product was the chloride-ate complex **4.4** along with the triflimidate-ate complex **4.5** (**Scheme IV.50, A**). As a benchmark reaction, we decided to perform a similar reaction in toluene instead of CH_2Cl_2 to prevent the chloride abstraction and using triflidic acid instead of triflimidic acid, the 10-triflimidate-9-sulfonium-10-boratriptycene-ate complex (**4.5**) formed after the protodeborylation being far too stable. A hindered base, diisopropylamine in this case, was added to favor the substitution of the fluoride while preventing the formation of a stable adduct with the Lewis acid (**Scheme IV.50, B**).



Scheme IV.50 : **A.** Preliminary observations of the fluoride abstraction from fluoroalkane. **B.** Attempt of Csp^3–F bond cleavage promoted by 9-sulfonium-10-boratriptycene as Lewis acid.

Unexpectedly, the desired fluoride-ate complex **4.7** was only detected by ^{19}F NMR spectroscopy (δ = –236.1) as a minor product and could not even be isolated despite 1-fluorononane was used in large excess. The major product turned out to be the 10-tolyl-9-sulfonium-10-boratriptycene-ate complex (**4.8**), resulting from the C–H borylation of toluene (**Scheme IV.50, B**). The product was obtained as a mixture of *meta*- and *para*-isomers which does not follow the classical regioselectivity pattern for a S_EAr reaction. Even though the borylation product **4.8** is only obtained in low yield (13%), such a reaction is of major interest since it consists in a transition-metal-free C–H borylation of an unactivated arene. The reaction was then reproduced without 1-fluorononane which led to a slightly increased yield (22%) (**Scheme IV.51**, **4.8**). Using benzene or even fluorobenzene as solvent led to the borylation of benzene (**Scheme IV.51, 4.9**) and fluorobenzene (**Scheme IV.51, 4.10**) respectively. The observed borylation of fluorobenzene demonstrated the propensity of the 9-sulfonium-10-boratriptycene to perform Csp^2–H borylations rather than Csp^2–F

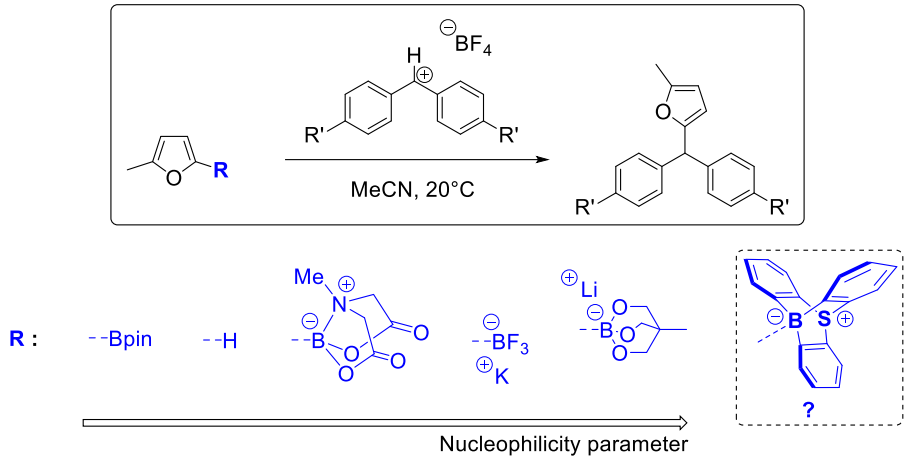
abstractions. In this context, the initial project of performing Csp^3– and Csp^2–F functionalizations mediated by our Lewis acid was set aside and attention was devoted to the development of Csp^2–H borylation reactions.



Scheme IV.51 : Preliminary observation of Csp^2–H borylation of toluene, benzene and fluorobenzene.

As aforementioned, Csp^2–H borylation of arenes is an ongoing research area of increasing importance since it allows the one-step transformation of C–H bonds into C–B bonds which can then be used for further transformations and the synthesis of value-added products.[39,56] In the present case, the proposed reaction presents an additional advantage compared to other reported methods. Indeed, the borylation product obtained is an aryl-boron-ate complex, whereas most of other methods provide boronic esters, such as aryl pinacol boronate or catechol boronate.[32,39,42] Mayr and co-workers demonstrated that, considering a boron compound containing an aromatic ring directly linked to the boron atom, the nucleophilicity parameter of the aryl ring can be increased up to six orders of magnitude while switching from a trivalent boron to a tetravalent boron species and even up to 13 orders of magnitude in boron-ate complexes (**Scheme IV.52**).[57] Therefore, the synthesis of an aryl-boron-ate complex by direct Csp^2–H borylation could be

a powerful tool for the further functionalization of the borylated aromatic ring via deborylative S_EAr reactions additionally to cross-coupling reactions.



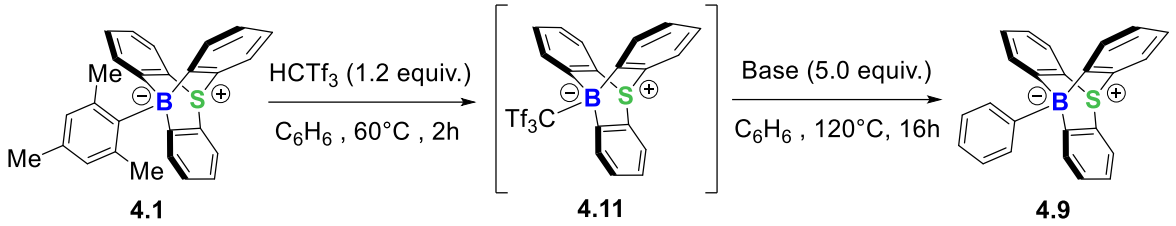
Scheme IV.52 : Nucleophilicity of aryl substituted boron species.[57]

IV.3. Optimization

Once demonstration was done of the ability of 9-sulfonium-10-boratriptycene to perform Csp^2–H borylations of arenes, we decided to investigate in more detail this interesting reactivity. The investigation started with the optimization of the borylation reaction conditions. This proceeds in two steps: *i)* the *in-situ* generation of the Lewis acid from 10-mesityl-9-sulfonium-10-boratriptycene-ate complex and formation of the corresponding triflide-ate complex, *ii)* the addition of the Brønsted base allowing the borylation reaction to occur. Therefore, the most important parameters to be optimized are the Brønsted base and the reaction time and temperature for the first and second steps. The substrate being used as solvent, benzene was selected as standard since it is inexpensive and provides a single borylation product, allowing an easy determination of the NMR yields by ^1H NMR spectroscopy using an appropriate internal standard. The optimization started by selecting the most appropriate Brønsted base (**Table IV.5**). The time and temperature for the first and second steps were arbitrarily fixed to be 60°C (**T_1**) /2h (**t_1**) and 120°C (**T_2**) /16h (**t_2**)

respectively. The reactions were performed in sealed Schlenk tubes, allowing to withstand the pressure as benzene is warmed above its boiling point.

Table IV.5 : Optimization of the Brønsted base for Csp^2–H borylation with *in-situ* generated 10-triflide-9-sulfonium-10-boratriptycene-ate complex.



4.1 **4.11** **4.9**

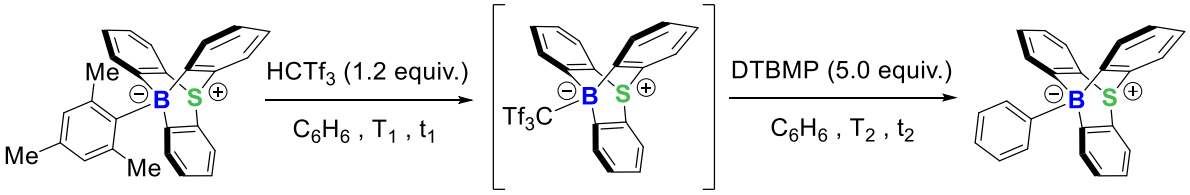
Entry	**Base**	**Yield** (%)
1	*i*Pr$_2$NH	24
2	TMPH	21
3	P(*o*-tolyl)$_3$	8
4	PMes$_3$	0
5	2,6-di*ter*butyl-4-methylpyridine (DTBMP)	55[a]

Yields are ^{1}H NMR yields obtained using 4-bromoanisole as internal standard. [a]: isolated yield

The first notable feature is the almost complete absence of borylation product using a hindered phosphine as Brønsted base (**Table IV.5**, entry **3** (8%) and **4** (0%)). At first sight this is surprising since hindered phosphines such as P(*o*-tolyl)$_3$ are commonly used in FLP chemistry for the heterolytic splitting of H_2 as well as for hydrogenation reactions in combination with B(C_6F_5)$_3$.[58,59] However, it has been reported by Stephan and co-workers that the combination of Lewis acids such as B(C_6F_5)$_3$ and hindered phosphines such as PMes$_3$ could lead to radical oxidation of the phosphine via single electron transfer.[60,61] In our case, the extreme Lewis acidity of the 9-sulfonium-10-boratriptycene combined with the prevented formation of a Lewis adduct with the phosphine could lead to radical oxidation of the phosphine, preventing the borylation reaction. However, sufficient

investigations have not been performed to prove this reactivity. With hindered alkylamines, the yields did not exceed 24%, and variety of byproducts were formed. Unfortunately, none of them could be identified at that stage neither any adduct with the Lewis base (**Table IV.5**, entry **1** and **2**). The best Brønsted base was the highly hindered 2,6-diterbutyl-4-methylpyridine (DTBMP), increasing the yield up to 55% (**Table IV.5**, entry **5**). After selecting DTBMP as best base, the reaction temperature and time were optimized (**Table IV.6**).

Table IV.6 : Optimization of the temperature and reaction time for Csp^2–H borylation with *in-situ* generated 10-triflide-9-sulfonium-10-boratriptycene-ate complex.



4.1 **4.11** **4.9**

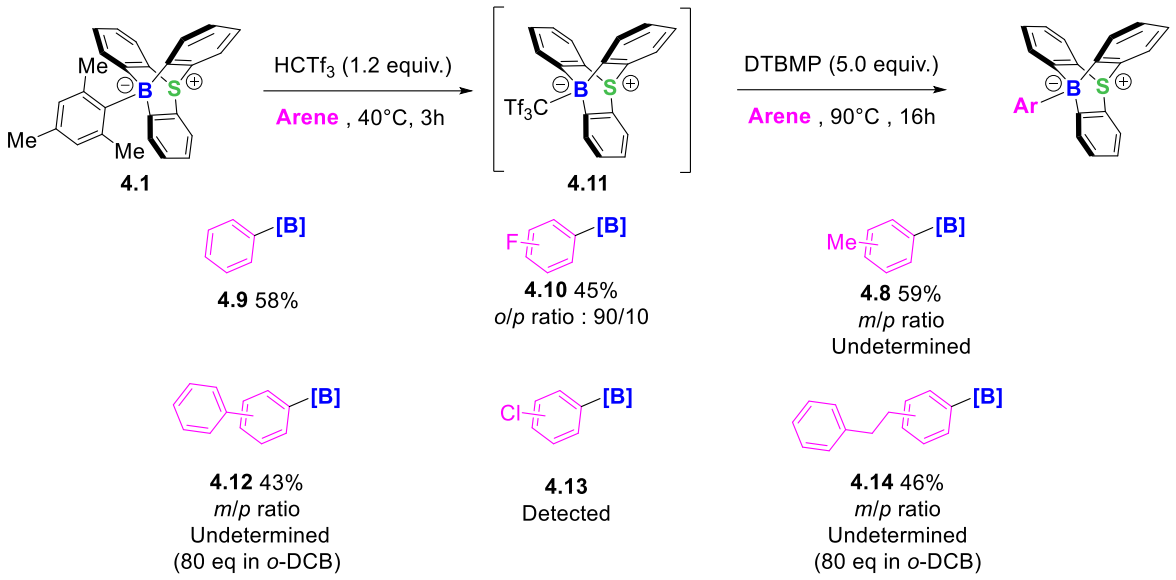
Entry	T_1 (°C)	T_2 (°C)	t_1 (h)	t_2 (h)	Yield (%)
1	60	120	2	16	55
2	60	140	2	16	31
3	100	120	1	0.25	traces
4	100	120	1	16	38
5	100	110	1	72	46
6	100	110	2	16	20
7	80	100	2	16	51
8	40	90	3	16	58
9	r.t.	100	3	16	48

Yields are ^{1}H NMR yields obtained using 4-bromoanisole as internal standard.

The first thing to note is that a slight increase of 20°C, from 120°C to 140°C, led to drastic decreased yield compared to the previous 55% (**Table IV.6**, entry **1** (55%) and **2** (31%)). It is also crucial to note that the borylation

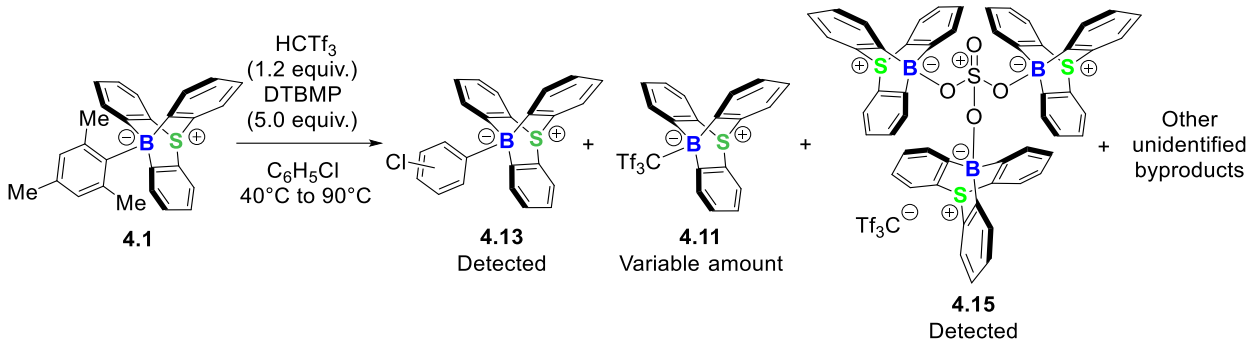
reaction is relatively slow and requires at least several hours to be considered completed (**Table IV.6**, entry **3**). An increase in temperature for the protodeborylation step, despite a shorter reaction time, also led to drastically lowered yield (**Table IV.6**, entry **4** (38%) and **6** (20%)). An increase of 8% points is observed between **Table IV.6** entries **4** (38%) and **5** (46%) keeping the borylation part at 110°C for 72h instead of 16h. Importantly, a decreased temperature for the protodeborylation part led to an increased yield, similar to the yield obtained using the so far best conditions

(**Table IV.6**, entry **7** (51%)). However, a slight warming (40°C) of the reaction during protodeborylation step is still required to speed up the generation of the triflide-ate complex (**Table IV.6**, entry **8** and **9**). With the best conditions identified (**Table IV.6**, entry **8**), the yield was only increased by 3% points, but these conditions are nevertheless more convenient and milder compared to the previous ones (**Table IV.6**, entry **1**). The optimization step was stopped at that stage, and we attended to develop a scope of borylated arenes. It was rapidly noted that the best yields were obtained with toluene with only 59% yield (**Scheme IV.53**). A range of 40% to 50% was obtained with other unactivated arene but switching from unactivated to deactivated such as chlorobenzene led to drastic yield drop with a borylation product only detectable by ^{11}B and ^{1}H NMR (**Scheme IV.53**).

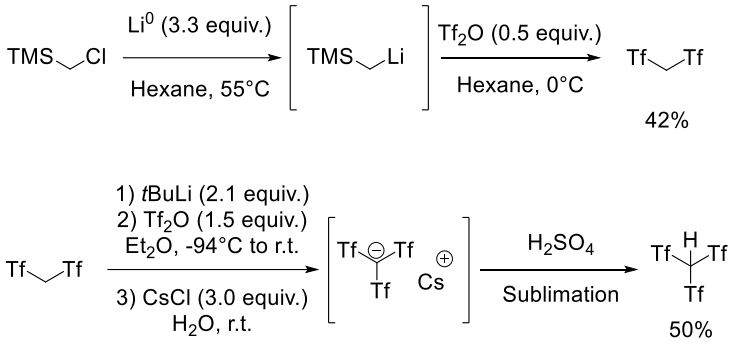


Scheme IV.53 : Scope of Csp^2–H borylation with *in-situ* generated 10-triflide-9-sulfonium-10-boratriptycene-ate complex and DTBMP as Brønsted base.

Only few byproducts were observed and their formation remained difficult to explain. It was postulated that under the conditions used for borylations, the triflide anion could decompose despite no clear evidence have been highlighted instead of tris(10-hydroxy-9-sulfonium-10-boratriptycene)oxosuflonium triflide **4.15**, which could be unambiguously characterized by single crystal X-ray diffraction analysis (**Scheme IV.54**). This interesting compound could arise from sulfuric acid remaining as impurity in the triflidic acid used. Even though this compound **4.15** was only obtained on 1mg scale, the presence of other impurities could not be excluded. Furthermore, triflidic acid being highly expensive (1g/500€), it had to be synthesized in the lab and care had to be taken during the purification step to avoid the presence of sulfuric acid in the final product (**Scheme IV.55**). It is also important to note that, as presented before, the protodeborylation step requires several hours under heating due to the extreme insolubility of the acid in most organic solvent, drastically slowing down the protodeborylation step. This several hours warming, even under mild conditions, might lead to the formation of byproducts.



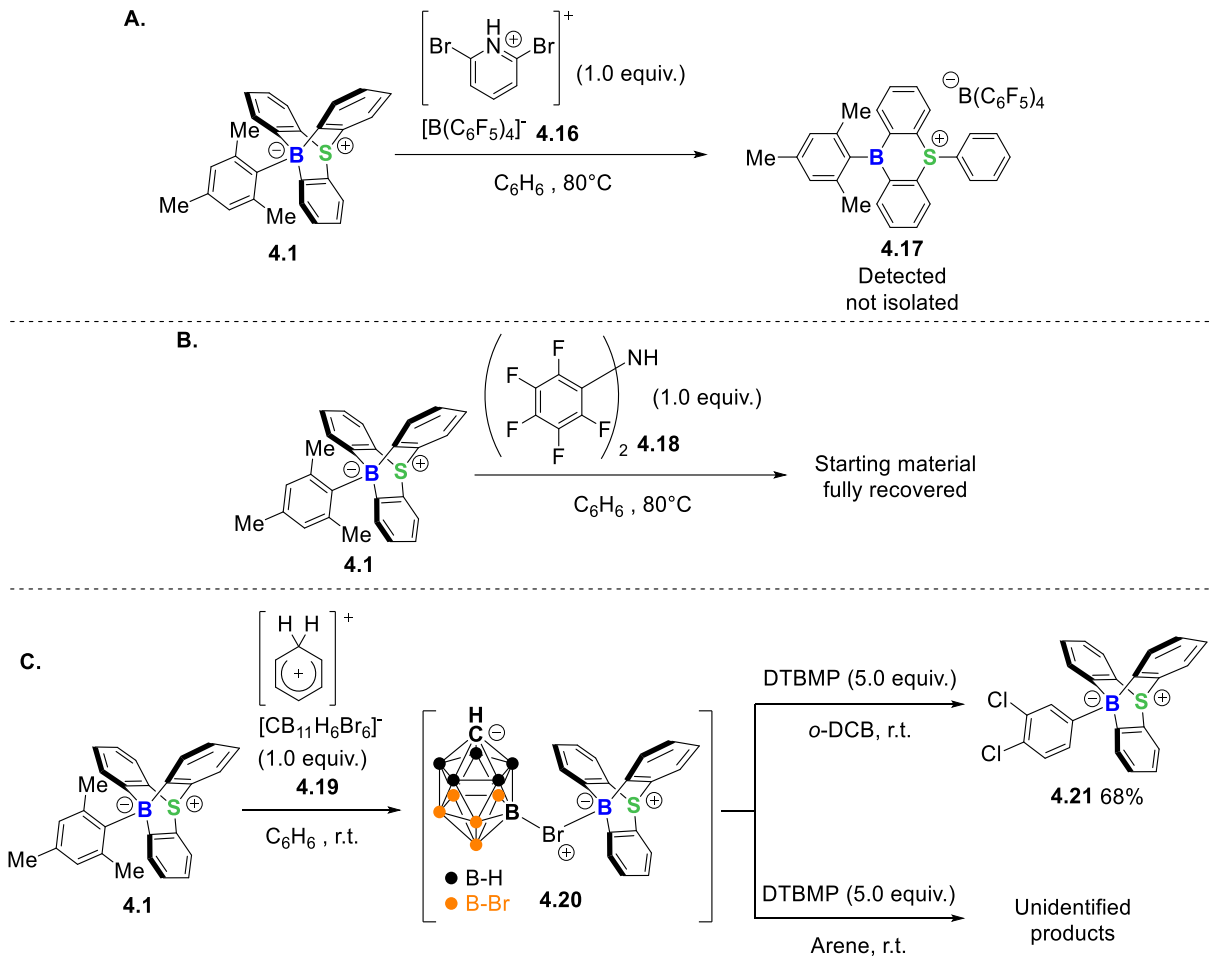
Scheme IV.54 : Attempted Csp^2–H borylation of chlorobenzene and detected side products.



Scheme IV.55 : Synthesis of triflidic acid.

Considering these facts, we decided to start over again and select another Brønsted acid to perform the protodeborylation. Unfortunately, triflidic acid was so far the only acid enabling a protodeborylation and the subsequent reversible formation of the "ate"-complex with the corresponding base. Investigations to identify a more suitable Brønsted acid started, supported by the extensive work of Leito and co-workers on the evaluation of pK_a's of a wild variety of Brønsted acids.[62] The criteria required a sufficiently strong Brønsted acid to perform a relatively fast protodeborylation along with a sufficiently weakly and/or hindered corresponding base to prevent the coordination with the 9-sulfonium-10-boratriptycene, or at least to make the coordination reversible under these experimental conditions. As presented in the previous chapter, 2,6-dibromopyridinium tetrakis(pentafluorophenyl)borane **4.16** was attempted but only provided decomposition of the starting material **4.17** (**Scheme IV.56, A**). Bis(pentafluorophenyl)amine **4.18** was synthesized and attempted as well,

but did not perform the protodeborylation (**Scheme IV.56, B**).[63] Reported by Reed and co-workers as a weakly coordinating anion (WCA), the pentacyanocyclopentadienide ion was synthesized however, the corresponding acid was not reported under its pure form and attempts to synthesize it remained unsuccessful.[64,65] Furthermore, salts involving this anion were reported to be insoluble in most organic solvents which was an issue already encountered with the triflide ion.[64] Next, the closest available derivative of carborane acid, benzenium 7,8,9,10,11,12-hexabromo-*closo*-carbododecaborate (hexabromocarborate) **4.19** was synthesized and tested (**Scheme IV.56, C.**).[66] As presented in the previous chapter, this acid led to relatively clean and fast protodeborylation however, the suggested "ate"-complex **4.20** formed with the hexabromocarborate ion precipitate in benzene or toluene and was found to be poorly soluble in other polyfluorinated arenes. Therefore, in order to use this strategy in the borylation reactions, the precipitate "ate"-complex **4.20** has to be filtered in glovebox, leading to substantial loss of product, prior to be used. Besides 1,2-dichlorobenzene which is able to solubilize the "ate"-complex **4.20** but prone to undergo borylation (**4.21)** upon addition of an external Brønsted base, polyhalogenated aromatic were not able to significantly solubilize the "ate"-complex **4.20** and the borylation products could barely be detected regardless of the conditions (**Scheme IV.56, C**). This strategy was rapidly abandoned due to the complexity of the reaction conditions and the apparent limited scope.

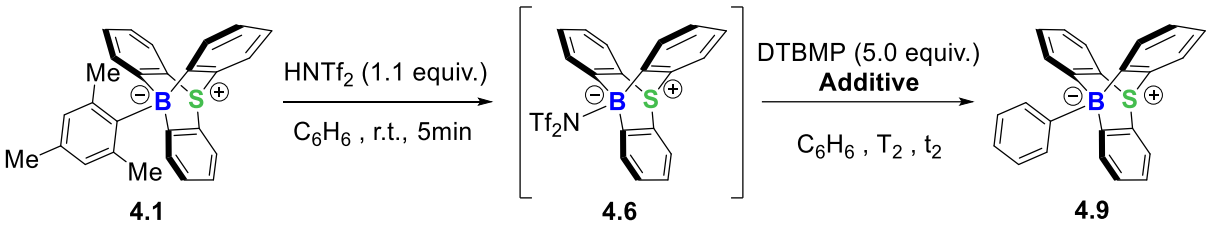


Scheme IV.56 : Attempted generation of 9-sulfonium-10-boratriptycene with - **A.** tetrakis(pentafluorophenyl)borate 2,6-dibromopyridinium (**4.16**) – **B.** bis(pentafluorophenyl)amine (**4.18**) – **C.** benzenium 7,8,9,10,11,12-hexabromo-*closo*-carbododecaborate (**4.19**) – as Brønsted acids.

It was already noted that triflimidic acid led to a clean and fast protodeborylation followed by the formation of an irreversible "ate"-complex **4.6**. The idea came to our mind that this "ate"-complex **4.6** could potentially be dissociated by addition of an additive acting as a Lewis acid and decreasing the interaction between the triflimidate ion and the 9-sulfonium-10-boratriptycene by coordinating the triflimidate moiety. Following this idea, the easily accessible $NaB(C_6F_5)_4$ was used as additional Lewis acid. The first attempt immediately provided promising results since the yield increased from 0% without the salt to 47% with one equivalent of $NaB(C_6F_5)_4$

(**Table IV.7**, entry **3**). Since triflimidic acid is commercially available and relatively cheap and $NaB(C_6F_5)_4$ easy to synthesize on gram scale[67], the use of these reagents was much more convenient than the use of triflidic acid. The reaction was also more convenient from a practical point of view since the protodeborylation is completed within seconds. It was therefore decided to optimize these new conditions to compare with the previous ones (**Table IV.7**).

Table IV.7 : Optimization of the reaction conditions for Csp^2–H borylation using *in-situ* formed 10-triflimidate-9-sulfonium-10-boratriptycene-ate complex combined with alkali tetrakis(pentafluorophenyl)borate as additives and DTBMP as as Brønsted base.



4.1 **4.6** **4.9**

	Additive	**T_2** (°C)	**t_2** (h)	**Yield** (%)
1	/	100	16	0
2	/	120	72	0
3	$NaB(C_6F_5)_4$ (1.0 equiv.)	100	16	47
4	$NaB(C_6F_5)_4$ (1.3 equiv.)	80	16	52
5	$NaB(C_6F_5)_4$ (1.3 equiv.)	60	16	67
6	$NaB(C_6F_5)_4$ (1.3 equiv.)	40	16	30
7	$NaB(C_6F_5)_4$ (1.3 equiv.)	r.t.	72	15
8	$NaB(C_6F_5)_4$ (1.5 equiv.)	60	16	73
9	$NaB(C_6F_5)_4$ (2.0 equiv.)	60	16	74
10	$LiB(C_6F_5)_4$ (1.5 equiv.)	60	16	6

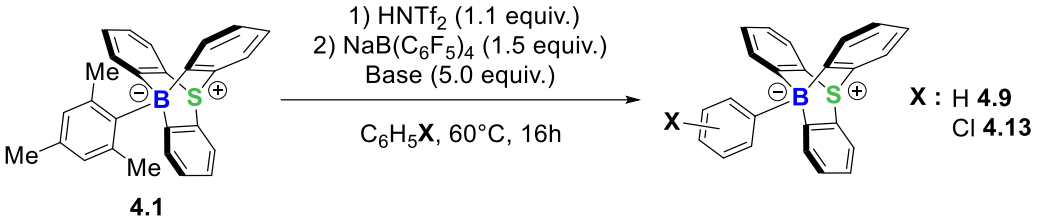
Yields are ^1H NMR yields obtained using 4-bromoanisole as internal standard.

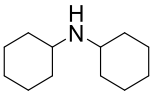
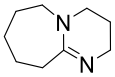
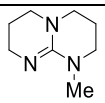
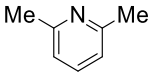
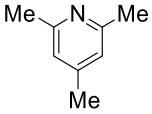
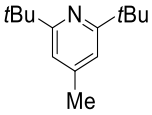
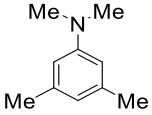
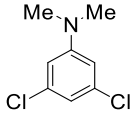
It can immediately be noted that the temperature has a significant impact on the borylation reaction. A temperature above 60°C led to reduced yields

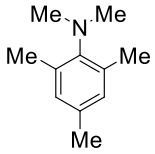
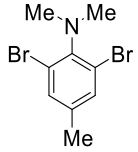
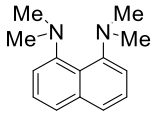
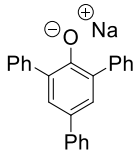
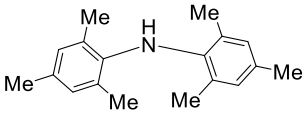
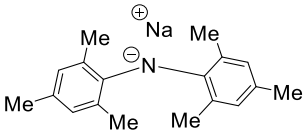
and formation of unidentified byproducts while a temperature below 60°C led to a reduced borylation rate with remaining triflimidate-ate complex (**4.6**) observed in the crude (**Table IV.7**, entry **3** (47%) to **7** (15%)). The amount of additive is also crucial, the best yields being obtained using 1.5 and 2.0 equivalents (**Table IV.7**, entry **8** (73%), **9** (74%)). The reaction conditions presented in entry **8** were selected as they provide the best yield with minimal amount of additive. Surprisingly, $LiB(C_6F_5)_4$ turned out to be less efficient than the corresponding sodium salt with only 6% yield obtained, even though lithium cation is generally considered as stronger Lewis acid than sodium cation (**Table IV.7**, entry **10**). Indeed, according to the work of Pomeli and co-workers, the affinity of triflimidate ion is stronger for lithium cation than sodium cation.[68] So far, no definitive explanation could be provided concerning the reduced activity of $LiB(C_6F_5)_4$ against $NaB(C_6F_5)_4$.

Since the reaction conditions changed, we decided to start the optimization again based on this new combination of triflimidic acid and $NaB(C_6F_5)_4$. We therefore decided to optimize again the choice of the Brønsted base (**Table IV.8**). Since one of the limitations encountered was the impossibility to efficiently borylate deactivated arenes such as haloarenes, the different Brønsted bases will be tested on benzene and chlorobenzene as substrates.

Table IV.8 : Optimization of the Brønsted base used for Csp^2–H borylation with *in-situ* generated 10-triflimidate-9-sulfonium-10-boratriptycene-ate complex (**4.6**) and $NaB(C_6F_5)_4$ as additive.



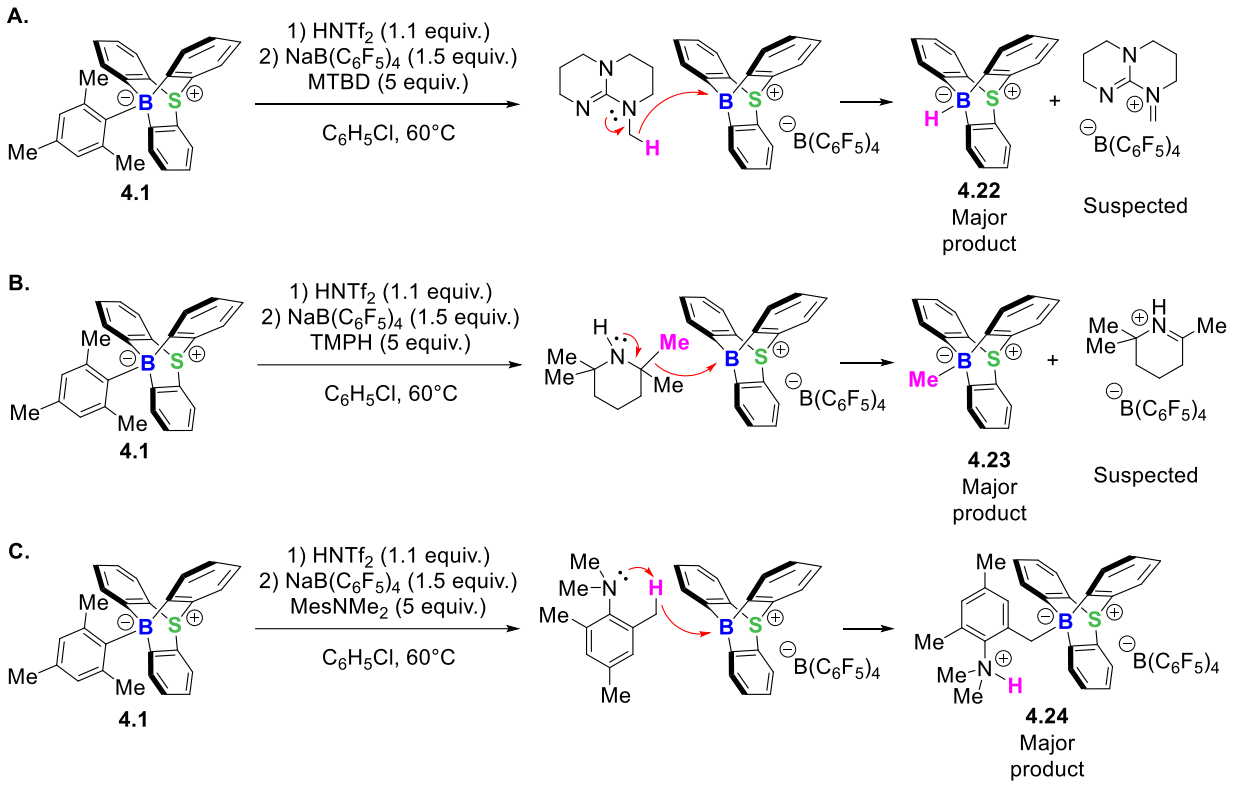
Entry	Base	Solvent	Yield (%)
1		C_6H_6	55
		C_6H_5Cl	Detected*
2		C_6H_6	45
		C_6H_5Cl	Detected*
3		C_6H_6	/
		C_6H_5Cl	0
4		C_6H_6	21
		C_6H_5Cl	0
5		C_6H_6	51
		C_6H_5Cl	Detected*
6		C_6H_6	48
		C_6H_5Cl	0
7		C_6H_6	45
		C_6H_5Cl	0
8		C_6H_6	74
		C_6H_5Cl	Detected*
9		C_6H_6	91
		C_6H_5Cl	85[a]
10		C_6H_6	88
		C_6H_5Cl	Detected*

11		C_6H_6	41
		C_6H_5Cl	0
12		C_6H_6	89
		C_6H_5Cl	Detected*
13		C_6H_6	15
		C_6H_5Cl	/
14		C_6H_6	/
		C_6H_5Cl	Detected*
15		C_6H_6	61
		C_6H_5Cl	Detected*
16		C_6H_6	11
		C_6H_5Cl	0

Yields are ^{1}H NMR yields obtained using 4-bromoanisole as internal standard. *Detected means that a signal corresponding to the desired product was detected by ^{11}B NMR but could not be isolated nor unambiguously detected by ^{1}H NMR. [a] : isolated yield

Considering the wide variety of Brønsted bases attempted, the first important feature is the apparent absence of correlation between the structure of the base and the yield. At first sight, aniline derivatives (**Table IV.8**, entries **9-12**) provided good results with benzene as substrate while a single one, *N*,*N*,3,5-tetramethylaniline (TMA) (**Table IV.8**, entry **9**), provided good results as well with chlorobenzene (85%). In most cases, no clear evidence of the formation of a major side product was observed. However, in some cases, interesting side products could be isolated which allowed a deeper understanding of the reactivity of the 9-sulfonium-10-boratriptycene. Indeed, using MTBD (**Table IV.8**, entry **5**) or the proton

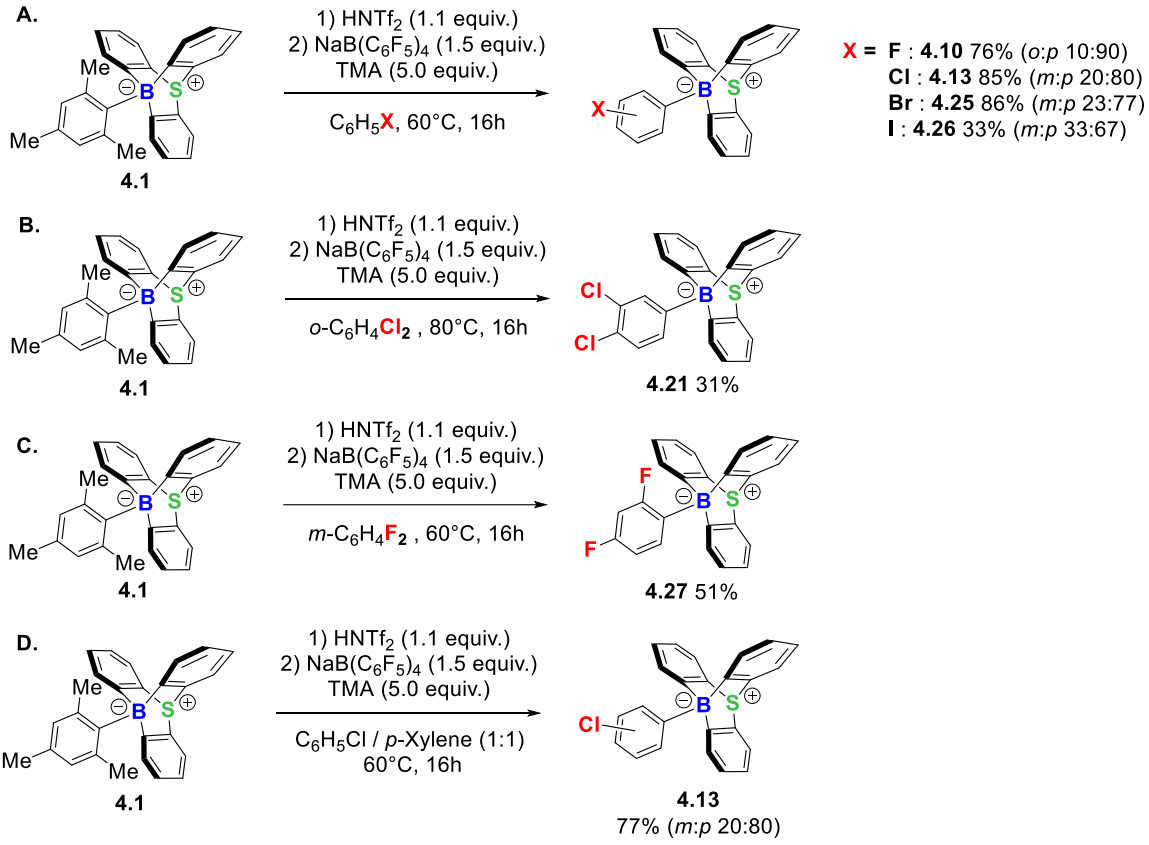
sponge (**Table IV.8**, entry **13**), the major side product was the 10-hydrido-9-sulfonium-10-boratriptycene-ate complex **4.22** (**Scheme IV.57, A**), resulting from the hydride abstraction from a methyl substituent. Such reactivity has already been reported between alkyl amines and $B(C_6F_5)_3$.[69–72] With alkyl amines as TMPH (**Table IV.8**, entry **1**) and DIPEA (**Table IV.8**, entry **3**), the formation of 10-methyl-9-sulfonium-10-boatriptycene-ate complex (**4.23**) was totally unexpected (**Scheme IV.57, B**). This product can only come from the abstraction of a methyl substituent from the base. Unfortunately, the corresponding iminium could not be isolated or observed. Even though the methyl-ate complex **4.23** was only obtained in a range of 4 to 20%, this stands as the first example of Csp^3–Csp^3 bond abstraction with a boron Lewis acid. Using 2,4,6-trisubstituted aniline derivatives (**Table IV.8**, entry **11**, **12**), the hydride abstraction was observed as very minor product. However with *N*,*N*,2,4,6-pentamethylaniline (**Table IV.8**, entry **11**), the major side product was found to be the product of Csp^3–H borylation of the *ortho*-methyl substituent (**4.24**) (**Scheme IV.57, C**). Once again, this product was totally unexpected and stands as the first example of Csp^3–H borylation using triarylboranes.[71] Despite being of great interest this reactivity has not been studied in more details in this thesis but should be under investigation afterwards.



Scheme IV.57 : Major side reactions observed between the 9-sulfonium-10-boratriptycene and Brønsted bases attempted during the optimization process.

Considering the good to excellent results obtained with TMA (**Table IV.8**, entry **9**, C_6H_6 = 91%, C_6H_5Cl = 85%), this base was selected to pursue the optimization. Few other substrates were then tackled, especially more deactivated arenes, in order to evaluate the limitations of this method (**Scheme IV.58**). The borylation of monohalogenated arenes proceeded with good yields (76 to 86%) except for iodobenzene (**4.26** 36%) (**Scheme IV.58, A**). This drastically lowered yield could come from disproportionation of iodobenzene under strong Lewis acidic conditions. A similar observation was reported by Ingleson and co-workers as they observed the generation of benzene during the electrophilic borylation of bromobenzene using borenium ions.[32] According to Olah and co-workers, benzene can be generated from haloarenes, especially bromo- and iodobenzene, by disproportionation in presence of a strong Lewis acid such as $AlCl_3$.[73] Even though we did not observe the formation of benzene due to evaporation to

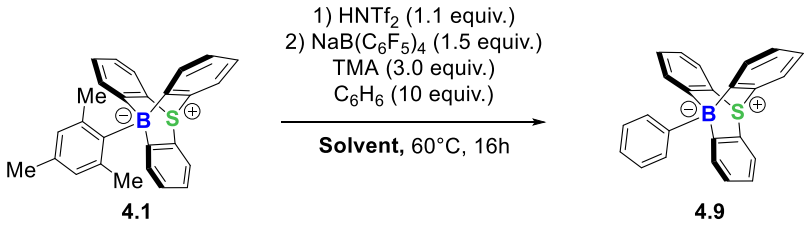
dryness of the crude, nor the borylation of benzene due to the large excess of iodobenzene in the medium against the *in-situ* formed benzene, this could stand as a reasonable hypothesis to explain the lowered yield with iodobenzene. Two dihalogenated arenes, 1,3-difluoro- and 1,2-dichlorbenzene, could be borylated with decent yields (**4.27** 51% and **4.21** 31% respectively) (**Scheme IV.58, A, B**). Surprisingly, the borylation of *p*-xylene turned out to be unsuccessful even though this arene is more nucleophilic than benzene. Furthermore, performing the reaction in a 1:1 mixture of *p*-xylene and chlorobenzene only led to the borylation of chlorobenzene (**Scheme IV.58, D**). This selectivity is totally unusual and could only be attributed to the steric hindrance induced by the methyl substituents on *p*-xylene.



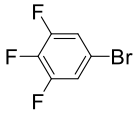
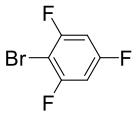
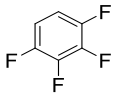
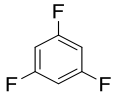
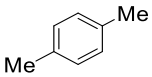
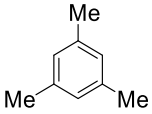
Scheme IV.58 : Csp^2–H borylation of haloarenes using corresponding haloarenes as solvent and competition reaction using 1:1 mixture of *p*-xylene and chlorobenzene as solvent.

Considering that even very weakly nucleophilic arenes such as 1,2-dichlorobenzene could be borylated, we decided to push further the optimization of our reaction conditions. So far, the substrates were used as solvent which reduces the applicability of the method, restricting the scope to liquid substrates. The next step of the optimization consisted in identifying an unreactive solvent and reducing the amount of substrate for maximizing the yields with minimum amount of substrate (**Table IV.9**). As starting point, it was decided to pursue the optimization based on 10 mg of starting 10-mesityl-9-sulfonium-10-boratriptycene-ate complex **4.1**, 1.1 equivalents of $HNTf_2$ and 10 equivalents of benzene. The temperature and reaction time were kept as previously optimized, 60°C and 16h respectively. Besides polyfluorinated benzene derivatives, only few polysubstituted arenes could be suitable as solvent due to their generally high melting and boiling points as well as their cost.

Table IV.9 : Optimization of the solvent used for Csp^2–H borylation with *in-situ* generated 10-triflimidate-9-sulfonium-10-boratriptycene-ate complex (**4.1**) and $NaB(C_6F_5)_4$ as additive.



4.1 **4.9**

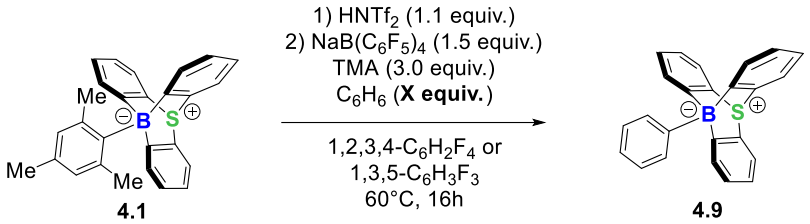
Entry	Solvent	Substrate concentration (mol.L^{-1})	Yield (%)
1		0.52	4
2		0.52	42
3		0.52	48
4		0.52	47
5		0.52	6
6		0.52	5

Yields are ^{1}H NMR yields obtained using 4-bromoanisole as internal standard

Aromatic hydrocarbons are not adequate for this reaction (**Table IV.9**, entries **5**, **6**), mostly due to the insolubility of the starting material and the Brønsted acid, leading to incomplete protodeborylation. Halogenated solvents are more suitable but strongly deactivated or hindered arenes are required. The best yields were obtained with 1,2,3,4-tetrafluorobenzene (**Table IV.9**, entry **3**), which is able to efficiently solubilize the starting materials allowing a fast and convenient protodeborylation. However, this

compound is relatively expensive to be extensively used as solvent. Therefore, much cheaper 1,3,5-trifluorobenzene was tested and, despite the slightly reduced solubility of the starting materials in this solvent, the yields obtained were similar or identical (**Table IV.9**, entries **3**, **4**). This was further confirmed performing other borylation experiments, therefore 1,3,5-trifluoro and 1,2,3,4-tetrafluorobenzene were used equally. With the most adequate solvent identified, the amount of base and substrate were the following parameters to optimize (**Table IV.10**). By varying the amount of benzene, the impact of the concentration of substrate was also evaluated.

Table IV.10 : Optimization of the amount of benzene as substrate used for Csp^2–H borylation with *in-situ* generated 10-triflimidate-9-sulfonium-10-boratriptycene-ate complex (**4.1**) and $NaB(C_6F_5)_4$ as additive.



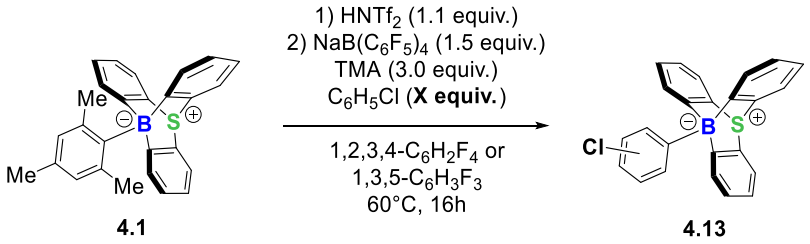
4.1 **4.9**

	Solvent Volume (mL)	**Benzene equivalents**	**Concentration** ($mol.L^{-1}$)	**Yield** (%)
1	0.50	10	0.49	48
2	1.0	20	0.49	51
3	0.50	20	0.94	66
4	1.0	40	0.94	74
5	0.50	30	1.35	85
6	1.0	60	1.35	90
7	0.50	40	1.73	86
8	1.0	80	1.73	88
9	0.50	50	2.08	89
10	1.0	100	2.08	86

Yields are ^1H NMR yields obtained using 4-bromoanisole as internal standard

It appeared clear that the concentration of benzene is more important than the equivalents. However, maintaining a steady concentration and doubling the solvent volume and the equivalents always led to slightly increased yields, except for the highest concentrations of substrates (**Table IV.10**, entries **9**, **10**). It can be hypothesized that this slight yield increase, despite a steady concentration of substrate, might be due to a better solubilization of the reagents. The best conditions considered were 30 equivalents of substrate, for a concentration of 1350 mmol.L^{-1} since it provides the best yields for a minimum amount of substrate (**Table IV.10**, entry **5** (85%)). Unfortunately, these conditions were then attempted with chlorobenzene as substrate which only provided 29% yield. This clearly revealed that a second optimization is required for deactivated arenes (**Table IV.11**). In this case, the yields are isolated yields since it was impossible to use any signal of the desired product from the crude ^{1}H NMR spectrum to determine a ^{1}H NMR yield.

Table IV.11 : Optimization of the amount of chlorobenzene as substrate used for Csp^{2}–H borylation with *in-situ* generated 10-triflimidate-9-sulfonium-10-boratriptycene-ate complex (**4.1**) and NaB(C_6F_5)$_4$ as additive.



4.1 **4.13**

	Solvent volume (mL)	**Chlorobenzene equivalents**	**Concentration** (mol.L^{-1})	**Yield** (%)
1	1.5	30	1.33	29
2	1.5	40	1.70	34
3	1.5	50	2.04	58
4	1.5	60	2.35	61
5	1.5	80	2.90	66

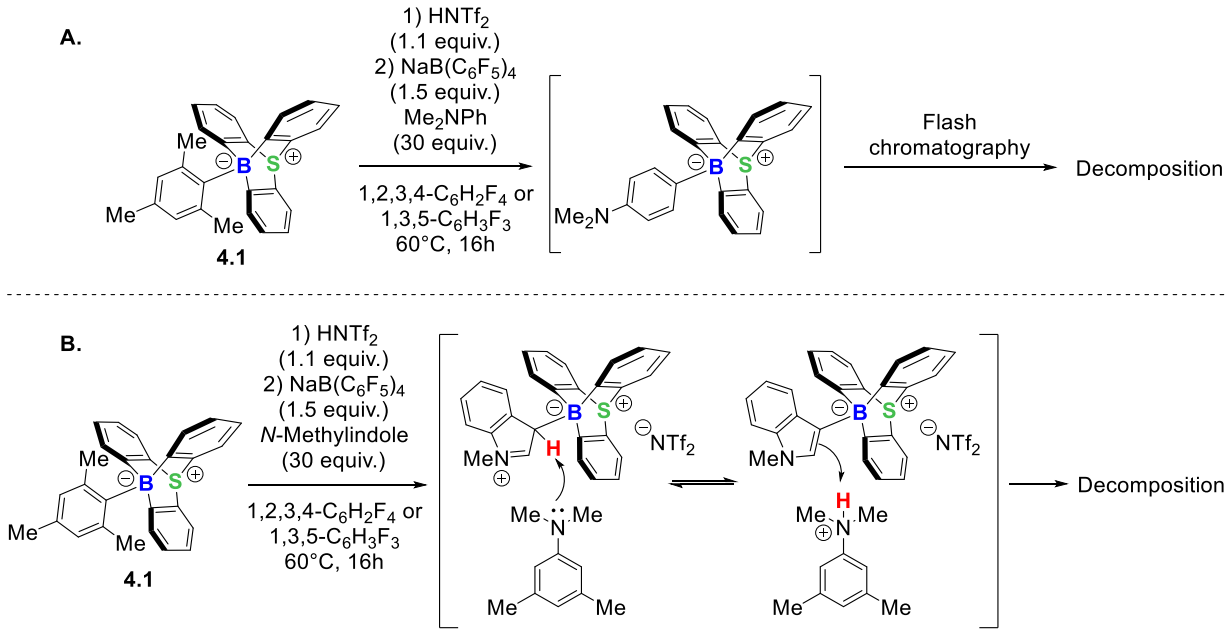
Unfortunately, the yield could not be drastically increased with chlorobenzene. Still, 66% (**Table IV.11**, entry **5**) can be considered good since only few methods allow this type of transformation. It was noted that increasing the amount of base up to 5.0 equivalents led to small increase of yield, especially with deactivated arenes. More importantly, increasing the amount of base does not seem to have a deleterious effect. Therefore, to standardize the conditions and maximize the yields, the substrate scope was developed with 5.0 equivalents of base.

IV.4. Substrate scope

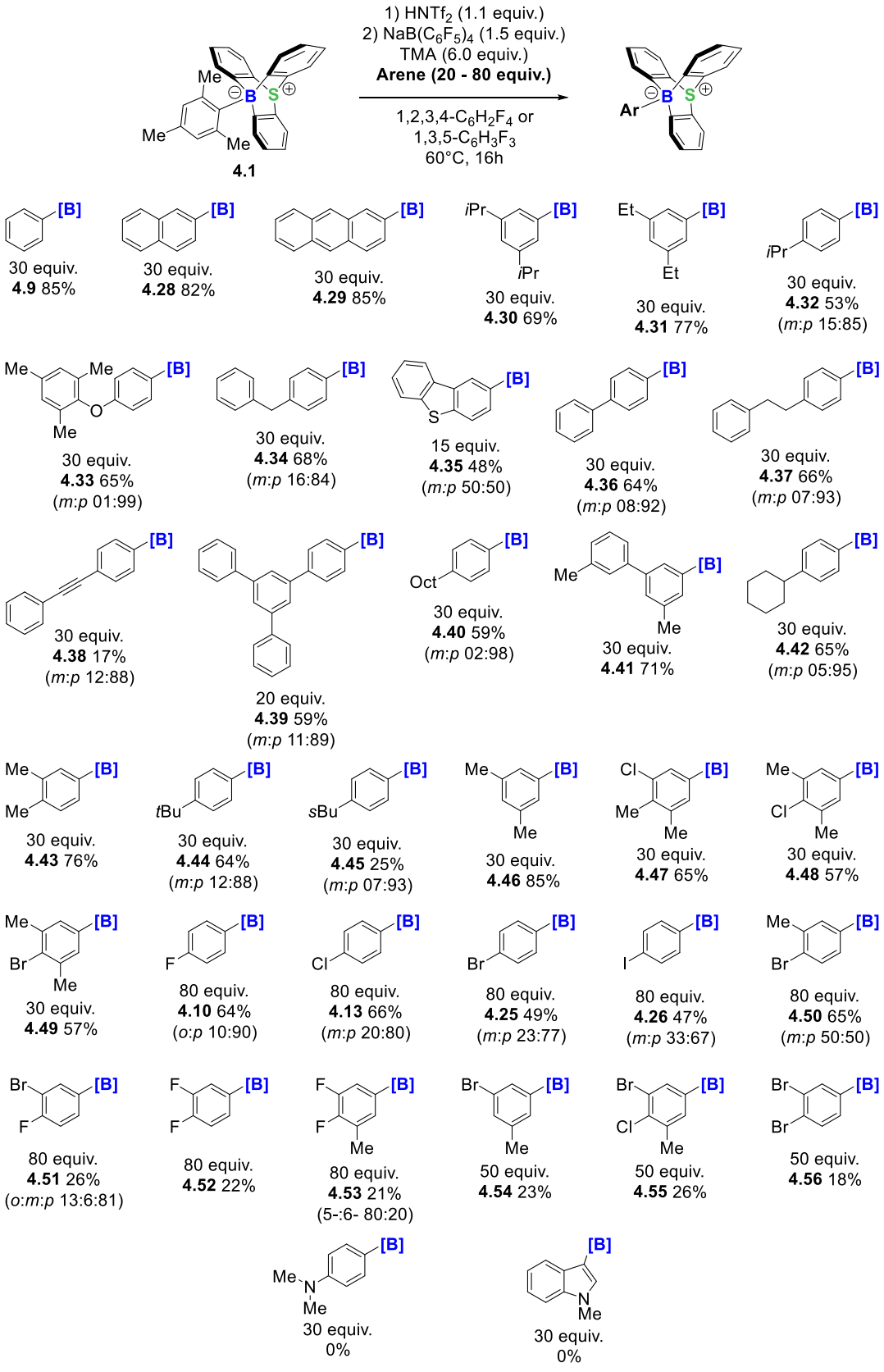
With the best conditions in hands for unactivated and deactivated arenes, a scope of substrates was developed. This started with unactivated arenes. It is important to note that, in the case of solid substrates, the equivalents may deviate from previously established conditions due to poor solubility of the substrate or too large amount of solid substrate required to reach 30 equivalents, as stated as standard conditions.

A large range of substrates could be borylated from unactivated to deactivated arenes. Surprisingly, activated arenes such as *N*,*N*-dimethylaniline (**Scheme IV.59, A**) and *N*-methylindole (**Scheme IV.59, B**) could not be borylated. In the case of *N*,*N*-dimethylaniline, a signal (–9.1 in ^{11}B NMR) that may correspond to the borylation product was observed but after flash chromatography no product could be recovered. This may come from a decomposition of the product on acidic silica by protodeborylation, however this hypothesis could not be confirmed (**Scheme IV.59, A**). With a so large excess of *N*,*N*-dimethylaniline, a substantial amount of the borohydride **4.22** resulting from the abstraction of an hydride from a methyl substituent was obtained while this product is rarely detected with only 5.0 equivalents of TMA,

although structurally similar. Concerning *N*-methylindole, the borylation product was not detected (**Scheme IV.59, B**). This could come from the formation of a stable Lewis adduct with the substrate despite no evidence of this adduct was observed.[32] Another plausible hypothesis stands for a reversible borylation/protodeborylation of the product, the protonated TMA formed being possibly able to protonate the "ate"-complex which led to protodeborylation. Another hypothesis for both cases is that the Lewis basic nitrogen would coordinate the Lewis acidic sodium cation, preventing abstraction of the triflimidate ion from the boron.[74–76] However, this hypothesis seems less realistic since the only product obtained would be the triflimidate-ate complex, which is not the case. Furthermore, this coordination of the sodium should also occur with the 5.0 equivalents of TMA added in every borylation reaction.

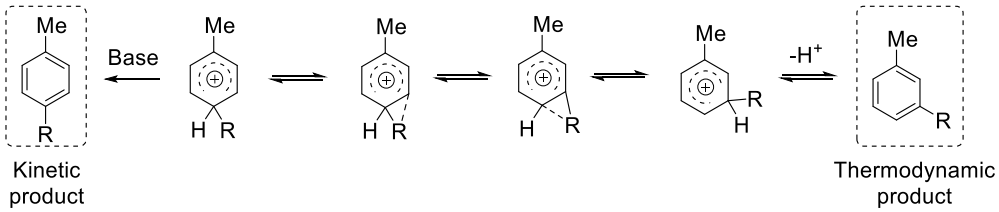


Scheme IV.59 : Suggested side reactions precluding the isolation Csp^2–H borylation product of **A.** *N,N*-dimethylaniline and **B.** *N*-methylindole.



Scheme IV.60 : Scope of Csp^2–H borylation.

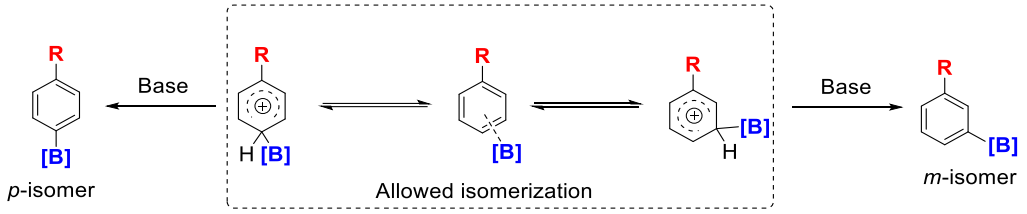
An important feature to note is the formation, for most of monosubstituted substrates, of *meta*- and *para*-isomers (**Scheme IV.60**). In all these cases, the preponderant formation of the *para*-isomer is according to S_EAr regioselectivity since the directing groups used in these cases are either inductive donor or inductive attractor but mesomeric donors. However, the formation of the *meta*-isomer is more intriguing. This was already observed by Ingleson and co-workers for example with toluene and was attributed to the formation of the thermodynamic product of the S_EAr reaction.[32] The formation of *m*-isomer has been widely reported in hydrocarbon chemistry during alkylations of arenes under thermodynamic control. Indeed, performing acid catalyzed alkylation of toluene in absence of base ultimately leads to the formation of *m*-isomer as the major or even as the exclusive product (**Scheme IV.61**).[77]



Scheme IV.61 : Isomerization of 1,4-disusbtituted arenium ion into 1,3-disubstituted arenium ion

The *m*:*p* ratios are in the range of 01:99 to 15:85 for activated arenes and 20:80 to 33:67 for haloarenes (**Scheme IV.60**). Interestingly, this method provides a much higher *para*-selectivity than previously reported electrophilic borylation methods. The formation of *meta*-isomers suggests two important mechanistic features: 1) the deprotonation by TMA is relatively slow and occurs after the isomerization and the formation of the thermodynamic product or 2) the deprotonation by TMA is reversible, as illustrated in the case of *N*-methylindole. The second hypothesis is improbable since we demonstrated that protonated TMA does not induce protodeborylation in the reaction time considered (16h). Under these reaction conditions, the isomerization of the *para*- into the *meta*-isomer can

be explained by the presence of a π- and a σ-complex between the 9-sulfonium-10-boratriptycene and the aromatic substrate which are in equilibrium. Therefore, the equilibrium constant between the π- and σ-complex could influence the final ratio of *para*- and *meta*-isomers **(Scheme IV.62**).[78,79]



Scheme IV.62 : Illustrated probable equilibrium between σ- and π-complexes with 9-sulfonium-10-boratriptycene leading to the formation of *m*- and *p*-isomers.

IV.5. Mechanistic investigations

IV.5.1 Experimental investigations

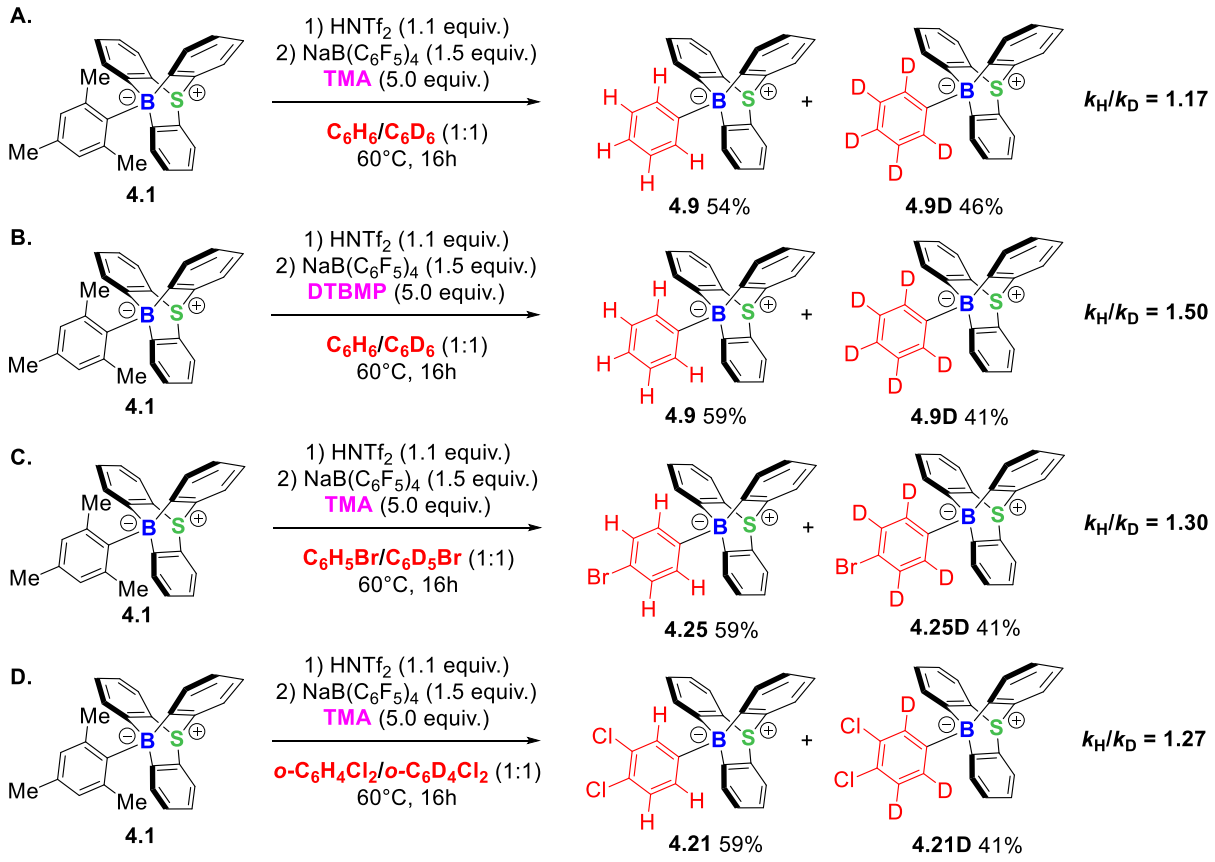
Kinetic isotope effect experiments

One of the most classical and commonly used tool to probe the mechanism of electrophilic borylation reactions is the determination of the kinetic isotope effect (KIE).[80,81] This consists in measuring the changes in the reaction rate when an atom, commonly hydrogen, is replaced by an isotope, commonly deuterium. This experiment could provide information of which bond is broken during the rate determining step by determining the ratio between the reaction rate constant of the formation of the hydrogenated product (k_H) and that of the deuterated product (k_D). This can be extended to the ratio between the amount of hydrogenated versus deuterated product.

$$\mathrm{KIE} = \frac{k_H}{k_D} = \frac{\mathrm{P}_H}{\mathrm{P}_D}$$

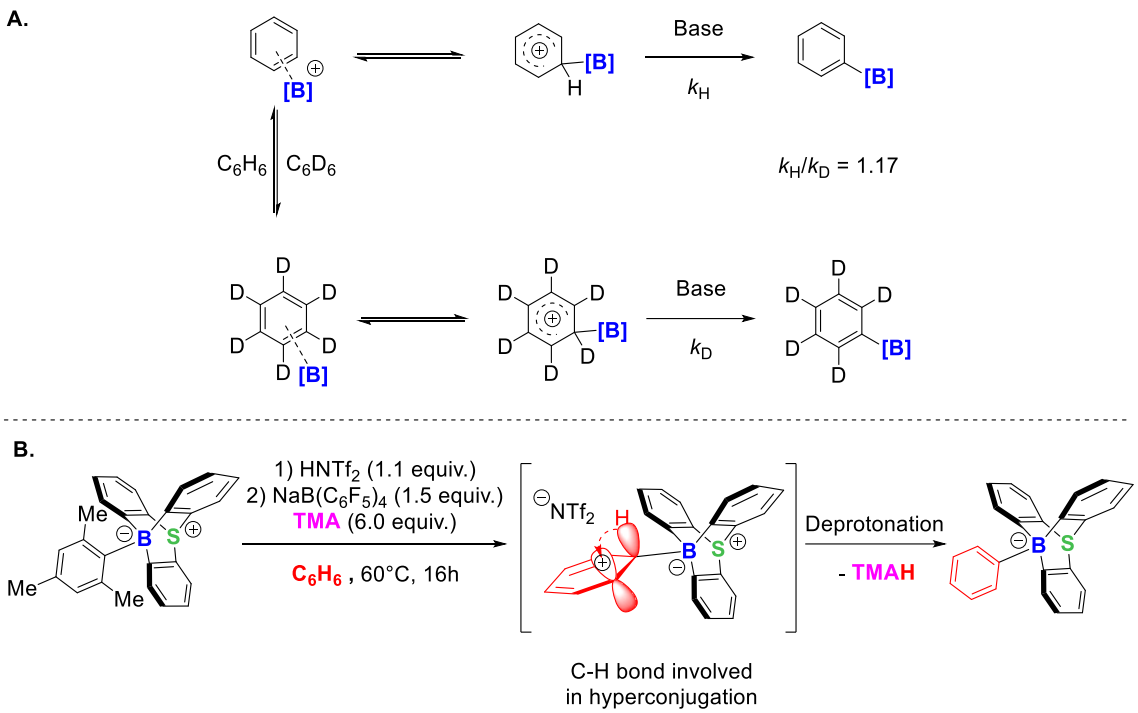
Two types of H/D KIE could be observed: the primary KIE or the secondary KIE. The primary KIE can indicate that the X–H/D bond is broken during the rate determining step. Values for a primary KIE can be expected to be about 6.5 to 7, even though typical experimental KIEs are much lower. The secondary KIE can be observed if the isotope replacement has been made far from the reactive center or in bonds that only change their hybridization in the rate determining step. For secondary KIEs, the values are lower and expected to be 1.1 – 1.2 for normal KIEs and 0.8 – 0.9 for inverse KIEs. It is important to note that, the replacement of a C–H bond by a C–D bond can also influence equilibria. Therefore, when equilibria are presents, a $k_H/k_D \neq 0$ can be observed which is called equilibrium isotope effect (EIE).[81]

We evaluated the H/D KIE under the form of intramolecular competition experiments by performing the borylation reaction using the substrate as solvent in a 1:1 molar ratio of hydrogenated/deuterated substrate. This type of intermolecular competition can provide information on whether as a C–H/D bond from the substrate is broken during the rate determining step. It is important to note that the absence of KIE indicates that the C–H/D bond cleavage does not occur during the rate determining step. However, the observation of a KIE does not prove that the C–H/D bond cleavage occurs during the rate determining step, it is also possible that the C–H/D bond cleavage occurs during the product determining step, which can be different from the rate determining step. Several experiments were conducted, varying the substrate and the Brønsted base (**Scheme IV.63**).



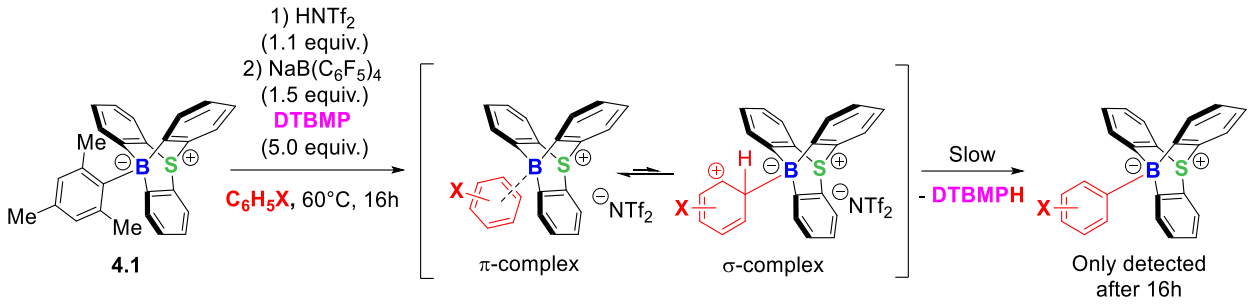
Scheme IV.63 : KIE experiments.

The first experiment performed was conducted using TMA as proton scavenger and only presents a very small k_H/k_D (1.17) (**Scheme IV.63, A**). Such a k_H/k_D suggests a secondary isotope effect rather than a primary one and therefore suggests that the deprotonation is not the rate determining step. It was already mentioned that a σ- and a π-complex between the 9-sulfonium-10-boratriptycene and the arene is present in equilibrium prior to the deprotonation step, this k_H/k_D might indicate an EIE (**Scheme IV.64, A**). Indeed, such a range of k_H/k_D has been observed for EIE in transition-metal-catalyzed C–H borylation.[81] A secondary KIE could also be observed when the C–H/D bond is involved in hyperconjugation during the rate determining step (**Scheme IV.64, B**). This could be the case upon formation of the σ-complex.



Scheme IV.64 : **A.** Illustrated equilibrium between π- and σ-complexes with C_6H_6 and C_6D_6 **B.** Illustrated involvement of the C–H bond into hyperconjugation before deprotonation.

The second experiment was conducted with DTBMP as Brønsted base. In these conditions, a more significant k_H/k_D was observed (1.50) which could suggest a primary KIE (**Scheme IV.63, B.**). This could suggest that the deprotonation is the rate determining step which would not be surprising considering the extreme steric hindrance of the DTBMP. It has already been demonstrated that the steric hindrance of DTBMP reduces its pK_a and leads to a kinetically disfavored protonation.[82] This could easily explain the absence of borylation with DTBMP using deactivated arenes as substrates. Indeed, since the formation of the σ-complex is reversible and the deprotonation is slow with DTBMP, the formation of aryl-ate complexes from weakly nucleophilic arenes would be extremely slow and potentially leading to the formation of decomposition or side products instead (**Scheme IV.65**).



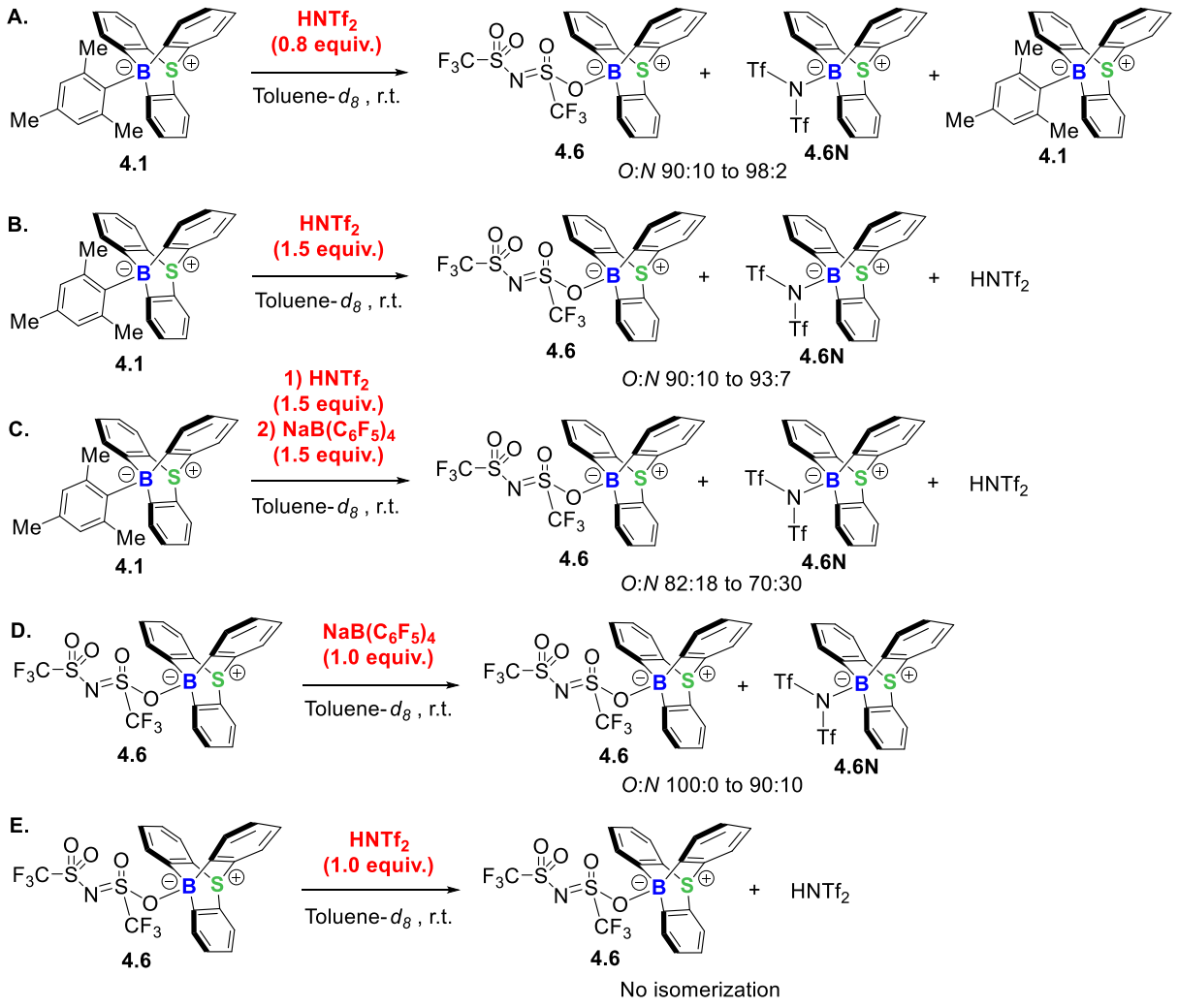
Scheme IV.65 : Illustration of absence of Csp^2-H borylation of deactivated arenes using DTBMP as proton scavenger.

The third and fourth experiments conducted show similar k_H/k_D than with the first experiment (1.30 and 1.27) (**Scheme IV.63, C, D**). In these cases, TMA was used as base and deactivated haloarenes were used as solvents. Even though the k_H/k_D values are slightly increased compared to the one obtained during the first experiment, suggesting the deprotonation as the rate determining step in this case would be absurd. Indeed, it can easily be reasoned that the acidic proton in the σ-complex formed from a haloarene would be more acidic than with benzene. Such k_H/k_D values might still correspond to a secondary KIE resulting from the involvement of the C–H/D bond in hyperconjugation with the adjacent carbocation. Furthermore, since the carbocation formed in the σ-complex is less stabilized due to the inductive electron-withdrawing character of halogens, the hyperconjugation could be stronger, leading to an increased k_H/k_D value. However, these k_H/k_D values can still suggest an EIE.

Determination of the reactive species

Although, the 9-sulfonium-10-boratriptycene could not be isolated or characterized so far under its free trivalent form, reactions occurring at the boron atom imply its generation but rather as a transient species. Therefore, it can be suggested that the reactive species for electrophilic borylation is not the free 9-sulfonium-10-boratriptycene but rather a coordinated species that immediately forms a σ-complex while the coordinated leaving group is

removed. We previously demonstrated that addition of $NaB(C_6F_5)_4$ on the 10-triflimidate-9-sulfonium-10-boratriptycene-ate complex **4.6** led to the formation of a reactive species competent to perform the electrophilic borylation. Thus, a ^{19}F NMR spectroscopic investigation was conducted in order to identify the nature of this reactive intermediate.



Scheme IV.66 : Evaluation of the conditions required for a reversible and dynamic formation of 10-triflimidate-9-sulfonium-10-boratriptycene-ate complex **4.6**.

To start this investigation, 10-mesityl-9-sulfonium-10-boratriptycene-ate complex **4.1** was treated with 0.8 equiv. of $HNTf_2$ in toluene-d_8. The crude was analyzed by ^{19}F, ^{11}B and ^{1}H NMR spectroscopy directly after mixing the products then after 16h and 40h (**Scheme IV.66, A**; **Figure IV.30**). As

expected, all analysis revealed an incomplete conversion of the starting material since a substoichiometric amount of acid is used. The immediate analysis showed four signals in ^{19}F NMR, the two major signals corresponding to the *O*-isomer triflimidate-ate complex **4.6** along with the *N*-isomer **4.6N** in a 90:10 ratio. The last very minor signal was attributed to impurities from $HNTf_2$. After 16h and 40h, the ^{19}F NMR spectra were similar, the amount of *N*-isomer **4.6N** being considerably reduced compared to the *O*-isomer **4.6** (98:2 *O*:*N* ratio). The apparent lability of the *N*-isomer **4.6N** explains the impossibility to isolate this isomer. However, another minor and apparently labile species appeared and is so far unidentified.

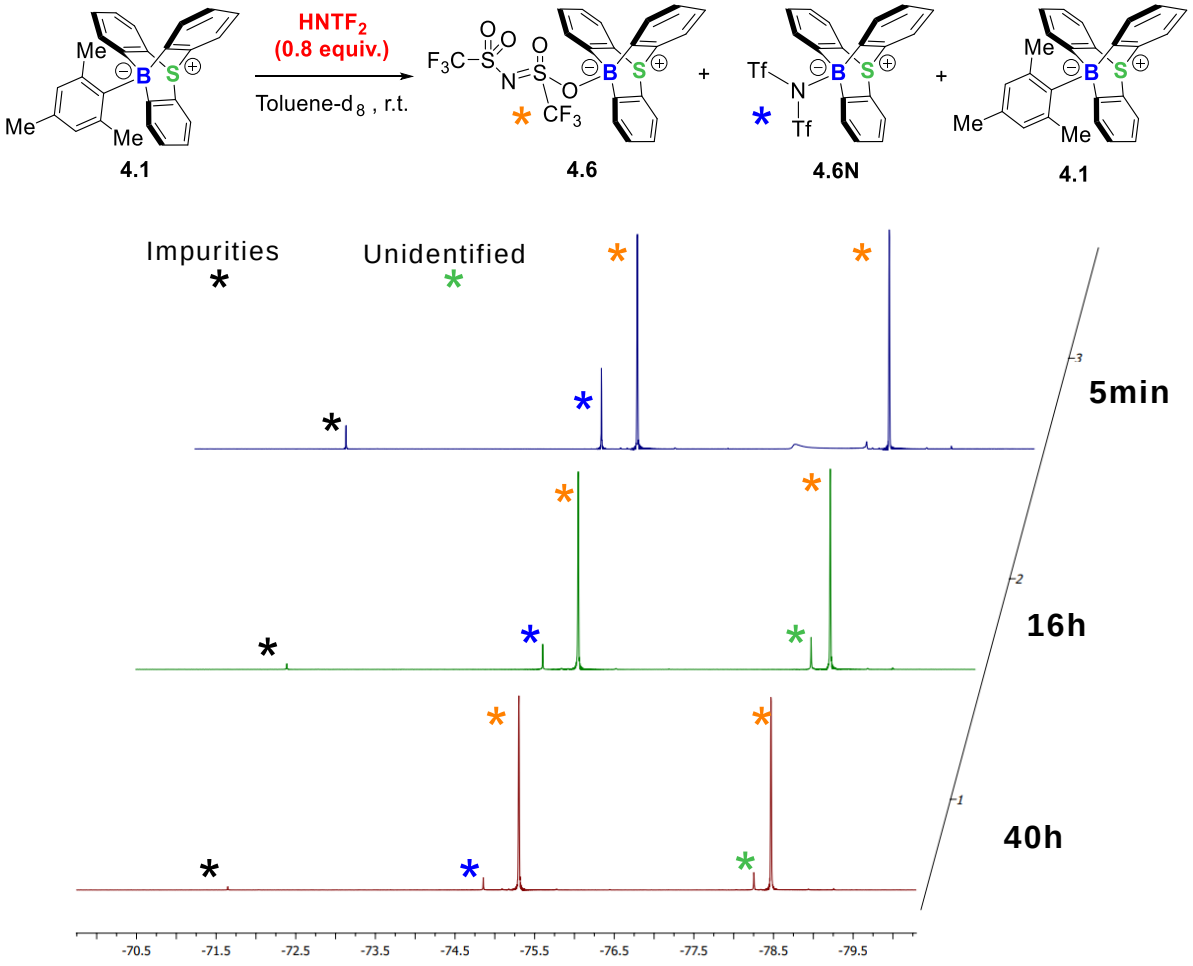


Figure IV.30 : Evolution of the crude resulting from the protodeborylation of 10-mesityl-9-sulfonium-10-boratriptycene-ate complex with 0.8 equiv. of triflimidic acid followed by ^{19}F NMR.

Next, the protodeborylation was performed using 1.5 equiv. of $HNTf_2$ and NMR analysis were recorded directly after mixing the reagents, after 16h and 40h (**Scheme IV.66, B**; **Figure IV.31**). The major product is still the *O*-isomer **4.6** in a similar ratio with the *N*-isomer **4.6N**. As expected, a large amount of remaining triflimidic acid is found. The amount of *N*-isomer **4.6N** decreases progressively to reach 93:7 ratio. However, no formation of previously unidentified product is observed as well as slower conversion of the *N*-isomer **4.6N** into the *O*-isomer **4.6** which might indicate that in presence of an excess of $HNTf_2$, the isomerization of the *N*-isomer **4.6N** into the *O*-isomer **4.6** is now in equilibrium, which is not the case with a default of $HNTf_2$.

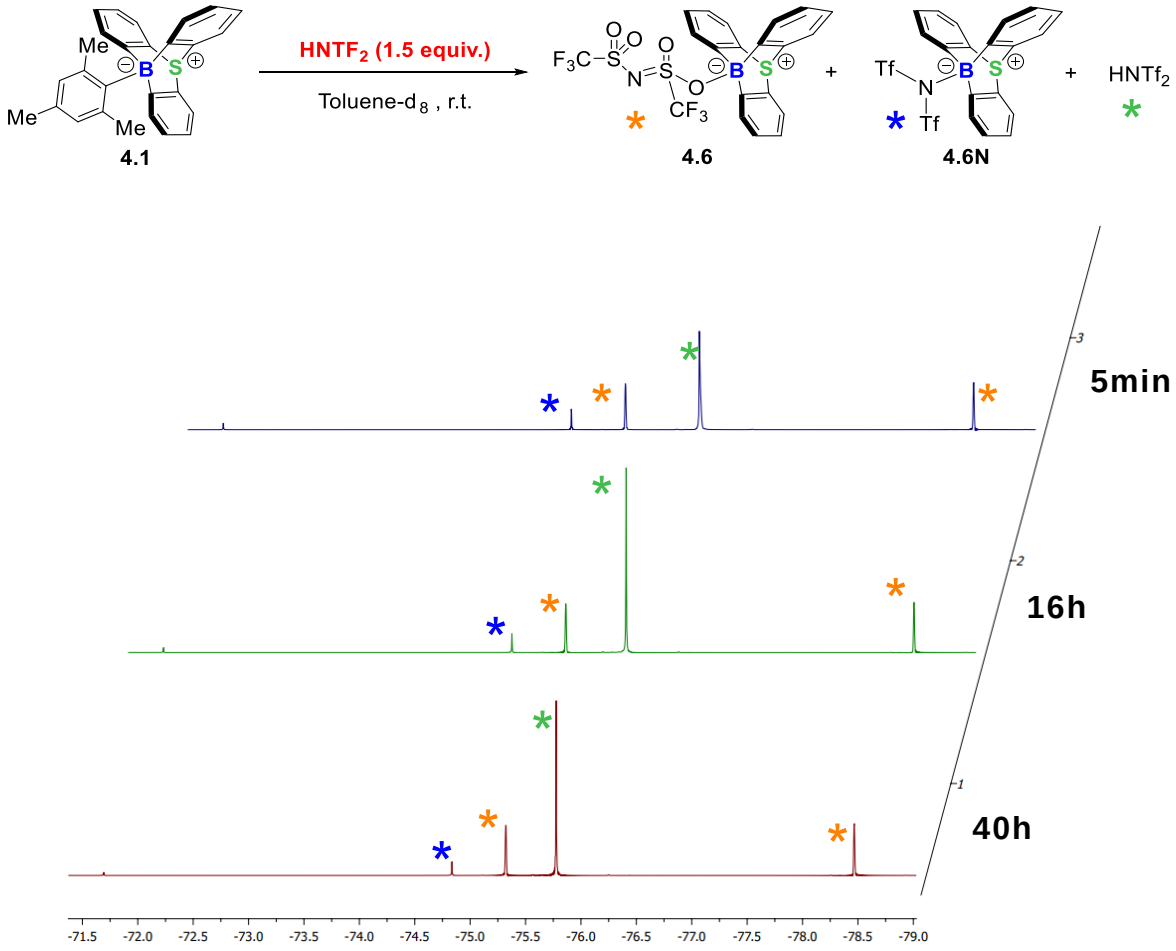


Figure IV.31 : Evolution of the crude resulting from the protodeborylation of 10-mesityl-9-sulfonium-10-boratriptycene-ate complex **4.1** with 1.5 equiv. of $HNTf_2$ followed by ^{19}F NMR.

Next, the same reaction was reproduced and 1.5 equiv. of $NaB(C_6F_5)_4$ was further added (**Scheme IV.66, C**; **Figure IV.32**). In these conditions, the *O*/*N*-isomer ratio is considerably decreased to reach 82:18 and even 70:30 after 16h, suggesting that in presence of sodium cation the *O*-isomer **4.6** is still the kinetic product but no longer the thermodynamic product. However, it is important to note that after 40h the *O*- **4.6** or *N*-isomers **4.6N** are no longer detected. The only observed product if the remaining $HNTf_2$ and a lot of signals suggesting a decomposition of the $B(C_6F_5)_4$ anion are observed. Therefore, the absence of *O*- **4.6** and *N*-isomers **4.6N** can come from a decomposition of the products as well as their precipitation. It seems then clear that the addition of sodium cation allows the formation of an equilibrium between the *O*- **4.6** and *N*-isomers **4.6N** which implies coordination/decoordination sequences of the triflimidate on the boron Lewis acidic center. This was confirmed by mixing the purified *O*-isomer **4.6** with $NaB(C_6F_5)_4$, showing a slow generation of the *N*-isomer **4.6N**. However, under these conditions, the generation seems slower than when the *N*-isomer **4.6N** is already present in the reaction medium. On the other hand, addition of $HNTf_2$ on the pure *O*-isomer **4.6** does not lead to formation of the *N*-isomer **4.6N**.

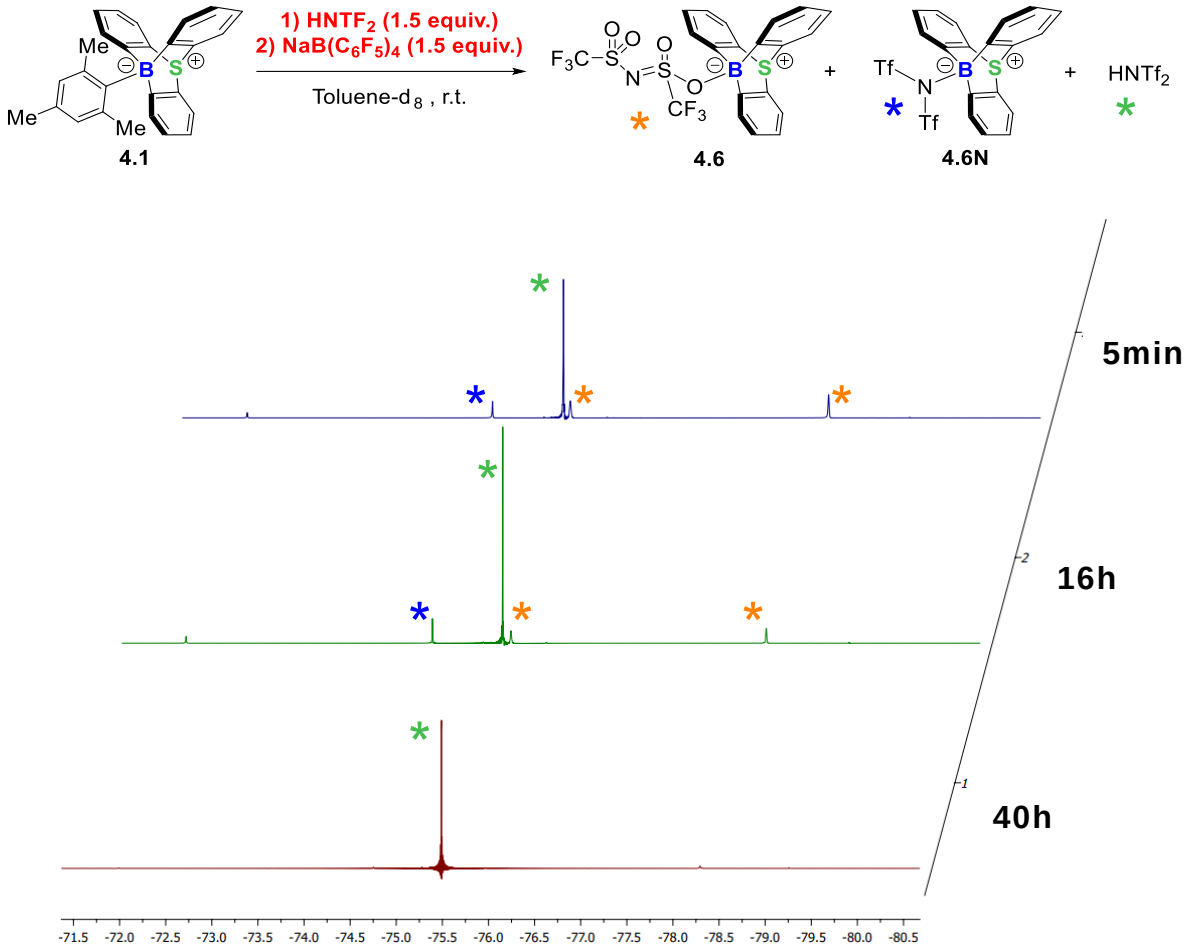
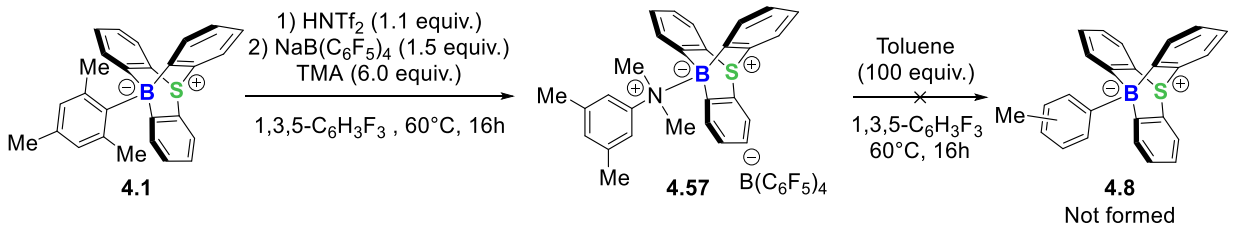


Figure IV.32 : Evolution of the crude resulting from the protodeborylation of 10-mesityl-9-sulfonium-10-boratriptycene-ate complex **4.1** with 1.5 equiv. of $HNTf_2$ and $NaB(C_6F_5)_4$ followed by ^{19}F NMR.

To conclude these first experiments, it was already demonstrated that the triflimidate-ate complex *O*-isomer **4.6** is the thermodynamic product and these experiments showed that the *N*-isomer **4.6N** slowly isomerizes into the *O*-isomer **4.6** even without sodium additive. It could then be hypothesized that the *N*-isomer **4.6N** plays a key role in the borylation reaction. Unfortunately, this product can only be reached *in-situ* and could never be isolated.

Several unexpected observations were then made, providing new insights on the reaction mechanism. First, while it was considered that TMA did not react with the 9-sulfonium-10-boratriptycene, the adduct **4.57** was isolated. We observed that, under the conditions employed to develop the borylation scope, if the substrate was too poorly reactive to be borylated, the major product formed was the Lewis adduct with TMA **4.57**. This was surprising, since borylation reactions of deactivated arene were performed using this Brønsted base, suggesting that the borylation reaction takes place before the formation of the adduct **4.57** or that the adduct **4.57** is reversible and can reform the active species. Considering the propensity of boron Lewis acids to bind Lewis bases, the first hypothesis is difficult to envision. We then decided to evaluate the reversibility of the adduct formation (**Scheme IV.67**). The borylation conditions were then reproduced without addition of reactive substrate. After 16h, toluene was added as substrate to the medium. In those conditions, the observation of the 10-tolyl-9-sulfonium-10-boratriptycene-ate complex **4.8** would mean that the TMA Lewis adduct **4.57** is reversible under the reaction conditions. On the other hand, absence of borylation product would mean that, when it takes place, the borylation takes place before forming the TMA Lewis adduct **4.57** which is irreversible under the reaction conditions.

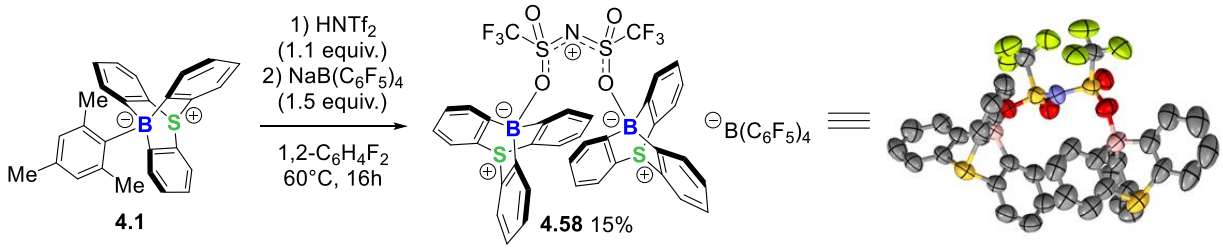


Scheme IV.67 : Evaluation of the reversible character of 10-(*N*,*N*,3,5-tetramethylaniline)-9-sulfonium-10-boratriptycene Lewis adduct (**4.57**).

This test reaction showed barely detectable borylation of toluene, suggesting that the TMA Lewis adduct **4.57** can not reform the reactive species under

these reaction conditions (**Scheme IV.67**). This observation remained difficult to understand since it suggests that the formation of a Lewis adduct, which should be almost instantaneous, is slower than the borylation of deactivated arenes such as 1,2-dichlorobenzene. This observation totally rules out the involvement of the uncomplexed 9-sulfonium-10-boratriptycene.

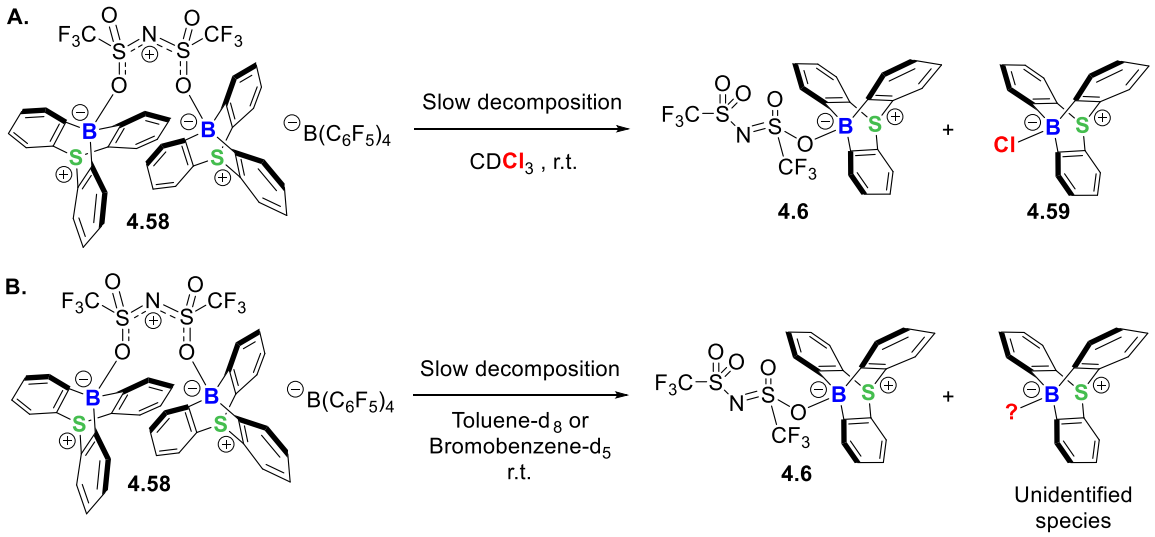
Fortuitously, while investigating the borylation reaction mechanism, we observed that without addition of a proton scavenger, the reaction led to the formation of a triflimidate bridged dimer **4.58**, with two 9-sulfonium-10-boratriptycene units linked to a single triflimidate ion (**Scheme IV.68, 4.58**). Since triflimidate ion is considered as a weakly coordinating anion (WCA), the formation of this dimer was totally unexpected. The relatively high chemical robustness of this compound was remarkable since it can be purified by flash chromatography undergoing only minimal decomposition. This product consists in the first boron equivalent of protonated triflimidic acid but this aspect will be discussed in a following chapter.



Scheme IV.68 : Synthesis of tetrakis(pentafluorophenyl)borate bis(10-trifluoromethylsulfonyl-9-sulfonium-10-boratriptycene)iminium **4.58** and X-ray structure with counteranion omitted for clarity.

This dimeric species provides crucial insights on the borylation process as the unanticipated formation of the 10-chloro- (**4.59**) and the 10-triflimidate-ate (**4.6**) complexes was observed after several hours in $CDCl_3$ (**Scheme IV.69, A**). After several hours in toluene-d_8 or bromobenzene-d_5 unidentified products are formed (**Scheme IV.69, B**) suggesting that this

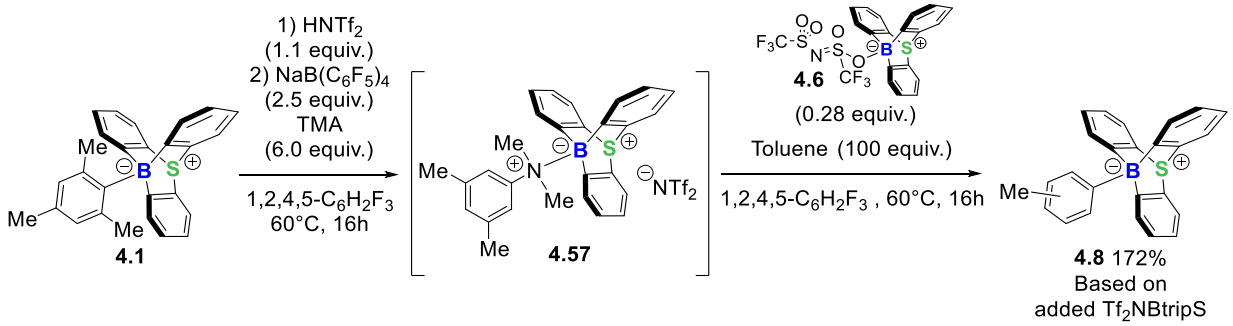
dimer could be displaced towards any Lewis adduct or "ate"-complex without requiring any internal or external stimuli. It was then hypothesized that this dimer could be the reactive species performing the borylation reaction or at least a reservoir of reactive Lewis acid.



Scheme IV.69 : Reactivity of bis(10-trifluoromethylsulfonyl-9-sulfonium-10-boratriptycene)iminium ion towards haloalkanes and aromatic solvents.

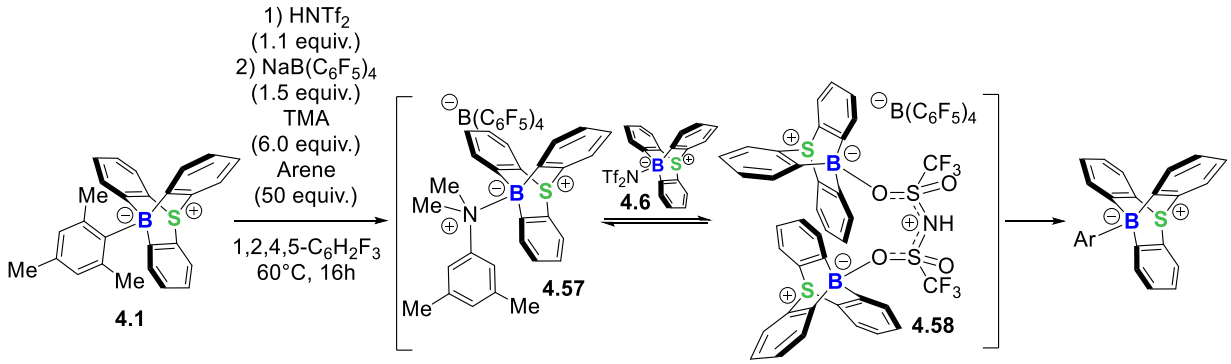
Though the TMA adduct **4.57** is not able to perform the borylation and was so far considered irreversible, this adduct could be in equilibrium with the triflimidate-bridged dimer **4.58**. It was hypothesized that the triflimidate ion plays a key role in the mechanism and the only reason why the TMA adduct **4.57** was so far considered irreversible is due to the absence of remaining triflimidate ion in the medium. Indeed, $NaB(C_6F_5)_4$ is used to reduce the energy of the triflimidate-boron bond and help triflimidate to dissociate from the boron but also causes the precipitation of $NaNTf_2$ which is much less soluble than $NaB(C_6F_5)_4$ in aromatic solvents. Therefore, in absence of triflimidate ion in the medium to reform the triflimidate-bridged dimer **4.58** or the triflimidate-ate complex **4.6**, the formation of TMA Lewis adduct **4.57** is a dead end. In order to evaluate this hypothesis, we decided to redo the previously presented control experiment but this time, a small amount of

triflimidate-ate complex **4.6** was added concomitantly with toluene (**Scheme IV.70**).



Scheme IV.70 : Evaluation of the reversible character of 10-(*N*,*N*,3,5-tetramethylaniline)-9-sulfonium-10-boratriptycene Lewis adduct **4.57** upon addition of additional 10-triflimidate-9-sulfonium-10-boratriptycene-ate complex **4.6**.

Against all odds, 10-tolyl-9-sulfonium-10-boratriptycene-ate complex **4.8** was obtained with 172% yield with respect to the additionally added triflimidate-ate complex **4.6** (**Scheme IV.70**). This totally precludes the formation of borylation product only from the additional triflimidate-ate complex **4.6** and implies that a non-negligible fraction of the TMA Lewis adduct **4.57** was converted into the triflimidate-bridged dimer **4.58**, allowing borylation of toluene (**Scheme IV.71**). However, this may reasonably be hypothesized that the borylation is concomitant to the formation of the adduct, the two reactions proceeding in parallel.



Scheme IV.71 : Illustration of the equilibrium between 10-(*N*,*N*,3,5-tetramethylaniline)-9-sulfonium-10-boratriptycene Lewis adduct **4.57** and bis(10-trifluoromethylsulfonyl-9-sulfonium-10-boratriptycene)iminium **4.58**.

This last experiment concludes the experimental mechanistic investigations about borylation reactions with the 9-sulfonium-10-boratriptycene. These experiments showed that the donor-free Lewis acid is probably not present in the reaction medium, only complexed forms of the Lewis acid in equilibrium with one another are present. Some of these complexed forms are able to undergo borylations and some are not. It was showed that TMA used as proton scavenger was able to form a Lewis adduct with the Lewis acid and that this Lewis adduct **4.57** was only reversible in presence of triflimidate-ate complex **4.6**. The triflimidate ion plays a key role in the reaction since it makes the TMA Lewis adduct **4.57** reversible and allows the formation of a triflimidate-bridged dimer **4.58** which could be the active species in the borylation mechanism.

IV.5.2 Quantum chemical investigation

In order to complete the experimental investigation of the electrophilic borylation mechanism, quantum chemical investigations were performed by Dr. Aurélien Chardon in collaboration with Prof. Dr. Raphaël Robiette from the Université Catholique de Louvain (UCL). This DFT analysis was performed at M062X/6-311G(d) level of theory (**Figure IV.33**). First of all, this investigation confirmed the hypothesis that the TMA Lewis adduct can be in equilibrium with the triflimidate-bridged dimer. However, it was demonstrated that the addition of $NaB(C_6F_5)_4$ over the triflimidate-ate complex (**I**) led to the formation of a complex (**II**) which is 80 $kJ.mol^{-1}$ more stable than the starting triflimidate-ate complex. Considering these calculations, generating the "ate"-complex (**III**) between the 9-suflonium-10-boratriptycene and the $B(C_6F_5)_4$ anion from the $[NaB(C_6F_5)_4{\cdot}Tf_2NBtripS]$ complex (**II**) requires 131 $kJ.mol^{-1}$ instead of 51 $kJ.mol^{-1}$ starting from the triflimidate-ate complex (**I**). The "ate"-complex (**III**) between the 9-suflonium-10-boratriptycene and the $B(C_6F_5)_4$ anion can be considered as the closest form from the free 9-sulfonium-10-boratritpcyene. This result suggests that it would be easier to generate the free Lewis acid without addition of $NaB(C_6F_5)_4$. Despite these energy values are inconsistent with the experimental results, it must be noted that the DFT calculations do not consider the insolubility of $NaNTf_2$ in the reaction medium, which appeared to be the driving force of the borylation reaction. Then, the DFT analysis showed that, from the 10-tetrakis(pentafluorophenyl)borate-9-sulfonium-10-boratriptycene-ate complex (**III**) (51 $kJ.mol^{-1}$), a more stable π-complex (**V**) (46 $kJ.mol^{-1}$) can be formed with benzene, via a σ-complex (**IV**) transition state (68 $kJ.mol^{-1}$). Regarding the very small gap between these σ- (**IV**) and π-complex (**V**) with benzene, it can be considered that these species are in equilibrium with one another. Surprisingly, the DFT analysis showed that the rate determining step of the borylation reaction is the

deprotonation of the Wheland intermediate (**VI**) by TMA (TS=112.8 kJ.mol^{-1}) to form the final phenyl-ate complex (**VII**). This contradicts the absence of primary KIE observed with TMA, since the absence of KIE indicates that the C–H bond is not broken during the rate determining step. However, it must be noted that, during the experiments, TMA was used in large excess which increases the deprotonation rate. However, the value obtained by DFT calculation explains the need of several equivalents of TMA and the almost complete absence of reactivity observed with a single equivalent of TMA. Considering the DFT analysis and the reaction conditions, it can be considered that the borylation reaction proceeds by the replacement of the triflimidate ion, which precipitate under the form of $NaNTf_2$, by benzene which forms a σ- (**IV**) or π-complex (**V**) to stabilize the highly electrophilic boron species. Once this σ- (**IV**) or π-complex (**V**) formed and in equilibrium with one another, the irreversible deprotonation with TMA present in large excess leads to the formation of the phenyl-ate complex (**VII**) as final product.

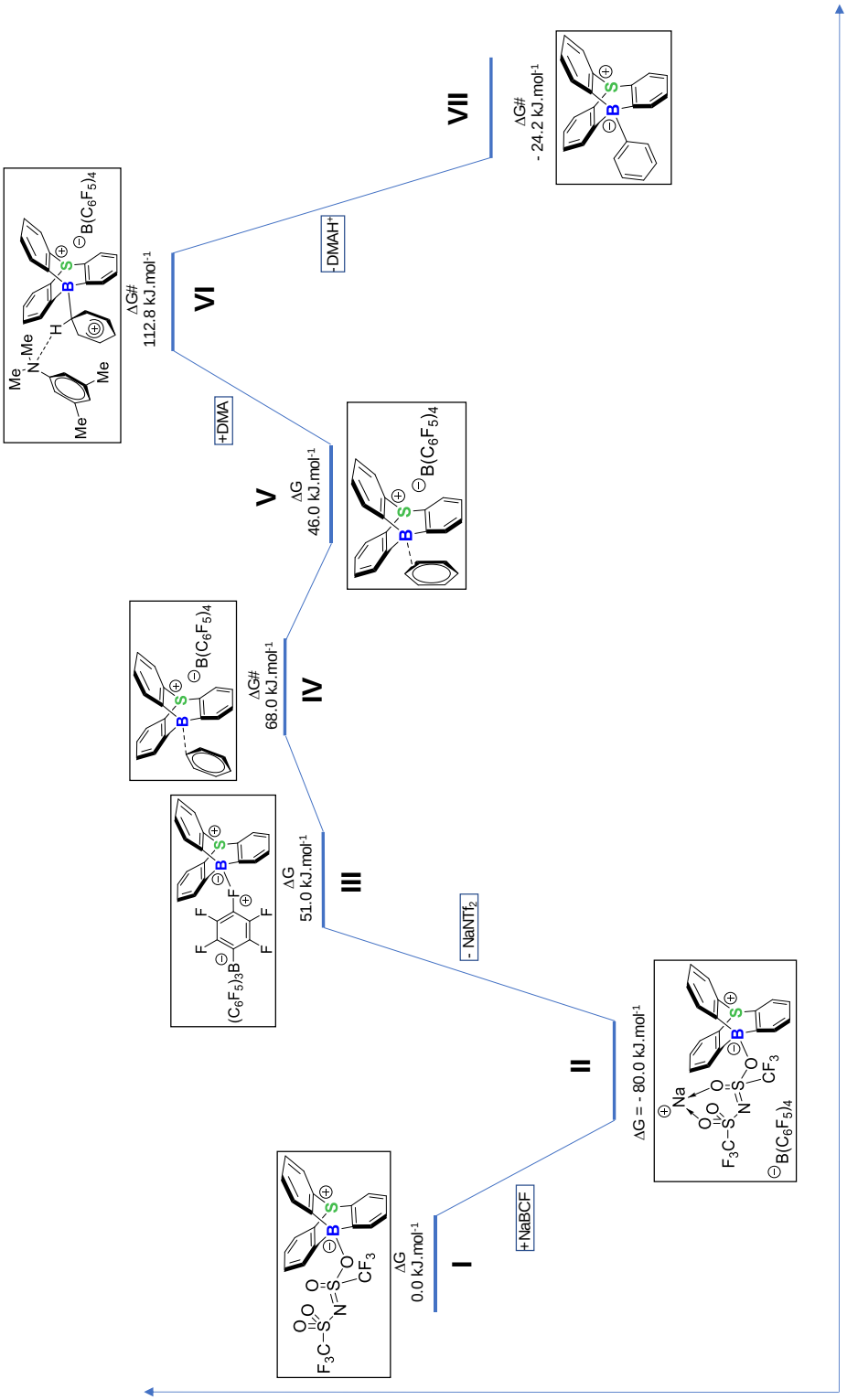
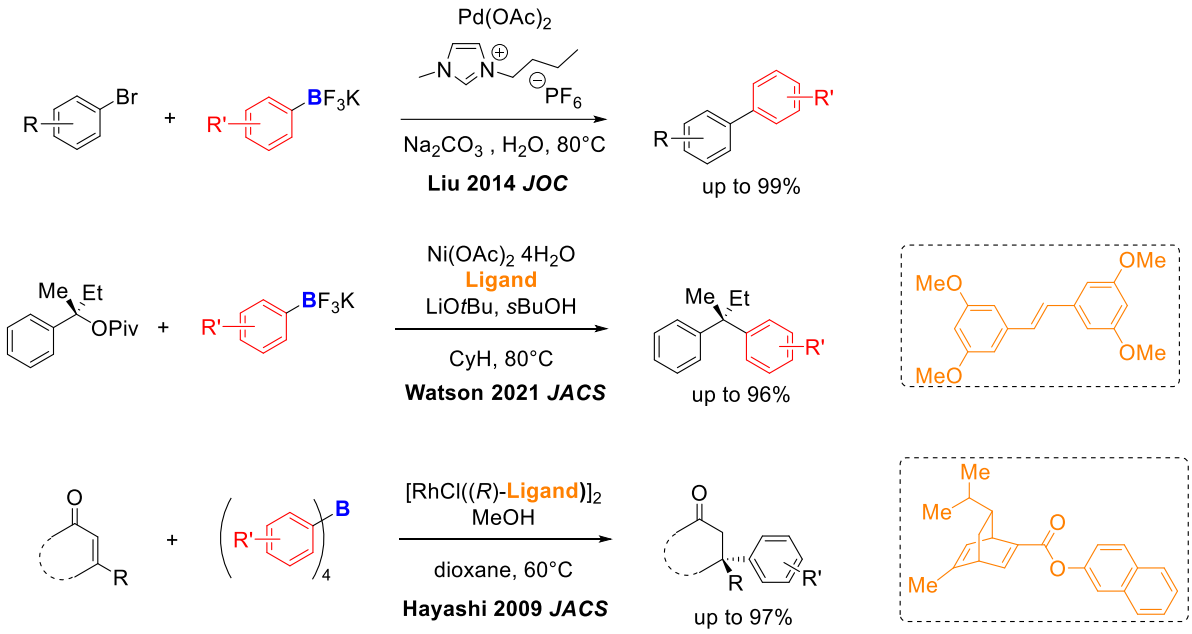


Figure IV.33 : Energy diagram of Csp^2–H borylation using the combination of 10-triflimidate-9-sulfonium-10-boratriptycene-ate complex **4.6**, $NaB(C_6F_5)_4$ and TMA.

IV.6. Aromatic Csp²-B functionalization

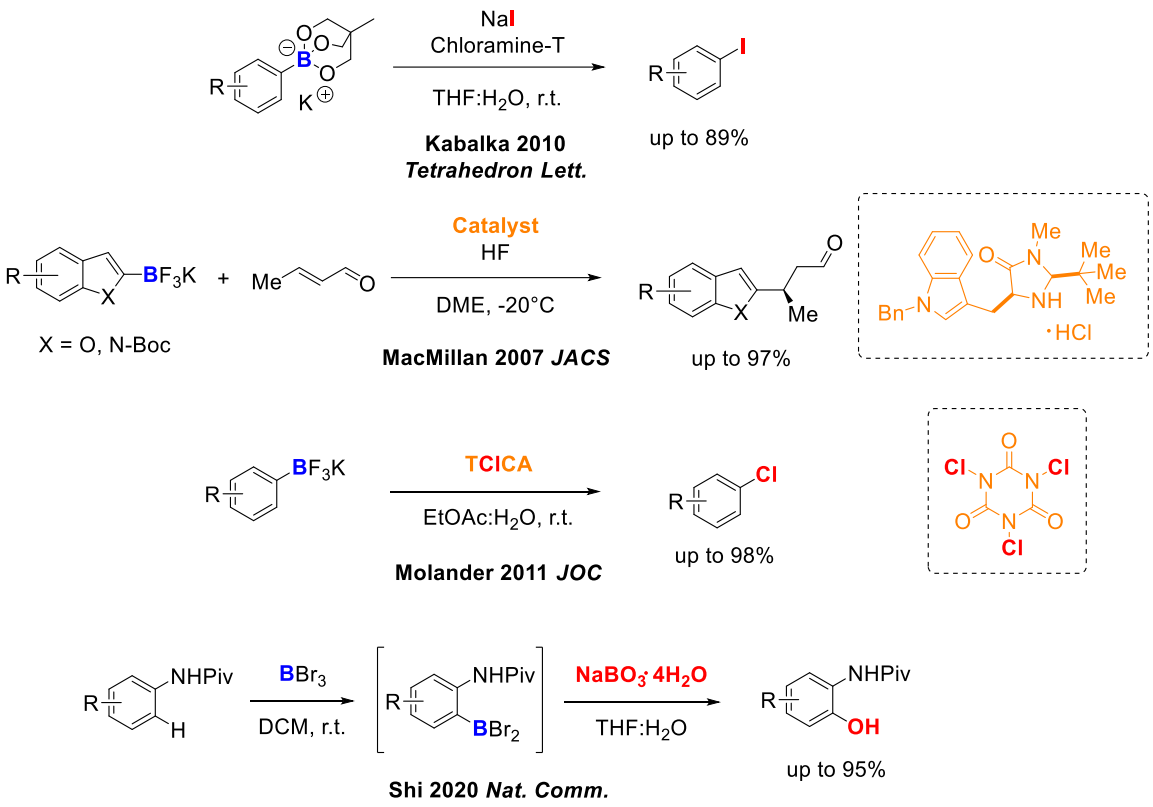
The Suzuki-Miyaura coupling reaction stands as a major and already one of the most important synthetic transformations developed in the last 50 years. This reaction allowing the formation of C–C bonds from C–B and C–X bonds, the demand of organoboron compounds skyrocketed.[2,5] The Suzuki-Miyaura cross-coupling and other transition metal mediated reactions are by far the most widely used methods for the functionalization of C–B bonds. Initially developed with boronic acids, loads of improvements have been made allowing the use of boronic esters, MIDA boronates or even trifluoroborate salts (**Scheme IV.72**).[83–88]



Scheme IV.72 : Selected examples of Suzuki-Miyaura type reactions using various arylborate salts.

However, the polarity of the $C^{\delta-}–B^{\delta+}$ bond and the propensity of aromatic organoboron to deborylate in presence of electrophiles have been used for the development of metal-free C–B bond and especially Csp²–B bonds functionalization (**Scheme IV.73**).[89–93] Indeed, as presented in a previous section, it has been demonstrated that the nucleophilicity of aromatic organoborate is increased up to 10^{13} compared to trivalent aromatic

organoboron species.[57] Following this statement, aromatic trifluoroborates, boronates, tetraarylborate or triarylhaloborate have been used as directing group for the *ipso*- or *ortho*-functionalization of Csp^2–B bonds (**Scheme IV.73**). Among the most important transition-metal-free reactions are the Petasis reaction, halogenation, electrophilic borylation and 1,2-migration reactions.

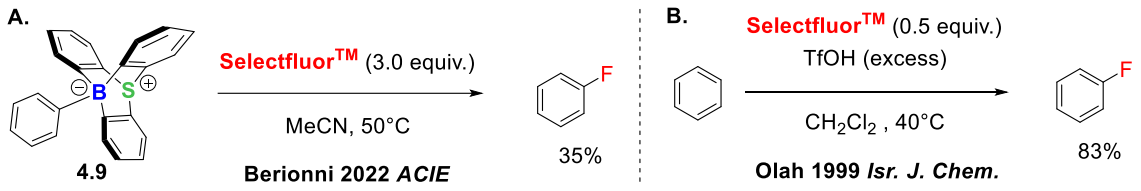


Scheme IV.73 : Selected examples of transition-metal-free regioselective functionalization of arylborates salts.

IV.6.1 *Ipso*-Csp^2–B halogenation

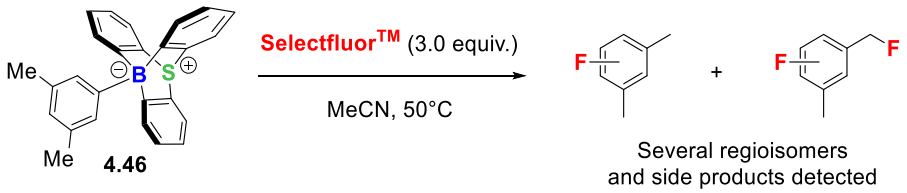
Based on the statement that, in tetrarylborates, the nucleophilicity of aromatic rings is increased compared to equivalent unsubstituted arenes, we decided to attempt functionalizing the 10-aryl-9-sulfonium-10-boratriptycene-ate complexes with electrophiles. We already demonstrated that treating 10-phenyl-9-sulfonium-10-boratriptycene-ate complex **4.9** with

Selectfluor® led to the formation of fluorobenzene with a decent yield of 35% (**Scheme IV.74, A**).[94] This Csp^2–B bond functionalization seemed promising since Selectfluor® does not fluorinate benzene unless it is mixed with triflic acid (**Scheme IV.74, B**).[95]



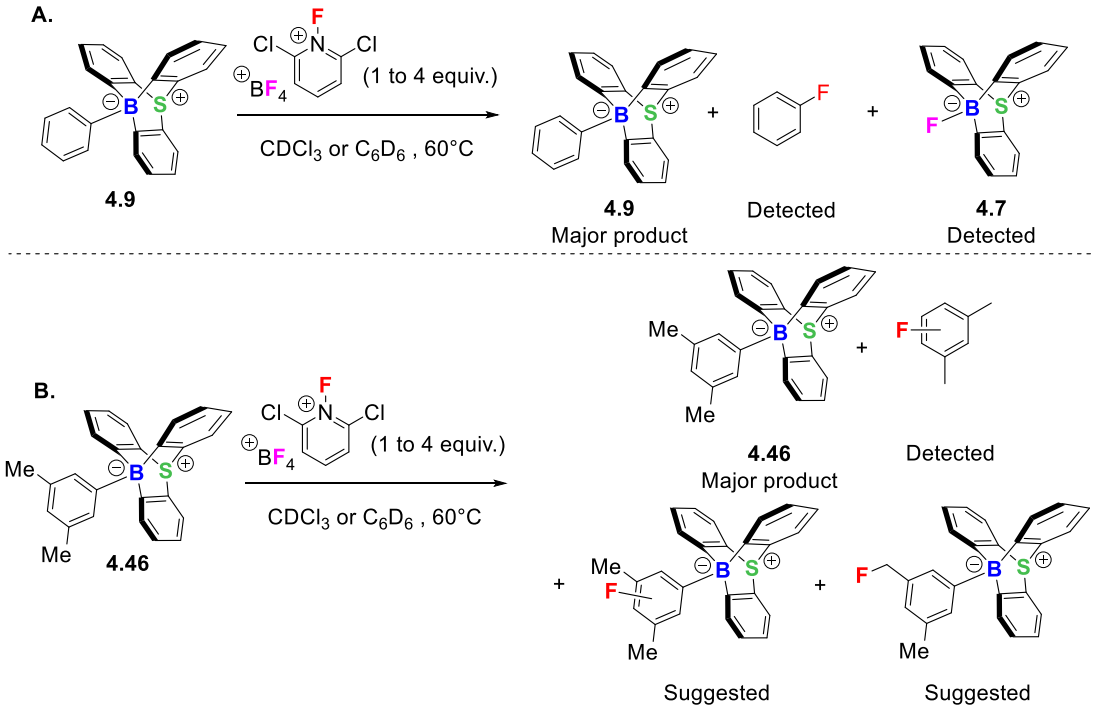
Scheme IV.74 : **A.** Synthesis of fluorobenzene by treatment of 10-phenyl-9-sulfonium-10-boratriptycene-ate complex **3.9** with Selectfluor™, **B.** Monofluorination of benzene using Selectfluor™ and triflic acid.

We then selected 10-(3,5-dimethylphenyl)-9-sulfonium-10-boratriptycene-ate complex **4.46** as model substrate since it would allow an easy evaluation of the fluorination regioselectivity. 10-Mesityl-9-sulfonium-10-boratriptycene-ate complex **4.1** was also used as model substrate for some reactions to qualitatively evaluate the conversion of the starting material by ^{19}F NMR. While the reaction with the phenyl-ate complex **4.9** provided clean ^{19}F NMR spectrum, the reaction with the 3,5-dimethylphenyl-ate complex **4.46** provided a totally messy ^{19}F NMR spectrum with several signals between –110 and –120ppm which is the typical range for monofluorinated benzene derivatives (**Scheme IV.75**).[94,95] This apparently unselective reaction implies the formation of a mixture of several fluorinated arenes, demonstrating that the reaction is not regioselective nor chemoselective.



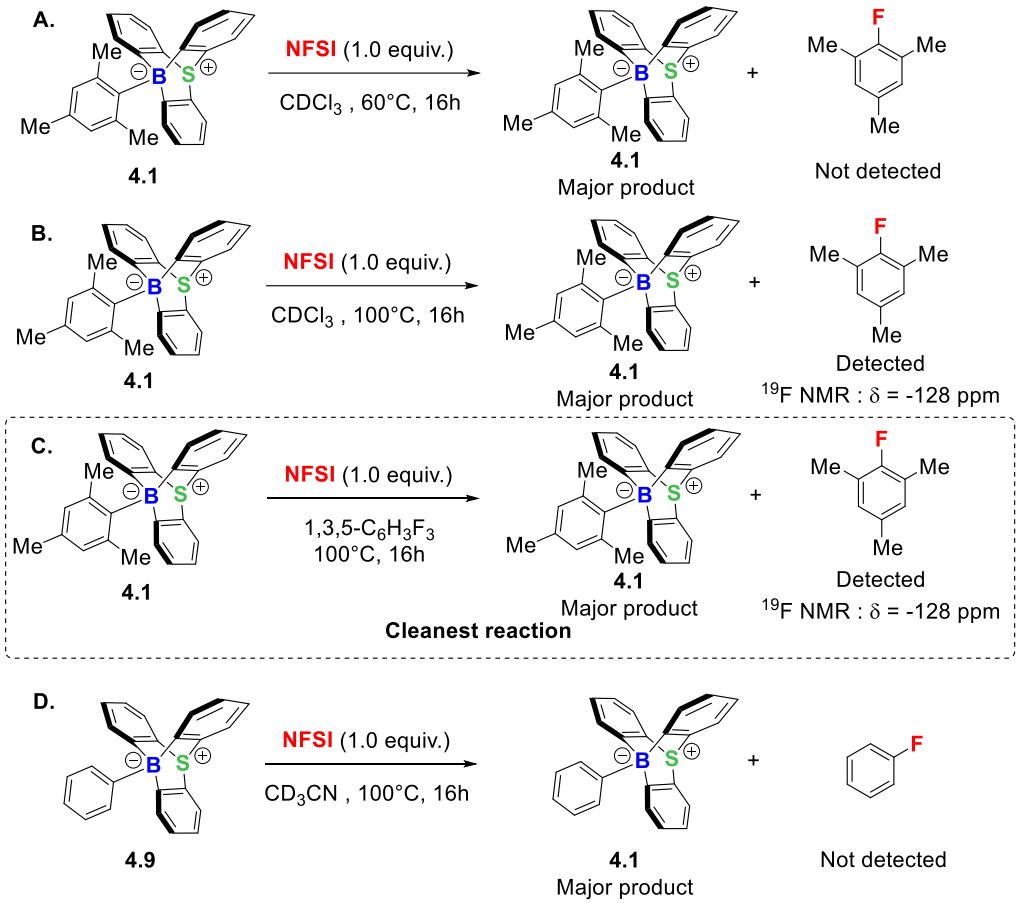
Scheme IV.75 : Unselective fluorination of 10-(3,5-dimethylphenyl)-9-sulfonium-10-boratriptycene-ate complex **4.46** with Selectfluor™.

Considering that Selectfluor® is a powerful oxidant and is very prone to single electron transfer (SET) at high temperature, we hypothesized that radical side reactions may take place under these conditions and lead to the formation of a wide variety of Csp^2–F and Csp^3–F bonds containing species.[96–98] We then evaluated other electrophilic fluorinating reagents. *N*-Fluoropyridinium salts were then used and especially *N*-fluoro-2,6-dichloropyridinium tetrafluoroborate. The fluorination reaction was attempted using 10-phenyl- **4.9** and 10-(3,5-dimethylphenyl)-9-sulfonium-10-boratriptycene-ate **4.46** complexes revealing in both cases a very low conversion (**Scheme IV.76, A, B**). The ^{19}F NMR spectra were relatively clean however, in the case of 3,5-dimethylphenyl-ate complex **4.46**, several additional signals were detected in ^{11}B NMR suggesting the formation of byproducts without undergoing the deborylation (**Scheme IV.76, B**). This again suggests a complete absence of regioselectivity, and these products were observed even under light exclusion conditions.



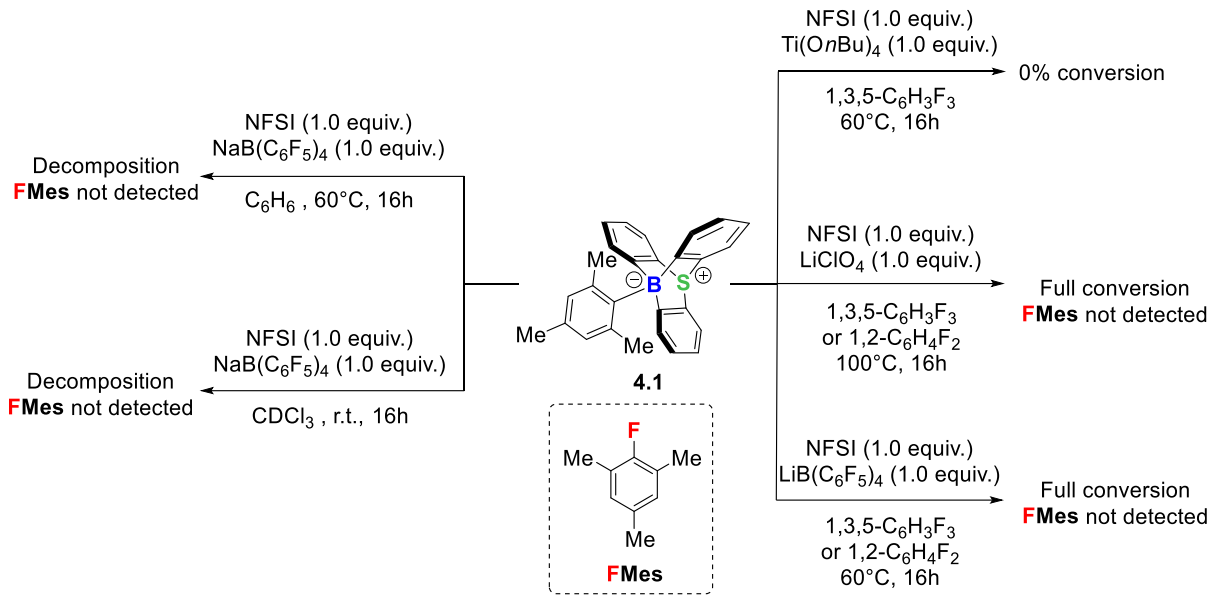
Scheme IV.76 : Attempted regioselective fluorodeborylation of 10-phenyl- **4.9** and 10-(3,5-dimethylphenyl)-9-sulfonium-10-boratriptycene-ate **4.46** complexes with *N*-fluoro-2,6-dichloropyridinium tetrafluoroborate.

Considering the undesired reactivity, *N*-fluoropyridinium salts were put aside and attention was devoted to cheaper *N*-fluorobenzenesulfonimide (NFSI) (**Scheme IV.77**).[97,98] A first fluorination test was attempted by mixing 1.0 equiv. of NFSI with the mesityl-ate complex **4.1** in $CDCl_3$ at 60°C (**Scheme IV.77, A**). At first sight, the crude was promising since it provided clean ^{11}B and ^{19}F NMR. However, the major product observed by ^{19}F NMR shows a chemical shift at –136.3 ppm while fluoromesitylene has a reported chemical shift of –128.0 ppm, using $CFCl_3$ as reference.[95] The reaction temperature was then increased to 100°C leading to the formation of a compound that could correspond to fluoromesitylene but still with a low conversion (**Scheme IV.77, B**). The reaction time was then increased from 16h to 72h leading to the appearance of several signals in ^{19}F NMR with still apparent low conversion according to ^{11}B NMR. Several solvents were then tested in similar conditions, all leading to relatively clean reactions with a small amount of fluoromesitylene likely formed but with very low conversions. Interestingly, the reaction using 1,3,5-trifluorobenzene provided the cleanest results despite a very low conversion (**Scheme IV.77, C**). Unfortunately, while performing a reaction with the 10-phenyl-9-sulfonium-10-boratriptycene-ate complex (**4.9**) no trace of fluorobenzene was observed (**Scheme IV.77, D**).



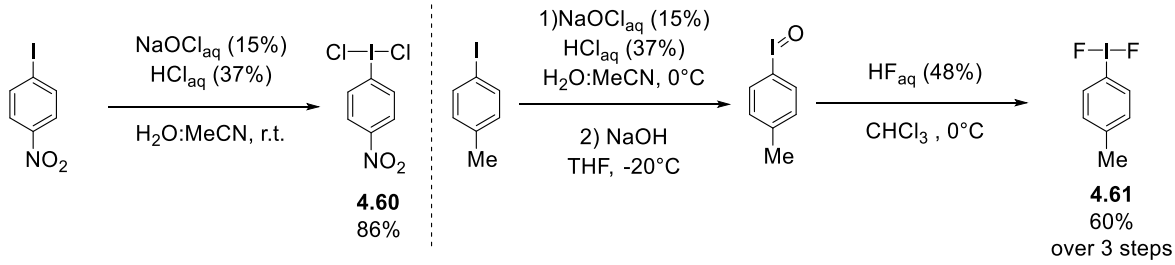
Scheme IV.77 : Attempted regioselective fluorodeborylation of 10-mesityl- **4.1** and 10-phenyl-9-sulfonium-10-boratriptycene-ate complexes **4.9** with NFSI.

Considering the very low conversions for all attempted reactions with NFSI, Lewis acidic additive were added to increase its electrophilicity.[99–101] Altough several types of Lewis acids have been used, no real improvement has been observed. In some cases, the addition of a Lewis acid showed no evident effect on the reaction while in some other cases, this led to complete decomposition of the starting material without formation of the desired fluorination product (**Scheme IV.78**).

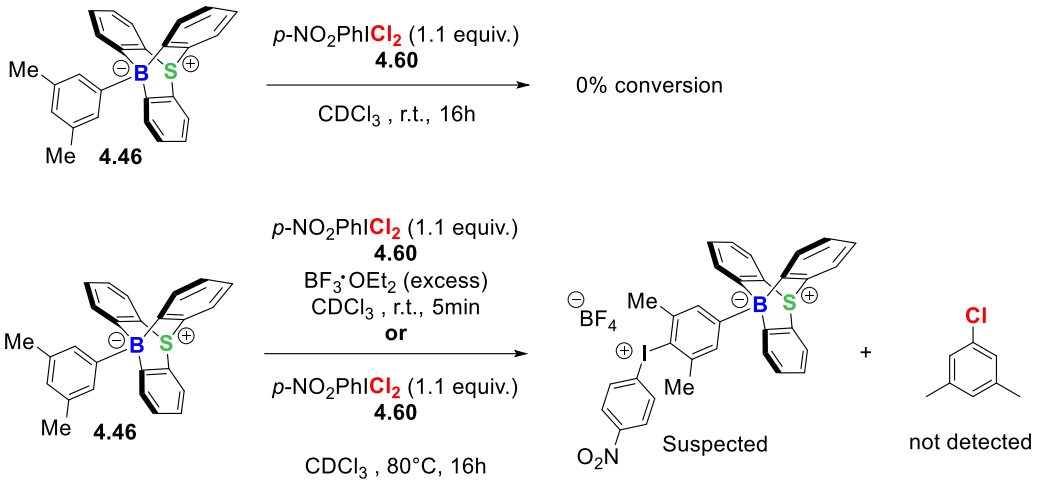


Scheme IV.78 : Attempted regioselective fluorodeborylation of 10-mesityl-9-sulfonium-10-boratriptycene-ate complex (**4.1**) with NFSI and various Lewis acids as NFSI activators

Next, hypervalent iodine reagents were succinctly evaluated with dichloro(aryl)- and difluoro(aryl)-λ^3-iodanes as chlorinating and fluorinating agents respectively. For this purpose, dichloro(*p*-nitrophenyl)- **4.60** and difluoro(*p*-tolyl)-λ^3-iodane **4.61** were prepared and tested on aryl-boron-ate complexes (**Scheme IV.79**).[102–107]

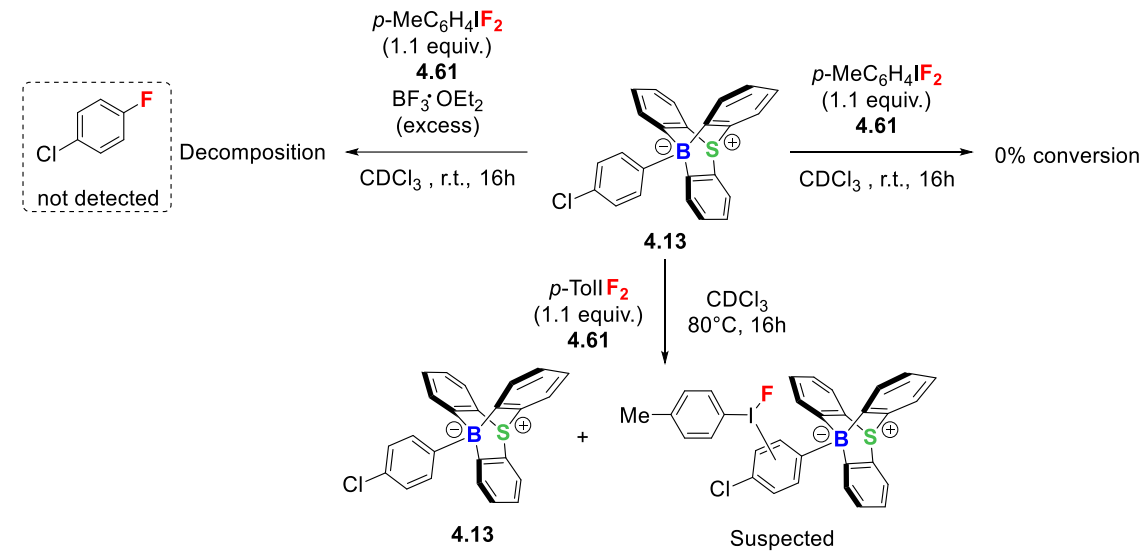


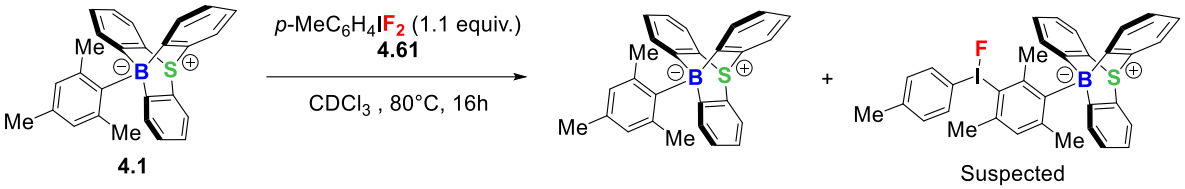
Scheme IV.79 : Synthesis of **A.** dichloro(4-nitrophenyl)-λ^3-iodane **4.60** and **B.** difluoro(*p*-tolyl)-λ^3-iodane **4.61**.



Scheme IV.80 : Attempted regioselective chlorodeborylation of 10-(3,5-dimethylphenyl)-9-sulfonium-10-boratriptycene-ate complexe **4.46** using dichloro(4-nitrophenyl)-λ^3-iodane **4.60**.

Using dichloro(aryl)-λ^3-iodane, the desired 3,5-dimethylchlorobenzene could not be detected and the crude ^{11}B NMR showed the formation of side products suggesting that the starting "ate"-complex **4.46** was functionalized without breaking the C–B bond (**Scheme IV.80**). Regarding the lack of selectivity observed with the 3,5-dimethylphenyl-ate complex, the fluorination reactions using *p*-tolylIF$_2$ were attempted with the chlorophenyl-ate complex, hypothesizing that the inductive attractive effect of chlorine would reduce the nucleophilicity of the aromatic ring and direct the reaction on *ipso*-position to the C–B bond (**Scheme IV.81**).

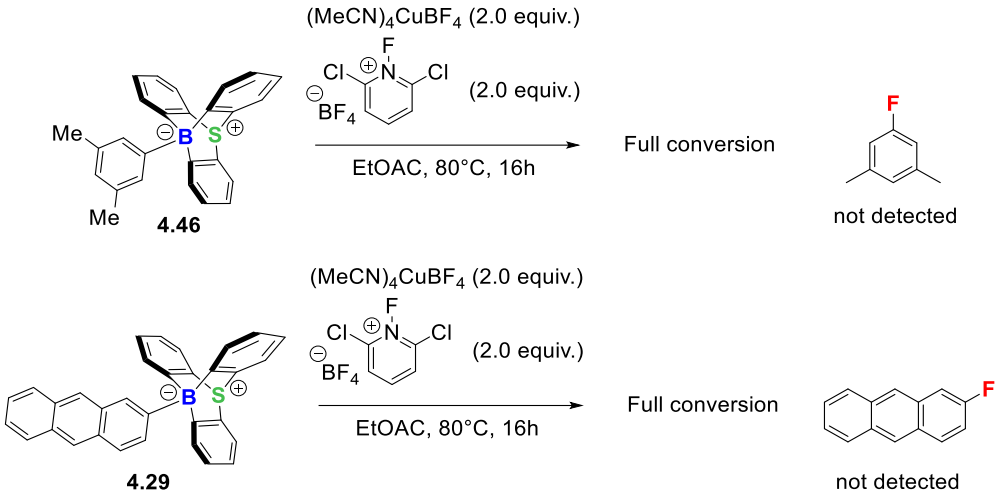




Scheme IV.81 : Attempted regioselective fluorodeborylation of 10-(4-chlorophenyl)- **4.13** and 10-mesityl-9-sulfonium-10-boratriptycene-ate complexes **4.1** using difluoro(*p*-tolyl)-λ^3-iodane **4.61**.

Unfortunately, similar results were obtained with dichloro- and difluoro(aryl)-λ^3-iodanes, showing no trace of desired chlorinated or fluorinated arene as well as a complete lack of reactivity observed on C–B bond *ipso*-position (**Scheme IV.81**).

Since in the few cases where fluorination was observed, the desired product was only detected by ^{19}F NMR with less than 10% yield, this fluorination project was put aside. Based on the fluorination methodology described by Sanford and co-workers, two more attempts were made using an electrophilic copper reagent as catalyst (**Scheme IV.82**).[108] To maximize the chances of success, the copper catalyst was used in stoichiometric amount. However, the desired fluorinated product was never detected.

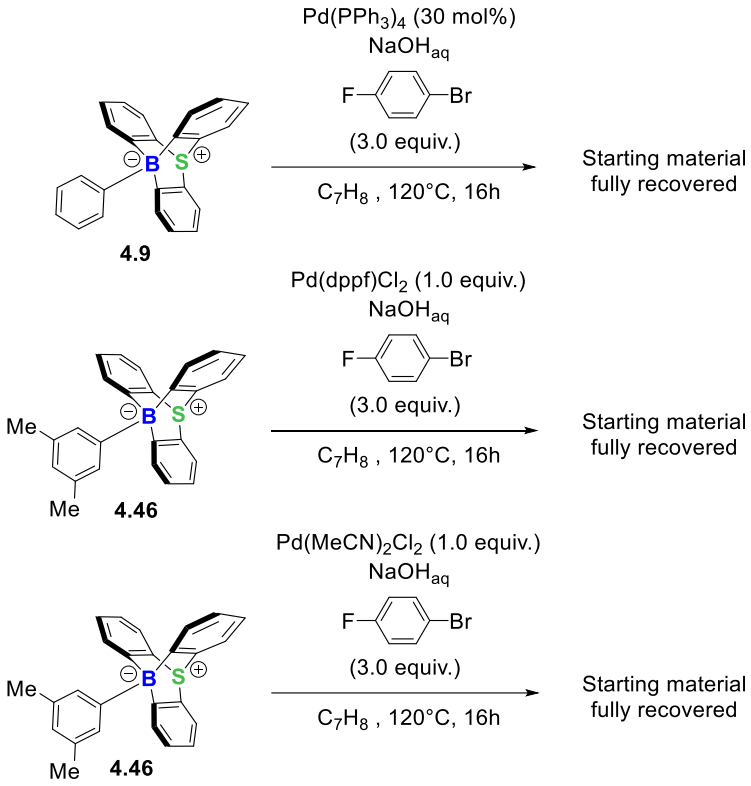


Scheme IV.82 : Attempted copper catalyzed regioselective fluorination of 10-aryl-9-sulfonium-10-boratriptycene-ate complexes

IV.6.2 Suzuki-Miyaura cross coupling

It was then attempted to transfer the exocyclic aryl substituent from our aryl-boron-ate complexes via Suzuki-Miyaura coupling. However, against all odds, even under harsh conditions the starting material was fully recovered. At first sight, this absence of reactivity was surprising since tetra aryl-borates are reactive substrates for Suzuki-Miyaura cross-coupling reactions (**Scheme IV.83**). However, we reasoned that, in our aryl-ate complexes, the C–B *ipso*-position is extremely hindered which might prevent the transmetallation step. Furthermore, it has already been demonstrated that, in classical conditions, hydroxy substituents on the aryl boronic acid or on the *in-situ* formed aryl-boronates play an important role by coordinating the palladium and assisting the transmetallation step. However, in our case the formation of a complex between the boron and the palladium species is impossible since it would imply the breaking of one of the four C–B bonds. It is also important to note that aryl-boron-ate complexes used for Suzuki-Miyaura can be *in-situ* hydrolyzed to form aryl-boronic acid derivatives. In

our, case the triptycene scaffold does not undergo hydrolysis or protodeborylation under basic conditions or even under aqueous acidic conditions. Considering these features, it can be rationalized that our 10-aryl-9-sulfonium-10-boratriptycene-ate complexes do not undergo Suzuki-Miyaura cross-coupling.

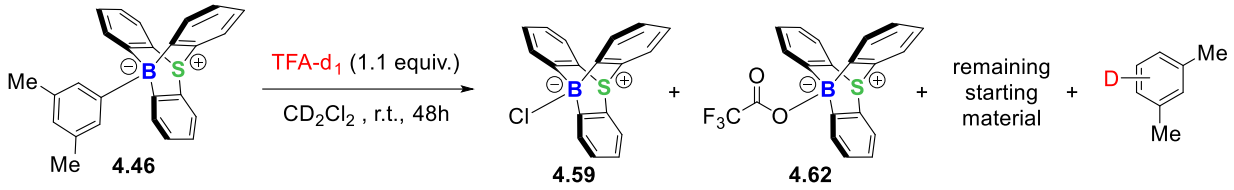


Scheme IV.83 : Attempted aryl transfer from 10-aryl-9-sulfonium-10-boratriptycene-ate complex via Suzuki-Miyaura coupling reactions.

IV.6.3 *Ipso*-Csp²-B deuteration

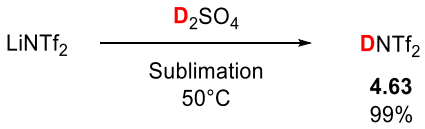
So far, only protodeborylation reactions using strong Brønsted acids provided clean heterolytic cleavage of the exocyclic C–B bond while releasing the corresponding arene. Considering these facts, the idea came in mind that, using deuterated Brønsted acids, it would be possible to regioselectively deuterate the *ipso*-C–B position via deuterodeborylation. For preliminary experiments, it was decided to treat the 10-(3,5-dimethylphenyl)-9-sulfonium-10-boratriptycene-ate complex **4.46** with

commercially available trifluoroacetic acid-d_1 to evaluate the selectivity of the protodeborylation reaction (**Scheme IV.84**). Unfortunately, the reaction turned out to be unexpectedly slow regardless of the solvent used. Furthermore, the ^{1}H NMR spectra were difficult to analyzed since a wide variety of side products involving the 9-sulfonium-10-boratriptycene moiety were present.



Scheme IV.84 : Attempted regioselective deuterodeborylation with TFA-d_1.

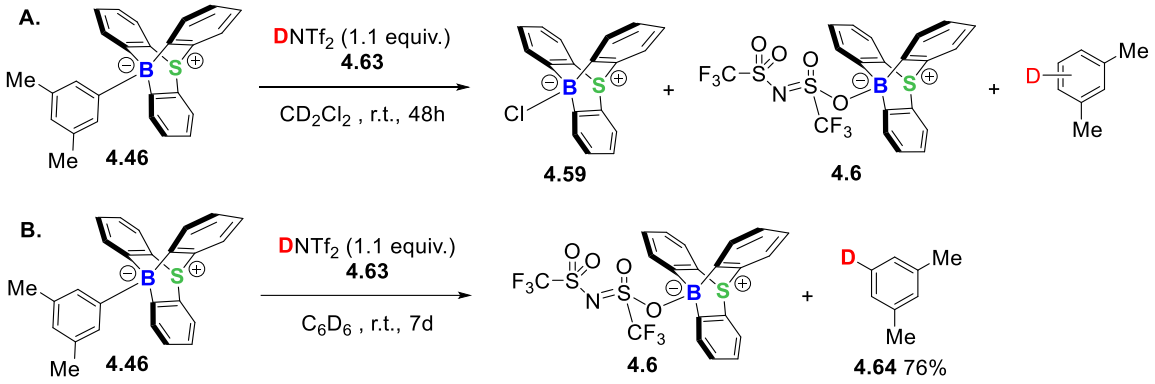
These disappointing results prompted us to switch from trifluoroacetic acid-d_1 to stronger Brønsted acids to speed up the reaction. We also reasoned that, the stronger the acid, the faster the reaction and probably the better the regioselectivity will be since the most nucleophilic site should be in *ispo*-position to the C–B bond. Since protodeborylation with triflimidic acid led to fast and clean reactions, it was decided to synthesize triflimidic acid-d_1 **4.63**. This could conveniently and quantitatively be obtained by sublimation of a mixture of lithium or sodium triflimidate and D_2SO_4 (**Scheme IV.85**).



Scheme IV.85 : Synthesis of triflimidic acid-d_1.

The deuterodeborylation was then attempted, treating the 10-(3,5-dimethylphenyl)-9-sulfonium-10-boratriptycene-ate complex **4.46** with $DNTf_2$ **4.63** in CD_2Cl_2 (**Scheme IV.86, A**). The reaction led to a fast and clean deborylation however, due to the formation of the 10-chloride- **4.59**

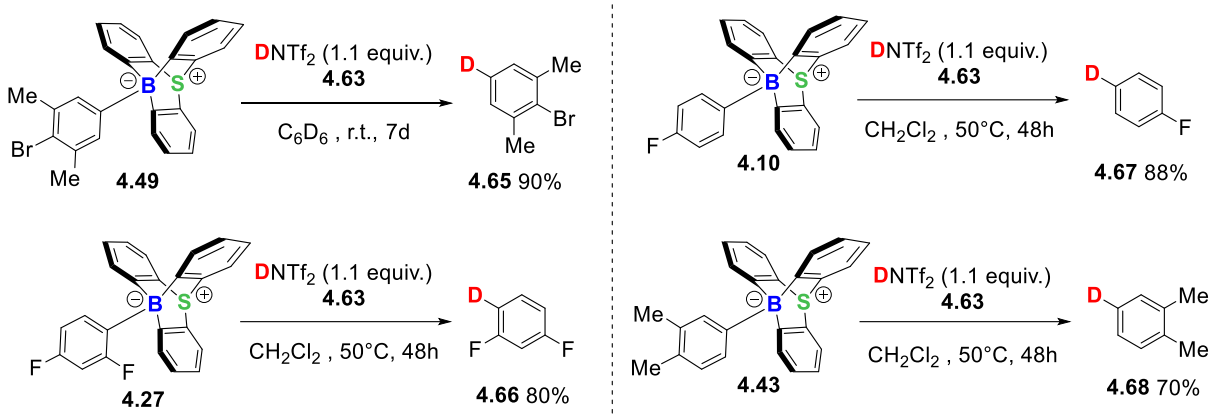
and 10-triflimidate-9-sulfonium-10-boratriptycene-ate **4.6** complexes, the ^{1}H NMR aromatic region was crowded and signals resulting from monodeuterated 1,3-dimethylbenzene were difficult to identify. Therefore, the selectivity and deuteration yield could not be unambiguously determined. The reaction was then performed in benzene-d_6 as solvent (**Scheme IV.86, B**). These conditions led to clean deuterodeborylation with only the 10-triflimidate-9-sulfonium-10-boratriptycene-ate complex **4.6** formed, drastically reducing the number of signals in the ^{1}H NMR aromatic region. However, the reaction turned out to be extremely slow, requiring one week at room temperature to reach completion. Using the signals of the 9-sulfonium-10-boratriptycene scaffold as internal standard, the formation of 1,3-dimethyl-5-deuterobenzene **4.64** could be unambiguously characterized with 76% yield.



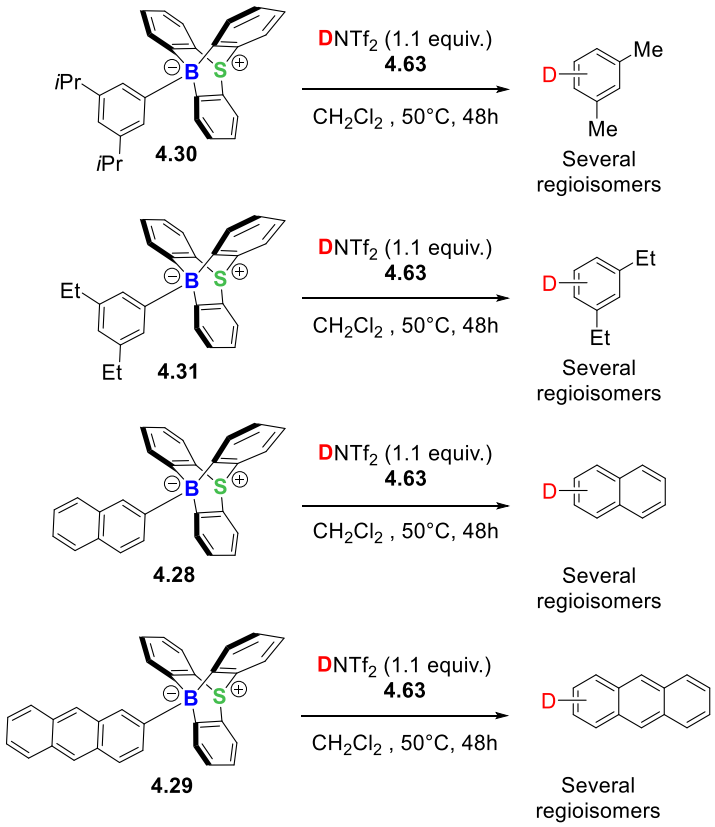
Scheme IV.86 : Optimization and achieved regioselective monodeuteration of 1,3-dimethylbenzene via deuterodeborylation of 10-(3,5-dimethylphenyl)-9-sulfonium-10-boratriptycene-ate complex **4.46**.

Another substrate could then be regioselectively monodeuterated following this strategy, 2,6-dimethyl-1-bromobenzene, affording 2,6-dimethyl-1-bromo-4-deuterobenzene **4.65** (**Scheme IV.87**). However, with other polyaromatic or alkyl-substituted substrates, a site selective deuteration could not be demonstrated via ^{1}H NMR. The reactions were then performed again in non-deuterated solvents and the crude was analyzed by ^{2}D NMR revealing a complete absence of selectivity with polyaromatic and alkyl-

substituted substrates (**Scheme IV.88**). However, with halogen-substituted substrates a clean deuterodeborylation was observed showing a single signal in the ^{2}D NMR aromatic region (**Scheme IV.87**).



Scheme IV.87 : Examples of regioselective monodeuteration of aromatic substrate via deuterodeborylation of 10-aryl-9-sulfonium-10-boratriptycene-ate complexes. Yields determined using aromatic signals of the triptycene scaffold or acetonitrile-d_3 as internal standard.



Scheme IV.88 : Attempted unselective monodeuteration of aromatic substrates.

So far, the regioselective monodeuteration of five aromatic substrates could be achieved with good yields. This demonstrated that the 9-sulfonium-10-boratriptycene moiety could act as a directing group to selectively functionalize aromatic substrates linked to the boron atom.

IV.7. Conclusion

Despite being reported for the first time more than 60 years ago, metal-free C–H borylations of arenes gained increasing interest for two decades with the extensive development of cationic boron species and other boron electrophiles and superelectrophiles. The borylation of heteroarenes and electron-rich arenes have been more extensively reported while the borylation of unactivated and electron-depleted arenes remains challenging and still stands as the topic of major scientific articles published in 2022. In this context, we report in this chapter a Csp^2–H borylation methodology using a new pyramidal trivalent boron Lewis acid, 9-sulfonium-10-boratriptycene. A full optimization of the reaction conditions was performed, and a scope of aromatic substrates was developed. Using readily available boron Lewis acids and commercially available cheap reagents, this method allows the borylation of unactivated arenes such as benzene and alkyl-substituted benzene derivatives as well as electron depleted haloarenes such as 1,2-dichlorobenzene. The Lewis acid used as borylating agent showing a unique reactivity, a full mechanistic investigation was performed experimentally and a complementary DFT study was performed by Dr. Aurélien Chardon and Prof. Dr. Raphaël Robiette to elucidate the mechanism of this borylation reaction. This mechanistic investigation confirmed that the 9-sulfonium-10-boratriptycene is never present as a trivalent species but forms σ- and π-complexes that are in equilibrium with each other in the reaction medium. After developing a scope of substrates, the functionalization of these tetraarylborate species was attempted. In a first

instance, regioselective mono-fluorinations and chlorinations were attempted and remained unsuccessful regardless of the fluorinating agents used. Every attempt led to a very limited of conversion, complete decomposition of the starting material or unselective functionalization. Suzuki-Miyaura coupling reactions also failed using 10-aryl-9-sulfonium-10-boratriptycene-ate complexes as substrates, leading to complete recovery of the starting material. This absence of reactivity is likely due to the triptycene scaffold and the impossibility of the aryl-boron-ate complex to *in-situ* hydrolyze into the corresponding aryl boronic acid.

Finally, regioselective mono-deuteration were attempted via deuterodeborylation of the 10-aryl-9-sulfonium-10-boratriptycene-ate complexes. Using deuterated Brønsted superacid $DNTf_2$, several substrates could be regioselectively mono-deuterated. Despite the inapplicability of the deuteration methodology to the more electron rich substrates of our borylation scope, several xylene and haloarene derivatives could be regioselectively deuterated with good yields. This work provides a new transition-metal-free Csp^2–H borylation methodology and stands as the first example of Csp^2–H borylation using a triarylborane as electrophilic borylating agent.

The mechanistic study provides new insights into the reactivity of 9-boratriptycene Lewis acids. This revealed that these boron Lewis acids have a greater propensity to form σ- and π-complexes with aromatic species than to form stable Lewis adducts with Lewis bases. These results obtained via the mechanistic investigation and during the functionalization part, once again demonstrated that embedding a boron atom into a triptycene scaffolds confers to the boron atom a unique reactivity which is partially due to the steric protection of one lobe of the empty p_z-orbital, when the acid is considered "free", and the σ^*-orbital, when considering a Lewis adduct or

"ate"-complex. This might provide new insights for considering electrophilic borylation reactions as well as the mechanism of Lewis acid-base exchanges in general.

In the following chapter, the ability of 9-sulfonium-10-boratriptycene to form stable "ate"-complexes with weakly coordinating anions was used to synthesize borylated equivalents of protonated Brønsted superacids.

IV.8. Reference

[1] T. W. Lyons, M. S. Sanford, *Chem. Rev.* **2010**, *110*, 1147–1169.
[2] A. Suzuki, *Angew. Chem. Int. Ed.* **2011**, *50*, 6722–6737.
[3] N. Miyaura, K. Yamada, A. Suzuki, *Tetrahedron Lett.* **1979**, *20*, 3437–3440.
[4] D. G. Hall, *Boronic Acids*, Wiley-VCH Verlag GmbH & Co., Weinheim, Germany, **2011**.
[5] I. A. I. Mkhalid, J. H. Barnard, T. B. Marder, J. M. Murphy, J. F. Hartwig, *Chem. Rev.* **2010**, *110*, 890–931.
[6] A. Ros, R. Fernández, J. M. Lassaletta, *Chem. Soc. Rev.* **2014**, *43*, 3229–3243.
[7] K. M. Waltz, X. He, C. Muhoro, J. F. Hartwig, *J. Am. Chem. Soc.* **1995**, *117*, 11357–11358.
[8] K. M. Waltz, J. F. Hartwig, *Science* **1997**, *277*, 211–213.
[9] H. Chen, S. Schlecht, T. C. Semple, J. F. Hartwig, *Science* **2000**, *287*, 1995–1997.
[10] C. N. Iverson, M. R. Smith, *J. Am. Chem. Soc.* **1999**, *121*, 7696–7697.
[11] J. Y. Cho, M. K. Tse, D. Holmes, R. E. Maleczka, M. R. Smith, *Science* **2002**, *295*, 305–308.
[12] T. Ishiyama, J. Takagi, K. Ishida, N. Miyaura, N. R. Anastasi, J. F. Hartwig, *J. Am. Chem. Soc.* **2002**, *124*, 390–391.
[13] T. Ishiyama, H. Isou, T. Kikuchi, N. Miyaura, *Chem. Commun.* **2010**, *46*, 159–161.
[14] M. J. S. Dewar, V. P. Kubba, R. Pettit, *J. Chem. Soc.* **1958**, *3073*, 3073–3076.
[15] M. J. S. Dewar, R. Dietz, *J. Chem. Soc.* **1959**, 2728–2730.
[16] E. L. Muetterties, *J. Am. Chem. Soc.* **1959**, *81*, 2597–2597.
[17] E. L. Muetterties, *J. Am. Chem. Soc.* **1960**, *82*, 4163–4166.
[18] M. J. S. Dewar, C. Kaneko, M. K. Bhattacharjee, *J. Am. Chem. Soc.* **1962**, *84*, 4884–4887.
[19] R. Köster, *Angew. Chemie Int. Ed.* **1964**, *3*, 174–185.
[20] B. W. Müller, *Helv. Chim. Acta* **1978**, *61*, 325–327.
[21] M. A. Grassberger, F. Turnowsky, J. Hildebrandt, *J. Med. Chem.* **1984**, *27*, 947–953.
[22] S. Oda, K. Ueura, B. Kawakami, T. Hatakeyama, *Org. Lett.* **2020**, *22*, 700–704.
[23] T. S. De Vries, E. Vedejs, *Organometallics* **2007**, *26*, 3079–3081.
[24] T. S. De Vries, A. Prokofjevs, E. Vedejs, *Chem. Rev.* **2012**, *112*, 4246–4282.
[25] T. S. De Vries, A. Prokofjevs, J. N. Harvey, E. Vedejs, *J. Am. Chem. Soc.* **2009**, *131*, 14679–14687.
[26] A. Prokofjevs, J. W. Kampf, E. Vedejs, *Angew. Chem. Int. Ed.* **2011**, *50*, 2098–2101.
[27] A. Prokofjevs, J. Jermaks, A. Borovika, J. W. Kampf, E. Vedejs,

Organometallics **2013**, *32*, 6701–6711.
[28] J. Lv, X. J. Zhang, M. Wang, Y. Zhao, Z. Shi, *Chem. Eur. J.* **2022**, *28*, e202104100.
[29] O. Sadek, A. Le Gac, N. Hidalgo, S. Mallet-Ladeira, K. Miqueu, G. Bouhadir, D. Bourissou, *Angew. Chem. Int. Ed.* **2022**, *61*, e202110102.
[30] A. Del Grosso, R. G. Pritchard, C. A. Muryn, M. J. Ingleson, *Organometallics* **2010**, *29*, 241–249.
[31] A. Del Grosso, P. J. Singleton, C. A. Muryn, M. J. Ingleson, *Angew. Chem. Int. Ed.* **2011**, *50*, 2102–2106.
[32] V. Bagutski, A. Del Grosso, J. A. Carrillo, I. A. Cade, M. D. Helm, J. R. Lawson, P. J. Singleton, S. A. Solomon, T. Marcelli, M. J. Ingleson, *J. Am. Chem. Soc.* **2013**, *135*, 474–487.
[33] A. Del Grosso, J. Ayuso Carrillo, M. J. Ingleson, *Chem. Commun.* **2015**, *51*, 2878–2881.
[34] Q. Yin, H. F. T. Klare, M. Oestreich, *Angew. Chem. Int. Ed.* **2017**, *56*, 3712–3717.
[35] M. A. Légaré, M. A. Courtemanche, É. Rochette, F. G. Fontaine, *Science* **2015**, *349*, 513–516.
[36] J. Lv, X. Chen, X. S. Xue, B. Zhao, Y. Liang, M. Wang, L. Jin, Y. Yuan, Y. Han, Y. Zhao, Y. Lu, J. Zhao, W.-Y. Sun, K. N. Houk, Z. Shi, *Nature* **2019**, *575*, 336–340.
[37] S. A. Iqbal, J. Cid, R. J. Procter, M. Uzelac, K. Yuan, M. J. Ingleson, *Angew. Chem. Int. Ed.* **2019**, *58*, 15381–15385.
[38] S. Rej, N. Chatani, *J. Am. Chem. Soc.* **2021**, *143*, 2920–2929.
[39] S. Rej, N. Chatani, *Angew. Chem. Int. Ed.* **2022**, *61*, e202209539.
[40] J. Pahl, E. Noone, M. Uzelac, K. Yuan, M. J. Ingleson, *Angew. Chem. Int. Ed.* **2022**, *61*, e202206230.
[41] T. Brückner, B. Ritschel, J. O. C. Jiménez-Halla, F. Fantuzzi, D. Duwe, C. Markl, R. D. Dewhurst, M. Dietz, H. Braunschweig, *Angew. Chem. Int. Ed.* **2023**, *62*, e202213284.
[42] X. Tan, X. Wang, Z. H. Li, H. Wang, *J. Am. Chem. Soc.* **2022**, *144*, 23286–23291.
[43] J. Atzrodt, V. Derdau, T. Fey, J. Zimmermann, *Angew. Chem. Int. Ed.* **2007**, *46*, 7744–7765.
[44] J. Atzrodt, V. Derdau, W. J. Kerr, M. Reid, *Angew. Chem. Int. Ed.* **2018**, *57*, 1758–1784.
[45] J. Atzrodt, V. Derdau, W. J. Kerr, M. Reid, *Angew. Chem. Int. Ed.* **2018**, *57*, 3022–3047.
[46] D. Hesk, *J. Label. Compd. Radiopharm.* **2020**, *63*, 247–265.
[47] T. He, H. F. T. Klare, M. Oestreich, *J. Am. Chem. Soc.* **2022**, *144*, 4734–4738.
[48] W. J. Kerr, G. J. Knox, L. C. Paterson, *J. Label. Compd. Radiopharm.* **2020**, *63*, 281–295.
[49] D. Whitaker, J. Burés, I. Larrosa, *J. Am. Chem. Soc.* **2016**, *138*, 8384–

8387.
[50] G. Q. Hu, E. C. Li, H. H. Zhang, W. Huang, *Org. Biomol. Chem.* **2020**, *18*, 6627–6633.
[51] W. Li, D. Yuan, G. Wang, Y. Zhao, J. Xie, S. Li, C. Zhu, *J. Am. Chem. Soc.* **2019**, *141*, 3187–3197.
[52] G. Q. Hu, J. W. Bai, E. C. Li, K. H. Liu, F. F. Sheng, H. H. Zhang, *Org. Lett.* **2021**, *23*, 1554–1560.
[53] S. Duttwyler, C. Douvris, N. L. P. Fackler, F. S. Tham, C. A. Reed, K. K. Baldridge, J. S. Siegel, *Angew. Chem. Int. Ed.* **2010**, *49*, 7519–7522.
[54] O. Allemann, S. Duttwyler, P. Romanato, K. K. Baldridge, J. S. Siegel, *Science* **2011**, *332*, 574–577.
[55] B. Shao, A. L. Bagdasarian, S. Popov, H. M. Nelson, *Science* **2017**, *355*, 1403–1407.
[56] S. A. Iqbal, J. Pahl, K. Yuan, M. J. Ingleson, *Chem. Soc. Rev.* **2020**, *49*, 4564–4591.
[57] G. Berionni, B. Maji, P. Knochel, H. Mayr, *Chem. Sci.* **2012**, *3*, 878–882.
[58] M. Trunk, J. F. Teichert, A. Thomas, *J. Am. Chem. Soc.* **2017**, *139*, 3615–3618.
[59] J. Dupré, A. C. Gaumont, S. Lakhdar, *Org. Lett.* **2017**, *19*, 694–697.
[60] L. Liu, L. L. Cao, Y. Shao, G. Ménard, D. W. Stephan, *Chem* **2017**, *3*, 259–267.
[61] L. L. Liu, L. L. Cao, D. Zhu, J. Zhou, D. W. Stephan, *Chem. Commun.* **2018**, *54*, 7431–7434.
[62] A. Kütt, T. Rodima, J. Saame, E. Raamat, V. Mäemets, I. Kaljurand, I. A. Koppel, R. Y. Garlyauskayte, Y. L. Yagupolskii, L. M. Yagupolskii, E. Bernhardt, H. Willner, I. Leito, *J. Org. Chem.* **2011**, *76*, 391–395.
[63] M. Schorpp, T. Heizmann, M. Schmucker, S. Rein, S. Weber, I. Krossing, *Angew. Chem. Int. Ed.* **2020**, *59*, 9453–9459.
[64] C. Richardson, C. A. Reed, *Chem. Commun.* **2004**, *4*, 706–707.
[65] T. Sakai, S. Seo, J. Matsuoka, Y. Mori, *J. Org. Chem.* **2013**, *78*, 10978–10985.
[66] C. A. Reed, *Acc. Chem. Res.* **2010**, *43*, 121–128.
[67] F. Forster, T. T. Metsänen, E. Irran, P. Hrobárik, M. Oestreich, *J. Am. Chem. Soc.* **2017**, *139*, 16334–16342.
[68] O. Bortolini, C. Chiappe, T. Ghilardi, A. Massi, C. S. Pomelli, *J. Phys. Chem. A* **2015**, *119*, 5078–5087.
[69] J. M. Farrell, Z. M. Heiden, D. W. Stephan, *Organometallics* **2011**, *30*, 4497–4500.
[70] T. Voss, T. Mahdi, E. Otten, R. Fröhlich, G. Kehr, D. W. Stephan, G. Erker, *Organometallics* **2012**, *31*, 2367–2378.
[71] G. Q. Chen, G. Kehr, C. G. Daniliuc, M. Bursch, S. Grimme, G. Erker, *Chem. Eur. J.* **2017**, *23*, 4723–4729.
[72] S. Basak, L. Winfrey, B. A. Kustiana, R. L. Melen, L. C. Morrill, A. P.

Pulis, *Chem. Soc. Rev.* **2021**, *50*, 3720–3737.
[73] G. A. Olah, W. S. Tolgyesi, R. E. A. Dear, *J. Org. Chem.* **1962**, *27*, 3441–3449.
[74] G. Rabe, H. W. Roesky, D. Stalke, F. Pauer, G. M. Sheldrick, *J. Organomet. Chem.* **1991**, *403*, 11–19.
[75] H. Giese, T. Habereder, H. Nöth, W. Ponikwar, S. Thomas, M. Warchhold, *Inorg. Chem.* **1999**, *38*, 4188–4196.
[76] N. Davison, K. Zhou, P. G. Waddell, C. Wills, C. Dixon, S. Hu, E. Lu, *Inorg. Chem.* **2022**, *61*, 3674–3682.
[77] G. A. Olah, G. K. Surya Prakash, K. Wade, Á. Molnár, R. E. Williams *Hydrocarbon Chemistry 2nd Edition*, Wiley-VCH Verlag GmbH & Co., Weinheim, Germany, **2011**.
[78] G. A. Olah, *Acc. Chem. Res.* **1970**, *4*, 240–248.
[79] T. Stuyver, D. Danovich, F. De Proft, S. Shaik, *J. Am. Chem. Soc.* **2019**, *141*, 9719–9730.
[80] E. M. Simmons, J. F. Hartwig, *Angew. Chem. Int. Ed.* **2012**, *51*, 3066–3072.
[81] M. Gómez-Gallego, M. A. Sierra, *Chem. Rev.* **2011**, *111*, 4857–4963.
[82] C. F. Bernasconi, D. J. Carre, *J. Am. Chem. Soc.* **1979**, *101*, 2707–2709.
[83] G. A. Molander, N. Ellis, *Acc. Chem. Res.* **2007**, *40*, 275–286.
[84] G. A. Molander, D. E. Petrillo, *Org. Lett.* **2008**, *10*, 1795–1798.
[85] S. Darses, J. P. Genet, *Chem. Rev.* **2008**, *108*, 288–325.
[86] L. Liu, Y. Dong, B. Pang, J. Ma, *J. Org. Chem.* **2014**, *79*, 7193–7198.
[87] R. Shintani, Y. Tsutsumi, M. Nagaosa, T. Nishimura, T. Hayashi, *J. Am. Chem. Soc.* **2009**, *131*, 13588–13589.
[88] J. Xu, O. P. Bercher, M. P. Watson, *J. Am. Chem. Soc.* **2021**, *143*, 8608–8613.
[89] M. R. Akula, M. L. Yao, G. W. Kabalka, *Tetrahedron Lett.* **2010**, *51*, 1170–1171.
[90] S. Lee, D. W. C. MacMillan, *J. Am. Chem. Soc.* **2007**, *129*, 15438–15439.
[91] G. A. Molander, L. N. Cavalcanti, *J. Org. Chem.* **2011**, *76*, 7195–7203.
[92] J. Lv, B. Zhao, Y. Yuan, Y. Han, Z. Shi, *Nat. Commun.* **2020**, *11*, 1–8.
[93] G. Pattison, *Org. Biomol. Chem.* **2019**, *17*, 5651–5660.
[94] A. Osi, D. Mahaut, N. Tumanov, L. Fusaro, J. Wouters, B. Champagne, A. Chardon, G. Berionni, *Angew. Chem. Int. Ed.* **2022**, *61*, e202112342
[95] T. Shamma, H. Buchholz, G. K. S. Prakash, G. A. Olah, *Isr. J. Chem.* **1999**, *39*, 207–210.
[96] P. T. Nyffeler, S. G. Durón, M. D. Burkart, S. P. Vincent, C.-H. Wong, *Angew. Chem. Int. Ed.* **2004**, *44*, 192–212.
[97] A. S. Kiselyov, *Chem. Soc. Rev.* **2005**, *34*, 1031–1037.
[98] G. S. Lal, G. P. Pez, R. G. Syvret, *Chem. Rev.* **1996**, *96*, 1737–1756.
[99] K. Fukushi, S. Suzuki, T. Kamo, E. Tokunaga, Y. Sumii, T. Kagawa, K.

Kawada, N. Shibata, *Green. Chem.* **2016**, *18*, 1864–1868.
[100] F. Xie, C. Du, Y. Pang, X. Lian, C. Xue, Y. Chen, X. Wang, M. Cheng, C. Guo, B. Lin, et al., *Tetrahedron Lett.* **2016**, *57*, 5820–5824.
[101] Q. Gu, E. Vessally, *RSC Adv.* **2020**, *10*, 16756–16768.
[102] J. Tao, G. K. Murphy, *Synthesis* **2019**, *51*, 3055–3059.
[103] E. A. Patrick, Y. Yang, W. E. Piers, L. Maron, B. S. Gelfand, *Chem. Commun.* **2021**, *57*, 8640–8643.
[104] J. C. Sarie, C. Thiehoff, R. J. Mudd, C. G. Daniliuc, G. Kehr, R. Gilmour, *J. Org. Chem.* **2017**, *82*, 11792–11798.
[105] J. C. Sarie, J. Neufeld, C. G. Daniliuc, R. Gilmour, *Synthesis* **2019**, *51*, 4408–4416.
[106] S. Shu, Y. Li, J. Jiang, Z. Ke, Y. Liu, *J. Org. Chem.* **2019**, *84*, 458–462.
[107] A. Granados, Z. Jia, M. del Olmo, A. Vallribera, *Eur. J. Org. Chem.* **2019**, *2019*, 2812–2818.
[108] Y. Ye, M. S. Sanford, *J. Am. Chem. Soc.* **2013**, *135*, 4648–4651.

Chapter V

From Proton to Boron: The Lewis Analogs of Protonated Brønsted Super Acids

Check for updates

Chemistry–A European Journal | Research Article
doi.org/10.1002/chem.202301146

Chemistry Europe
European Chemical Societies Publishing

www.chemeurj.org

From Proton to Boron: The Lewis Analogs of Protonated Brønsted Super Acids

Arnaud Osi,[a] Nikolay Tumanov,[a] Luca Fusaro,[a] Johan Wouters,[a] Guillaume Berionni,[a] and Aurélien Chardon*[a]

Dedicated to Prof. Alain Krief for his 80th birthday.

Abstract: Isolation and characterization of highly reactive intermediates are crucial to understand the nature of chemical reactivity. Accordingly, the reactivity of weakly coordinating anions (WCA), usually used to stabilized cationic super electrophiles are of fundamental interest. When a variety of WCA are known to form stable σ-complexes with a proton, inducing Brønsted super acidity, bis-coordinated weak-coordinated anions are much more elusive and considered as long-sought reactive species. In this work, the chemistry of borylated sulfate, triflimidate and triflate anions were scouted in details with the aim of synthetizing the unique analogs of protonated Brønsted superacids. Those complexes were formed by successive borylation with a 9-boratriptycene derived Lewis super acid paired with a weak coordinated anion, characterized in solution and in the solid state and exhibit unique structures and reactivities.

Introduction

Back in the 1960's, stronger electrophiles emerged with the replacement of sulfate or halide by triflate ion $[CF_3SO_3]^-$ owing to its weaker coordinating properties. Before the 1990's, and the emergence of X-ray crystallography, one can assume that triflate anion, along with other anions such as $[BF_4]^-$, $[ClO_4]^-$, $[AlX_4]^-$ and $[MX_6]^-$ did not interact with their paired cation and were therefore considered as "noncoordinating anions".[1] It turned out that these anions were actually coordinated to the electrophilic center. The demonstration being done that an anion with no coordinating ability was elusive, the term "noncoordinating" anions was subsequently replaced by "weakly coordinating" anion (WCA),[2] those included perfluorinated tetra-arylborates salts,[3] perfluoroalkyl aluminates or halogenated icosahedral carboranes extensively developed by Reed.[4,5]

Interestingly, some anions such has halides or hydrides have shown the ability of coordinating two electrophiles forming halonium species and some of them such as fluoronium or chloronium cations have been observed and isolated as bridged species resulting from the coordination of two boranes,[6] silylium,[7] borenium or carbeniums ions (Figure 1).[8,9] However, twofold coordination of weaker coordinating anions is much more elusive.[10] For instance, it took almost twenty years after the isolation of protonated sulfuric acid by Minkwitz in 2002,[11] until evidence of the existence of heavier silylated analog was provided by Schulz in 2021 (Figure 1, VII).[12] In contrast, multicoordinated WCA with Lewis acids are unknown outside group XIV, presumably because of the lack of sufficiently Lewis superacid aside silylium cations.[7,13] However, coercing main-group Lewis acids into a cage-shaped or pyramidal scaffold result in a strong decrease of the reorganization energy upon reaction with Lewis bases.[14]

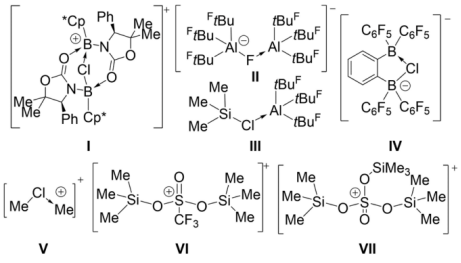


Figure 1. Selected examples of twofold coordination of halides (**I**–**V**) and weakly coordinating anions (**VI** and **VII**) with electrophiles.

This makes pyramidal organoboron Lewis acids, and especially those derived from 9-boratriptycene significantly more Lewis acidic than their trigonal planar counterparts.[15]

We recently reported the synthesis of the 9-sulfonium-10-boratriptycene **2** (Figure 2A) and demonstrated its ability to activate strong chemical bond such as Csp^2–H, Csp^3–H and Csp^3–Csp^3 bonds.[15d] Stimulated by this work, we envisioned to use it as a stabilizing Lewis super acid to access multi-coordinated WCA. Here we report the validation of this

[a] A. Osi, Dr. N. Tumanov, Dr. L. Fusaro, Prof. Dr. J. Wouters, Prof. Dr. G. Berionni, Dr. A. Chardon
Chemistry Department
Namur Institute of Structured Matter
University of Namur
61 rue de Bruxelles, 5000 Namur (Belgium)
E-mail: aurelien.chardon@unamur.be

Supporting information for this article is available on the WWW under https://doi.org/10.1002/chem.202301146

© 2023 Wiley-VCH GmbH

A. Osi, N. Tumanov, L. Fusaro, J. Wouters, G. Berionni, A. Chardon, *Chem. Eur. J.* **2023**, e202301146

V.1. Introduction

Back in the 1960's, stronger electrophiles emerged with the replacement of sulfate or halide ions by the triflate ion $[CF_3SO_3]^-$ owing to its weaker coordinating properties. Before the 1990's, and the emergence of X-ray crystallography, one can assume that the triflate anion, along with other anions such as $[BF_4]^-$, $[ClO_4]^-$, $[AlX_4]^-$ and $[MX_6]^-$ did not interact with their paired cation and were therefore considered as "noncoordinating anions".[1–3] It turned out that these anions were actually coordinated to the electrophilic center. The demonstration being done that an anion with no coordinating ability was elusive, the term "noncoordinating" anion was subsequently replaced by "weakly coordinating" anion (WCA),[4–7] those included perfluorinated tetra-arylborate salts, perfluoroalkyl aluminates[8–11] or halogenated icosahedral carboranes extensively developed by Reed.[12–14]

Interestingly, some anions such has halides or hydrides have shown the ability of coordinating two electrophiles forming halonium species and some of them such as fluoronium or chloronium cations have been observed and isolated as bridged species resulting from the coordination of two boranes,[15–23] silylium,[24–29] borenium[30–36] or carbenium ions (**Figure V.34**).[37–42] However, twofold coordination of weaker coordinating anions is much more elusive.[43–46] For instance, it took almost twenty years after the isolation of protonated sulfuric acid by Minkwitz in 2002,[47] until the synthesis of a heavier silylated analog was achieved by Schulz in 2021 (**Figure V.34**, **VII**).[48] In contrast, multicoordinated WCA with Lewis acids are unknown outside group XIV, presumably because of the lack of sufficiently strong Lewis superacids aside silylium cations.[24,49,50] However, coercing main-group Lewis acids into a cage-shaped or pyramidal scaffold results in a strong decrease of the reorganization energy upon reaction with Lewis bases.[51–53] This makes pyramidal organoboron Lewis acids, and

especially those derived from 9-boratriptycene, significantly more Lewis acidic than their trigonal planar counterparts.[54–57]

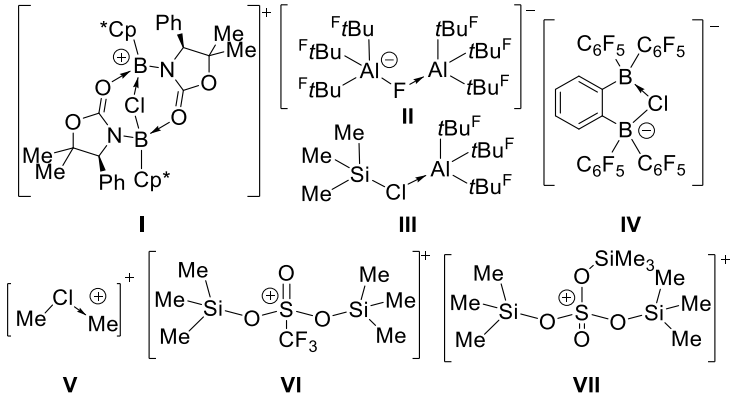


Figure V.34 : Selected examples of twofold coordination of halides (**I-V**) and weak coordinated anions (**VI** and **VII**) with electrophiles.

We recently reported the synthesis of the 9-sulfonium-10-boratriptycene **5.2** (**Figure V.35**, **A**) and demonstrated its ability to activate strong chemical bonds such as Csp^2–H, Csp^3–H and Csp^3–Csp^3 bonds.[57] Stimulated by this work, we envisioned to use it as a stabilizing Lewis super acid to access multicordinated WCA. Here we report the validation of this hypothesis for the preparation and characterization of *per*-borylated sulfate, triflimidate and triflate anions as heavier analogs of protonated Brønsted super acids. Those entries open a new family of WCA stabilized Lewis acids, which were isolated as stable crystalline materials under super acidic conditions.

V.2. Synthesis of mono-, bis- and tris-borylated sulfate

Starting with the synthesis of 9-sulfonium-10-boratriptycene-methylsulfate **5.3**, the protodeboronation of ate-complex **5.1** with various amounts of H_2SO_4 was examined and mostly yielded starting material and unidentified decomposition byproducts. As we recently demonstrated that the Lewis acid **5.2** could be generated from the corresponding triflimidate-ate complex

upon addition of $NaB(C_6F_5)_4$,[57] sequential quenching of *in-situ* generated 9-sulfonium-10-boratriptycene **5.2** with excess Me_2SO_4 followed by subsequent demethylation on silica gel allowed the synthesis of (9-sulfonium-10-boratriptycene)methylsulfate **5.3** with 78% yield (**Figure V.35, A**). Next, the demethylation was attempted and revealed to be less straightforward than expected since only partial methyl transfer was observed even in presence of an excess of pyridine. Quantitative methyl transfer was only observed in presence of a large excess of *N*-methylpyrolidine (NMP) affording **5.4** in 61% yield (**Figure V.35, A**).

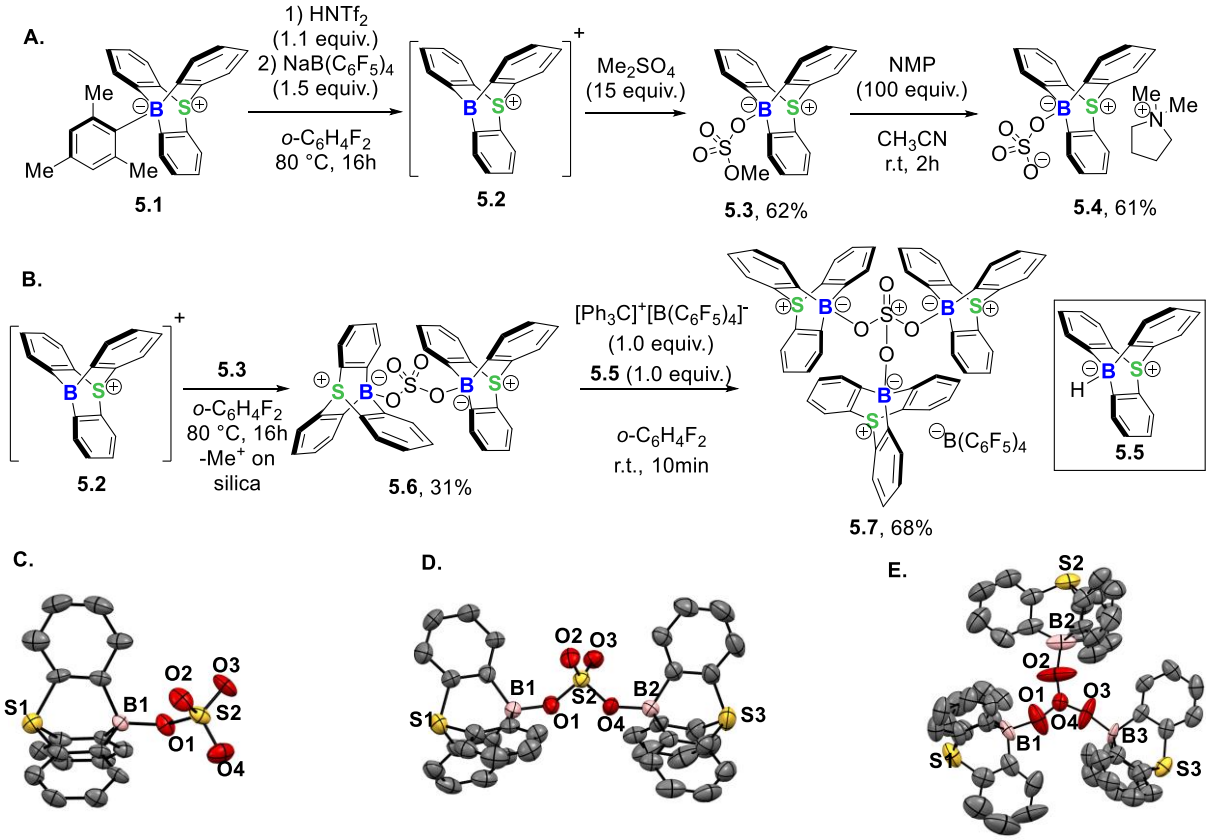


Figure V.35 : **A.** Synthesis of **5.3** by protodeboronation of **5.1** using the $HNTf_2/NaB(C_6F_5)_4$ couple followed by quench with Me_2SO_4; subsequent demethylation with *N*-methylpyrolidine to form anionic complex **5.4**; **B.** Synthesis of **5.6** and of **5.7** by trapping **5.6** with *in-situ* generated 9-sulfonium-10-boratriptycene **5.2**. Molecular structures; of **C.** anionic complex **5.4**; **D.** bisborylated sulfate **5.6**; **E.** trisborylated sulfate **5.7**. H-atoms and counter anion/cation are omitted for clarity; thermal ellipsoids are represented with a 50% probability level.

The bis(9-sulfonium-10-boratriptycene)sulfate **5.6** was secured with 31% yield upon reaction of **5.3** with *in-situ* generated 9-sulfonium-10-boratriptycene **5.2** (**Figure V.35**, **B**). We then devoted our attention to the preparation of the trisborylated derivative **5.7**, the group XIII analog of protonated sulfuric acid. Subsequently, hydride abstraction from borohydride **5.5** with a stoichiometric amount of $[Ph_3C]^+[B(C_6F_5)_4]^-$ followed by treatment with **5.6** cleanly afforded compound **5.7** (**Figure V.35, B**). According to ^{11}B NMR spectroscopy, compound **5.7** showed one broad singlet at 8.4 ppm, slightly deshielded compared to that of **5.6** (δ = 1.6) which indicate no evidence for the splitting of the ^{11}B NMR chemical shift of **5.7**.

Upon successive borylations, the B–O bond lengths are slightly elongated from $[(BTripS)_1SO_4]^-$ [1.494(10) Å]] to $[(BTripS)_2SO_4]$ [1.506(5) Å] and $[(BTripS)_3SO_4]^+$ [1.527(10) Å]. Conversely, the pyramidalization angle decreases upon coordination, indicating the highest donor free character at boron along $[(BTripS)_3SO_4]^+$ (α = 21.6°) > $[(BTripS)_2SO_4]$ (α = 22.9°) > $[(BTripS)_1SO_4]^-$ (α = 23.4°) (**Table V.12**).

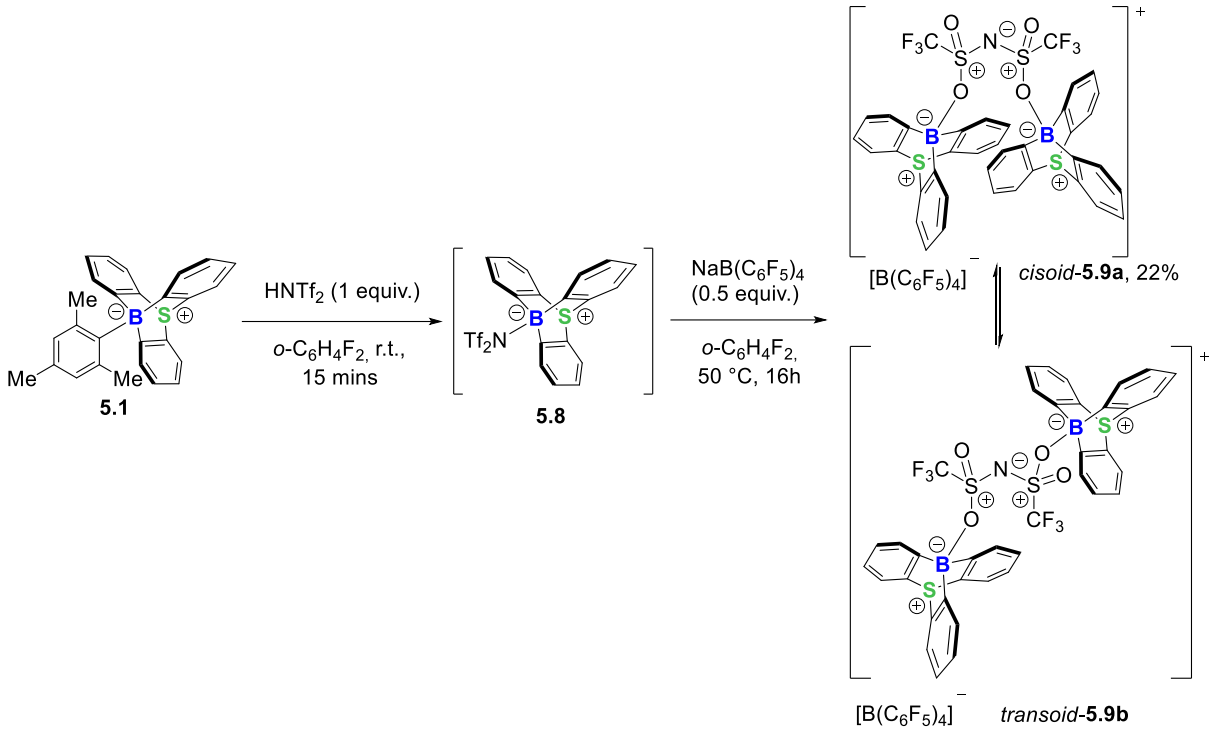
Quantum chemical calculations at M06-2X/6-311G(d) level of theory were thus undertaken by Dr. Aurélien Chardon to evaluate the evolution of the net partial charges of the sulfur atom and the $[SO_4]$ moieties upon successive borylations. As a consequence of the delocalization over the $[SO_4]$ entity, the calculated partial net charges at sulfur show no significant change with calculated values of $[(BTripS)_1SO_4]^-$ 2.57*e*, $[(BTripS)_2SO_4]$ 2.62*e* and $[(BTripS)_3SO_4]^+$ 2.69*e*. For the sulfate, the partial charges strongly increased upon successive borylation along $[SO_4]^{2-}$ < -1.45 $[(BTripS)SO_4]^-$ < -1.10 $[(BTripS)_2SO_4]^-$ < -0.85 $[(BTripS)_3SO_4]^-$ (**Table V.12**).

In line with this, formal charge transfers upon mono (0.54*e*), bis (0.90*e*) and tris-borylation (1.14*e*) are exceeding by far that of $[SiMe_3]^+$,[48] showing the unrivalled high electron affinity of 9-sulfonium-10-boratriptycene. A comparison of these borylated sulfate salts with related silylium equivalents reveals the differences between non-VSEPR boron Lewis acids and silylium cations, despite their close Lewis acidic properties.[57–59] Whereas the tris(trimethylsilyl)oxosulfonium **VII** likely behaved as a $[TMS]^+$ reservoir, the borylated analog **5.7** showed a surprising high stability both in the solid state and in solution, this is presumably due to the steric protection of the B–O σ*-orbital paired with the high dissociation enthalpy of the B–O bond.

V.3. Synthesis of bis-borylated triflimidate

Encouraged by the generation of a tris-borylated sulfate and intrigued by its unusual stability towards ambient conditions, we then targeted the synthesis of bisborylated triflimidate and triflate cations, the heavier analogs of the protonated triflimidic and triflic acids.[60]

It was then assumed that reacting the triflimidate-ate complex **5.8** with half an equivalent of $NaB(C_6F_5)_4$ would provide half an equivalent of the Lewis acid, which would react with the remaining starting material to form the desired compound **5.9** (**Scheme V.89**). After 16h at 50 °C, ^{11}B NMR analysis showed a complete consumption of the starting material, but most significantly, the ^{19}F NMR spectrum revealed a shielding and a splitting of the signals observed previously for **5.8** (from signals at δ = –75.0 and –78.2 in **5.8**, to two independent signals at δ = –71.6 and –74.0 in a 5:1 ratio in **5.9**). Similar observations were derived from ^1H NMR spectroscopy where two triptycene units were detected with the same ratio (See the Supporting information).



Scheme V.89 : Synthesis of $[(BtripS)_2NTf_2]^+$ **5.9**

We therefore hypothesized that these two systems are best represented as *cisoid*-**5.9a** and *transoid*-**5.9b** forms of the bis-borylated triflimidate **5.9** (**Scheme V.89**).

After removal of the sodium salt upon fast filtration over SiO_2 under air, cationic complex **5.9a** was isolated as an air stable white powder in 22% yield. X-ray crystallographic analysis confirmed the formation of the bis-borylated triflimide anion and showed a *cisoid* conformation with respect to the CF_3 groups, in accordance with others η^2-O,O[Yt]$^{2+}$ bonded triflimide complexes, but in sharp contrast with the Tf_2NH acid or triflimide anion which both prefer *transoid* like conformation (**Figure V.36**).[61–64] Owing to the twofold coordination, the pyramidalization at boron likely decreases for **5.9a** (α = 21.1°) with respect to that of **5.8** (α = 22.4°). Both B–O bond lengths have found to be slightly longer than that of **5.8** [1.55 Å] but are still in the range for an NTf_2–O moiety bound to tricoordinate boron.[65] While the prevalence of the *cisoid* form **5.9a** in the solution and in the solid-state

are still in question, the stacked conformation is likely due to π–π-stacking interaction between two benzene rings of each triptycenes scaffolds with interplanar distance of 3.72Å (**Figure V.36**, **B**). As a consequence, the S3–N1–S2 angle [123.7(5)°] are slightly smaller than that of the triflimidate-ate complex **5.8** (124.4°) and deviated from 4.5° to that of η^2-O,O[Yb]$^{2+}$ bonded triflimide complexes (see the SI for molecular structure of **5.8**).[44]

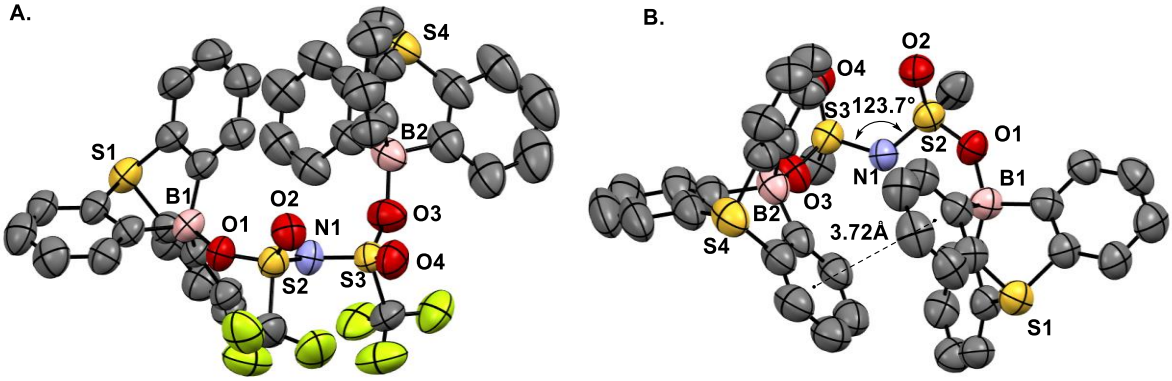


Figure V.36 : **A.** molecular structure of **5.9a** and **B.** its corresponding side view where fluorine atoms have been omitted for clarity. Counter anion and H-atoms are omitted for clarity, thermal ellipsoids are represented with a 50% probability level.

V.4. Synthesis of bis-borylated trilfate

Protodeboronation of the ate-complex **5.1** with a stoichiometric amount of triflic acid (TfOH) cleanly provides the triflate complex **5.10** with 74% yield (**Figure V.37**, **A, B**). Next, treatment of a solution of **5.10** with equimolar *in-situ* generated 9-sulfonium-10-boratriptycene **5.2** in C_6F_6 resulting in a solution from which a solid precipitated, after 15 min the solid was collected by filtration and washed with additional C_6F_6. Clean formation of the bis-borylated triflate cation was observed by ^{19}F NMR spectroscopy with one signal at -71.7 ppm, the associated ^{11}B NMR spectra expectedly indicated a broad singlet at 12.3 ppm. Compound **5.11** was found to have limited stability in solution, gradually decomposing into a mixture of chloride-boron-ate complex and complex **5.10** upon dissolution in CD_2Cl_2 (See the SI). Despite its high reactivity in σ-donating aromatic solvents, unambiguous evidence for the structure of **5.11** was provided by crystallographic characterization (see **Table V.12** for the key geometrical parameters). Expectedly, both B–O bonds are longer [1.562(2) Å] than that in **5.9** [1.542(3) Å], leading to a decrease of the pyramidalization at boron from 22.5° in **5.10** to 21.4° in **5.11**, reflecting the weak and covalent nature of these B–O interactions. In addition, the steric repulsion between the two triptycene units in **5.11** causes an opening of the B–O–S angle up to 21° (**Figure V.37**, **C**).

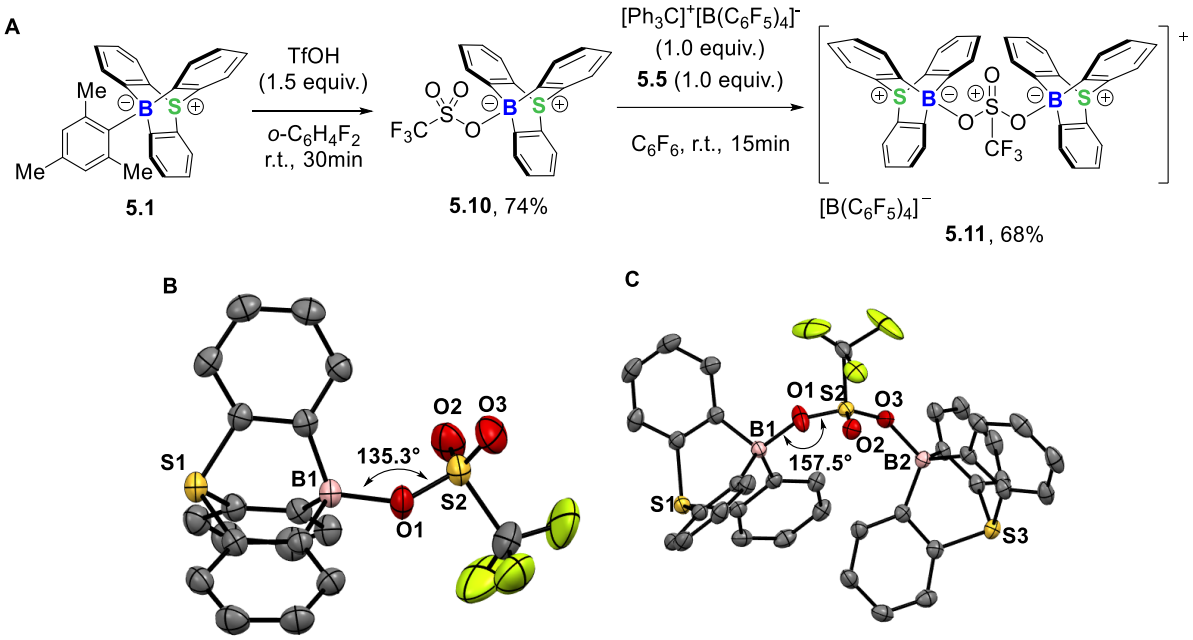


Figure V.37 : Synthesis of **A.** the triflate complex **5.10** and the bis-borylated triflate cation **5.11**; and **B.** Molecular structure of **5.10** and **C.** molecular structure of **5.11** in the solid state.

V.5. Quantum chemical investigations

Next, quantum chemical calculations showed a severe increase of the formal charge transfer at sulfur upon successive borylations of the triflate anion from 0.426*e* in **5.10** to 0.696*e* in **5.11** (**Table V.12**). This is corroborated by the high FIA of **5.11** in the gas phase (419 kJ.mol^{-1}) which, although lower than that of SbF_5 and $B(C_6F_5)_3$ is one of the highest calculated for a tetra-coordinated organoboron compound (**Table V.12**).[58]

Table V.12 : Selected bond lengths [Å] and angles [°], ^{11}B NMR data [ppm], formal charge at sulfur $q_{(S)}$ [*e*], anion formal charge $q_{(anion)}$ [*e*], anion charge transfer $\Delta q^{tot}_{CT,T+}$ [*e*], non isodesmic FIA [kJ mol^{-1}] and pyramidalization angle α (°).

	$[(BTripS)SO_4]^-$ **5.4**	$[(BTripS)_2SO_4]$ **5.6**	$[(BTripS)_3SO_4]^+$ **5.7**	$[(BTripS)Tf_2N]$ **5.8**	$[(BTripS)_2Tf_2N]^+$ **5.9a**	$[(BTripS)TfO]$ **5.10**	$[(BTripS)_2TfO]^+$ **5.11**
$S–O_{(-B)}$	1.560	1.522-1.530	1.387-1.420	1.41-1.47	1.456-1496	1.504	1.495-1.504
B–O	1.490	1.503-1.510	1.515-1.539	1.55	1.567-1.622	1.542	1.562
B–O–S	131.5	130.2-130.6	156.4-161.0	129.4[d]	141.5-142.1	135.3	134.4-146.4
$\delta[^{11}B]$	-1.0	1.6	8.5	6.0[15d]	11.7	3.6	12.3
$q_{(S)}$[c]	2.55	2.62	2.69	2.17	2.19	2.28	2.32
$q_{(anion)}$[c]	-1.45	-1.10	-0.85	-0.60	-0.28	-0.57	-0.30
$\Delta q^{tot}_{CT,T+}$[c]	0.55	0.90	1.15	0.40	0.72	0.42	0.70
FIA	/	17.1	334.2	156.0	371	66.9	418.7
α[b]	23.4	22.9	21.6	22.4[d]	21.2	22.5	21.4

[a] Cf. -2 in $[SO_4]^{2-}$, -1 in $[TfO]^-$ and -1 in $[Tf_2N]^-$. [b] Pyramidalization angle in degree: defined as the angle between one B-C bond and the plane spanned by the *ipso*-carbon atoms of the triptycene benzene rings. [c] Derived from quantum chemical calculation at M06-2X/6-311G(d) level of theory.

V.6. Conclusion

In essence, the Lewis acidic properties of the 9-sulfonium-10-boratriptycene enables the stabilization of tris-borylated sulfate and bis-borylated triflimide and triflate anions as unique analogs of the corresponding protonated Brønsted super acids. In the case of sulfate derivatives, computational analysis confirmed a stronger formal charge transfer upon successive borylation than that of silylated sulfuric acid. When the tris-borylated sulfate is highly stable in solution and in the solid state, the corresponding bis-borylated triflate anion is labile in solution and could serve as a Lewis super acid reservoir. Further studies concerning the chemical behavior of such electrophiles are currently under investigation and will be reported in due course.

V.7. References

[1] W. Beck, K. Sünkel, *Chem. Rev.* **1988**, *88*, 1405–1421.
[2] S. H. Strauss, *Chem. Rev.* **1993**, *93*, 927–942.
[3] M. Bochmann, *Angew. Chemie Int. Ed.* **1992**, *31*, 1181–1182.
[4] I. Krossing, I. Raabe, *Angew. Chem. Int. Ed.* **2004**, *43*, 2066–2090.
[5] I. M. Riddlestone, A. Kraft, J. Schaefer, I. Krossing, *Angew. Chem. Int. Ed.* **2018**, *57*, 13982–14024.
[6] S. F. Rach, F. E. Kuhn, *Chem. Rev.* **2009**, *109*, 2061–2080.
[7] W. E. Geiger, F. Barrière, *Acc. Chem. Res.* **2010**, *43*, 1030–1039.
[8] I. Krossing, *Chem. Eur. J.* **2001**, *7*, 490–502.
[9] I. Krossing, *Comprehensive Inorganic Chemistry II,* Elsevier Ltd. **2013**.
[10] I. Krossing, A. Reisinger, *Eur. J. Inorg. Chem.* **2005**, 1979–1989.
[11] A. Martens, P. Weis, M. C. Krummer, M. Kreuzer, A. Meierhöfer, S. C. Meier, J. Bohnenberger, H. Scherer, I. Riddlestone, I. Krossing, *Chem. Sci.* **2018**, *9*, 7058–7068.
[12] C. A. Reed, *Acc. Chem. Res.* **1998**, *31*, 133–139.
[13] C. A. Reed, *Acc. Chem. Res.* **2010**, *43*, 121–128.
[14] S. P. Fisher, A. W. Tomich, S. O. Lovera, J. F. Kleinsasser, J. Guo, M. J. Asay, H. M. Nelson, V. Lavallo, *Chem. Rev.* **2019**, *119*, 8262–8290.
[15] H. E. Katz, *Organometallics* **1987**, *6*, 1134–1136.
[16] L. Englert, A. Stoy, M. Arrowsmith, J. H. Muessig, M. Thaler, A. Deißenberger, A. Häfner, J. Böhnke, F. Hupp, J. Seufert, J. Mies, A. Damme, T. Dellermann, K. Hammond, T. Kupfer, K. Radacki, T. Thiess, H. Braunschweig, *Chem. Eur. J.* **2019**, *25*, 8612–8622.
[17] S. P. Lewis, L. D. Henderson, B. D. Chandler, M. Parvez, W. E. Piers, S. Collins, *J. Am. Chem. Soc.* **2005**, *127*, 46–47.
[18] M. Melaimi, F. P. Gabbaï, *J. Am. Chem. Soc.* **2005**, *127*, 9680–9681.
[19] S. Solé, F. P. Gabbaï, *Chem. Commun.* **2004**, *4*, 1284–1285.
[20] M. J. Sgro, J. Dömer, D. W. Stephan, *Chem. Commun.* **2012**, *48*, 7253–7255.
[21] B. R. Barnett, C. E. Moore, A. L. Rheingold, J. S. Figueroa, *J. Am. Chem. Soc.* **2014**, *136*, 10262–10265.
[22] M. A. Légaré, C. Pranckevicius, H. Braunschweig, *Chem. Rev.* **2019**, *119*, 8231–8261.
[23] T. W. Hudnall, C. W. Chiu, F. P. Gabbaï, *Acc. Chem. Res.* **2009**, *42*, 388–397.
[24] H. F. T. Klare, L. Albers, L. Süsse, S. Keess, T. Müller, M. Oestreich, *Chem. Rev.* **2021**, *121*, 5889–5985.
[25] R. Panisch, M. Bolte, T. Müller, *J. Am. Chem. Soc.* **2006**, *128*, 9676–9682.
[26] A. Merk, L. Bührmann, N. Kordts, K. Görtemaker, M. Schmidtmann, T. Müller, *Chem. Eur. J.* **2021**, *27*, 3496–3503.
[27] A. Sekiguchi, Y. Murakami, N. Fukaya, Y. Kabe, *Chem. Lett.* **2004**, *33*, 530–531.

[28] T. Müller, *Angew. Chem. Int. Ed.* **2001**, *40*, 3033–3036.
[29] P. Romanato, S. Duttwyler, A. Linden, K. K. Baldridge, J. S. Siegel, *J. Am. Chem. Soc.* **2010**, *132*, 7828–7829.
[30] A. Prokofjevs, J. W. Kampf, A. Solovyev, D. P. Curran, E. Vedejs, *J. Am. Chem. Soc.* **2013**, *135*, 15686–15689.
[31] D. N. Shih, R. Boobalan, Y. H. Liu, R. J. Chein, C. W. Chiu, *Inorg. Chem.* **2021**, *60*, 16266–16272.
[32] B. Inés, M. Patil, J. Carreras, R. Goddard, W. Thiel, M. Alcarazo, *Angew. Chem. Int. Ed.* **2011**, *50*, 8400–8403.
[33] C. Bonnier, W. E. Piers, A. A. S. Ali, A. Thompson, M. Parvez, *Organometallics* **2009**, *28*, 4845–4851.
[34] T. A. Engesser, M. R. Lichtenthaler, M. Schleep, I. Krossing, *Chem. Soc. Rev.* **2016**, *45*, 789–799.
[35] T. S. De Vries, A. Prokofjevs, E. Vedejs, *Chem. Rev.* **2012**, *112*, 4246–4282.
[36] W. E. Piers, S. C. Bourke, K. D. Conroy, *Angew. Chem. Int. Ed.* **2005**, *44*, 5016–5036.
[37] E. S. Stoyanov, I. V. Stoyanova, F. S. Tham, C. A. Reed, *J. Am. Chem. Soc.* **2010**, *132*, 4062–4063.
[38] S. Duttwyler, C. Douvris, N. L. P. Fackler, F. S. Tham, C. A. Reed, K. K. Baldridge, J. S. Siegel, *Angew. Chem. Int. Ed.* **2010**, *49*, 7519–7522.
[39] K. F. Hoffmann, A. Wiesner, C. Müller, S. Steinhauer, H. Beckers, M. Kazim, C. R. Pitts, T. Lectka, S. Riedel, *Nat. Commun.* **2021**, *12*, 5275
[40] S. Hämmerling, G. Thiele, S. Steinhauer, H. Beckers, C. Müller, S. Riedel, *Angew. Chem. Int. Ed.* **2019**, *58*, 9807–9810.
[41] M. D. Struble, M. T. Scerba, M. Siegler, T. Lectka, *Science* **2013**, *340*, 57–60.
[42] R. R. Naredla, D. A. Klumpp, *Chem. Rev.* **2013**, *113*, 6905–6948.
[43] Y. Hasegawa, T. Ohkubo, K. Sogabe, Y. Kawamura, Y. Wada, N. Nakashima, S. Yanagida, *Angew. Chem. Int. Ed.* **2000**, *39*, 357–360.
[44] A. V. Mudring, A. Babai, S. Arenz, R. Giernoth, *Angew. Chem. Int. Ed.* **2005**, *44*, 5485–5488.
[45] G. Schultz, I. Hargittai, R. Seip, *Z. Naturforsch. A.* **1981**, *36*, 917–918.
[46] A. Wirth, O. Moers, A. Blaschette, P. G. Jones, *Z. Anorg. Allg. Chem.* **1998**, *624*, 991–998.
[47] R. Minkwitz, R. Seelbinder, R. Schöbel, *Angew. Chem. Int. Ed.* **2002**, *41*, 111–114.
[48] K. Bläsing, R. Labbow, A. Schulz, A. Villinger, *Angew. Chem. Int. Ed.* **2021**, *60*, 13798–13802.
[49] A. Schulz, J. Thomas, A. Villinger, *Chem. Commun.* **2010**, *46*, 3696–3698.
[50] L. P. Press, B. J. McCulloch, W. Gu, C.-H. Chen, B. M. Foxman, O. V. Ozerov, *Chem. Commun.* **2015**, *51*, 14034–14037.
[51] G. Bouhadir, D. Bourissou, *Chem. Soc. Rev.* **2004**, *33*, 210–217.

[52] A. Chardon, A. Osi, D. Mahaut, A. Ben Saida, G. Berionni, *Synlett* **2020**, *31*, 1639–1648.
[53] L. A. Mück, A. Y. Timoshkin, G. Frenking, *Inorg. Chem.* **2012**, *51*, 640–646.
[54] A. Chardon, A. Osi, D. Mahaut, T. H. Doan, N. Tumanov, J. Wouters, L. Fusaro, B. Champagne, G. Berionni, *Angew. Chem. Int. Ed.* **2020**, *59*, 12402–12406.
[55] A. Ben Saida, A. Chardon, A. Osi, N. Tumanov, J. Wouters, A. I. Adjieufack, B. Champagne, G. Berionni, *Angew. Chem. Int. Ed.* **2019**, *58*, 16889–16893.
[56] D. Mahaut, A. Chardon, L. Mineur, G. Berionni, B. Champagne, *ChemPhysChem* **2021**, *22*, 1958–1966.
[57] A. Osi, D. Mahaut, N. Tumanov, L. Fusaro, J. Wouters, B. Champagne, A. Chardon, G. Berionni, *Angew. Chem. Int. Ed.* **2022**, *61*, e202112342.
[58] L. Greb, *Chem. Eur. J.* **2018**, *24*, 17881–17896.
[59] H. Großekappenberg, M. Reißmann, M. Schmidtmann, T. Müller, *Organometallics* **2015**, *34*, 4952–4958.
[60] T. Soltner, N. R. Goetz, A. Kornath, *Eur. J. Inorg. Chem.* **2011**, 3076–3081.
[61] W. Zhao, J. Sun, *Chem. Rev.* **2018**, *118*, 10349–10392.
[62] S. Antoniotti, V. Dalla, E. Duñach, *Angew. Chem. Int. Ed.* **2010**, *49*, 7860–7888.
[63] A. Haas, C. Klare, P. Betz, J. Bruckmann, C. Krüger, Y.-H. Tsay, F. Aubke, *Inorg. Chem.* **1996**, *35*, 1918–1925.
[64] P. Johansson, S. P. Gejji, J. Tegenfeldt, J. Lindgren, *Electrochim. Acta* **1998**, *43*, 1375–1379.
[65] C. R. P. Millet, J. Pahl, E. Noone, K. Yuan, G. S. Nichol, M. Uzelac, M. J. Ingleson, *Organometallics* **2022**, *41*, 2638–2647.

Chapter VI

A Selenenium-Bridged 10-Boratriptycene Lewis Acid

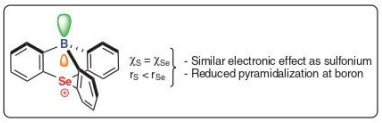
Synthesis A. Osi et al. Paper

A Selenenium-Bridged 10-Boratriptycene Lewis Acid

Arnaud Osi
Nikolay Tumanov
Johan Wouters
Aurélien Chardon*
Guillaume Berionni*

Department of Chemistry, NISM Institute, University of Namur, 61 Rue de Bruxelles, 5000 Namur, Belgium

Dedicated to Prof Alain Krief for his 80th birthday.



Received: 21.03.2022
Accepted after revision: 02.05.2022
Published online: 02.05.2022
DOI: 10.1055/a-1840-5680; Art ID: ss-2022-t0143-op

Abstract A non-planar triarylborane and a new member of the boratriptycene family bearing a selenium atom in bridgehead position of triptycene scaffold was generated and isolated as a boron-'ate' complex paired with a weakly coordinating anion. With similar electronegativity while possessing longer atom radius with respect to sulfur, the introduction a selenium atom, in the form of a selenenium moiety, at the bridgehead of a triptycene scaffold allows a very precise modification of the pyramidalization of the boron atom environment. Experimental and computational evaluation of the Lewis acidity of this new boratriptycene derivative gave qualitative information on how a modification of the pyramidalization of the boron environment affects alone Lewis acidity parameters of such pyramidal triarylborane.

Key words Lewis acids, main-group chemistry, organoboron compounds, triptycene, acidity scale

Owing to their countless applications in material sciences, catalysis, and drug design, trivalent boron compounds are prototypical Lewis acids.[1] In contrast to trialkyl- or trihaloboranes, triarylboranes are tunable platforms for the development of structurally diverse Lewis acids covering a wide range of Lewis acidic properties and applications ranging from anion carriers to catalysts, supramolecular materials, frustrated Lewis pairs, and activators for Ziegler–Natta polymerization.[2] While triarylboranes with well-known propeller-like structures are prototypical Lewis acids, two electronic and structural factors, known as reorganization energy and π-backdonation, can drastically modify their Lewis acidity and lead to novel classes of boron Lewis acids with unforeseen properties.[3] By constraining the central boron and substituent into a planar shape, the reorganization energy and π-backdonation are increased, leading to reduced Lewis acidity at boron.[4] In contrast, constraining the boron atom into a pyramidal trigonal geometry decreases the reorganization energy and π-backdonation, drastically increasing the boron Lewis acidity.[3c,h]

Since 2012, increasing attention has been devoted to non-planar Lewis acids since quantum chemical calculations highlighted 9-boratriptycene and its group XIII analogues for their extraordinary Lewis acidity and potential for the activation and complexation of unreactive small molecules.[3,5] It has been reported that, by preventing p-π conjugation while lowering the reorganization energy with a pre-pyramidalized boron compound, the Lewis acidity of perfluorinated triarylboranes can be reached without the introduction of electron-withdrawing substituents.[6a] Using the 9-boratriptycene **1** as reference, we demonstrated that switching from carbon to a cationic phosphorous bridgehead triptycene scaffold **2** leads to a dramatic increase in Lewis acidity, approaching and even surpassing triarylsilylium species.[6b] Very recently, we reported the generation of the transient sulfonium-bridged analogue **3** of the 9-boratriptycene **1** and, for the first time, the high reactivity of

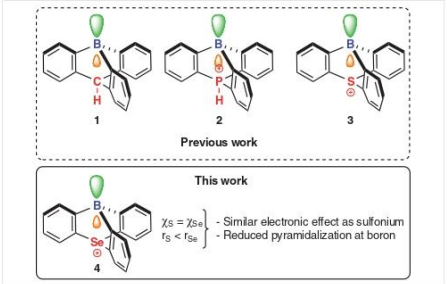


Figure 1 Previous work on 9-boratriptycene derivatives and new selenenium derivative in this work

© 2022. Thieme. All rights reserved.
Georg Thieme Verlag KG, Rüdigerstraße 14, 70469 Stuttgart, Germany

Downloaded by: University of Namur. Copyrighted material.

A.Osi, N. Tumanov, J. Wouters, A. Chardon, G. Berionni, *Synthesis* **2022**, *55*, 347.

VI.1. Introduction

Owing to their countless applications in materials science, catalysis, and drug design, trivalent boron compounds are prototypical Lewis acids.[1–4] In contrast to trialkyl- or trihaloboranes, triarylboranes are tunable platforms for the development of structurally diverse Lewis acids covering a wide range of Lewis acidic properties and applications ranging from anion carriers to catalysts, supramolecular materials, frustrated Lewis pairs, and activators for Ziegler–Natta polymerization.[5–14] While triarylboranes with well-known propeller-like structures are prototypical Lewis acids, two electronic and structural factors, known as reorganization energy and π-backdonation, can drastically modify their Lewis acidity and lead to novel classes of boron Lewis acids with unforeseen properties.[15–25] By constraining the central boron and substituents into a planar shape, the reorganization energy and π-backdonation are increased, leading to reduced Lewis acidity at boron.[26,27] In contrast, constraining the boron atom into a pyramidal trigonal geometry decreases the reorganization energy and π-backdonation, drastically increasing the boron Lewis acidity.[18,22]

Since 2012, increasing attention has been devoted to non-planar Lewis acids since quantum chemical calculations highlighted the 9-boratriptycene and its group XIII analogues for their extraordinary Lewis acidity and potential for the activation and complexation of unreactive small molecules.[18,20,28,29] It has been reported that, by preventing p–π- conjugation while lowering the reorganization energy with a pre-pyramidalized boron compound, the Lewis acidity of perfluorinated triarylboranes can be reached without the introduction of electron-withdrawing substituents.[30] Using the 9-boratriptycene **6.1** as reference, we demonstrated that switching from carbon to a cationic

phosphorous bridgehead triptycene scaffold **6.2** leads to a dramatic increase in Lewis acidity, approaching and even surpassing triarylsilylium species.[31] Very recently, we reported the generation of the transient sulfonium-bridged analogue **6.3** of the 9-boratriptycene **6.1** and, for the first time, the high reactivity of such peculiar species in several challenging chemical transformations.[32] With a Lewis acidity further exceeding the previously reported 9-boratriptycene derivatives, the sulfonium derivative showed a propensity to activate several strong and weakly reactive bonds such as Csp^2–H, Csp^3–H, Csp^3–Csp^3, and Csp^3–Si bonds.

In the context of the development of new pyramidal organoboranes and of the investigation of the structural features affecting the Lewis acidity of such pyramidal boron Lewis acids, we have been stimulated to synthesize a selenium derivative of the 9-boratriptycene. With similar electronegativity as sulfur but with a 35% longer atomic radius leading to longer C–Se than C–S bonds, the replacement of a sulfur bridgehead triptycene with a selenium one will lead to decreased pyramidalization at the boron atom.[33,34] Such single modification will allow the impact of a modification of the boron pyramidalization on the Lewis acidity of 9-boratriptycene derivatives to be directly evaluated (**Figure VI.38**).

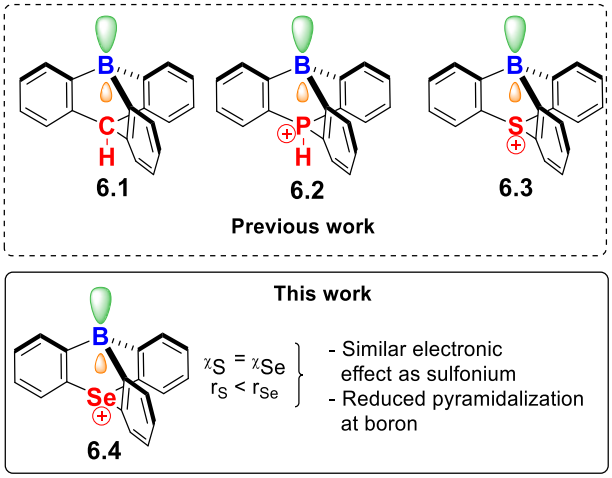
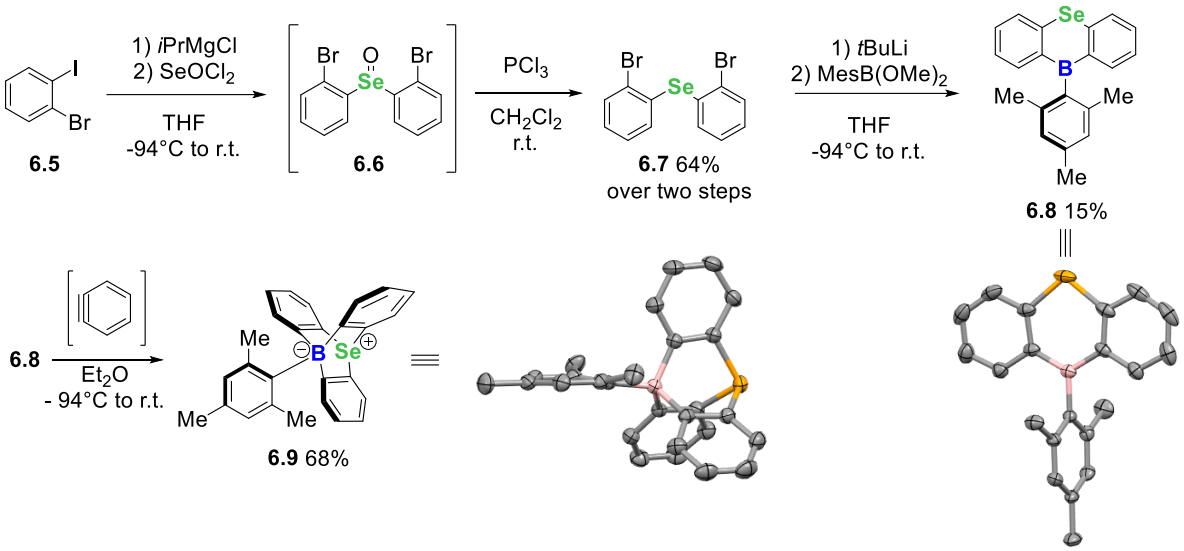


Figure VI.38 : Previous work on 9-boratriptycene derivatives and new selenenium derivative in this work.

VI.2. Synthesis of precursors and and generation of the 9-selenenium-10-boratriptycene.

Although prepared for the first time in 1929, the chemistry of selenenium and especially triarylselenenium species is relatively underdeveloped.[34] Without any established procedure, we decided to transpose our recently reported strategy to produce **6.3** for reaching the selenenium derivative **6.4**. The synthesis started with the reaction of 2-bromophenyl Grignard reagent with selenium oxychloride followed by reduction of the formed selenoxide **6.6** with PCl_3 to produce **6.7** (**Scheme VI.90**). The triarylborane **6.8** was prepared from bis(2-bromophenyl)selenide **6.7** with reduced yield compared to the sulfur derivative. The borane then undergoes a [4+2] cycloaddition with *in-situ* generated benzyne to form the triptycene scaffold, providing the mesityl-boron-ate complex **6.9** in good yield. Its structure was unambiguously confirmed by a single-crystal X-ray diffraction analysis. Unlike as for the triarylborane **6.8**, the borate **6.9** was obtained with a similar yield to that of the sulfonium analogue of **6.9** which may come from higher nucleophilicity of the selenium in the

precursor **6.8**, due to reduced π-conjugation between selenium and sp^2-hybridized carbon atoms, compared to sulfur.[34]



Scheme VI.90 : Synthesis of 10-mesityl-10***H***-9-selena-boraanthracene **6.8** and cycloaddition with benzyne to form 10-mesityl-9-selenenium-10-boratriptycene-ate complex **6.9** and their respective molecular structures.

X-ray diffraction analysis allowed the evaluation of the boron atom pyramidalization which is defined by the distance between the boron atom and the plane spanned by the three *ipso*-carbon atoms of the triptycene scaffold. With a distance of [0.703 Å], the selenenium derivative **6.9** is significantly less pyramidalized than the reported sulfonium analogue [0.678 Å], due to the longer C–Se bonds (mean value 1.928 Å) at the bridgehead position of the triptycene scaffold (**Figure VI.39**) compared to C–S bonds (mean value 1.789 Å).

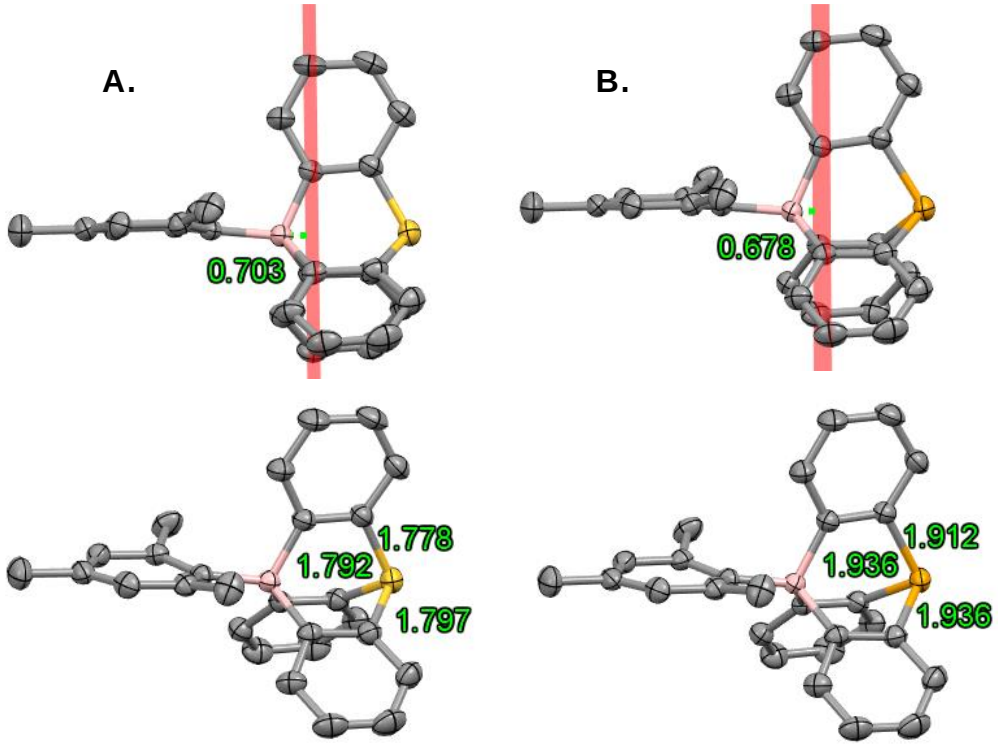
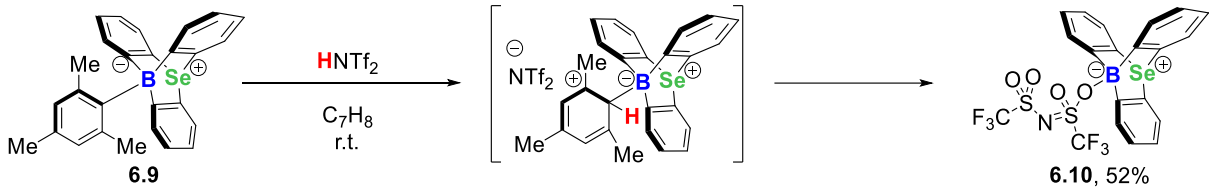


Figure VI.39 : Molecular structures of the **A.** 10-mesityl-9-sulfonium-10-boratriptycene-ate complex and **B.** ate-complex **6.9**, demonstration of the pyramidalization correlated with C–S or C–Se bond length. H-atoms and solvate molecules are omitted for clarity; thermal ellipsoids are represented with 50% probability level; bond lengths [Å].

The treatment of selenium-borate **6.9** with triflimidic acid led to clean *ipso*-protonation of the mesityl moiety followed by release of mesitylene and formation of the boron-triflimidate complex **6.10** (**Scheme VI.91**) as a mixture of *O*- and *N*-isomer with a 93:7 ratio as determined by ^{19}F NMR spectroscopy. Although the *O*-isomer is the thermodynamic product, this apparent excellent selectivity is surprising as an 87:13 isomer ratio is obtained with the sulfonium derivative. This might be explained by a reduced Lewis acidity of the selenenium derivative compared to the sulfonium one, leading to the favored formation of the thermodynamic product. The slightly increased steric hindrance around the boron atom coming from the orientation of the *ortho*-hydrogen atoms, pointing slightly more towards the boron in the selenenium derivative than in the sulfonium one, might also lead to the preferred formation of

the

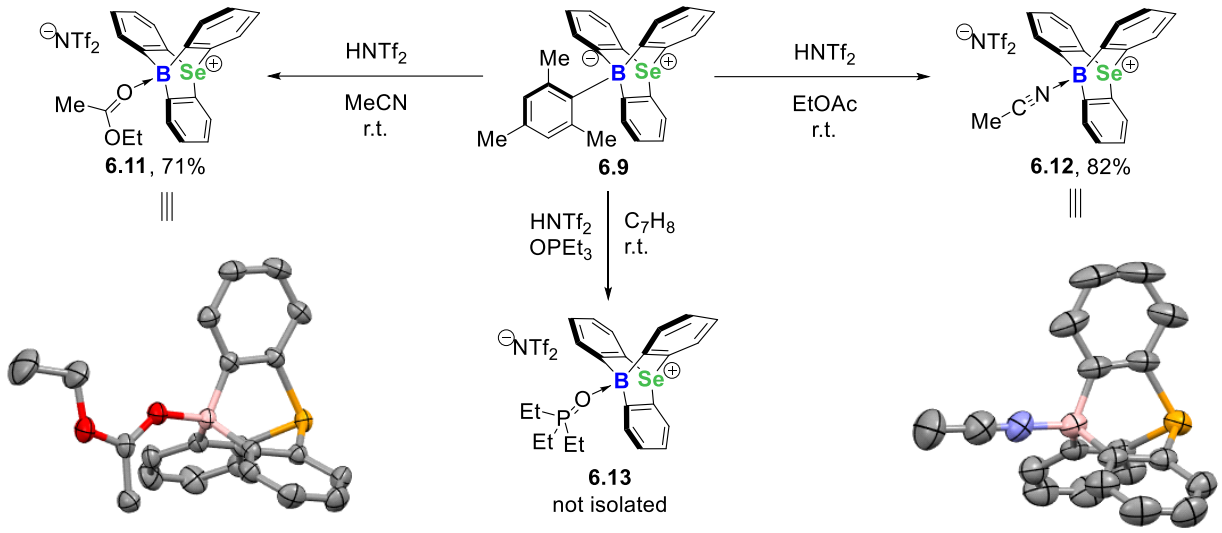
O-isomer, being less sterically demanding. After purification, only the *O*-isomer could be obtained with 52% yield, demonstrating the exceptional ability of 9-selenenium-10-boratriptycene to bind weakly coordinating anions.



Scheme VI.91 : Protodeborylation of **6.9** with $HNTf_2$ and formation of 10-tri-flimidate-9-selenenium-10-boratriptycene-ate complex **6.10**

VI.3. Evaluation of the 9-selenenium-10-boratriptycene Lewis acidity.

Performing the protodeborylation in ethyl acetate or acetonitrile, respectively, as reaction solvent provided the corresponding Lewis adducts **6.11** and **6.12** (**Scheme VI.92**) which were unambiguously characterized by X-ray diffraction analysis. In the solid state, a B–O bond of 1.541(3) Å is calculated, slightly longer than the sulfonium derivative (1.537(9) Å) although shorter than the phosphonium derivative (1.548(3) Å).[31,32]



Scheme VI.92 : Formation of the Lewis adducts **6.11, 6.12, 6.13** via protodeborylation of **6.9** and molecular structures of **6.11** and **6.12,** counter-anion and hydrogen atoms have been omitted for clarity.

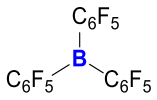
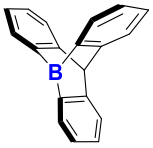
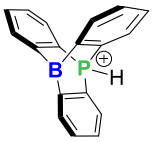
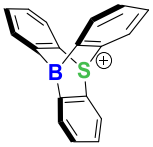
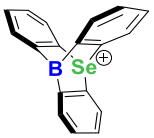
IR spectroscopy showed that the CN stretching vibration of **6.12** (2373 cm^{-1}) is slightly higher to that of **6.3** (2345 cm^{-1}),[32] whereas the $\nu_{C=O}$ of **6.11** (1592 cm^{-1}) is similar to that of **6.2**-EtOAc (1580 cm^{-1}),[31] suggesting similar Lewis acidic properties. A closer look at the carboxyl moiety of the coordinated ethyl acetate moiety revealed that the C=O bond is elongated (1.263(3) Å) compared to free ethyl acetate (1.203 Å)[35–37] while the carbonyl C–O bond (1.288(3) Å) is considerably shortened (1.345 Å).[38] In such Lewis adduct, the ethyl acetate is therefore electronically and geometrically closer to an oxocarbenium species than a classical carbonyl.[39] The ^{31}P NMR measurement of the Lewis adduct with $OPEt_3$, generated *in-situ* with $HNTf_2$ in presence of $OPEt_3$ in CD_2Cl_2, showed a chemical shift of $\delta = 80.5$, corresponding to an acceptor number (AN) of 87 following the Gutmann–Beckett method,[40] thus exceeding the Lewis acidity of tris(perfluorotolyl)borane (AN = 85) and approaching that of cationic electrophilic phosphonium $[(C_6F_5)_3PF]^+$ (AN=89).[41–45] The Lewis acidity value obtained with the Gutmann–

Beckett method put the selenenium derivative between the phosphonium and the sulfonium ones, in line with the ν_{CN} values.

All quantum chemical calculations were performed by Dr. Aurélien Chardon. Upon coordination with NH_3 a RE of 51 kJ mol^{-1} is calculated for **6.4**, which is slightly higher than in **6.3** and consistent with the reduce pre-pyramidalization of the boron atom in **6.4**. Expectedly, the RE increase up to 90 and 91 kJ mol^{-1} upon coordination with F^- and H^- respectively (**Table VI.13**). Accordingly, the NH_3, FIA, and HIA affinities are slightly lower in the case of **6.4** but still comparable to that of 9-sulfonium-10-boratriptycene **6.3** (**Table VI.13**). This is showing that the reduced prepyramidalization of the boron atom in **6.4**, even if inducing a slightly higher RE upon complexation with Lewis bases, has only a limited impact on the Lewis acidic properties of **6.4**. Since coulombic attraction and charge effects contribution are reduced in condensed phases, the non-isodesmic FIA of **6.3** and **6.4** have also been calculated in CH_2Cl_2 and showed an expected substantial reduction of the initial gas-phase values from 854 to 521 kJ mol^{-1} and from 845 to 512 kJ mol^{-1} for **6.3** and **6.4** respectively (**Table VI.13**).

The slightly reduced Lewis acidity of the 9-selenenium-10-boratriptycene compared to sulfonium derivative provides qualitative evidences that the pyramidalization at the boron atom affects the Lewis acidity of boratriptycene derivatives. Even though the longer C–Se bonds than C–S induces structural reorganization leading to increased steric hindrance on the boron atom, due to *ortho*-hydrogen atoms pointing towards the boron atom, the impact on the determined Lewis acidity could be neglected due to the limited size of the Lewis bases used as probes.

Table VI.13 : Pyramidalization Angle Derived from Quantum Chemical Calculation Using the M06-2X Exchange-Correlation Functional and the 6-311G(d) Atomic Basis Set[a].

		 6.1	 6.2	 6.3	 6.4
α^{b}	0°	15.5°	13.9°	13.4°	12.7°
Acceptor number	85	77	84.7	88.4	87
RE:[d] F^-	132	87	83	88	90
RE:[d] H^-	144	92	92	89	91
RE:[d] NH_3	97	45	45	49	51
FIA[e] (ΔH_0/kJ·mol^{-1})	466	476	845 (513)	854 (521)	845 (512)
HIA[e] (ΔH_0/kJ·mol^{-1})	516	496	871	880	869 (438)
NH_3 (ΔH_0/kJ·mol^{-1})	159	159	263	263	256

[a] Values in parenthesis correspond to non-isodesmic values in CH_2Cl_2 (IEFPCM solvation model).
[b] α is the pyramidalization angle, as defined by the angle between one Ar-B bond and the plane formed by the 3 triptycene ipso carbon atom.
[c] Calculated acceptor number derived from ^{31}P NMR measurements with $OP(Et)_3$ as Lewis base probe.
[d] Gas phase reorganization energies (RE) upon complexation with Lewis bases and hydride, fluoride and ammonia affinities $-\Delta H^0$ (kJ mol^{-1}).
[e] Pseudo-isodesmic reactions have been used, with the HIA of $HSiMe_3$ and FIA of $FSiMe_3$ as the anchor point evaluated at the G3 reference level.[46][47][48]

VI.4. Conclusion

In conclusion, demonstration has been made a few years ago that constraining an archetypal planar triarylborane into a pyramidal organization leads to a drastic increase of Lewis acidity. This was illustrated with the 9-boratriptycene **6.1** and the cationic phosphonium **6.2** and sulfonium **6.3** derivatives presented a strong propensity to borylate inert C–H bonds. Despite understanding the factors affecting the Lewis acidity of boranes, exclusively modifying a single one without affecting the other remains a complex undertaking. Here we describe the synthesis and characterization of a selenenium derivative of the 9-boratriptycene

family. With reduced pyramidalization of the boron atom and similar electronegativity of the selenium with respect to sulfur, this provides a deeper understanding of how the pyramidalization of the boron atom affects the Lewis acidity.

VI.5. References

[1] A. Wakamiya, S. Yamaguchi, *Bull. Chem. Soc. Jpn.* **2015**, *88*, 1357–1377.
[2] W. E. Piers, *Adv. Organomet. Chem.* **2005**, *52*, 1–76.
[3] W. E. Piers, T. Chivers, *Chem. Soc. Rev.* **1997**, *26*, 345–354.
[4] S. M. Berger, M. Ferger, T. B. Marder, *Chem. Eur. J.* **2021**, *27*, 7043–7058.
[5] M. A. Légaré, C. Pranckevicius, H. Braunschweig, *Chem. Rev.* **2019**, *119*, 8231–8261.
[6] M. Li, J. S. Fossey, T. D. James, *Boron: Sensing, Synthesis and Supramolecular Self-assembly*, RSC, Cambridge, **2015**.
[7] C. R. Wade, A. E. J. Broomsgrove, S. Aldridge, F. P. Gabbaï, *Chem. Rev.* **2010**, *110*, 3958–3984.
[8] G. Erker, *Dalton Trans.* **2005**, 1883–1890.
[9] F. Jäkle, *Chem. Rev.* **2010**, *110*, 3985–4022.
[10] A. Lorbach, A. Hübner, M. Wagner, *Dalton Trans.* **2012**, *41*, 6048–6063.
[11] L. Ji, S. Griesbeck, T. B. Marder, *Chem. Sci.* **2017**, *8*, 846–863.
[12] M. Hirai, N. Tanaka, M. Sakai, S. Yamaguchi, *Chem. Rev.* **2019**, *119*, 8291–8331.
[13] D. W. Stephan, G. Erker, *Angew. Chem. Int. Ed.* **2010**, *49*, 46–76.
[14] D. W. Stephan, *Science* **2016**, *354*, 1248–1256.
[15] B. D. Rowsell, R. J. Gillespie, G. L. Heard, *Inorg. Chem.* **1999**, *38*, 4659–4662.
[16] F. Bessac, G. Frenking, *Inorg. Chem.* **2003**, *42*, 7990–7994.
[17] K. M. Marczenko, J. A. Zurakowski, M. B. Kindervater, S. Jee, T. Hynes, N. Roberts, S. Park, U. Werner-Zwanziger, M. Lumsden, D. N. Langelaan, S. S. Chitnis, *Chem. Eur. J.* **2019**, *25*, 16414–16424.
[18] L. A. Mück, A. Y. Timoshkin, G. Frenking, *Inorg. Chem.* **2012**, *51*, 640–646.
[19] E. I. Davydova, T. N. Sevastianova, A. Y. Timoshkin, *Coord. Chem. Rev.* **2015**, *297–298*, 91–126.
[20] D. Mahaut, A. Chardon, L. Mineur, G. Berionni, B. Champagne, *ChemPhysChem* **2021**, *22*, 1958–1966.
[21] M. Henkelmann, A. Omlor, M. Bolte, V. Schünemann, H.-W. Lerner, J.

Noga, P. Hrobárik, M. Wagner, *Chem. Sci.* **2022**, *13*, 1608–1617.
[22] A. Chardon, A. Osi, D. Mahaut, A. Ben Saida, G. Berionni, *Synlett* **2020**, *31*, 1639–1648.
[23] F. Ebner, H. Wadepohl, L. Greb, *J. Am. Chem. Soc.* **2019**, *141*, 18009–18012.
[24] F. Ebner, L. Greb, *Chem* **2021**, *7*, 2151–2159.
[25] M. B. Kindervater, K. M. Marczenko, U. Werner-Zwanziger, S. S. Chitnis, *Angew. Chem. Int. Ed.* **2019**, *58*, 7850–7855.
[26] Z. Zhou, A. Wakamiya, T. Kushida, S. Yamaguchi, *J. Am. Chem. Soc.* **2012**, *134*, 4529–4532.
[27] T. Kushida, C. Camacho, A. Shuto, S. Irle, M. Muramatsu, T. Katayama, S. Ito, Y. Nagasawa, H. Miyasaka, E. Sakuda, N. Kitamura, Z. Zhou, A. Wakamiya, S. Yamaguchi, *Chem. Sci.* **2014**, *5*, 1296–1304.
[28] L. A. Mück, A. Y. Timoshkin, M. Von Hopffgarten, G. Frenking, *J. Am. Chem. Soc.* **2009**, *131*, 3942–3949.
[29] A. Y. Timoshkin, K. Morokuma, *Phys. Chem. Chem. Phys.* **2012**, *14*, 14911.
[30] A. Chardon, A. Osi, D. Mahaut, T. H. Doan, N. Tumanov, J. Wouters, L. Fusaro, B. Champagne, G. Berionni, *Angew. Chem. Int. Ed.* **2020**, *59*, 12402–12406.
[31] A. Ben Saida, A. Chardon, A. Osi, N. Tumanov, J. Wouters, A. I. Adjieufack, B. Champagne, G. Berionni, *Angew. Chem. Int. Ed.* **2019**, *58*, 16889–16893.
[32] A. Osi, D. Mahaut, N. Tumanov, L. Fusaro, J. Wouters, B. Champagne, A. Chardon, G. Berionni, *Angew. Chem. Int. Ed.* **2022**, *61*,e202112342.
[33] D. Perrone, M. Monteiro, J. C. Nunes, *Selenium: Chemistry, Analysis, Function and Effects, Chaptre 1*, RSC, London, **2015**.
[34] T. Wirth, *Organoselenium Chemistry*, Wiley VCH, **2011**.
[35] M. F. Lappert, *J. Chem. Soc.* **1962**, 542–548.
[36] I. R. Beattie, T. Gilson, *J. Chem. Soc.* **1964**, 2292–2295.
[37] K. F. Purcell, R. S. Drago, *J. Am. Chem. Soc.* **1966**, *88*, 919–924.
[38] R. J. Woods, C. W. Andrews, J. P. Bowen, *J. Am. Chem. Soc.* **1992**, *114*, 859–864.
[39] J. Andres, A. Arnau, J. Bertran, E. Silla, *J. Mol. Struct.* **1985**, *120*, 315–320.
[40] I. B. Sivaev, V. I. Bregadze, *Coord. Chem. Rev.* **2014**, *270–271*, 75–88.
[41] U. Mayer, V. Gutmann, W. Gerger, *Monatsh. Chem.* **1975**, *106*, 1235–1257.
[42] V. Gutmann, *Coord. Chem. Rev.* **1976**, *18*, 225–255.
[43] M. A. Beckett, G. C. Strickland, J. R. Holland, K. Sukumar Varma, *Polymer* **1996**, *37*, 4629–4631.
[44] P. Erdmann, L. Greb, *Angew. Chem. Int. Ed.* **2022**, *61*, e202114550.
[45] D. Roth, J. Stirn, D. W. Stephan, L. Greb, *J. Am. Chem. Soc.* **2021**,

143, 15845–15851.
[46] Y. Zhao, D. G. Truhlar, *Theor. Chem. Acc.* **2008**, *120*, 215–241.
[47] H. Böhrer, N. Trapp, D. Himmel, M. Schleep, I. Krossing, *Dalton Trans.* **2015**, *44*, 7489–7499.
[48] L. Greb, *Chem. Eur. J.* **2018**, *24*, 17881–17896.

Chapter VII

General Conclusions and Perspectives

VII.1. Conclusion

This work was dedicated to the development of non-planar boron Lewis acids which represent an underdeveloped class of Lewis acids with predicted remarkable reactivity and Lewis acidic properties. More specifically, attention was devoted to the development of 9- and 10-boratriptycenes which are cage-shaped non-planar triarylboranes in which a boron atom is embedded in the bridgehead position of a triptycene scaffold. Concomitantly with the beginning of this thesis, the synthesis of a member of the boratriptycene family was reported by Sawamura and co-workers and Berionni and co-workers respectively.[1,2] However, the 9-phosphonium-10-boratriptycene was only reported under the form of Lewis adducts or boron-ate complexes with Lewis bases, only providing a glimpse of its reactivity.

The research started with the synthesis of the parent 9-boratriptycene which consists in the "simplest" boratriptycene derivative with a structure containing only a single boron atom as heteroatom. A bench stable and storable precursor could be obtained under the form of a 9-aryl-9-boratriptycene-ate complex which undergoes fast and clean generation of the Lewis acid by protodeborylation in presence of a Brønsted superacid (**Figure VII.40, A, B**). It was observed that, in solution, the free Lewis acid, formed by protodeborylation reaction, was in equilibrium with complexes formed with the solvent and the weakly coordinating triflimidate ion (**Figure VII.40, B**).[3] Despite extensive efforts, the free 9-boratriptycene could not be isolated. This experimental work supported by a complete DFT study performed by Damien Mahaut allowed to rationalize the origin and the parameters influencing the exceptional Lewis acidity of the 9-boratriptycene and its derviatives. Previous DFT studies predicted that the increased Lewis acidity compared to other triarylboranes came from the preorganized pyramidal geometry of the boron atom which lead to reduced

reorganization energy upon coordination with a Lewis base (**Figure VII.40, C**).[4] This feature was confirmed with our work but it was additionally demonstrated that the absence of π–p_z-conjugation plays a key role in the increased Lewis acidity (**Figure VII.40, D**).

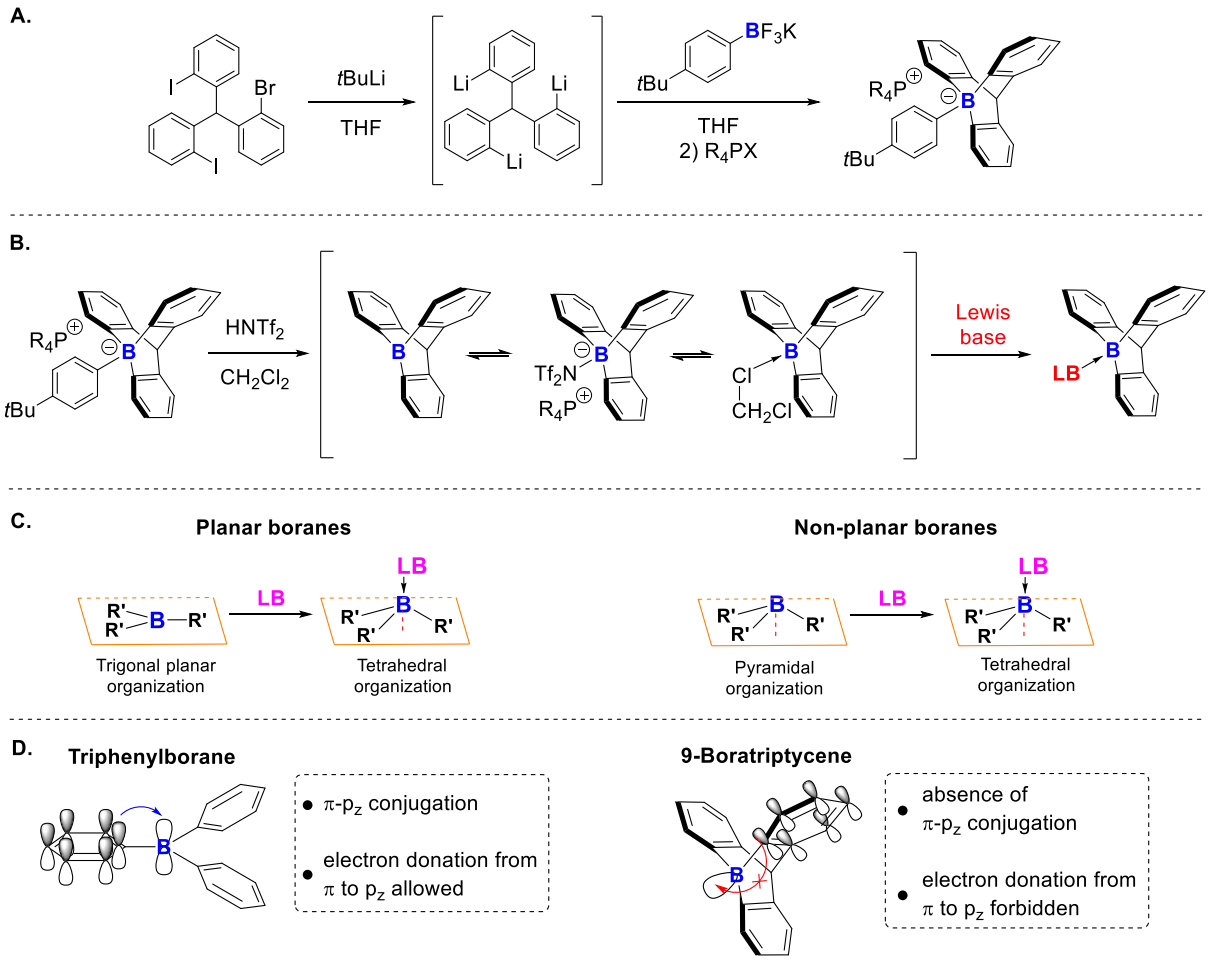


Figure VII.40 : **A.** Synthesis of 9-aryl-9-boratriptycene-ate complex, **B.** Generation of the 9-boratriptycene, **C.** Illustration of the reorganization energy for planar and non-planar boranes, **D.** Illustration of presence and absence of π–p_z-conjugation in triphenylborane and 9-boratriptycene.

Unfortunately, once *in-situ* generated, the 9-boratriptycene was difficult to handle due to its propensity to bind traces of water and immediately decompose via protodeborylation. This prompt us to develop a new boratriptycene derivative which would exhibit greater stability toward protodeborylation of the triptycene scaffold.

The 9-phosphonium-10-boratriptycene being already described, we decided to switch from phosphorus to sulfur in bridgehead position. Attention was then devoted to the synthesis of 9-sulfonium-10-boratriptycene, the sulfonium bridgehead allowing a significant increase of Lewis acidity while preventing protodeborylation of the triptycene scaffold by reducing the electron density on the aromatic rings. Once again, a bench stable precursor of the Lewis acid was synthesized, allowing clean and fast generation upon protodeborylation with Brønsted superacids (**Figure VII.41, A**). Due to the extreme Lewis acidity of this 9-sulfonium-10-boratriptycene, which reaches the one of silylium ions, strong and stable boron-ate complexes are formed even with weakly coordinating anions such as triflimidate of triflide ions, precluding the isolation of the free Lewis acid.[5]

Attempts to isolate the donor-free 9-sulfonium-10-boratriptycene by boron-to-carbon hydride transfer or boron-to-silicon fluoride transfer led to the formation of bench stable hydride- or fluoride-bridged dimer respectively (**Figure VII.41, B**, **C**). A deeper investigation led to the conclusion that the unexpected stability of the bridged dimers and boron-ate complexes with WCA came from a steric protection of the σ*-B–X (X=WCA) orbital due to the triptycene scaffold. This protection precludes any substitution at the boron center and requires the transient formation of the free Lewis acid prior to the formation of a new Lewis adduct or boron-ate complex (**Figure VII.41, D**). Furthermore, additional experiments suggested that the donor-free 9-sulfonium-10-boratriptycene could not be isolated and could only exist in solution as a transient species in equilibrium with Lewis adducts or boron-ate complexes.

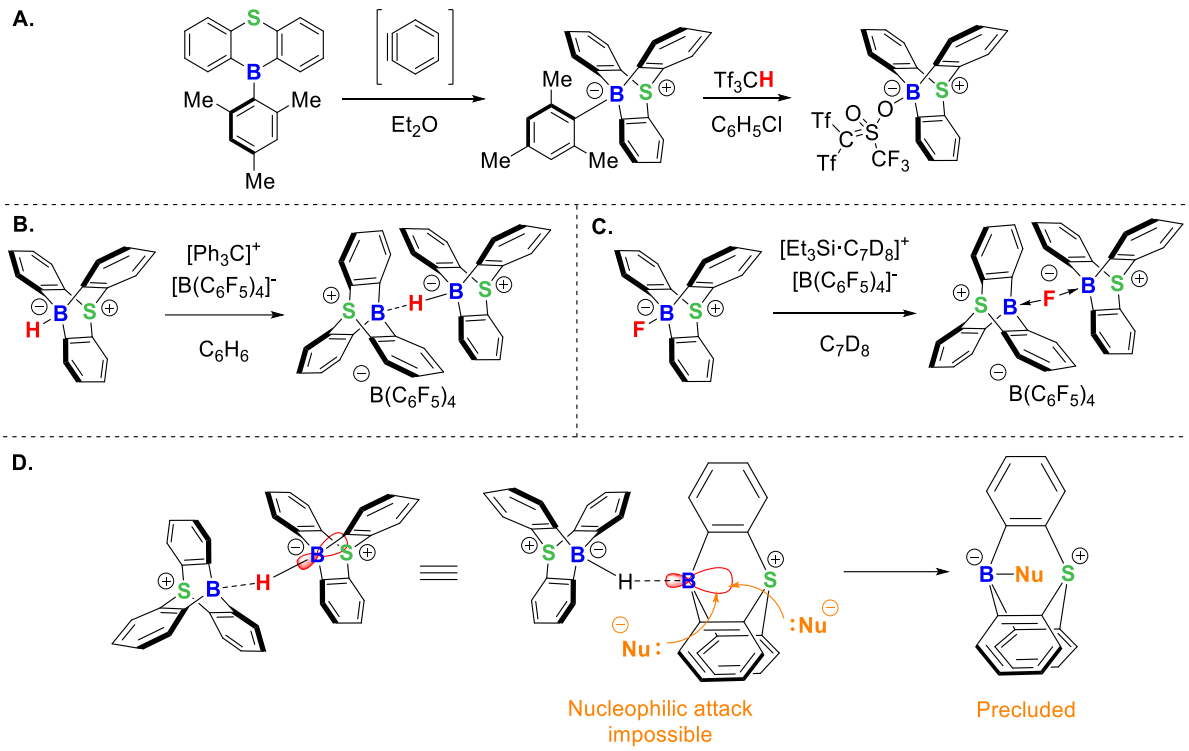


Figure VII.41 : **A.** Synthesis of 9-sulfonium-10-boratritycene precursor and protodeborylation with triflidic acid, **B.** Boron-to-carbon hydride transfer and formation of the hydride-bridged dimer, **C.** Boron-to-silicon fluoride transfer and formation of the fluoride-bridged dimer, **D.** Illustration of the kinetic protection.

While attempting to generate the donor-free 9-sulfonium-10-boratriptycene, the propensity of this Lewis acid to perform Csp^2–H borylation of arenes was observed. A full optimization of the reaction conditions was then performed, and a scope of aromatic substrates was developed (**Figure VII.42, A**). Meanwhile, the initial objective of performing Csp^2–F abstraction reactions was set aside considering the propensity of the 9-sulfonium-10-boratriptycene to borylate fluorinated arenes instead of performing Csp^2–F abstraction. Using readily available boron Lewis acids and commercially available cheap reagents, this method allows the borylation of unactivated arenes such as benzene and alkyl-substituted benzene derivatives as well as electron depleted haloarenes such as 1,2-dichlorobenzene.

The Lewis acid used as borylating agent showing a unique reactivity, a full mechanistic investigation was performed experimentally and a complementary DFT study was performed by Dr. Aurélien Chardon to elucidate the mechanism of this reactions. This mechanistic investigation confirmed that the 9-sulfonium-10-boratriptycene is never present as a trivalent species, but forms σ- and π-complexes that are in equilibrium with each other in the reaction medium. After expanding the scope of substrates and obtaining a series of boron-aryl-ate complexes, their functionalization was attempted. In a first instance, regioselective mono-fluorination and chlorination reactions were attempted and remained unsuccessful regardless of the chlorinating or fluorinating agent used. Every attempt led to absence of conversion, complete decomposition of the starting material or unselective functionalization. Against all odds, Suzuki-Miyaura coupling reactions also failed using 10-aryl-9-sulfonium-10-boratriptycene-ate complexes as substrates, leading to complete recovery of the starting material. This absence of reactivity is likely due to the triptycene scaffold and the impossibility of the aryl-ate complex to *in-situ* hydrolyze into the corresponding aryl-boronic acid. Finally, regioselective mono-deuteration were attempted via deuterodeborylation of the 10-aryl-9-sulfonium-10-boratriptycene-ate complexes. Using deuterated Brønsted superacid $DNTf_2$, several substrates could be regioselectively mono-deuterated (**Figure VII.42, B.**). Despite the inapplicability of the deuteration methodology to the more electron rich substrates of our borylation scope, several xylene and haloarene derivatives could be regioselectively deuterated with good yields.

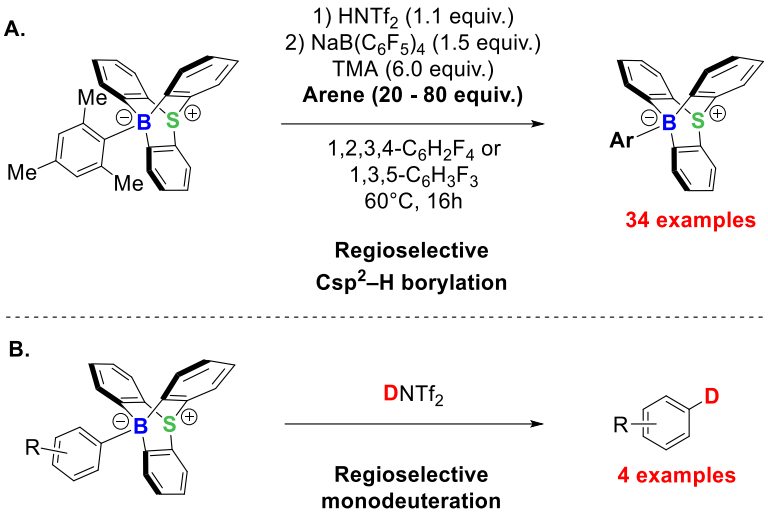
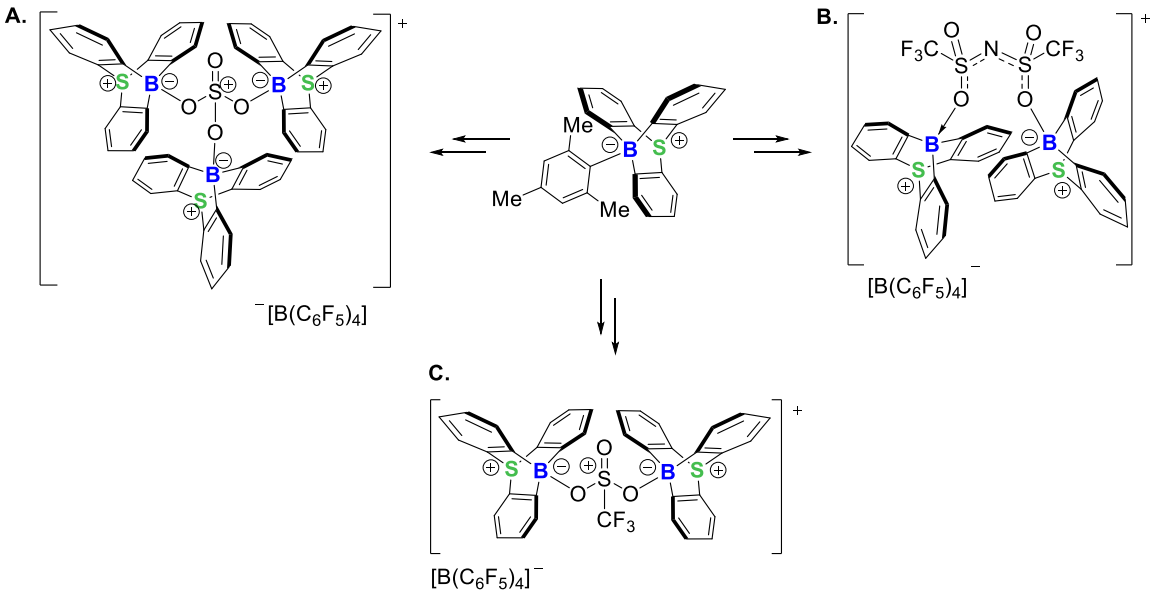


Figure VII.42 : **A.** Optimized conditions of Csp^2–H borylation of arenes and **B.** Regioselective monodeuterations of aryl-boron-ate complexes.

This work provides a new transition-metal-free Csp^2–H borylation methodology and stands as the first examples of Csp^2–H borylation using a triarylborane as electrophilic borylating agent. The mechanistic study provides new insights into the reactivity of the 9-boratriptycene Lewis acids. This revealed that these boron Lewis acids have a greater propensity to form σ- and π-complex with aromatic species than to form stable Lewis adduct with Lewis bases. These results obtained via the mechanistic investigation and during the functionalization part, once again demonstrated that embedding a boron atom into a triptycene scaffold confers to the boron atom a unique reactivity which is partially due to the steric protection of one lobe of the empty p_z-orbital, when the acid is considered "free", and the σ^*-orbital, when considering a Lewis adduct or "ate"-complex. This might provide new insights for considering electrophilic borylation reactions as well as the mechanism of Lewis acid-base exchanges in general.

Despite the 9-sulfonium-10-boratriptycene could not be isolated as donor-free nor as a boron-ate complex with a carborate ion, its propensity to bind WCA could be exploited. Borylated equivalents of protonated sulfuric, triflic and triflimidic acid could be synthesized (**Scheme VII.93**). The tris-

borylated sulfate and bis-borylated triflimidate are remarkably stable in solution and ambient conditions, once again demonstrating the steric protection of the σ^* B–X orbital, already discussed. Complementary DFT analysis were performed by Dr. Aurélien Chardon for evaluating the charge density on the boron and sulfur atoms of these complexes. The FIA of these species was also evaluated, revealing exceptional Lewis acidities, in the range of $B(C_6F_5)_3$, for bench stable species.



Scheme VII.93 : **A.** Tris-borylated sulfate, **B.** Bis-borylated triflimidate and **C.** Bis-borylated triflate.

As presented in Chapter II, two major factors are linked to the increased Lewis acidity of 9-boratriptycene derivatives compared to classical triaryl boranes: 1) the prepyramidalization of the boron atom reducing the reorganization energy upon coordination with a Lewis base and 2) the absence of π–p_z-conjugation. In order to isolate the impact of the boron atom prepyramidalization on the Lewis acidity, we decided to synthesize the 9-selenenium-10-boratriptycene. Indeed, with an increased atomic radius and almost identical electronegativity compared to sulfur, switching from sulfur to selenium in the bridgehead position would only impact the

pyramidalization of the boron atom. The 9-selenenium-10-boratriptycene was then synthesized with a similar methodology as the sulfonium derivative and its Lewis acidity was evaluated experimentally and *via* DFT investigation, performed by Dr. Aurélien Chardon (**Figure VII.43**).[6] As predicted, a slightly decreased Lewis acidity is observed compared to the sulfonium derivative. These results suggest that the pyramidalization is a crucial parameter for explaining the increased Lewis acidity of the 9- and 10-boratriptycene derivatives, however the degree of pyramidalization is not proportional to the increase of Lewis acidity.

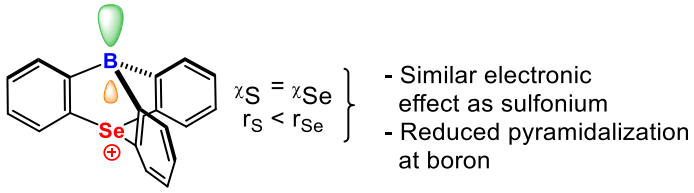


Figure VII.43 : Influence of replacement of the sulfonium by selenenium bridgehead.

The results obtained during this thesis led to the publication of several articles in high impact factor journals and shed light on non-planar boranes and especially 9- and 10-boratriptycene derivatives which, before this work, were only theoretical curiosities. Before this work, the only pyramidal boron Lewis acid was 1-boraadamantane which was mostly used as Lewis adduct and its reactivity as Lewis acid remained underexplored. With the synthesis and complete study of these species, a deeper understanding of the factors influencing the Lewis acidity of boranes in general was provided. With this work, we demonstrated that structural deformation of the Lewis acid has a similar and even stronger impact on Lewis acidity than strong electron withdrawing substituents. This additional knowledge could help the design of future Lewis acids by allowing a fine tuning of their properties according to the desired applications. This work on the factors influencing the Lewis acidity of boron compounds could also influence other aspects of boron chemistry by allowing to predict more precisely the properties of novel organoboron compounds based on their structure. More generally, this work

provides new insights into the structure-properties relationship of Lewis acids.

As it was demonstrated that the cage-shaped scaffold allows a fantastic steric stabilization of the Lewis acidic center, it can easily be envisioned to use this interesting property to modify the reactivity of a wide variety of species, far beyond the field of Lewis acids. Indeed, constraining a reactive center into a cage-shaped structure for increasing its stability towards nucleophilic substitution reaction is a concept that might find applications far beyond the field of Lewis acids.

This work takes part to and feeds a research area that has been extensively carried out between the 70’s and 90’s then almost ignored since 2010’s. This work helped to regain interest for boron Lewis acids and most widely for main-group compounds exhibiting unusual geometries.

VII.2. Perspectives

The first and most obvious perspective would be to further extend the 9- and 10-boratriptycenes family. However, considering the work presented in this thesis on the Lewis acidic properties of 9- and 10-boratriptycenes, it might also be of interest to investigate the properties and reactivity of the heteroatom in bridgehead position (**Figure VII.44**).

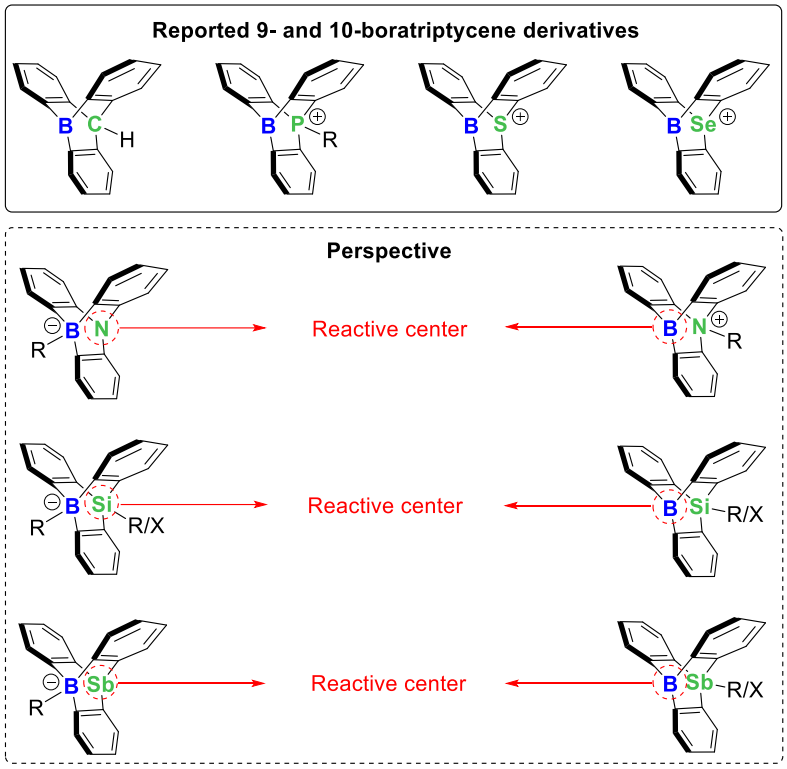


Figure VII.44 : Perspectives of extension of 9- and 10-boratriptycene family.

An important perspective of this work concerns the pursuit of the Csp^2–H borylations and functionalizations. A complementary computational evaluation would be of interest to determine if a Brønsted base could perform better than *N*,*N*,3,5-tetramethylaniline. Indeed, one of the identified limitations for the borylation of strongly electron depleted haloarenes is the competition between the Csp^2–H borylation and the formation of the Lewis adduct. Even though several Brønsted bases have already been screened, a

computational screening of other Brønsted bases being more hindered to reduce the association with the 9-sulfonium-10-boratritpycene while allowing a fast deprotonation of the arenium ion once it is formed. Additionally, an investigation of the impact of substituents *ortho* to the boron atom on the Csp^2–H borylation could also be of interest (**Figure VII.45**).

Considering the introduction of substituents on the triptycene scaffold, it might also be of interest to introduce electron-withdrawing substituents on the aromatic rings of the triptycene scaffold. This might increase the Lewis acidity of the boron Lewis acid while further reducing its propensity to undergo protodeborylation of the triptycene scaffold. These modifications and optimizations could allow to further reduce the amount of arene substrate required for the borylation reaction, increasing the interest of the method.

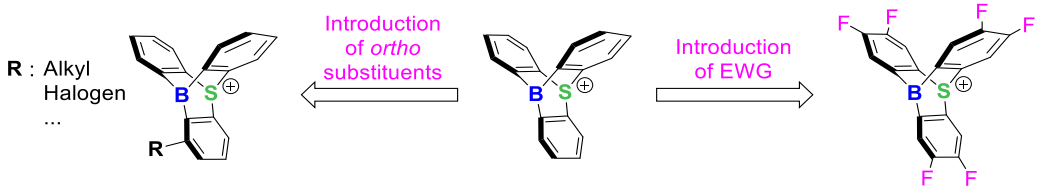
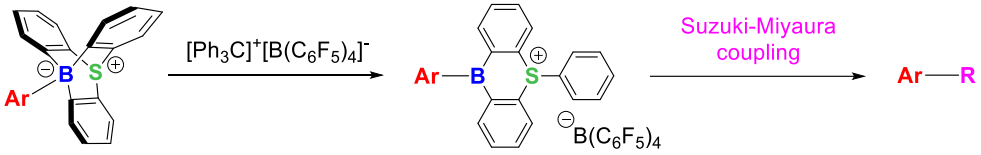


Figure VII.45 : Perspective of triptycene scaffold functionalization.

Considering the functionalization of the exocyclic ring from our 10-aryl-9-sulfonium-10-boratriptycene-ate complexes, it might be of interest to attempt Suzuki-Miyaura coupling in the conditions developed by Carrow and co-workers.[7,8] It might also be envisioned to use a very particular reactivity observed when treating 10-mesityl-9-sulfonium-10-boratriptycene-ate complex with tritylium ion or 2,6-dibromopyridinium tetrakis(pentafluorophenyl)borate. As previously mentioned, under these conditions a breaking of a C–B bond from the triptycene scaffold is observed. This reactivity could be used for allowing the functionalization of the exocyclic ring via Suzuki-Miyaura coupling for example (**Scheme VII.94**).

The opening of the triptycene scaffold could reduce the steric hindrance around the reactive boron center while the sulfonium moiety could reduce the reactivity of three of the four aromatic rings therefore directing the reactivity on the aromatic ring to functionalize.



Scheme VII.94 : Perspective of exocyclic ring functionalization via Suzuki-Miyaura coupling reaction.

It would also be a great interest to investigate more extensively the Csp^3–H borylation reaction, which has been observed during the optimization of the Csp^2–H borylation conditions. This type of reactivity remains underexplored in frustrated Lewis pair chemistry with only few examples reported so far. The reactivity on few other substrates should be evaluated, in case of successful attempts, a complete optimization and mechanistic investigation should be carried out (**Figure VII.46**).

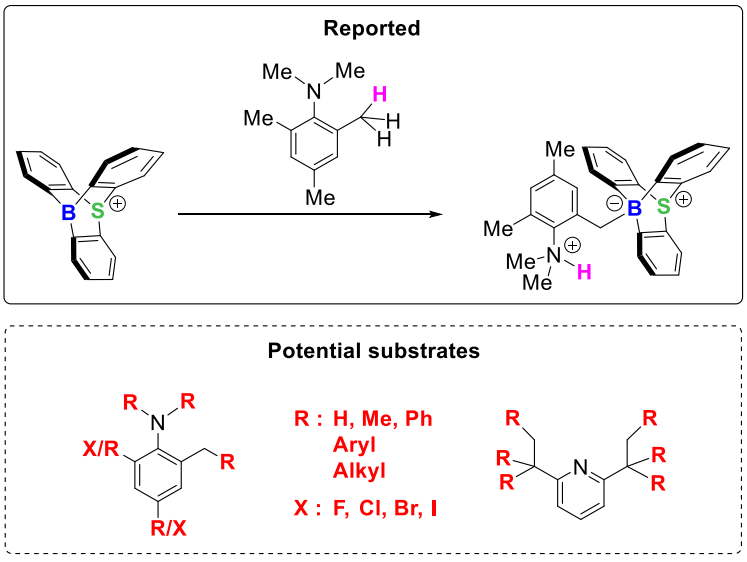
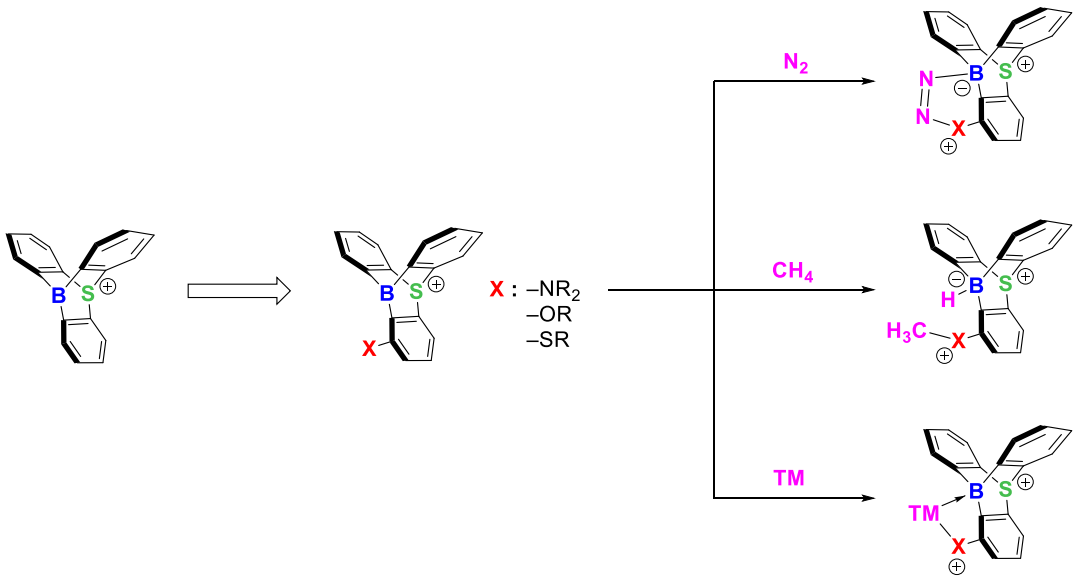


Figure VII.46 : Potential substrates for the development of Csp^3–H

Another interesting perspective to increase the versatility of 9-sulfonium-10-boratriptycene and, by extension, other members of the boratriptycene family, would be the introduction of Lewis basic functions on the triptycene scaffold. By introducing a Lewis basic center in *ortho*-position of the boron atom, an intramolecular FLP system involving a Lewis superacid could be developed. This could open new perspectives for the activation and functionalization of highly stable molecules such as methane or molecular nitrogen. This type of bifunctional system could also find application as bidentate ligands in the field of transition-metals (**Scheme VII.95**). Such type of ambiphilic ligands have found wide application to tune the reactivity of transition metals, by coordination to the metal center or by cooperative reactivity.[9] In the present case, a coordination of the boratriptycene moiety to the metal center might be expected leading to an increased electrophilicity of the metal center. By further tuning substituents surrounding the boron center, it might be possible to preclude the coordination of the boron to the metal and design a system combining the extreme Lewis acidity of the 9-boratriptycene derivatives with the reactivity of transition metals.



Scheme VII.95 : Perspective of development of bifunctional system for the activation of N_2, CH_4 or as ligand for transition-metals.

Far from the Lewis acids area, extensive attention should be devoted to the synthesis of new complexes such as the molecular oxide bis-anion. Indeed, these species may exhibit unexpected properties as ligands, in transition-metal complexes for instance (**Figure VII.47**). These complexes could then find applications far beyond the field of frustrated Lewis pairs or Lewis acids.

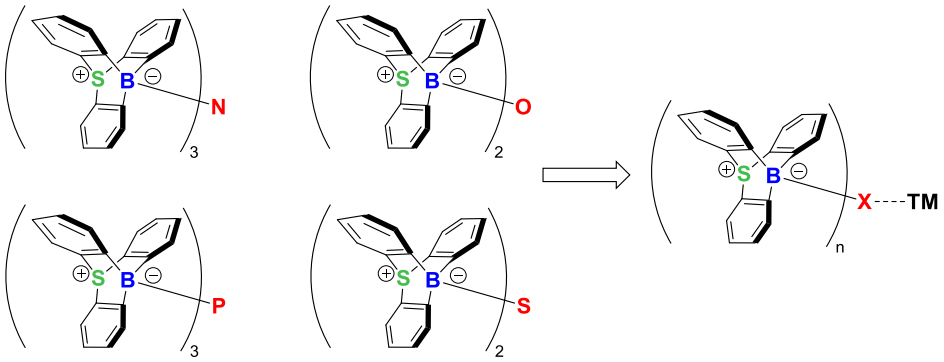


Figure VII.47 : Structures and potential applications of the molecular oxide bis-anion and nitrogen, sulfur and phosphorus derivatives as ligands.

VII.3. References

[1] S. Konishi, T. Iwai, M. Sawamura, *Organometallics* **2018**, *37*, 1876–1883.

[2] A. Ben Saida, A. Chardon, A. Osi, N. Tumanov, J. Wouters, A. I. Adjieufack, B. Champagne, G. Berionni, *Angew. Chem. Int. Ed.* **2019**, *58*, 16889–16893.

[3] A. Chardon, A. Osi, D. Mahaut, T. H. Doan, N. Tumanov, J. Wouters, L. Fusaro, B. Champagne, G. Berionni, *Angew. Chem. Int. Ed.* **2020**, *59*, 12402–12406.

[4] L. A. Mück, A. Y. Timoshkin, G. Frenking, *Inorg. Chem.* **2012**, *51*, 640–646.

[5] A. Osi, D. Mahaut, N. Tumanov, L. Fusaro, J. Wouters, B. Champagne, A. Chardon, G. Berionni, *Angew. Chem. Int. Ed.* **2022**, *61*, DOI 10.1002/anie.202112342.

[6] A. Osi, N. Tumanov, J. Wouters, A. Chardon, G. Berionni, *Synth.* **2023**, *55*, 347–353.

[7] L. Chen, D. R. Sanchez, B. Zhang, B. P. Carrow, *J. Am. Chem. Soc.* **2017**, *139*, 12418–12421.

[8] L. Chen, H. Francis, B. P. Carrow, *ACS Catal.* **2018**, *8*, 2989–2994.

[9] G. Bouhadir, D. Bourissou, *Chem. Soc. Rev.* **2016**, *45*, 1065–1079.

Supporting Information

Content

II.1. General laboratory procedure 250

II.1.1. Analytical methods 250

II.1.2. Material 251

II.2. Preparation of starting materials. 252

II.3. Generation of 9-boratriptycene **2.9** in solution (CD_2Cl_2). 256

II.4. Generation of 9-boratriptycene **2.9** in solution using tetrabutylphosphonium as a counter cation (CD_2Cl_2 and benzene-*d6*) 259

II.5. Synthesis of 9-boratriptycene Lewis adducts **2.16**-**2.23**. 264

9-boratriptycene-etherate Lewis adduct **2.16** 264

9-boratriptycene-pyridine Lewis adduct **2.17** 265

9-boratriptycene-triphenylphosphine Lewis adduct **2.18** 266

9-boratriptycene-9-phosphatriptycene Lewis adduct **2.19** 267

9-boratriptycene-*tert*butyl diphenylphosphine Lewis adduct **2.20** 268

9-boratriptycene-MeCN Lewis adduct **2.22** 273

9-boratriptycene-EtOAc Lewis adduct **2.23** 274

II.6. Generation of Gutmann-Beckett Lewis adduct **2.21**. 275

II.7. Competitions reactions. 277

II.8. Quantum chemical calculations 282

II.9. Thermal analysis of Lewis adducts **2.16**-**2.17**: 285

II.10. Crystallographic parameters: 286

II.11. References 289

III.1. Preparation of starting materials. 291

Bis-(2,2'-bromophenyl)sulfide **S3.2** 291

10-Mesityl-10***H***-9-thia-10-boraanthracene **3.2** 292

10-Mesityl-9-sulfonium-10-boratriptycene **3.3** 293

Bis(trifluoromethylsulfonyl)methane **S3.3** 294

Tris(trifluoromethanesulfonyl)methane **S3.4** 295

III.2. Synthesis of compounds **3.4**-**3.8**, **3.24a** 296
10-Triflide-9-sulfonium-10-boratriptycene-ate complex **3.4**.....296
10-Hydrido-9-sulfonium-10-boratriptycene-ate complex **3.5** 298
Tetrakis(pentafluorophenyl)borate 10,10'-hydronium-bis(9-sulfonium-10-boratriptycene) **3.6**.....299
10-Fluoro-9-sulfonium-10-boratriptycene-ate complex **3.7** 302
Tetrakis(pentafluorophenyl)borate 10,10’-fluoronium-bis(9-sulfonium-10-boratriptycene) **3.8**.....303
10,10’-Oxybis-9-sulfonium-10-boratriptycene-ate complex **3.24a**.....304
III.3. Synthesis of compounds **3.9**-**3.19** 305
10-Phenyl-9-sulfonium-10-boratriptycene-ate complex **3.9**.....305
10-Tolyl-9-sulfonium-10-boratriptycene-ate complex **3.10**.....306
10-(3,5-Dimethylphenyl)-9-sulfonium-10-boratriptycene-ate complex **3.11**.....308
10-Fluoro-9-sulfonium-10-boratriptycene-ate complex **3.12** 309
10-(Chlorophenyl)-9-sulfonium-10-boratriptycene-ate complex **3.13**.....310
10-(Bromophenyl)-9-sulfonium-10-boratriptycene-ate complex **3.14**.....311
10-(Iodophenyl)-9-sulfonium-10-boratriptycene-ate complex **3.15**.....312
10-(2,4-Difluorophenyl)-9-sulfonium-10-boratriptycene-ate complex **3.16**.....314
10-(3,4-Dichlorophenyl)-9-sulfonium-10-boratriptycene-ate complex **3.17** 315
10-(4-chloro-3,5-dimethylphenyl)-9-sulfonium-10-boratriptycene-ate complex **3.18** 316
10-Bis(trifluoromethylsulfonyl)imide-9-sulfonium-10-boratriptycene-ate complex **3.19** 317
III.4. Synthesis of ate-complexe **3.21** derived from activation of Csp^3–H bond. 318
10-((*N,N*-dimethylamino-3,5-dimethylphenyl)methyl)-9-sulfonium-10-boratriptycene-ate complex **3.21**.....318
III.5. Synthesis of ate-complexes **3.22**-**3.23** derived from cleavage of Csp^3–Si bond. 320

From cleavage of Si-Me bond in $PhSiMe_3$: 320

10-methyl-9-sulfonium-10-boratriptycene-ate complex **3.22** 320

From cleavage of Si-Me bond in $(Me_3Si)_3SiH$: 321

From cleavage of Si-Et bond in $(Et_3Si)_2O$: 321

10-ethyl-9-sulfonium-10-boratriptycene-ate complex **3.23** 321

III.6. Synthesis of ate complexe **3.19** derived from cleavage of Csp^3–Csp^3 bond. .. 323

10-methyl-9-sulfonium-10-boratriptycene-ate complex **3.22** 323

III.7. Protocols and NMR monitoring of selected reactions. 325

Reactivity of borohydride **3.5** toward Brønsted acids: 325

Reactivity of 10-hydrido-9-sulfonium-10-boratriptycene-ate **3.6** complex towards SIMes and $HNTf_2$: 327

Generation of Gutmann–Beckett Lewis adduct: 330

Lewis acidity study by infrared spectroscopy: 331

Competitive Csp^2-H activation of C_6H_5Cl toward *p*-xylene: 335

Regeneration of triflimidate-complexe **3.19** by protodeboronation of ate-complexe **3.9** with $HNTf_2$: 336

Formation of C_6H_5F by *ipso*-fluorodeboronation of ate-complexe **3.9** with Selectfluor®: 339

Crude ^{11}B NMR analysis for the Csp^3-Si bond cleavage in $Ph\text{-}SiMe_3$: 340

III.8. Attempted generation of 9-sulfonium-10-boratriptycene (**3.2**) with 2,6-dibromopyridinium (**3.25**, **3.26**). 340

III.9. Synthesis of tritylium and benzenium 7,8,9,10,11,12-hexabromo-carbadodecaborate.....345

III.10. Hydride abstraction from 10-hydrido-9-sulfonium-10-boratriptycene in σ-donating solvent and borylation.....350

III.10.1 Using $[Ph_3C]^+[B(C_6F_5)_4]^-$ as hydride abstractor. 350

III.10.2 Using $[Ph_3C][CB_{11}H_6Br_6]$ 356

III.11. Quantum chemical calculations 359
III.12. Crystallographic parameters: 364
III.13. References 370
IV.1. Csp^2–H borylation optimization with substrate as solvent 373
IV.1.1 Brønsted base optimization using $HCTf_3$. 373
IV.1.2 Temperature and reaction time using $HCTf_3$ and DTBMP. 374
IV.1.3 Optimization of $B(C_6F_5)_4$ alkali salt, temperature and reaction time using $HNTf_2$. 375
IV.1.4 Optimization of Brønsted base with combination of $HNTf_2$ and $NaB(C_6F_5)_4$. 376
IV.2. Csp^2–H borylation optimization with reduced amount of substrate 379
IV.2.1 Optimization of the solvent 379
IV.2.2 Optimization of the required equivalents and concentration of benzene as substrate 380
IV.2.3 Optimization of the required equivalents and concentration of chlorobenzene as substrate 382
IV.3. Synthetic procedures. 383
IV.3.1 General procedure for volatile substrates (**GP1**): 383
10-aryl-9-sulfonium-10-boratriptycene-ate complex 383
IV.3.2 General procedure for solid or non-volatile substrates (**GP2**): 383
IV.4 Kinetic isotope effect 413
IV.4.1 Isotope effect with benzene as substrate and TMA as Brønsted base. 413
IV.4.2 Isotope effect with benzene as substrate and TBDMP as Brønsted base. 414
IV.4.3 Isotope effect with bromobenzene as substrate and TMA as Brønsted base. 415
IV.4.4 Isotope effect with 1,2-dichlorobenzene as substrate and TMA as Brønsted base. 416
IV.5 Determination of the active species 418
IV.5.1 Protodeborylation with 0.8 equivalents of triflimidic acid 418

IV.5.2 Protodeborylation with 1.5 equivalents of triflimidic acid.....421

IV.5.3 Protodeborylation with 1.5 equivalents of triflimidic acid and $NaB(C_6F_5)_4$...425

IV.5.4 Addition of 1.0 equivalent of $NaB(C_6F_5)_4$ over 10-triflimidate-9-sulfonium-10-boratriptycene-ate complex **4.6** *O*-isomer. 429

IV.5.5 Addition of 0.1 equivalent of $HNTf_2$ over 10-triflimidate-9-sulfonium-10-boratriptycene-ate complex **4.6** *O*-isomer. 431

IV.6. Synthesis of tetrakis(pentafluorophenyl)borate bis(10-trifluoromethylsulfonyl-9-sulfonium-10-boratriptycene)iminium..... 432

IV.7. Slow chloride abstraction from $CDCl_3$ with tetrakis(pentafluorophenyl)borate bis(10-trifluoromethylsulfonyl-9-sulfonium-10-boratriptycene)iminium..... 433

IV.8. Demonstration of the 10-(*N*,*N*,3,5-tetramethylaniline)-9-sulfonium-10-boratriptycene Lewis adduct reversibility. 436

IV.9. Deuteration..... 437

IV.10. NMR spectra of synthesized compounds 444

IV.11 Quantum chemical calculations..... 502

IV.12. References..... 502

V.1. Preparation of starting materials. 504

(9-Sulfonium-10-boratriptycene)-10-methylsulfate **5.3** 504

N,*N*-Dimethylpyrolidinium (9-sulfonium-10-boratriptycene)-10-sulfate **5.4**.....505

Bis(9-sulfonium-10-boratriptycene)-10-sulfate **5.6** 506

Tetrakis(pentafluorophenyl)borate tris(10-oxo-9-sulfonium-10-boratriptycene)sulfoxonium **5.7** 507

Tetrakis(pentafluorophenyl)borate bis(10-trifluoromethylsulfonyl-9-sulfonium-10-boratriptycene)imminium **5.9**.....508

10-Triflate-9-sulfonium-10-boratriptycene-ate complex **5.10**.....509

Tetrakis(pentafluorophenyl)borate bis(10-oxy-9-sulfonium-10-boratriptycene)trifluoromethyloxosulfonium **5.11** 510

V.2. Protocols and NMR monitoring of selected reactions:..... 512

Decomposition of **5.11** in $CDCl_3$: 512

Csp^2-H borylation of C_6H_5F: 514

V.3. NMR spectra of synthesized compounds 515

V.4. Crystallographic parameters 528
V.5. Quantum chemical calculations..... 532
V.6. References..... 535
VI.1. Preparation of starting materials. 537
VI.2. Generation of Gutmann-Beckett Lewis adduct **6.13**..... 543
VI.3. Quantum chemical calculations..... 544
VI.4. Crystallographic parameters 544
VI.5. References..... 546

II.1. General laboratory procedure

II.1.1. Analytical methods

NMR spectra were recorded on 400 or 500 MHz NMR JEOL spectrometer. The observed signals are reported in parts per million (ppm) relative to the residual signal of the non-deuterated solvent for ^{1}H and ^{13}C NMR spectra.

The following abbreviations are used to describe multiplicities s = singlet, d = doublet, t = triplet, q = quartet, quin = quintuplet, br = broad, m = multiplet. The external references considered as 0.0 ppm are borontrifluoride etherate ($BF_3{\cdot}Et_2O$) for ^{11}B NMR, trichloromonofluoromethane ($CFCl_3$) for ^{19}F NMR and H_3PO_4 (85%) for ^{31}P NMR.

Flash chromatography was performed using silica gel Silica Flash® 40-63 micron (230-400 mesh) from Sigma-Aldrich. TLC detection was accomplished by irradiation with a UV lamp at 265 or 313 nm.

Melting points were determined on a Büchi B-545 device and are not corrected.

Infrared spectra were recorded on a PerkinElmer FT-IR Spectrometer.

UV-VIS absorption spectra were recorded by Cary 5000 UV-Vis-NIR Spectrophotometer. Photoluminescence spectra were recorded by Cary Eclipse Fluorescence Spectrophotometer.

In some case, HRMS were detected as sum of the desired product and *trans*-2-[3-(4-*tert*-butylphenyl)-2-methyl-2-propenylidene]malononitrile (DCTB), constituent of the matrix.

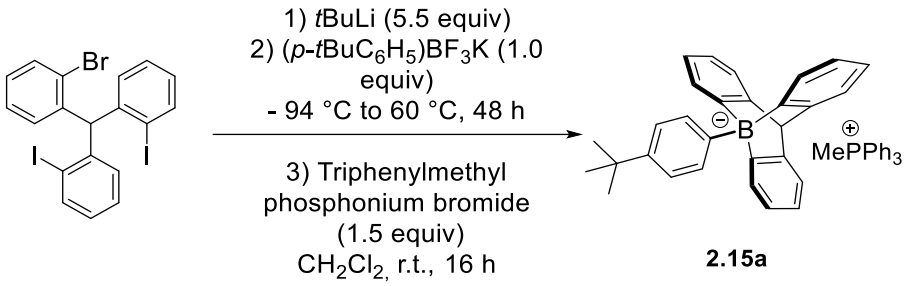
II.1.2. Material

4Å Molecular sieves were dried at 400 °C under high vacuum for 3 days and stored in a high performance glove box. Diethylether, tetrahydrofuran, toluene and dichloromethane were dried with an MBraun solvent purification system and stored under argon. CD_2Cl_2 was dried over preactivated 4Å molecular sieves and stored in a glove box, all others solvents were stored over preactivated 4Å molecular sieves and stored in a glove box prior to use. Others reagents and chemicals were purchased from Sigma-Aldrich, Alfa Aesar, TCI and Fluorochem and used without further purification. Tetraethylammonium-trispentafluorophenyl-borohydride, tetrabutylammonium-trispentafluorophenyl-fluoroborate,[S2.1a] trispentafluorophenylboron-triphenylphosphine Lewis adduct,[S2.1b] 2,2'-((2-and bromophenyl)methylene)bis(iodobenzene) was prepared according to literature procedure.[S2.1c]

Unless otherwise stated all the reactions were performed under an atmosphere of argon using classical Schlenk line technique or in a high performance NC6glovebox.

II.2. Preparation of starting materials.

methyltriphenyl phosphonium 9-(*p*-*t*BuC$_6$H$_5$)-9-boratriptycene-“ate” complex **2.15a**



2.15a

A solution of *t*BuLi (1.9 M in pentane, 7.5 mL, 14.3 mmol, 5.5 equiv) was added dropwise to a solution of 2,2'-((2-bromophenyl)methylene)bis(iodobenzene) (1.5 g, 2.6 mmol, 1.0 equiv) in THF (20 mL) at -94 °C. After 3 h at -94 °C, potassium-(*p*-*t*BuC$_6$H$_5$)trifluoroborate (0.63 mg, 2.6 mmol, 1.0 equiv) was added portionwise as a solid under a vigorous flux of Ar. After 10 min, the cooling bath is removed, a condenser is set up under Ar and the mixture is warmed at 50 °C. After 48 h, the brown mixture is evaporated to dryness and then diluted in CH_2Cl_2 (20 mL) and filtered to remove the inorganic salts. Methyltriphenyl phosphonium bromide (1.4 g, 3.9 mmol, 1.5 equiv.) was added as a solid and the mixture was vigorously stirred at room temperature. After 16 h, the mixture was filtered to remove the inorganic salts. The filtrate was concentrated under reduced pressure and purified *via* silica gel chromatography (CH_2Cl_2/pentane from 1:1 to 3:1) affording methyltriphenyl phosphonium 9-(*p*-*t*BuC$_6$H$_5$)-9-boratriptycene-“ate” complex **2.15a** (27% over 2 steps, 0.46 g, 0.69 mmol) as a pale yellow powder.

TLC: R_f = 0.25 (CH_2Cl_2/pentane 25:75)

^{1}H NMR (400 MHz, $CDCl_3$) δ (ppm) = 8.13 (d, *J* = 7.4 Hz, 2H), 7.63 (t, *J* = 7.1 Hz, 3H), 7.49 (d, *J* = 8.0 Hz, 2H), 7.40 (d, *J* = 6.9 Hz, 3H), 7.36-7.33 (m, 6H), 7.20 (d, *J* = 7.0 Hz, 3H), 7.08 (dd, *J* = 13.3, 7.5 Hz, 6H), 6.61 (t, *J* = 7.1 Hz, 3H), 6.41 (t, *J* = 7.1 Hz, 3H), 5.35 (s, 1H), 1.49 (s, 9H), 0.35 (d, *J* = 12.6 Hz, 3H).

^{13}C NMR (101 MHz, $CDCl_3$) δ (ppm) = 151.0 (Cq), 145.1 (Cq), 134.9 (d, *J* = 2.7 Hz, CH), 133.0 (d, *J* = 10.5 Hz, CH), 130.3 (d, *J* = 12.6 Hz, CH), 129.8 (CH), 123.6 (d, *J* = 2.9 Hz, CH), 123.1 (CH), 122.5 (CH), 121.4 (CH), 119.6 (CH), 118.8 (CH), 61.8 (CH),

34.5 (Cq), 32.1 (CH_3), 5.1 (d, J = 56.6 Hz, CH_3). The carbon directly attached to the boron atom on the triptycene core was not detected, likely due to quadrupolar relaxation.

^{11}B NMR (128 MHz, $CDCl_3$) δ (ppm) = -11.6

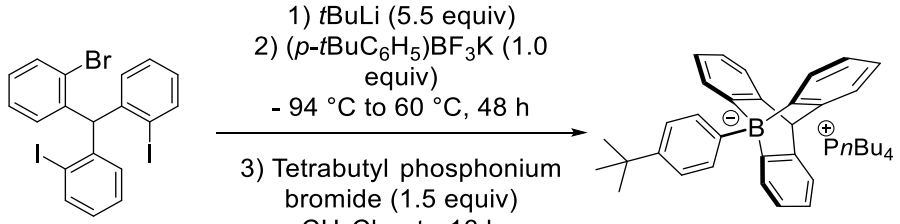
^{31}P NMR (162 MHz, $CDCl_3$) δ (ppm) = 21.8

HRMS (ESI$^-$) (*m/z*): calc. for $[C_{29}H_{26}{}^{10}B]$: 384.21584 $[M+H]^+$; found: 384.21718.

IR (neat, ATR): $\tilde{\nu}$ / cm^{-1} = 3038, 2956, 2902, 2861, 1439, 1269, 1114, 883.

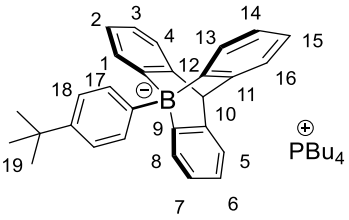
M.p. (CH_2Cl_2/pentane): 140-142 °C

tetrabutyl phosphonium 9-(*p*-*t*BuC_6H_5)-9-boratriptycene-"ate" complex **2.15b**



2.15b

A solution of *t*BuLi (1.9 M in pentane, 7.5 mL, 14.3 mmol, 5.5 equiv) was added dropwise to a solution of 2,2'-((2-bromophenyl)methylene)bis(iodobenzene) (1.5 g, 2.6 mmol, 1.0 equiv) in THF (20 mL) at -94 °C. After 3 h at -94 °C, potassium-(*p*-*t*BuC_6H_5)trifluoroborate (630 mg, 2.6 mmol, 1.0 equiv) was added portionwise as a solid under a vigorous flux of Ar. After 10 min, the cooling bath is removed, a condenser is set up under Ar and the mixture is warmed at 50 °C for 48 h. After 48 h, the brown mixture is evaporated to dryness then diluted in CH_2Cl_2 (20 mL) and filtered to remove the inorganic salts. Tetrabutyl phosphonium bromide (1.6 g, 3.9 mmol, 1.5 equiv) was added to the filtrate as a solid and the mixture is vigorously stirred at room temperature. After 16 h, the mixture was filtered to remove the inorganic salts. The filtrate was concentrated under reduced pressure and purified *via* silica gel chromatography (CH_2Cl_2/pentane from 1:1 to 3:1) affording tetrabutyl phosphonium 9-(*p*-*t*BuC_6H_5)-9-boratriptycene-"ate" complex **2.15b** (19% over 2 steps, 0.32 g, 0.49 mmol) as pale yellow powder.



TLC: R_f = 0.30 (CH_2Cl_2/pentane 25:75)

^{1}H NMR (400 MHz, $CDCl_3$) δ (ppm) = 8.02 (d, *J* = 7.8 Hz, 2H, H_{17}), 7.44 (d, *J* = 7.8 Hz, 3H, H_1, H_8, H_{13}), 7.40 (d, *J* = 8.2 Hz, 2H, H_{18}), 7.18 (dd, *J* = 6.9, 1.3 Hz, 3H, H_4, H_5, H_{16}), 6.70-6.61 (m, 6H, H_2, H_3, H_6, H_7, H_{14}, H_{15}), 5.29 (s, 1H, H_{10}), 1.41 (s, 9H, H_{19}), 1.20-1.10 (m, 8H, *n*Bu), 0.89-0.76 (m, 28H, *n*Bu).

^{13}C NMR (101 MHz, $CDCl_3$) δ (ppm) = 150.6 (Cq), 145.1 (Cq), 135.6 (CH), 129.5 (CH), 123.4 (CH), 123.3 (CH), 122.7 (CH), 121.3 (CH), 61.6 (CH), 34.4 (Cq), 32.0 (CH_3), 23.7 (d, *J* = 11.5 Hz, CH_2), 23.6 (CH_2), 17.3 (d, *J* = 47.3 Hz, CH_2), 13.8 (CH_3) The carbon directly attached to the boron atom on the triptycene core was not detected, likely due to quadrupolar relaxation.

^{11}B NMR (128 MHz, $CDCl_3$) δ (ppm) = -11.9

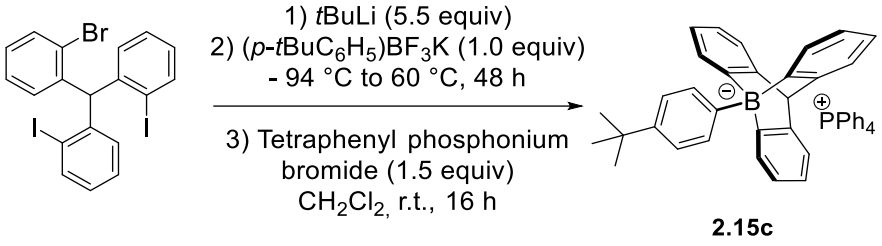
^{31}P NMR (162 MHz, $CDCl_3$) δ (ppm) = 32.6

HRMS (ESI$^-$) (*m/z*): calc. for [$C_{29}H_{26}{}^{10}B$]: 384.21584 $[M+H]^+$; found: 384.21720.

IR (neat, ATR): $\tilde{\nu}$ / cm^{-1} = 3044, 2962, 2873, 1446, 1269, 907.

M.p. (CH_2Cl_2/pentane): 212-216 °C.

tetraphenyl phosphonium 9-(*p*-*t*BuC_6H_5)-9-boratriptycene-“ate” complex **2.15c**



2.15c

A solution of *t*BuLi (1.9 M in pentane, 7.5 mL, 14.3 mmol, 5.5 equiv) was added dropwise to a solution of 2,2'-((2-bromophenyl)methylene)bis(iodobenzene) (1.5 g, 2.6 mmol, 1.0 equiv) in THF (20 mL) at -94 °C. After 3h at -94 °C, potassium-(*p*-

*t*BuC$_6$H$_5$)trifluoroborate (630 mg, 2.6 mmol, 1.0 equiv) was added portionwise as a solid under a vigorous flux of Ar. After 10 min, the cooling bath is removed, a condenser is set up under Ar and the mixture is warmed at 50 °C for 48 h. After 48 h, the brown mixture is evaporated to dryness then diluted in dichloromethane (20 mL) and filtered to remove the inorganic salts. Tetraphenyl phosphonium bromide (1.6 g, 3.9 mmol, 1.5 equiv.) are added to the filtrate as a solid and the mixture is vigorously stirred at room temperature. After 16h, the mixture was filtered to remove the inorganic salts. The filtrate was concentrated under reduced pressure and purified *via* silica gel chromatography (CH_2Cl_2/pentane from 50:50 to 75:25) affording tetraphenyl phosphonium 9-(*p*-*t*BuC$_6$H$_5$)-9-boratriptycene-"ate" complex **2.15c** (30% over 2 steps, 0.56 g, 0.78 mmol) as a white powder.

Single crystals suitable for X-ray diffraction analysis were obtained by a slow evaporation of a saturated solution of **2.15c** in CH_2Cl_2.

TLC: R_f = 0.25 (CH_2Cl_2/pentane 25:75)

^{1}H NMR (400 MHz, CD_2Cl_2) δ (ppm) = 8.00 (d, *J* = 6.1 Hz, 2H), 7.82-7.74 (m, 4H), 7.63-7.55 (m, 8H), 7.51-7.41 (m, 10H), 7.34 (d, *J* = 6.5 Hz, 2H), 7.22-7.15 (m, 2H), 6.69-6.59 (m, 6H), 5.30 (s, 1H), 1.45 (s, 9H).

^{13}C NMR (101 MHz, CD_2Cl_2) δ (ppm) = 163.9 (dd, *J* = 87.5, 44.0 Hz, Cq), 150.7 (Cq), 145.2 (Cq), 136.0 (CH), 135.8 (CH), 134.7 (d, *J* = 10.2 Hz, CH), 130.9 (d, *J* = 12.7 Hz, CH), 129.3 (CH), 129.3 (CH), 128.5 (CH), 125.6 (CH), 123.6 (CH), 122.9 (CH), 122.6 (CH), 121.5 (CH), 118.2 (Cq), 117.3 (Cq), 61.6 (CH), 34.5 (Cq), 31.9 (CH_3).

^{11}B NMR (128 MHz, CD_2Cl_2) δ (ppm) = -11.8

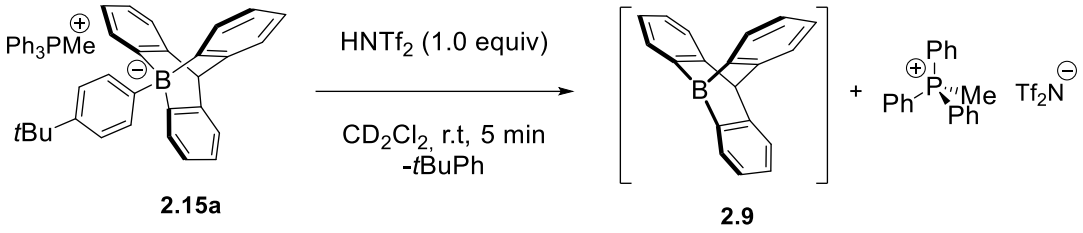
^{31}P NMR (162 MHz, CD_2Cl_2) δ (ppm) = 23.7

HRMS (ESI$^-$) (*m/z*): calc. for [$C_{29}H_{26}{}^{10}B$]: 384.21584 $[M+H]^+$; found: 384.21741.

IR (neat, ATR): $\tilde{\nu}$ / cm^{-1} = 3037, 2962, 2866, 1433, 1276, 1098, 907.

M.p. (CH_2Cl_2/pentane): 266-270 °C

II.3. Generation of 9-boratriptycene **2.9** in solution (CD_2Cl_2).



2.15a **2.9**

In a glove box, Tf_2NH (10.0 mg, 37.7 μmol, 1.0 equiv) was added to a solution of triphenylmethylphosphonium-9-*tert*butylphenyl-9-boratriptycene-"ate"-complex **2.15a** (25 mg, 37.7 μmol, 1.0 equiv) in CD_2Cl_2 (0.65 mL). The initial colorless mixture turns immediately to deep yellow (Photo SII.1). After 5 min, the solution was transferred in a JYoung NMR tube and directly submitted to ^1H and ^{11}B NMR spectroscopy measurements (Figures SII.1 and SII.2). The ^1H NMR analysis show the presence of 2 new signals: δ (ppm in CD_2Cl_2) = 6.78-6.74 (m, 6H), 7.57-7.54 (m, 3H); as well as *tert*-butylbenzene δ (ppm in CD_2Cl_2) = 1.33 (s). The ^{11}B NMR analysis show a single signal at – 11.6 ppm (CD_2Cl_2) corresponding to the remaining starting material **2.15a**.

Next, the solution was washed with benzene-*d6* to remove the remaining starting material and *tert*-butylbenzene. The resulting deep red solution (Photo SII.2) was then submitted to ^1H and ^{11}B NMR analysis (Figures SII.3 and SII.4). The ^1H NMR spectra appear cleaner and show only the presence of 9-boratriptycene **2.9**: δ (ppm in CD_2Cl_2) = 7.61-7.53 (m, 3H), 7.24-7.17 (m, 3H), 6.85-6.71 (m, 6H), 5.27 (s, 1H); and triphenylmethylphosphinium triflimidate: δ (ppm in CD_2Cl_2) = 7.89-7.81 (m, 3H), 7.73-7.64 (m, 6H), 7.51-7.39 (m, 6H), 2.29 (d, *J* = 13.1 Hz, 3H). The ^{11}B NMR spectra (CD_2Cl_2) shows a very broad signal at 60.9 ppm coherent with a three coordinated environment but significantly downshifted to that calculated using the gauge including atomic orbital density functional theory [GIAO-DFT] method at the B3LYP/6-311+G(2d,p)//M06-2X/6-311G(d) level of theory (91.7 ppm, see the quantum chemical calculation section). Unfortunately, and despite numerous attempts no crystal suitable or X-ray diffraction analysis was obtained due to very fast decomposition into the corresponding borinic acid.

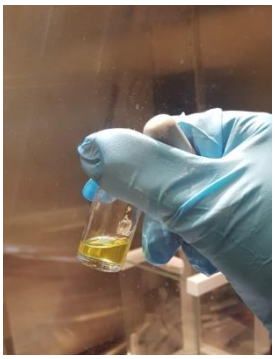
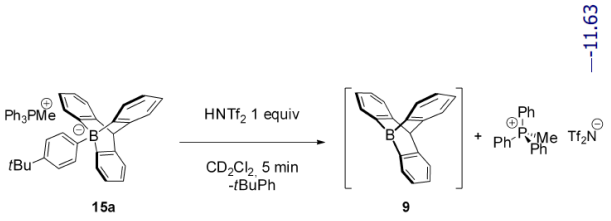


Photo SII.1

Figure SII.1: ^{1}H NMR spectra (400 MHz, 25°C, CD_2Cl_2)



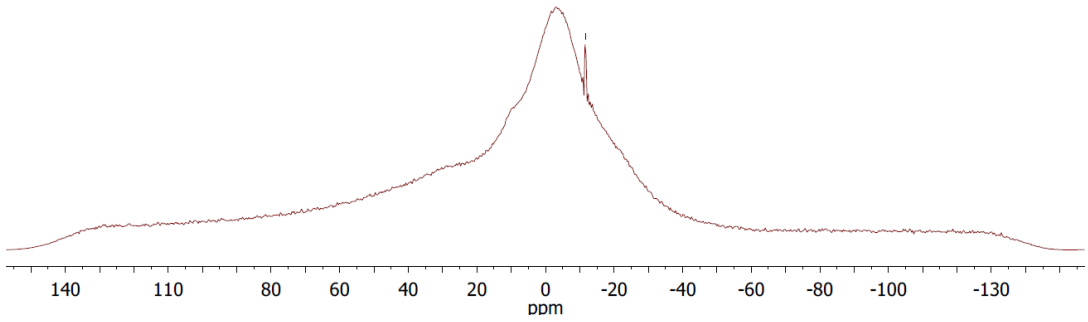


Figure SII.2: ^{11}B NMR spectra (128 MHz, 25°C, CD_2Cl_2)

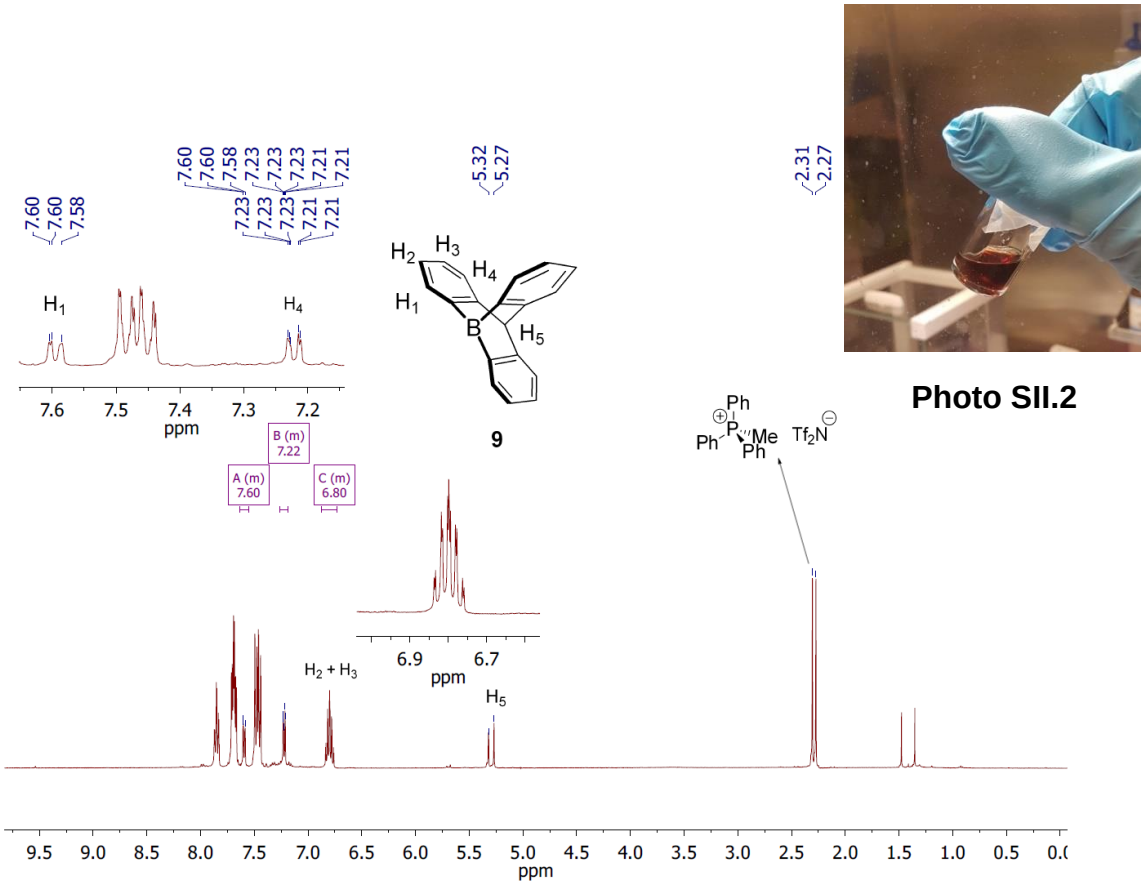


Photo SII.2

Figure SII.3: ^{1}H NMR spectra (400 MHz, 25°C, CD_2Cl_2)

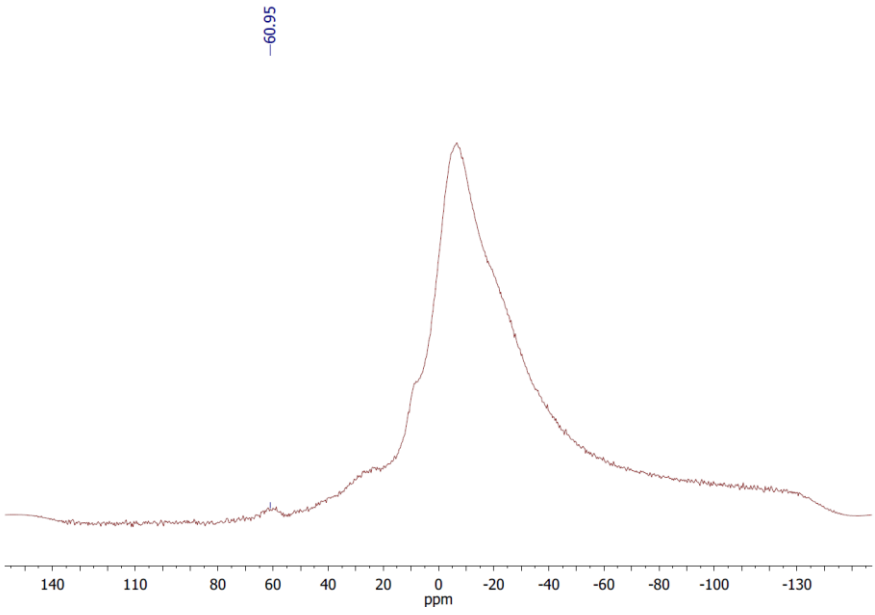
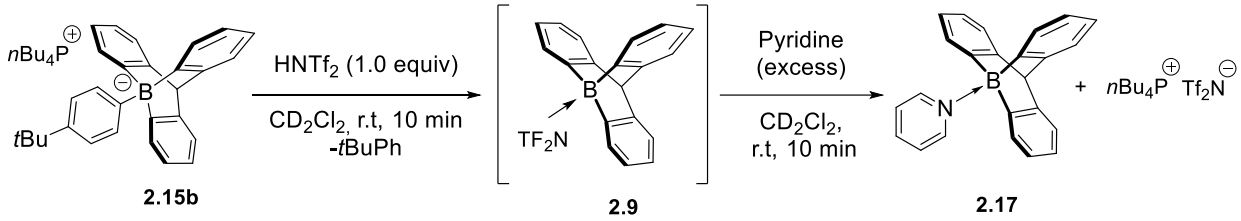


Figure SII.4: ^{11}B NMR spectra (128 MHz, 25°C, CD_2Cl_2)

II.4. Generation of 9-boratriptycene **2.9** in solution using tetrabutylphosphonium as a counter cation (CD_2Cl_2 and benzene-*d6*).

In CD_2Cl_2:



In a glove box, Tf_2NH (11.0 mg, 38.7 μmol, 1.0 equiv) was added to a solution of tetrabutylphosphonium-9-*tert*butylphenyl-9-boratriptycene-"ate"-complex **2.15b** (25 mg, 38.7 μmol, 1.0 equiv) in CD_2Cl_2 (0.65 mL). The initial colorless mixture turns immediately to yellow. After 10 min, the solution was directly submitted to ^{11}B and ^{19}F NMR spectroscopy (CD_2Cl_2). The ^{11}B NMR spectra shows a very broad signal at 60.1 ppm coherent with what we previously observed in the case of **2.15a** (See section II.3), a small signal was also detected at 8.2 ppm (Figure SII.5) which have been attributed to the NTf_2-9-boratriptycene complex (*O*-isomer) according to quantum chemical calculations (See section II.8). The ^{19}F NMR analysis show 2 sharp signals: δ (ppm in CD_2Cl_2) = -76.0 (s), -78.8 (s), indicating the formation of the Tf_2N-9-boratriptycene (*O*-isomer). A broad signal at – 78.9 ppm was also observed (*N*-isomer, Figure SII.6). Those observations are coherent witch the formation of **2.9** as a complex with the NTf_2^-. Next, an excess of pyridine was added to confirm the displacement of the triflimidate by a stronger Lewis base. The ^{19}F NMR analysis show that the broad signal at -78.9 ppm disappear to let the place of a very sharp signal at -79.3 ppm ("uncoordinated" triflimidate) who confirm the displacement of the triflimidate by the pyridine (Figure SII.7). This displacement was also confirmed by submitting the sample to ^{11}B NMR analysis where the previous signals at 60.1 and 8.2 ppm was no more detected, a single sharp peak was observed at -1.50 ppm who confirm the presence of the 9-boratriptycene-pyridine Lewis adduct **2.17** (Figure SII.8).

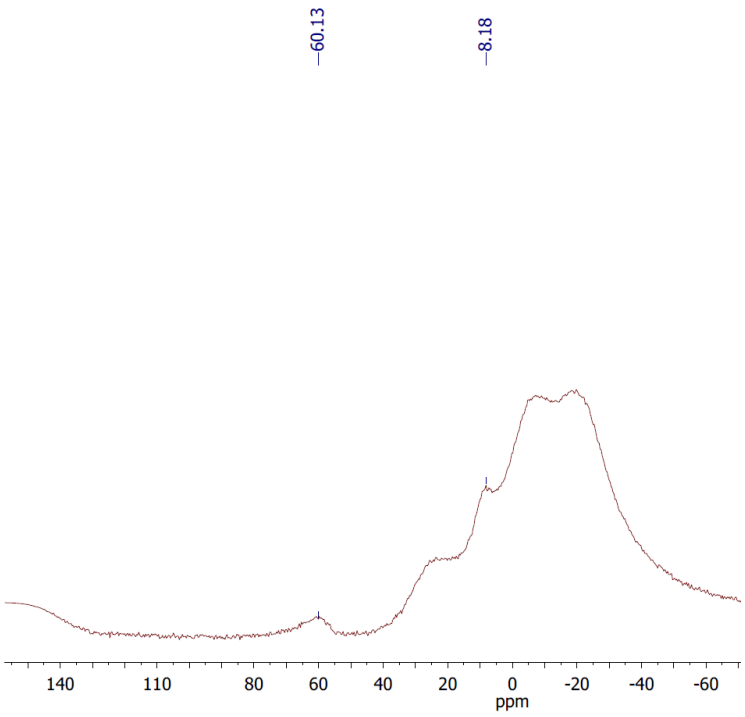


Figure SII.5: ^{11}B NMR spectra (128 MHz, 25°C, CD_2Cl_2)

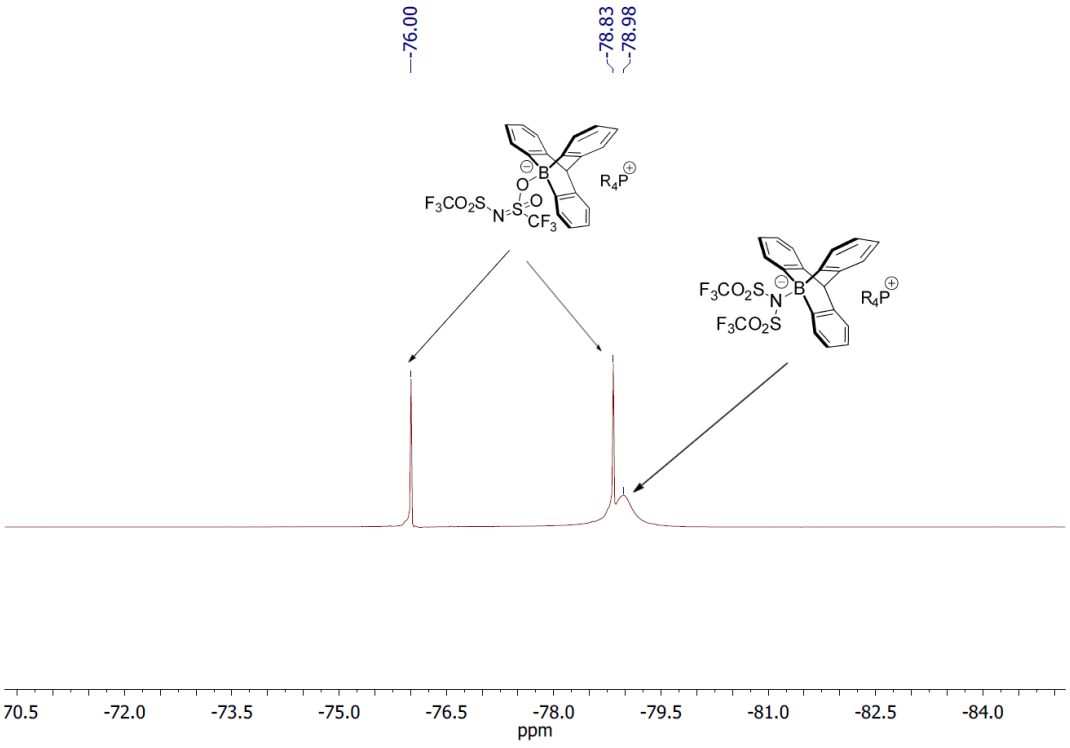


Figure SII.6: ^{19}F NMR spectra (376 MHz, 25°C, CD_2Cl_2)

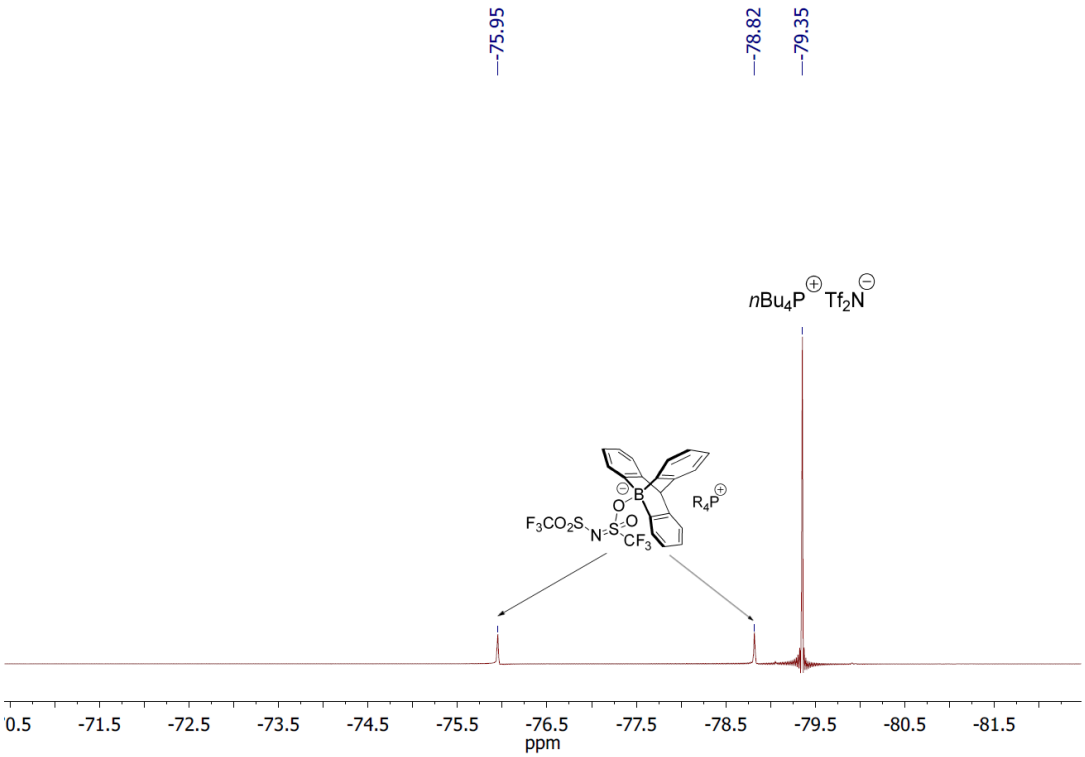


Figure SII.7: ^{19}F NMR spectra after adding pyridine (376 MHz, 25°C, CD_2Cl_2)

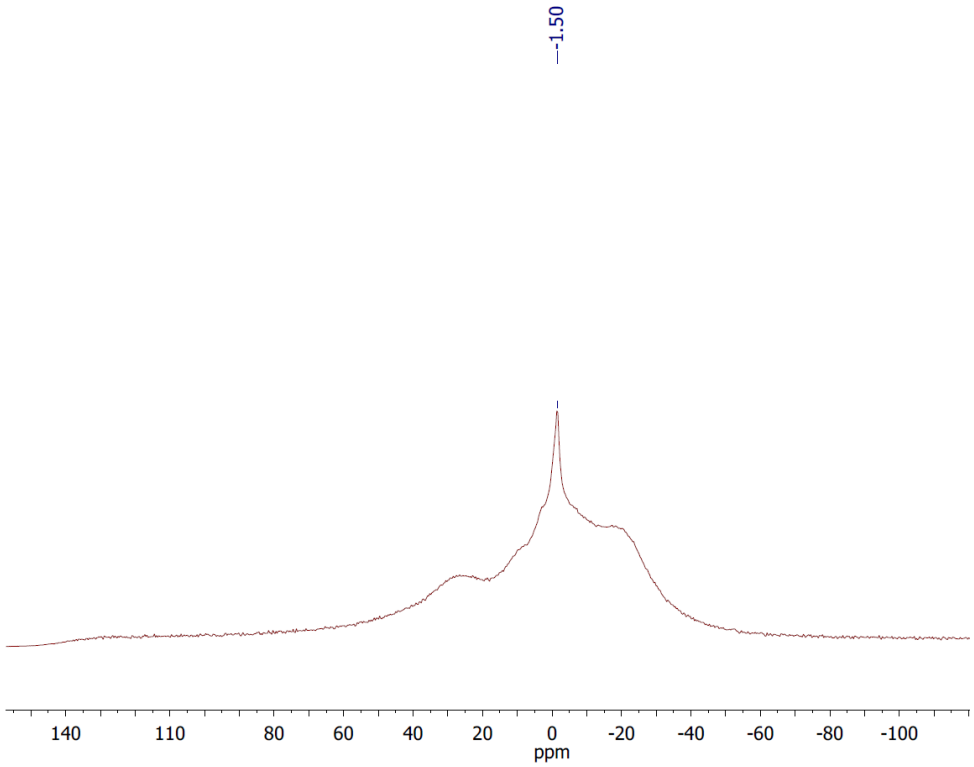
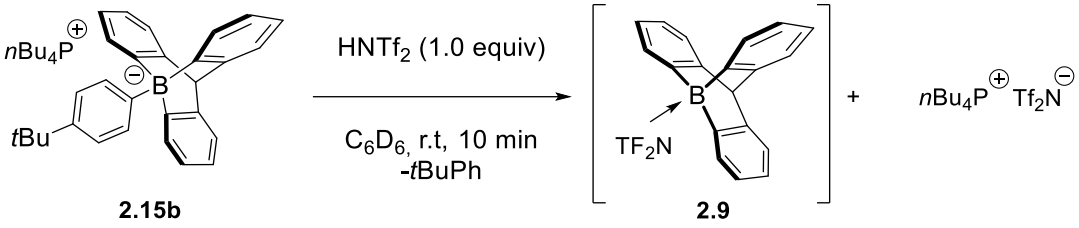


Figure SII.8: ^{11}B NMR spectra after adding pyridine (128 MHz, 25°C, CD_2Cl_2)

In benzene-*d*6:



2.15b **2.9**

In a glove box, Tf_2NH (10.9 mg, 38.7 μmol, 1.0 equiv) was added to a solution of tetrabutylphosphonium-9-*tert*butylphenyl-9-boratriptycene-"ate"-complex **2.15b** (25 mg, 38.7 μmol, 1.0 equiv) in benzene-*d6* (0.65 mL). The initial colorless mixture turns immediately to yellow. After 10 min, the solution was put in the fridge and let at 0 °C for 1h which lead to a phase separation. The yellow mother liquor was removed and the resulting purple mixture was washed with benzene-*d6* (3* 1 mL) and then submitted to NMR spectroscopy (CD_2Cl_2). The ^1H NMR analysis show the presence of the triflimidate-9-boratriptycene complex: δ (ppm in CD_2Cl_2) = 6.87-6.83 (m, 6H), 7.24-7.24 (m, 3H), 7.56-7.53 (m, 3H) ((Figure SII.9). Traces of the starting material was also detected. The ^{19}F NMR analysis show 2 sharp signals: δ (ppm in CD_2Cl_2) = -76.0 (s), -78.8 (s), indicating the formation of the Tf_2N-9-boratriptycene (*N*-isomer). The signal corresponding to the "free" triflimidate was also detected: δ (ppm in CD_2Cl_2) = -76.4 (s), (Figure SII.10). The ^{11}B NMR analysis is silent.

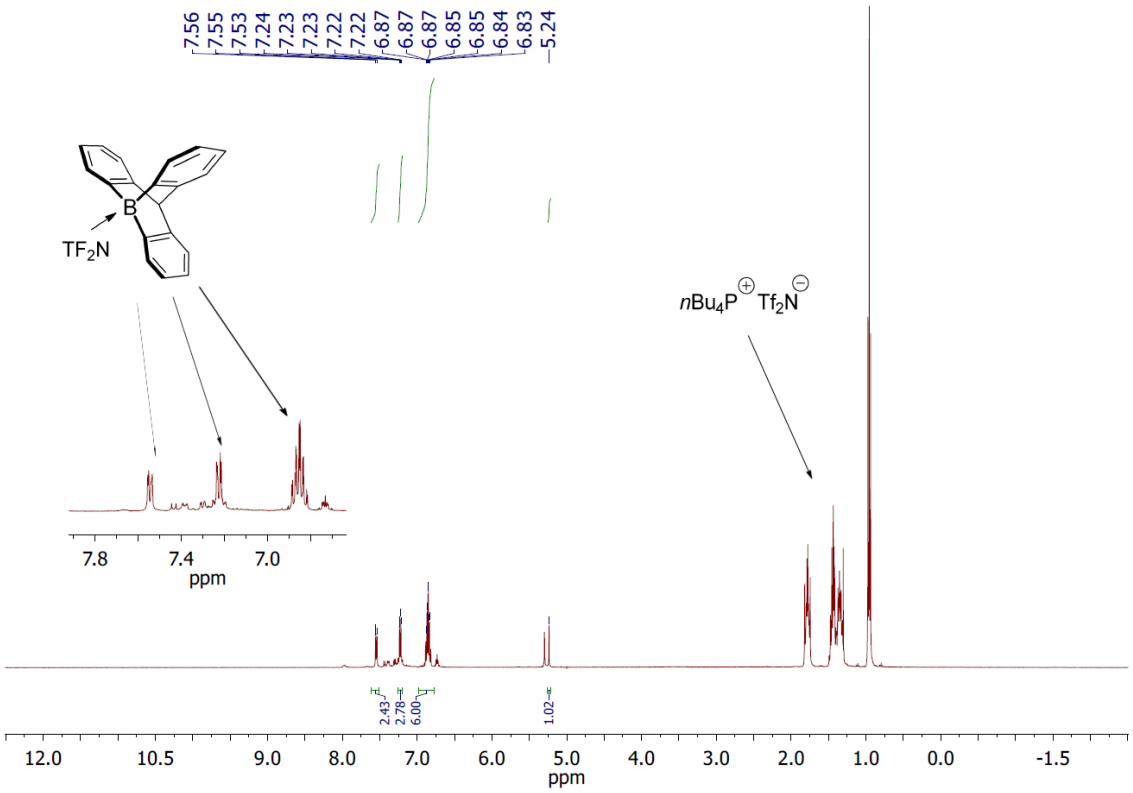


Figure SII.9: ^{1}H NMR spectra (400 MHz, 25°C, CD_2Cl_2)

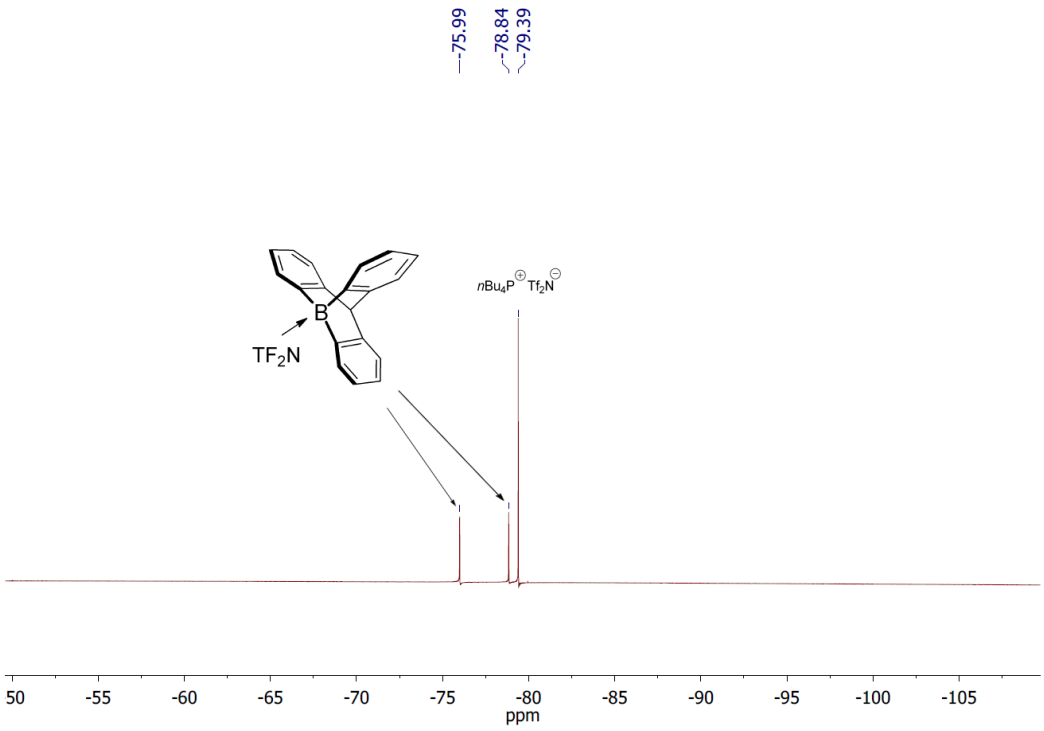
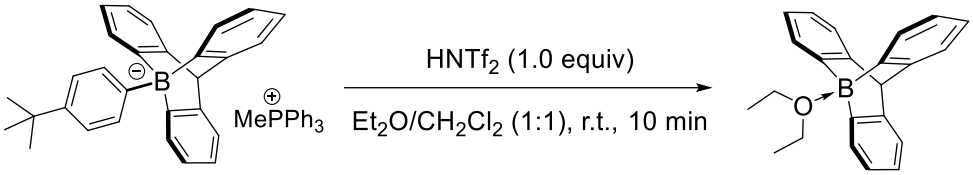


Figure SII.10: ^{19}F NMR spectra (376 MHz, 25°C, CD_2Cl_2)

II.5. Synthesis of 9-boratriptycene Lewis adducts **2.16**-**2.23**.

9-boratriptycene-etherate Lewis adduct **2.16**



2.15a **2.16**

In a glove box, a solution of methyltriphenyl phosphonium 9-(4-*t*BuPh)-9-boratriptycene-"ate" complex **2.15a** (180 mg, 0.27 mmol, 1 equiv) in CH_2Cl_2/Et_2O (3.0 mL, 1:1) is added to solid bis(trifluoromethane)sulfonimide (76 mg, 0.27 mmol, 1 equiv) and the reaction is stirred at room temperature. After 10 min, the mixture is concentrated under reduced pressure and purified *via* silica gel chromatography (CH_2Cl_2/pentane 1:1) affording 9-boratriptycene-etherate Lewis adduct **2.16** (81%, 71 mg, 0.22 mmol) as a white solid.

Single crystals suitable for X-ray diffraction analysis were obtained by a slow evaporation of a saturated solution of **2.16** in CH_2Cl_2 at 0 °C.

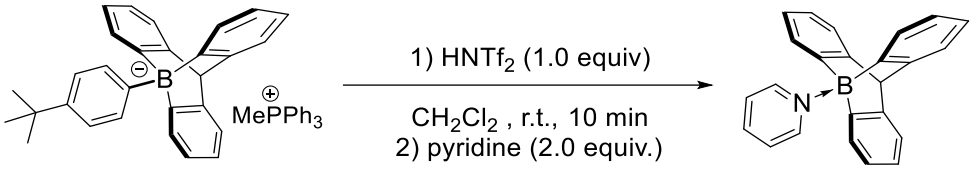
TLC: R_f = 0.4 (CH_2Cl_2/pentane)

^{1}H NMR (400 MHz, $CDCl_3$) δ (ppm) = 7.39-7.35 (m, 3H), 7.34-7.30 (m, 3H), 6.93-6.86 (m, 6H), 5.27 (s, 1H), 5.16 (q, *J* = 7.1 Hz, 4H), 1.97 (t, *J* = 7.1 Hz, 6H).
^{13}C NMR (101 MHz, $CDCl_3$) δ (ppm) = 148.3 (Cq), 125.6 (CH), 124.1 (CH), 124.0 (CH), 123.7 (CH), 78.2 (CH_2), 60.0 (CH), 29.9 (CH_3).

^{11}B NMR (128 MHz, $CDCl_3$) δ (ppm) = 10.9

HRMS (ESI) (*m/z*): calc. for $[C_{23}H_{23}{}^{10}BO]$: 326.18420 $[M+H]^+$; found: 326.17101.
IR (neat, ATR): $\tilde{\nu}$ / cm^{-1} = 3283, 2921, 2866, 1597, 1446, 1269, 1173, 962.
M.p. (CH_2Cl_2): 170-174 °C (decomposition).

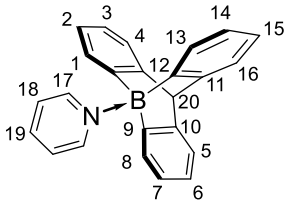
9-boratriptycene-pyridine Lewis adduct **2.17**



2.15a **2.17**

In a glove box, a solution of methyltriphenyl phosphonium 9-(4-*t*BuPh)-9-boratriptycene-"ate" complex **2.15a** (180 mg, 0.27 mmol, 1.0 equiv) in CH_2Cl_2 (3.0 mL) is added to solid bis(trifluoromethane)sulfonimide (76 mg, 0.27 mmol, 1.0 equiv) and the reaction is stirred at room temperature. After 10 min, pyridine (42 µl, 0.54 mmol, 2.0 equiv) is added and the reaction is stirred for 1 min. The crude mixture is concentrated under reduced pressure and purified *via* silica gel chromatography (CH_2Cl_2/pentane 25:75) affording 9-boratriptycene-pyridine Lewis adduct **2.17** (78%, 70 mg, 0.21 mmol) as a yellow solid.

Single crystals suitable for X-ray diffraction analysis were obtained by a slow evaporation of a saturated solution of **2.17** in (CH_2Cl_2/pentane 1:1).



TLC: R_f = 0.4 (CH_2Cl_2/pentane, 25:75)

^{1}H NMR (400 MHz, CD_2Cl_2) δ (ppm) = 9.37 (dd, *J* = 6.7, 1.5 Hz, 2H, H_{17}), 8.39-8.33 (m, 1H, H_{19}), 8.03-7.96 (m, 2H, H_{18}), 7.40-7.34 (m, 3H, H_1, H_8, H_{13}), 7.04-6.99 (m, 3H, H_4, H_5, H_{16}), 6.97-6.85 (m, 6H, H_2, H_3, H_6, H_7, H_{14}, H_{15}), 5.42 (s, 1H, H_{20})

^{13}C NMR (101 MHz, CD_2Cl_2) δ (ppm) = 149.2 (Cq), 147.7 (CH), 142.0 (CH), 127.0 (CH), 125.6 (CH), 124.2 (CH), 124.0 (CH), 60.5 (CH). The carbon directly attached to the boron atom on the triptycene core was not detected, likely due to quadrupolar relaxation.

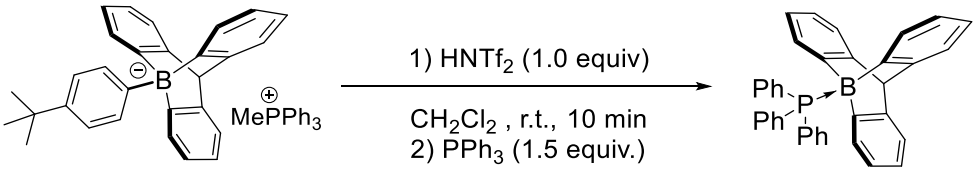
^{11}B NMR (128 MHz, CD_2Cl_2) δ (ppm) = -1.6

HRMS (ESI) (*m/z*): calc. for [$C_{24}H_{19}N^{10}B$]: 331.16414 $[M+H]^+$; found: 331.16428.

IR (neat, ATR): $\tilde{\nu}$ / cm^{-1} = 3037, 2921, 2866, 1453, 1269, 1146, 900.

M.p. (CH_2Cl_2/pentane): 298-302 °C (decomposition).

9-boratriptycene-triphenylphosphine Lewis adduct **2.18**



2.15a **2.18**

In a glove box, a solution of methyltriphenyl phosphonium 9-(4-*t*BuPh)-9-boratriptycene-"ate" complex **2.15a** (30 mg, 0.045 mmol, 1.0 equiv) in CH_2Cl_2 (1.0 mL) is added to solid bis(trifluoromethane)sulfonimide (12.7 mg, 0.045 mmol, 1.0 equiv) and the reaction is stirred at room temperature. After 10 min, triphenylphosphine (18 mg, 0.090 mmol, 1.5 equiv) is added and the reaction is stirred for 1 min. The mixture is concentrated under reduced pressure and diethylether (5 mL) was added. The solid is filtrated, washed with diethylether (2 x 5 mL) and then purified *via* silica gel chromatography (CH_2Cl_2/pentane 25:75) affording 9-boratriptycene-triphenylphosphine Lewis adduct **2.18** (65%, 15 mg, 0.029 mmol) as a white solid.

Single crystals suitable for X-ray diffraction analysis were obtained by a slow evaporation of a saturated solution of **2.18** in CH_2Cl_2.

TLC: R_f = 0.42 (CH_2Cl_2/pentane 25:75)

^{1}H NMR (400 MHz, CD_2Cl_2) δ (ppm) = 7.70-7.58 (m, 9H), 7.50-7.43 (m, 6H), 7.36 (d, *J* = 7.3 Hz, 3H), 6.87 (td, *J* = 7.4, 1.2 Hz, 3H), 6.81 (d, *J* = 7.1 Hz, 3H), 6.59 (td, *J* = 7.4, 1.2 Hz, 3H), 5.45 (s, 1H).

^{13}C NMR (101 MHz, CD_2Cl_2) δ (ppm) = 149.9 (d, *J* = 11.4 Hz, Cq), 134.9 (d, *J* = 10.3 Hz, CH), 132.6 (d, *J* = 2.1 Hz, CH), 130.6 (d, *J* = 2.9 Hz, CH), 129.7 (d, *J* = 10.6 Hz, CH), 126.3 (Cq), 124.0 (d, *J* = 2.2 Hz, CH), 123.9 (CH), 123.5 (CH), 61.3 (CH). The carbon directly attached to the boron atom on the triptycene core was not detected, likely due to quadrupolar relaxation.

^{11}B NMR (128 MHz, CD_2Cl_2) δ (ppm) = -11.9

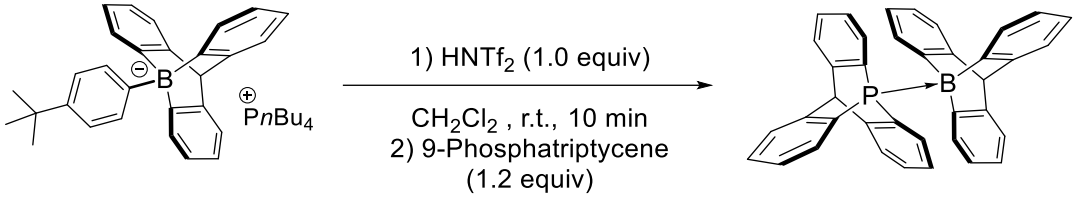
^{31}P NMR (162 MHz, CD_2Cl_2) δ (ppm) = 4.6

HRMS (ESI) (*m/z*): calc. for $[C_{37}H_{29}{}^{10}BP]$: 514.21308 $[M+H]^+$; found: 514.21341.

IR (neat, ATR): $\tilde{\nu}$ / cm^{-1} = 3044, 2955, 2866, 1433, 1269, 1096, 907.

M.p. (CH_2Cl_2): 278-281 °C (decomposition).

9-boratriptycene-9-phosphatriptycene Lewis adduct **2.19**



2.15b **2.19**

In a glove box, a solution of tetrabutylphosphonium 9-(4-*t*BuPh)-9-boratriptycene-"ate" complex **2.15b** (30 mg, 0.047 mmol, 1.0 equiv) in CH_2Cl_2/toluene (2.0 mL, 1:1) is added to solid bis(trifluoromethane)sulfonimide (13.1 mg, 0.047 mmol, 1.0 equiv) and the reaction is stirred at room temperature. After 10 min, a solution of 9-phosphatriptycene (15 mg, 0.055 mmol, 1.2 equiv) in CH_2Cl_2 (0.5 mL) is added and the reaction is stirred for 1 min. The mixture is concentrated under reduced pressure and purified *via* silica gel chromatography (CH_2Cl_2/pentane 10:90) affording pure 9-boratriptycene-9-phosphatriptycene Lewis adduct **2.19** (61%, 15 mg, 0.029 mmol) as a pale yellow solid.

Single crystals suitable for X-ray diffraction analysis were obtained by a phase gas diffusion of pentane into of a saturated solution of **2.19** in CH_2Cl_2/toluene (90:10) at 0 °C.

TLC: R_f = 0.20 (CH_2Cl_2/pentane 10:90)

^{1}H NMR (400 MHz, $CDCl_3$) δ (ppm) = 7.84-7.77 (m, 6H), 7.53-7.48 (m, 3H), 7.41-7.37 (m, 3H), 7.14-7.06 (m, 6H), 6.97 (td, *J* = 7.4, 1.1 Hz, 3H), 6.70 (td, *J* = 7.3, 1.1 Hz, 3H), 5.95 (s, 1H), 5.66 (s, 1H).

^{13}C NMR (101 MHz, $CDCl_3$) δ (ppm) = 149.3 (d, *J* = 12.8 Hz, Cq), 148.1 (Cq), 133.3 (d, *J* = 14.8 Hz, CH), 130.8 (CH), 129.1 (d, *J* = 6.1 Hz, CH), 129.0 (d, *J* = 53.4 Hz, CH), 126.5 (CH), 126.4 (CH), 124.2 (CH), 124.1 (CH), 123.6 (CH). The carbon directly

attached to the boron atom on the triptycene core was not detected, likely due to quadrupolar relaxation, as well as the carbon on the bridgehead position of the triptycene scaffolds.

^{11}B NMR (128 MHz, $CDCl_3$) δ (ppm) = -15.8

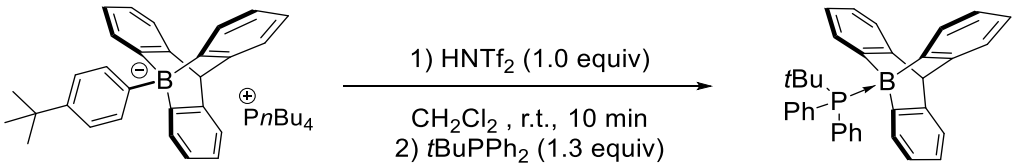
^{31}P NMR (162 MHz, $CDCl_3$) δ (ppm) = -28.8

HRMS (ESI) (*m/z*): calc. for [$C_{38}H_{27}{}^{10}BP$]: 524,19743 $[M+H]^+$; found: 524.19780.

IR (neat, ATR): $\tilde{\nu}$ / cm^{-1} = 3044, 2922, 2855, 1439, 1269, 1120, 910, 734.

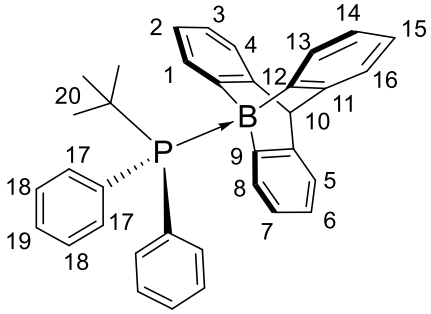
M.p. (toluene/pentane): 332-334 °C (decomposition).

9-boratriptycene-*tert*butyl diphenylphosphine Lewis adduct **2.20**



2.15b **2.20**

In a glove box, a solution of tetrabutylphosphonium 9-(4-*t*BuPh)-9-boratriptycene-"ate" complex **2.15b** (92 mg, 0.143 mmol, 1.0 equiv) in CH_2Cl_2 (3.0 mL) is added to solid bis(trifluoromethane)sulfonimide (40.1 mg, 0.143 mmol, 1.0 equiv) and the reaction is stirred at room temperature. After 10 min, a solution of *tert*butyl diphenylphosphine (45 mg, 0.185 mmol, 1.3 equiv) in CH_2Cl_2 (1.0 mL) is added and the reaction is stirred for 1 min. The mixture is concentrated under reduced pressure and purified *via* silica gel chromatography (CH_2Cl_2/pentane 20:80) affording 9-boratriptycene-*tert*butyl diphenylphosphine Lewis adduct **2.20** (63%, 44 mg, 0.089 mmol) as a white solid.



2.20

TLC: R_f = 0.20 (CH_2Cl_2/pentane 20:80)

^{1}H NMR (400 MHz, $CDCl_3$) δ (ppm) = 8.20 – 8.15 (m, H_{17}, 4H), 7.49-7.44 (m, H_1, H_{13}, H_{19}, 4H), 7.42 (dt, *J* = 7.3, 1.3 Hz, H_4, H_{16}, 2H), 7.35-7.31 (m, H_5, H_{18}, 5H), 6.96 (td, *J* = 7.3, 1.1 Hz, H_3, H_{15}, 2H), 6.80 (td, *J* = 7.3, 1.3 Hz, H_2, H_{14}, 2H), 6.78 (td, *J* = 7.3, 1.3 Hz, H_7 or H_6, 1H), 6.47 (d, *J* = 6.9 Hz, H_7 or H_6, 1H), 6.37 (td, *J* = 7.3, 1.2 Hz, H_8, 1H), 5.48 (s, H_{10}, 1H), 1.69 (d, *J* = 14.8, H_{20}, 9H).

^{13}C NMR (101 MHz, $CDCl_3$) δ (ppm) = 149.5 (Cq), 136.9 (d, *J* = 8.6 Hz, CH), 132.4 (CH), 131.8 (CH), 128.3 (d, *J* = 9.6 Hz, CH), 123.9 (d, *J* = 9.4 Hz, CH), 123.3 (CH), 122.8 (CH), 122.6 (CH), 61.6 (CH), 33.1 (d, *J* = 4.0 Hz, CH_3), 29.9 (Cq). The carbon directly attached to the boron atom on the triptycene core was not detected, likely due to quadrupolar relaxation.

^{11}B NMR (128 MHz, $CDCl_3$) δ (ppm) = -9.4

^{31}P NMR (162 MHz, $CDCl_3$) δ (ppm) = 19.1

HRMS (ESI) (*m/z*): calc. for [$C_{35}H_{33}{}^{10}BP$]: 494.24438 $[M+H]^+$; found: 494.24420.

IR (neat, ATR): $\tilde{\nu}$ / cm^{-1} = 3051, 2921, 2846, 1433, 1085, 886, 729.

M.p. : 265-269 °C (decomposition).

The absence of rotation around the P-B bond was unambiguously ensure by ^{1}H-1D TOCSY and ^{1}H NOE NMR experiments see Figures SII.11-SII.15, and temperature dependent ^{1}H NMR spectroscopy (Figure SII.16).

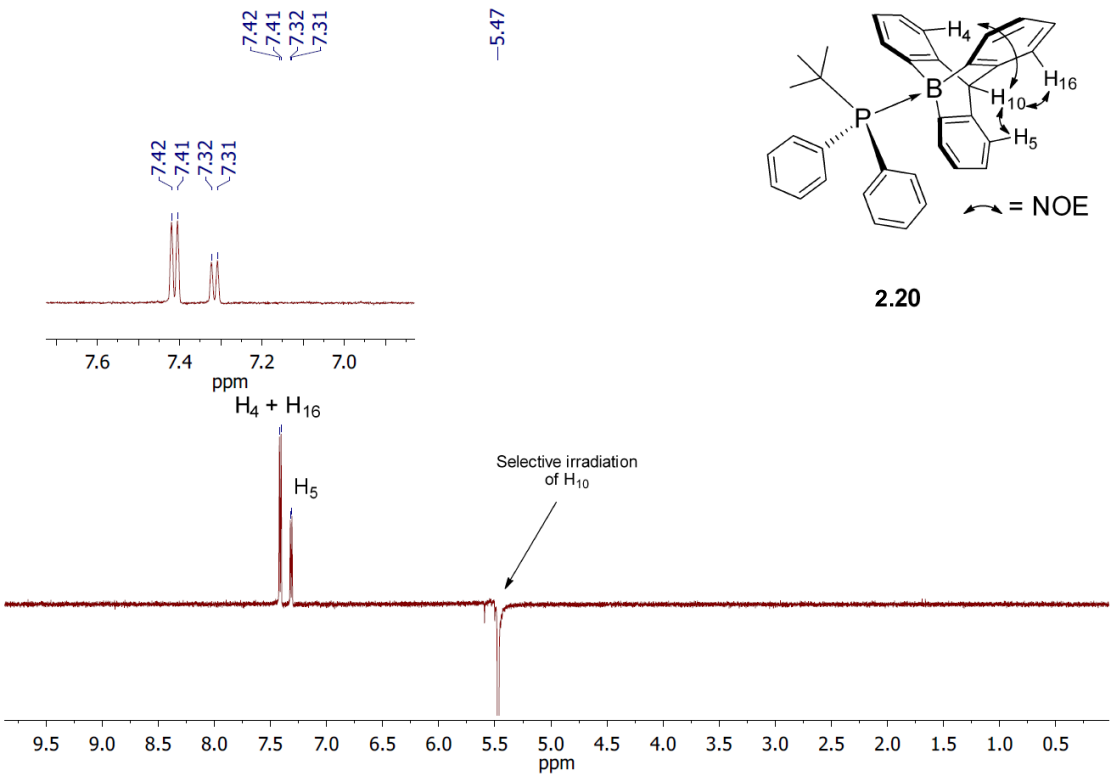


Figure SII.11: NOE selective 1D experiment of H_{10} (500 MHz, 25°C, $CDCl_3$)

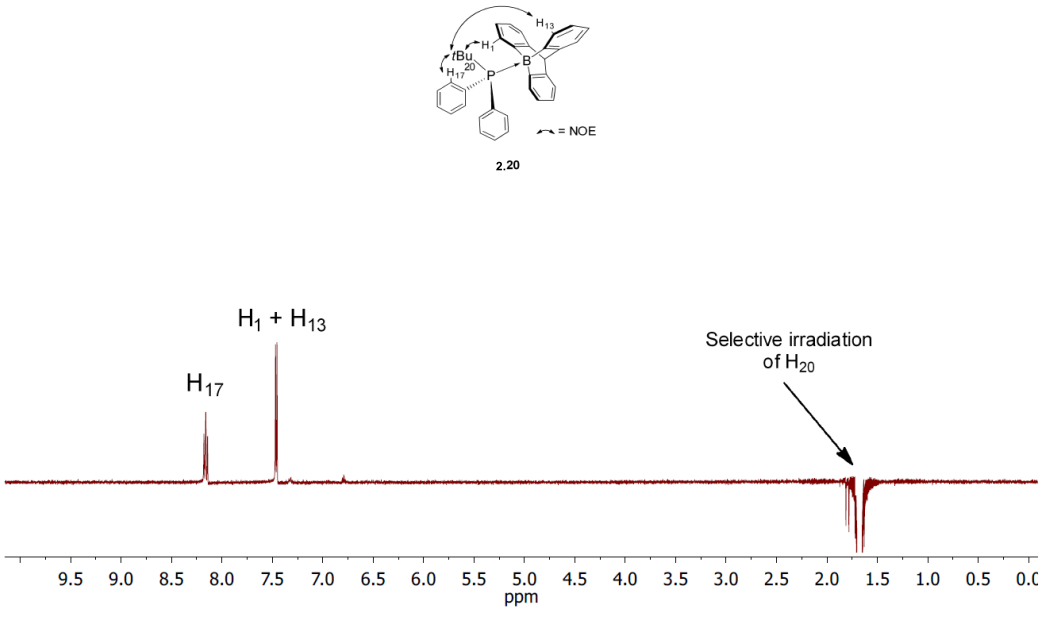


Figure SII.12: NOE selective 1D experiment of H_{20} (500 MHz, 25°C, $CDCl_3$)

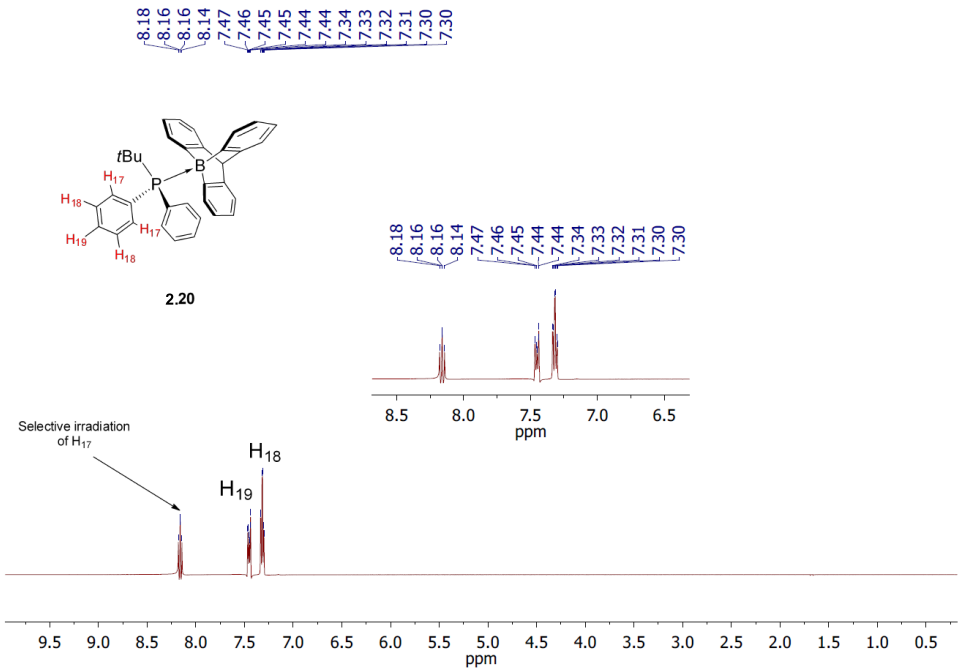


Figure SII.13: TOCSY selective 1D experiment of H_{17} showing the spin system of the phosphine aryl substituent (in red).

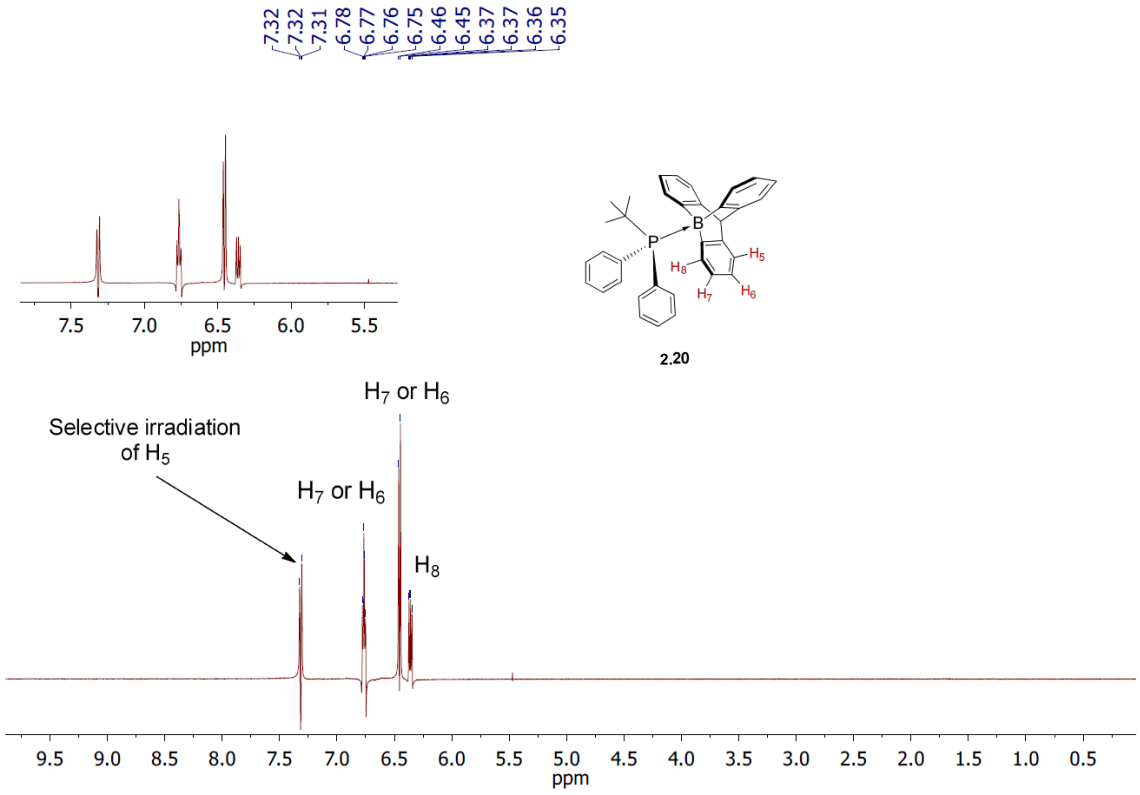


Figure SII.14: TOCSY selective 1D experiment of H_5 showing the spin system of the aryl ring of 9-boratriptycene (in red).

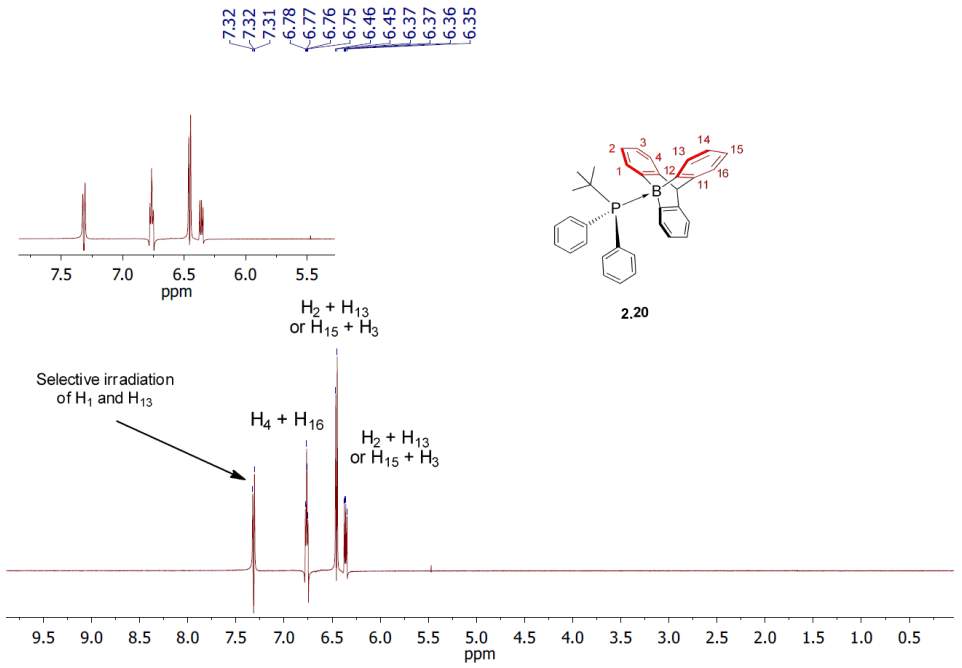


Figure SII.15: TOCSY selective 1D experiment of H_1 and H_{13} showing the spin system of the two aryl rings of 9-boratriptycene (in red).

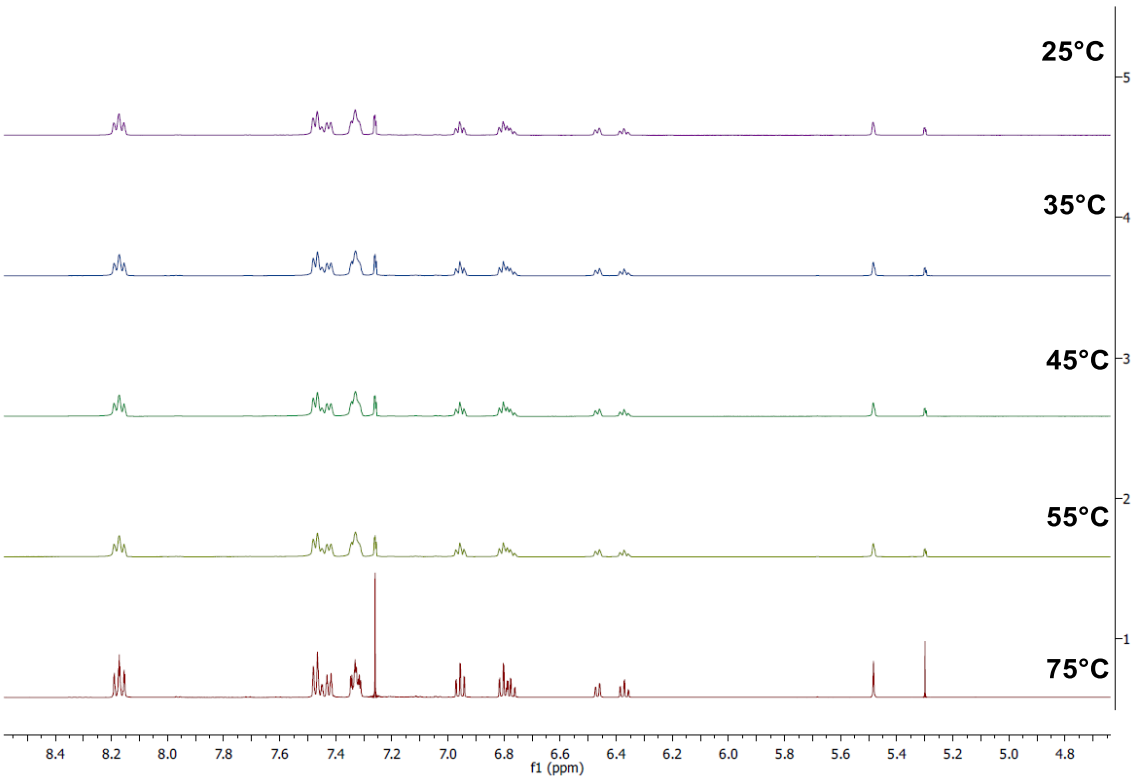
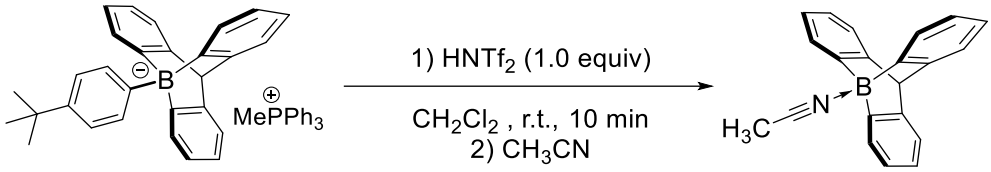


Figure SII.16: Temperature dependent ^{1}H NMR analysis of **20** (500 MHz, $CDCl_3$).

9-boratriptycene-MeCN Lewis adduct **2.22**



2.15a **2.22**

A solution of methyltriphenyl phosphonium 9-(4-*t*BuPh)-9-boratriptycene-"ate" complex **2.15a** (30 mg, 0.045 mmol, 1.0 equiv) in CH_2Cl_2 (1.0 mL) is added to solid bis(trifluoromethane)sulfonimide (12.7 mg, 0.045 mmol, 1.0 equiv) and the reaction is stirred at room temperature. After 10 min, acetonitrile is added (1.5 mL). The mixture is concentrated under reduced pressure and diethylether (5 mL) was added. The solid is filtrated and washed with diethylether (2 x 5 mL) and then purified *via* silica gel chromatography (CH_2Cl_2/pentane 25:75) affording 9-boratriptycene-MeCN Lewis adduct **2.22** (63%, 8.3 mg, 0.029 mmol) as a pale yellow solid.

Single crystals suitable for X-ray diffraction analysis were obtained by a slow evaporation of a saturated solution of **2.22** in CH_2Cl_2.

TLC: R_f = 0.30 (CH_2Cl_2/pentane 25:75)

^{1}H NMR (400 MHz, CD_2Cl_2) δ (ppm) = 7.39-7.35 (m, 3H), 7.33-7.28 (m, 3H), 6.97-6.89 (m, 6H), 5.34 (s, 1H), 2.81 (s, 3H).

^{13}C NMR (101 MHz, CD_2Cl_2) δ (ppm) = 147.5 (Cq), 124.8 (CH), 124.2 (CH), 124.0 (CH), 123.9 (CH), 59.1 (CH), 3.5 (CH_3). The carbon directly attached to the boron atom on the triptycene core was not detected, likely due to quadrupolar relaxation. The quaternary carbon of the CN triple bond was also not observed.

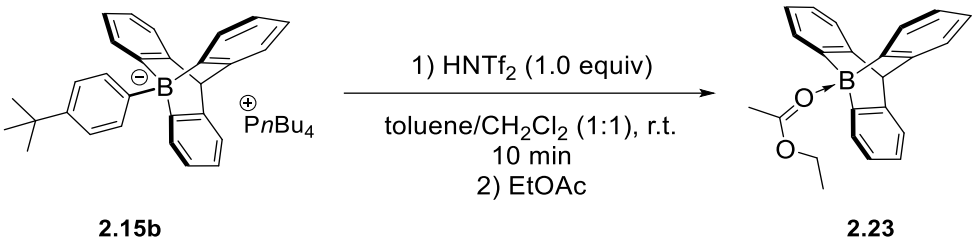
^{11}B NMR (128 MHz, CD_2Cl_2) δ (ppm) = -7.6

HRMS: The title compound cannot be detected by mass spectroscopy.

IR (neat, ATR): $\tilde{\nu}$ / cm^{-1} = 3044, 2955, 2921, 2866, 2337 (CN), 1433, 1269, 1098.

M.p. (CH_2Cl_2): 240-242 °C (decomposition).

9-boratriptycene-EtOAc Lewis adduct **2.23**



2.15b **2.23**

In a glove box, a solution of tetrabutylphosphonium 9-(4-*t*BuPh)-9-boratriptycene-"ate" complex (30 mg, 0.047 mmol, 1.0 equiv) **2.15b** in CH_2Cl_2/toluene (2.0 mL, 1:1) is added to solid bis(trifluoromethane)sulfonimide (13.1 mg, 0.047 mmol, 1.0 equiv). After 10 min, EtOAc was added (1.5 mL). The mixture is left overnight at room temperature and then filtrated affording 9-boratriptycene-EtOAc Lewis adduct **2.23** (39%, 6.1 mg, 0.018 mmol) as colourless crystals suitable for X-ray diffraction analysis.

TLC: The title compound is not stable on silica gel, decomposition was observed when performing flash column chromatography and TLC (checked by 2D TLC).

^{1}H NMR (400 MHz, $CDCl_3$) δ (ppm) = 7.36-7.32 (m, 3H), 7.17-7.12 (m, 3H), 6.92-6.84 (m, 6H), 5.39 (s, 1H), 5.05 (q, *J* = 7.2 Hz, 2H), 2.83 (s, 3H), 1.72 (t, *J* = 7.1 Hz, 3H).

^{13}C NMR (101 MHz, $CDCl_3$) δ (ppm) = 186.1 (Cq, C=O), 147.7 (Cq), 124.5 (CH), 123.9 (CH), 123.8 (CH), 123.5 (CH), 68.9 (CH_2), 59.3 (CH), 22.34 (CH_3), 14.01 (CH_3). The carbon directly attached to the boron atom on the triptycene core was not detected, likely due to quadrupolar relaxation.

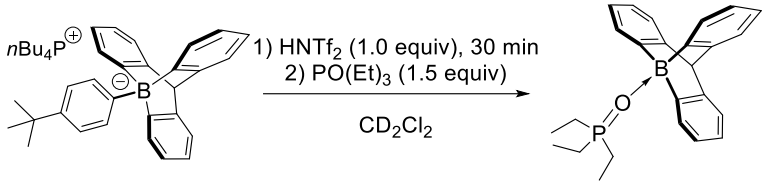
^{11}B NMR (128 MHz, $CDCl_3$) δ (ppm) = 5.7

HRMS (ESI) (*m/z*): calc. for $[C_{23}H_{22}{}^{10}BO_2]$: 340.17437 $[M+H]^+$; found: 340.17446.

IR (neat, ATR): $\tilde{\nu}$ / cm^{-1} = 3044, 2962, 2866, 1603 (C=O), 1433, 1187, 1033.

M.p. (CH_2Cl_2/toluene): 184-187 °C (decomposition).

II.6. Generation of Gutmann-Beckett Lewis adduct **2.21**.



2.15b **2.21**

In a glove box, a solution of tetrabutylphosphonium-10-*tert*butylphenyl-10-boratriptycene “ate”-complex **2.15b** (30 mg, 47 μmol, 1.0 equiv) in 0.500 mL of CD_2Cl_2 was added to Tf_2NH (13.1 mg, 47.0 μmol, 1.0 equiv) in a small vial. The initially homogenous colorless solution turn to deep yellow and finally purple. After 15 min at room temperature $PO(Et)_3$ (7.0 mg, 47 μmol, 1.0 equiv) was added as a solution in CD_2Cl_2 (0.25 mL). The ^{31}P NMR analysis show a signal at 75.0 ppm for the Lewis adduct **2.21** (Figure SII.17) which correspond to an acceptor number of 76.2. Same result was obtained in a presence of 0.3 equivalent of $OPEt_3$ (Figure SII.18).

In order to obtain suitable crystals for X-ray diffraction analysis the procedure was modified as following.

In a glove box, a solution of tetrabutylphosphonium-10-*tert*butylphenyl-10-boratriptycene “ate”-complex **2.15b** (30 mg, 47 μmol, 1.0 equiv) in 0.60 mL of toluene was added to Tf_2NH (13.0 mg, 47 μmol, 1.0 equiv) in a small vial. The initially homogenous colorless solution became biphasic. The upper yellow layer was removed and the resulting deep purple lower phase was washed with toluene (3 x 1 mL). Then, $PO(Et)_3$ (7.0 mg, 47 μmol, 1.0 equiv) was added as a solution in toluene (0.25 mL). Single crystals suitable for X-ray diffraction analysis were obtained by a slow evaporation of a saturated solution of **2.21** in CH_2Cl_2/toluene.

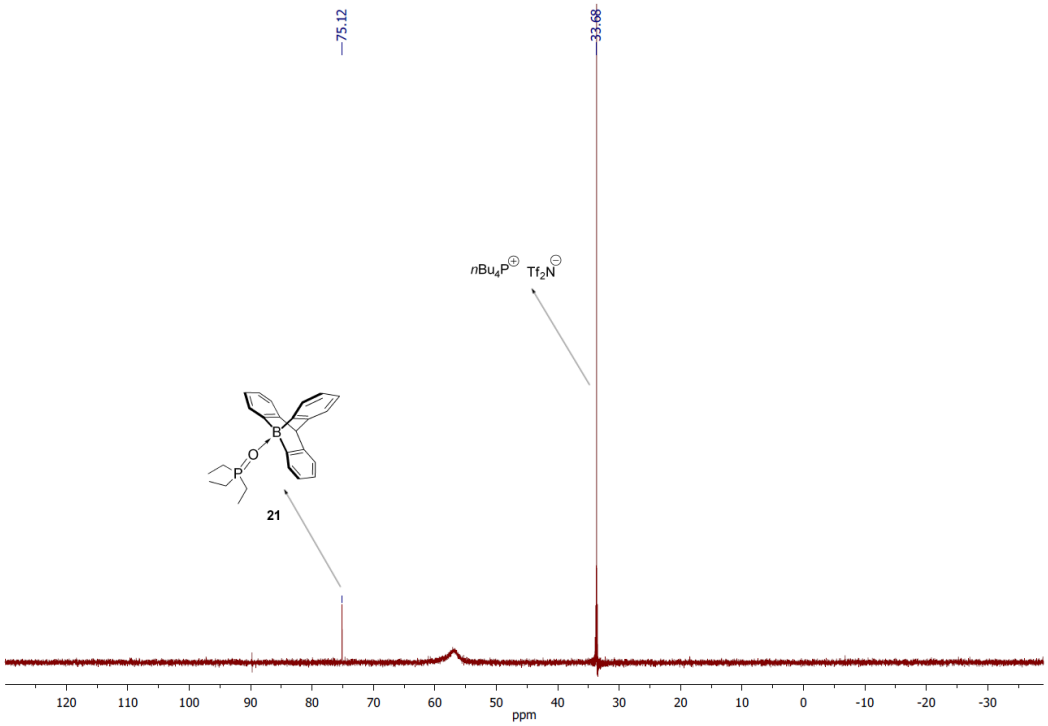


Figure SII.17: ^{31}P NMR spectra (202 MHz, 25°C, CD_2Cl_2)

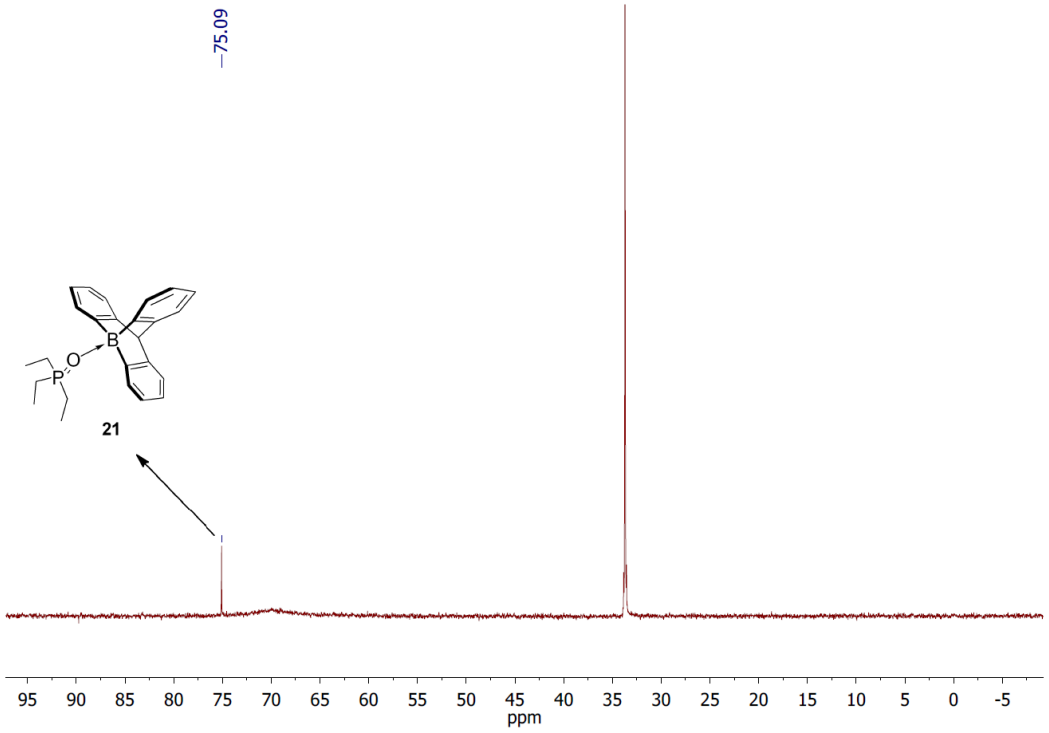
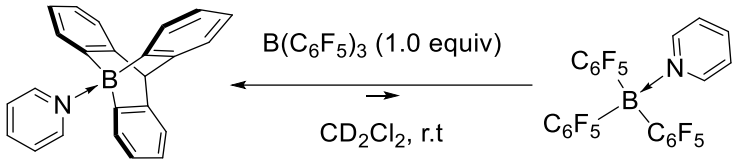


Figure SII.18: ^{31}P NMR spectra (0.3 equiv of $OPEt_3$, 500 MHz, 25°C, CD_2Cl_2)

II.7. Competitions reactions.



2.17

In a glove box, 9-boratriptycene-pyridine Lewis adduct **2.17** (4.0 mg, 12.0 μmol, 1.0 equiv) was added as a solid to a solution of trispentafluorophenylborane (6.2 mg, 12.0 μmol, 1.0 equiv) in CD_2Cl_2 (0.65 mL). After 1h, The NMR tube was vigorously shake and submitted to ^{1}H, ^{19}F and ^{11}B NMR spectroscopy. The ^{1}H NMR spectra only show the presence of the 9-boratriptycene-pyridine Lewis adduct **2.17** δ (ppm in CD_2Cl_2) = 9.36 (d, *J* = 5.2 Hz, 2H), 8.50-8.18 (m, 1H), 7.98 (ddd, *J* = 8.7, 4.4, 3.6 Hz, 2H), 7.41-7.28 (m, 3H), 7.05-6.97 (m, 3H), 6.96-6.75 (m, 2H), (Figure SII.20). However, the ^{19}F NMR spectra show trace amounts of the known pyridine-trispentafluorophenylboron Lewis adduct,[S2.2] δ (ppm in CD_2Cl_2) = -131.7 (br), -157.3 (t, *J* = 20.3 Hz), -163.8 (br) (Figure SII.21-SII.22), “donor free” trispentafluorophenylboron was detected as a major product δ (ppm in CD_2Cl_2) = -128.4 (br), -144.1 (br), -161.0 (br). ^{11}B NMR analysis only show the signals of the “donor” free trispentafluorophenylboron δ (ppm in CD_2Cl_2) = 58.8 ppm and 9-boratriptycene-pyridine Lewis adduct **2.17** δ (ppm in CD_2Cl_2) = -1.71 (Figure SII.23).

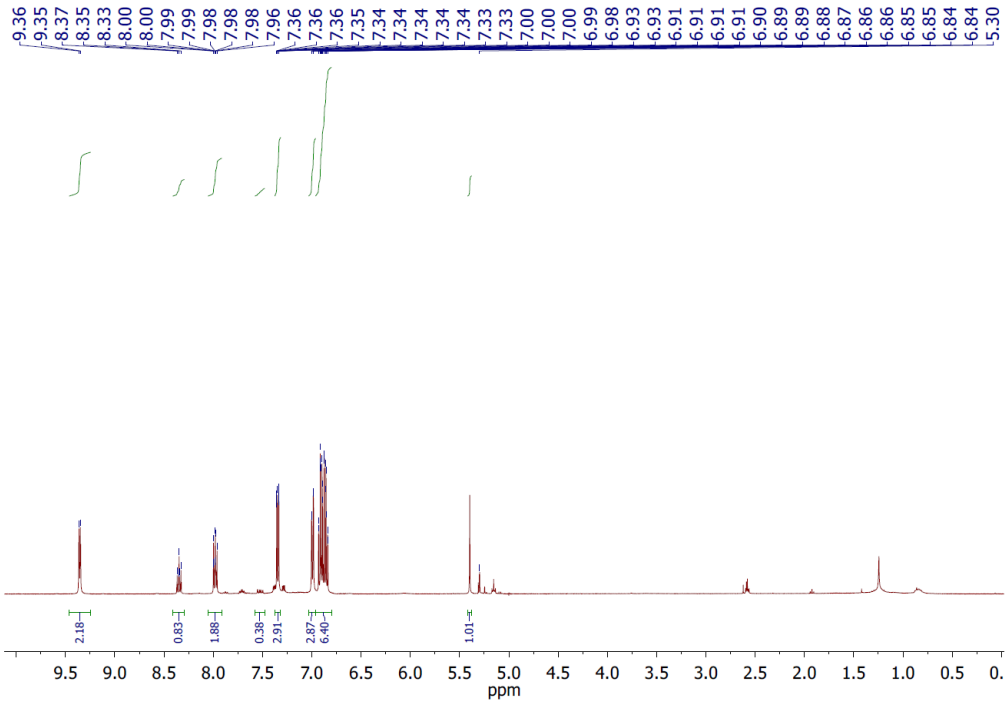


Figure SII.19: ^{1}H NMR spectra (400 MHz, 25°C, CD_2Cl_2)

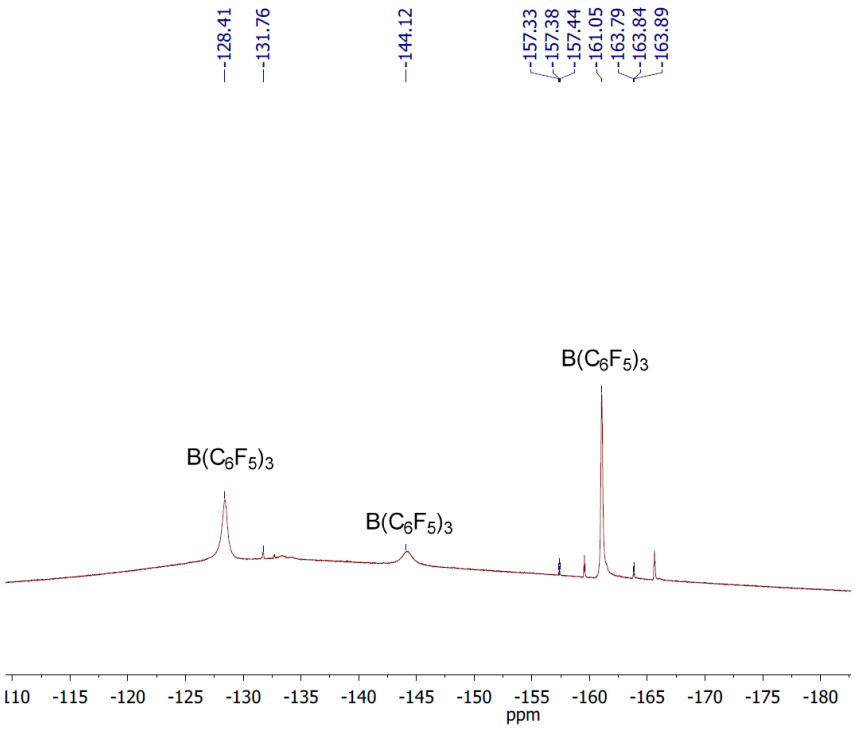


Figure SII.20: ^{19}F NMR spectra (376 MHz, 25°C, CD_2Cl_2)

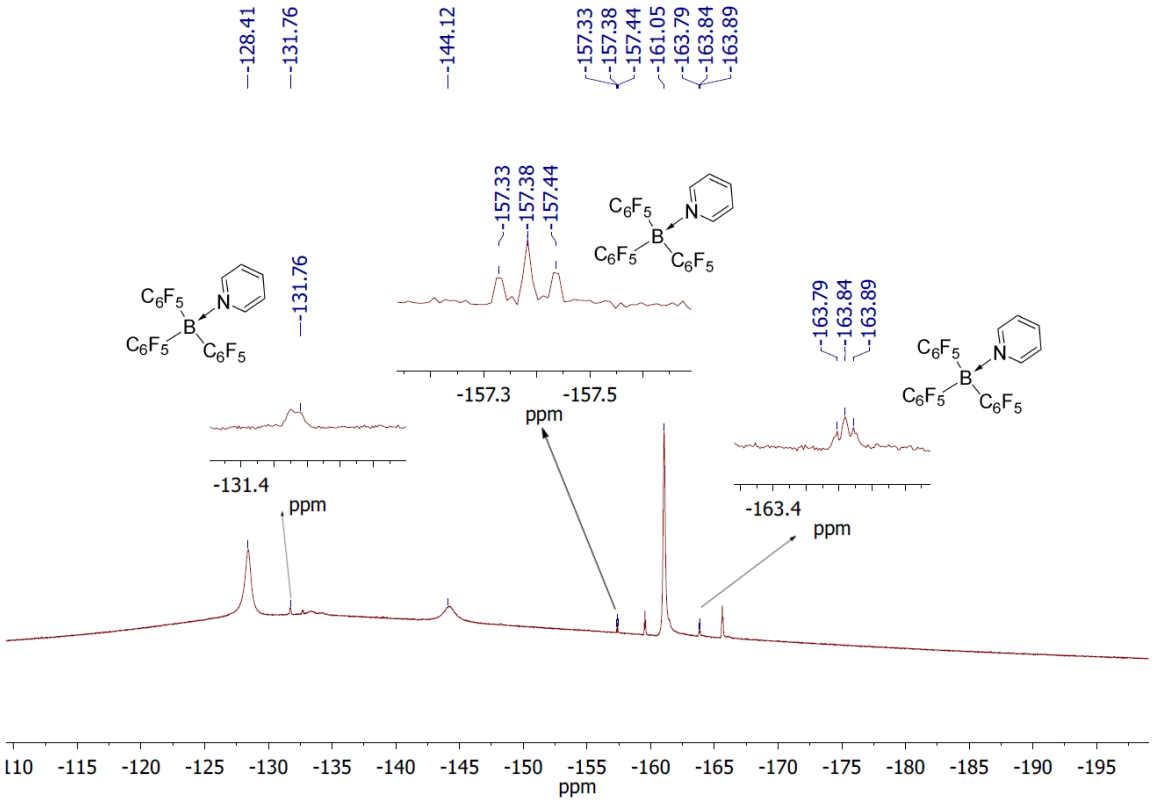


Figure SII.22: ^{19}F NMR spectra (376 MHz, 25°C, zoom in CD_2Cl_2)

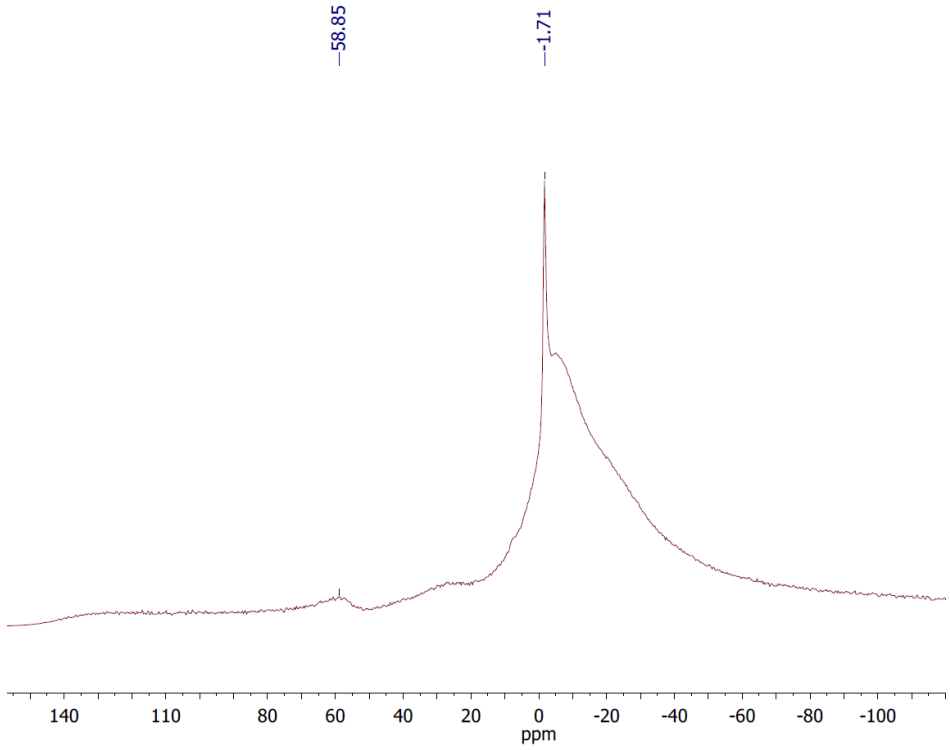
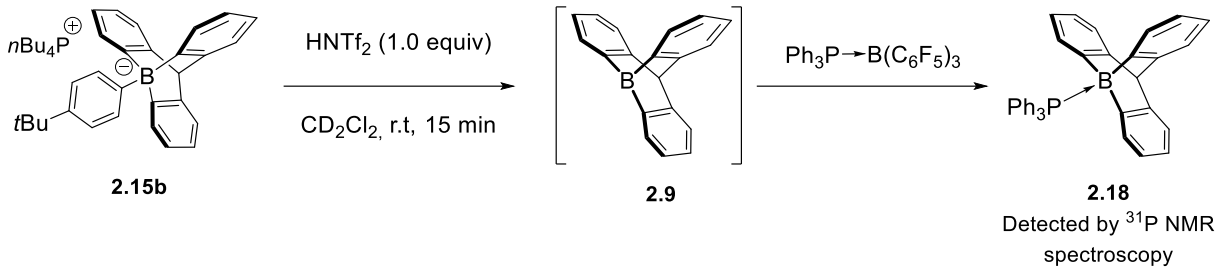


Figure SII.23: ^{11}B NMR spectra (128 MHz, 25°C, CD_2Cl_2)



2.15b **2.9** **2.18**

Detected by ^{31}P NMR spectroscopy

In a glove box, Tf_2NH (10.9 mg, 38.7 μmol, 1.0 equiv) was added to a solution of tetrabutylphosphonium-9-*tert*butylphenyl-9-boratriptycene-"ate"-complex **2.15b** (25 mg, 38.7 μmol, 1.0 equiv) in CD_2Cl_2 (0.65 mL). After 15 min, triphenylphosphine-trispentafluorophenyl Lewis adduct (31 mg, 40 μmol, 1.0 equiv) was added as a solution in CD_2Cl_2 (0.1 mL). After 1h, ^{31}P NMR spectra only show the presence of the triphenylphosphine-trispentafluorophenyl Lewis adduct: δ (ppm in CD_2Cl_2) = 1.96 ppm, meaning that no transfer take place after 1h (Figure SII.24). However, after 24h a substantial amount of the 9-boratriptycene-triphenylphosphine Lewis adduct **2.18** was detected by ^{31}P NMR spectroscopy δ (ppm in CD_2Cl_2) = 4.50 ppm showing that the triphenylphopshine is slowly displace from the trispentafluorophenylboron to the 9-boratriptycene (Figure SII.25).

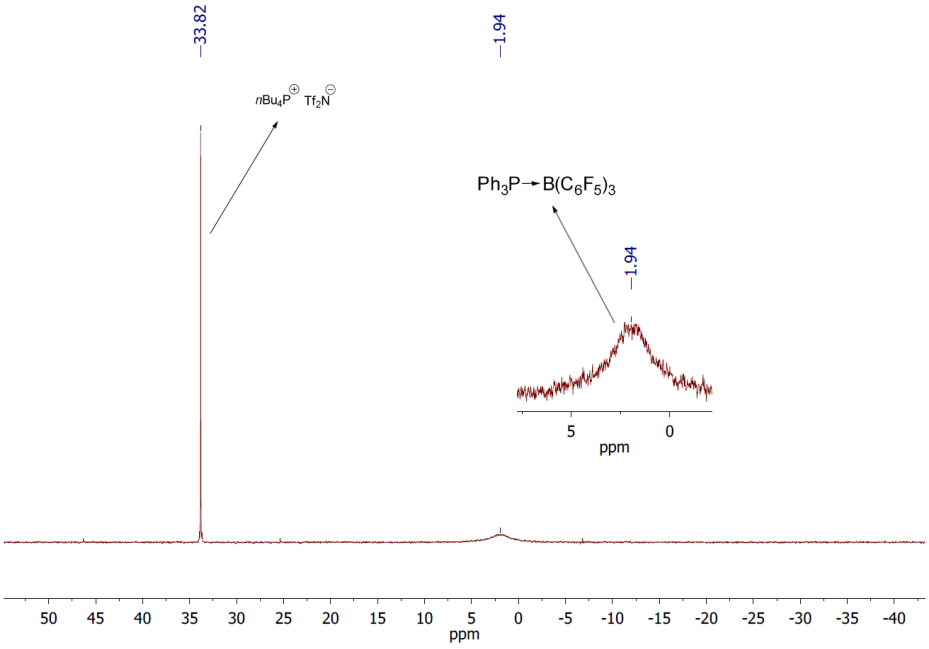


Figure SII.24: ^{31}P NMR spectra (202 MHz, 25°C, CD_2Cl_2) after 1h.

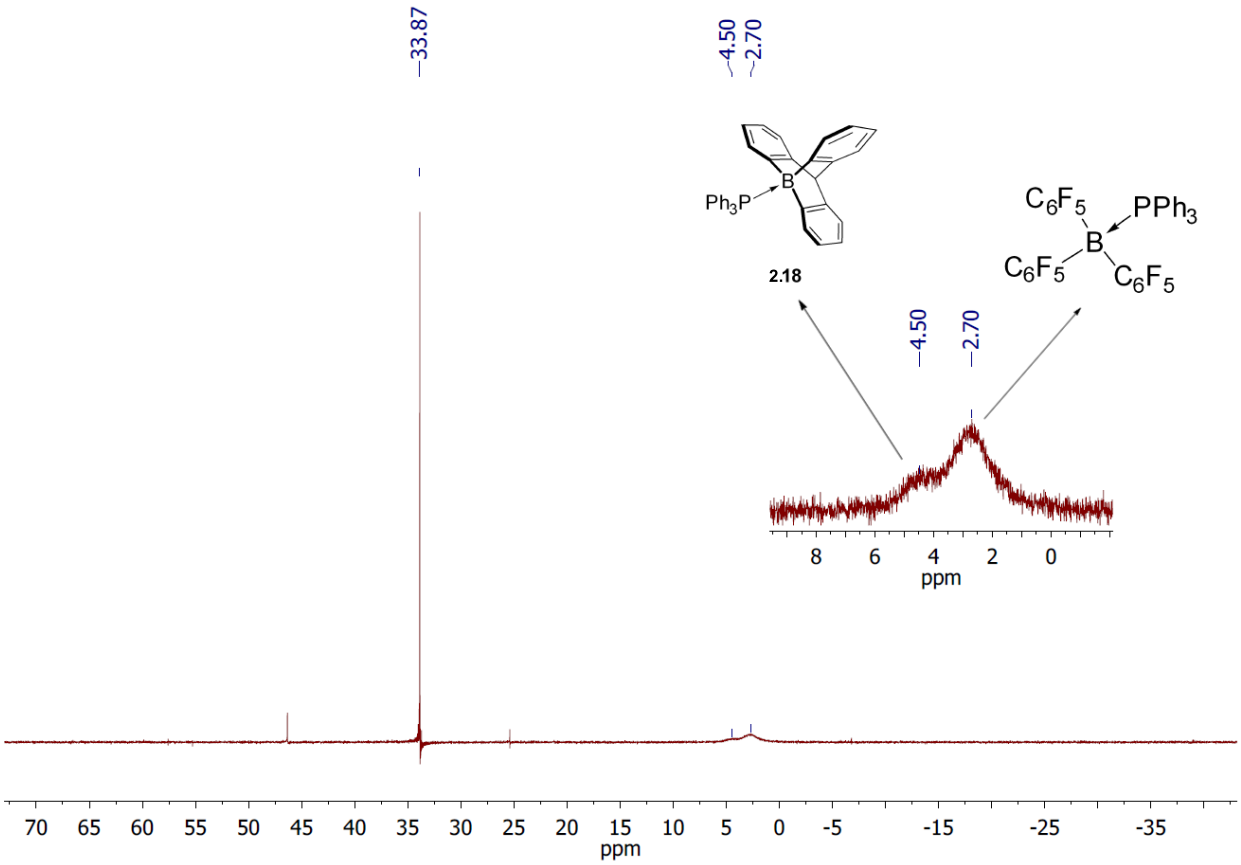


Figure SII.25: ^{31}P NMR spectra (202 MHz, 25°C, CD_2Cl_2) after 24h.

8. Quantum chemical calculations

Calculation methods

Using the Gaussian16 package[S2.3], geometry optimizations and vibrational frequency calculations were performed at the M06-2X/6-311G(d) level of theory. The geometry optimizations were performed using a tight convergence threshold on the residual forces on the atoms (1.5×10^{-5} Hartree/Bohr or Hartree/radian). For each compound, all vibrational frequencies are real, demonstrating that the structures are minima on the potential energy surface. When indicated, solvent (CH_2Cl_2) effects were modelled using the Polarizable Continuum Model put into Integral Equation Formalism (IEFPCM).[S2.4] For fluoride (FIA) and hydride (HIA) affinities, isodesmic reactions were employed, using respectively G3 $FSiMe_3 \rightarrow SiMe_3^+ + F^-$ and $HSiMe_3 \rightarrow SiMe_3^+ + H^-$ as anchor points, according to the scheme of Krossing.[S2.5] The natural atomic orbital and natural bond orbital analysis was performed in gas phase using the Gaussian NBO 3.1 program[S2.6] at the M06-2X/6-311G(d) level of theory, on optimized structures. NMR chemical shifts (obtained using the GIAO method) were evaluated at the B3LYP/6-311+G(2d,p) level of theory on structures optimized at the M06-2X/6-311G(d) level of theory, in both cases simulating CH_2Cl_2 as solvent.

^{11}B NMR predictions

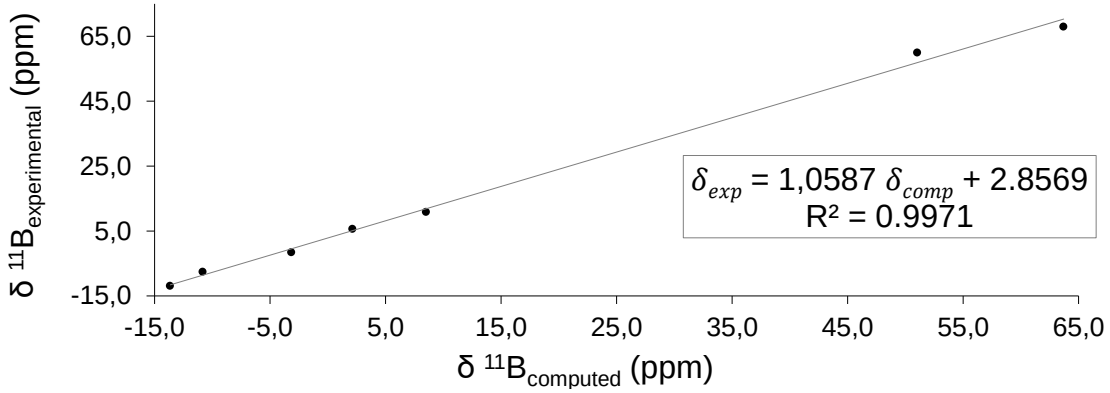


Figure SII.26: Calibration between experimental and computed values for boron NMR.

Table SII.1: Data for the calibration of ^{11}B NMR and predicted experimental chemical shift of 9-boratriptycene **2.9**. The computed isotropic magnetic shielding tensor of the reference compound for ^{11}B NMR (F_3B-OEt_2) is 100.4 ppm.

Compound	δ_{comp} ^{11}B (ppm)	δ_{exp} ^{11}B (ppm)
2.9-Pyridine (CH_2Cl_2)	-3.2	-1.5
2.9-OEt_2 (CH_2Cl_2)	8.5	10.9
2.9-MeCN (CH_2Cl_2)	-10.8	-7.6
2.9-PPh_3 (CH_2Cl_2)	-13.6	-11.9
2.9-AcOEt (CH_2Cl_2)	2.2	5.7
BPh_3 **2.25** (CH_2Cl_2)	51.0	60.0
$B(C_6F_5)_3$ **2.26** (CH_2Cl_2)	63.7	68.0
2.9 (CH_2Cl_2)	84.9	**Predicted: 92 ppm**

Global and local electrophilicity indexes

The global electrophilicity index (ω, in eV) was first introduced by Parr.[S2.7] and is defined as:

$$\omega\ (eV) = {\chi^2}/{2\eta} \text{ with } \chi\ (eV) = {-1}/{2}\ (E_{HOMO} + E_{LUMO}) \text{ and } \eta\ (eV) = E_{LUMO} - E_{HOMO}$$

where χ is the electronegativity of Mulliken and η the chemical hardness. The local electrophilicity index ω_X can be defined as the product of the global electrophilicity ω with a local Fukui function f_k^+ (on the atomic site *k*):[S2.8]

$$\omega_X(eV) = \omega . f_k^+$$

the latter Fukui function can be conveniently expressed from the electron population of atom *k* in the system of N and N+1 electrons:[S2.9]

$$f_k^+ = Q_k(N+1) - Q_k(N) = \Delta Q_k$$

Table SII.2 presents the determined global and local electrophilicity indexes for a selection of boron Lewis acids.

Table SII.2: Global (ω) and local (ω_B, on the boron atom) electrophilicity indexes for several Lewis acids. Structures are optimized at the M06-2X/6-311G(d) level of theory. The energies of the frontier orbitals are obtained as the energies of the corresponding Kohn-Sham orbitals. The natural charges of the boron Q_B (N) and Q_B (N+1) are obtained after NBO analysis (respectively with charge=0, spin multiplicity=1 and charge=-1, spin multiplicity=2) on the same structures and at the same level of theory.

Compounds	Global Electrophilicity Index			Local (boron) electrophilicity index			
	E_{HOMO} (eV)	E_{LUMO} (eV)	**ω (eV)**	Q_B (N+1)	Q_B (N)	ΔQ_B	**ω_B (eV)**
2.1	-8.650	0.600	**0.88**	0.41	1.06	-0.65	**-0.57**
2.9	-7.434	-0.640	**1.20**	-0.25	1.00	-1.25	**-1.50**
2.24	-7.381	-0.240	**1.02**	-0.33	0.88	-1.21	**-1.23**
2.25 BPh_3	-8.172	-1.122	**1.53**	0.50	0.93	-0.42	**-0.65**
2.26 $B(C_6F_5)_3$	-9.002	-2.780	**2.79**	0.44	0.88	-0.44	**-1.23**
BEt_3	-9.131	0.485	**0.97**	0.43	1.12	-0.69	**-0.67**

II.9. Thermal analysis of Lewis adducts **2.16**-**2.17**:

TGA/DSC Thermal analysis of Lewis adducts **2.16** and **2.17** have been carried out on a Mettler Toledo TGA/DSC 3+ SF/1000 apparatus. The measurements were done under an atmosphere of N_2 (80 mL/min), both samples were heated from 25 to 500 °C at heating rate of 10 °C/min.

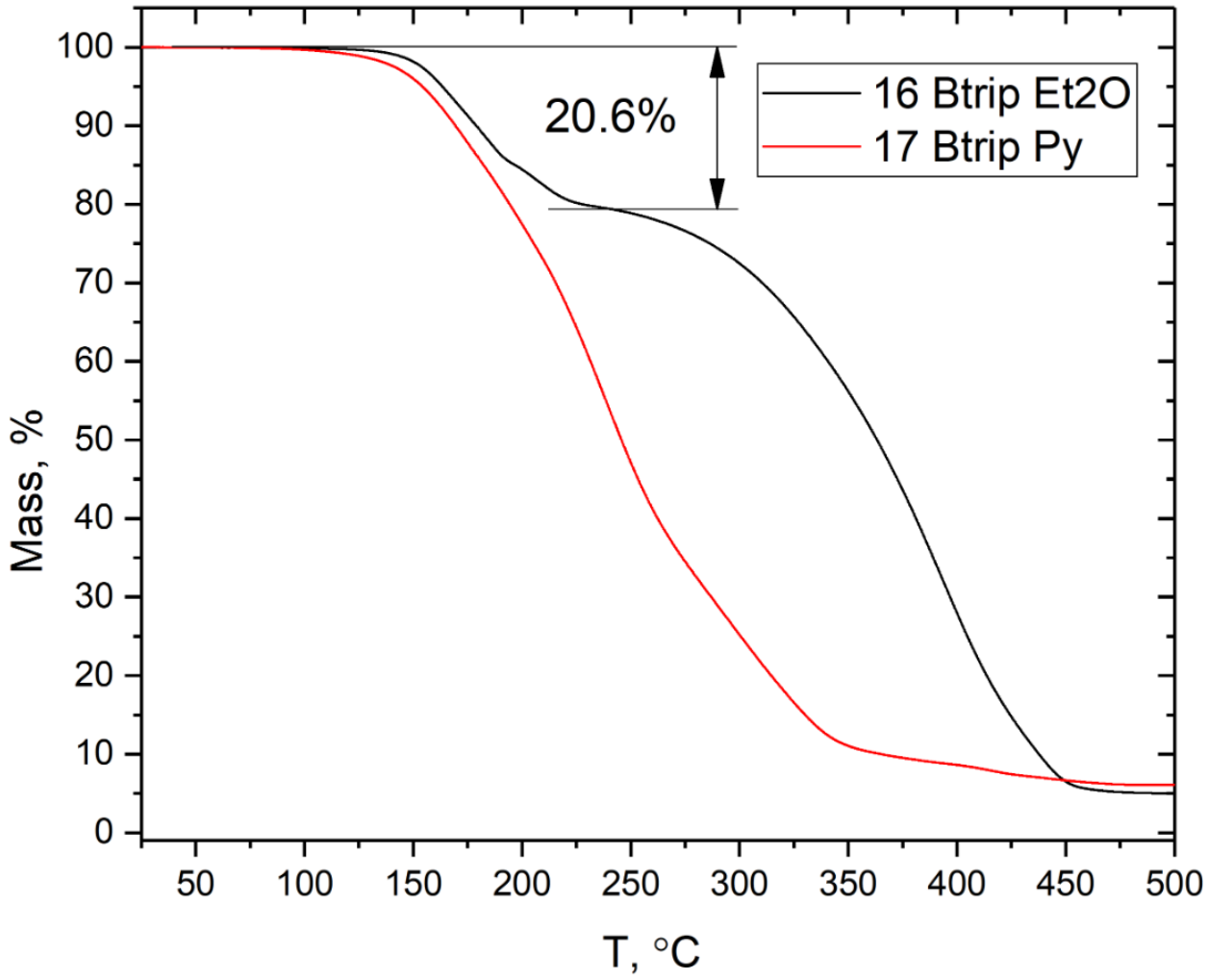


Figure SII.30: Thermal gravimetric analysis of compounds **2.16** (black) and **2.17** (red).

II.10. Crystallographic parameters:

The crystal structures were determined from single-crystals X-ray diffraction data collected using an Oxford Diffraction Gemini Ultra R diffractometer (Cu Kα radiation, fine-focus sealed tube, multilayer mirror). The data were integrated using the CrysAlisPro software.[S2.10] The structures were solved by the dual-space algorithm implemented in SHELXT,[S2.11] and refined by full-matrix least squares on $|F|^2$ using SHELXL-2018/3,[S2.12] the shelXLe,[S2.13] and Olex2 software.[S2.14] Non-hydrogen atoms were refined anisotropically; and hydrogen atoms in most of the cases were located from the difference Fourier map but placed on calculated positions in riding mode with equivalent isotropic temperature factors fixed at 1.2 times U_{eq} of the parent atoms (1.5 times U_{eq} for methyl groups).

	2.15c	**2.16**	**2.17**	**2.18**
Chemical formula	$C_{29}H_{26}B^-$ $\cdot C_{24}H_{20}P^+$	$C_{23}H_{23}BO$	$C_{24}H_{18}BN$	$C_{37}H_{28}BP\cdot CH_2Cl_2$
M_r	724.68	326.22	331.20	599.30
Crystal system, space group	Triclinic, $P\bar{1}$	Orthorhombic, $Pmn2_1$	Orthorhombic, *Pnma*	Trigonal, $R\bar{3}c$:*H*
Temperature (K)	295	295	100	100
a, *b*, *c* (Å)	13.2077 (4), 13.3525 (5), 13.8714 (6)	10.4920 (4), 8.4112 (3), 9.9365 (4)	20.4336 (7), 10.1425 (4), 8.1572 (3)	13.4252 (4), 13.4252 (4), 58.0611 (11)
α, β, γ (°)	66.928 (4), 62.820 (4), 77.557 (3)	90, 90, 90	90, 90, 90	90, 90, 120
V (Å^3)	2000.14 (15)	876.89 (6)	1690.56 (10)	9062.7 (6)
Z	2	2	4	12
μ (mm^{-1})	0.87	0.55	0.56	2.63
Crystal size (mm)	0.50 × 0.23 × 0.08	0.36 × 0.14 × 0.11	0.39 × 0.12 × 0.11	0.29 × 0.18 × 0.03
Absorption correction	Analytical			
T_{min}, T_{max}	0.771, 0.944	0.912, 0.966	0.866, 0.953	0.679, 0.914
No. of measured, independent and observed [$I > 2\sigma(I)$] reflections	18600, 7067, 6211	2361, 1240, 911	4930, 1577, 1429	10159, 1800, 1590
R_{int}	0.031	0.040	0.024	0.049
$(\sin\theta/\lambda)_{max}$ (Å^{-1})	0.598	0.599	0.597	0.598
$R[F^2 > 2\sigma(F^2)]$, $wR(F^2)$, *S*	0.040, 0.114, 1.03	0.053, 0.185, 1.13	0.039, 0.102, 1.04	0.053, 0.147, 1.04
No. of reflections	7067	1240	1577	1800
No. of parameters	499	153	133	145
No. of restraints	0	10	0	16
$\Delta\rho_{max}$, $\Delta\rho_{min}$ (e Å^{-3})	0.22, -0.28	0.18, -0.21	0.37, -0.20	0.40, -0.45
CCDC deposition number	1986932	1986933	1986934	1986935

	2.19	**2.21**	**2.22**	**2.23**
Chemical formula	$C_{38}H_{26}BP \cdot 2(C_7H_8)$	$C_{25}H_{28}BOP$	$C_{21}H_{16}BN \cdot CH_2Cl_2$	$C_{23}H_{21}BO_2 \cdot 1.5(C_7H_8)$
M_r	708.63	386.25	378.08	478.41
Crystal system, space group	Monoclinic, $P2_1/n$	Monoclinic, $C2$	Monoclinic, $P2_1/c$	Monoclinic, $C2/c$
Temperature (K)	100	295	295	100
a, b, c (Å)	11.3312 (6), 10.8435 (5), 15.5434 (8)	18.1814 (2), 11.05567 (11), 11.36083 (13)	12.48707 (14), 13.97455 (15), 12.29219 (14)	24.8027 (3), 15.66116 (19), 13.97831 (18)
α, β, γ (°)	90, 96.883 (5), 90	90, 106.9535 (12), 90	90, 101.7559 (11), 90	90, 101.4805 (13), 90
V (Å^3)	1896.05 (16)	2184.37 (5)	2100.01 (4)	5321.08 (12)
Z	2	4	4	8
μ (mm^{-1})	0.91	1.19	2.80	0.55
Crystal size (mm)	0.26 × 0.22 × 0.15	0.40 × 0.19 × 0.10	0.41 × 0.37 × 0.06	0.68 × 0.15 × 0.12
Absorption correction	Analytical			
T_{min}, T_{max}	0.839, 0.907	0.762, 0.901	0.431, 0.844	0.654, 1.000
No. of measured, independent and observed [$I > 2\sigma(I)$] reflections	9221, 3353, 2825	10048, 3876, 3780	10972, 3726, 3249	14312, 4670, 4329
R_{int}	0.067	0.017	0.018	0.020
$(\sin\theta/\lambda)_{max}$ (Å^{-1})	0.598	0.597	0.597	0.597
$R[F^2 > 2\sigma(F^2)]$, $wR(F^2)$, S	0.073, 0.211, 1.10	0.044, 0.128, 1.03	0.056, 0.176, 1.06	0.036, 0.094, 1.04
No. of reflections	3353	3876	3726	4670
No. of parameters	245	256	236	430
No. of restraints	0	1	0	85
$\Delta\rangle_{max}$, $\Delta\rangle_{min}$ (e Å^{-3})	0.58, -0.37	0.35, -0.20	0.37, -0.49	0.24, -0.16
Absolute structure parameter	–	0.000 (6)	–	–
CCDC deposition number	1986936	1986937	1986938	1986939

II.11. References

[S2.1] a) V. Morozova, P. Mayer, G. Berionni, *Angew. Chem. Int. Ed.* **2015**, *54*, 14508; c) H. Jacobsen, H. Berke, S. Döring, G. Kehr, G. Erker, R. Fröhlich, O. Meyer, *Organometallics*, **1999**, *18*, 1724; c) A. Ben Saida, A. Chardon, A. Osi, N. Tumanov, J. Wouters, A. I. Adjeufack, B. Champagne, G. Berionni, *Angew. Chem. Int. Ed,* **2019**, *58*, 16889;

[S2.2] N. A. Shcherbina, I. V. Kazakov, N. Yu. Gugin, A. S. Lisovenko, A. V. Pomogaeva, Yu. V. Kondrat'ev, V. V. Suslonov, *Russ. J. Gen. Chem.,* **2019**, *89*, 1162.

[S2.3] Gaussian 16, Revision B.01, M. J. Frisch, G. W. Trucks, H. B. Schlegel, G. E. Scuseria, M. A. Robb, J. R. Cheeseman, G. Scalmani, V. Barone, G. A. Petersson, H. Nakatsuji, X. Li, M. Caricato, A. V. Marenich, J. Bloino, B. G. Janesko, R. Gomperts, B. Mennucci, H. P. Hratchian, J. V. Ortiz, A. F. Izmaylov, J. L. Sonnenberg, D. Williams-Young, F. Ding, F. Lipparini, F. Egidi, J. Goings, B. Peng, A. Petrone, T. Henderson, D. Ranasinghe, V. G. Zakrzewski, J. Gao, N. Rega, G. Zheng, W. Liang, M. Hada, M. Ehara, K. Toyota, R. Fukuda, J. Hasegawa, M. Ishida, T. Nakajima, Y. Honda, O. Kitao, H. Nakai, T. Vreven, K. Throssell, J. A. Montgomery, Jr., J. E. Peralta, F. Ogliaro, M. J. Bearpark, J. J. Heyd, E. N. Brothers, K. N. Kudin, V. N. Staroverov, T. A. Keith, R. Kobayashi, J. Normand, K. Raghavachari, A. P. Rendell, J. C. Burant, S. S. Iyengar, J. Tomasi, M. Cossi, J. M. Millam, M. Klene, C. Adamo, R. Cammi, J. W. Ochterski, R. L. Martin, K. Morokuma, O. Farkas, J. B. Foresman, and D. J. Fox, Gaussian, Inc., Wallingford CT, **2016**.

[S2.4] J. Tomasi, B. Mennucci, R. Cammi, *Chem. Rev.* **2005**, *105*, 2999

[S2.5] H. Böhrer, N. Trapp, D. Himmel, M. Schleep, I. Krossing, *Dalton Trans.* **2015**, *44*, 7489.

[S2.6] E. D. Glendening, A. E. Reed, J. E. Carpenter, F. Weinhold, NBO Version 3.1.

[S2.7] R. G. Parr, L. V. Szentpály, S. Liu, *J. Am. Chem. Soc.* **1999**, *121*, 1922.

[S2.8] a) P. Pérez, A. Toro-Labbé, A. Aizman, R. Contreras, *J. Org. Chem.* **2002**, *67*, 4747; b) E. Chamorro, P. K. Chattaraj, P. Fuentealba, *J. Phys. Chem. A.* **2003**, *107*, 7068; c) P. K. Chattaraj, U. Sarkar, D. R. Roy, *Chem. Rev.* **2006**, *106*, 2065.

[S2.9] W. Yang, W. J. Mortier, *J. Am. Chem. Soc.* **1986**, *108*, 5708.

[S2.10] Rigaku Oxford Diffraction. CrysAlis PRO. Rigaku Oxford Diffraction: Oxford, UK

2018.

[S2.11] G. M. Sheldrick, *Acta Crystallogr. Sect. A Found. Adv.* **2015**, *71*, 3.

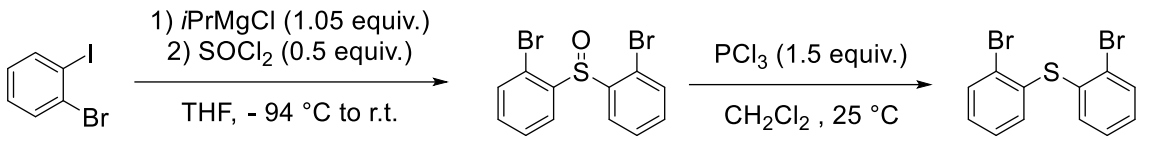
[S2.12] G. M. Sheldrick, *Acta Crystallogr. Sect. C Struct. Chem.* **2015**, *71*, 3.

[S2.13] C. B. Hübschle, G. M. Sheldrick, B. Dittrich, *J. Appl. Crystallogr.* **2011**, *44*, 1281.

[S2.14] O. V. Dolomanov, L. J. Bourhis, R. J. Gildea, J. A. K. Howard, Puschmann, H. *J. Appl.Crystallogr.* **2009**, *42*, 339.

III.1. Preparation of starting materials.

Bis-(2,2'-bromophenyl)sulfide **S3.2**



S3.1 **S3.2**

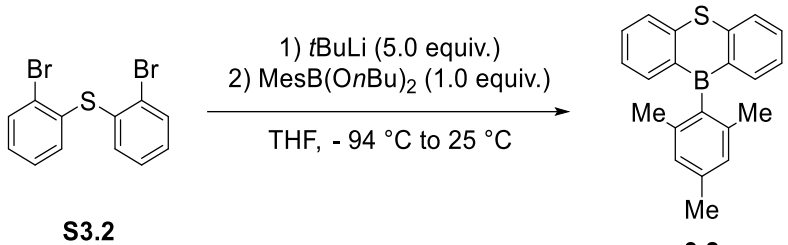
71% over two steps

The title compound is known and fully described.[S1] A solution of *i*PrMgCl (2.0 M in THF, 98 ml, 197 mmol, 1.05 equiv.) was added dropwise to a solution of 1-iodo-2-bromobenzene (24 ml, 187 mmol, 1.0 equiv.) in THF (200 ml) at – 94 °C over the course of 1h30. Then, $SOCl_2$ (6.8 ml, 94 mmol, 0.5 equiv.) was added and the reaction was stirred for further 1h30 at – 94 °C. The reaction was quenched by addition of 100 ml of saturated NH_4Cl, the organic layer was collected and the aqueous layer was extracted with Et_2O (3 × 80 ml). The combined organic layers were dried with $MgSO_4$ and concentrated under reduced pressure. The crude was poured into hexane and filtrated affording bis(2,2'-bromophenyl)sulfoxide **S3.1** as colorless/slightly yellow solid which was used in the next step without further purification.

To solution of bis(2,2'-bromophenyl)sulfoxide **S3.1** in CH_2Cl_2 (150 ml) at room temperature was added PCl_3 (280 mmol, 24 ml, 1.5 equiv.). After 72h at room temperature, the mixture was concentrated under reduced pressure, diluted in CH_2Cl_2, filtered over silica gel plug followed by subsequent evaporation to dryness. The crude mixture was purified by flash column chromatography (hexane) affording pure bis(2,2'-bromophenyl)sulfide **S3.2** as colorless crystalline solid (22.9 g, 66.5 mmol, 71% yield). ^{1}H NMR data is consistent with one reported in the literature.[S1]

^{1}H NMR (400 MHz, $CDCl_3$) δ (ppm) = 7.63 (d, *J* = 7.8 Hz, 2H), 7.25-7.21 (m, 2H), 7.16-7.11 (m, 4H).

10-Mesityl-10***H***-9-thia-10-boraanthracene **3.2**



S3.2

3.2
33%

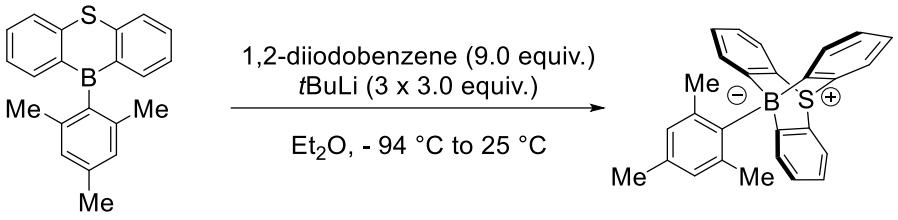
10-Mesityl-10***H***-9-thia-10-boraanthracene was prepared according to a modified literature procedure.[S2] A solution of *t*BuLi (1.9 M in pentane, 15.3 ml, 29 mmol, 5.0 equiv.) was added dropwise to a solution of bis(2,2'-bromophenyl)sulfide **S3.2** (2.0 g, 5.8 mmol, 1.0 equiv.) in THF (20 ml) at – 94 °C. The reaction was stirred for 30 min at – 94 °C then allowed to warm at room temperature for further 30 min. A solution of MesB(O*n*Bu)$_2$ (5.8 mmol, 1.0 equiv.) in THF (15 ml) was subsequently added dropwise. After stirring at room temperature for 16h, the reaction was quenched with saturated NH_4Cl, the organic layer is collected and the aqueous phase was extracted with EtOAc (3 x 50 mL). The combined organic layers are dried over $MgSO_4$ and concentrated under reduced pressure. The crude mixture was poured in *i*PrOH and the resulting precipitate was filtered and washed with *i*PrOH affording 10-mesityl-10***H***-9-thia-10-boraanthracene **3.2** (0.60 g, 1.9 mmol, 33% yield) as a pale-yellow powder. ^{1}H, ^{13}C and ^{11}B NMR data are consistent with those reported in the literature.[S2]

^{1}H NMR (400 MHz, $CDCl_3$) δ (ppm) = 7.88 (dd, *J* = 7.7, 1.5 Hz, 2H), 7.79 (d, *J* = 8.1 Hz, 2H), 7.65-7.60 (m, 2H), 7.33-7.27 (m, 2H), 6.95 (s, 2H), 2.41 (s, 3H), 1.94 (s, 6H).

^{13}C NMR (101 MHz, $CDCl_3$) δ (ppm) = 144.5, 139.8, 138.9, 136.9, 132.3, 127.1, 125.4, 124.8, 23.0, 21.4. The carbon atoms directly attached to the boron atom were not detected, likely due to quadrupolar relaxation.

^{11}B NMR (128 MHz, $CDCl_3$) δ (ppm) = 58.6 (br)

10-Mesityl-9-sulfonium-10-boratriptycene **3.3**



3.2 **3.3**
46%

Under Ar atmosphere, a solution of *t*BuLi (1.9 M in pentane, 2.5 ml, 4.8 mmol, 3.0 equiv.) was added dropwise to a solution of 10-mesityl-10***H***-9-thia-10-boraanthracene **3.2** (0.50 g, 1.6 mmol, 1.0 equiv.) and 1,2-diiodobenzene (1.9 ml, 14.3 mmol, 9.0 equiv.) in Et_2O (30 ml) at – 94 °C. The reaction was subsequently allowed to warm at room temperature. After 9h, the reaction was cooled again at – 94 °C and a solution of *t*BuLi (1.9 M in pentane, 2.5 ml, 4.8 mmol, 3.0 equiv.) was added dropwise. The reaction was subsequently allowed to warm at room temperature. After another 9h, the reaction was cooled at – 94 °C and a solution of *t*BuLi (1.9 M in pentane, 2.5 ml, 4.8 mmol, 3.0 equiv.) was added dropwise for the third time. The reaction was subsequently allowed to warm at room temperature and stirred for another 9h. The crude was evaporated to dryness, dissolved in CH_2Cl_2 (100ml) and washed with water (50 mL) in order to remove inorganic salts. The organic phase was washed with brine, dried with $MgSO_4$, filtered and evaporated to dryness. The crude was poured into Et_2O, the resulting precipitate was filtrated and washed with Et_2O. The resulting powder was recovered, dissolved in CH_2Cl_2 and dropped on a silica gel plug and subsequently washed with hexane (200 ml). The silica residue was further washed with CH_2Cl_2 (200 ml). The CH_2Cl_2 phase was evaporated to dryness affording 10-mesityl-9-sulfonium-10-boratriptycene **3.3** (0.29 g, 0.74 mmol, 46% yield) as a colorless to pale yellow powder.

Single crystals suitable for X-ray diffraction analysis were obtained by a slow evaporation of a saturated solution of **3.3** in CH_2Cl_2.

^{1}H NMR (500 MHz, $CDCl_3$) δ (ppm) = 7.73 (m, 6H), 7.16 (td, *J* = 7.3, 1.1 Hz, 3H), 7.05 (s, 2H), 7.01 (td, *J* = 7.4, 1.4 Hz, 3H), 2.43 (s, 3H), 2.04 (s, 6H).

^{13}C NMR (126 MHz, $CDCl_3$) δ (ppm) = 143.6 (Cq), 135.8 (CH), 134.2 (Cq), 133.8 (Cq), 129.6 (CH), 128.2 (CH), 127.2 (CH), 123.7 (CH), 26.9 (CH_3), 21.1 (CH_3). The carbon atoms directly attached to the boron atom on the triptycene core were not detected, likely due to quadrupolar relaxation.

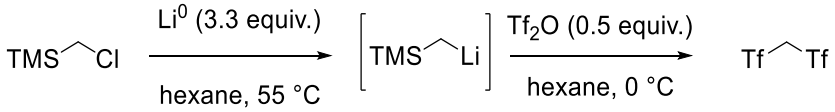
^{11}B NMR (160 MHz, $CDCl_3$) δ (ppm) = -8.7 (s)

HRMS (MALDI$^-$) (*m/z*): calc. for [$C_{27}H_{23}{}^{11}BS$]: 390.1614 [M]$^+$; found: 390.1580.

IR (neat, ATR): $\tilde{\nu}$ / cm^{-1} = 3058, 2924, 2847, 1642, 1513, 1460, 1427, 1293, 1260, 1083, 982, 891.

M.p. (CH_2Cl_2): 277-279 °C

Bis(trifluoromethylsulfonyl)methane **S3.3**



S3.3
42%

Bis(trifluoromethylsulfonyl)methane **S3.3** was synthesized according to a modified literature procedure.[S3]

Under an argon atmosphere, (chloromethyl)trimethylsilane (11.5 ml, 82.4 mmol, 1.1 equiv.) was added to a suspension of thermally activated Li^0 (1.70 g, 247 mmol, 3.3 equiv.) in hexane. The mixture was sonicated and warmed at 50 °C. After 16h at 50 °C, the cloudy purple solution is filtered via cannula to remove remaining Li^0 and LiCl salts. The solution of $TMSCH_2Li$ is then cooled at 0 °C and triflic anhydride (6.2 ml, 37.5 mmol, 0.5 equiv.), freshly distilled over P_2O_5, was added over the course of 1h via a syringe pump. After 40 min at 0 °C, the reaction is allowed to warm at room temperature for 2h. The reaction is quenched with saturated $NaHCO_3$ (80 ml). The organic layer is removed and the cloudy aqueous phase is back extracted with CH_2Cl_2 (3 × 60 ml. The

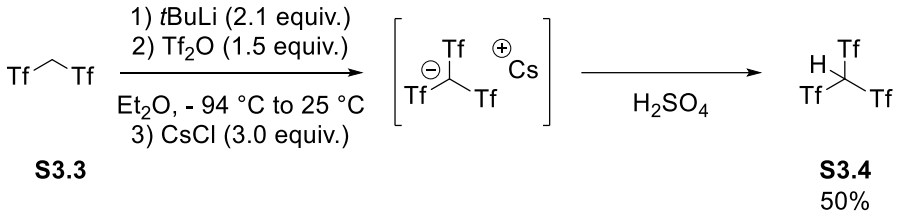
aqueous phase is then acidified with concentrated HCl (12M, 50 ml). The aqueous phase was further extracted with CH_2Cl_2 (3 × 60 ml) and the combined organic phases are dried over $MgSO_4$, filtered and concentrated under reduced pressure forming a yellow oily residue with small crystals. The crude is transferred in a sublimating appartus and sublimed (50 °C to 70 °C, 1 to 0.1 mbar) affording pure bis(trifluoromethylsulfonyl)methane **S3.3** (2.2 g, 16 mmol, 42% yield) as colorless crystalline solid. ^{1}H, ^{13}C and ^{19}F NMR data are consistent with one reported in the literature.[S3]

^{1}H NMR (400 MHz, $CDCl_3$) δ (ppm) = 4.96 (s, 2H).

^{13}C NMR (101 MHz, $CDCl_3$) δ (ppm) = 118.8 (q, J_{C-F} = 328 Hz), 64.2.

^{19}F NMR (386 MHz, $CDCl_3$) δ (ppm) = -13.0 (s, 6F)

Tris(trifluoromethanesulfonyl)methane **S3.4**



S3.3 **S3.4** 50%

Tris(trifluoromethanesulfonyl)methane **S3.4** was synthesized according to a modified literature procedure.[S3]

Under an argon atmosphere, a solution of *t*BuLi (1.9 M in pentane, 4.0 ml, 7.6 mmol, 2.1 equiv.) was added to a solution of bis(trifluoromethylsulfonyl)methane (1.0 g, 3.6 mmol, 1.0 equiv.) in Et_2O (25 ml) at – 94 °C. After 30 min at – 94 °C, Tf_2O (0.90 ml, 5.4 mmol, 1.5 equiv.) was added over the course of 40 min at – 94 °C. After further 40 min at – 94 °C, the reaction was allowed to warm at room temperature. After 2h, the reaction mixture is concentrated under reduced pressure. The yellow residue was treated with saturated $NaHCO_3$ (60 ml) and extracted with CH_2Cl_2 (3 × 60 ml). The aqueous phase was acidified with concentrated HCl (12M, 50 ml). The acidified aqueous phase was

extracted with CH_2Cl_2 (3 × 60 ml). The combined organic phases were thrown away and the acidified aqueous phase was further extracted with Et_2O (3 × 60 ml). The combined ethereal phases were combined, dried over $MgSO_4$, filtered and concentrated under reduced pressure. The yellow oily residue was mixed with CsCl (1.76 g, 10.8 mmol, 3.0 equiv.) in water (10 ml) and stirred for 3 min until complete precipitation of cesium tris(trifluoromethanesulfonyl)methide. The precipitate was filtered and washed with water. Cesium tris(trifluoromethanesulfonyl)methide was transferred into a sublimating funnel, mixed with concentrated H_2SO_4 (99.9 %, 2 ml, 10 equiv.) and sublimed (100 °C to 120 °C, 1 to 0.1 mbar). After 16h, the sublimating funnel is transferred in the glovebox, sublimed triflidic acid was recovered and immediately submitted to second sublimation under the same conditions in order to remove all traces of remaining sulfuric acid, affording pure tris(trifluoromethylsulfonyl)methane **S3.4** as a colorless glassy highly hygroscopic and corrosive solid (0.74 g, 1.8 mmol, 50% yield) and stored in a capped vial in glovebox. ^{13}C and ^{19}F NMR data are consistent with one reported in the literature.[S3]

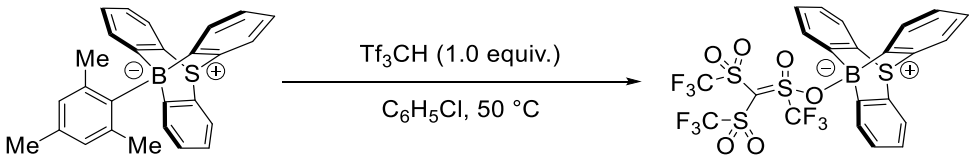
Note: Second sublimation is required to remove all traces of sulfuric acid and sulfate impurities. If purchased from suppliers, triflidic acid should be submitted to sublimation prior to be used.

^{13}C NMR (101 MHz, $CDCl_3$) δ (ppm) = 122.6 (q, *J* = 326 Hz).

^{19}F NMR (386 MHz, $CDCl_3$) δ (ppm) = -78.4 (s, 9F).

III.2. Synthesis of compounds **3.4**-**3.8**, **3.24a**

10-Triflide-9-sulfonium-10-boratriptycene-ate complex **3.4**



3.3 **3.4** 41%

In a glovebox, $HCTf_3$ (106 mg, 0.256 mmol, 1.0 equiv) was added to a suspension of 10-mesityl-9-sulfonium-10-boratriptycene-ate complex **3.3** (100 mg, 0.256 mmol, 1.0 equiv.) in C_6H_5Cl (4 ml). The reaction is stirred at 50 °C out of the glovebox in a Schlenk tube. After 16h, the crude was evaporated to dryness and purified via flash column chromatography (hexane/CH_2Cl_2 60:40) affording 10-triflide-9-sulfonium-10-boratriptycene-ate complex **3.4** (72 mg, 0.10 mmol, 41 % yield) as a colorless powder.

Single crystals suitable for X-ray diffraction analysis were obtained by a slow evaporation of a saturated solution of **3.4** in C_6H_5F.

Note: Triflidic acid is relatively insoluble in most organic solvents, therefore the reaction has to be stirred for several hours. Warming the reaction at 50 °C helps increasing the solubility and is low enough to avoid reaction with the solvent.

TLC: R_f = 0.40 (hexane/CH_2Cl_2 50:50)

^{1}H NMR (400 MHz, $(CD_3)_2CO$) δ (ppm) = 8.14-8.11 (m, 3H), 7.96 (dd, *J* = 7.4, 0.9 Hz, 3H), 7.52 (td, *J* = 7.4, 1.1 Hz, 3H), 7.33 (td, *J* = 7.6, 1.3 Hz, 3H).

^{13}C NMR (126 MHz, $CDCl_3$) δ (ppm) = 131.7 (CH), 130.7 (Cq), 130.6 (CH), 127.9 (CH), 126.3 (CH). The carbon atoms directly attached to the boron atom on the triptycene core were not detected, likely due to quadrupolar relaxation as well as carbon of the trifluoromethyl substituents.

^{11}B NMR (128 MHz, acetone-d_6) δ (ppm) = 10.7 (br)

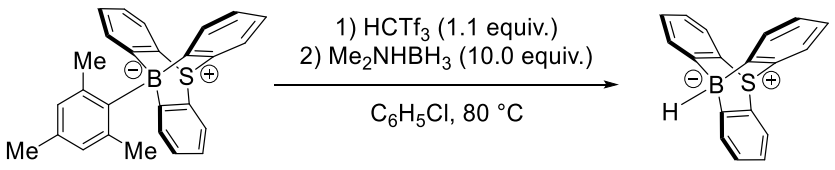
^{19}F NMR (386 MHz, acetone-d_6) δ (ppm) = -69.8 (br), -76.2 (br), -77.4 (s), -78.3 (br).

HRMS (MALDI$^-$) (*m/z*): Could not be determined due to decomposition during injection.

IR (neat, ATR): $\tilde{\nu}$ / cm^{-1} = 3058, 2986, 2909, 1432, 1393, 1379, 1331, 1221, 1202, 1130, 1063, 982, 958, 819, 753.

M.p. (C_6H_5F): 195-197 °C (dec)

10-Hydrido-9-sulfonium-10-boratriptycene-ate complex **3.5**



3.3 **3.5** 45%

In a glovebox, $HCTf_3$ (116 mg, 0.282 mmol, 1.1 equiv.) was added to a suspension of 10-mesityl-9-sulfonium-10-boratriptycene-ate complex **3.3** (100 mg, 0.256 mmol, 1.0 equiv.) in C_6H_5Cl (4 ml). The reaction is stirred at 80 °C out of the glovebox in a Schlenk tube. After 1h30, Me_2NHBH_3 (151 mg, 2.56 mmol, 10.0 equiv.) was added as a solid under Ar and the reaction was stirred at 80 °C. After 16h, the reaction was evaporated to dryness, purification *via* flash column chromatography (hexane/CH_2Cl_2 90:10) afforded 10-hydrido-9-sulfonium-10-boratriptycene-ate complex **3.5** (32 mg, 0.12 mmol, 45 % yield) as a colorless powder.

Single crystals suitable for X-ray diffraction analysis were obtained by a slow evaporation of a saturated solution of **3.5** in CH_2Cl_2.

TLC: R_f = 0.90 (hexane/CH_2Cl_2 50:50)

^{1}H NMR (500 MHz, $CDCl_3$) δ (ppm) = 7.98-7.93 (br, 3H), 7.71 (d, *J* = 7.7 Hz, 3H), 7.26-7.22 (m, 3H), 7.03 (td, *J* = 7.5, 1.4 Hz, 3H), 3.75 (q, *J* = 199.3 Hz, 1H).

^{13}C NMR (126 MHz, $CDCl_3$) δ (ppm) = 134.6 (CH), 133.9 (Cq), 130.4 (CH), 127.4 (CH), 124.1 (CH). The carbon atoms directly attached to the boron atom on the triptycene core were not detected, likely due to quadrupolar relaxation.

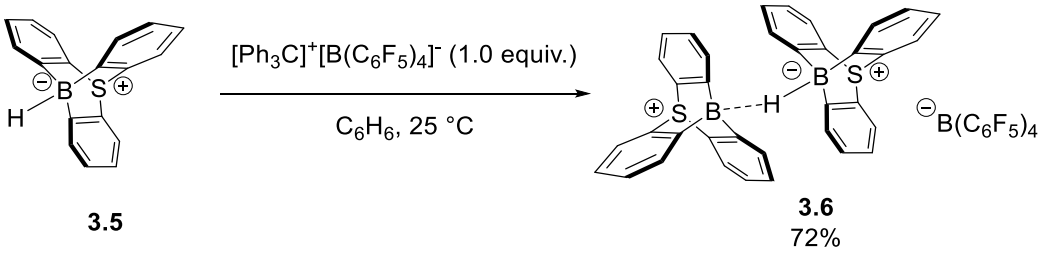
^{11}B NMR (160 MHz, $CDCl_3$) δ (ppm) = -10.7 (d, *J* = 99.4 Hz)

HRMS (MALDI $^-$) (*m/z*): calc. for $[C_{35}H_{31}{}^{11}BN_2S]$: 522.2301 $[M+DCTB]^+$; found: 522.2297.

IR (neat, ATR): $\tilde{\nu}$ / cm^{-1} = 3048, 2971, 2919, 2857, 2398, 1575, 1432, 1374, 1293, 1260, 1183, 1130, 1016, 882.

M.p. (CH_2Cl_2): 310-312 °C

Tetrakis(pentafluorophenyl)borate 10,10'-hydronium-bis(9-sulfonium-10-boratriptycene) **3.6**



3.5

3.6
72%

In a glovebox, triphenylcarbenium tetrakis(pentafluorophenyl)borate (32.7 mg, 0.0356 mmol, 1.0 equiv.) was added as a solid in a vial containing to a suspension of 10-hydrido-9-sulfonium-10-boratriptycene-ate complex **3.5** (10.0 mg, 0.0367 mmol, 1.0 equiv.) in C_6H_6 (1.0 ml) at room temperature. After stirring for 10 minutes, the precipitate was filtrated and washed with C_6H_6 (3 x 1 mL) affording tetrakis(pentafluorophenyl)borate 10,10'-hydronium-bis(9-sulfonium-10-boratriptycene) **3.6** (32 mg, 0.0264 mmol, 72%) as a colorless to pale orange powder.

Single crystals suitable for X-ray diffraction analysis were obtained by a slow evaporation of a saturated solution of **3.6** in C_6H_6.

Note: The same result can be obtained using 0.5 equiv. of triphenylcarbenium tetrakis(pentafluorophenyl)borate. Addition of a large excess of triphenylcarbenium tetrakis(pentafluorophenyl)borate leads to the formation of the same product.

^{1}H NMR (500 MHz, $CDCl_3$) δ (ppm) = 8.02 (dd, *J* = 7.6, 1.1 Hz, 6H), 7.76 (dd, *J* = 7.1, 1.4 Hz, 6H), 7.33 (td, *J* = 7.5, 1.5 Hz, 6H), 7.30-7.26 (m, 6H), 1.25 (br s, 1H).

^{13}C NMR (126 MHz, $CDCl_3$) δ (ppm) =132.9 (CH), 131.9 (CH), 128.7 (CH), 128.5 (Cq), 127.1 (CH). The carbon atoms directly attached to the boron atom on the triptycene core were not detected, likely due to quadrupolar relaxation. The carbons attached to the tetrakis(pentafluorophenyl)borate anion were not detected due to the very poor solubility of **3.7**.

^{11}B NMR (160 MHz, $CDCl_3$) δ (ppm) = 8.8 (br), -17.6 (s)

^{19}F NMR (483 MHz, $CDCl_3$) δ (ppm) = -132.4 (s, 8F), -163.0 (t, *J* = 20.6 Hz, 4F), -166.7 (t, 18.0 Hz, 8F).

HRMS (MALDI$^-$) (*m/z*): calc. for $[C_{36}H_{25}{}^{11}B_2S_2]$: 543.1584 $[M]^+$; found: 543.1591.

IR (neat, ATR): $\tilde{\nu}$ / cm^{-1} = 3058, 2924, 2312, 1642, 1503, 1456, 1427, 1374, 1264, 1145, 1078, 968.

M.p. (C_6H_6): 206-209 °C (dec)

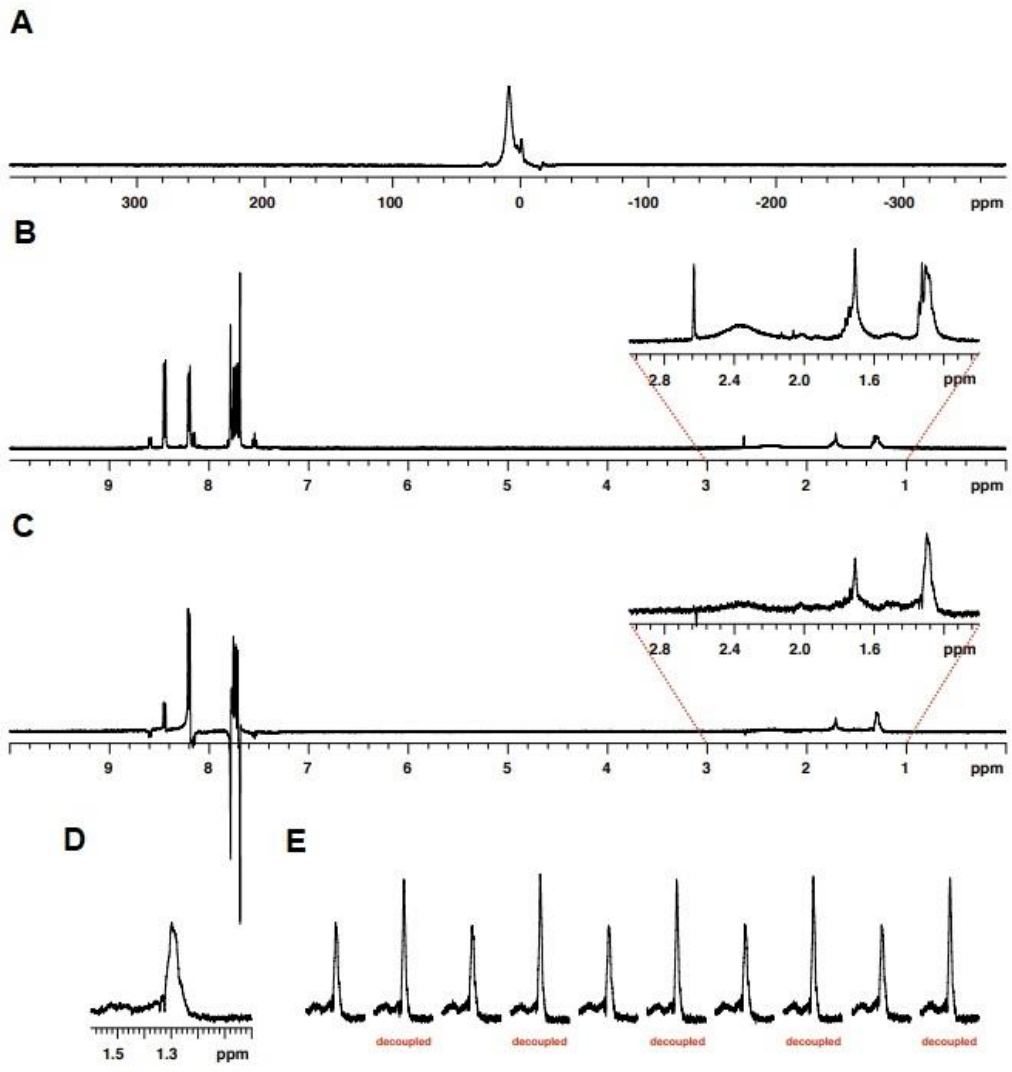


Figure SIII.1. Selected NMR spectra of **3.6** after quick washed of the crude reaction mixture with C_6D_6: (**A**) ^{11}B NMR of **3.7** (128 MHz, 55 °C, C_6D_5Br); (**B**) quantitative ^{1}H NMR spectra of **3.7** (400 MHz, 55 °C, C_6D_5Br); (**C**) inversion recovery ^{1}H NMR spectra (400 MHz, 55 °C, C_6D_5Br) with optimized parameters to suppress signals

superimposed with the B-H signal in **3.6** at δ_{ppm} = 1.3; (**D**) and (**E**) zoom of the 1.5-1.2 ppm region, showed increasing intensity of the B–H signal in **3.7** when the boron is decoupled.

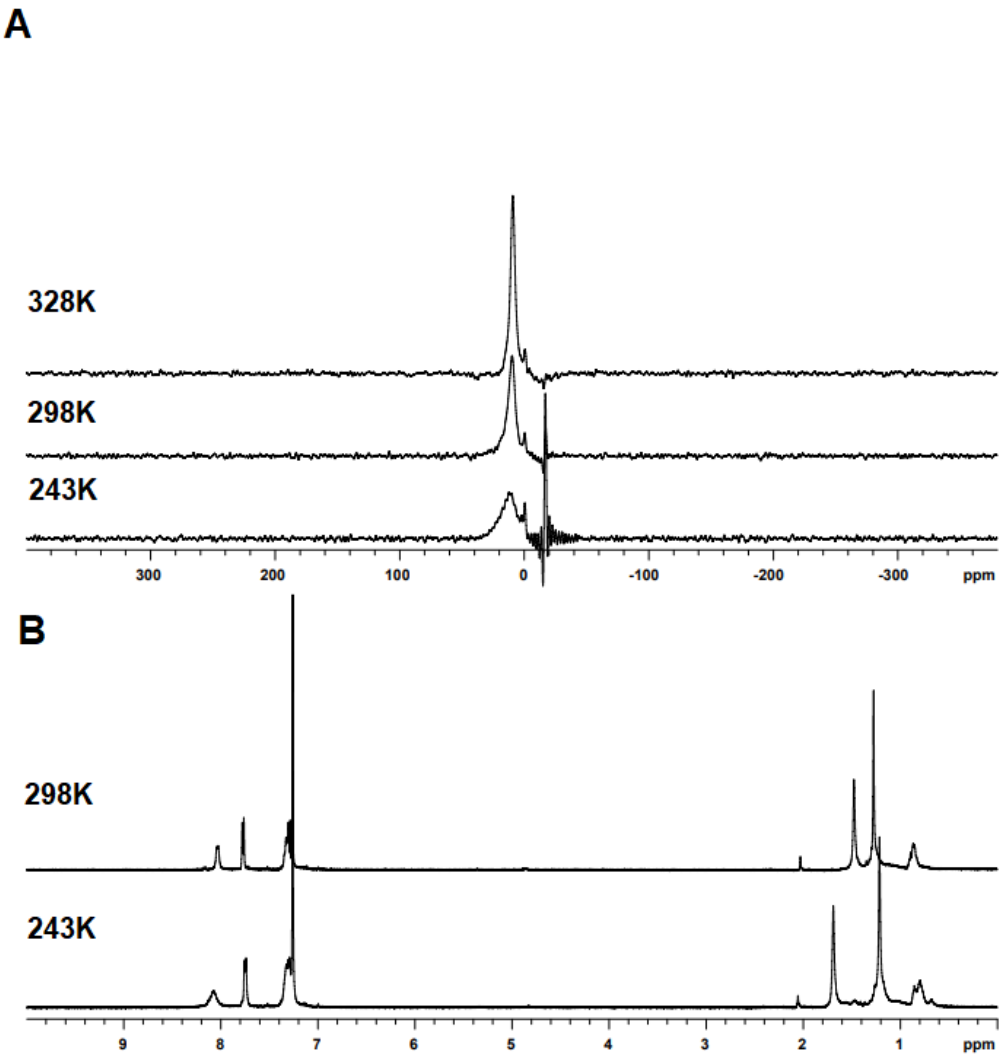
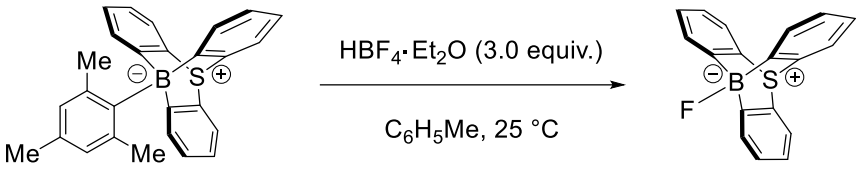


Figure SIII.2. ^{11}B (**A**, 128 MHz) and ^{1}H (**B**, 128 MHz) NMR spectra ($CDCl_3$) of **3.6** recorded at variable temperature. At increasing temperature, the ^{11}B signal becomes sharper. No signals due to slow exchange on the chemical shift time scale were observed in the studied temperature range. The analysis was stopped at – 30 °C due to the poor solubility of **3.6** at lower temperature.

10-Fluoro-9-sulfonium-10-boratriptycene-ate complex **3.7**



3.3 **3.7** 73%

Tetrafluoroboric acid diethylether complex (0.10 ml, 0.77 mmol, 3.0 equiv.) was added to a solution of 10-mesityl-9-sulfonium-10-boratriptycene-ate complex **3.3** (0.10 g, 0.26 mmol, 1.0 equiv.) in toluene (5 ml) and stirred vigorously. After 3h at room temperature, the mixture was evaporated to dryness and the crude was purified via flash column chromatography (hexane/CH_2Cl_2 60:40) affording 10-fluoro-9-sulfonium-10-boratriptycene-ate complex **3.7** (56 mg, 0.19 mmol, 75% yield) as a colorless powder.

TLC: R_f = 0.40 (hexane/CH_2Cl_2 50/50)

^{1}H NMR (500 MHz, $CDCl_3$) δ (ppm) = 8.02 (d, *J* = 7.2 Hz, 3H), 7.71 (d, *J* = 7.7 Hz, 3H), 7.34 (td, *J* = 7.3, 1.0 Hz, 3H), 7.08 (td, *J* = 7.6, 1.4 Hz, 3H).

^{13}C NMR (126 MHz, $CDCl_3$) δ (ppm) = 131.8 (d, *J* = 6.6 Hz, Cq), 130.7 (CH), 130.6 (CH), 127.3 (d, *J* = 2.1 Hz, CH), 124.6 (CH). The carbon atoms directly attached to the boron atom on the triptycene core were not detected, likely due to quadrupolar relaxation.

^{11}B NMR (160 MHz, $CDCl_3$) δ (ppm) = 2.4 (d, *J* = 54.2 Hz)

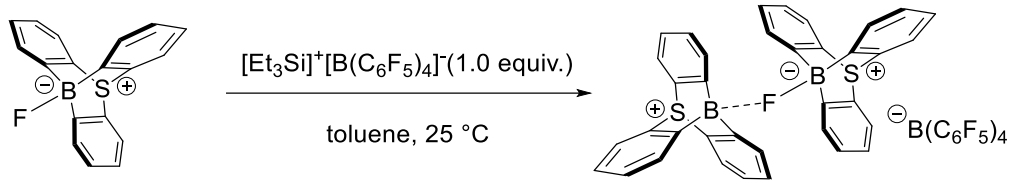
^{19}F NMR (483 MHz, $CDCl_3$) δ (ppm) = -236.1 (m)

HRMS (MALDI$^-$) (*m/z*): calc. for [$C_{18}H_{12}{}^{11}BFS$]: 290.0737 $[M]^+$; found: 290.0742.

IR (neat, ATR): $\tilde{\nu}$ / cm^{-1} = 3048, 2957, 2919, 2857, 1723, 1570, 1427, 1293, 1255, 1188, 1152, 1006.

M.p. (CH_2Cl_2): 307-309 °C

Tetrakis(pentafluorophenyl)borate 10,10'-fluoronium-bis(9-sulfonium-10-boratriptycene) **3.8**



3.7 **3.8** 81%

In a glovebox, triphenylcarbenium tetrakis(pentafluorophenyl)borate (32 mg, 0.034 mmol, 1.0 equiv.) was added to a solution of Et_3SiH (4.4 mg, 0.038 mmol, 1.1 equiv.) in toluene (1.0 ml) leading to a deep orange solution. The reaction is stirred until complete color fading. The solution of *in situ* generated triethylsilylium tetrakis(pentafluorophenyl)borate was added to a suspension of 10-fluoro-9-sulfonium-10-boratriptycene-ate complex **3.7** (10 mg, 0.034 mmol, 1.0 equiv.) in toluene. After 10 min, the precipitate was filtered and washed with toluene (2 x 1 mL) and pentane (2 x 1 mL) affording tetrakis(pentafluorophenyl)borate 10,10'-fluoronium-bis(9-sulfonium-10-boratriptycene) **3.8** (17 mg, 0.014 mmol, 81% yield) as a colorless powder.

Single crystals suitable for X-ray diffraction analysis were obtained by a slow evaporation of a saturated solution of **3.8** in CH_2Cl_2.

Note: The same result can be obtained using 0.5 equiv. of triethylsilyl tetrakis(pentafluorophenyl)borate. Addition of a large excess of triethylsilyl tetrakis(pentafluorophenyl)borate leads to the formation of the same product.

^{1}H NMR (500 MHz, $CDCl_3$) δ (ppm) = 7.99 (d, *J* = 7.6 Hz, 6H), 7.88 (d, *J* = 7.1 Hz, 6H), 7.35 (t, *J* = 7.2 Hz, 6H), 7.31 (t, *J* = 7.4 Hz, 6H).

^{13}C NMR (126 MHz, $CDCl_3$) δ (ppm) = 151.1 (Cq), 150.8 (Cq), 148.3 (Cq, $^{1}J_{C\text{-}F}$ = 244.7 Hz), 136.4 (Cq, $^{1}J_{C\text{-}F}$ = 223.4 Hz), 131.9 (CH), 131.2 (Cq), 131.1 (Cq), 129.8 (CH), 128.7 (CH), 127.0 (CH). One carbon of the tetrakis(pentafluorophenyl)borate was not detected.

^{11}B NMR (160 MHz, $CDCl_3$) δ (ppm) = 13.5 (br), -17.6 (s)

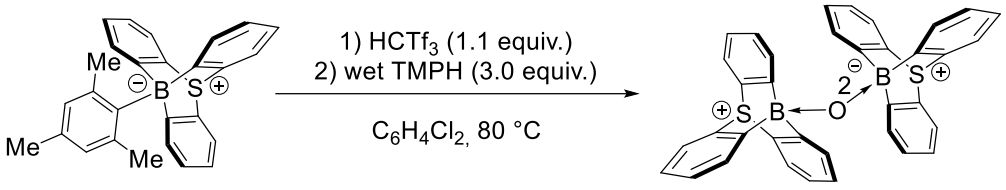
^{19}F NMR (483 MHz, $CDCl_3$) δ (ppm) = -132.4 (d, *J* = 10.2, 10F), -163.0 (t, *J* = 20.6 Hz, 5F), -166.6 (t, *J* = 18.1, 10F), -250.1 (s, 1H).

HRMS (MALDI$^-$) (*m/z*): calc. for $[C_{36}H_{24}{}^{11}B_2FS_2]$: 561.1490 $[M]^+$; found: 561.1479.

IR (neat, ATR): $\tilde{\nu}$ / cm^{-1} = 3058, 2909, 1642, 1513, 1460, 1374, 1269, 1150, 1083, 973, 901.

M.p. (CH_2Cl_2): 192-196 °C (dec)

10,10'-Oxybis-9-sulfonium-10-boratriptycene-ate complex **3.24a**



3.3 **3.24a** 26%

In a glovebox, $HCTf_3$ (35 mg, 0.085 mmol, 1.1 equiv.) was added to a suspension of 10-mesityl-9-sulfonium-10-boratriptycene-ate complex **3.3** (30 mg, 0.077 mmol, 1.0 equiv.) in *o*-$C_6H_4Cl_2$ (2.0 ml) in a Schlenk tube. The reaction was stirred out of the glovebox at 80 °C. After 1h30 at 80°C, the reaction was cooled at room temperature and wet TMPH (0.040 ml, 0.23 mmol, 3.0 equiv.) was added. After 16h at 373K, the reaction was evaporated to dryness and the crude was purified via flash column chromatography (hexane/CH_2Cl_2 70:30) affording 10,10'-oxybis-9-sulfonium-10-boratriptycene-ate complex **3.24a** (5.6 mg, 0.010 mmol, 26% yield) as a colorless powder.

Single crystals suitable for X-ray diffraction analysis were obtained by a slow evaporation of a saturated solution of **3.24a** in CH_2Cl_2.

Note : 10,10'-oxybis-9-sulfonium-10-boratriptycene-ate complex **3.24a** has been initially obtained as a side-product of CH activation and was not reproducible. The

present procedure is a reproducible synthesis of 10,10'-oxybis-9-sulfonium-10-boratriptycene-ate complex **3.24a**.

TLC: R_f = 0.6 (hexane/CH_2Cl_2 50:50)

^{1}H NMR (400 MHz, $CDCl_3$) δ (ppm) = 8.19 (d, *J* = 7.1 Hz, 6H), 7.75 (d, *J* = 7.6 Hz, 6H), 7.12 (t, *J* = 7.2 Hz, 6H), 7.02 (td, *J* = 7.5, 1.5 Hz, 6H).

^{13}C NMR (101 MHz, $CDCl_3$) δ (ppm) = 134.1 (CH), 129.9 (Cq), 126.9 (CH), 123.8 (CH), 119.4 (CH). The carbon atoms directly attached to the boron atom on the triptycene core were not detected, likely due to quadrupolar relaxation.

^{11}B NMR (128 MHz, $CDCl_3$) δ (ppm) = -0.4

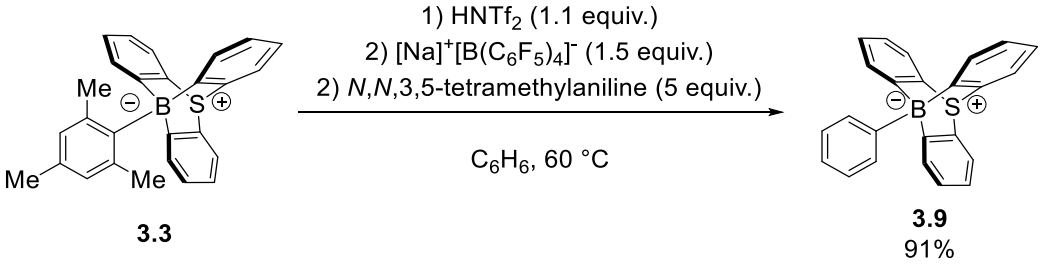
HRMS (MALDI$^-$) (*m/z*): calc. for $[C_{36}H_{25}{}^{11}B_2OS_2]$: 559.1533 $[M+H]^+$; found: 559.1527.

IR (neat, ATR): $\tilde{\nu}$ / cm^{-1} = 3048, 2962, 2919, 2852, 1723, 1432, 1374, 1288, 1250, 1126, 1073, 1016.

M.p. (CH_2Cl_2): 295-297 °C (dec)

III.3. Synthesis of compounds **3.9**-**3.19**

10-Phenyl-9-sulfonium-10-boratriptycene-ate complex **3.9**



3.3 → **3.9** 91%

In a glovebox, $HNTf_2$ (24 mg, 0.085 mmol, 1.1 equiv.) was added as a solid to a suspension of 10-mesityl-9-sulfonium-10-boratriptycene-ate complex **3.3** (30 mg, 0.077 mmol, 1.0 equiv.) in C_6H_6 (2.0 ml) in a Schlenk tube. After 5 min, *N*,*N*,3,5-tetramethylaniline (57 mg, 0.38 mmol, 5.0 equiv.) and sodium tetrakis(pentafluorophenyl)borate (81 mg, 0.115 mmol, 1.5 equiv.) were added. The reaction was stirred out of the glovebox at 60 °C. After 16h, the reaction mixture was

evaporated to dryness. The crude was dissolved in CH_2Cl_2 and trifluoroacetic acid was added dropwise. Purification by flash column chromatography (hexane/CH_2Cl_2 95:5) afforded 10-(phenyl)-9-sulfonium-10-boratriptycene-ate complex **3.9** (24 mg, 0.070 mmol, 91% yield) as a colorless solid.

Single crystals suitable for X-ray diffraction analysis were obtained by a slow evaporation of a saturated solution of **3.9** in CH_2Cl_2.

TLC: R_f = 0.90 (hexane/CH_2Cl_2 50:50)

^{1}H NMR (500 MHz, $CDCl_3$) δ (ppm) = 8.10 (d, *J* = 6.9 Hz, 2H), 7.86 (d, *J* = 7.3 Hz, 3H), 7.77 (d, *J* = 7.6 Hz, 3H), 7.56 (t, *J* = 7.5 Hz, 2H), 7.39 (t, *J* = 7.3 Hz, 1H), 7.23 (td, *J* = 7.4, 1.2 Hz, 3H), 7.06 (td, *J* = 7.5, 1.4 Hz, 3H).

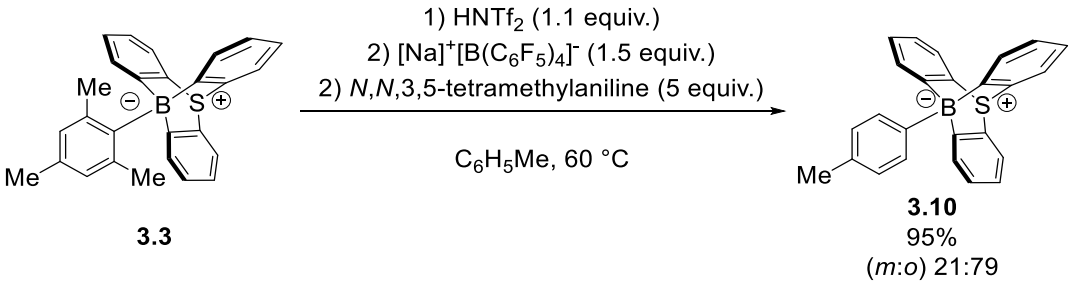
^{13}C NMR (126 MHz, $CDCl_3$) δ (ppm) = 135.8 (CH), 134.5 (CH), 134.3 (CH), 130.2 (CH), 127.7 (CH), 124.9 (CH), 224.2 (CH). The carbon atoms directly attached to the boron atom on the triptycene core were not detected, likely due to quadrupolar relaxation.

^{11}B NMR (160 MHz, $CDCl_3$) δ (ppm) = -9.3 (s).

HRMS (MALDI $^-$) (*m/z*): calc. for $[C_{41}H_{35}{}^{11}BN_2S]$: 598.2614 $[M+DCTB]^+$; found: 598.2607.

IR (neat, ATR): $\tilde{\nu}$ / cm^{-1} = 3048, 2919, 2852, 2388, 1733, 1642, 1508, 1460, 1432, 1260, 1188, 1083, 882.

10-Tolyl-9-sulfonium-10-boratriptycene-ate complex **3.10**



In a glovebox, $HNTf_2$ (24 mg, 0.085 mmol, 1.1 equiv.) was added as a solid to a suspension of 10-mesityl-9-sulfonium-10-boratriptycene-ate complex **3.3** (30 mg, 0.077

mmol, 1.0 equiv.) in C_6H_5Me (2.0 ml) in a Schlenk tube. After 5 min, *N*,*N*,3,5-tetramethylaniline (57 mg, 0.38 mmol, 5.0 equiv.) and sodium tetrakis(pentafluorophenyl)borate (81 mg, 0.115 mmol, 1.5 equiv.) were added. The reaction was stirred out of the glovebox at 60 °C. After 16h, the reaction mixture was evaporated to dryness. The crude was dissolved in CH_2Cl_2 and trifluoroacetic acid was added dropwise. Purification by flash column chromatography (hexane/CH_2Cl_2 95:5) afforded 10-(tolyl)-9-sulfonium-10-boratriptycene-ate complex **3.10** (26 mg, 0.073 mmol, 95% yield) as a colorless solid.

Note: 10-tolyl-9-sulfonium-10-boratriptycene-ate complex **3.10** was obtained as an inseparable mixture of two isomers (*m*:*p*) with 21:79 ratio.

TLC: R_f = 0.90 (hexane/CH_2Cl_2 50:50)

^{1}H NMR (500 MHz, $CDCl_3$) δ (ppm) = *meta* isomer: 7.96 (s, 1H), 7.91 (br, 1H), 7.48 (t, *J* = 7.4 Hz, 1H), 7.25 (td, *J* = 7.2, 1.2 Hz, 3H), 7.24 (d, *J* = 7.2 Hz, 1H), 7.07 (t, *J* = 7.5 Hz, 3H), 2.53 (s, 3H). *para* isomer: 8.01 (d, *J* = 7.5 Hz, 2H), 7.88 (d, *J* = 7.4 Hz, 3H), 7.77 (d, *J* = 7.6 Hz, 3H), 7.41 (d, *J* = 7.5 Hz, 2H), 7.24 (td, *J* = 7.3, 1.2 Hz, 3H), 7.07 (td, *J* = 7.4, 1.4 Hz, 3H), 2.52 (s, 3H)

^{13}C NMR (126 MHz, $CDCl_3$) δ (ppm) = 136.6, 136.5, 135.8, 134.5, 134.5 (Cq), 134.4, 134.3, 134.0 (Cq), 132.8, 130.1, 128.5, 127.7, 125.6, 124.2, 124.1, 22.3 (CH_3), 21.5 (CH_3), 135.8 (CH), 134.5 (CH), 134.3 (CH), 130.2 (CH), 127.7 (CH), 124.9 (CH), 224.2 (CH). The carbon atoms directly attached to the boron atom on the triptycene core were not detected, likely due to quadrupolar relaxation.

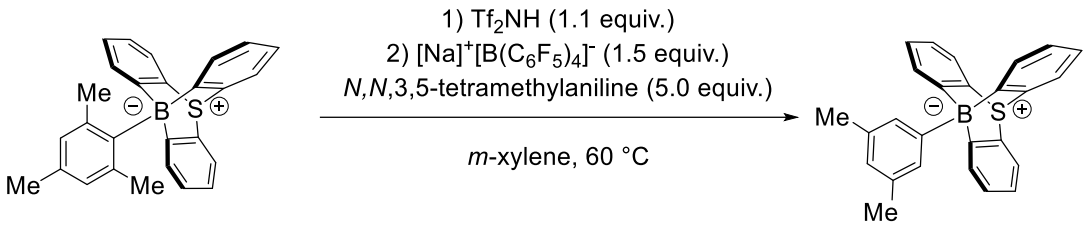
^{11}B NMR (160 MHz, $CDCl_3$) δ (ppm) = -9.3 (s).

HRMS (MALDI $^-$) (*m/z*): calc. for $[C_{42}H_{37}{}^{11}BN_2S]$: 612.2771 $[M+DCTB]^+$; found: 612.2778.

IR (neat, ATR): $\tilde{\nu}$ / cm^{-1} = 3053, 2933, 1647, 1513, 1456, 1264, 1145, 1083, 973.

M.p. (CH_2Cl_2): 240-242 °C

10-(3,5-Dimethylphenyl)-9-sulfonium-10-boratriptycene-ate complex **3.11**



3.3 **3.11** 79%

In a glovebox, $HNTf_2$ (24 mg, 0.085 mmol, 1.1 equiv.) was added as a solid to a suspension of 10-mesityl-9-sulfonium-10-boratriptycene-ate complex **3.3** (30 mg, 0.077 mmol, 1.0 equiv.) in *m*-xylene (2.0 ml) in a Schlenk tube. After 5 min, *N,N,*3,5-tetramethylaniline (57 mg, 0.38 mmol, 5.0 equiv.) and sodium tetrakis(pentafluorophenyl)borate (81 mg, 0.115 mmol, 1.5 equiv.) were added. The reaction was stirred out of the glovebox at 60 °C. After 16h, the reaction mixture was evaporated to dryness. The crude was dissolved in CH_2Cl_2 and trifluoroacetic acid was added dropwise. Purification by flash column chromatography (hexane/CH_2Cl_2 95:5) afforded 10-(3,5-dimethylphenyl)-9-sulfonium-10-boratriptycene-ate complex **3.11** (23 mg, 0.061 mmol, 79% yield) as a colorless solid.

TLC: R_f = 0.90 (hexane/CH_2Cl_2 50:50)

^{1}H NMR (500 MHz, $CDCl_3$) δ (ppm) = 7.89 (d, *J* = 7.4 Hz, 3H), 7.76 (d, *J* = 7.6 Hz, 3H), 7.73 (s, 2H), 7.24 (t, *J* = 6.4 Hz, 3H), 7.80-7.43 (m, 4H), 2.48 (s, 6H).

^{13}C NMR (126 MHz, $CDCl_3$) δ (ppm) = 163.0, 136.6 (Cq), 134.6 (Cq), 134.5, 133.6, 130.2, 127.7, 126.6, 124.2, 22.1 (CH_3)

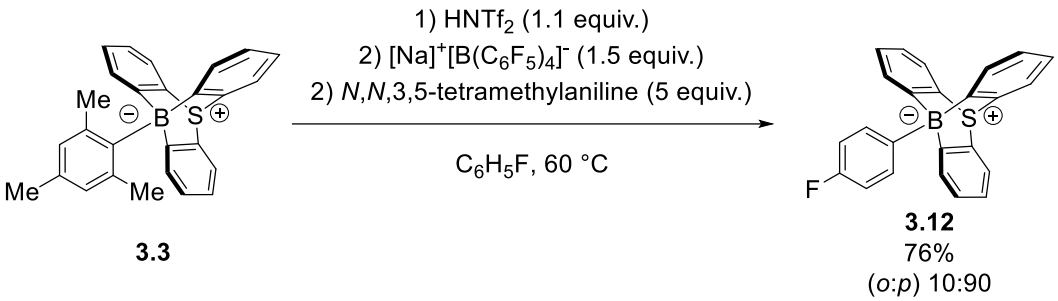
^{11}B NMR (160 MHz, $CDCl_3$) δ (ppm) = -9.3 (s)

HRMS (MALDI $^-$) (*m/z*): calc. for $[C_{43}H_{39}{}^{10}BN_2S]$: 625.2963 $[M+DCTB]^+$; found: 625.2951.

IR (neat, ATR): $\tilde{\nu}$ / cm^{-1} = 3043, 1581, 1422, 1297, 1254, 1169, 1032, 941, 864, 816, 753.

M.p. (CH_2Cl_2/pentane): >300°C

10-Fluoro-9-sulfonium-10-boratriptycene-ate complex **3.12**



In a glovebox, $HNTf_2$ (24 mg, 0.085 mmol, 1.1 equiv.) was added as a solid to a suspension of 10-mesityl-9-sulfonium-10-boratriptycene-ate complex **3.3** (30 mg, 0.077 mmol, 1.0 equiv.) in C_6H_5F (2.0 ml) in a Schlenk tube. After 5 min, *N*,*N*,3,5-tetramethylaniline (57 mg, 0.38 mmol, 5.0 equiv.) and sodium tetrakis(pentafluorophenyl)borate (81 mg, 0.115 mmol, 1.5 equiv.) were added. The reaction was stirred out of the glovebox at 60 °C. After 16h, the reaction mixture was evaporated to dryness. The crude was dissolved in CH_2Cl_2 and trifluoroacetic acid was added dropwise. Purification by flash column chromatography (hexane/CH_2Cl_2 95:5) afforded 10-(fluoro)-9-sulfonium-10-boratriptycene-ate complex **3.12** (26 mg, 0.073 mmol, 95% yield) as a colorless solid.

Note: 10-fluoro-9-sulfonium-10-boratriptycene-ate complex **3.12** was obtained as an inseparable mixture of two isomers (*o*:*p*) with 10:90 ratio.

TLC: R_f = 0.90 (hexane/CH_2Cl_2 50:50)

^{1}H NMR (500 MHz, $CDCl_3$) δ (ppm) = 8.06-8.00 (m, 2H), 7.80 (d, *J* = 7.4 Hz, 3H), 7.77 (dd, *J* = 7.6, 0.6 Hz, 3H), 7.27-7.22 (m, 5H), 7.07 (dt, *J* = 7.5, 1.4 Hz, 3H).

^{13}C NMR (126 MHz, $CDCl_3$) δ (ppm) = 161.4 (d, *J* = 242.2 Hz, Cq), 136.9 (6.2 Hz, CH), 134.4 (Cq), 134.0 (CH), 130.3 (CH), 127.8 (CH), 124.3 (CH), 114.3 (d, *J* = 18.1 Hz, CH). The carbon atoms directly attached to the boron atom on the triptycene core were not detected, likely due to quadrupolar relaxation.

^{11}B NMR (160 MHz, $CDCl_3$) δ (ppm) = -9.5 (s, *p*-isomer), -10.0 (s, *o*-isomer).

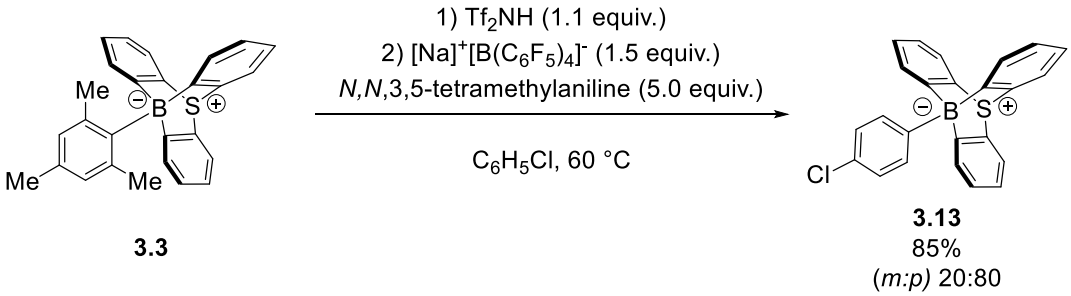
^{19}F NMR (483 MHz, $CDCl_3$) δ (ppm) = -115.0 (s, *o*-isomer), -119.2 (s, *p*-isomer).

HRMS (MALDI $^{-}$) (*m/z*): calc. for $[C_{41}H_{34}{}^{11}BN_2FS]$: 616.2520 $[M+DCTB]^+$; found: 616.2526.

IR (neat, ATR): $\tilde{\nu}$ / cm^{-1} = 3053, 2981, 2914, 2852, 1575, 1427, 1293, 1260, 1183, 1126, 1006, 882, 796.

M.p. (CH_2Cl_2): 254-256 °C

10-(Chlorophenyl)-9-sulfonium-10-boratriptycene-ate complex **3.13**



3.3

3.13
85%
(*m:p)* 20:80

In a glovebox, $HNTf_2$ (24 mg, 0.085 mmol, 1.1 equiv.) was added as a solid to a suspension of 10-mesityl-9-sulfonium-10-boratriptycene-ate complex **3.3** (30 mg, 0.077 mmol, 1.0 equiv.) in C_6H_5F (2.0 ml) in a Schlenk tube. After 5 min, *N*,*N*,3,5-tetramethylaniline (57 mg, 0.38 mmol, 5.0 equiv.) and sodium tetrakis(pentafluorophenyl)borate (81 mg, 0.115 mmol, 1.5 equiv.) were added. The reaction was stirred out of the glovebox at 60 °C. After 16h, the reaction mixture was evaporated to dryness. The crude was dissolved in CH_2Cl_2 and trifluoroacetic acid was added dropwise. Purification by flash column chromatography (hexane/CH_2Cl_2 95:5) afforded 10-(chloro)-9-sulfonium-10-boratriptycene-ate complex **3.13** (25 mg, 0.065 mmol, 85% yield) as a colorless solid.

Note: 10-chloro-9-sulfonium-10-boratriptycene-ate complex **3.13** was obtained as an inseparable mixture of two isomers (*m*:*p*) with 20:80 ratio.

TLC: R_f = 0.90 (hexane/CH_2Cl_2 50:50)

^{1}H NMR (500 MHz, $CDCl_3$) δ (ppm) = *meta* isomer: 8.09 (s, 1H), 7.96 (d, *J* = 7.5 Hz, 1H), 7.83-7.76 (m, 6H), 7.49 (t, *J* = 7.7 Hz, 1H), 7.38 (d, *J* = 7.8 Hz, 1H), 7.27-7.22 (m,

3H), 7.08 (t, *J* = 7.5 Hz, 3H). *para* isomer: 8.03 (d, *J* = 7.5 Hz, 2H), 7.83-7.76 (m, 6H), 7.53 (dd, *J* = 8.1, 1.3 Hz, 2H), 7.27-7.22 (m, 3H), 7.08 (t, *J* = 7.5 Hz, 3H).

^{13}C NMR (126 MHz, $CDCl_3$) δ (ppm) = 137.1, 134.5, 134.0, 130.3,127.8, 127.7, 124.4, 124.3. The carbon atoms directly attached to the boron atom on the triptycene core were not detected, likely due to quadrupolar relaxation.

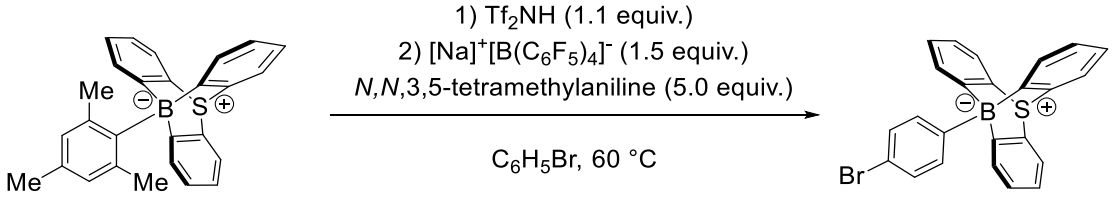
^{11}B NMR (160 MHz, $CDCl_3$) δ (ppm) = -9.5 (s)

HRMS (MALDI $^{-}$) (*m/z*): calc. for $[C_{41}H_{34}{}^{11}BN_2SCl]$: 632.2224 $[M+DCTB]^+$; found: 632.2239.

IR (neat, ATR): $\tilde{\nu}$ / cm^{-1} = 3053, 2991, 2919, 2852, 1594, 1427, 1370, 1293, 1255, 1150, 1011, 858.

M.p. (CH_2Cl_2): 255-262 °C

10-(Bromophenyl)-9-sulfonium-10-boratriptycene-ate complex **3.14**



3.3

3.14
86%
(*m*:*p*) 23:77

In a glovebox, $HNTf_2$ (24 mg, 0.085 mmol, 1.1 equiv.) was added as a solid to a suspension of 10-mesityl-9-sulfonium-10-boratriptycene-ate complex **3.3** (30 mg, 0.077 mmol, 1.0 equiv.) in C_6H_5Br (2.0 ml) in a Schlenk tube. After 5 min, *N,N,*3,5-tetramethylaniline (57 mg, 0.38 mmol, 5.0 equiv.) and sodium tetrakis(pentafluorophenyl)borate (81 mg, 0.115 mmol, 1.5 equiv.) were added. The reaction was stirred out of the glovebox at 60 °C. After 16h, the reaction mixture was evaporated to dryness. The crude was dissolved in CH_2Cl_2 and trifluoroacetic acid was added dropwise. Purification by flash column chromatography (hexane/CH_2Cl_2 95:5) afforded 10-(bromo)-9-sulfonium-10-boratriptycene-ate complex **3.14** (28 mg, 0.066 mmol, 86% yield) as a colorless solid.

Note: 10-bromo-9-sulfonium-10-boratriptycene-ate complex **3.14** was obtained as an inseparable mixture of two isomers (*m*:*p*) with 23:77 ratio.

TLC: R_f = 0.90 (hexane/CH_2Cl_2 50:50)

^{1}H NMR (500 MHz, $CDCl_3$) δ (ppm) = *meta* isomer: 8.24 (s, 1H), 8.11-7.98 (m, 1H), 7.82-7.76 (m, 6H), 7.53 (ddd, *J* = 7.9, 2.1, 1.1 Hz, 1H), 7.42 (t, *J* = 7.6 Hz, 1H), 7.28-7.24 (m, 3H), 7.08 (t, *J* = 7.5 Hz, 3H). *para* isomer: 7.96 (d, *J* = 7.8 Hz, 2H), 7.82-7.76 (m, 6H), 7.67 (d, *J* = 8.3 Hz, 2H), 7.24 (td, *J* = 7.4, 1.2 Hz, 3H), 7.08 (td, *J* = 7.5, 1.5 Hz, 3H).

^{13}C NMR (126 MHz, $CDCl_3$) δ (ppm) = 137.6, 134.4, 134.0, 130.7, 130.3, 127.8, 124.4. The carbon atoms directly attached to the boron atom on the triptycene core were not detected, likely due to quadrupolar relaxation.

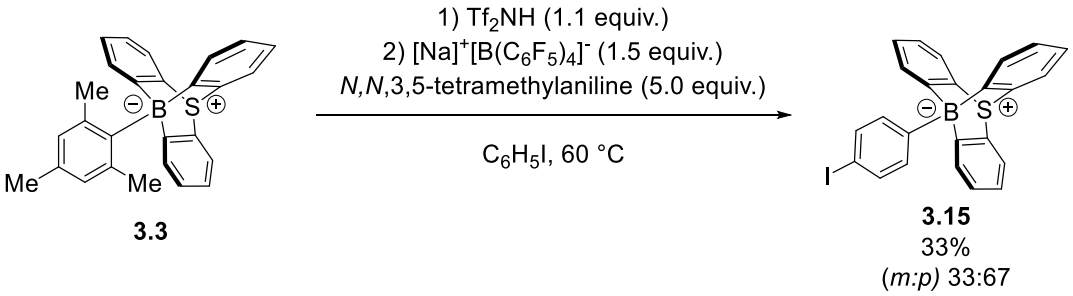
^{11}B NMR (160 MHz, $CDCl_3$) δ (ppm) = -9.4 (s)

HRMS (MALDI $^-$) (*m/z*): calc. for $[C_{41}H_{34}{}^{11}BN_2SBr]$: 676.1719 $[M+DCTB]^+$; found: 676.1730.

IR (neat, ATR): $\tilde{\nu}$ / cm^{-1} = 3053, 2976, 2919, 2852, 1570, 1422, 1293, 1255, 1188, 1068, 1001, 886.

M.p. (CH_2Cl_2/pentane): 256-261 °C (dec)

10-(Iodophenyl)-9-sulfonium-10-boratriptycene-ate complex **3.15**



3.3

3.15
33%
(*m:p)* 33:67

In a glovebox, $HNTf_2$ (24 mg, 0.085 mmol, 1.1 equiv.) was added as a solid to a suspension of 10-mesityl-9-sulfonium-10-boratriptycene-ate complex **3** (30 mg, 0.077 mmol, 1.0 equiv.) in iodobenzene (2.0 ml) in a Schlenk tube. After 5 min, *N,N,*3,5-tetramethylaniline (57 mg, 0.38 mmol, 5.0 equiv.) and sodium

tetrakis(pentafluorophenyl)borate (81 mg, 0.115 mmol, 1.5 equiv.) were added. The reaction was stirred out of the glovebox at 60 °C. After 16h, the reaction mixture was evaporated to dryness. The crude was dissolved in CH_2Cl_2 and trifluoroacetic acid was added dropwise. Purification by flash column chromatography (hexane/CH_2Cl_2 95:5) afforded 10-(3,5-dimethylphenyl)-9-sulfonium-10-boratriptycene-ate complex **3.15** (12 mg, 0.025 mmol, 33% yield) as a colorless solid.

Note: 10-iodo-9-sulfonium-10-boratriptycene-ate complex **3.15** was obtained as an inseparable mixture of two isomers (*m*:*p*) with 33:67 ratio.

TLC: R_f = 0.90 (hexane/CH_2Cl_2 50:50)

^{1}H NMR (500 MHz, $CDCl_3$) δ (ppm) = *meta* isomer: 8.44 (s, 1H), 8.03 (d, *J* = 7.4 Hz, 1H), 7.80-7.76 (m, 6H), 7.73 (ddd, *J* = 7.8, 1.8, 1.1 Hz, 1H), 7.30 (t, *J* = 7.6 Hz, 1H), 7.26 (t, *J* = 7.4 Hz, 3H), 7.08 (t, *J* = 7.5 Hz, 3H). *para* isomer: 7.87 (d, *J* = 8.3 Hz, 2H), 7.83 (d, *J* = 8.1 Hz, 2H), 7.80-7.76 (m, 6H), 7.24 (td, *J* = 7.4, 1.2 Hz, 3H), 7.08 (td, *J* = 7.5, 1.4 Hz, 3H).

^{13}C NMR (126 MHz, $CDCl_3$) δ (ppm) = 162.6, 144.3, 137.9, 136.6, 134.7, 134.4 (Cq), 134.3 (Cq), 134.0, 133.9, 133.9, 130.4, 130.3, 127.9, 124.4, 124.3, 91.0

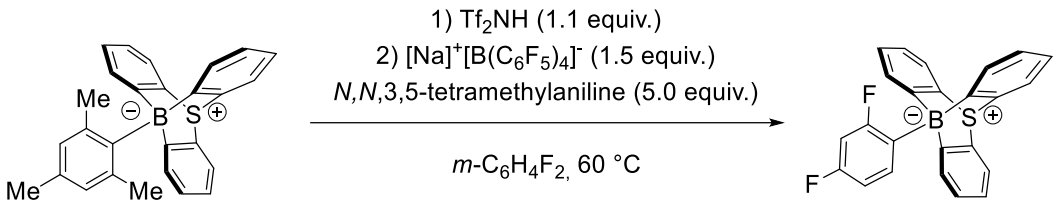
^{11}B NMR (160 MHz, $CDCl_3$) δ (ppm) = -9.5 (s), -9.7 (s)

HRMS (MALDI $^-$) (*m/z*): calc. for $[C_{41}H_{34}{}^{10}BN_2SI]$: 723.1617 $[M+DCTB]^+$; found: 723.1599.

IR (neat, ATR): $\tilde{\nu}$ / cm^{-1} = 3049, 2925, 2242, 1574, 1478, 1435, 1297, 1259, 1192, 1005, 905, 752.

M.p. (CH_2Cl_2/pentane): 252-254°C

10-(2,4-Difluorophenyl)-9-sulfonium-10-boratriptycene-ate complex **3.16**



3.3 **3.16** 51%

In a glovebox, $HNTf_2$ (24 mg, 0.085 mmol, 1.1 equiv.) was added as a solid to a suspension of 10-mesityl-9-sulfonium-10-boratriptycene-ate complex **3.3** (30 mg, 0.077 mmol, 1.0 equiv.) in *m*-$C_6H_4F_2$ (2.0 ml) in a Schlenk tube. After 5 min, *N,N,*3,5-tetramethylaniline (57 mg, 0.38 mmol, 5.0 equiv.) and sodium tetrakis(pentafluorophenyl)borate (81 mg, 0.115 mmol, 1.5 equiv.) were added. The reaction was stirred out of the glovebox at 60 °C. After 16h, the reaction mixture was evaporated to dryness and the crude was purified by flash column chromatography (hexane/CH_2Cl_2 90:10) affording 10-(2,4-difluorophenyl)-9-sulfonium-10-boratriptycene-ate complex **3.16** (15 mg, 0.039mmol, 61% yield) as a colorless powder.

TLC: R_f = 0.90 (hexane/CH_2Cl_2 50:50)

^{1}H NMR (500 MHz, $CDCl_3$) δ (ppm) = 8.30-8.24 (m, 1H), 7.76 (d, *J* = 7.7 Hz, 3H), 7.76-7.73 (m, 3H), 7.26-7.22 (m, 3H), 7.11-7.04 (m, 4H), 6.96 (td, *J* = 9.9, 2.5 Hz, 1H).

^{13}C NMR (126 MHz, $CDCl_3$) δ (ppm) = 136.8 (dd, *J* = 14.3, 8.3 Hz), 134.1, 134.0 (Cq), 130.3, 127.7, 124.4, 110.5 (d, *J* = 17.1 Hz), 103.6 (dd, *J* = 31.2, 22.9 Hz). The carbon atoms directly attached to the boron atom on the triptycene core were not detected, likely due to quadrupolar relaxation.

^{11}B NMR (160 MHz, $CDCl_3$) δ (ppm) = -10.1 (s)

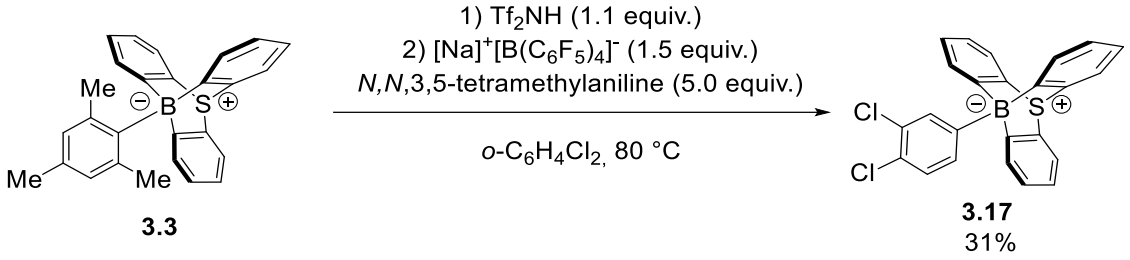
^{19}F NMR (483 MHz, $CDCl_3$) δ (ppm) = -91.5 (s, 1F), -115.8 (quintet, *J* = 8.4 Hz, 1F).

HRMS (MALDI $^-$) (*m/z*): calc. for $[C_{41}H_{33}{}^{11}BN_2SF_2]$: 634.2426 $[M+DCTB]^+$; found: 634.2435.

IR (neat, ATR): $\tilde{\nu}$ / cm^{-1} = 3048, 2924, 2852, 1642, 1589, 1513, 1456, 1432, 1264, 1126, 1078, 968, 843.

M.p. (CH_2Cl_2/pentane): 217-221 °C

10-(3,4-Dichlorophenyl)-9-sulfonium-10-boratriptycene-ate complex **3.17**



3.3 → **3.17** 31%

In a glovebox, $HNTf_2$ (24 mg, 0.085 mmol, 1.1 equiv.) was added as a solid to a suspension of 10-mesityl-9-sulfonium-10-boratriptycene-ate complex **3.3** (30 mg, 0.077 mmol, 1.0 equiv.) in *o*-C_6H_4Cl (2.0 ml) in a Schlenk tube. After 5 min, *N,N,*3,5-tetramethylaniline (57 mg, 0.38 mmol, 5.0 equiv.) and sodium tetrakis(pentafluorophenyl)borate (81 mg, 0.115 mmol, 1.5 equiv.) were added. The reaction was stirred out of the glovebox at 80 °C. After 16h, the reaction mixture was evaporated to dryness. The crude was dissolved in CH_2Cl_2 and trifluoroacetic acid was added dropwise. Purification by flash column chromatography (hexane/CH_2Cl_2 95:5) afforded 10-(3,4-dichlorophenyl)-9-sulfonium-10-boratriptycene-ate complex **3.17** (25 mg, 0.065 mmol, 31% yield) as a colorless solid.

Single crystals suitable for X-ray diffraction analysis were obtained by a slow evaporation of a saturated solution of **3.17** in CH_2Cl_2.

TLC: R_f = 0.90 (hexane/CH_2Cl_2 50:50)

^{1}H NMR (500 MHz, $CDCl_3$) δ (ppm) = 8.16 (s, 1H), 7.87 (d, *J* = 7.9 Hz, 1H), 7.78 (d, *J* = 7.6 Hz, 3H), 7.75 (d, *J* = 7.4 Hz, 3H), 7.60 (d, *J* = 8.0 Hz, 1H), 7.25 (td, *J* = 7.3, 0.8 Hz, 3H), 7.09 (td, *J* = 7.5, 1.3 Hz, 3H).

^{13}C NMR (126 MHz, $CDCl_3$) δ (ppm) = 137.2, 135.2, 134.3 (Cq), 133.8, 130.4, 129.6, 128.6 (Cq), 127.9, 124.5. The carbon atoms directly attached to the boron atom on the triptycene core were not detected, likely due to quadrupolar relaxation.

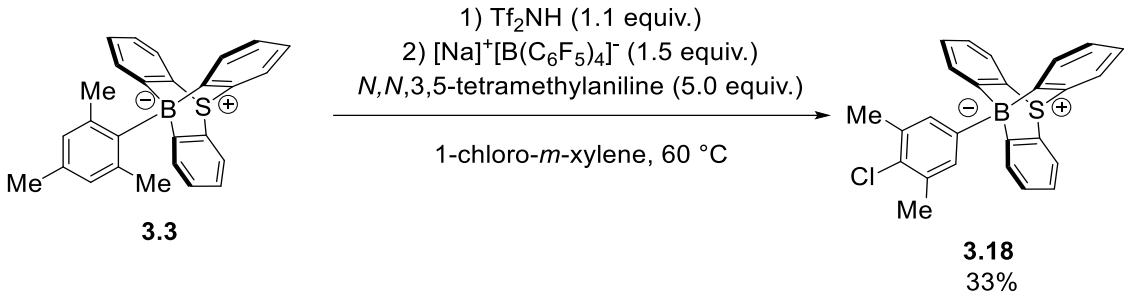
^{11}B NMR (160 MHz, $CDCl_3$) δ (ppm) = -9.7 (s)

HRMS (MALDI $^-$) (*m/z*): calc. for $[C_{41}H_{33}{}^{11}BN_2SCl_2]$: 666.1835 $[M+DCTB]^+$; found: 666.1817.

IR (neat, ATR): $\tilde{\nu}$ / cm^{-1} = 3058, 2919, 1847, 1570, 1432, 1298, 1260, 1183, 1130, 1016, 920, 886.

M.p. (CH_2Cl_2/pentane): 248-252 °C

10-(4-chloro-3,5-dimethylphenyl)-9-sulfonium-10-boratriptycene-ate complex **3.18**



3.3 → **3.18** 33%

In a glovebox, $HNTf_2$ (24 mg, 0.085 mmol, 1.1 equiv.) was added as a solid to a suspension of 10-mesityl-9-sulfonium-10-boratriptycene-ate complex **3.3** (30 mg, 0.077 mmol, 1.0 equiv.) in 1-chloror-*m*-xylene (2.0 ml) in a Schlenk tube. After 5 min, *N,N,*3,5-tetramethylaniline (57 mg, 0.38 mmol, 5.0 equiv.) and sodium tetrakis(pentafluorophenyl)borate (81 mg, 0.115 mmol, 1.5 equiv.) were added. The reaction was stirred out of the glovebox at 60 °C. After 16h, the reaction mixture was evaporated to dryness. The crude was dissolved in CH_2Cl_2 and trifluoroacetic acid was added dropwise. Purification by flash column chromatography (hexane/CH_2Cl_2 95:5) afforded 10-(3,5-dimethylphenyl)-9-sulfonium-10-boratriptycene-ate complex **3.18** (12 mg, 0.025 mmol, 33% yield) as a colorless solid.

TLC: R_f = 0.90 (hexane/CH_2Cl_2 50:50)

^{1}H NMR (500 MHz, $CDCl_3$) δ (ppm) = 7.84 (d, *J* = 7.4 Hz, 3H), 7.81 (s, 2H), 7.78 (d, *J* = 7.7 Hz, 3H), 7.26 (t, *J* = 7.4 Hz, 3H), 7.08 (t, *J* = 7.5 Hz, 3H), 2.54 (s, 6H).

^{13}C NMR (126 MHz, $CDCl_3$) δ (ppm) = 162.7, 136.0, 134.8 (Cq), 134.4 (Cq), 134.2, 131.5 (Cq), 130.3, 127.8, 124.3, 21.2 (CH_3).

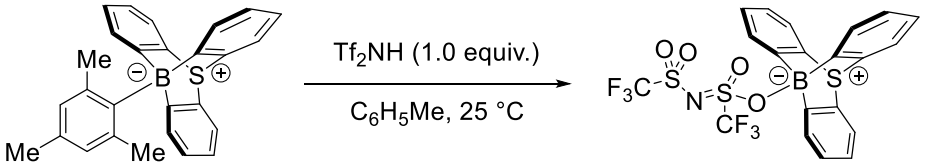
^{11}B NMR (160 MHz, $CDCl_3$) δ (ppm) = -9.6 (s)

HRMS (MALDI $^{-}$) (*m/z*): calc. for $[C_{43}H_{38}{}^{10}BN_2SCl]$: 659.2574 $[M+DCTB]^+$; found: 659.2588.

IR (neat, ATR): $\tilde{\nu}$ / cm^{-1} = 3047, 2980, 1571, 1436, 1292, 1258, 1172, 1124, 1052, 955, 859, 753.

M.p. (CH_2Cl_2/pentane): >300°C

10-Bis(trifluoromethylsulfonyl)imide-9-sulfonium-10-boratriptycene-ate complex **3.19**



3.3 **3.19** 81%

In a glovebox, $HNTf_2$ (24 mg, 0.085 mmol, 1.1 equiv.) was added as a solid to a suspension of 10-mesityl-9-sulfonium-10-boratriptycene-ate complex **3.3** (30 mg, 0.077 mmol, 1.0 equiv.) in toluene (2.0 ml) in a Schlenk tube. The reaction was stirred for 5 min and then evaporated to dryness. Purification *via* flash column chromatography (hexane/CH_2Cl_2 70:30) afforded 10-bis(trifluoromethylsulfonyl)imide-9-sulfonium-10-boratriptycene-ate complex **3.19** (34 mg, 0.062 mmol, 81% yield) as a colorless solid.

TLC: R_f = 0.5 (hexane/CH_2Cl_2 50:50)

^{1}H NMR (400 MHz, $CDCl_3$) δ (ppm) = 8.09 (dd, *J* = 7.4, 1.0 Hz, 3H), 7.80 (d, *J* = 7.3 Hz, 3H), 7.43 (t, *J* = 7.3 Hz, 3H), 7.19 (td, *J* = 7.8, 1.3 Hz, 3H).

^{13}C NMR (101 MHz, $CDCl_3$) δ (ppm) = 131.6, 131.0 (Cq), 130.9, 127.8, 126.0. The carbon atoms directly attached to the boron atom on the triptycene core were not detected, likely due to quadrupolar relaxation.

^{11}B NMR (128 MHz, $CDCl_3$) δ (ppm) = 6.0 (br)

^{19}F NMR (386 MHz, $CDCl_3$) δ (ppm) = -75.0, -78.2

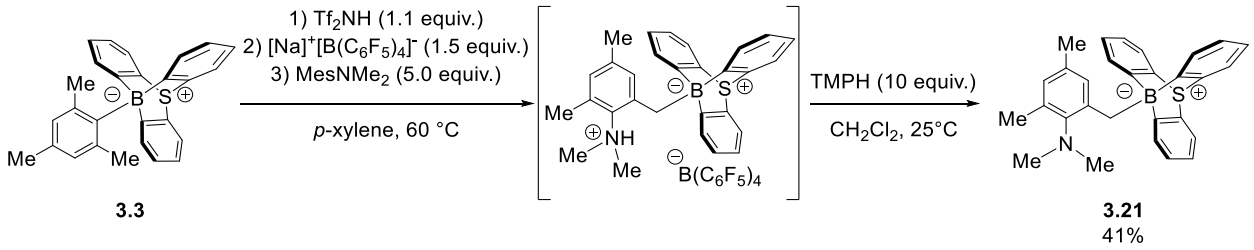
HRMS (MALDI$^-$) (*m/z*): Could not be determined due to decomposition during injection.

IR (neat, ATR): $\tilde{\nu}$ / cm^{-1} = 3062, 2914, 1432, 1379, 1326, 1207, 1135, 1102, 1044, 853, 796.

M.p. ($CHCl_3$): 236-238 °C

III.4. Synthesis of ate-complexe **3.21** derived from activation of Csp^3–H bond.

10-((*N,N*-dimethylamino-3,5-dimethylphenyl)methyl)-9-sulfonium-10-boratriptycene-ate complex **3.21**



In a glovebox, $HNTf_2$ (24 mg, 0.085 mmol, 1.1 equiv.) was added as a solid to a suspension of 10-mesityl-9-sulfonium-10-boratriptycene-ate complex **3.3** (30 mg, 0.077 mmol, 1.0 equiv.) in *p*-xylene (2.0 ml) in a Schlenk tube. After 5 min, *N,N*-dimethyl-mesitylaniline (63 mg, 0.39 mmol, 5.0 equiv.) and sodium tetrakis(pentafluorophenyl)borate (81 mg, 0.115 mmol, 1.5 equiv.) were added. The reaction was stirred out of the glovebox at 60 °C during 16h, then the reaction mixture was evaporated to dryness and the crude was purified by preparative TLC affording a crude mixture of 10-((*N,N*-dimethylamonium-3,5-dimethylphenyl)methyl)-9-sulfonium-10-boratriptycene-ate complex tetrakis(pentafluorophenyl)borate. The crude was dissolved in CH_2Cl_2 and TMPH (0.13

ml, 0.77 mmol, 10 equiv.) was added. After 2h, the crude was evaporated to dryness and purified via preparative TLC affording 10-((*N,N*-dimethylamino-3,5-dimethylphenyl)methyl)-9-sulfonium-10-boratriptycene-ate complex **3.21** (14 mg, 0.031 mmol, 41% yield) as a colorless powder.

Single crystals suitable for X-ray diffraction analysis were obtained by a slow evaporation of a saturated solution of **3.21** in (CH_2Cl_2/pentane 1:1).

TLC: R_f = 0.3 (hexane/CH_2Cl_2 50/50)

^{1}H NMR (500 MHz, $CDCl_3$) δ (ppm) = 7.75 (m, 6H), 7.16 (t, *J* = 7.3 Hz, 3H), 7.03 (td, *J* = 7.4, 0.9 Hz, 3H), 6.85 (s, 1H), 6.80 (s, 1H), 3.13 (s, 6H), 3.07 (s, 2H), 2.39 (s, 3H), 1.92 (s, 3H).

^{13}C NMR (126 MHz, $CDCl_3$) δ (ppm) = 144.9 (Cq), 136.7 (Cq), 134.7 (Cq), 134.1, 133.2 (Cq), 131.8, 130.0, 127.6, 127.4, 123.9, 43.0 (CH_3), 29.9 (CH_3), 21.1 (CH_3), 19.6 (CH_3). The carbon atoms directly attached to the boron atom on the triptycene core were not detected, likely due to quadrupolar relaxation.

^{11}B NMR (160 MHz, $CDCl_3$) δ (ppm) = -11.2 (s).

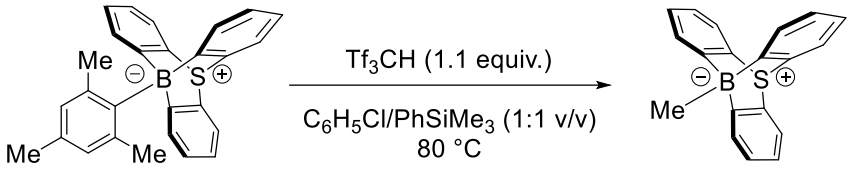
HRMS (MALDI$^-$) (*m/z*): calc. for [$C_{29}H_{28}{}^{11}BNS$]: 433.2036 $[M]^+$; found: 433.2027.

IR (neat, ATR): $\tilde{\nu}$ / cm^{-1} = 3053, 2952, 2924, 2852, 1733, 1671, 1556, 1432, 1379, 1298, 1260, 1116, 1047, 753.

III.5. Synthesis of ate-complexes **3.22**-**3.23** derived from cleavage of Csp^3–Si bond.

From cleavage of Si-Me bond in $PhSiMe_3$:

10-methyl-9-sulfonium-10-boratriptycene-ate complex **3.22**



3.3 | **3.22** 51%

In a glovebox, $HCTf_3$ (35 mg, 0.085 mmol, 1.1 equiv.) was added as a solid to a suspension of 10-mesityl-9-sulfonium-10-boratriptycene-ate complex **3.3** (30 mg, 0.077 mmol, 1.0 equiv.) in C_6H_5Cl (1.0 ml) and $PhSiMe_3$ (1.0 ml) in a Schlenk tube. The reaction was stirred out of the glovebox at during 16h at 80 °C, then the reaction mixture was evaporated to dryness and the crude was purified via flash chromatography (hexane/CH_2Cl_2 90:10) affording 10-methyl-9-sulfonium-10-boratriptycene-ate complex **3.22** (11 mg, 0.039 mmol, 51% yield) as a colorless powder.

TLC: R_f = 0.90 (hexane/CH_2Cl_2 50/50)

^{1}H NMR (500 MHz, $CDCl_3$) δ (ppm) = 7.82 (d, *J* = 7.1 Hz, 3H), 7.71 (d, *J* = 7.6 Hz, 3H), 7.27 (td, *J* = 7.3, 1.1 Hz, 3H), 7.03 (td, *J* = 7.5, 1.4 Hz, 3H), 0.81 (s, 3H).

^{13}C NMR (101 MHz, $CDCl_3$) δ (ppm) = 134.6 (CH), 132.2 (Cq), 130.2 (CH), 127.3 (CH), 123.9 (CH). The carbon atoms directly attached to the boron atom on the triptycene core were not detected, likely due to quadrupolar relaxation.

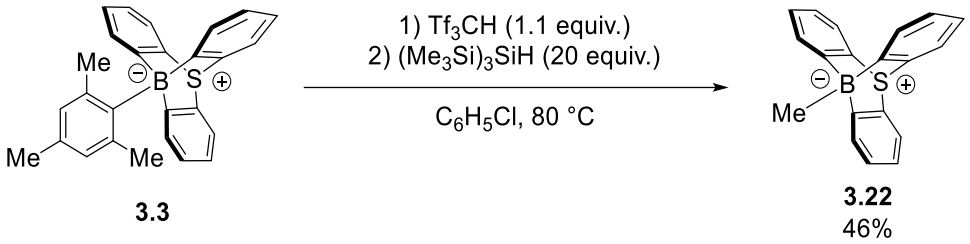
^{11}B NMR (128 MHz, $CDCl_3$) δ (ppm) = -12.6

HRMS (MALDI $^-$) (*m/z*): calc. for $[C_{36}H_{33}{}^{11}BN_2S]$: 536.2458 $[M+DCTB]^+$; found: 536.2442.

IR (neat, ATR): $\tilde{\nu}$ / cm^{-1} = 3053, 2919, 2852, 1723, 1570, 1432, 1370, 1293, 1255, 1188, 1001, 886.

M.p. (CH_2Cl_2): 254-256 °C

From cleavage of Si-Me bond in $(Me_3Si)_3SiH$:

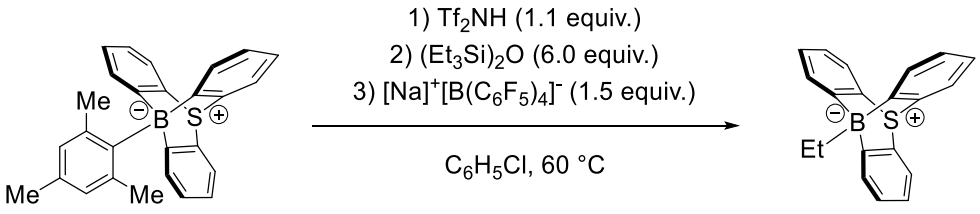


3.3 **3.22** 46%

In a glovebox, $HCTf_3$ (35 mg, 0.085 mmol, 1.1 equiv.) was added as a solid to a suspension of 10-mesityl-9-sulfonium-10-boratriptycene-ate complex **3.3** (30 mg, 0.077 mmol, 1.0 equiv.) in C_6H_5Cl (2.0 ml) in a Schlenk tube. The reaction was stirred out of the glovebox at 80 °C. After 1h30 at 80 °C, $(Me_3Si)_3SiH$ (0.71 ml, 2.3 mmol, 20 equiv.) was added. After 16h at 80 °C, the reaction was evaporated to dryness and the crude was purified via flash chromatography (hexane/CH_2Cl_2 90:10) affording 10-methyl-9-sulfonium-10-boratriptycene-ate complex **3.22** (10 mg, 0.035 mmol, 46% yield) as a colorless powder. ^1H and ^{11}B NMR data are consistent with the one described above.

From cleavage of Si-Et bond in $(Et_3Si)_2O$:

10-ethyl-9-sulfonium-10-boratriptycene-ate complex **3.23**



3.3 **3.23** 83%

In a glovebox, $HNTf_2$ (24 mg, 0.085 mmol, 1.1 equiv.) was added as a solid to a suspension of 10-mesityl-9-sulfonium-10-boratriptycene-ate complex **3.3** (30 mg, 0.077 mmol, 1.0 equiv.) in C_6H_5Cl (2.0 ml) in a Schlenk tube. After 5 min, $(Et_3Si)_2O$ (114 mg, 0.46 mmol, 6.0 equiv.) and sodium tetrakis(pentafluorophenyl)borate (81 mg, 0.115 mmol, 1.5 equiv.) were added. The reaction was stirred out of the glovebox at 60 °C. After 16h, the reaction mixture was evaporated to dryness and the crude was purified by flash chromatography (hexane/CH_2Cl_2 90:10) affording pure 10-ethyl-9-sulfonium-10-boratriptycene-ate complex **3.23** (19 mg, 0.064 mmol, 83% yield) as a colorless solid.

TLC: R_f = 0.90 (hexane/CH_2Cl_2 50/50)

^{1}H NMR (500 MHz, $CDCl_3$) δ (ppm) = 7.90 (d, *J* = 7.2 Hz, 3H), 7.70 (dd, *J* = 7.7, 0.5 Hz, 3H), 7.26 (td, *J* = 7.3, 1.1 Hz, 3H), 7.03 (td, *J* = 7.5, 1.4 Hz, 3H), 1.62-1.53 (br, 5H).

^{13}C NMR (101 MHz, $CDCl_3$) δ (ppm) = 135.0 (Cq), 133.0, 130.1, 127.5, 123.8, 11.5 (CH_3). The carbon atoms directly attached to the boron atom on the triptycene core were not detected, likely due to quadrupolar relaxation.

^{11}B NMR (128 MHz, $CDCl_3$) δ (ppm) = -10.9

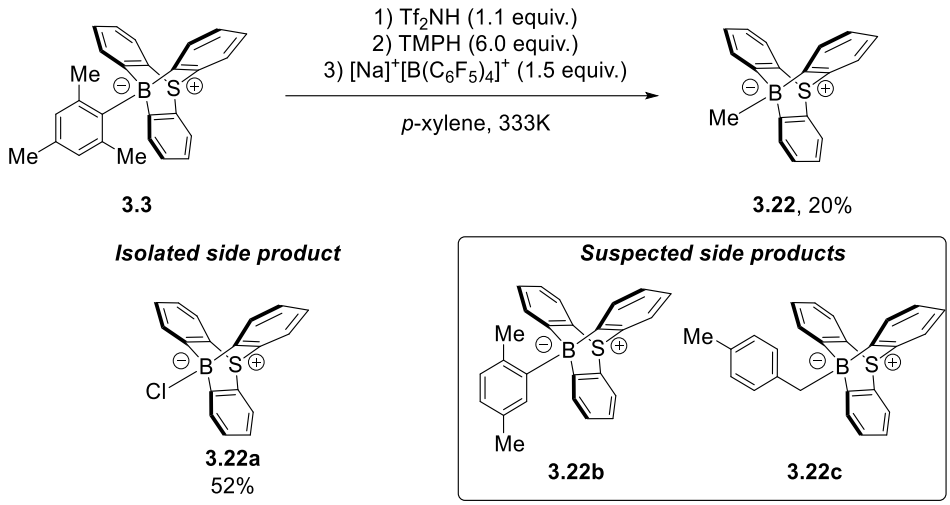
HRMS (MALDI $^-$) (*m/z*): calc. for $[C_{37}H_{35}{}^{11}BN_2SB]$: 550.2614 $[M+DCTB]^+$; found: 550.2598.

IR (neat, ATR): $\tilde{\nu}$ / cm^{-1} = 3048, 2924, 2842, 1566, 1432, 1365, 1293, 1260, 1188, 1121, 1073, 1001, 882.

M.p. (CH_2Cl_2): 211-213 °C

III.6. Synthesis of ate complexe **3.19** derived from cleavage of Csp^3–Csp^3 bond.

10-methyl-9-sulfonium-10-boratriptycene-ate complex **3.22**



In a glovebox, $HNTf_2$ (24 mg, 0.085 mmol, 1.1 equiv.) was added to a suspension of 10-mesityl-9-sulfonium-10-boratriptycene-ate complex **3.3** (30 mg, 0.077 mmol, 1.0 equiv.) in *m*-$C_6H_4F_2$ (2.0 ml) in a sealed Schlenk tube. After 5 min, TMPH (65 mg, 0.46 mmol, 6.0 equiv.) and sodium tetrakis(pentafluorophenyl)borate (81 mg, 0.115 mmol, 1.5 equiv.) were added. The reaction was stirred out of the glovebox at 333K. After 72h, the reaction mixture was evaporated to dryness and directly submitted to ^{11}B NMR spectroscopy, where four major signals have been observed (Figure S3). Two of them have been isolated and are the chloroborane-complex **3.22a** (52%) which results to the decomposition of the triflimidate complex **3.19** in presence of $[Na]^+[B(C_6F_5)_4]^-$ upon addition of chloroform, and the methyl-ate complex **3.22** (4.5 mg, 0.015 mmol, 20% yield) which results to a formal methyl anion abstraction from TMPH. Crystals suitable for X-ray diffraction analysis were obtained by a slow evaporation of a saturated solution of **3.22** in CH_2Cl_2.

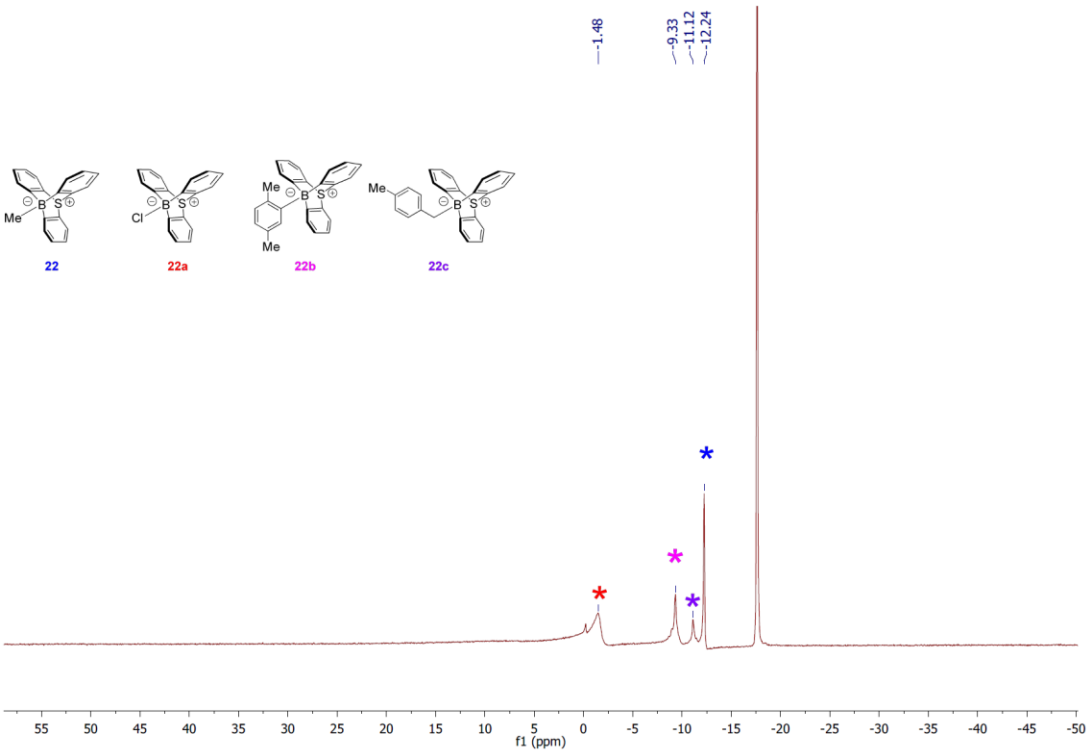


Figure SIII.3. ^{11}B (160 MHz, $CDCl_3$) NMR spectra of the crude reaction mixture, showing the presence of four products.

III.7. Protocols and NMR monitoring of selected reactions.

Reactivity of borohydride **3.5** toward Brønsted acids:

In a glovebox, a solution of HCl in Et_2O (0.05 mL, 2M, 0.1 mmol, 3 equiv.) was added to a solution of 10-hydrido-9-sulfonium-10-boratriptycene-ate complex **3.5** (10 mg, 0.035 mmol, 1.0 equiv.) in $CDCl_3$ (0.7 ml). The ^{11}B NMR analysis showed no reaction after 1 week (Figure SIII.4).

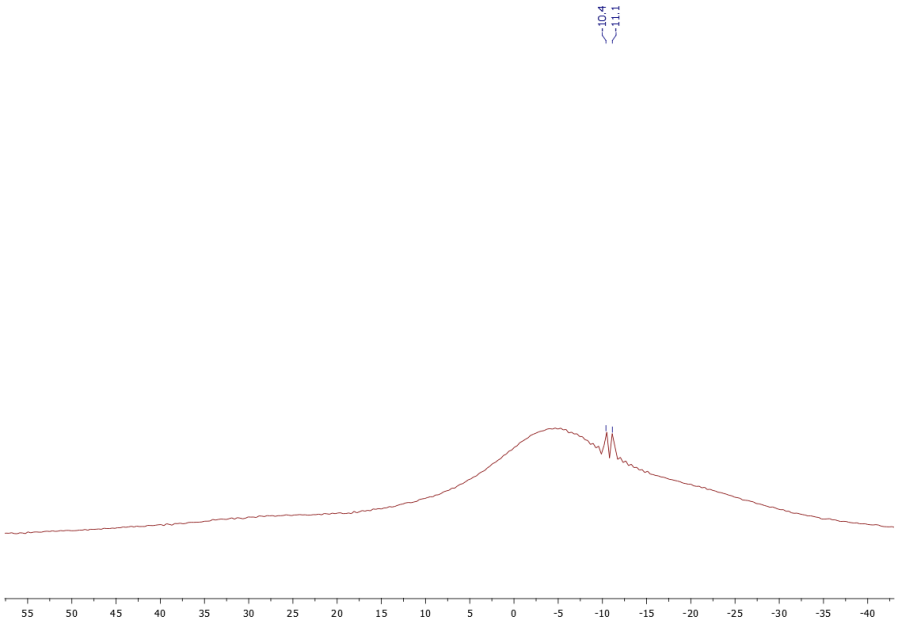


Figure SIII4. ^{11}B NMR spectra (128MHz, 25 °C, C_6D_6) for the reaction of borohydride **3.5** with HCl.

Similar results were obtained using $HNTf_2$. In a glovebox, $HNTf_2$ (7.5 mg, 0.027 mmol, 1.5 equiv.) was added as a solid to a solution of 10-hydrido-9-sulfonium-10-boratriptycene-ate complex **3.5** (5 mg, 0.018 mmol, 1.0 equiv.) in benzene-d_6 (0.7 ml). ^{11}B and ^{1}H NMR analysis showed no conversion of the borohydride **3.5** (Figure S5-S6).

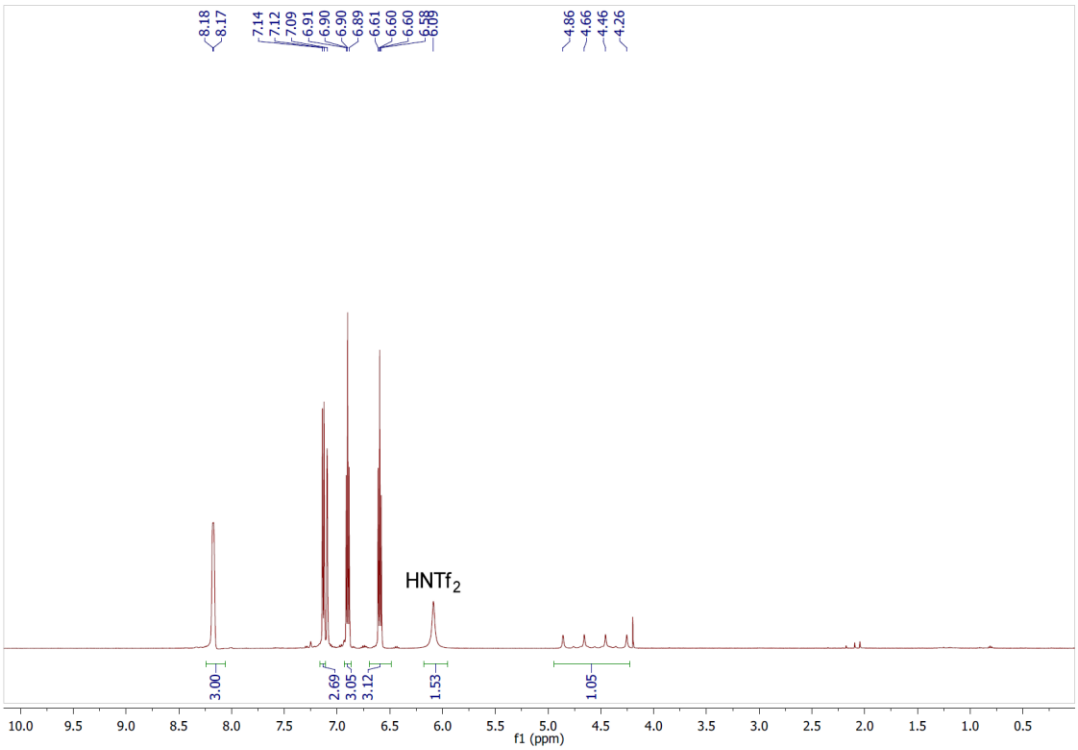


Figure SIII.5. ^{1}H NMR spectra (500 MHz, 25 °C, C_6D_6) for the reaction of borohydride **3.5** with $HNTf_2$.

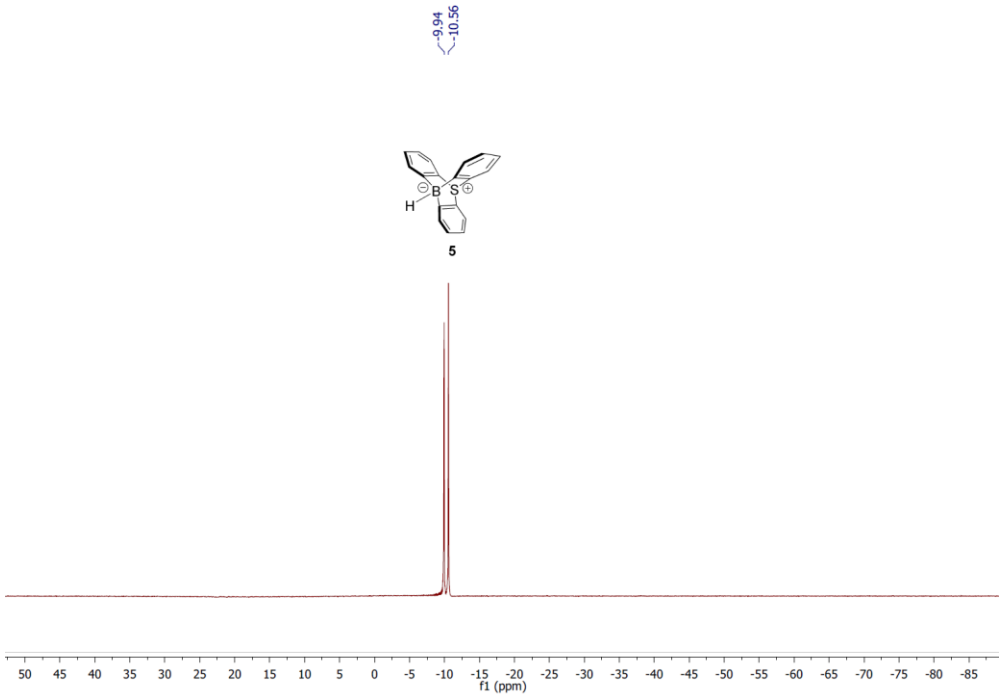


Figure SIII.6. ^{11}B NMR spectra (160 MHz, 25 °C, C_6D_6) for the reaction of borohydride **3.5** with $HNTf_2$.

Reactivity of 10-hydrido-9-sulfonium-10-boratriptycene-ate **3.6** complex towards SIMes and $HNTf_2$:

In a glovebox, 1,3-bis(mesityl)-2-imidazolidinylidene (2.0 mg, 0.0065 mmol, 1.0 equiv.) was added as a solid to a suspension of tetrakis(pentafluorophenyl)borate 10,10'-hydronium-bis(9-sulfonium-10-boratriptycene) **3.6** (8.0 mg, 0.0065 mmol, 1.0 equiv.) in C_6H_5Me and then vigorously stirred. After 16h, a crystalline precipitate appeared and was filtered and washed with small amount of *n*-pentane (1 mL) affording pure recovered starting material **3.6** (7.8 mg, 0.0064 mmol, 99%). The ^{1}H and ^{11}B NMR analysis are consistent with one reported above.

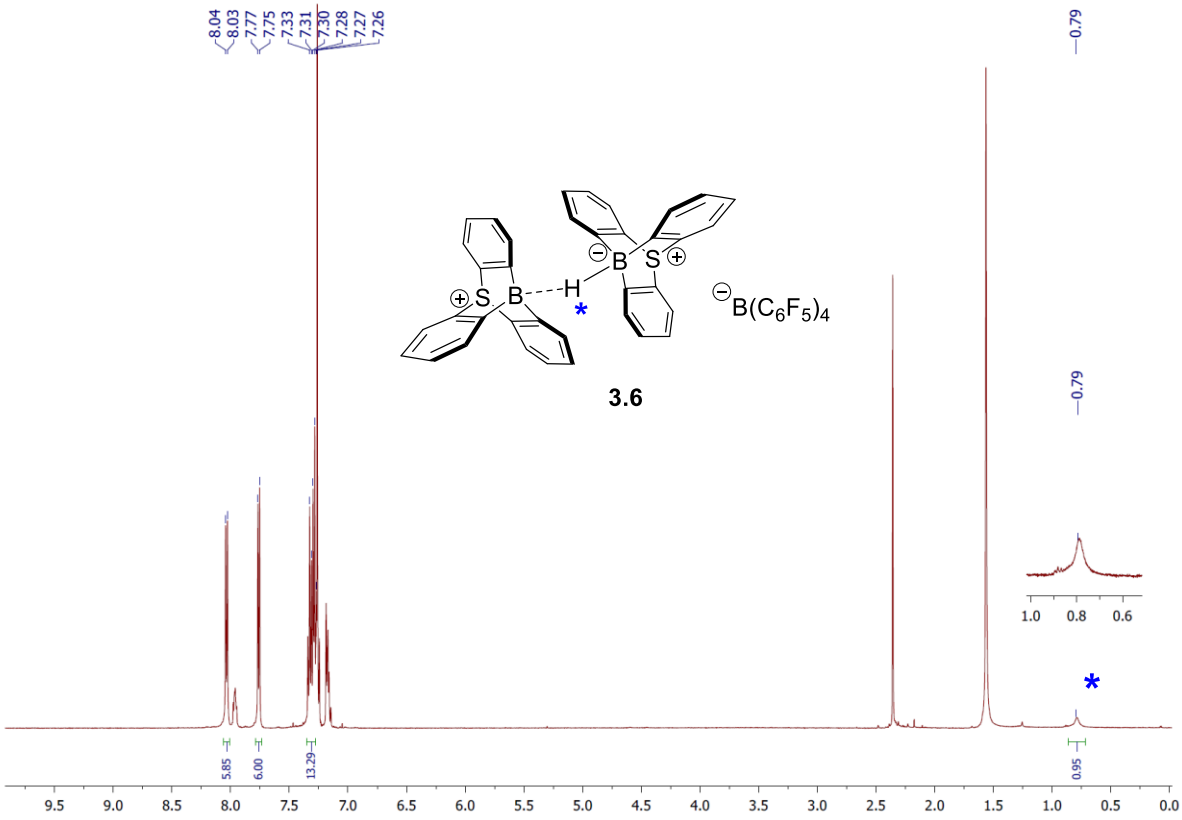


Figure SIII.7. ^{1}H NMR spectra (500 MHz, 25 °C, toluene-d_8) of the recovered starting material after the reaction of **3.6** with IMes.

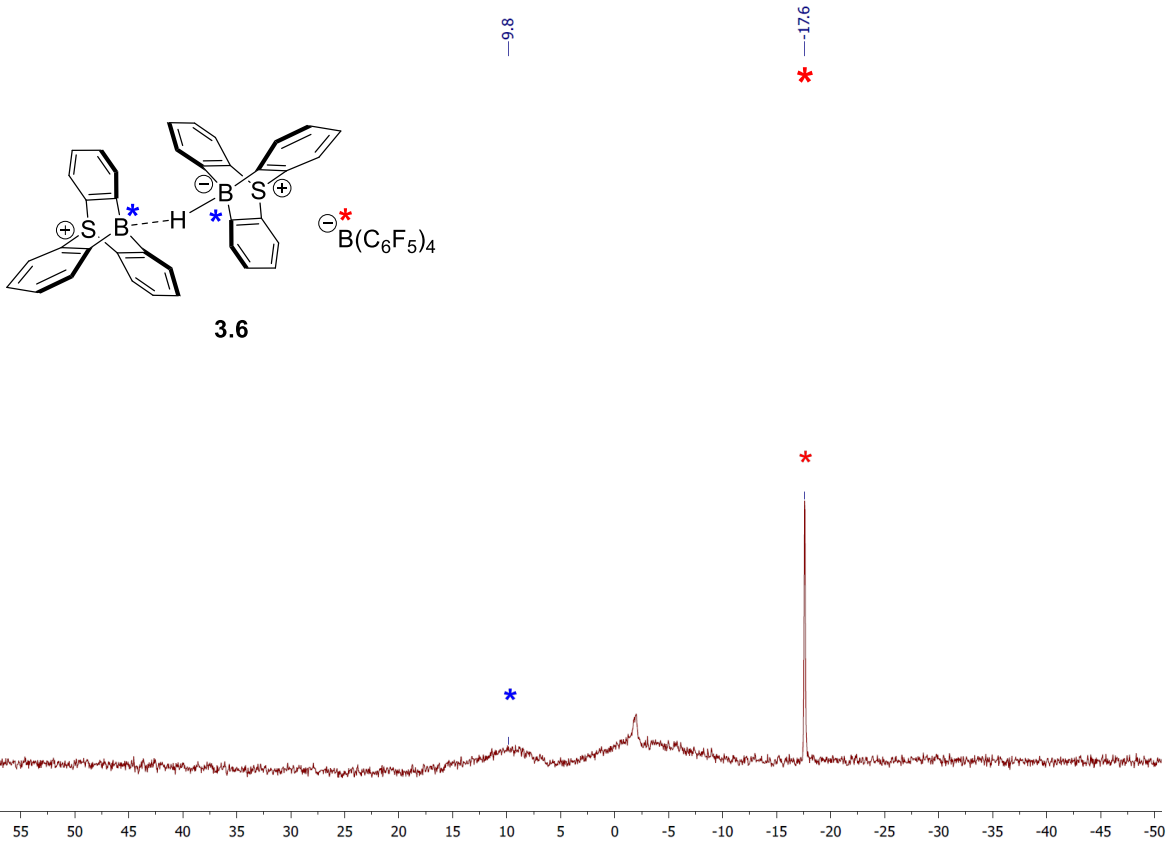


Figure SIII.8. ^{11}B NMR spectra (160 MHz, 25 °C, toluene-d_8) of the recovered starting material after the reaction of **3.6** with IMes.

In a glovebox, $HNTf_2$ (1.1 mg, 0.004 mmol, 1.0 equiv.) was added as a solid to a suspension of tetrakis(pentafluorophenyl)borate 10,10'-hydronium-bis(9-sulfonium-10-boratriptycene) **3.6** (5.0 mg, 0.004 mmol, 1.0 equiv.) in a mixture of $CDCl_3/C_6D_6$ (1:1 v/v) and then vigorously stirred. After 1h the resulting solution was directly submitted to ^1H and ^{19}F NMR spectroscopy. ^1H NMR spectra (Figure SIII.9) showed the absence of reactivity of **3.6** toward $HNTf_2$, similar conclusion was deduced from ^{19}F NMR spectra where only unreacted $HNTf_2$ and tetrakis(pentafluorophenyl)borate anion have been observed (Figure SIII.10).

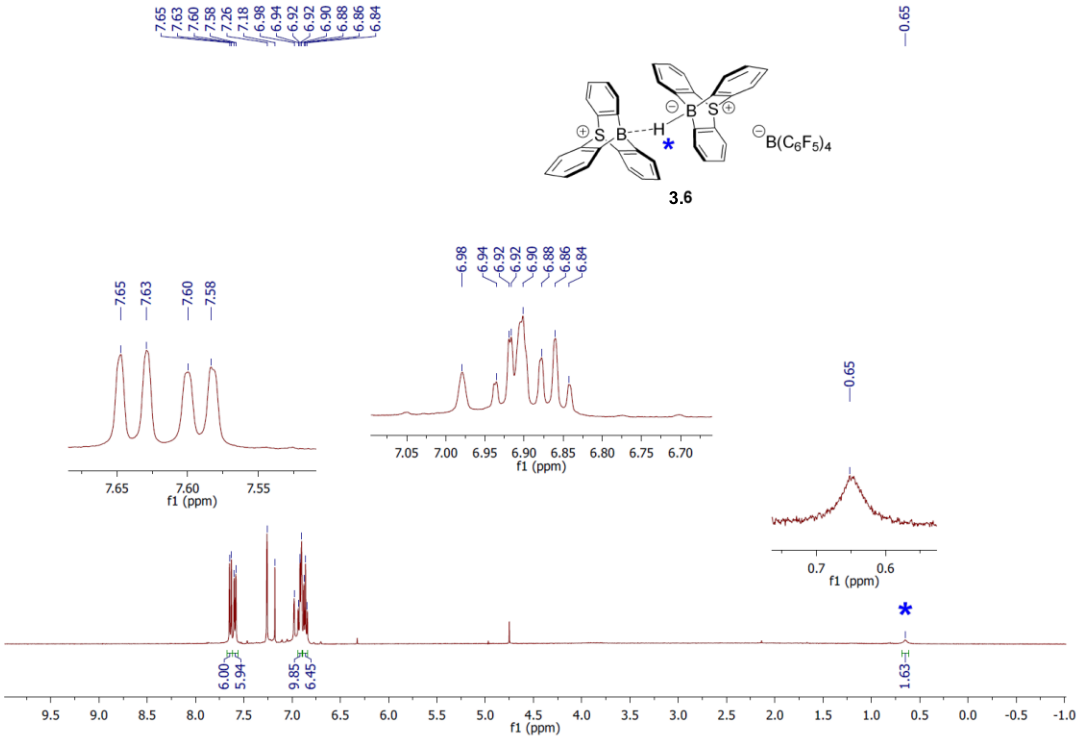


Figure SIII.9. ^{1}H NMR spectra (500 MHz, 25 °C, $CDCl_3/C_6D_6$) for the reaction of **3.6** with $HNTf_2$.

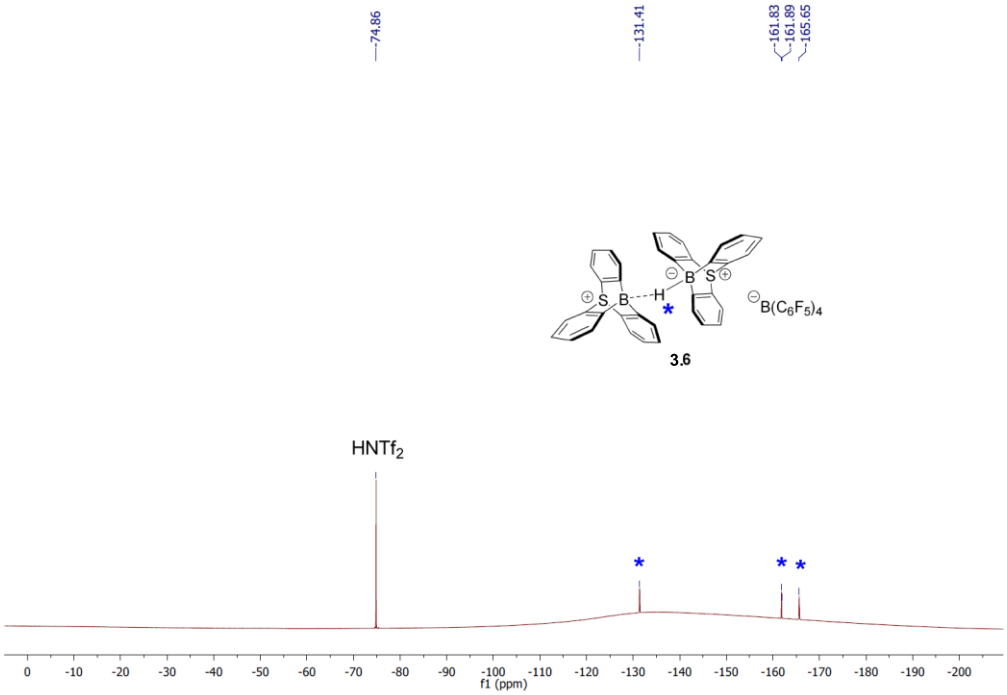
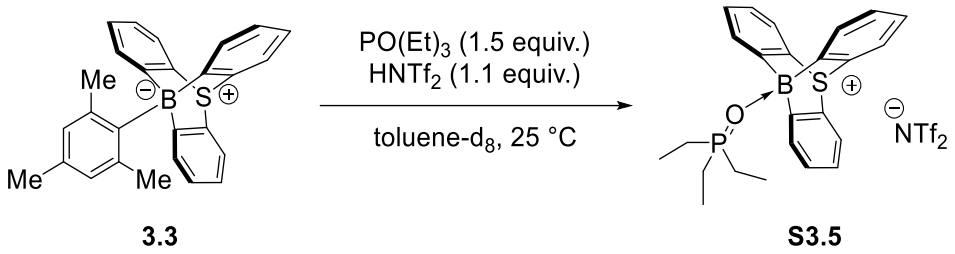


Figure SIII.10. ^{19}F NMR spectra (470 MHz, 25 °C, $CDCl_3/C_6D_6$) for the reaction of **3.6** with $HNTf_2$.

Generation of Gutmann–Beckett Lewis adduct:



3.3 **S3.5**

In a glovebox, $HNTf_2$ (7.9 mg, 0.028 mmol, 1.1 equiv.) was added as a solid to a solution of $OP(Et)_3$ (5.2 mg, 0.038 mmol, 1.5 equiv.) in toluene-d_8 (0.7 ml). After 2 min, 10-mesityl-9-sulfonium-10-boratriptycene-ate complex **3.3** (10 mg, 0.028 mmol, 1.0 equiv.) was added as a solid and the turbid mixture was stirred until being homogeneous. The ^{31}P NMR analysis show a signal at 81.2 ppm for the Lewis adduct **S3.5** (Figure SIII.11) which correspond to an acceptor number (AN) of 88.8. A broad signal at 74.7 ppm correspond to an excess of protonated $PO(Et)_3$.

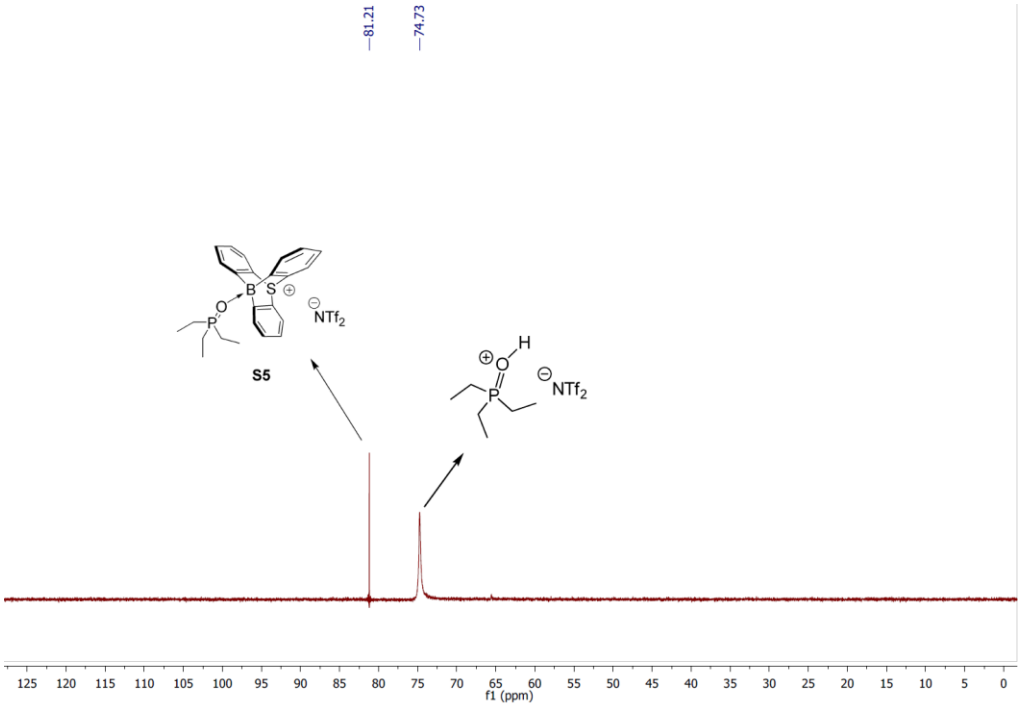
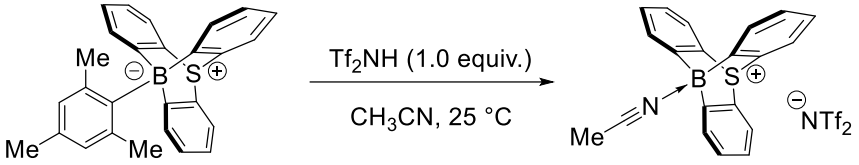


Figure SIII.11. ^{31}P NMR spectra (202 MHz, 25 °C, toluene-d_8) for the reaction of **3.3** with $O(PEt)_3$.

Lewis acidity study by infrared spectroscopy:

Triflimidate-9-sulfonium-10-boratriptycene-acetonitrile Lewis adduct **S3.6**



3.3 **S3.6** 68%

In a glovebox, $HNTf_2$ (14 mg, 0.051 mmol, 1.0 equiv.) was added as a solid to a suspension of 10-mesityl-9-sulfonium-10-boratriptycene-ate complex **3.3** (20 mg, 0.051 mmol, 1.0 equiv.) in CH_3CN (2.0 ml). After 10 min, the crude was evaporated to dryness and washed with Et_2O (3 x 3 mL) affording triflimidate-9-sulfonium-10-boratriptycene-acetonitrile Lewis adduct **S3.6** (21 mg, 0.035 mmol, 68%) as colorless solid.

Single crystals suitable for X-ray diffraction analysis were obtained by a slow evaporation of a saturated solution of **S3.6** in CH_2Cl_2/acetone (50/50).

^{1}H NMR (400 MHz, CD_2Cl_2) δ (ppm) = 7.92 (d, *J* = 7.7 Hz, 3H), 7.87 (d, *J* = 7.3, 0.9 Hz, 3H), 7.49 (td, *J* = 7.4, 1.0 Hz, 3H), 7.29 (td, *J* = 7.6, 1.3 Hz, 3H), 3.36 (s, 3H).

^{13}C NMR (101 MHz, CD_2Cl_2) δ (ppm) = 132.1, 132.0, 129.9, 129.0, 127.0, 4.5 (CH_3). The carbon atoms directly attached to the boron atom on the triptycene core were not detected, likely due to quadrupolar relaxation.

^{11}B NMR (128 MHz, CD_2Cl_2) δ (ppm) = -6.5

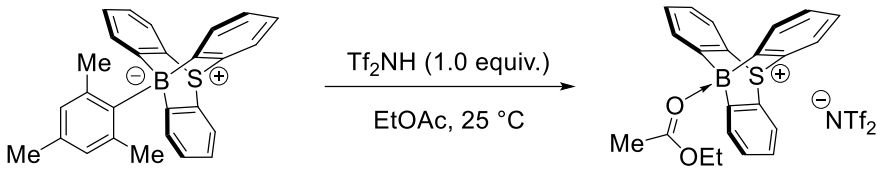
^{19}F NMR (386 MHz, CD_2Cl_2) δ (ppm) = -79.4

HRMS (MALDI$^-$) (*m/z*): The title compound rapidly decomposed after the injection

IR (neat, ATR): $\tilde{\nu}$ / cm^{-1} = 3047, 2985, 2932, 2345, 1585, 1432, 1350, 1225, 1181, 1143, 1056, 859, 749.

M.p. (CH_2Cl_2): 255-257°C

Triflimidate-9-sulfonium-10-boratriptycene-ethylacetate Lewis adduct **S3.7**



3.3 **S3.7** 71%

In a glovebox, $HNTf_2$ (14 mg, 0.051 mmol, 1.0 equiv.) was added as a solid to a suspension of 10-mesityl-9-sulfonium-10-boratriptycene-ate complex **3.3** (20 mg, 0.051 mmol, 1.0 equiv.) in EtOAc (2.0 ml). After 10 min, the crude was evaporated to dryness and washed with Et_2O (3 x 3 mL) affording triflimidate-9-sulfonium-10-boratriptycene-ethylacetate Lewis adduct **S3.7** (23 mg, 0.036 mmol, 71%) as a colorless solid. Traces of 10-triflimidate-9-sulfonium-10-boratriptycene-ate complex remained after washing with Et_2O and could not be removed.

Single crystals suitable for X-ray diffraction analysis were obtained by a slow evaporation of a saturated solution of **S3.7** in $CHCl_3$/acetone (50/50).

^{1}H NMR (400 MHz, CD_2Cl_2) δ (ppm) = 7.96 (d, *J* = 7.7 Hz, 3H), 7.64 (dd, *J* = 7.3, 0.8 Hz, 3H), 7.47 (td, *J* = 7.4, 1.0 Hz, 3H), 7.29 (td, *J* = 7.7, 1.3 Hz, 3H), 5.19 (br, 2H), 2.84 (br, 3H), 1.76 (br, 3H), 1.57 (br, 3H).

^{13}C NMR (101 MHz, CD_2Cl_2) δ (ppm) = 188.0 (C=O), 132.1, 131.7, 129.6, 129.4, 126.8, 28.7, 13.9. The carbon atoms directly attached to the boron atom on the triptycene core were not detected, likely due to quadrupolar relaxation. The CH_2 carbon atom could not be observed.

^{11}B NMR (128 MHz, CD_2Cl_2) δ (ppm) = 2.82

^{19}F NMR (386 MHz, CD_2Cl_2) δ (ppm) = -79.4

HRMS (MALDI$^-$) (*m/z*): The title compound rapidly decomposed after the injection

IR (neat, ATR): $\tilde{\nu}$ / cm^{-1} = 3043, 2975, 2913, 2845, 1585, 1432, 1340, 1191, 1124, 1052, 869, 753

M.p. (CH_2Cl_2): 192-195°C

Discussion:

IR spectroscopy showed that the CN stretching vibration of **S3.6** (2345 cm^{-1}) is higher than that of 9-boratriptycene **3.1** (2337 cm^{-1})[S4] and highly blue shifted by 96 cm^{-1} with respect to free CH_3CN.[S5] The $\nu_{C=O}$ stretching vibration in **S3.7** (1585 cm^{-1}) also indicated that **3.1** is a stronger Lewis acid than 9-boratriptycene (1603 cm^{-1}) and comparable than that of 9-phosphonium-10-boratriptycene (1581 cm^{-1}).[S4,S7]

In the solid state (Figure SIII.12), the B-N bond length of [1.548(3) Å] in **S3.6** is significantly shorter that values of previously reported 9-boratriptycene-MeCN Lewis adducts,[S4,S7] consistent with the more electron-deficient boron center in **3.1**. In the case of **S3.7**, the most striking structural parameters are the C4-O1 and C4-O2 bond lengths. Indeed, with [1.258(8) Å] and [1.284(8) Å], both are slightly shorter than that of the corresponding 9-phosphonium-10-boratriptycene-EtOAt Lewis adduct which displayed bond lengths of [1.257(4) Å] and [1.295(4) Å] for C4-O1 and C4-O2 respectively.[S7] Therefore, the later structural parameters as well as the highly deshielded ^1H NMR chemical shift of H1 at δ = 5.19 ppm showed that the properties of coordinated EtOAc in **S3.7** are more closer to a dioxocarbenium cation than that of classical-EtOAc Lewis adducts.[S8]

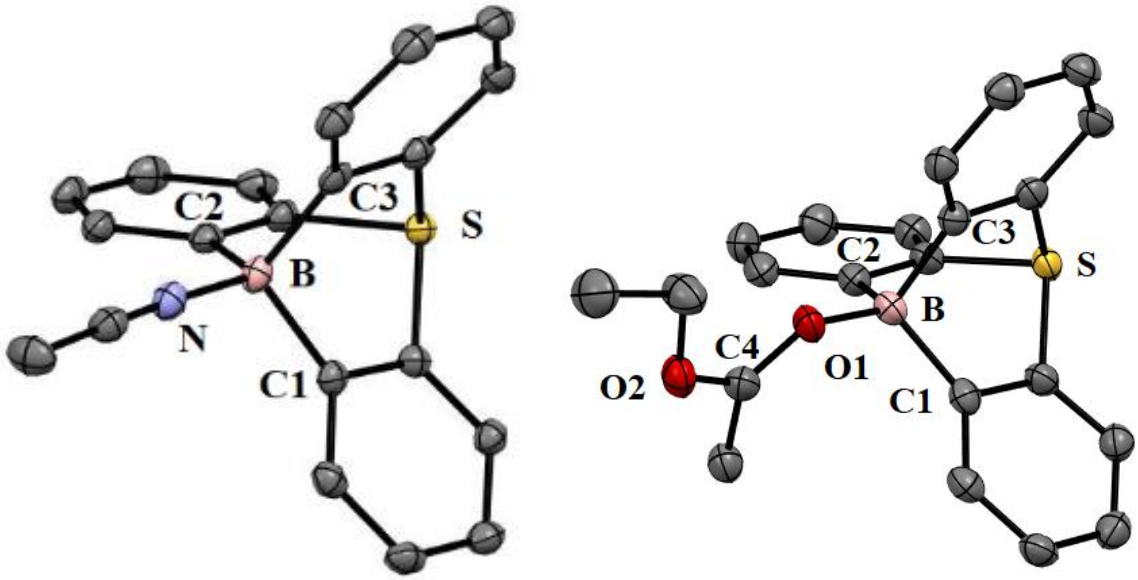
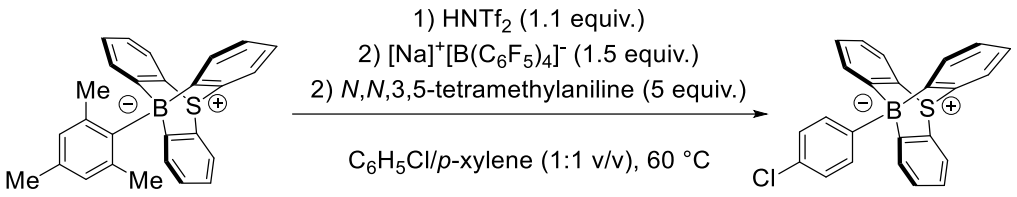


Figure SIII.12. Molecular structures of **S3.6** and **S3.7**. Selected bond lengths in Å; (**S3.6**): B-N 1.548(3); B-C1 1.616(4); B-C2 1.615(4); B-C3 1.615(3). (**S3.7**): B-O1 1.537(9); B-C1 1.626(7); B-C2 1.622(7); B-C3 1.625(7). H-atoms and counter-anions are omitted for clarity; thermal ellipsoids are represented with a 50% probability level

Competitive Csp^2-H activation of C_6H_5Cl toward *p*-xylene:



3.3 **3.13**, 77%

In a glovebox, $HNTf_2$ (16 mg, 0.056 mmol, 1.1 equiv.) was added as a solid to a suspension of 10-mesityl-9-sulfonium-10-boratriptycene-ate complex **3.3** (20 mg, 0.051 mmol, 1.0 equiv.) in a mixture of C_6H_5Cl/*p*-xylene (1:1 (v/v) total 2.0 ml) in a Schlenk tube. After 5 min, *N*,*N*,3,5-tetramethylaniline (38 mg, 0.255 mmol, 5.0 equiv.) and sodium tetrakis(pentafluorophenyl)borate (54 mg, 0.076 mmol, 1.5 equiv.) were added. The reaction was stirred out of the glovebox at 60 °C. After 16h, the reaction mixture was evaporated to dryness and directly submitted to NMR spectroscopy, ^{11}B NMR spectra showed the selective formation of ate-complexe **3.13** (Figure S13). Next, the crude was dissolved in CH_2Cl_2 and trifluoroacetic acid was added dropwise. Purification by flash column chromatography (hexane/CH_2Cl_2 95:5) afforded 10-(chloro)-9-sulfonium-10-boratriptycene-ate complex **3.13** (15 mg, 0.039 mmol, 76% yield) as a colorless solid.

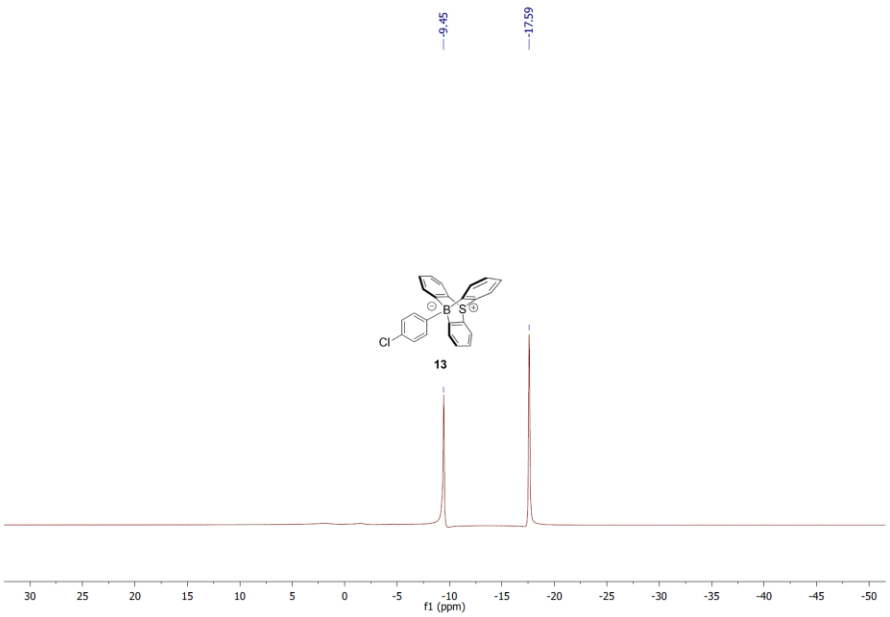
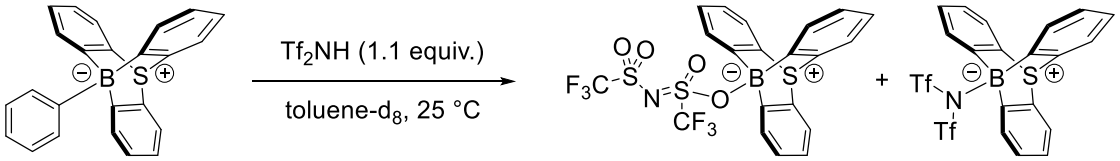


Figure SIII.13. ^{11}B NMR spectra (160 MHz, 25 °C, $CDCl_3$) for the reaction of **3.1** toward a mixture of C_6H_5Cl/*p*-xylene.

<u>Regeneration of triflimidate-complexe **3.19** by protodeboronation of ate-complexe **3.9** with $HNTf_2$:</u>



3.9 **3.19** major **S3.8** minor

In a glovebox, $HNTf_2$ (4.3 mg, 0.021 mmol, 1.1 equiv.) was added as a solid to a solution of 10-phenyl-9-sulfonium-10-boratriptycene-ate complex **3.9** (5 mg, 0.014 mmol, 1.0 equiv.) in toluene-d_8 (0.750 ml) in a glass vial. The reaction was stirred for 16h and then submitted to NMR spectroscopy. ^1H NMR analysis showed clean formation of triflimidate-complex **3.19** as well as the formation of C_6H_6 resulting to the protodeboronation of **3.9,** the *N*-isomer **S3.8** are also detected (10%) (Figure SIII.14). ^{19}F NMR analysis showed the formation of complex **3.19** and traces of the corresponding *N*-isomer **S3.8** as well as unreacted $HNTf_2$ (Figure SIII.15). ^{11}B NMR analysis indicate the formation of complex **3.19** and traces of unreacted **3.9** (Figure SIII.16).

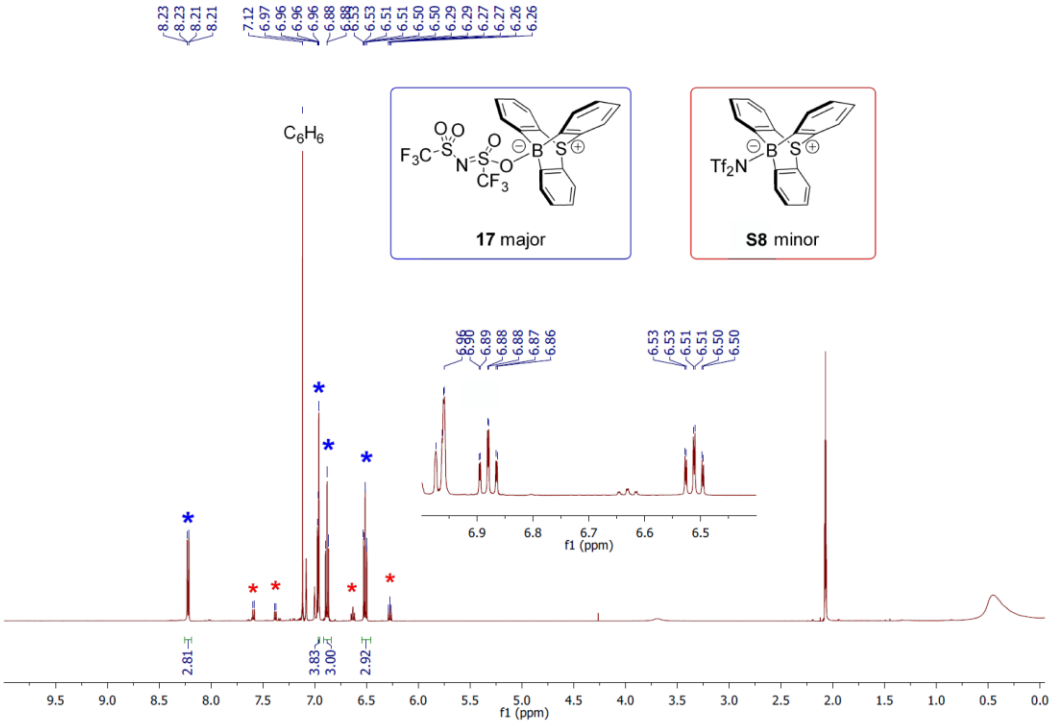


Figure SIII.14. ^{1}H NMR spectra (500 MHz, 25 °C, toluene-d_8) for the reaction of **3.9** with $HNTf_2$.

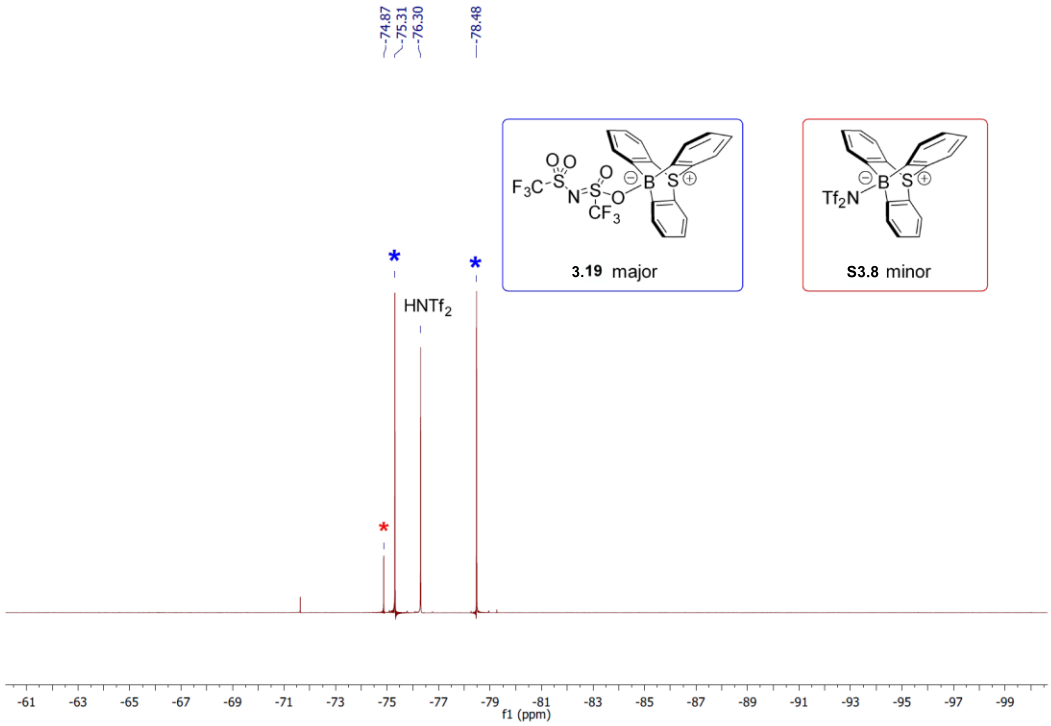


Figure SIII.15. ^{19}F NMR spectra (470 MHz, 25 °C, toluene-d_8) for the reaction of **3.9** with $HNTf_2$.

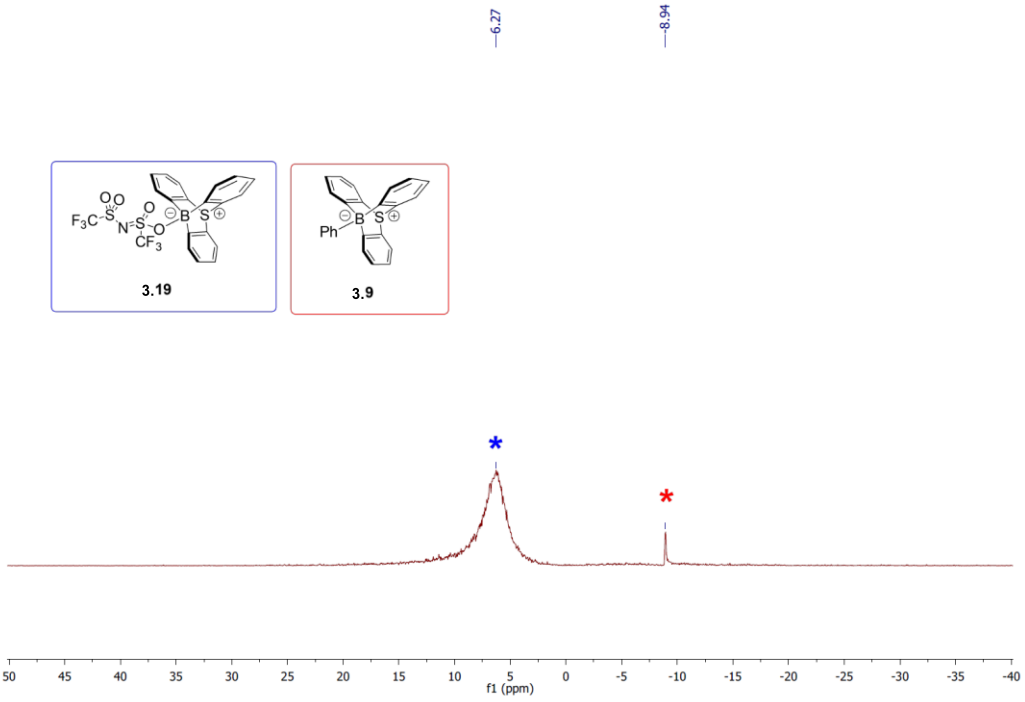
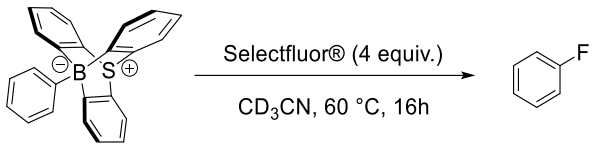


Figure SIII.16. ^{11}B NMR spectra (160 MHz, 25 °C, toluene-d_8) for the reaction of **3.13** with $HNTf_2$.

Formation of C_6H_5F by *ipso*-fluorodeboronation of ate-complexe **3.9** with Selectfluor®:



3.9

Under an argon atmosphere, Selectfluor® (18 mg, 0.057 mmol, 4.0 equiv.) was added as a solid to a solution of 10-phenyl-9-sulfonium-10-boratriptycene-ate complex **3.9** (5 mg, 0.014 mmol, 1.0 equiv.) in CD_3CN (2.0 ml). After 16h at 60 °C, the reaction mixture was cooldown at 25 °C and $C_6H_5CF_3$ (2 mg, 0.014 mmol, 1 equiv.) was added as an internal standard. The mixture was then directly submitted to ^{19}F NMR spectroscopy showing the formation of PhF with 35% NMR yield (Figure SIII.17).

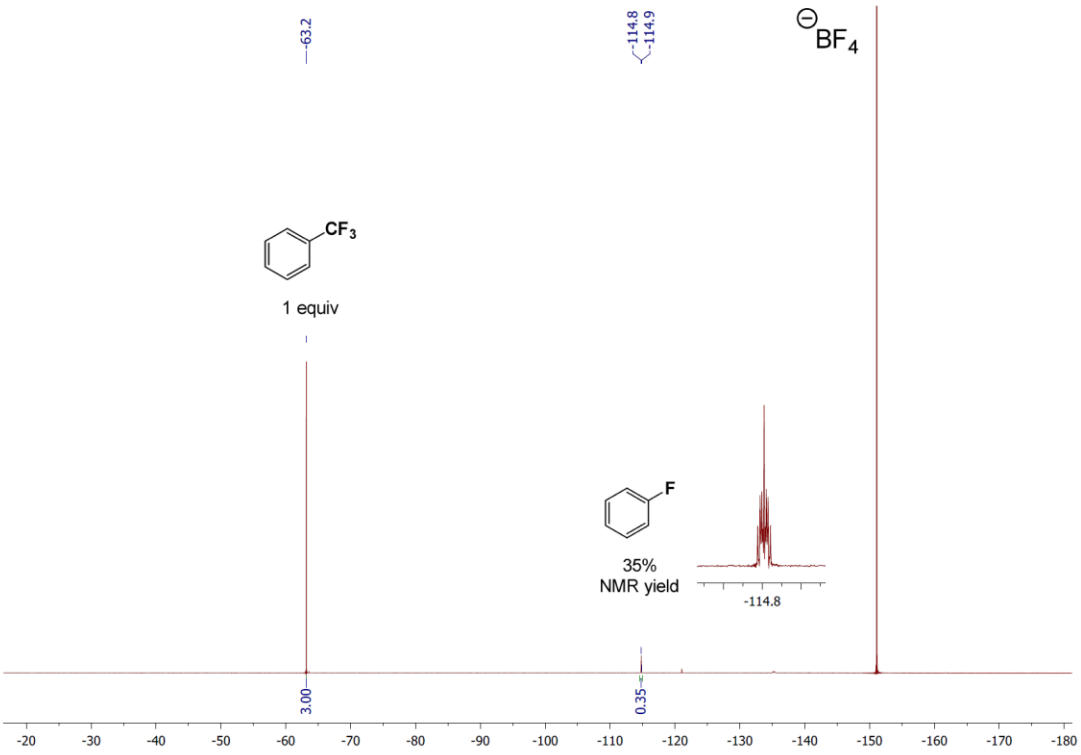


Figure SIII.17. ^{19}F NMR spectra (470 MHz, 25 °C, CD_3CN) for the reaction of **3.9** with Selectfluor® at 60 °C yielding C_6H_5F with an NMR yield of 35%.

Crude ^{11}B NMR analysis for the Csp^3-Si bond cleavage in Ph-SiMe$_3$:

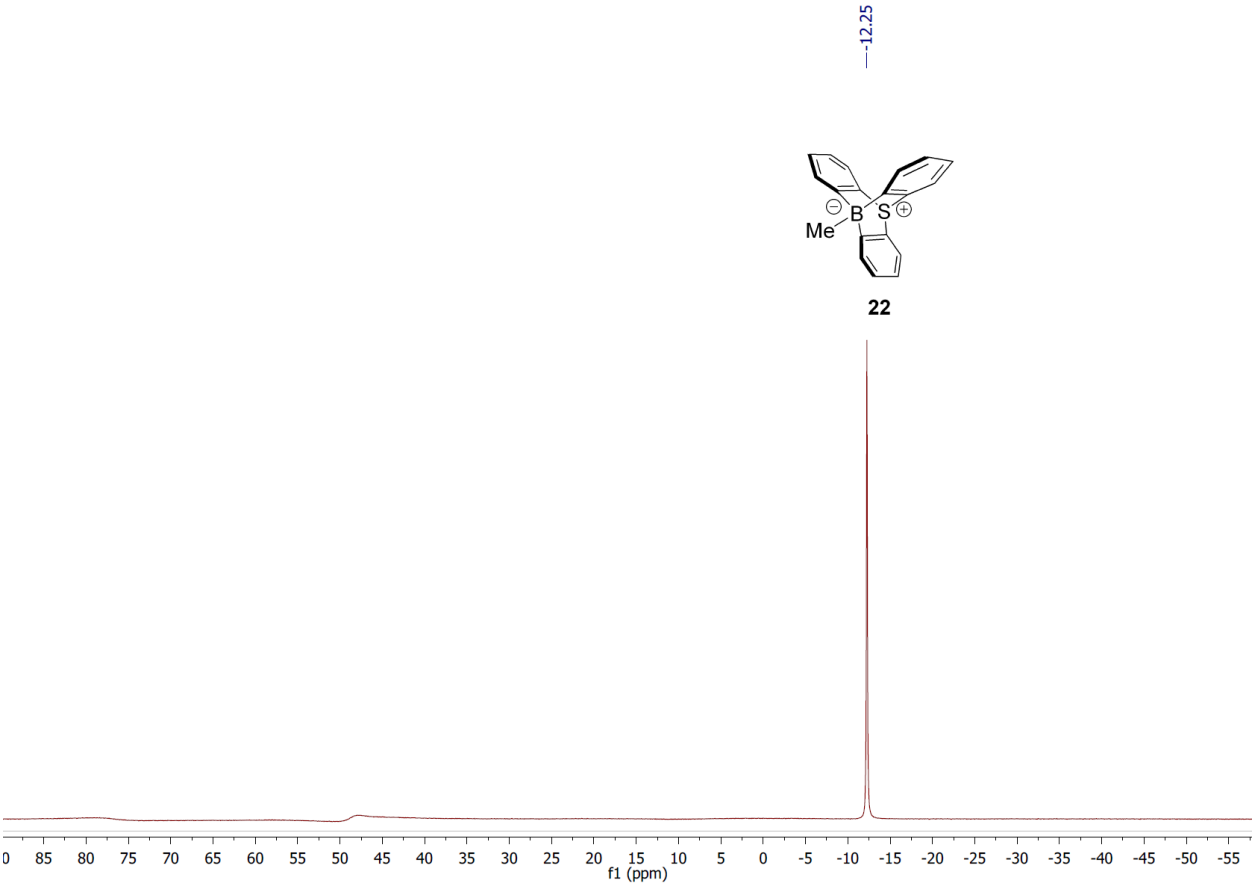
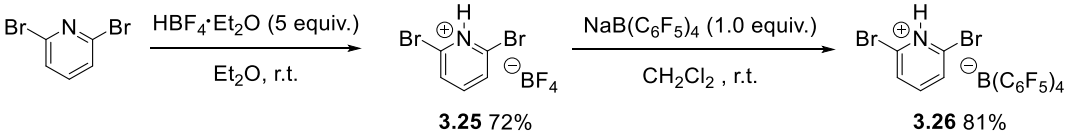


Figure SIII.18. ^{11}B NMR spectra (160 MHz, 25 °C, $CDCl_3$) for the reaction of **3.2** with Ph-SiMe$_3$ at 80 °C yielding selectively ate-complexe **3.22**.

III.8. Attempted generation of 9-sulfonium-10-boratriptycene (**3.2**) with 2,6-dibromopyridinium (**3.25**, **3.26**).

2,6-dibromopyridinium tetrafluoroborate (**3.25**) and tetrakis(pentafluorophenyl)borate (**3.26**)



3.25 72% **3.26** 81%

Synthesized according to a modified literature procedure.[S9] To a solution of 2,6-dibromopyridine (1.2 g, 5.0 mmol, 1.0 equiv.) in dry Et_2O (10 ml) was added a solution of HBF_4 in Et_2O (54 wt %, 0.80 ml, 6.0 mmol, 1.2 equiv.) at 0°C to give a white

precipitate. The mixture was allowed to warm at room temperature and filtered. The solid was washed with Et_2O then dried under vacuum affording pure 2,6-dibromopyridinium tetrafluoroborate (**3.25**) as a white solid (1.2 g, 3.6 mmol, 72%).

^{1}H NMR (500 MHz, DMSO) δ (ppm) = 13.52 (s, 1H), 7.73 – 7.70 (m, 3H).

^{19}F NMR (471 MHz, DMSO) δ (ppm) = -148.2 (s)

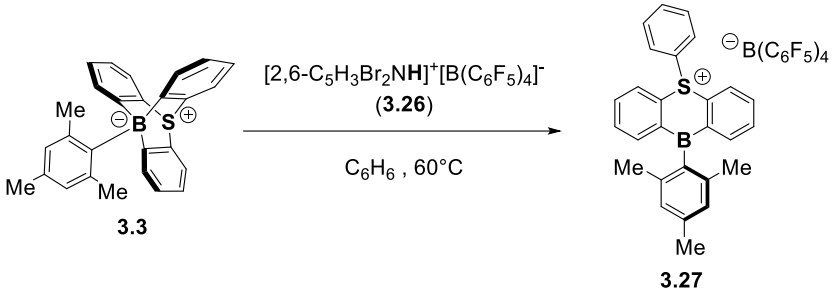
Under Ar atmosphere, to a suspension of 2,6-dibromopyridinium tetrafluoroborate (**3.25**) (1.0 g, 3.0 mmol, 1.0 equiv.) in dry CH_2Cl_2 was added sodium tetrakis(pentafluorophenyl)borate (2.2 g, 3.0 mmol, 1.0 equiv.). The mixture was stirred overnight and then filtered. The filtrate was evaporated to dryness affording pure 2.6-dibromopyridinium tetrakis(pentafluorophenyl)borate as a white solid (2.2 g, 2.4 mmol, 81%).

^{1}H NMR (500 MHz, $CDCl_3$) δ (ppm) = 11.52 (s, 1H), 7.62 – 7.59 (m, 3H).

^{19}F NMR (471 MHz, $CDCl_3$) δ (ppm) = -132.4 (d, *J* = 10.2, 8F), -163.0 (t, *J* = 20.6 Hz, 4F), -166.6 (t, *J* = 18.1, 8F)

^{11}B NMR (160 MHz, $CDCl_3$) δ (ppm) = -17.6 (s)

Protodeborylation with 2,6-dibromopyridinium tetrakis(pentafluorophenyl)borate



3.3 **3.27**

In a glovebox, 2,6-dibromopyridinium tetrakis(pentafluorophenyl)borate (**3.26**) (24 mg, 0.027 mmol, 1.05 equiv.) was added to a solution of 10-mesityl-9-suflonium-10-boratriptycene-ate complex (**3.3**) (10 mg, 0.26 mmol, 1.0 equiv.) in C_6H_6. The reaction was stirred at 60°C for 16h then evaporated to dryness and directly analyzed by NMR

spectroscopy. NMR analysis revealed the decomposition of suggest the opening of the triptycene scaffold.

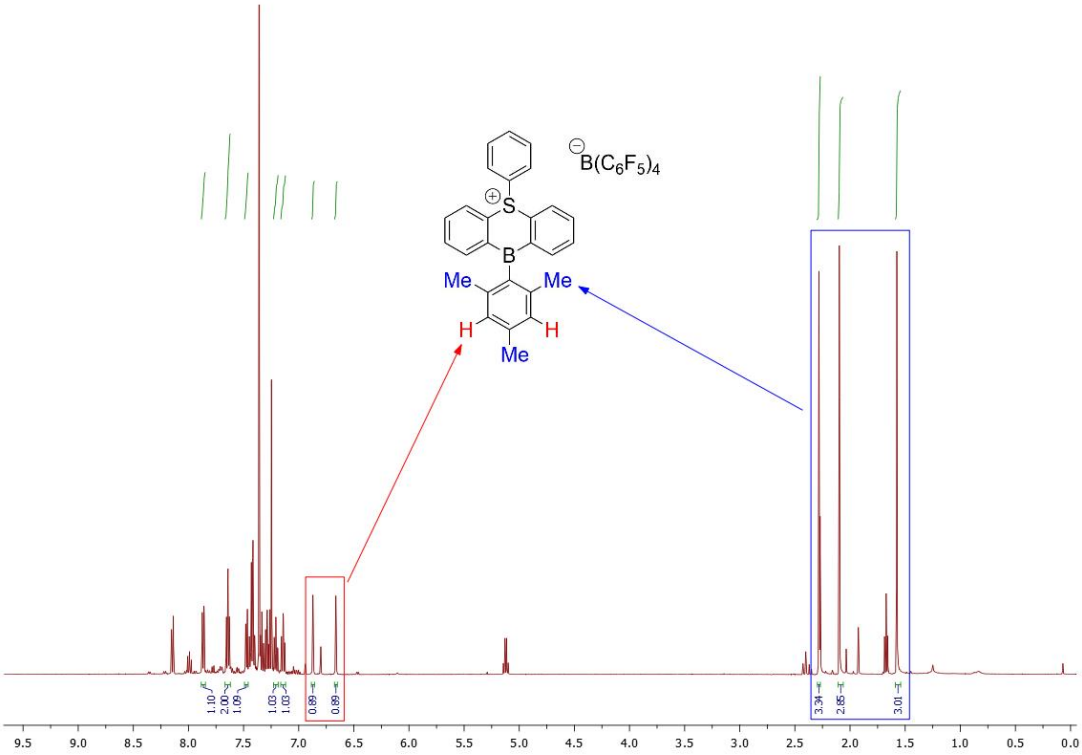


Figure SIII.19. ^{1}H NMR spectra (500 MHz, 25 °C, $CDCl_3$) for the crude reaction of **3.3** with **3.26** at 60 °C.

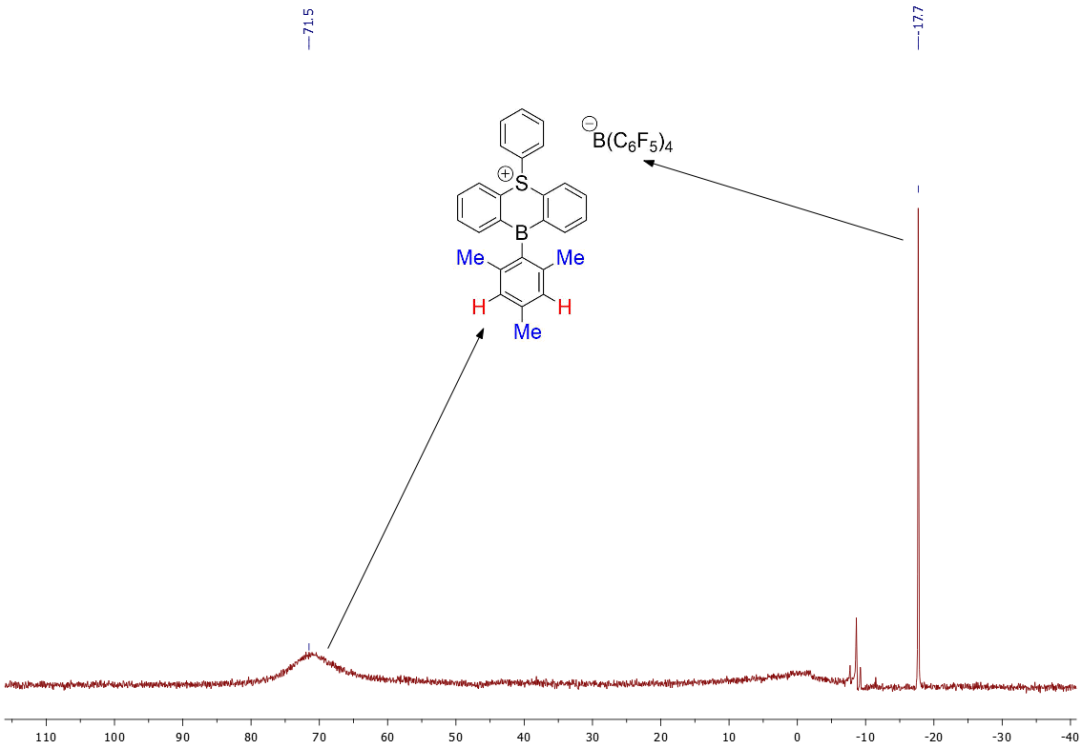
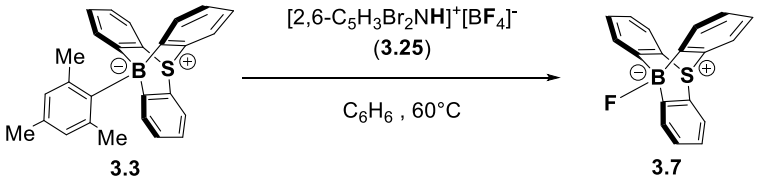


Figure SIII.20. ^{11}B NMR spectra (160 MHz, 25 °C, $CDCl_3$) for the crude reaction of **3.3** with **3.26** at 60 °C.

Protodeborylation with 2,6-dibromopyridinium tetrafluoroborate



In a glovebox, 2,6-dibromopyridinium tetrafluoroborate (**3.25**) (8.7 mg, 0.027 mmol, 1.05 equiv.) was added to a solution of 10-mesityl-9-suflonium-10-boratriptycene-ate complex (**3.3**) (10 mg, 0.26 mmol, 1.0 equiv.) in C_6H_6. The reaction was stirred at 60°C for 16h then evaporated to dryness and directly analyzed by NMR spectroscopy. The presence of a signal at δ = –236.1 unambiguously demonstrates the formation of product **3.7**, showing that under these condition the 9-sulfonium-10-boratriptycene can be generated.

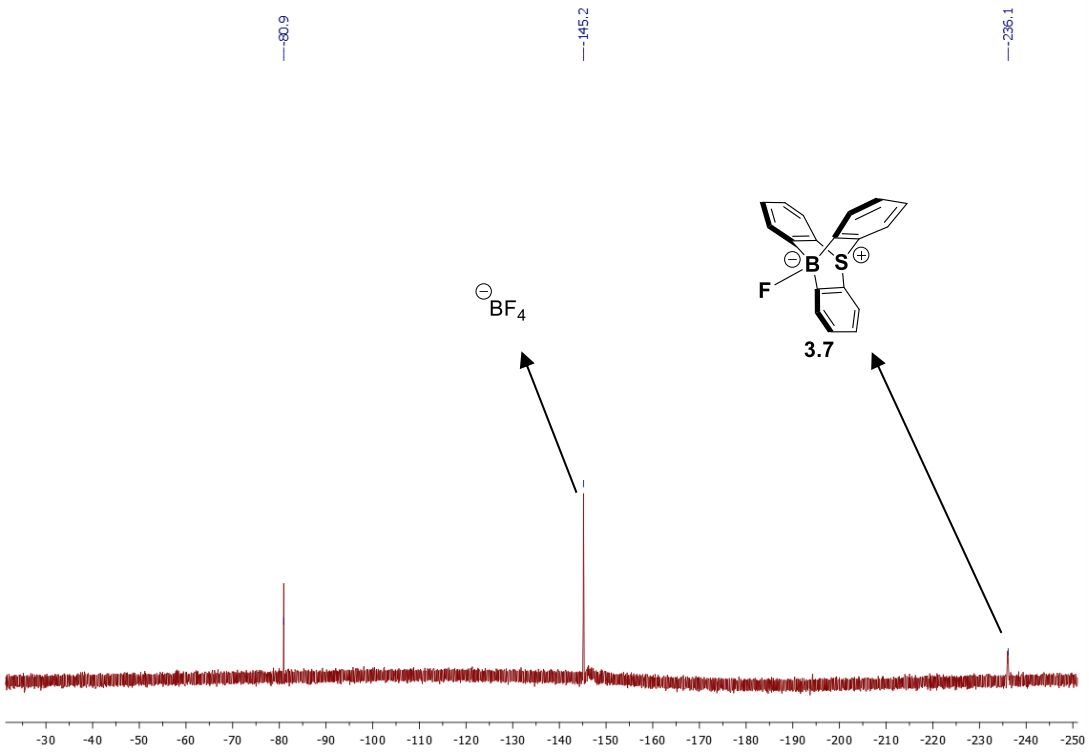
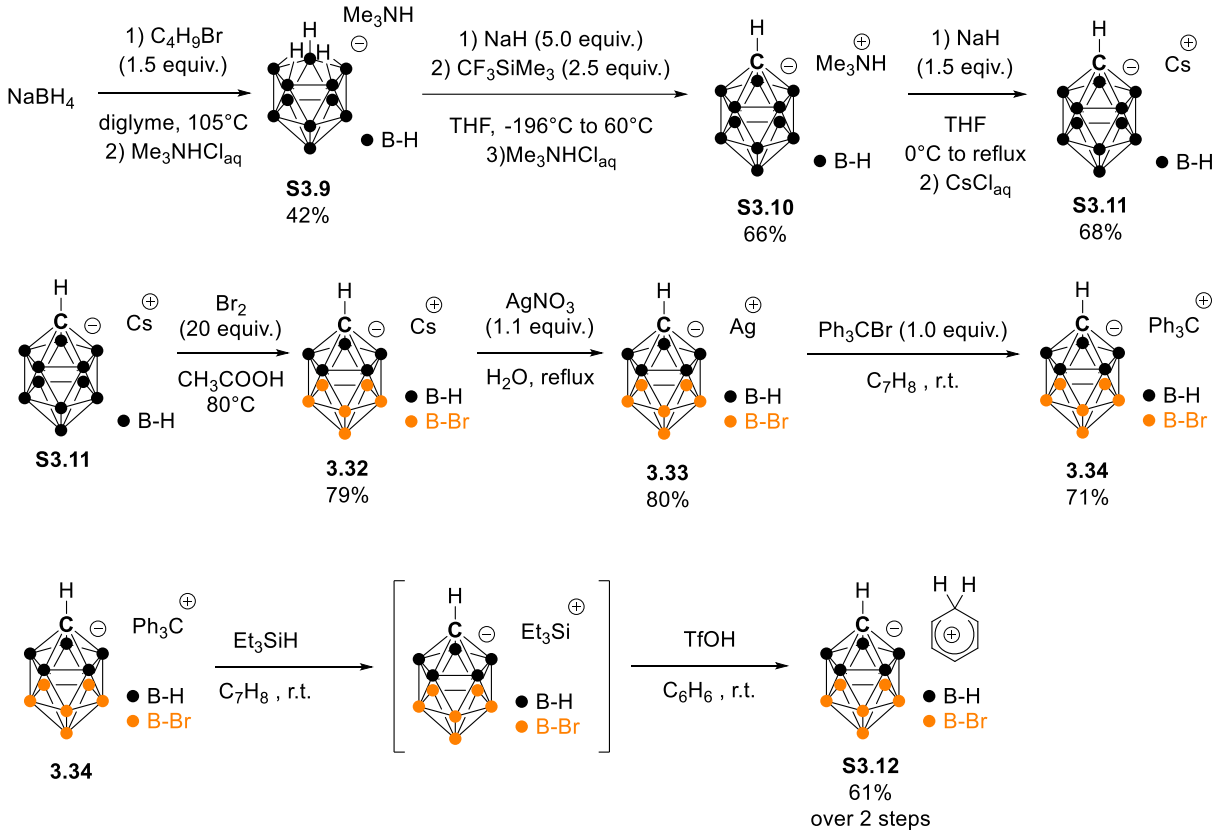


Figure SIII.21. ^{19}F NMR spectra (471 MHz, 25 °C, $CDCl_3$) for the crude reaction of **3.3** with **3.25** at 60 °C.

III.9. Synthesis of tritylium and benzenium 7,8,9,10,11,12-hexabromo-carbadodecaborate.

The synthesis was adapted from literature procedures[S24, S25, S26, S27].



Step 1: $NaBH_4$ to $[Me_3NH][B_{11}H_{14}]$

In a dry three neck flask equipped with a condenser and a dropping funnel, bromobutane (127 ml, 1.2 mol, 1.5 equiv.) was added dropwise (20 ml/h) to a suspension of $NaBH_4$ (30g, 0.79 mol, 1.0 equiv.) in dry diglyme (200 ml) warmed a 105°C. The yellow solution was stirred and heated for further 1h after completion of the addition of bromobutane. The reaction was then allowed to cool down to room temperature, the mixture was filtered and the precipitate was washed with dry diglyme (2x30ml). The filtrate was recovered and the diglyme was distilled under reduced pressure (!!! Temperature should not exceed 95°C). The residue was mixed with aqueous Me_3NHCl (14 g in 150 ml of H_2O). The aqueous solution was extracted with DCM (3x100 ml). The combined organic layers were dried with $MgSO_4$ and concentrated under reduced pressure. The partially liquid residue was poured into

deionized water and the precipitated was filtered and washed with H_2O then Et_2O affording pure $[Me_3NH]^+$ $[B_{11}H_{14}]^-$ **S3.9** (6.4 g, 0.033 mol, 42%) as a pale yellow powder.

^{1}H NMR (500 MHz, CD_3CN) δ (ppm) = 2.82 (s, 9H), 2.5 – 0.4 (m, 11H),

^{11}B NMR (160 MHz, CD_3CN) δ (ppm) = -14.2, -16.1, -16.7.

Step 2: $[Me_3NH][B_{11}H_{14}]$ to $[Me_3NH][CB_{11}H_{11}]$

Under Ar in a 500 ml Ace high pressure vessel equipped with a PTFE screw cap, NaH (60% in mineral oil) (8.1 g, 0.20 mol, 5.6 equiv.) was added in three portions at 0°C to a solution of $[Me_3NH][B_{11}H_{14}]$ **S3.9** (7.0 g, 0.036 mol, 1.0 equiv.) in dry THF (200 ml). The mixture was then stirred at 0°C for 5 min then allowed to warm at room temperature. The mixture was concentrated under reduced pressure (300 mbar) for 30 min at room temperature. Additional dry THF (100 ml) was added. The reaction is then frozen at -196°C and CF_3SiMe_3 (14.5 ml, 0.098 mol, 2.7 equiv.) was added, the flask was quickly sealed with a PTFE scree cap, shaken for 1 min and allowed to warm at room temperature for 45 min. The reaction was then heated at 60°C in pre heated oil bath and stirred for 3 days at 60°C. The reaction was then cooled at 0°C and the PTFE screw cap was carefully removed (pressure released). The reaction was then quenched by dropwise addition of water until gas evolution stopped. The volatiles were removed under reduced pressure. The crude oil was diluted with 150 ml of water and the pH was adjusted to neutral via addition of aqueous HCl. The aqueous phase was then extracted with pentane (2x80 ml) to remove the mineral oil. Me_3NHCl (7g, 0.072 mol, 2.0 equiv.) was added leading to formation of a white precipitate. The mixture was extracted with Et_2O (3x100 ml) then EtOAc (3x100 ml). The combined organic layers were dried over $MgSO_4$ and evaporated to dryness. The resulting brown oil was poured into water (50 ml) and additional Me_3NHCl (5 g) were added. The precipitate was filtered and washed with small amount of water and Et_2O. The desired $[Me_3NH][CB_{11}H_{12}]$ was recovered as a beige powder. The filtrate was concentrated again under reduced pressure, filtered and washed with small amount of water and Et_2O. This procedure is repeated until desired product could be obtained. After combination of fractions, the desired $[Me_3NH][CB_{11}H_{12}]$ **S3.10** (5.0g, 0.024 mol, 66%) was obtained as a beige powder.

^{1}H NMR (500 MHz, acetone-d_6) δ (ppm) = 3.21 (s, 9H), 2.24 (s, 1H), 2.10-1.0 (m, 11H),

^{11}B NMR (160 MHz, acetone-d_6) δ (ppm) = -6.7, -13.2, -16.3.

Step 3: $[Me_3NH][CB_{11}H_{11}]$ to $CsCB_{11}H_{11}$

Under Ar, NaH (60%, 1.4 g, 36 mmol, 1.5 equiv.) was added at 0°C to a solution of dried $[Me_3NH][CB_{11}H_{12}]$ **S3.10** (4.6g, 22 mmol, 1.0 equiv.) in dried THF (50 ml). The reaction was then refluxed overnight. The reaction was then cooled at 0°C and quenched by dropwise addition of water. The volatiles were removed under reduced pressure and the residue was diluted with 50 ml of water. The aqueous phase was washed with pentane to remove mineral oil. CsCl (5.6 g, 36 mmol, 1.5 equiv.) was added and the resulting precipitate was filtered affording $CsCB_{11}H_{12}$ **S3.11** (4g, 15 mmol, 68%) as a beige powder.

^{1}H NMR (500 MHz, acetone-d_6) δ (ppm) = 2.23 (s, 1H), 2.10-1.0 (m, 11H),

^{11}B NMR (160 MHz, acetone-d_6) δ (ppm) = -7.2 (d, J = 138 Hz), -13.7 (d, J = 136 Hz), -16.8 (d, J = 150 Hz).

Step 4: $CsCB_{11}H_{11}$ to $CsCB_{11}H_6Br_6$

$CsCB_{11}H_{12}$ **S3.11** (4g, 14 mmol, 1.0 equiv.) and glacial acetic acid (50 ml) were placed in a 500 ml three-neck round bottom flask equipped with a condenser and a dropping funnel and containing a teflon stir bar. A hose fitted with a funnel was attached to the condenser and minimally submerged into an aqueous solution of NaOH and Na_2SO_3. Bromine (15 ml) was added over the course of 15 min and the dropping funnel was washed with glacial acetic acid (5 ml) which is added to the reaction mixture. The dropping funnel was the removed and the neck closed. The mixture was stirred for 24h at 80°C. The volatiles were removed under reduced pressure to reach a final volume of approximately 10 ml. Water (200 ml) was then added and the solution was heated to boiling. Na_2SO_3 (2 g) and NaOH (0.5 g) were added to raise the pH to 6-7. Any insoluble material remaining after 5 minutes of boiling were removed via hot filtration through a frit. CsCl (2.0g, 12 mmol, 0.85 equiv.) was added to the boiling solution and the solution was the slowly cooled to room temperature then transferred in an ice bath.

The solution was then filtered affording $CsCB_{11}H_6Br_6$ **3.32** (8.2g, 11 mmol, up to 79% after several precipitation/recrystallization) as white powder.

^{11}B NMR (160 MHz, acetone-d_6) δ (ppm) = -2.9 (s), -10.9 (s), -21.2 (d, *J* = 167 Hz).

Step 5: $CsCB_{11}H_6Br_6$ to $AgCB_{11}H_6Br_6$

$CsCB_{11}H_6Br_6$ **3.32** (4.0g, 5.3 mmol, 1.0 equiv.) was dissolved in boiling deionized water (100 ml). When completely dissolved, one drop of concentrated HNO_3 was added. $AgNO_3$ (1.0g, 5.9 mmol, 1.1 equiv.) was dissolved in a minimum amount of deionized water and the solution was added to the boiling solution under low ambient light. A white precipitate appeared and the mixture was boiled and stirred for further 15 min then allowed to cool to room temperature. The precipitate is filtered on a glass frit and the white powder is air dried for 10 minutes. The powder was then transferred in a Schlenk tube wrapped in Al foil and heated at 90°C under dynamic vacuum for 5h. The Schlenk was then transferred in glovebox. The purity of the product was judged by the success of its use in the trityl salt preparation.

Step 6: $AgCB_{11}H_6Br_6$ to $[Ph_3C][CB_{11}H_6Br_6]$

In glovebox, $AgCB_{11}H_6Br_6$ **3.33** (3.0 g, 4.1 mmol) was added to a 100 ml round bottom flask and dry toluene was added to cover the solid. The slurry was stirred and dry acetonitrile was added dropwise until dissolution. A solution of tritylbromide (1.3 g, 4.1 mmol, 1.0 equiv.) was in toluene (2.0 ml) was prepared and added to the $AgCB_{11}H_6Br_6$ solution. The solution turned red and was stirred for 2h then filtered through a frit glass. The precipitate was washed with small aliquots of dry toluene:acetonitrile (4:1). The volume of the filtrate was reduced to a few mLs under vacuum and the precipitate was collected and washed with small amounts of dry toluene and dry hexane affording pure $[Ph_3C][CB_{11}H_6Br_6]$ **3.34** (2.6g, 3.0 mmol, 74%) as a red crystalline powder.

^{1}H NMR (500 MHz, $CDCl_3$) δ (ppm) = 8.24 (t, *J* = 7.5 Hz, 3H), 7.85 (d, *J* = 7.9 Hz, 6H), 7.62 (d, *J* = 8.3 Hz, 6H).

^{11}B NMR (160 MHz, $CDCl_3$) δ (ppm) = -2.9 (s), -10.9 (s), -21.2 (d, *J* = 167 Hz).

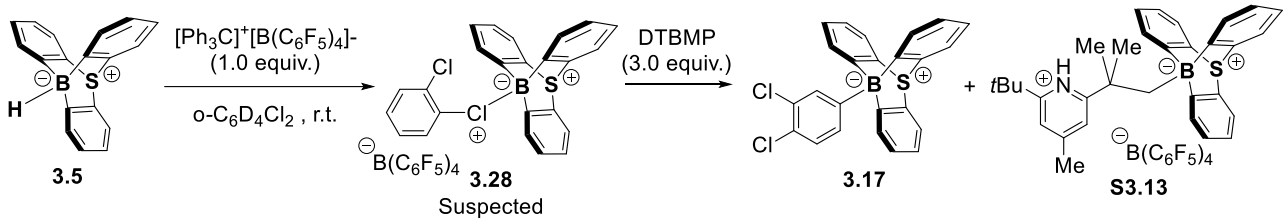
Step 7: $[Ph_3C][CB_{11}H_6Br_6]$ to $[C_6H_7][CB_{11}H_6Br_6]$

In glovebox, $[Ph_3C][CB_{11}H_6Br_6]$ **3.34** (300 mg, 0.35 mmol, 1.0 equiv.) was mixed with toluene (2.0 ml) and few drops of Et_3SiH were added. The organge solution is stirred until becoming colorless. Hexane (0.5 ml) was added and a precipitate formed. The precipitate was filtered and washed with small amount of hexane. The precipitate was immediately transferred in a 5 ml round bottom flask and covered with benzene (1.5 ml). Few drops of triflic acid were added and a yellow precipitate formed. The precipitate was filtered and washed with benzene and hexane affording $[C_6H_7][CB_{11}H_6Br_6]$ **S3.12** (148 mg, 0.21 mmol, 61%) as a yellow powder and was used without further purification.

III.10. Hydride abstraction from 10-hydrido-9-sulfonium-10-boratriptycene in σ-donating solvent and borylation

III.10.1 Using $[Ph_3C]^+[B(C_6F_5)_4]^-$ as hydride abstractor.

In *o*-$C_6D_4Cl_2$



In glovebox, tritylium tetrakis(pentafluorophenyl)borate (16 mg, 0.018 mmol, 1.0 equiv.) was added to a suspension of 10-hydrido-9-sulfonium-10-boratriptycene-ate complex (**3.5**) (5.0 mg, 0.018 mmol, 1.0 equiv.) in *o*-$C_6D_4Cl_2$. The mixture was stirred 5 min at room temperature and analyzed by NMR spectroscopy. The ^{11}B and ^{1}H NMR suggest the formation of a complexed 9-sulfonium-10-boratriptycene species with almost quantitative boron-to-carbon hydride transfer. Then DTBMP (14 mg, 0.054 mmol, 3.0 equiv.) was added and the crude was analyzed again by NMR spectroscopy. After addition of DTBMP, the broad signal previously present in ^{11}B NMR vanished and two new signals suggesting the formation of two “ate”-complexes appeared. The formation of “ate”-complexes demonstrate the labile character of the complex formed prior to the addition of DTBMP and the ability of this complex to generate the 9-sulfonium-10-boratriptycene which can then borylate 1,2-dichlorobenzene.

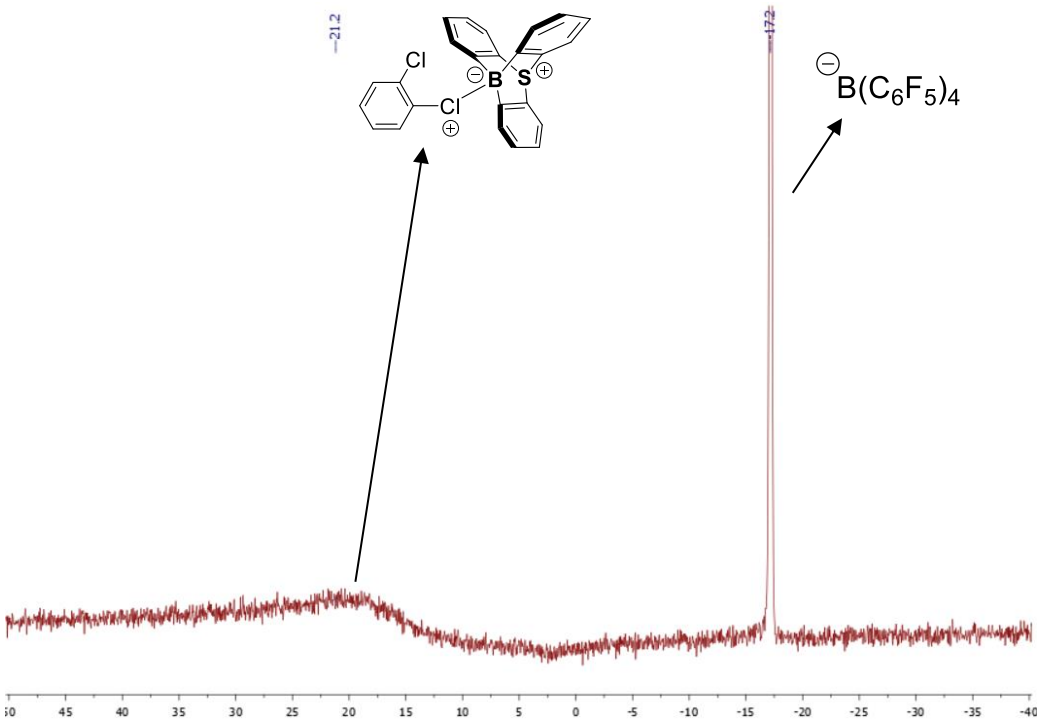


Figure SIII.22. ^{11}B NMR spectra (160 MHz, 25 °C, *o*-$C_6D_4Cl_2$) for the crude reaction of **3.5** with tritylium tetrakis(pentafluorophenyl)borate at 25 °C before addition of DTBMP.

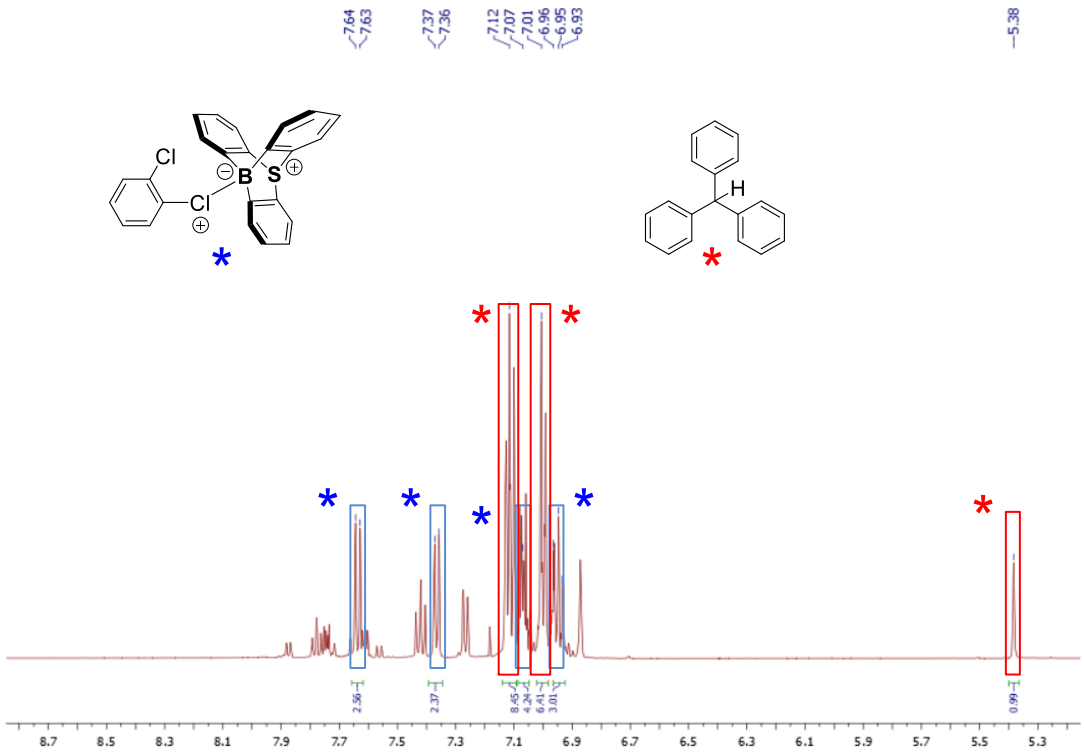


Figure SIII.23. ^{1}H NMR spectra (500 MHz, 25 °C, *o*-$C_6D_4Cl_2$) for the crude reaction of **3.5** with tritylium tetrakis(pentafluorophenyl)borate at 25 °C before addition of DTBMP.

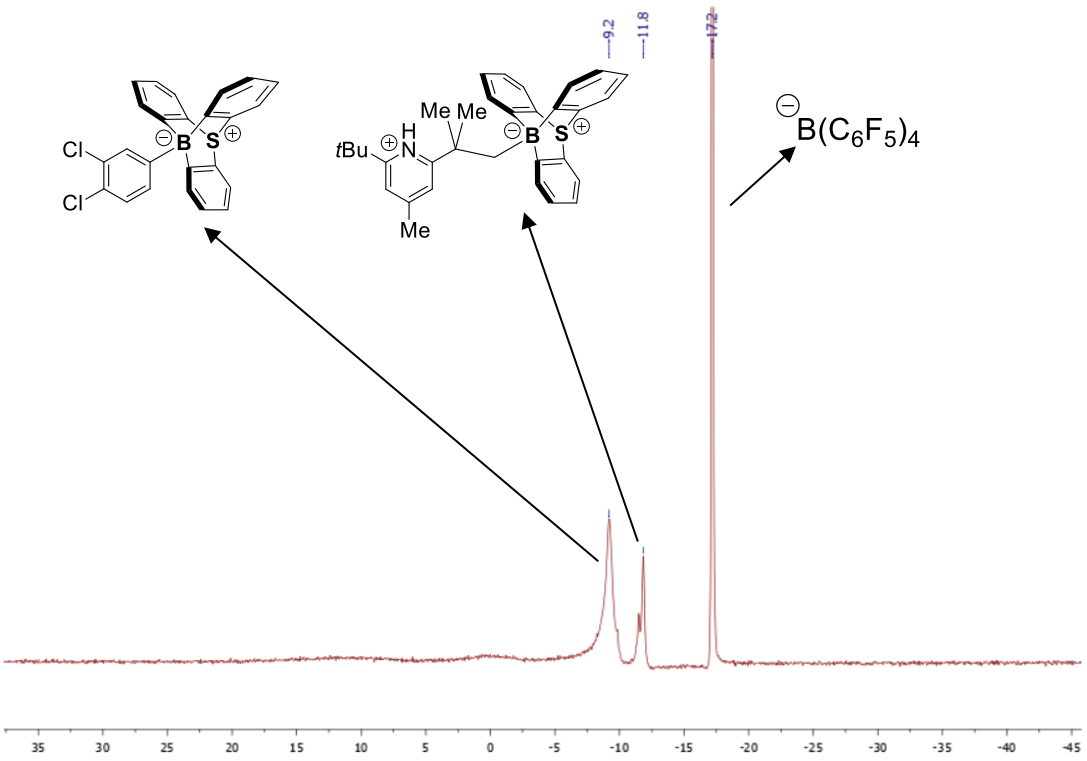
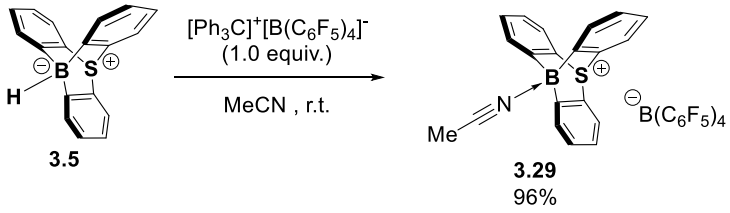


Figure SIII.24. ^{11}B NMR spectra (160 MHz, 25 °C, *o*-$C_6D_4Cl_2$) for the crude reaction of **3.5** with tritylium tetrakis(pentafluorophenyl)borate at 25 °C after addition of DTBMP.

In MeCN



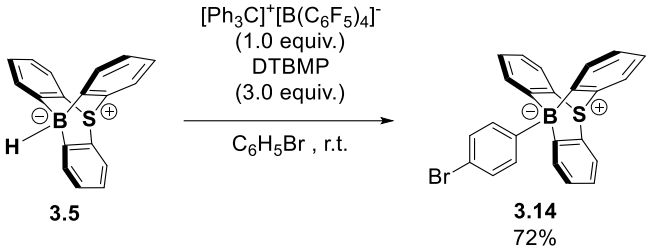
In glovebox, tritylium tetrakis(pentafluorophenyl)borate (16 mg, 0.018 mmol, 1.0 equiv.) was added to a suspension of 10-hydrido-9-sulfonium-10-boratriptycene-ate complex (**3.5**) (5.0 mg, 0.018 mmol, 1.0 equiv.) in MeCN. The mixture was stirred 10 min at room temperature and evaporated to dryness. The crude was washed with small amount of pentane affording pure tetrakis(pentafluorophenyl)borate 9-sulfonium-10-boratriptycene-acetonitrile Lewis adduct (**3.29**) (17 mg, 0.017 mmol, 96%).

^{1}H NMR (400 MHz, $CDCl_3$) δ (ppm) = 7.92 (d, *J* = 7.7 Hz, 3H), 7.87 (d, *J* = 7.3, 0.9 Hz, 3H), 7.49 (td, *J* = 7.4, 1.0 Hz, 3H), 7.29 (td, *J* = 7.6, 1.3 Hz, 3H), 3.36 (s, 3H).

^{11}B NMR (128 MHz, $CDCl_3$) δ (ppm) = -6.5, -17.6 (s)

^{19}F NMR (386 MHz, $CDCl_3$) δ (ppm) = -132.4 (d, *J* = 10.2, 8F), -163.0 (t, *J* = 20.6 Hz, 4F), -166.6 (t, *J* = 18.1, 8F)

In bromobenzene



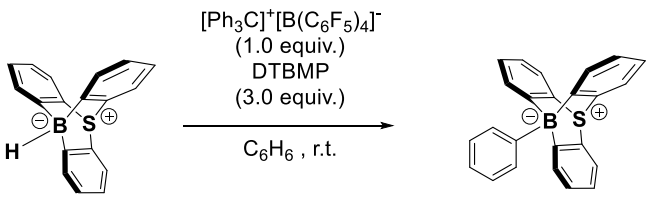
3.5 **3.14** 72%

In glovebox, tritylium tetrakis(pentafluorophenyl)borate (33 mg, 0.036 mmol, 1.0 equiv.) was added to a suspension of 10-hydrido-9-sulfonium-10-boratriptycene-ate complex (**3.5**) (10 mg, 0.036 mmol, 1.0 equiv.) and DTBMP (33 mg, 0.11 mmol, 3.0 equiv.) in bromobenzene. After stirring for 20 min, the crude was evaporated to dryness and purification by flash chromatography affording pure 10-(4-bromophenyl)-9-sulfonium-10-boratriptycene-ate complex (11 mg, 0.026 mmol, 72%) as a white powder. 10-(4-bromophenyl)-9-sulfonium-10-boratriptycene-ate complex was obtained as a mixture of *m* and *p*-isomers (23:77).

^{1}H NMR (500 MHz, $CDCl_3$) δ (ppm) = *meta* isomer: 8.24 (s, 1H), 8.11-7.98 (m, 1H), 7.82-7.76 (m, 6H), 7.53 (ddd, *J* = 7.9, 2.1, 1.1 Hz, 1H), 7.42 (t, *J* = 7.6 Hz, 1H), 7.28-7.24 (m, 3H), 7.08 (t, *J* = 7.5 Hz, 3H). *para* isomer: 7.96 (d, *J* = 7.8 Hz, 2H), 7.82-7.76 (m, 6H), 7.67 (d, *J* = 8.3 Hz, 2H), 7.24 (td, *J* = 7.4, 1.2 Hz, 3H), 7.08 (td, *J* = 7.5, 1.5 Hz, 3H).

^{11}B NMR (160 MHz, $CDCl_3$) δ (ppm) = -9.4 (s)

In benzene



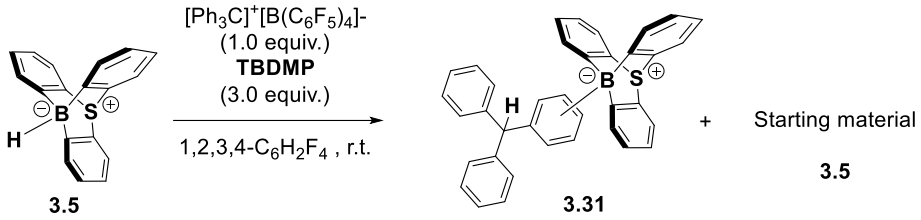
3.5 **3.9** 96%

In glovebox, tritylium tetrakis(pentafluorophenyl)borate (33 mg, 0.036 mmol, 1.0 equiv.) was added to a suspension of 10-hydrido-9-sulfonium-10-boratriptycene-ate complex (**3.5**) (10 mg, 0.036 mmol, 1.0 equiv.) and DTBMP (33 mg, 0.11 mmol, 3.0 equiv.) in benzene. After stirring for 20 min, the crude was evaporated to dryness and purification by flash chromatography affording pure 10-phenyl-9-sulfonium-10-boratriptycene-ate complex (12 mg, 0.035 mmol, 96%) as a white powder.

^{1}H NMR (500 MHz, $CDCl_3$) δ (ppm) = 8.10 (d, *J* = 6.9 Hz, 2H), 7.86 (d, *J* = 7.3 Hz, 3H), 7.77 (d, *J* = 7.6 Hz, 3H), 7.56 (t, *J* = 7.5 Hz, 2H), 7.39 (t, *J* = 7.3 Hz, 1H), 7.23 (td, *J* = 7.4, 1.2 Hz, 3H), 7.06 (td, *J* = 7.5, 1.4 Hz, 3H).

^{11}B NMR (160 MHz, $CDCl_3$) δ (ppm) = -9.3 (s).

<u>In 1,2,3,4-tetrafluorobenzene</u>



In glovebox, tritylium tetrakis(pentafluorophenyl)borate (16 mg, 0.018 mmol, 1.0 equiv.) was added to a suspension of 10-hydrido-9-sulfonium-10-boratriptycene-ate complex (**3.5**) (5.0 mg, 0.018 mmol, 1.0 equiv.) and DTBMP (14 mg, 0.054 mmol, 3.0 equiv.) in 1,2,3,4-$C_6H_2F_4$. The mixture was stirred 2h at room temperature and analyzed by NMR spectroscopy. The formation of the 10-trityl-9-sulfonium-10-boratriptycene-ate complex is suggested by NMR analysis, however the regioselectivity could not be unambiguously determined.

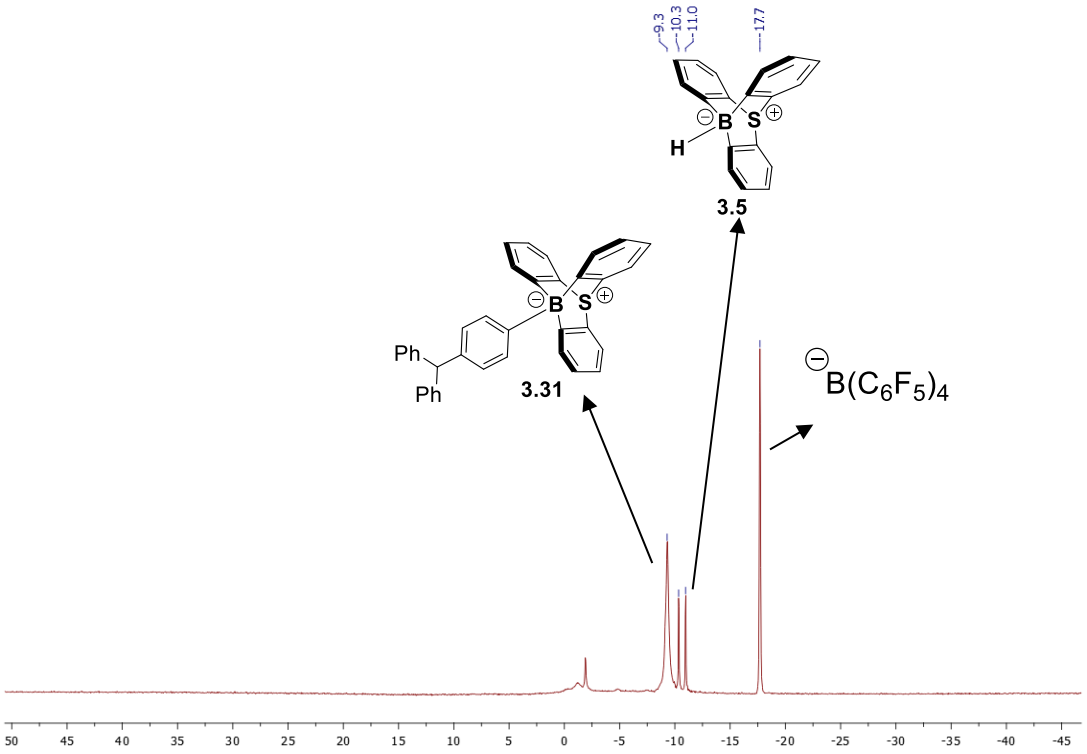
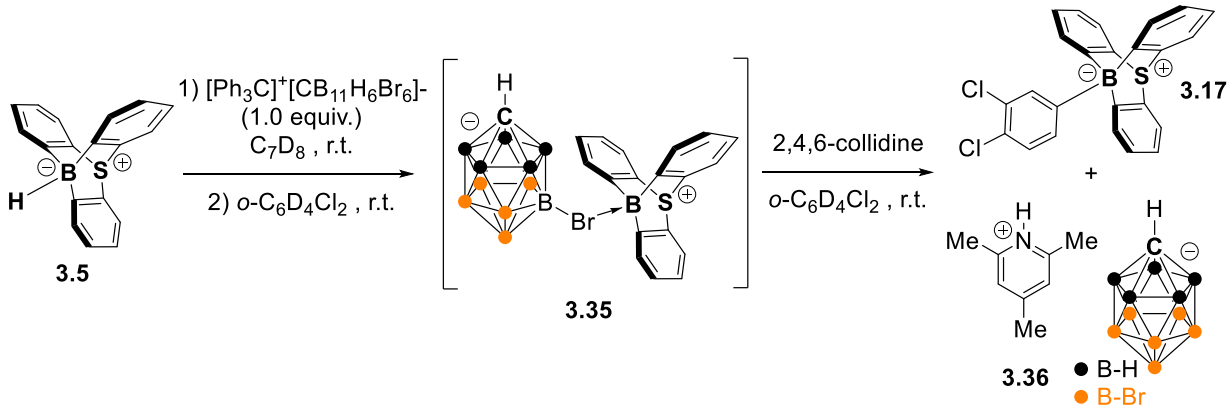


Figure SIII.25. ^{11}B NMR spectra (160 MHz, 25 °C, $CDCl_3$) for the crude reaction of **3.5** with tritylium tetrakis(pentafluorophenyl)borate in 1,2,3,4-$C_6H_2F_4$ in presence of DTBMP at 25 °C.

III.10.2 Using $[Ph_3C][CB_{11}H_6Br_6]$



In glovebox, $[Ph_3C][CB_{11}H_6Br_6]$ **3.35** (15.4 mg, 0.018 mmol, 1.0 equiv.) was added to a suspension of 10-hydrido-9-sulfonium-10-boratriptycene-ate complex **3.5** (5.0 mg, 0.018 mmol, 1.0 equiv.) in toluene-d_8. The mixture was stirred 5 min and a sticky precipitate formed. The precipitate was washed with toluene-d_8 then dissolved in *o*-$C_6D_4Cl_2$ and analyzed by NMR. The ^{11}B and ^{1}H NMR analysis suggest the formation of a complexed 9-sulfonium-10-boratriptycene species and the desymmetrization of the signals corresponding to hexabromocarbadodecaborate suggest the formation of an "ate"-complex with the 9-sulfonium-10-boratriptycene. After analysis, one drop of 2,4,6-collidine was added in the NMR tube and the mixture was analyzed by NMR again. The NMR analysis unambiguously show the borylation of 1,2-dichlorobenzene present as solvent, revealing the labile character of the complexed species present in solution prior to the addition of 2,4,6-collidine.

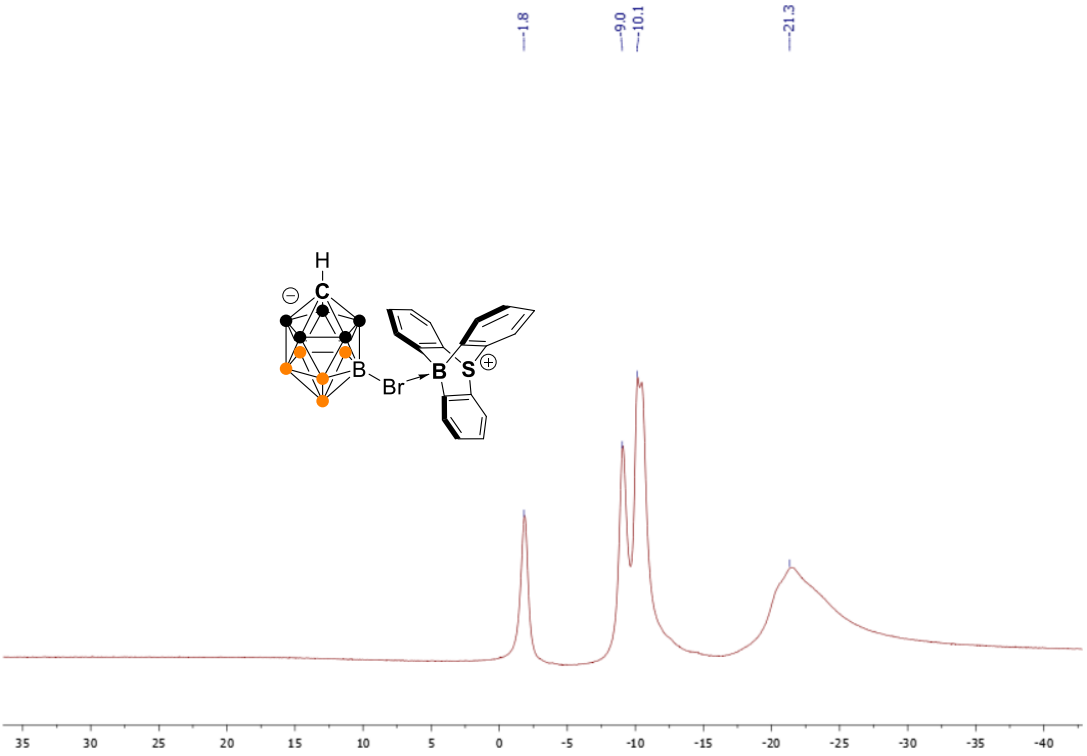


Figure SIII.26. ^{11}B NMR spectra (160 MHz, 25 °C, *o*-$C_6D_4Cl_2$) for the crude reaction of **3.5** with [Ph_3C][$CB_{11}H_6Br_6$] **3.34** in C_7D_8 at 25 °C before addition of 2,4,6-collidine.

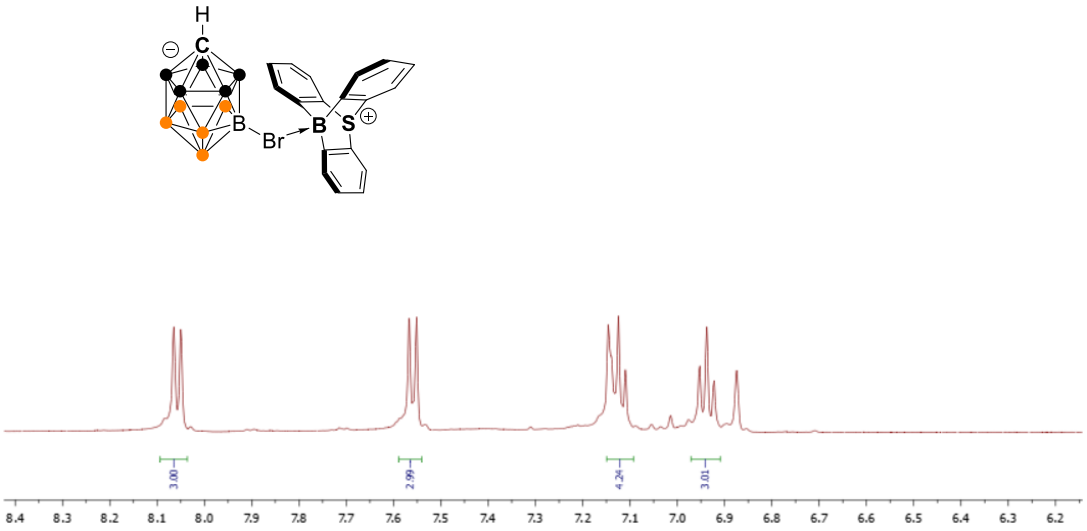


Figure SIII.27. ^{1}H NMR spectra (500 MHz, 25 °C, *o*-$C_6D_4Cl_2$) for the crude reaction of **3.5** with [Ph_3C][$CB_{11}H_6Br_6$] **3.34** in C_7D_8 at 25 °C before addition of 2,4,6-collidine.

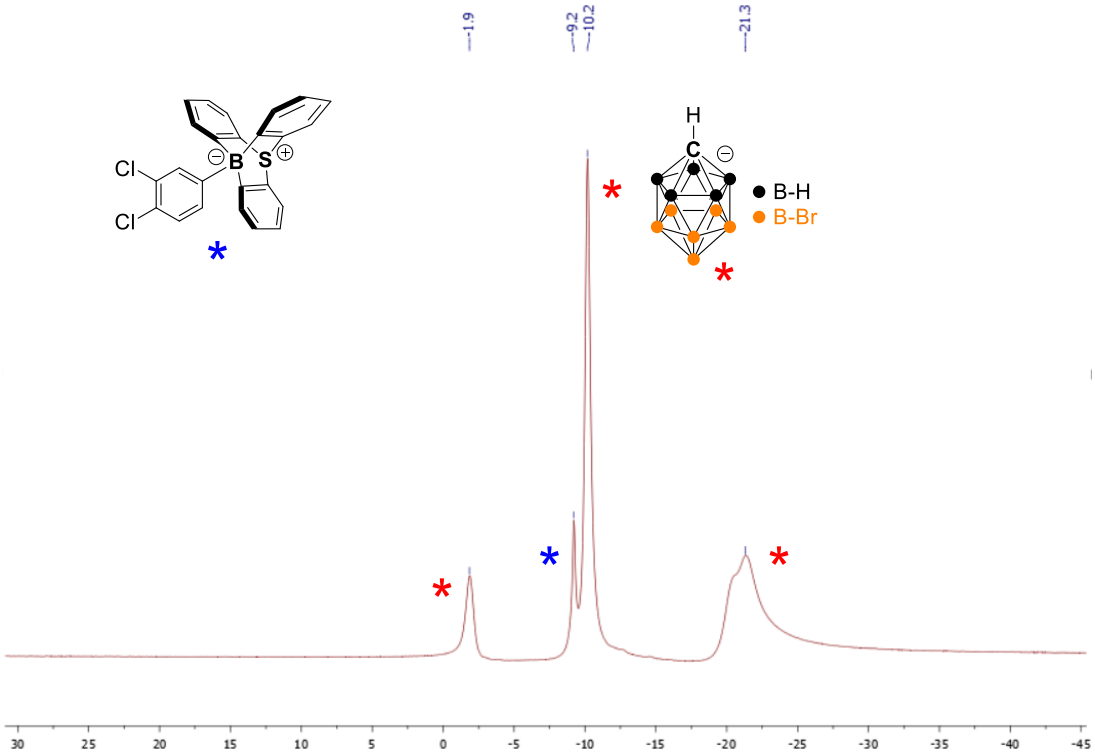


Figure SIII.28. ^{11}B NMR spectra (160 MHz, 25 °C, *o*-$C_6D_4Cl_2$) for the crude reaction of **3.5** with $[Ph_3C][CB_{11}H_6Br_6]$ **3.34** in C_7D_8 at 25 °C after addition of 2,4,6-collidine.

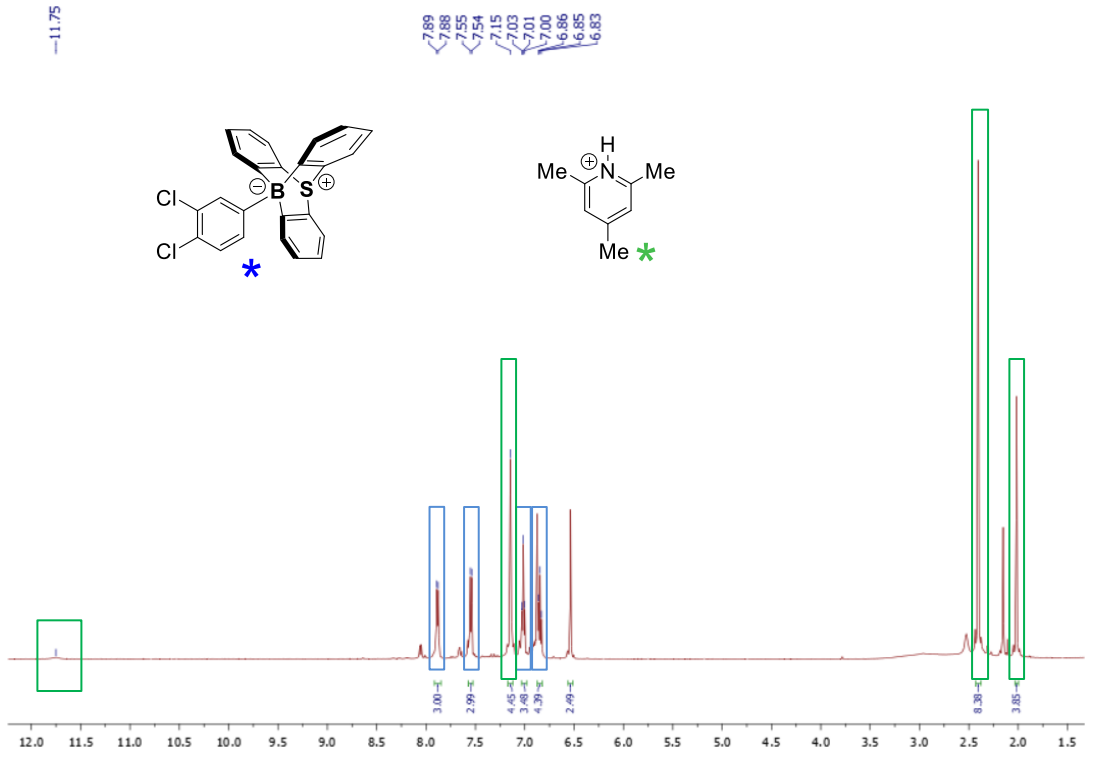


Figure SIII.29. ^{1}H NMR spectra (500 MHz, 25 °C, *o*-$C_6D_4Cl_2$) for the crude reaction of **3.5** with $[Ph_3C][CB_{11}H_6Br_6]$ **3.34** in C_7D_8 at 25 °C after addition of 2,4,6-collidine.

III.11. Quantum chemical calculations

Full geometry optimizations and vibrational frequency calculations were performed, using the Gaussian16 package,[S9] at the M06-2X/6-311G(d) level of theory. A tight convergence threshold on the residual forces of the atoms (1.5×10^{-5} Hartree/Bohr or Hartree/radian) was used for geometry optimizations. For each investigated compound, all vibrational frequencies are real, demonstrating that these structures are minima on the potential energy surface. Solvent effects for dichloromethane (CH_2Cl_2) were considered using the Polarizable Continuum Model put into Integral Equation Formalism by Tomasi and coworkers (IEFPCM).[S15] Fluoride (FIA) and Hydride Ion Affinities (HIA) were computed according to the scheme of Krosing, *via* isodesmic reactions, using respectively $FSiMe_3 \rightarrow SiMe_3^+ + F^-$ ($\Delta H^0 = 958 kJ\ mol^{-1}$) and $HSiMe_3 \rightarrow SiMe_3^+ + H^-$ ($\Delta H^0 = 959\ kJ\ mol^{-1}$) evaluated at the G3 level as anchor points.[S16] Consequently, the initial M06-2X/6-311G(d) FIA and HIA values were corrected by -119.1 $kJ.mol^{-1}$ and -32.3 $kJ.mol^{-1}$ respectively. The global electrophilicity (ω) index is used as a descriptor of Lewis acidity and is defined as:

$$\omega\ (eV) = {\chi^2}/{2\eta} \text{ with } \chi\ (eV) = {-1}/{2}\ (\varepsilon_{HOMO} + \varepsilon_{LUMO}) \text{ and } \eta\ (eV) = \varepsilon_{LUMO} - \varepsilon_{HOMO}$$

where χ is the electronegativity of Mulliken and η the chemical hardness.[S17] The local electrophilicity index ω_k is defined as the product of the global electrophilicity ω with a local Fukui function f_k^+ (on the atomic site *k*),[S18,S19] which can in turn be expressed from the electron population of atom *k* in the system of N and N+1 electrons:[S20]

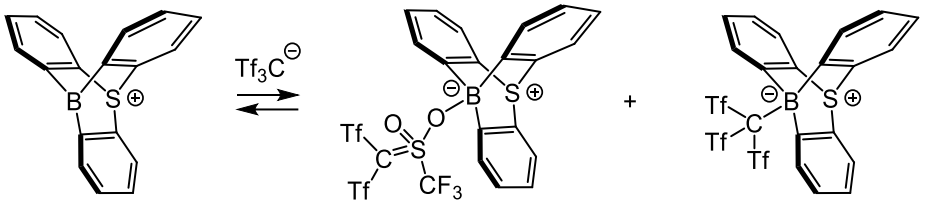
$$\omega_k(eV) = \omega\ f_k^+$$
$$f_k^+ = Q_k(N+1) - Q_k(N) = \Delta Q_k$$

The natural atomic orbital and natural bond orbital analysis was performed using the Gaussian NBO 3.1 program at the M06-2X/6-311G(d) level of theory,[S21] simulating CH_2Cl_2 as solvent on optimized structures. NMR chemical shifts (obtained using the GIAO method) were evaluated at the B3LYP/6-311+G(2d,p) level of theory on structures optimized at the M06-2X/6-311G(d) level of theory, in both cases simulating CH_2Cl_2 as solvent.[S22,S23]

Table SIII.1. Lewis acidity characterization of 9-sulfonium-10-boratriptycene **3.1** and other Lewis acids. Gas phase affinities, $-\Delta H^0$ ($kJ.mol^{-1}$), of the complexation of selected Lewis acids with typical Lewis bases (hydride for HIA, fluoride for FIA, ammonia, triphenylphosphine, and pyridine), as well as global (w, in eV) and local (boron, w_B, in eV) electrophilicity indices of the Lewis acids. Enthalpies for HIA and FIA are corrected via isodesmic reactions.

Lewis acids	Affinities with Lewis bases and global/ local electrophilicities						
	HIA	FIA	NH_3	PPh_3	C_6H_5N	ω	ω_B
9-sulfonium-10-boratriptycene (**3.2**)	880	854	263	270	269	4.91	-2.28
$B(C_6F_5)_3$ (*17*)	514	466	159	133	144	2.79	-1.23
Ph_3C^+	886	-	-	-	-	-	-

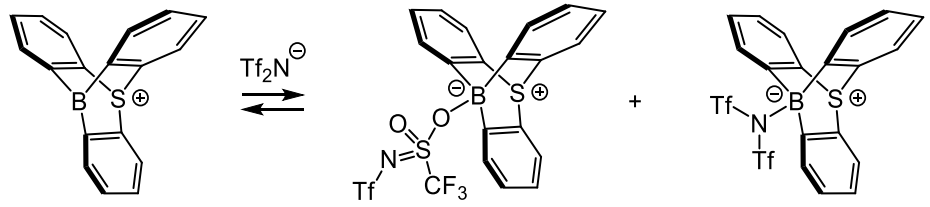
Table SIII.2. State functions of equilibria of triflide anion $[CTf_3]^-$ with the 9-sulfonium-10-boratriptycene (**3.1**) at the IEFPCM(CH_2Cl_2)/M06-2X/6-311G(d) level of theory. All energies are given in $kJ.mol^{-1}$ except entropies in $J.mol.K^{-1}$.



3.1 | **3.4** *O*-isomer | **S3.9** *C*-isomer

Complexation with CTf_3^-	ΔE	ΔH^0	ΔS^0	ΔG^0
CTf_3^- (**S3.9**)	-72	-67	-235	4
CTf_3^- (**3.4**)	-205	-199	-193	-142

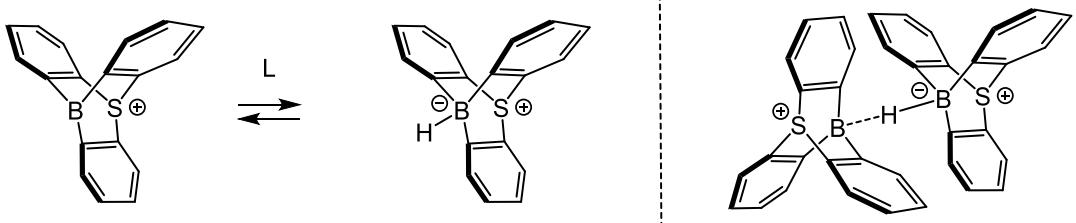
Table SIII.3. State functions of equilibria of triflimide anion $[NTf_2]^-$ with the 9-sulfonium-10-boratriptycene **3.1** at the IEFPCM(CH_2Cl_2)/M06-2X/6-311G(d) level of theory. All energies are given in kJ.mol^{-1} except entropies in J.mol.K^{-1}.



3.1 | **3.19** *O*-isomer | **S3.8** *N*-isomer

Complexation with NTf_2^-	ΔE	ΔH^0	ΔS^0	ΔG^0
NTf_2^- (**S3.8**)	-213	-206	-221	-140
NTf_2^- (**3.19**)	-226	-220	-188	-164

Table SIII.4. State functions of equilibria of the 9-sulfonium-10-boratriptycene **3.1** with hydride anion and **3.6** at the IEFPCM(CH_2Cl_2)/M06-2X/6-311G(d) level of theory. All energies are given in kJ.mol^{-1} except entropies in J.mol.K^{-1}.



3.1 | **3.5** L = H^- | **S3.10** L = **3.5**

Complexation with hydride or borohydride **3.5**	ΔE	ΔH^0	ΔS^0	ΔG^0
L = H^-	-466	-449	-108	-417
L = **3.5**	-175	-169	-174	-117

Natural bonding orbitals in **3.24a**

Inspection of the NBO reveals that there are four lone pairs at the oxygen atom (Figure S30): two are of 100% 2p character while the others are of 88.5% 2s-11.5% 2p and 11.5% 2p-88.5% 2s respectively. Both boron empty orbitals are sp2 hybridized, and possess natural charges of 0.701e for B1 and 0.703e for B2 as well as a comparable electron occupancy of 0.4e. The partial charge at the oxygen atom has a significant negative value (- 1.0e) which is in accordance with its total valence electron occupancy of 7.0e.

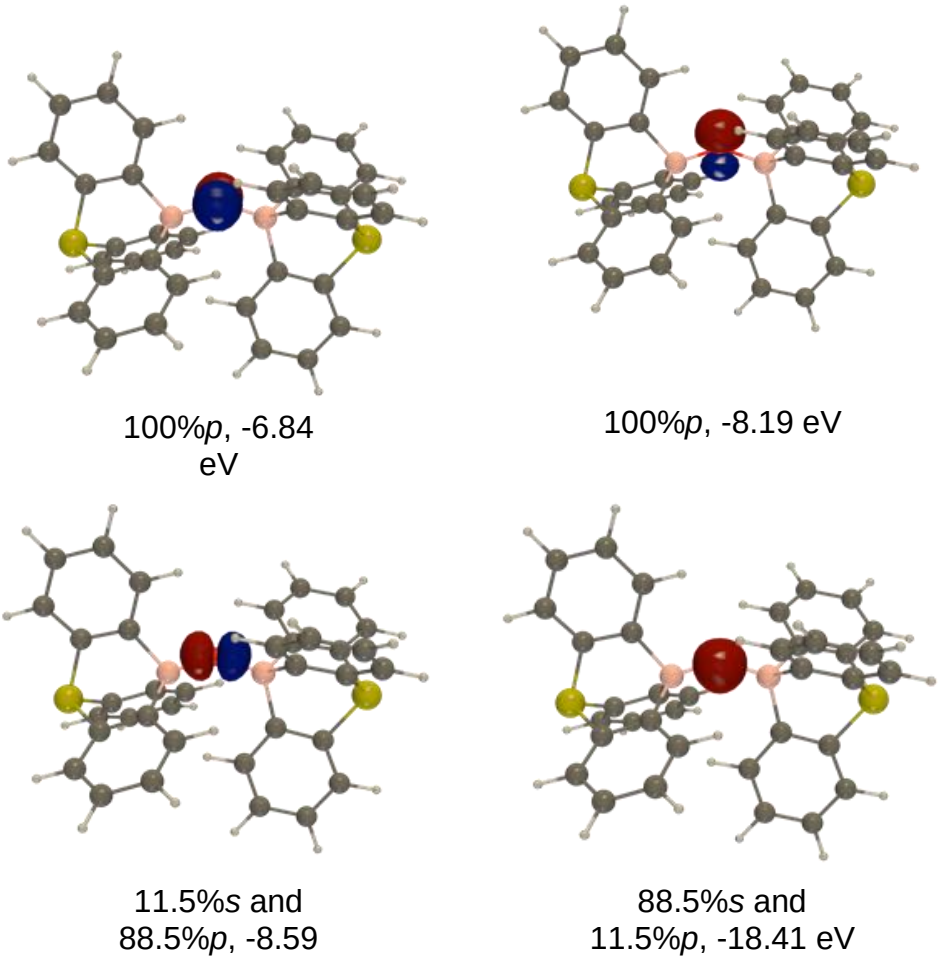
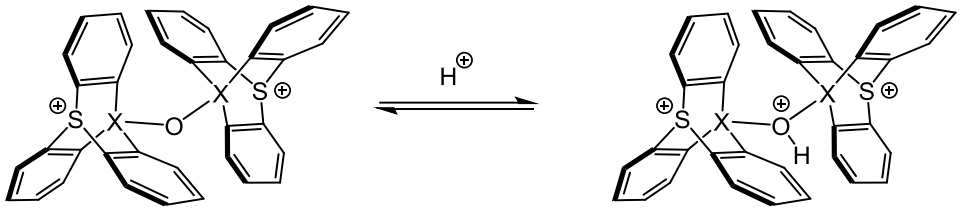


Figure SIII.30. Plot of the oxygen lone pairs of **3.24a** in decreasing order of energy from left to right, with corresponding s/p character (negligible d character is omitted for clarity) and energy in eV: the isovalue for all structures is of 0.1 a.u.

Table SIII.5. Calculated proton affinity of the 10,10'-oxybis-9-sulfonium-10-boratriptycene-ate complex **3.24a**, [C] and [Si] derivatives **S3.11** and **S3.12** at the IEFPCM(CH_2Cl_2)/M06-2X/6-311G(d) level of theory. All energies are given in $kJ.mol^{-1}$ except entropies in $J.mol.K^{-1}$. Gas phase values are given in parenthesis



3.24a: X = B
S3.11: X = C
S3.12: X = Si

S3.13: X = **B**
S3.14: X = **Si**
S3.15: X = **C**

Proton affinity	ΔE	ΔH^0	ΔS^0	ΔG^0
X = B	-755 (-1053)	-726 (-1020)	-136 (-104)	-685 (-989)
X = C, **S3.11**	-429 (-273)	-400 (-249)	-116 (-100)	-366 (-219)
X = Si, **S3.10 S3.6**	-421 (-253)	-391 (-230)	-138 (-123)	-350 (-194)

III.12. Crystallographic parameters:

The crystal structures were determined from single-crystal X-ray diffraction data collected using an Oxford Diffraction Gemini Ultra R diffractometer (Cu Kα radiation with multilayer mirror or Mo Kα radiation with graphite monochromator). The data were integrated using the CrysAlisPro software.[S24] The structures were solved by the dual-space algorithm implemented in SHELXT,[S25] and refined by full-matrix least squares on $|F|^2$ using SHELXL-2018/3,[S26] the shelXLe,[S27] and Olex2 software.[S28] Non-hydrogen atoms were refined anisotropically; and hydrogen atoms in most of the cases were located from the difference Fourier map but placed on calculated positions in riding mode with equivalent isotropic temperature factors fixed at 1.2 times U_{eq} of the parent atoms (1.5 times U_{eq} for methyl groups).

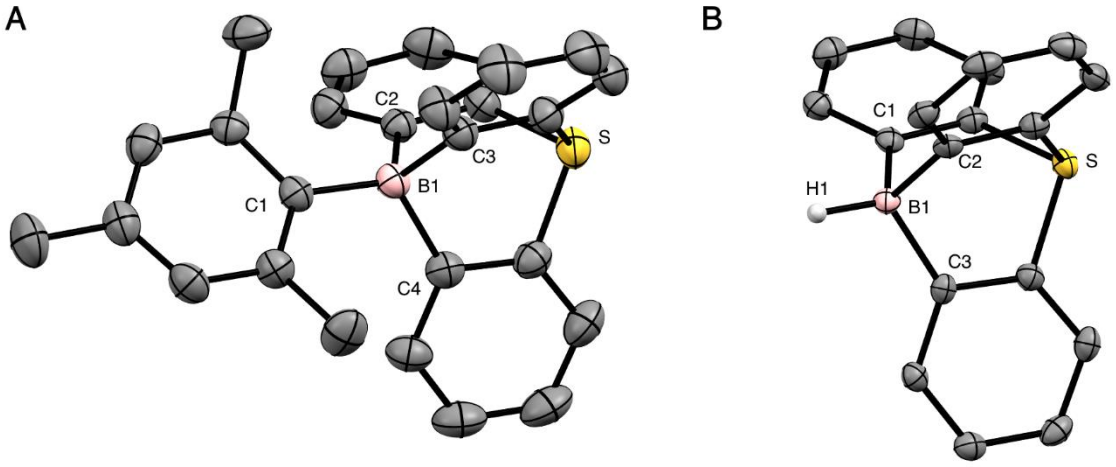


Figure SIII.31. Molecular structures of (**A**) 10-mesityl-9-sulfonium-10-boratriptycene **3.3**; (**B**) 10-hydrido-9-sulfonium-10-boratriptycene-ate complex **3.5**. Ellipsoids represent 50% probability. Hydrogen atoms (except the boron-bound hydrogen in **3.5**) are omitted for clarity. Selected distances in Å; (**A**): B1-C1 1.630(2), B1-C2 1.656(2), B1-C3 1.635(2), B1-C4 1.663(2); (**B**) H1-B1 1.150(2), B1-C1 1.636(3), B1-C2 1.635(3), B1-C3 1.629(3).

Table SIII.6. Crystal data and structure refinement for compounds **3.4-3.7**.

	3.3	**3.4**	**3.5**	**3.6**
Chemical formula	$C_{27}H_{23}BS$	$C_{22}H_{12}BF_9O_6S_4$	$C_{18}H_{13}BS$	$C_{24}BF_{20}^{-}\cdot C_{36}H_{25}B_2S_2^{+}\cdot 2(CH_2Cl_2)$
M_r	390.32	682.37	272.15	1392.20
Crystal system, space group	Monoclinic, $P2_1/n$	Orthorhombic, $Pca2_1$	Orthorhombic, $P2_12_12_1$	Tetragonal, $P4_2/n$
Temperature (K)	295	295	100	295
a, b, c (Å)	8.98084 (17), 18.2960 (5), 12.5117 (3)	16.2758 (2), 11.28554 (15), 14.45228 (17)	8.19051 (11), 8.24243 (10), 20.6095 (3)	19.48215 (19), 19.48215 (19), 15.2732 (2)
α, β, γ (°)	90, 93.0908 (19), 90	90, 90, 90	90, 90, 90	90, 90, 90
V (Å^3)	2052.84 (8)	2654.61 (6)	1391.34 (3)	5797.00 (14)
Z	4	4	4	4
Radiation type	Mo $K\alpha$	Cu $K\alpha$		
μ (mm^{-1})	0.17	4.25	1.91	3.49
Crystal size (mm)	0.56 × 0.44 × 0.09	0.27 × 0.17 × 0.05	0.60 × 0.40 × 0.20	0.52 × 0.34 × 0.06
Absorption correction	Analytical			Gaussian
T_{min}, T_{max}	0.934, 0.985	0.482, 0.819	0.556, 0.751	0.297, 1.000
No. of measured, independent and observed [$I > 2\sigma(I)$] reflections	13116, 6273, 4923	19921, 4286, 4133	6352, 2455, 2401	16738, 5120, 4302
R_{int}	0.017	0.027	0.024	0.037
θ_{max} (°)	30.5	67.1	67.1	67.0
$(\sin\theta/\lambda)_{max}$ (Å^{-1})	0.714	0.597	0.597	0.597
$R[F^2 > 2\sigma(F^2)]$, $wR(F^2)$, S	0.044, 0.126, 1.04	0.028, 0.071, 1.06	0.026, 0.069, 1.07	0.044, 0.122, 1.03
No. of reflections	6273	4286	2455	5120
No. of parameters	265	578	185	413
No. of restraints	0	385	0	0
H-atom treatment	constrained		mixed	
$\Delta\rho_{max}$, $\Delta\rho_{min}$ (e·Å^{-3})	0.26, -0.28	0.18, -0.17	0.22, -0.20	0.62, -0.49
Absolute structure	–	Flack x determined using 1695 quotients	Flack x determined using 966 Cryst. B69 (2013) 249-259).	–
Absolute structure parameter	–	-0.015 (7)	-0.003 (8)	–
CCDC deposition number	2094921	2094922	2094923	2094924

Table SIII.7. Crystal data and structure refinement for compounds **3.6a-3.8**.

	3.6a	**3.6b**	**3.6c**	**3.8**
Chemical formula	$C_{36}H_{25}B_2S_2^+ \cdot BF_4^- \cdot CHCl_3$	$2(C_{24}BF_{20}^-) \cdot 2(C_{36}H_{25}B_2S_2^+) \cdot 3(C_7H_8)$	$C_{24}BF_{20}^- \cdot C_{36}H_{25}B_2S_2^+ \cdot 3(C_6H_6)$	$C_{36}H_{24}B_2FS_2^+ \cdot C_{24}BF_{20}^- \cdot 2.84(CHCl_3)$
M_r	749.48	1360.55	1456.67	1579.58
Crystal system, space group	Triclinic, $P\bar{1}$	Triclinic, $P\bar{1}$	Monoclinic, $C2/c$	Triclinic, $P\bar{1}$
Temperature (K)	295	100	100	295
a, b, c (Å)	11.9583 (6), 13.0556 (5), 13.1122 (6)	14.5171 (6), 25.8935 (11), 33.3610 (13)	25.5512 (7), 14.7595 (4), 34.5527 (7)	14.7475 (9), 15.2428 (7), 15.9694 (8)
α, β, γ (°)	114.071 (4), 107.101 (4), 92.097 (4)	69.824 (4), 88.833 (4), 89.528 (4)	90, 101.955 (2), 90	99.787 (4), 93.642 (5), 113.458 (5)
V (Å^3)	1757.49 (15)	11768.4 (9)	12747.9 (6)	3210.8 (3)
Z	2	8	8	2
Radiation type	Cu $K\alpha$			
μ (mm^{-1})	3.88	1.79	1.70	4.95
Crystal size (mm)	0.18 × 0.15 × 0.02	0.42 × 0.11 × 0.08	0.31 × 0.13 × 0.09	0.25 × 0.15 × 0.02
Absorption correction	Analytical	Multi-scan	Analytical	
T_{min}, T_{max}	0.585, 0.943	0.840, 1.000	0.695, 0.872	0.455, 0.906
No. of measured, independent and observed [$I > 2\sigma(I)$] reflections	15949, 6219, 5141	57563, 57563, 31848	23890, 8333, 7056	6914, 3866, 2924
R_{int}	0.036	/	0.032	0.033
θ_{max} (°)	67.2	67.4	67.2	40.3
$(\sin\theta/\lambda)_{max}$ (Å^{-1})	0.598	0.599	0.598	0.419
$R[F^2 > 2\sigma(F^2)]$, $wR(F^2)$, S	0.052, 0.148, 1.04	0.053, 0.133, 0.85	0.045, 0.121, 1.11	0.065, 0.191, 1.04
No. of reflections	6219	57563	8333	3866
No. of parameters	481	3711	929	960
No. of restraints	21	1128	0	252
H-atom treatment	mixed			constrained
$\Delta\rho_{max}$, $\Delta\rho_{min}$ (e·Å^{-3})	0.38, -0.40	0.60, -0.36	0.38, -0.28	0.50, -0.66
Absolute structure parameter				
CCDC deposition number	2094925	2094926	2094927	2094928

Table SIII.8. Crystal data and structure refinement for compounds **3.9**-**S3.7**

	3.9	**3.17**	**S3.6**	**S3.7**
Chemical formula	$C_{24}H_{17}BS$	$C_{24}H_{15}BCl_2S$	$C_{20}H_{15}BNS^{+}\cdot C_2F_6NO_4S_2^{-}$	$C_{22}H_{20}BO_2S^{+}\cdot C_2F_6NO_4S_2^{-}$
M_r	348.24	417.13	592.35	639.40
Crystal system, space group	Orthorhombic, *Pnma*	Orthorhombic, $Pna2_1$	Monoclinic, $P2_1$	Triclinic, *P*1
Temperature (K)	100	295	100	100
a, *b*, *c* (Å)	15.2306 (5), 13.5916 (5), 8.8267 (4)	13.8031 (3), 8.3478 (2), 22.0059 (5)	8.18280 (16), 13.79365 (19), 11.4446 (2)	8.5150 (9), 13.530 (1), 13.6287 (13)
α, β, γ (°)	90, 90, 90	90, 90, 90		62.285 (9), 74.800 (9), 75.847 (8)
V (Å^3)	1827.20 (12)	2535.65 (10)	1211.12 (4)	1327.5 (2)
Z	4	4	2	2
Radiation type	Cu $K\alpha$	Mo $K\alpha$	Cu $K\alpha$	Cu $K\alpha$
μ (mm^{-1})	1.57	0.34	3.55	3.33
Crystal size (mm)	0.52 × 0.28 × 0.06	0.44 × 0.40 × 0.03	0.46 × 0.33 × 0.14	0.27 × 0.13 × 0.07
Absorption correction	Gaussian	Analytical	Analytical	Gaussian
T_{min}, T_{max}	0.489, 1.000	0.840, 0.984	0.560, 0.809	0.445, 1.000
No. of measured, independent and observed [$I > 2\sigma(I)$] reflections	5487, 1694, 1514	20709, 7734, 5649	11634, 4291, 4253	8120, 8120, 6585
R_{int}	0.038	0.019	0.028	0.065
θ_{max} (°)	67.0	32.8	67.0	66.6
$(\sin\theta/\lambda)_{max}$ (Å^{-1})	0.597	0.761	0.597	0.595
$R[F^2 > 2\sigma(F^2)]$, $wR(F^2)$, *S*	0.045, 0.132, 1.03	0.037, 0.103, 1.00	0.023, 0.060, 1.06	0.066, 0.219, 1.10
No. of reflections	1694	7734	4291	8120
No. of parameters	133	255	480	373
No. of restraints	0	1	599	0
H-atom treatment	constrained	constrained	constrained	constrained
$\Delta\rho_{max}$, $\Delta\rho_{min}$ (e·Å^{-3})	0.42, -0.32	0.17, -0.16	0.20, −0.20	0.71, −0.42

Absolute structure	–	Refined as a perfect inversion twin.	Refined as a perfect inversion twin.	-
CCDC deposition number	2094929	2094930	2104327	21043276

Table SIII.9. Crystal data and structure refinement for compounds **3.21**

	3.21, polymorph I	**3.21**, polymorph II	**3.22**	**3.24a**
Chemical formula	$C_{29}H_{28}BNS$	$C_{29}H_{28}BNS$	$C_{19}H_{15}BS$	$7(C_{36}H_{24}B_2OS_2)\cdot 7(C_6H_6)$
M_r	433.39	433.39	286.18	4454.79
Crystal system, space group	Triclinic, $P\bar{1}$	Triclinic, $P\bar{1}$	Trigonal, $R\bar{3}$:*H*	Trigonal, $R\bar{3}$
Temperature (K)	295	295	295	295
a, *b*, *c* (Å)	9.1621 (7), 14.1607 (15), 18.4967 (18)	8.5764 (12), 11.9342 (18), 12.3727 (16)	12.0575 (4), 12.0575 (4), 17.7431 (6)	40.4314 (8), 40.4314 (8), 12.2458 (4)
α, β, γ (°)	84.893 (8), 86.200 (7), 84.327 (8)	78.384 (12), 78.978 (11), 74.042 (13)	90, 90, 120	90, 90, 120
V (Å^3)	2374.6 (4)	1180.2 (3)	2233.94 (18)	17336.2 (10)
Z	4	2	6	3
Radiation type	Cu $K\alpha$	Cu $K\alpha$	Cu $K\alpha$	Cu $K\alpha$
μ (mm^{-1})	1.32	1.32	1.81	1.71
Crystal size (mm)	0.20 × 0.03 × 0.02	0.13 × 0.08 × 0.02	0.34 × 0.27 × 0.05	0.33 × 0.22 × 0.03
Absorption correction	Analytical	Analytical	Analytical	Analytical
T_{min}, T_{max}	0.973, 0.996	0.901, 0.969	0.687, 0.918	0.717, 0.944
No. of measured, independent and observed [$I > 2\sigma(I)$] reflections	25436, 8394, 5881	12476, 4147, 2968	5121, 879, 872	29516, 6836, 5309
R_{int}	0.068	0.048	0.026	0.050
θ_{max} (°)	67.5	66.6	67.0	67.0
$(\sin\theta/\lambda)_{max}$ (Å^{-1})	0.599	0.595	0.597	0.598
$R[F^2 > 2\sigma(F^2)]$, $wR(F^2)$, *S*	0.057, 0.160, 1.04	0.050, 0.140, 1.05	0.044, 0.111, 1.22	0.063, 0.198, 1.08
No. of reflections	8394	4147	879	6836
No. of parameters	586	294	135	604
No. of restraints	0	0	133	507
H-atom treatment	constrained	constrained	mixed	constrained
$\Delta\rho_{max}$, $\Delta\rho_{min}$ (e·Å^{-3})	0.23, -0.31	0.22, -0.36	0.20, -0.28	0.34, -0.66
Absolute structure	–	–	-	-
CCDC deposition number	2094931	2094932	2094933	2095204

III.13. References

[S3.1] I. S. Park, K. Matsuo, N. Aiwaza, T. Yasuda. T. *Adv. Funct. Mater.* **2018**, *28*, 1802031.

[S3.2] T. Agou, J. Kobayashi, T. Kawashima, T. *Chem. Eur. J.* **2007**, *13*, 8051.

[S3.3] F. J. Waller, A. G. M. Barret, D. C. Braddock, D. Ramprasad, R. M. McKinnel, A. J. P. White, D. J. Williams, R. Ducray, R. *J. Org. Chem*. **1999**, *64*, 2910.

[S3.4] A. Chardon, A. Osi, D. Mahaut, T-H. Doan N. Tumanov, L. Fusaro, J. Wouters, B. Champagne, G. Berionni, *Angew. Chem. Int. Ed.* **2020**, *59*, 12402.

[S3.5] M. F. Lappert, *J. Chem. Soc.* **1962**, *0*, 542.

[S3.6] A. Ben Saida, A. Chardon, A. Osi, N. Tumanov, J. Wouters, A. I. Adjeufack, B. Champagne, G. Berionni, *Angew. Chem. Int. Ed,* **2019**, *58*, 16889.

[S3.8] S. Chamberland, J. W. Ziller, K. A. Woerpel, *J. Am. Chem. Soc.* **2005**, *127*, 5322.

[S3.9] R. Guo, X. Qi, H. Xiang, P. Geaneotes, R. Wang, P. Liu, Y.-M. Wang, *Angew. Chem. Int. Ed.* **2020**, *59*, 16651

[S3.10] P. P. Belov, P. A. Storozhenko, N. S. Voloshina, M. G. Kuznetsova *Russ. J. Appl. Chem.* **2017**, 90, 1804.

[S3.11] L. Toom, A. Kütt, I. Leito *Dalton. Trans.* **2019**, 48, 7499.

[S3.12] N. Tanaka, Y. Shoji, T. Fukushima *Organometallics*, **2016**, 35, 2022

[S3.13] C. A. Reed *Acc. Chem. Res.* **2010**, 43, 121.

[S3.14] M. J. Frisch, G. W. Trucks, H. B. Schlegel, G. E. Scuseria, M. A. Robb, J. R. Cheeseman, G. Scalmani, V. Barone, G. A. Petersson, H. Nakatsuji, X. Li, M. Caricato, A. V. Marenich, J. Bloino, B. G. Janesko, R. Gomperts, B. Mennucci, H. P. Hratchian, J. V. Ortiz, A. F. Izmaylov, J. L. Sonnenberg, D. Williams-Young, F. Ding, F.Lipparini, F. Egidi, J. Goings, B. Peng, A. Petrone, T. Henderson, D. Ranasinghe, V. G. Zakrzewski, J. Gao, N. Rega, G. Zheng, W. Liang, M. Hada, M. Ehara, K. Toyota, R. Fukuda, J. Hasegawa, M. Ishida, T. Nakajima, Y. Honda, O. Kitao, H. Nakai, T. Vreven, K. Throssell, J. A. Montgomery, J. E. Peralta, Jr., F. Ogliaro, M. J. Bearpark, J. J. Heyd, E. N. Brothers, K. N. Kudin, V. N. Staroverov, T. A. Keith, R. Kobayashi, J. Normand, K. Raghavachari, A. P. Rendell, J. C. Burant, S. S. Iyengar, J. Tomasi, M. Cossi, J. M. Millam, M. Klene, C. Adamo, R. Cammi, J. W. Ochterski, R. L. Martin, K. Morokuma, O. Farkas, J. B. Foresman, D. J. Fox, *Gaussian 16 Rev, A.03* (Gaussian Inc., 2016).

[S3.15] J. Tomasi, B. Mennucci, Cammi, R. *Chem. Rev.* **2005**, *105* (8), 2999.

[S3.16] H. Böhrer, N. Trapp, D. Himmel, M. Schleep, I. Krossing, *Dalton Trans*. **2015**, *44*, 7489.

[S3.17] R. G. Parr, L. V. Szentpály, S. Liu, *J. Am. Chem. Soc*. **1999**, *121* (9), 1922.

[S3.18] P. Pérez, A. Toro-Labbé, A. Aizman, R. Contreras, *J. Org. Chem.* **2002**, *67* (14), 4747.

[S3.19] P. Chattaraj, K. U. Sarkar, D. R. Roy,. *Chem. Rev.* **2006**, *106* (6), 2065.

[S3.20] W. Yang, W. J. Mortier, *J. Am. Chem. Soc.* **1968**, *108* (19), 5708.

[S3.21] E. D. Glendening, A. E. Reed, J. E. Carpenter, F. Weinhold, *NBO Version 3.1*, (Gaussian Inc., 2003).

[S3.22] R. Ditchfield, *Mol. Phys*. **1974**, *27*, 789

[S3.23] K. Wolinski, J. F. Hinton, P. Pulay, *J. Am. Chem. Soc*. **1990**, *112* (23), 8251.

[S3.24] Rigaku Oxford Diffraction. *CrysAlis PRO*, (Rigaku Oxford Diffraction., 2018).

[S3.25] G. M. Sheldrick, *Acta Crystallogr. Sect. A Found. Adv,* **2015**, *71*, 3.

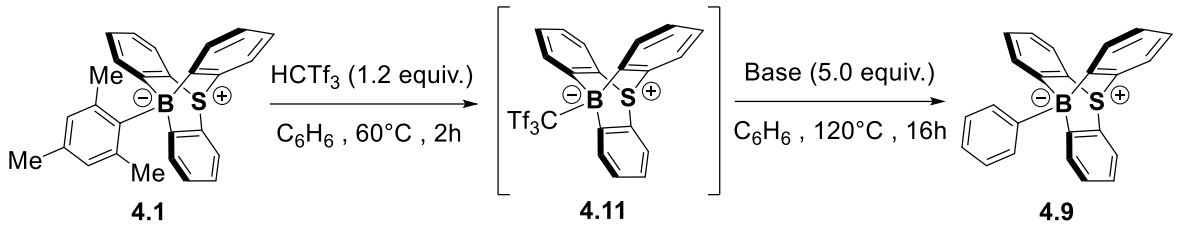
[S3.26] G. M. Sheldrick, *Acta Crystallogr. Sect. C Struct. Chem,* **2015**, *71*, 3.

[S3.27] C. B. Hübschle, G. M. Sheldrick, B. Dittrich, *J. Appl. Crystallogr,* **2011**, *44*, 1281.

[S3.28] O. V. Dolomanov, L. J. Bourhis, R. J. Gildea, J. A. K. Howard, H. Puschmann, *J. Appl.Crystallogr,* **2009**, *42*, 339.

IV.1. Csp^2–H borylation optimization with substrate as solvent

IV.1.1 Brønsted base optimization using $HCTf_3$.



4.1 **4.11** **4.9**

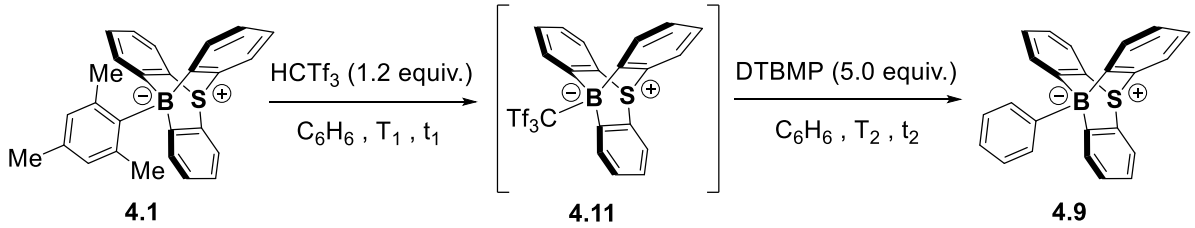
In glovebox, $HCTf_3$ (13 mg, 0.031 mmol, 1.2 equiv.) was added to a suspension of 10-mesityl-9-sulfonium-10-boratriptycene-ate complex **4.1** (10 mg, 0.026 mmol, 1.0 equiv.) in benzene (1.5 ml). The Schlenk tube was sealed with a glass stopper, stirred and warmed at 60°C out of the glovebox in an oil bath. After 2h, the glass stopper was removed and the Brønsted base (0.128 mmol, 5.0 equiv.) was added under a stream of Ar. The Schlenk tube was sealed with a glass stopper and warmed at 120°C. After 16h, the crude was evaporated to dryness, dissolved in $CDCl_3$ and ^1H and ^{11}B NMR spectra were recorded. The yields were determined using 4-bromoanisole as internal standard.

Table SIV.1 Optimization of Csp^2–H borylation condition using $HCTf_3$: selection of the Brønsted base.

Entry	**Base**	**Yield** (%)
1	*i*Pr_2NH	24
2	TMPH	21
3	P(*o*-tolyl)$_3$	8
4	$PMes_3$	0
5	2,6-di*ter*butyl-4-methylpyridine (DTBMP)	55[a]

Yields are ^1H NMR yields obtained using 4-bromoanisole as internal standard. [a]: isolated yield

IV.1.2 Temperature and reaction time using $HCTf_3$ and DTBMP.



4.1 **4.11** **4.9**

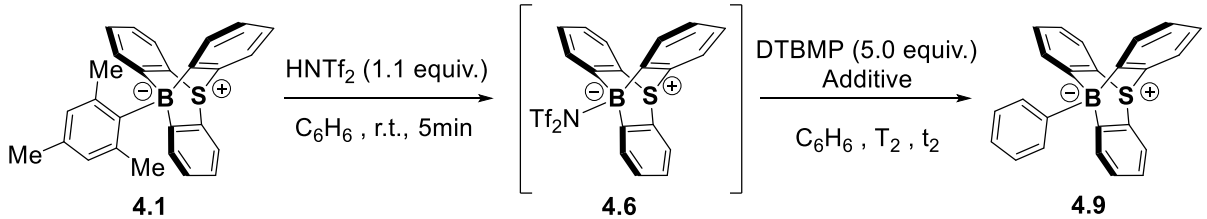
In glovebox, $HCTf_3$ (13 mg, 0.031 mmol, 1.2 equiv.) was added to a suspension of 10-mesityl-9-sulfonium-10-boratriptycene-ate complex **4.1** (10 mg, 0.026 mmol, 1.0 equiv.) in benzene (1.5 ml). The Schlenk tube was sealed with a glass stopper, stirred and warmed at 20 to 100°C out of the glovebox in an oil bath. After 1 to 3h, the glass stopper was removed and DTBMP (26 mg, 0.13 mmol, 5.0 equiv.) was added under a stream of Ar. The Schlenk tube was sealed with a glass stopper and warmed at 90 to 140°C. After 15min to 72h, the crude was evaporated to dryness, dissolved in $CDCl_3$ and ^{1}H and ^{11}B NMR spectra were recorded. The yields were determined using 4-bromoanisole as internal standard.

Table SIV.2 Optimization of Csp^2–H borylation condition using $HCTf_3$ and DTBMP: Selection of the reaction time and temperature.

Entry	Base	T_1 (°C)	T_2 (°C)	t_1 (h)	t_2 (h)	**Yield** (%)
1)		60	120	2	16	55
2)		60	140	2	16	31
3)		100	120	1	0.25	traces
4)		100	120	1	16	38
5)	DTBMP	100	110	1	72	46
6)		100	110	2	16	20
7)		80	100	2	16	51
8)		40	90	3	16	58
9)		r.t.	100	3	16	48

Yields are ^1H NMR yields obtained using 4-bromoanisole as internal standard.

IV.1.3 Optimization of $B(C_6F_5)_4$ alkali salt, temperature and reaction time using $HNTf_2$.



4.1 **4.6** **4.9**

In glovebox, $HNTf_2$ (7.9 mg, 0.028 mmol, 1.1 equiv.) was added to a suspension of 10-mesityl-9-sulfonium-10-boratriptycene-ate complex **4.1** (10 mg, 0.026 mmol, 1.0 equiv.) in benzene (1.5 ml). The reaction mixture was stirred 5 min and $B(C_6F_5)_4$ alkali salt (0.038 mmol, 1.5 equiv.) was added. After stirring for further 5 min, DTBMP (26 mg, 0.13 mmol, 5.0 equiv.) was added, the Schlenk tube was sealed with a glass stopper and put out of the glovebox. The mixture was stirred and warmed in an oil bath at 60 to

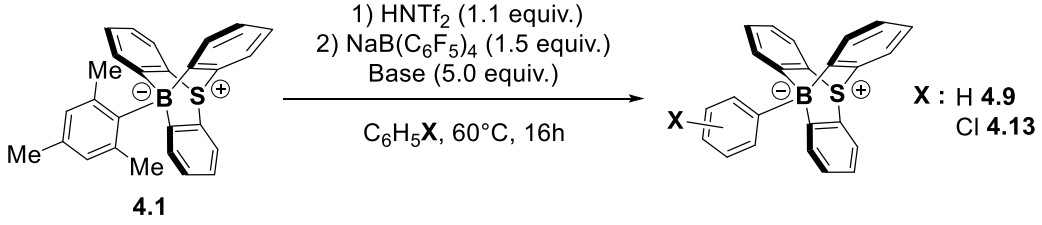
120°C. After 16 to 72h, the crude was evaporated to dryness, dissolved in $CDCl_3$ and ^1H and ^{11}B NMR spectra were recorded. The yields were determined using 4-bromoanisole as internal standard.

Table SIV.3 Optimization of Csp^2–H borylation condition using $HNTf_2$ and DTBMP: Selection of the reaction time and temperature and $B(C_6F_5)_4$ alkali salt.

	Additive	**T_2** (°C)	**t_2** (h)	**Yield** (%)
1)	/	100	16	0
2)	/	120	72	0
3)	$NaB(C_6F_5)_4$ (1.0 equiv.)	100	16	47
4)	$NaB(C_6F_5)_4$ (1.3 equiv.)	80	16	52
5)	$NaB(C_6F_5)_4$ (1.3 equiv.)	60	16	67
6)	$NaB(C_6F_5)_4$ (1.3 equiv.)	40	16	30
7)	$NaB(C_6F_5)_4$ (1.3 equiv.)	r.t.	72	15
8)	$NaB(C_6F_5)_4$ (1.5 equiv.)	60	16	73
9)	$NaB(C_6F_5)_4$ (2.0 equiv.)	60	16	74
10)	$LiB(C_6F_5)_4$ (1.5 equiv.)	60	16	6

Yields are ^1H NMR yields obtained using 4-bromoanisole as internal standard.

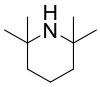
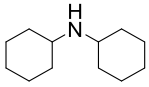
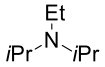
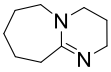
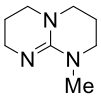
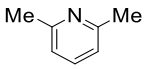
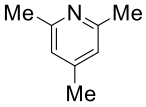
IV.1.4 Optimization of Brønsted base with combination of $HNTf_2$ and $NaB(C_6F_5)_4$.

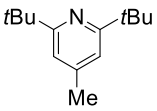
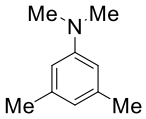
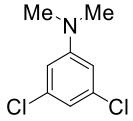
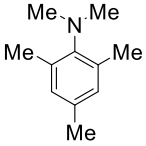
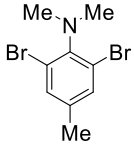
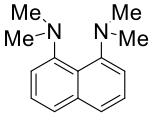
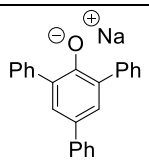
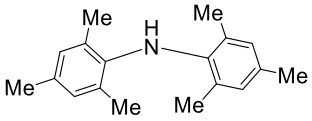
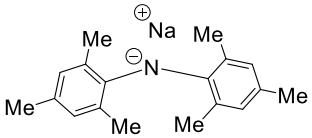


In glovebox, $HNTf_2$ (7.9 mg, 0.028 mmol, 1.1 equiv.) was added to a suspension of 10-mesityl-9-sulfonium-10-boratriptycene-ate complex **4.1** (10 mg, 0.026 mmol, 1.0 equiv.)

in benzene (1.5 ml) or chlorobenzene (1.5 ml). The reaction mixture was stirred 5 min and $NaB(C_6F_5)_4$ (28 mg, 0.038 mmol, 1.5 equiv.). After stirring for further 5 min, the Brønsted base (0.13 mmol, 5.0 equiv.) was added, the Schlenk tube was sealed with a glass stopper and put out of the glovebox. The mixture was stirred and warmed in an oil bath at 60°C. After 16h, the crude was evaporated to dryness, dissolved in $CDCl_3$ and ^1H and ^{11}B NMR spectra were recorded. The yields were determined using 4-bromoanisole as internal standard.

Table SIV.4 Optimization of Csp^2–H borylation condition using $HNTf_2$ and $NaB(C_6F_5)_4$: Selection of the Brønsted base.

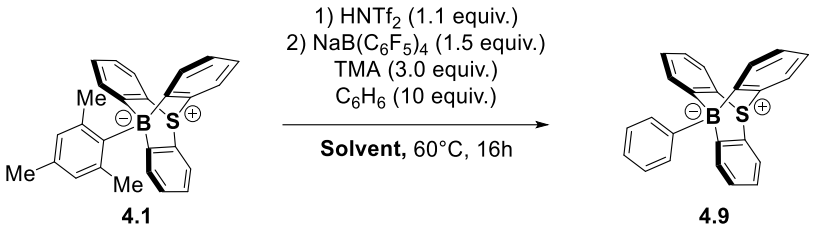
Entry	**Base**	**Solvent**	**Yield** (%)
1)		C_6H_6	55
		C_6H_5Cl	Detected*
2)		C_6H_6	45
		C_6H_5Cl	Detected*
3)		C_6H_6	/
		C_6H_5Cl	0
4)		C_6H_6	21
		C_6H_5Cl	0
5)		C_6H_6	51
		C_6H_5Cl	Detected*
6)		C_6H_6	48
		C_6H_5Cl	0
7)		C_6H_6	45
		C_6H_5Cl	0
8)		C_6H_6	74

		C_6H_5Cl	Detected
9)		C_6H_6 C_6H_5Cl	91 85[a]
10)		C_6H_6 C_6H_5Cl	88 Detected*
11)		C_6H_6 C_6H_5Cl	41 0
12)		C_6H_6 C_6H_5Cl	89 Detected*
13)		C_6H_6 C_6H_5Cl	15 /
14)		C_6H_6 C_6H_5Cl	/ Detected
15)		C_6H_6 C_6H_5Cl	61 Detected*
16)		C_6H_6 C_6H_5Cl	11 0

Yields are ^{1}H NMR yields obtained using 4-bromoanisole as internal standard. *Detected means that a signal corresponding to the desired product was detected by ^{11}B NMR but could not be isolated nor unambiguously detected by ^{1}H NMR. [a] : isolated yield

IV.2. Csp^2–H borylation optimization with reduced amount of substrate

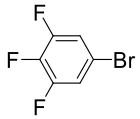
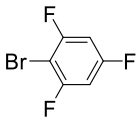
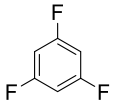
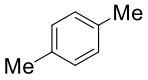
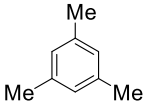
IV.2.1 Optimization of the solvent



4.1 **4.9**

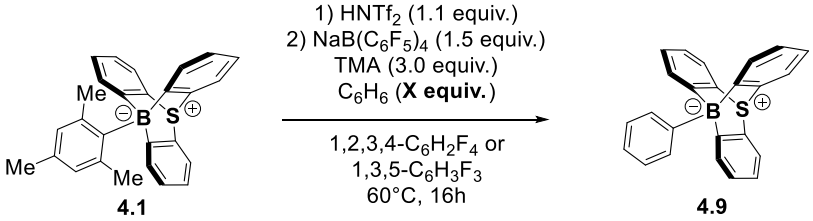
In glovebox, $HNTf_2$ (7.9 mg, 0.028 mmol, 1.1 equiv.) was added to a suspension of 10-mesityl-9-sulfonium-10-boratriptycene-ate complex **4.1** (10 mg, 0.026 mmol, 1.0 equiv.) and benzene (23 µl, 0.26 mmol, 10 equiv.) in aromatic solvent (0.50 ml). The reaction mixture was stirred 5 min and $NaB(C_6F_5)_4$ (28 mg, 0.038 mmol, 1.5 equiv.). After stirring for further 5 min, *N*,*N*,3,5-tetramethylaniline (13 µl, 0.13 mmol, 3.0 equiv.) was added, the Schlenk tube was sealed with a glass stopper and put out of the glovebox. The mixture was stirred and warmed in an oil bath at 60°C. After 16h, the crude was evaporated to dryness, dissolved in $CDCl_3$ and ^1H and ^{11}B NMR spectra were recorded. The yields were determined using 4-bromoanisole as internal standard.

Table SIV.5 Optimization of Csp^2–H borylation condition with reduced amount of benzene as substrate using $HNTf_2$ and $NaB(C_6F_5)_4$: Selection of the solvent

Entry	Solvent	Substrate concentration ($mol.L^{-1}$)	Yield (%)
1)		0.52	4
2)		0.52	42
3)		0.52	48
4)		0.52	47
5)		0.52	6
6)		0.52	5

Yields are ^1H NMR yields obtained using 4-bromoanisole as internal standard

IV.2.2 Optimization of the required equivalents and concentration of benzene as substrate



In glovebox, $HNTf_2$ (7.9 mg, 0.028 mmol, 1.1 equiv.) was added to a suspension of 10-mesityl-9-sulfonium-10-boratriptycene-ate complex **4.1** (10 mg, 0.026 mmol, 1.0 equiv.)

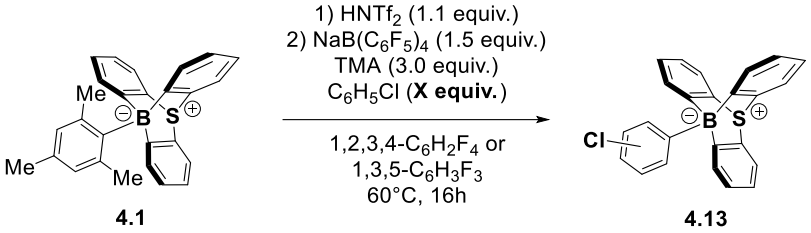
and benzene (23 µl to 0.23 ml, 0.26 to 2.8 mmol, 10 to 100 equiv.) in 1,2,3,4-tetrafluorobenzene or 1,3,5-trifluorobenzene (0.50 to 1.0 ml). The reaction mixture was stirred 5 min and $NaB(C_6F_5)_4$ (28 mg, 0.038 mmol, 1.5 equiv.). After stirring for further 5 min, *N*,*N*,3,5-tetramethylaniline (13 µl, 0.078 mmol, 3.0 equiv.) was added, the Schlenk tube was sealed with a glass stopper and put out of the glovebox. The mixture was stirred and warmed in an oil bath at 60°C. After 16h, the crude was evaporated to dryness, dissolved in $CDCl_3$ and ^1H and ^{11}B NMR spectra were recorded. The yields were determined using 4-bromoanisole as internal standard.

Table SIV.6 Optimization of Csp^2–H borylation condition with reduced amount of benzene as substrate using $HNTf_2$ and $NaB(C_6F_5)_4$: optimization of substrate concentration and equivalents.

	Solvent Volume (mL)	**Benzene equivalents**	**Concentration** ($mol.L^{-1}$)	**Yield** (%)
1)	0.50	10	0.49	48
2)	1.0	20	0.49	51
3)	0.50	20	0.94	66
4)	1.0	40	0.94	74
5)	0.50	30	1.35	85
6)	1.0	60	1.35	90
7)	0.50	40	1.73	86
8)	1.0	80	1.73	88
9)	0.50	50	2.08	89
10)	1.0	100	2.08	86

Yields are ^1H NMR yields obtained using 4-bromoanisole as internal standard

IV.2.3 Optimization of the required equivalents and concentration of chlorobenzene as substrate



4.1 **4.13**

In glovebox, $HNTf_2$ (24 mg, 0.084 mmol, 1.1 equiv.) was added to a suspension of 10-mesityl-9-sulfonium-10-boratriptycene-ate complex **4.1** (30 mg, 0.077 mmol, 1.0 equiv.) and chlorobenzene (0.23 ml to 0.62 ml, 2.3 to 6.1 mmol, 30 to 80 equiv.) in 1,2,3,4-tetrafluorobenzene or 1,3,5-trifluorobenzene (1.5 ml). The reaction mixture was stirred 5 min and $NaB(C_6F_5)_4$ (84 mg, 0.12 mmol, 1.5 equiv.). After stirring for further 5 min, *N*,*N*,3,5-tetramethylaniline (39 µl, 0.23 mmol, 3.0 equiv.) was added, the Schlenk tube was sealed with a glass stopper and put out of the glovebox. The mixture was stirred and warmed in an oil bath at 60°C. After 16h, the crude was evaporated to dryness and purified via flash chromatography, affording 10-(4-chlorophenyl)-9-sulfonium-10-boratriptycene-ate complex.

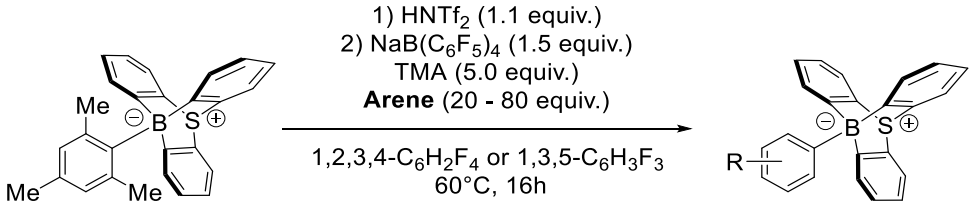
Table SIV.7 Optimization of Csp^2–H borylation condition with reduced amount of chlorobenzene as substrate using $HNTf_2$ and $NaB(C_6F_5)_4$: optimization of substrate concentration and equivalents

	Solvent volume (mL)	**Chlorobenzene equivalents**	**Concentration** ($mol.L^{-1}$)	**Yield** (%)
1)	1.5	30	1.33	29
2)	1.5	40	1.70	34
3)	1.5	50	2.04	58
4)	1.5	60	2.35	61
5)	1.5	80	2.90	66

IV.3. Synthetic procedures.

IV.3.1 General procedure for volatile substrates (**GP1**):

10-aryl-9-sulfonium-10-boratriptycene-ate complex



4.1

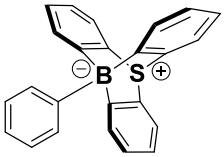
Under glovebox conditions in a Schlenk tube, $HNTf_2$ (40 mg, 0.14 mmol, 1.1 equiv.) was added to a suspension of 10-mesityl-9-sulfonium-10-boratritpycene-ate complex **4.1** (50 mg, 0.13, 1.0 equiv.) in 1,2,3,4-tetrafluorobenzene (3.0 ml) or 1,3,5-trifluorobenzene (3.0 ml). The reaction was stirred for 5min then $NaB(C_6F_5)_4$ (139 mg, 0.19 mmol, 1.5 equiv.) and stirred for further 5 min. 3,5,*N*,*N*-Tetramethylaniline (**TMA**) (105 µl, 0.64 mmol, 5.0 equiv.) and the aromatic substrate were added. The Schlenk tube was then sealed with a glass stopper, stirred and warmed in an oil bath at 60°C. After 16h, the volatiles were removed and the crude was dissolved in CH_2Cl_2, trifluoroacetic acid (54 µl, 0.70 mmol, 5.5 equiv.) was added and the solution was filtered over silica gel plug. The filtrate was evaporated to dryness and purified via flash chromatography (90:10 *n*-hexane/CH_2Cl_2) affording pure 10-aryl-9-sulfonium-10-boratriptycene-ate complex.

IV.3.2 General procedure for solid or non-volatile substrates (**GP2**):

Under glovebox conditions in a Schlenk tube, $HNTf_2$ (40 mg, 0.14 mmol, 1.1 equiv.) was added to a suspension of 10-mesityl-9-sulfonium-10-boratritpycene-ate complex **4.1** (50 mg, 0.13, 1.0 equiv.) in 1,2,3,4-tetrafluorobenzene (3.0 ml) or 1,3,5-trifluorobenzene (3.0 ml). The reaction was stirred for 5min then $NaB(C_6F_5)_4$ (139 mg, 0.19 mmol, 1.5 equiv.) and stirred for further 5 min. 3,5,*N*,*N*-Tetramethylaniline (**TMA**) (105 µl, 0.64 mmol, 5.0 equiv.) and the aromatic substrate were added. The Schlenk tube was then sealed with a glass stopper, stirred and warmed in an oil bath at 60°C.

After 16h, the volatiles were removed and the crude was dissolved in CH_2Cl_2, trifluoroacetic acid (54 µl, 0.70 mmol, 5.5 equiv.) was added and the solution was filtered over silica gel plug. The filtrate was evaporated to dryness then adsorbed on silica and settled on a silica gel plug. The silica was thoroughly washed with a mixture of *n*-hexane and CH_2Cl_2 (98:2). The removal of excess aromatic substrate was monitored by TLC. Once the excess aromatic substrate was removed, the silica gel plug was then washed with pure CH_2Cl_2 and the filtrate was recovered. The crude was then purified via flash chromatography (90:10 *n*-hexane/CH_2Cl_2) affording pure 10-aryl-9-sulfonium-10-boratriptycene-ate complex.

10-Phenyl-9-sulfonium-10-boratriptycene-ate complex 4.9.



According to **GP1** with the following quantities of benzene (343 µl, 3.8 mmol, 30 equiv.).[S1]

Yield: 85%

The ^{1}H, ^{13}C and ^{11}B NMR data are identical to that previously reported.

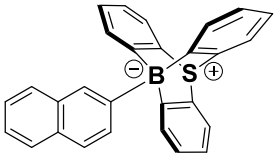
TLC: R_f = 0.9 (50:50 *n*-hexane/CH_2Cl_2)

^{1}H NMR (500 MHz, $CDCl_3$) δ (ppm) = 8.10 (d, *J* = 6.9 Hz, 2H), 7.86 (d, *J* = 7.3 Hz, 3H), 7.77 (d, *J* = 7.6 Hz, 3H), 7.56 (t, *J* = 7.5 Hz, 2H), 7.39 (t, *J* = 7.3 Hz, 1H), 7.23 (td, *J* = 7.4, 1.2 Hz, 3H), 7.06 (td, *J* = 7.5, 1.4 Hz, 3H).

^{13}C NMR (126 MHz, $CDCl_3$) δ (ppm) = 135.8 (CH), 134.5 (CH), 134.3 (CH), 130.2 (CH), 127.7 (CH), 124.9 (CH), 224.2 (CH). The carbon atoms directly attached to the boron atom on the triptycene core were not detected, likely due to quadrupolar relaxation.

^{11}B NMR (160 MHz, $CDCl_3$) δ (ppm) = -9.3 (s).

10-(2-Naphtyl)-9-sulfonium-10-boratriptycene-ate complex 4.28



According to **GP2** with the following quantities of naphtalene (492 mg, 3.8 mmol, 30 equiv.).

Yield: 82%

TLC: R_f = 0.9 (50:50 *n*-hexane/CH_2Cl_2)

^{1}H NMR (500 MHz, $CDCl_3$) δ (ppm) = 8.67 (s, 1H), 8.14 (d, *J* = 8.2 Hz, 1H), 8.00 (d, *J* = 8.3 Hz, 1H), 7.98-7.93 (m, 2H), 7.90 (d, *J* = 7.3 Hz, 3H), 7.80 (dd, *J* = 7.7, 0.9 Hz, 3H). 7.54-7.46 (m, 2H), 7.24 (td, *J* = 7.5, 1.1 Hz, 3H), 7.09 (td, *J* = 7.5, 1.4 Hz, 3H).

^{13}C NMR (126 MHz, $CDCl_3$) δ (ppm) = 162.9 (CB), 135.0 (CH), 134.5 (Cq), 134.3 (CH), 134.1 (Cq), 134.0 (CH), 132.1 (Cq), 130.3 (CH), 128.1 (CH), 127.8 (CH), 127.7 (CH), 126.1 (CH), 125.0 (CH), 124.7 (CH), 124.3 (CH).

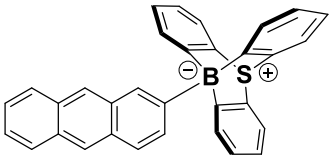
^{11}B NMR (160 MHz, $CDCl_3$) δ (ppm) = -9.1 (s).

HRMS (MALDI$^+$) (*m/z*): calc. for [$C_{28}H_{19}BNaS^+$] : 421.1198, [M^+] : 421.1206

IR (neat, ATR): $\tilde{\nu}$ / cm^{-1} = 3047, 1498, 1429, 1297, 1256, 1170, 1124, 946, 905, 810, 741.

M.p. : >300°C

10-(2-Anthracyl)-9-sulfonium-10-boratriptycene-ate complex 4.29



According to **GP2** with the following quantities of anthracene (686 mg, 3.8 mmol, 30 equiv.).

Yield: 85%

TLC: R_f = 0.9 (50:50 *n*-hexane/CH_2Cl_2)

^{1}H NMR (500 MHz, $CDCl_3$) δ (ppm) = 8.89 (s, 1H), 8.55 (d, *J* = 14.7 Hz, 2H), 8.16 (d, *J* = 8.5 Hz, 1H), 8.13-8.04 (m, 3H), 7.96 (d, *J* = 7.2 Hz, 3H), 7.81 (dd, *J* = 7.6, 0.9 Hz, 3 H), 7.48-7.43 (m, 2H), 7.26 (td, *J* = 7.4, 1.1 Hz, 3H), 7.10 (td, *J* = 7.5, 1.4 Hz, 3H).

^{13}C NMR (126 MHz, $CDCl_3$) δ (ppm) = 162.8 (CB), 135.1 (CH), 134.5 (Cq), 134.4 (CH), 133.6 (CH), 132.9 (Cq), 131.7 (Cq), 131.4 (Cq), 131.2 (Cq), 130.3 (CH), 128.4 (CH), 128.3 (CH), 127.8 (CH), 126.0 (CH), 126.0 (CH), 125.7 (CH), 125.6 (CH), 124.8 (CH), 124.6 (CH), 124.3 (CH), 120.5 (CH), 119.6 (CH), 110.7 (CH).

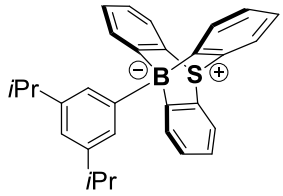
^{11}B NMR (160 MHz, $CDCl_3$) δ (ppm) = -9.1 (s).

HRMS (MALDI$^+$) (*m/z*): calc. for [$C_{32}H_{21}BNaS^+$] : 471.1355, [M^+] : 471.1347

IR (neat, ATR): $\tilde{\nu}$ / cm^{-1} = 3043, 2961, 2924, 1589, 1507, 1457, 1425, 1293, 1270, 1161, 1083, 978, 869, 746.

M.p. : 291°C (dec)

10-(3,5-Di*iso*propylphenyl)-9-sulfonium-10-boratriptycene-ate complex 4.30



According to **GP1** with the following quantities of 1,3-di*iso*priopylbenzene (729 µl, 3.8 mmol, 30 equiv.).

Yield: 69%

TLC: R_f = 0.9 (50:50 *n*-hexane/CH_2Cl_2)

^{1}H NMR (500 MHz, $CDCl_3$) δ (ppm) = 7.89 (d, *J* = 7.0 Hz, 3H), 7.80 (s, 2H), 7.77 (dd, *J* = 7.6, 0.8 Hz, 3H), 7.25 (td, *J* = 7.4, 1.3 Hz, 3H), 7.11 (t, *J* = 1.6 Hz, 1H), 7.07 (td, *J* = 7.5, 1.4 Hz, 3H), 3.05 (hept, *J* = 6.9 Hz, 2H), 1.39 (d, *J* = 6.9 Hz, 12H).

^{13}C NMR (126 MHz, $CDCl_3$) δ (ppm) = 163.3 (CB), 147.4 (Cq), 134.5 (CH), 131.4 (CH), 130.1 (CH), 130.1 (CH), 127.7 (CH), 124.1 (CH), 121.0 (CH), 34.7 (CH), 24.6 (CH_3).

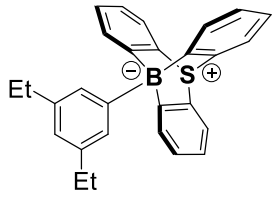
^{11}B NMR (160 MHz, $CDCl_3$) δ (ppm) = -9.0 (s).

HRMS (MALDI$^+$) (*m/z*): calc. for [$C_{30}H_{29}BNaS^+$] : 455.1981, [M^+] : 455.1973

IR (neat, ATR): $\tilde{\nu}$ / cm^{-1} = 3056, 2956, 1584, 1429, 1293, 1256, 1183, 1024, 873, 741.

M.p. : 226-228°C

10-(3,5-Diethylphenyl)-9-sulfonium-10-boratriptycene-ate complex 4.31



According to **GP1** with the following quantities of 1,3-diethylbenzene (597 µl, 3.8 mmol, 30 equiv.).

Yield: 77%

TLC: R_f = 0.9 (50:50 *n*-hexane/CH_2Cl_2)

^{1}H NMR (500 MHz, $CDCl_3$) δ (ppm) = 7.91 (d, *J* = 7.3 Hz, 3H), 7.82-7.77 (m, 5H), 7.25 (td, *J* = 7.4, 0.5 Hz, 3H), 7.10 (s, 1H), 7.07 (td, *J* = 7.3, 0.9 Hz, 3H), 2.81 (q, *J* = 7.6 Hz, 4H), 1.39 (t, *J* = 7.6 Hz, 6H).

^{13}C NMR (126 MHz, $CDCl_3$) δ (ppm) = 163.2 (CB), 143.0 (Cq), 134.5 (CH), 134.5 (CH), 132.8 (CH), 130.1 (CH), 127.7 (CH), 124.1 (CH), 124.0 (CH), 29.6 (CH_2), 16.3 (CH_3).

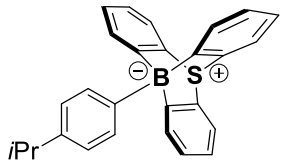
^{11}B NMR (160 MHz, $CDCl_3$) δ (ppm) = -9.1 (s).

HRMS (MALDI$^+$) (*m/z*): calc. for [$C_{28}H_{25}BNaS^+$] : 427.1668, [M^+] : 427.1674

IR (neat, ATR): $\tilde{\nu}$ / cm^{-1} = 2961, 2920, 1648, 1589, 1507, 1461, 1411, 1275, 1170, 1092, 978, 878, 755.

M.p. : 209-212°C

10-(4-*iso*propylphenyl)-9-sulfonium-10-boratriptycene-ate complex 4.32



According to **GP1** with the following quantities of *iso*propylbenzene (536 µl, 3.8 mmol, 30 equiv.).

Product obtained as inseparable mixture of two regioisomers (*m*:*p* 15:85)

Yield: 53%

TLC: R_f = 0.9 (50:50 *n*-hexane/CH_2Cl_2)

^{1}H NMR (500 MHz, $CDCl_3$) δ (ppm) = (*m*-isomer) 7.95 (d, *J* = 6.3 Hz, 2H), 7.77 (dd, *J* = 7.6, 0.9 Hz, 3H), 7.72 (t, *J* = 7.8 Hz, 2H), 7.51 (t, *J* = 7.7 Hz, 1H), 7.24 (dt, *J* = 7.3, 1.2 Hz, 3H), 7.07 (td, *J* = 7.5, 1.4 Hz, 3H), 3.07 (hept, *J* = 6.9 Hz, 1H), 1.39 (d, *J* = 6.9 Hz). (*p*-isomer) 8.03 (d, *J* = 7.8 Hz, 2H), 7.88 (d, *J* = 7.3 Hz, 3H), 7.77 (dd, *J* = 7.6, 0.9 Hz, 3H), 7.44 (d, *J* = 7.7 Hz, 2H), 7.24 (td, *J* = 6.7, 1.2 Hz, 3H), 7.06 (td, *J* = 7.4, 1.4 Hz, 3H), 3.07 (hept, *J* = 6.9 Hz, 1H), 1.42 (d, *J* = 6.9 Hz, 6H).

^{13}C NMR (126 MHz, $CDCl_3$) δ (ppm) = 163.1 (CB), 145.0 (Cq), 135.6 (CH), 134.5 (Cq), 134.4 (CH), 130.1 (CH), 127.7 (CH), 125.7 (CH), 124.1 (CH), 34.0 (CH), 24.4 (CH_3).

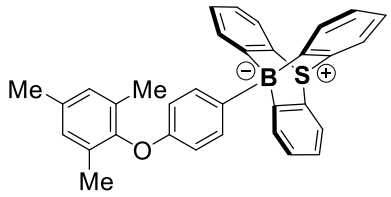
^{11}B NMR (160 MHz, $CDCl_3$) δ (ppm) = -9.3 (s).

HRMS (MALDI$^+$) (*m/z*): calc. for [$C_{27}H_{23}BNaS^+$] : 413.1511, [M^+] : 413.1507

IR (neat, ATR): $\tilde{\nu}$ / cm^{-1} = 3052, 2956, 1434, 1306, 1261, 1179, 1010, 892, 750.

M.p. : 211-214°C

10-((4-Mesityloxy)-4-phenyl)-9-sulfonium-10-boratriptycene-ate complex 4.33



According to **GP2** with the following quantities of mesityl-phenyl ether[S2] (815 mg, 3.8 mmol, 30 equiv.).

Product obtained as inseparable mixture of two regioisomers (*m*:*p* 01:99)

Yield: 65%

TLC: R_f = 0.9 (50:50 *n*-hexane/CH_2Cl_2)

^{1}H NMR (500 MHz, $CDCl_3$) δ (ppm) = (*p*-isomer) 7.95 (d, *J* = 8.4 Hz, 2H), 7.85 (d, *J* = 6.8 Hz, 3H), 7.76 (dd, *J* = 7.6, 0.7 Hz, 3H), 7.23 (td, *J* = 7.3, 1.1 Hz, 3H), 7.06 (td, *J* = 7.5, 1.4 Hz, 3H), 6.99 (d, *J* = 8.6 Hz, 2H), 6.97 (s, 2H), 2.35 (s, 3H), 2.28 (s, 6H).

^{13}C NMR (126 MHz, $CDCl_3$) δ (ppm) = 163.3 (CB), 155.8 (Cq), 149.7 (Cq), 136.7 (CH), 134.4 (Cq), 134.2 (CH), 134.0 (Cq), 131.6 (Cq), 130.1 (CH), 129.6 (CH), 127.7 (CH), 124.1 (CH), 114.1 (CH), 21.0 (CH_3), 16.8 (CH_3).

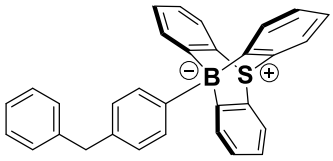
^{11}B NMR (160 MHz, $CDCl_3$) δ (ppm) = -9.4 (s).

HRMS (MALDI$^+$) (*m/z*): calc. for [$C_{33}H_{27}BONaS^+$] : 505.1773, [M^+] : 505.1762

IR (neat, ATR): $\tilde{\nu}$ / cm^{-1} = 3043, 2929, 1584, 1484, 1429, 1297, 1215, 1165, 1010, 887, 832, 741.

M.p. : 203°C (dec)

10-(4-diphenylmethane)-9-sulfonium-10-boratriptycene-ate complex 4.34



According to **GP2** with the following quantities of diphenylmethane (950 mg, 3.8 mmol, 30 equiv.).

Product obtained as inseparable mixture of two regioisomers (*m*:*p* 16:84)

Yield: 65%

TLC: R_f = 0.9 (50:50 *n*-hexane/CH_2Cl_2)

^{1}H NMR (500 MHz, $CDCl_3$) δ (ppm) = (*p*-isomer) 8.02 (d, *J* = 7.8 Hz, 2H), 7.86 (*J* = 6.8 Hz, 3H), 7.77 (dd, *J* = 7.7, 0.8 Hz, 3H), 7.43-7.35 (m, 5H), 7.28-7.25 (m, 2H), 7.23 (dt, *J* = 7.4, 1.1 Hz, 3H), 7.06 (td, *J* = 7.5, 1.4 Hz, 3H), 4.15 (s, 2H).

^{13}C NMR (126 MHz, $CDCl_3$) δ (ppm) = 163.1 (CB), 142.2 (Cq), 137.3 (Cq), 135.8 (CH), 134.4 (Cq), 134.3 (CH), 130.1 (CH), 129.3 (CH), 128.5 (CH), 128.2 (CH), 127.7 (CH), 126.0 (CH), 124.2 (CH), 42.1 (CH_2).

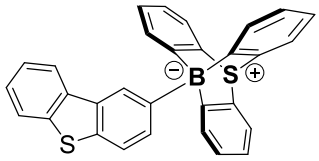
^{11}B NMR (160 MHz, $CDCl_3$) δ (ppm) = -9.3 (s).

HRMS (MALDI^{+}) (*m/z*): calc. for [$C_{31}H_{23}BNaS^{+}$] : 461.1511, [M^{+}] : 461.1502

IR (neat, ATR): $\tilde{\nu}$ / cm^{-1} = 3052, 2965, 2929, 1648, 1589, 1521, 1420, 1270, 1179, 1129, 1088, 978, 878, 750.

M.p. : 216-219°C

10-(2-dibenzothiophene)-9-sulfonium-10-boratriptycene-ate complex 4.35



According to **GP2** with the following quantities of dibenzothiophene (354 mg, 1.9 mmol, 15 equiv.).

Product obtained as inseparable mixture of two regioisomers (2-:3- 50:50)

Yield: 48%

TLC: R_f = 0.8 (50:50 *n*-hexane/CH_2Cl_2)

^{1}H NMR (500 MHz, $CDCl_3$) δ (ppm) = (2-isomer) 8.63 (s, 1H), 8.35 (d, *J* = 8.0 Hz, 1H), 8.16 (d, *J* = 8.0 Hz, 1H), 8.28-8.25 (m, 1H), 7.95-7.87 (m, 4H), 7.83-7.79 (m, 3H), 7.50-7.42 (m, 2H), 7.26 (tt, *J* = 7.3, 1.1 Hz, 3H), 7.10 (td, *J* = 7.5, 1.3 Hz, 3H). (3-isomer) 8.95 (s, 1H), 8.20 (d, *J* = 8.2 Hz, 1H), 8.05 (d, *J* = 8.0 Hz, 1H), 7.95-7.87 (m, 4H), 7.83-7.79 (m, 3H), 7.50-7.42 (m, 2H), 7.09 (td, *J* = 7.5, 1.3 Hz, 3H).

^{13}C NMR (126 MHz, $CDCl_3$) δ (ppm) = 132.6 (CB), 139.5 (Cq), 139.3 (Cq), 136.7 (Cq), 136.7 (Cq), 136.3 (Cq), 135.4 (CH), 135.1 (CH), 134.5 (Cq), 134.4 (Cq), 134.2 (CH), 132.9 (CH), 132.4 (CH), 130.3 (CH), 129.2 (CH), 129.1 (CH), 128.5 (CH), 128.4 (CH), 127.9 (CH), 127.8 (CH), 126.1 (CH), 126.0 (CH), 124.3 (CH), 124.2 (CH), 124.1 (CH), 123.0 (CH), 123.0 (CH), 121.9 (CH), 121.6 (CH), 121.3 (CH), 120.7 (CH).

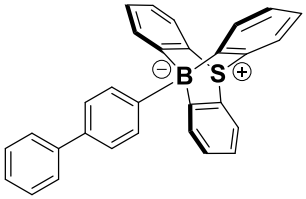
^{11}B NMR (160 MHz, $CDCl_3$) δ (ppm) = -9.0 (s).

HRMS (MALDI$^+$) (*m/z*): calc. for [$C_{30}H_{19}BNaS_2^+$] : 477.0919, [M^+] : 477.0926

IR (neat, ATR): $\tilde{\nu}$ / cm^{-1} = 3047, 2965, 2920, 1644, 1589, 1507, 1452, 1420, 1261, 1165, 1129, 1088, 974, 869, 746.

M.p. : 278-283°C

10-(4-biphenyl)-9-sulfonium-10-boratriptycene-ate complex 4.36



According to **GP2** with the following quantities of biphenyl (593 mg, 3.8 mmol, 30 equiv.).

Product obtained as inseparable mixture of two regioisomers (*m*:*p* 08:92)

Yield: 64%

TLC: R_f = 0.9 (50:50 *n*-hexane/CH_2Cl_2)

^{1}H NMR (500 MHz, $CDCl_3$) δ (ppm) = 8.19 (d, *J* = 7.5 Hz, 2H), 7.92 (d, *J* = 7.4 Hz, 3H), 7.84 (t, *J* = 7.2 Hz, 4H), 7.79 (d, *J* = 7.7 Hz, 3H), 7.51 (t, *J* = 7.3 Hz, 2H), 7.37 (td, *J* = 7.6, 1.1 Hz, 1H), 7.26 (t, *J* = 7.4 Hz, 3H), 7.09 (t, *J* = 7.5 Hz, 3H).

^{13}C NMR (126 MHz, $CDCl_3$) δ (ppm) = 162.8 (CB), 142.2 (Cq), 137.4 (Cq), 136.2 (CH), 134.5 (Cq), 134.3 (CH), 130.2 (CH), 128.8 (CH), 127.8 (CH), 127.2 (CH), 126.7 (CH), 126.3 (CH), 124.3 (CH).

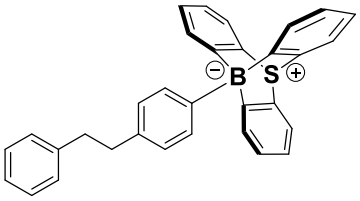
^{11}B NMR (160 MHz, $CDCl_3$) δ (ppm) = -9.3 (s).

HRMS (MALDI$^+$) (*m/z*): calc. for [$C_{32}H_{21}BNaS^+$] : 471.1355, [M^+] : 471.1359

IR (neat, ATR): $\tilde{\nu}$ / cm^{-1} = 3047, 1484, 1434, 1302, 1261, 1193, 1115, 1010, 892, 750.

M.p. : 283-285°C

10-(4-bibenzyl)-9-sulfonium-10-boratriptycene-ate complex 4.37



According to **GP2** with the following quantities of bibenzyl (700 mg, 3.8 mmol, 30 equiv.).

Product obtained as inseparable mixture of two regioisomers (*m*:*p* 07:93)

Yield: 66%

TLC: R_f = 0.9 (50:50 *n*-hexane/CH_2Cl_2)

^{1}H NMR (500 MHz, $CDCl_3$) δ (ppm) = 8.04 (d, *J* = 7.7 Hz, 2H), 7.88 (d, *J* = 7.3 Hz, 3H), 7.78 (d, *J* = 7.7 Hz, 3H), 7.43 (d, *J* = 7.8 Hz, 2H), 7.38-7.32 (m, 4H), 7.25 (td, *J* = 7.4, 1.0 Hz, 3H), 7.07 (td, *J* = 7.5, 1.3 Hz, 3H), 3.15-3.06 (m, 4H).

^{13}C NMR (126 MHz, $CDCl_3$) δ (ppm) = 163.3 (CB), 142.7 (Cq), 138.1 (Cq), 135.8 (CH), 134.4 (Cq), 134.3 (CH), 130.1 (CH), 128.7 (CH), 128.5 (CH), 128.4 (CH), 127.8 (CH), 127.7 (CH) 125.9 (CH), 124.2 (CH), 38.4 (CH_2), 38.2 (CH_2).

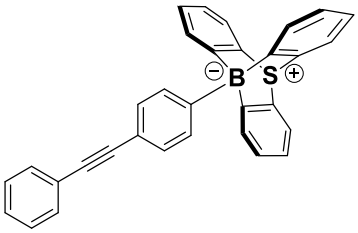
^{11}B NMR (160 MHz, $CDCl_3$) δ (ppm) = -9.3 (s).

HRMS (MALDI$^+$) (*m/z*): calc. for [$C_{32}H_{25}BNaS^+$] : 475.1668, [M^+] : 475.1667

IR (neat, ATR): $\tilde{\nu}$ / cm^{-1} = 3038, 2920, 1493, 1439, 1293, 1256, 1179, 1019, 901, 801, 750.

M.p. : 245-248°C

10-(4-diphenylacetylene)-9-sulfonium-10-boratriptycene-ate complex 4.38



According to **GP2** with the following quantities of diphenylacetylene (685 mg, 3.8 mmol, 30 equiv.).

Product obtained as inseparable mixture of two regioisomers (*m*:*p* 12:88)

Yield: 66%

TLC: R_f = 0.9 (50:50 *n*-hexane/CH_2Cl_2)

^{1}H NMR (500 MHz, $CDCl_3$) δ (ppm) = 8.09 (d, *J* = 8.0 Hz, 2H), 7.83 (dd, *J* = 7.4, 0.9 Hz, 3H), 7.78 (dd, *J* = 7.7, 0.9 Hz, 3H), 7.73 (d, *J* = 8.2 Hz, 2H), 7.63-7.59 (m, 2H), 7.40-7.32 (m, 3H), 7.25 (td, *J* = 7.4, 1.2 Hz, 3H), 7.08 (td, *J* = 7.5, 1.5 Hz, 3H).

^{13}C NMR (126 MHz, $CDCl_3$) δ (ppm) = 162.5 (CB), 135.7 (CH), 134.4 (Cq), 134.1 (CH), 131.8 (CH), 131.7 (CH), 130.8 (CH), 130.3 (CH), 128.4 (CH), 127.9 (CH), 127.8 (CH), 124.3 (CH), 119.3 (Cq), 91.0 (Cq), 88.3 (Cq).

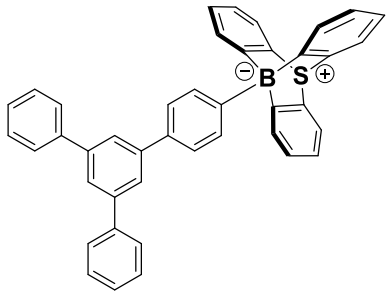
^{11}B NMR (160 MHz, $CDCl_3$) δ (ppm) = -9.3 (s).

HRMS (MALDI$^+$) (*m/z*): calc. for [$C_{32}H_{21}BNaS^+$] : 471.1355, [M^+] : 471.1351

IR (neat, ATR): $\tilde{\nu}$ / cm^{-1} = 3047, 2920, 1589, 1484, 1429, 1297, 1220, 1165, 1024, 892, 855, 810, 750.

M.p. : 254-257°C

10-(4-triphenylbenzene)-9-sulfonium-10-boratriptycene-ate complex 4.39



According to **GP2** with the following quantities of triphenylbenzene (785 mg, 2.5 mmol, 20 equiv.).

Product obtained as inseparable mixture of two regioisomers (*m*:*p* 11:89)

Yield: 59%

TLC: R_f = 0.9 (50:50 *n*-hexane/CH_2Cl_2)

^{1}H NMR (500 MHz, $CDCl_3$) δ (ppm) = 8.23 (d, *J* = 8.0 Hz, 2H), 8.04 (d, *J* = 1.7 Hz, 2H), 7.97-7.92 (m, 5H), 7.83 (dt, *J* = 1.7 Hz, 1H), 7.83-7.78 (m, 7H), 7.53 (t, *J* = 7.7 Hz, 4H), 7.42 (tt, *J* = 7.4,1.2 Hz, 2H), 7.2 (td, *J* = 7.4,1.2 Hz, 3H), 7.09 (td, *J* = 7.5, 1.3 Hz, 3H).

^{13}C NMR (126 MHz, $CDCl_3$) δ (ppm) = 162.7 (CB), 143.3 (Cq), 142.3 (Cq), 141.6 (Cq), 137.3 (Cq), 136.2 (CH), 134.4 (Cq), 134.2 (CH), 130.2 (CH), 128.9 (CH), 127.8 (CH), 127.5 (CH), 127.5 (CH), 126.4 (CH), 125.2 (CH), 124.6 (CH), 124.2 (CH).

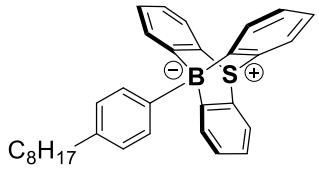
^{11}B NMR (160 MHz, $CDCl_3$) δ (ppm) = -9.2 (s).

HRMS (MALDI$^+$) (*m/z*): calc. for [$C_{42}H_{29}BKS^+$] : 615.1720, [M^+] : 615.1710

IR (neat, ATR): $\tilde{\nu}$ / cm^{-1} = 3052, 2910, 1584, 1498, 1425, 1293, 1256, 1199, 1015, 887, 746.

M.p. : 296°C (dec)

10-(4-octylphenyl)-9-sulfonium-10-boratriptycene-ate complex 4.40



According to **GP2** with the following quantities of octylbenzene (852 µl, 3.8 mmol, 30 equiv.).

Product obtained as inseparable mixture of two regioisomers (*m*:*p* 02:98)

Yield: 59%

TLC: R_f = 0.9 (50:50 *n*-hexane/CH_2Cl_2)

^{1}H NMR (500 MHz, $CDCl_3$) δ (ppm) = 8.01 (d, *J* = 7.7 Hz, 2H), 7.87 (d, *J* = 6.8 Hz, 3H), 7.77 (dd, *J* = 7.6, 0.7 Hz, 3H), 7.39 (d, *J* = 7.9 Hz, 2H), 7.23 (td, *J* = 7.4, 1.1 Hz, 3H), 7.06 (td, *J* = 7.5, 1.3 Hz, 3H), 2.79-2.74 (m, 2H), 1.84-1.75 (m, 2H), 1.52-1.45 (m, 2H), 1.45-1.30 (m, 8H), 0.92 (t, *J* = 6.9 Hz, 3H).

^{13}C NMR (126 MHz, $CDCl_3$) δ (ppm) = 163.5 (CB), 139.2 (Cq), 135.6 (CH), 134.4 (Cq), 134.3 (CH), 130.1 (CH), 127.7 (CH), 127.7 (CH), 124.1 (CH), 36.1 (CH_2), 32.1 (CH_2), 31.9 (CH_2), 29.8 (CH_2), 29.7 (CH_2), 29.5 (CH_2), 22.8 (CH_2), 14.3 (CH_3).

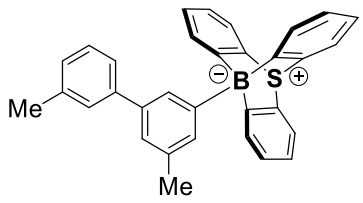
^{11}B NMR (160 MHz, $CDCl_3$) δ (ppm) = -9.3 (s).

HRMS (MALDI$^+$) (*m/z*): calc. for [$C_{32}H_{33}BNaS^+$] : 483.2294, [M^+] : 483.2285

IR (neat, ATR): $\tilde{\nu}$ / cm^{-1} = 2924, 2847, 1434, 1293, 1261, 1183, 1115, 1040, 896, 750.

M.p. : Could not be determined.

10-(5-(3,3'-dimethylbiphenyl))-9-sulfonium-10-boratriptycene-ate complex 4.41



According to **GP2** with the following quantities of 3,3'-dimethylbiphenyl (700 mg, 3.8 mmol, 30 equiv.).

Yield: 71%

TLC: R_f = 0.9 (50:50 *n*-hexane/CH_2Cl_2)

^{1}H NMR (500 MHz, $CDCl_3$) δ (ppm) = 8.10 (s, 1H), 7.96 (s, 1H), 7.93 (d, *J* = 6.8 Hz, 3H), 7.78 (dd, *J* = 7.6, 0.8 Hz, 3H), 7.56-7.53 (m, 2H), 7.46-7.44 (m, 1H), 7.33 (t, *J* = 8.0 Hz, 1H), 7.25 (td, *J* = 7.4, 1.2 Hz, 3H), 7.14 (d, *J* = 7.5 Hz, 1H), 7.08 (td, *J* = 7.5, 1.4 Hz, 3H), 2.58 (s, 3H), 2.42 (s, 3H).

^{13}C NMR (126 MHz, $CDCl_3$) δ (ppm) = 163.2 (CB), 143.3 (Cq), 140.3 (Cq), 138.1 (Cq), 137.0 (Cq), 135.5 (CH), 134.5 (Cq), 134.4 (CH), 132.0 (CH), 130.3 (CH), 128.6 (CH), 128.4 (CH), 127.7 (CH), 127.4 (CH), 124.8 (CH), 124.7 (CH), 124.2 (CH), 22.3 (CH_3), 21.8 (CH_3).

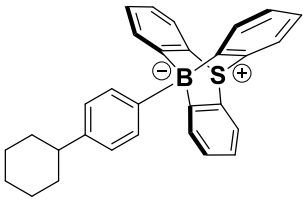
^{11}B NMR (160 MHz, $CDCl_3$) δ (ppm) = -9.1 (s).

HRMS (MALDI$^+$) (*m/z*): calc. for [$C_{32}H_{25}BNaS^+$] : 475.1668, [M^+] : 475.1663

IR (neat, ATR): $\tilde{\nu}$ / cm^{-1} = 3029, 1580, 1425, 1297, 1256, 1165, 1120, 955, 869, 787, 741.

M.p. :187-188 °C.

10-(4-cyclohexylphenyl)-9-sulfonium-10-boratriptycene-ate complex 4.42



According to **GP1** with the following quantities of cyclohexylbenzene (648 µl, 3.8 mmol, 30 equiv.).

Product obtained as inseparable mixture of two regioisomers (*m*:*p* 05:95)

Yield: 65%

TLC: R_f = 0.9 (50:50 *n*-hexane/CH_2Cl_2)

^{1}H NMR (500 MHz, $CDCl_3$) δ (ppm) = 8.01 (d, *J* = 7.8 Hz, 2H), 7.87 (d, *J* = 6.7 Hz, 3H), 7.76 (dd, *J* = 7.6, 0.8 Hz, 3H), 7.41 (d, *J* = 7.9 Hz, 2H), 7.23 (td, *J* = 7.3, 1.1 Hz, 3H), 7.06 (td, *J* = 7.5, 1.4 Hz, 3H), 2.65 (tt, *J* = 11.9, 3.3 Hz, 1H), 2.09 (d, *J* = 11.6 Hz, 2H), 1.90 (dt, *J* = 12.9, 3.1 Hz, 2H), 1.81 (d, *J* = 12.8 Hz, 1H), 1.61 (dq, *J* = 12.5, 2.9 Hz, 2H), 1.49 (tq, *J* = 12.8, 3.2 Hz, 2H), 1.34 (tq, *J* = 12.8, 3.6 Hz, 1H).

^{13}C NMR (126 MHz, $CDCl_3$) δ (ppm) = 163.2 (CB), 144.3 (Cq), 135.6 (CH), 1344 (Cq), 134.4 (CH), 130.1 (CH), 127.7 (CH), 126.1 (CH), 124.1 (CH), 44.5 (CH), 34.9 (CH_2), 27.3 (CH_2), 26.6 (CH_2).

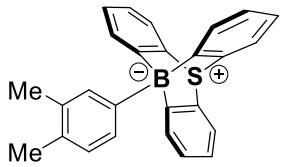
^{11}B NMR (160 MHz, $CDCl_3$) δ (ppm) = -9.3 (s).

HRMS (MALDI$^+$) (*m/z*): calc. for [$C_{30}H_{27}BNaS^+$] : 453.1824, [M^+] : 453.1828

IR (neat, ATR): $\tilde{\nu}$ / cm^{-1} = 3047, 2915, 2847, 1580, 1507, 1457, 1293, 1193, 1010, 869, 750.

M.p. :250-252 °C.

10-(4-(3,4-dimethylphenyl)-9-sulfonium-10-boratriptycene-ate complex 4.43



According to **GP1** with the following quantities of *o*-xylene (464 µl, 3.8 mmol, 30 equiv.).

Yield: 76%

TLC: R_f = 0.9 (50:50 *n*-hexane/CH_2Cl_2)

^{1}H NMR (500 MHz, $CDCl_3$) δ (ppm) = 7.93-7.88 (m, 4H), 7.84 (d, *J* = 7.3 Hz, 1H), 7.77 (dd, *J* = 7.6, 0.6 Hz, 3H), 7.36 (d, *J* = 7.4 Hz, 1H), 7.24 (td, *J* = 7.5, 1.1 Hz, 3H), 7.06 (td, *J* = 7.5, 1.4 Hz, 3H), 2.45 (s, 3H), 2.44 (s, 3H).

^{13}C NMR (126 MHz, $CDCl_3$) δ (ppm) = 163.3 (CB), 137.2 (CH), 135.3 (Cq), 134.5 (Cq), 134.4 (CH), 133.4 (CH), 132.7 (Cq), 130.1 (CH), 129.1 (CH), 127.7 (CH), 124.1 (CH), 20.4 (CH_3), 19.8 (CH_3).

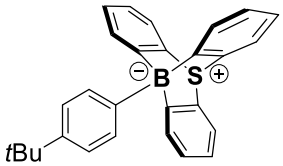
^{11}B NMR (160 MHz, $CDCl_3$) δ (ppm) = -9.3 (s).

HRMS (MALDI$^+$) (*m/z*): calc. for [$C_{26}H_{21}BNaS^+$] : 399.1355, [M^+] : 399.1354

IR (neat, ATR): $\tilde{\nu}$ / cm^{-1} = 3047, 1493, 1420, 1297, 1252, 1202, 1124, 1010, 937, 805, 750.

M.p. :266-268°C.

10-(4-(4-*ter*butylphenyl)-9-sulfonium-10-boratriptycene-ate complex 4.44



According to **GP1** with the following quantities of *ter*butylbenzene (597 µl, 3.8 mmol, 30 equiv.).

Product obtained as inseparable mixture of two regioisomers (*m*:*p* 12:88)

Yield: 64%

TLC: R_f = 0.9 (50:50 *n*-hexane/CH_2Cl_2)

^{1}H NMR (500 MHz, $CDCl_3$) δ (ppm) = (*m*-isomer) 8.12 (s, 1H), 7.97 (d, *J* = 7.3 Hz, 1H), 7.88-7.86 (m, 3H), 7.80-7.76 (m, 3H), 7.72 (dd, *J* = 7.5, 1.1 Hz, 1H), 7.53 (t, *J* = 7.5 Hz, 1H), 7.44 (d, *J* = 7.8 Hz, 1H), 7.27-7.22 (m, 3H), 7.10-7.05 (m, 3H), 1.45 (s, 9H). (*p*-isomer) 8.03 (d, *J* = 8.0 Hz, 2H), 7.89 (d, *J* = 7.4 Hz, 3H), 7.61-7.58 (m, 2H), 7.24 (td, *J* = 7.4, 1.2 Hz, 3H), 7.06 (td, *J* = 7.5, 1.4 Hz, 3H), 1.49 (s, 9H).

^{13}C NMR (126 MHz, $CDCl_3$) δ (ppm) = 163.3 (CB), 147.2 (Cq), 135.4 (CH), 134.4 (Cq), 134.4 (CH), 130.1 (CH), 127.7 (CH), 124.5 (CH), 124.1 (CH), 34.6 (Cq), 31.8 (CH_3).

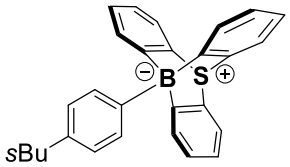
^{11}B NMR (160 MHz, $CDCl_3$) δ (ppm) = (*m*-isomer) -9.0 (s), (*p*-isomer) -9.3 (s).

HRMS (MALDI$^+$) (*m/z*): calc. for [$C_{28}H_{25}BNaS^+$] : 427.1668, [M^+] : 427.1662

IR (neat, ATR): $\tilde{\nu}$ / cm^{-1} = 2947, 2869, 1489, 1416, 1265, 1202, 1120, 1019, 869, 846, 814, 750.

M.p. :242-249 °C.

10-(4-(4-*sec*butylphenyl)-9-sulfonium-10-boratriptycene-ate complex 4.45



According to **GP1** with the following quantities of *sec*butylbenzene (598 µl, 3.8 mmol, 30 equiv.).

Product obtained as inseparable mixture of two regioisomers (*m*:*p* 07:93)

Yield: 25%

TLC: R_f = 0.9 (50:50 *n*-hexane/CH_2Cl_2)

^{1}H NMR (500 MHz, $CDCl_3$) δ (ppm) = 7.99 (d, *J* = 7.6 Hz, 2H), 7.86 (d, *J* = 7.2 Hz, 3H), 7.76 (d, *J* = 7.5 Hz, 3H), 7.37 (d, *J* = 7.9 Hz, 2H), 7.23 td, *J* = 7.3, 0.9 Hz, 3H), 7.05 (td, *J* = 7.5, 1.2 Hz, 3H), 2.72 (sext, *J* = 7.0 Hz, 1H), 1.83-1.63 (m, 2H), 1.39 (d, *J* = 7.0 Hz, 3H), 0.97 (t, *J* = 7.4 Hz, 3H).

^{13}C NMR (126 MHz, $CDCl_3$) δ (ppm) = 163.6 (CB), 143.8 (Cq), 135.5 (CH), 134.4 (Cq), 134.3 (CH), 130.0 (CH), 127.6 (CH), 126.3 (CH), 124.1 (CH), 41.5 (CH), 31.6 (CH_2), 21.9 (CH_3), 12.7 (CH_3).

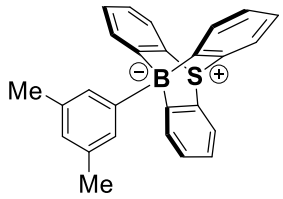
^{11}B NMR (160 MHz, $CDCl_3$) δ (ppm) = (*m*-isomer) -9.0 (s), (*p*-isomer) -9.3 (s).

HRMS (MALDI$^+$) (*m/z*): calc. for [$C_{28}H_{25}BNaS^+$] : 427.1668, [M^+] : 427.1659

IR (neat, ATR): $\tilde{\nu}$ / cm^{-1} = 3043, 2951, 2860, 1434, 1297, 1265, 1188, 1010, 896, 750.

M.p. :264°C (dec)

10-(5-(1,3-dimethylphenyl)-9-sulfonium-10-boratriptycene-ate complex 4.46



According to **GP1** with the following quantities of *m*-xylene (475 µl, 3.8 mmol, 30 equiv.).[S1]

Yield: 85%

The ^{1}H, ^{13}C and ^{11}B NMR data are identical to that previously reported.

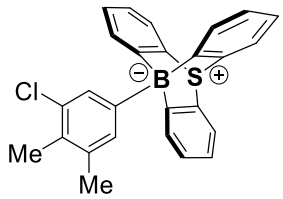
TLC: R_f = 0.9 (50:50 *n*-hexane/CH_2Cl_2)

^{1}H NMR (500 MHz, $CDCl_3$) δ (ppm) = 7.89 (d, *J* = 7.4 Hz, 3H), 7.76 (d, *J* = 7.6 Hz, 3H), 7.73 (s, 2H), 7.25 (t, *J* = 7.3 Hz, 3H), 7.09-7.04 (m, 4H), 2.48 (s, 6H).

^{13}C NMR (126 MHz, $CDCl_3$) δ (ppm) = 163.0 (CB), 136.6 (Cq), 134.5 (Cq), 134.5 (CH), 133.6 (CH), 130.2 (CH), 127.7 (CH), 126.6 (CH), 124.2 (CH), 22.1 (CH_3).

^{11}B NMR (160 MHz, $CDCl_3$) δ (ppm) = -9.3 (s).

10-(5-(2,3-dimethylchlorophenyl)-9-sulfonium-10-boratriptycene-ate complex 4.47



According to **GP1** with the following quantities of 2,3-dimethylchlorobenzene (492 µl, 3.8 mmol, 30 equiv.).

Yield: 65%

TLC: R_f = 0.9 (50:50 *n*-hexane/CH_2Cl_2)

^{1}H NMR (500 MHz, $CDCl_3$) δ (ppm) = 7.93 (s, 1H), 7.84 (d, *J* = 7.2 Hz, 3H), 7.76 (dd, *J* = 7.7, 0.8 Hz, 3H), 7.74 (s, 1H), 7.25 (td, *J* = 7.4, 1.2 Hz, 3H), 7.07 (td, *J* = 7.5, 1.4 Hz, 3H), 2.47 (s, 3H), 2.45 (s, 3H).

^{13}C NMR (126 MHz, $CDCl_3$) δ (ppm) = 137.3 (Cq), 135.8 (CH), 134.4 (Cq), 134.1 (CH), 133.7 (CH), 130.4 (Cq), 130.3 (CH), 127.8 (CH), 124.3 (CH), 21.4 (CH_3), 16.3 (CH_3).

The carbon atoms directly attached to the boron atom on the triptycene core were not detected, likely due to quadrupolar relaxation.

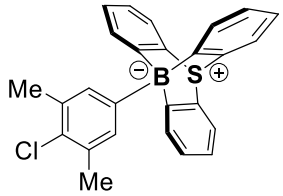
^{11}B NMR (160 MHz, $CDCl_3$) δ (ppm) = -9.6 (s).

HRMS (MALDI^{+}) (*m/z*): calc. for [$C_{26}H_{20}BNaSCl^{+}$] : 433.0965, [M^{+}] : 433.0958

IR (neat, ATR): $\tilde{\nu}$ / cm^{-1} = 3043, 1534, 1475, 1429, 1293, 1256, 1215, 1138, 1006, 969, 892, 801, 750.

M.p. : >300 °C

10-(4-(1-chloro-2,6-dimethylphenyl)-9-sulfonium-10-boratriptycene-ate complex 4.48



According to **GP1** with the following quantities of 2,6-dimethylchlorobenzene (510 µl, 3.8 mmol, 30 equiv.).[S1]

Yield: 57%

The ^{1}H, ^{13}C and ^{11}B NMR data are identical to that previously reported.

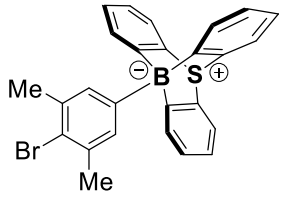
TLC: R_f = 0.9 (50:50 *n*-hexane/CH_2Cl_2)

^{1}H NMR (500 MHz, $CDCl_3$) δ (ppm) = = 7.84 (d, J = 7.4 Hz, 3H), 7.81 (s, 2H), 7.78 (d, J = 7.7 Hz, 3H), 7.26 (t, J = 7.4 Hz, 3H), 7.08 (t, J = 7.5 Hz, 3H), 2.54 (s, 6H).

^{13}C NMR (126 MHz, $CDCl_3$) δ (ppm) = = 162.7, 136.0, 134.8 (Cq), 134.4 (Cq), 134.2, 131.5 (Cq), 130.3, 127.8, 124.3, 21.2 (CH3).

^{11}B NMR (160 MHz, $CDCl_3$) δ (ppm) = -9.6 (s).

10-(4-(2,6-dimethylbromophenyl)-9-sulfonium-10-boratriptycene-ate complex 4.49



According to **GP1** with the following quantities of 2,6-dimethylbromobenzene (512 µl, 3.8 mmol, 30 equiv.).

Yield: 57%

TLC: R_f = 0.9 (50:50 *n*-hexane/CH_2Cl_2)

^{1}H NMR (500 MHz, $CDCl_3$) δ (ppm) = 7.85 (d, *J* = 7.3 Hz, 3H), 7.81 (s, 2H), 7.78 (dd, *J* = 7.7, 1.0 Hz, 3H), 7.26 (td, *J* = 7.6, 1.0 Hz, 3H), 7.08 (td, *J* = 7.4, 1.3 Hz, 3H), 2.58 (s, 6H).

^{13}C NMR (126 MHz, $CDCl_3$) δ (ppm) = 162.7 (CB), 136.8 (Cq), 135.9 (CH), 134.4 (Cq), 134.2 (CH), 130.3 (CH), 127.8 (CH), 124.5 (Cq), 124.3 (CH), 24.4 (CH_3).

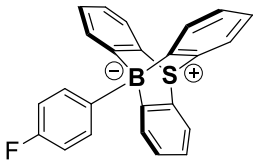
^{11}B NMR (160 MHz, $CDCl_3$) δ (ppm) = -9.5 (s).

HRMS (MALDI$^+$) (*m/z*): calc. for [$C_{26}H_{20}BNaS^{79}Br^+$] : 477.0460, [$M^+$] : 477.0458

IR (neat, ATR): $\tilde{\nu}$ / cm^{-1} = 3052, 1439, 1375, 1297, 1252, 1170, 1129, 1015, 955, 787, 750.

M.p. : >300 °C

10-(4-fluorophenyl)-9-sulfonium-10-boratriptycene-ate complex 4.10



According to **GP1** with the following quantities of fluorobenzene (966 µl, 10 mmol, 80 equiv.).[S1]

Product obtained as inseparable mixture of two regioisomers (*o*:*p* 10:90)

Yield: 64%

The ^{1}H, ^{13}C and ^{11}B NMR data are identical to that previously reported.

TLC: R_f = 0.9 (50:50 *n*-hexane/CH_2Cl_2)

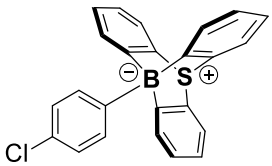
^{1}H NMR (500 MHz, $CDCl_3$) δ (ppm) = 8.06-8.00 (m, 2H), 7.80 (d, J = 7.4 Hz, 3H), 7.77 (dd, J = 7.6, 0.6 Hz, 3H), 7.27-7.22 (m, 5H), 7.07 (dt, J = 7.5, 1.4 Hz, 3H).

^{13}C NMR (126 MHz, $CDCl_3$) δ (ppm) = 161.4 (d, J = 242.2 Hz, Cq), 136.9 (6.2 Hz, CH), 134.4 (Cq), 134.0 (CH), 130.3 (CH), 127.8 (CH), 124.3 (CH), 114.3 (d, J = 18.1 Hz, CH). The carbon atoms directly attached to the boron atom on the triptycene core were not detected, likely due to quadrupolar relaxation.

^{11}B NMR (160 MHz, $CDCl_3$) δ (ppm) = -9.5 (s, p-isomer), -10.0 (s, o-isomer)

^{19}F NMR (483 MHz, $CDCl_3$) δ (ppm) = -115.0 (s, o-isomer), -119.2 (s, p-isomer)

10-(4-chlorophenyl)-9-sulfonium-10-boratriptycene-ate complex 4.13



According to **GP1** with the following quantities of chlorobenzene (1.04 ml, 10 mmol, 80 equiv.).[S1]

Product obtained as inseparable mixture of two regioisomers (*m*:*p* 20:80)

Yield: 66%

The ^{1}H, ^{13}C and ^{11}B NMR data are identical to that previously reported.

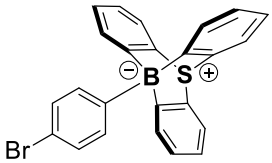
TLC: R_f = 0.9 (50:50 *n*-hexane/CH_2Cl_2)

^{1}H NMR (500 MHz, $CDCl_3$) δ (ppm) = (*m*-isomer) 8.09 (s, 1H), 7.96 (d, J = 7.5 Hz, 1H), 7.83- 7.76 (m, 6H), 7.49 (t, J = 7.7 Hz, 1H), 7.38 (d, J = 7.8 Hz, 1H), 7.27-7.22 (m, 3H), 7.08 (t, J = 7.5 Hz, 3H). (*p*-isomer) 8.03 (d, J = 7.5 Hz, 2H), 7.83-7.76 (m, 6H), 7.53 (dd, J = 8.1, 1.3 Hz, 2H), 7.27-7.22 (m, 3H), 7.08 (t, J = 7.5 Hz, 3H)

^{13}C NMR (126 MHz, $CDCl_3$) δ (ppm) = 137.1, 134.5, 134.0, 130.3,127.8, 127.7, 124.4, 124.3. The carbon atoms directly attached to the boron atom on the triptycene core were not detected, likely due to quadrupolar relaxation.

^{11}B NMR (160 MHz, $CDCl_3$) δ (ppm) = -9.5

10-(4-bromophenyl)-9-sulfonium-10-boratriptycene-ate complex 4.25



According to **GP1** with the following quantities of bromobenzene (1.07 ml, 10 mmol, 80 equiv.).[S1]

Product obtained as inseparable mixture of two regioisomers (*m*:*p* 23:77)

Yield: 49%

The ^{1}H, ^{13}C and ^{11}B NMR data are identical to that previously reported.

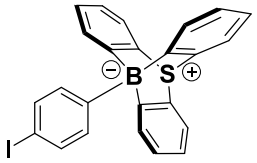
TLC: R_f = 0.9 (50:50 *n*-hexane/CH_2Cl_2)

^{1}H NMR (500 MHz, $CDCl_3$) δ (ppm) = (*m*-isomer) 8.24 (s, 1H), 8.11-7.98 (m, 1H), 7.82-7.76 (m, 6H), 7.53 (ddd, J = 7.9, 2.1, 1.1 Hz, 1H), 7.42 (t, J = 7.6 Hz, 1H), 7.28-7.24 (m, 3H), 7.08 (t, J = 7.5 Hz, 3H). (*p*-isomer) 7.96 (d, J = 7.8 Hz, 2H), 7.82-7.76 (m, 6H), 7.67 (d, J = 8.3 Hz, 2H), 7.24 (td, J = 7.4, 1.2 Hz, 3H), 7.08 (td, J = 7.5, 1.5 Hz, 3H).

^{13}C NMR (126 MHz, $CDCl_3$) δ (ppm) = 137.6, 134.4, 134.0, 130.7, 130.3, 127.8, 124.4. The carbon atoms directly attached to the boron atom on the triptycene core were not detected, likely due to quadrupolar relaxation.

^{11}B NMR (160 MHz, $CDCl_3$) δ (ppm) = -9.4

10-(4-iodophenyl)-9-sulfonium-10-boratriptycene-ate complex 4.26



According to **GP1** with the following quantities of iodobenzene (1.16 ml, 10 mmol, 80 equiv.).[S1]

Product obtained as inseparable mixture of two regioisomers (*m*:*p* 33:67)

Yield: 47%

The ^{1}H, ^{13}C and ^{11}B NMR data are identical to that previously reported.

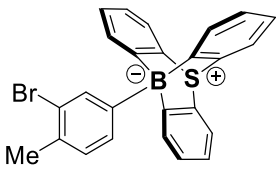
TLC: R_f = 0.9 (50:50 *n*-hexane/CH_2Cl_2)

^{1}H NMR (500 MHz, $CDCl_3$) δ (ppm) = (*m*-isomer) 8.44 (s, 1H), 8.03 (d, J = 7.4 Hz, 1H), 7.80- 7.76 (m, 6H), 7.73 (ddd, J = 7.8, 1.8, 1.1 Hz, 1H), 7.30 (t, J = 7.6 Hz, 1H), 7.26 (t, J = 7.4 Hz, 3H), 7.08 (t, J = 7.5 Hz, 3H). (*p*-isomer) 7.87 (d, J = 8.3 Hz, 2H), 7.83 (d, J = 8.1 Hz, 2H), 7.80-7.76 (m, 6H), 7.24 (td, J = 7.4, 1.2 Hz, 3H), 7.08 (td, J = 7.5, 1.4 Hz, 3H).

^{13}C NMR (126 MHz, $CDCl_3$) δ (ppm) = 162.6, 144.3, 137.9, 136.6, 134.7, 134.4 (Cq), 134.3 (Cq), 134.0, 133.9, 133.9, 130.4, 130.3, 127.9, 124.4, 124.3, 91.0

^{11}B NMR (160 MHz, $CDCl_3$) δ (ppm) = -9.5 (s), -9.7 (s)

10-(3-bromo-4-methylphenyl)-9-sulfonium-10-boratriptycene-ate complex 4.50



According to **GP2** with the following quantities of 2-bromotoluene (1.2 ml, 10 mmol, 80 equiv.).

Product obtained as inseparable mixture of two regioisomers (*m*:*p* 50:50)

Yield: 65%

TLC: R_f = 0.9 (50:50 *n*-hexane/CH_2Cl_2)

^{1}H NMR (500 MHz, $CDCl_3$) δ (ppm) = (3-bromo isomer) 8.27 (s, 1H), 7.82 (dd, *J* = 7.1, 1.9 Hz, 3H), 7.78 (d, *J* = 7.7 Hz, 3H), 7.76-7.73 (m, 1H), 7.43 (d, *J* = 7.5 Hz, 1H), 7.28-7.23 (m, 3H), 7.08 (t, *J* = 7.5 Hz, 3H), 2.56 (s, 3H). (4-bromo isomer) 7.98 (s, 1H), 7.90 (d, *J* = 7.3 Hz, 1H), 7.82 (dd, *J* = 7.1, 1.9 Hz, 3H), 7.78 (d, *J* = 7.7 Hz, 3H), 7.71 (d, *J* = 8.0 Hz, 1H), 7.28-7.23 (m, 3H), 7.08 (t, *J* = 7.5 Hz, 3H), 2.55 (s, 3H).

^{13}C NMR (126 MHz, $CDCl_3$) δ (ppm) = 162.5 (CB), 139.1 (CH), 138.4 (CH), 135.0 (CH), 134.8 (CH), 134.3 (Cq), 134.3 (Cq), 134.1 (CH), 134.0 (CH), 133.8 (Cq), 131.5 (CH), 130.4 (CH), 130.3 (CH), 130.3 (CH), 127.8 (CH), 124.3 (CH), 121.7 (CH), 23.4 (CH_3), 22.9 (CH_3).

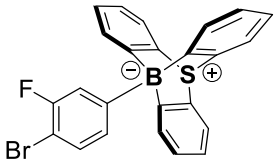
^{11}B NMR (160 MHz, $CDCl_3$) δ (ppm) = (4-bromo isomer) -9.5 (s) (3-bromo isomer) -9.7 (s).

HRMS (MALDI$^+$) (*m/z*): calc. for [$C_{25}H_{18}BS^{79}Br^+$] : 463.0303, [M^+] : 463.0305

IR (neat, ATR): $\tilde{\nu}$ / cm^{-1} = 3043, 2961, 2929, 1639, 1589, 1511, 1466, 1425, 1265, 1179, 1092, 983, 878, 760.

M.p. : 252-253°C

10-(3-(4-fluorobromophenyl)-9-sulfonium-10-boratriptycene-ate complex 4.51



According to **GP1** with the following quantities of 2-fluoro-bromobenzene (1.12 ml, 10 mmol, 80 equiv.).

Yield: 26%

TLC: R_f = 0.9 (50:50 *n*-hexane/CH_2Cl_2)

^{1}H NMR (500 MHz, $CDCl_3$) δ (ppm) = 8.24 (d, *J* = 7.3 Hz, 1H), 7.93 (s, 1H), 7.78 (d, *J* = 7.7 Hz, 3H), 7.75 (d, *J* = 7.3 Hz, 3H), 7.33-7.28 (m, 1H), 7.26 (td, *J* = 7.3, 1.1 Hz, 3H), 7.09 (td, *J* = 7.4, 1.2 Hz, 3H).

^{13}C NMR (126 MHz, $CDCl_3$) δ (ppm) = 140.0 (CH), 136.0 (d, *J* = 6.1 Hz, CF), 134.3 (Cq), 133.8 (CH), 130.4 (CH), 127.9 (CH), 124.5 (CH).

The carbon atoms directly attached to the boron atom on the triptycene core were not detected, likely due to quadrupolar relaxation.

^{11}B NMR (160 MHz, $CDCl_3$) δ (ppm) = -9.5 (s).

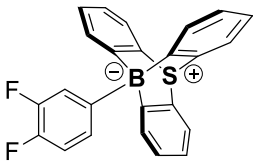
^{19}F NMR (483 MHz, $CDCl_3$) δ (ppm) = (*o*-isomer) -110.6, (*m*-isomer) -114.2, (*p*-isomer) -113.6.

HRMS (MALDI$^+$) (*m/z*): calc. for [$C_{24}H_{15}BNaSBrF^+$] : 467.0053, [M^+] : 467.0060

IR (neat, ATR): $\tilde{\nu}$ / cm^{-1} = 3047, 1571, 1480, 1429, 1297, 1261, 1234, 1183, 1047, 919, 801, 750.

M.p. : 265-267°C

10-(3-(*o*-difluorophenyl)-9-sulfonium-10-boratriptycene-ate complex 4.52



According to **GP1** with the following quantities of *o*-difluorobenzene (1.12 ml, 10 mmol, 80 equiv.).

Yield: 22%

TLC: R_f = 0.9 (50:50 *n*-hexane/CH_2Cl_2)

^{1}H NMR (500 MHz, $CDCl_3$) δ (ppm) = 7.87-7.81 (m, 1H), 7.80-8.71 (m, 7H), 7.36-7.28 (m, 1H), 7.26 (td, *J* = 7.3, 1.2 Hz, 3H), 7.09 (td, *J* = 7.5, 1.4 Hz, 3H).

^{13}C NMR (126 MHz, $CDCl_3$) δ (ppm) = 162.3 (CB), 134.3 (Cq), 133.8 (CH), 131.3 (CH), 130.4 (CH), 127.9 (CH), 124.4 (CH), 123.5 (d, *J* = 13.6 Hz, CF), 116.3 (d, *J* = 13.3 Hz, CF).

^{11}B NMR (160 MHz, $CDCl_3$) δ (ppm) = -9.7 (s).

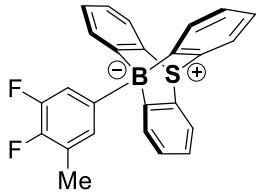
^{19}F NMR (483 MHz, $CDCl_3$) δ (ppm) = -141.1 (s), -144.6 (s)

HRMS (MALDI$^+$) (*m/z*): calc. for [$C_{24}H_{15}BNaSF_2^+$] : 407.0853, [M^+] : 407.0849

IR (neat, ATR): $\tilde{\nu}$ / cm^{-1} = 3047, 1603, 1502, 1429, 1384, 1265, 1151, 1120, 1019, 951, 805, 746.

M.p. : 250°C (dec)

10-(5-(1,2-difluoro-3-methylphenyl))-9-sulfonium-10-boratriptycene-ate complex 4.53



According to **GP1** with the following quantities of *o*-difluorobenzene (1.2 ml, 10 mmol, 80 equiv.).

Yield: 21%

TLC: R_f = 0.9 (50:50 *n*-hexane/CH_2Cl_2)

^{1}H NMR (500 MHz, $CDCl_3$) δ (ppm) = 7.80-7.75 (m, 6H), 7.69-7.58 (m, 2H), 7.26 (td, *J* = 6.9, 1.0 Hz, 3H), 7.08 (td, *J* = 7.5, 1.4 Hz, 3H), 2.45 (d, *J* = 1.9 Hz, 3H).

^{13}C NMR (126 MHz, $CDCl_3$) δ (ppm) = 162.5 (CB), 134.3 (Cq), 134.1, 133.9 (CH), 132.9, 130.3 (CH), 127.9 (CH), 127.7, 124.4 (CH), 124.3, 120.8 (d, *J* = 13.7 Hz, CF), 15.0 (CH_3).

^{11}B NMR (160 MHz, $CDCl_3$) δ (ppm) = (5-isomer) -9.7 (s), (6-isomer) -10.0 (s).

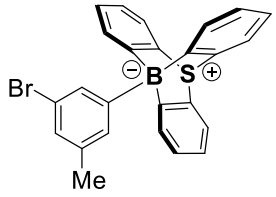
^{19}F NMR (483 MHz, $CDCl_3$) δ (ppm) = (5-isomer) -142.2 (dd, *J* = 20.7, 12.2 Hz, 1F), -149.1 (dt, *J* = 15.9, 7.4 Hz, 1F), (6-isomer) -123.6 (d, *J* = 21.8 Hz, 1H), -144.5 (d, *J* = 22.0 Hz, 1H).

HRMS (MALDI$^+$) (*m/z*): calc. for [$C_{25}H_{17}BNaSF_2^+$] : 421.1010, [M^+] : 421.1006

IR (neat, ATR): $\tilde{\nu}$ / cm^{-1} = 3047, 1603, 1507, 1420, 1384, 1302, 1261, 1156, 1033, 969, 755.

M.p. : 244°C (dec)

10-(3-(1-bromo-3-methylphenyl)-9-sulfonium-10-boratriptycene-ate complex 4.54



According to **GP1** with the following quantities of 3-bromotoluene (777 µl, 64 mmol, 50 equiv.).

Yield: 23%

TLC: R_f = 0.9 (50:50 *n*-hexane/CH_2Cl_2)

^{1}H NMR (500 MHz, $CDCl_3$) δ (ppm) = 8.00 (s, 1H), 7.83-7.78 (m, 4H), 7.77 (dd, *J* = 7.6, 0.8 Hz, 3H), 7.36 (s, 1H), 7.26 (td, *J* = 7.4, 1.2 Hz, 3H), 7.08 (td, *J* = 7.5, 1.4 Hz, 3H), 2.46 (s, 3H).

^{13}C NMR (126 MHz, $CDCl_3$) δ (ppm) = 135.2 (CH), 135.0 (CH), 134.4 (CH), 134.1 (CH), 130.4 (CH), 128.6 (CH), 127.8 (CH), 124.4 (CH), 21.8 (CH_3).

The carbon atoms directly attached to the boron atom on the triptycene core were not detected, likely due to quadrupolar relaxation.

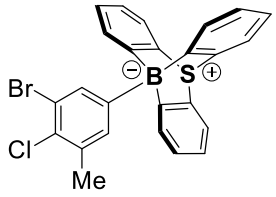
^{11}B NMR (160 MHz, $CDCl_3$) δ (ppm) = -9.6 (s).

HRMS (MALDI$^+$) (*m/z*): calc. for [$C_{25}H_{18}BNaS^{79}Br^+$] : 463.0303, [$M^+$] : 463.0290

IR (neat, ATR): $\tilde{\nu}$ / cm^{-1} = 3038, 1584, 1553, 1425, 1288, 1261, 1234, 1156, 960, 851, 810, 755.

M.p. : >300 °C

10-(5-(1-bromo-2chloro-3-methylphenyl)-9-sulfonium-10-boratriptycene-ate complex 4.55



According to **GP1** with the following quantities of 1-bromo-2-chloro-3-methylbenzene (1.32 g, 64 mmol, 50 equiv.).

Yield: 26%

TLC: R_f = 0.9 (50:50 *n*-hexane/CH_2Cl_2)

^{1}H NMR (500 MHz, $CDCl_3$) δ (ppm) = 8.18 (s, 1H), 7.86 (s, 1H), 7.78 (dd, *J* = 7.6, 1.0 Hz, 6H), 7.27 (td, *J* = 7.4, 1.1 Hz, 3H), 7.09 (td, *J* = 7.5, 1.3 Hz, 3H), 2.57 (s, 3H).

^{13}C NMR (126 MHz, $CDCl_3$) δ (ppm) = 162.2 (CB), 138.1 (CH), 137.2 (CH), 137.1 (Cq), 134.3 (Cq), 133.8 (CH), 130.5 (Cq), 130.4 (CH), 127.9 (CH), 124.5 (CH), 22.1 (CH_3).

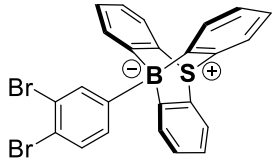
^{11}B NMR (160 MHz, $CDCl_3$) δ (ppm) = -9.8 (s).

HRMS (MALDI$^+$) (*m/z*): calc. for [$C_{25}H_{17}BNaSCl^{79}Br^+$] : 496.9914, [$M^+$] : 496.9901

IR (neat, ATR): $\tilde{\nu}$ / cm^{-1} = 3043, 1530, 1434, 1302, 1265, 1197, 1129, 1047, 965, 896, 846, 746.

M.p. : >300 °C

10-(5-(1,2-dibromophenyl)-9-sulfonium-10-boratriptycene-ate complex 4.56



According to **GP1** with the following quantities of *o*-dibromobenzene (773 µl, 64 mmol, 50 equiv.).

Yield: 18%

TLC: R_f = 0.9 (50:50 *n*-hexane/CH_2Cl_2)

^{1}H NMR (500 MHz, $CDCl_3$) δ (ppm) = 8.34 (s, 1H), 7.84 (d, *J* = 7.7 Hz, 1H), 7.79-773 (m, 7H), 7.27 (td, *J* = 7.4, 1.1 Hz, 3H), 7.09 (td, *J* = 7.5, 1.3 Hz, 3H).

^{13}C NMR (126 MHz, $CDCl_3$) δ (ppm) = 140.5 (CH), 136.0 (CH), 134.2 (Cq), 133.7 (CH), 132.9 (Cq), 130.4 (CH), 127.9 (CH), 124.4 (CH).

The carbon atoms directly attached to the boron atom on the triptycene core were not detected, likely due to quadrupolar relaxation.

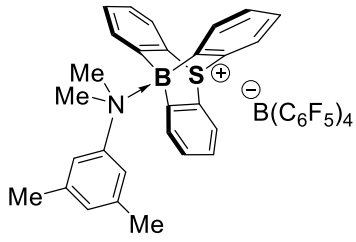
^{11}B NMR (160 MHz, $CDCl_3$) δ (ppm) = -9.8 (s).

HRMS (MALDI$^+$) (*m/z*): calc. for [$C_{24}H_{15}BNaS^{79}Br^+$] : 526.9252, [$M^+$] : 526.9236

IR (neat, ATR): $\tilde{\nu}$ / cm^{-1} = 3052, 2920, 2851, 1448, 1261, 1188, 1115, 1010, 905, 760.

M.p. : 257-259°C

10-(*N*,*N*,3,5-tetramethylaniline)-9-sulfonium-10-boratriptycene Lewis adduct tetrakis(pentafluorophenyl)borate 4.57



Under glovebox conditions in a Schlenk tube, $HNTf_2$ (40 mg, 0.14 mmol, 1.1 equiv.) was added to a suspension of 10-mesityl-9-sulfonium-10-boratritpycene-ate complex **1**

(50 mg, 0.13 mmol, 1.0 equiv.) in 1,2,3,4-tetrafluorobenzene (3.0 ml). The reaction was stirred for 5min then $NaB(C_6F_5)_4$ (139 mg, 0.19 mmol, 1.5 equiv.) and stirred for further 5 min. 3,5,*N*,*N*-Tetramethylaniline (**TMA**) (105 µl, 0.64 mmol, 5.0 equiv.). The Schlenk tube was then sealed with a glass stopper, stirred and warmed in an oil bath at 60°C. After 16h, the volatiles were removed and the crude was purified via flash chromatography (50:50 *n*-hexane/CH_2Cl_2) affording pure 10-(*N*,*N*,3,5-tetramethylaniline)-9-sulfonium-10-boratriptycene Lewis adduct tetrakis(pentafluorophenyl)borate (82 mg, 0.074 mmol, 58%).

Yield: 58%

TLC: R_f = 0.3 (50:50 *n*-hexane/CH_2Cl_2)

^{1}H NMR (500 MHz, $CDCl_3$) δ (ppm) = 8.05 (d, *J* = 7.6 Hz, 1H), 7.97 (d, *J* = 7.7 Hz, 1H), 7.94-7.91 (m, 2H), 7.53-7.45 (m, 3H), 7.33-7.25 (m, 7H), 7.08 (s, 3H), 4.21-4.17 (m, 6H), 2.32-2.03 (br, 6H).

^{13}C NMR (126 MHz, $CDCl_3$) δ (ppm) = 150.8, (Cq), 149.3 (Cq), 147.4 (Cq), 137.3 (CH), 135.4 (CH), 134.8 (CH), 134.7 (CH), 133.4 (CH), 133.1 (CH), 132.7 (Cq), 131.3 (CH), 131.2 (CH), 130.6 (CH), 130.6 (CH), 130.1 (CH), 129.2 (CH), 129.1 (CH), 126.7 (CH), 126.6 (CH), 126.5 (CH), 57.8 (CH_3), 57.7 (CH_3), 21.4 (CH_3).

The carbon atoms directly attached to the boron atom on the triptycene core were not detected, likely due to quadrupolar relaxation.

^{11}B NMR (160 MHz, $CDCl_3$) δ (ppm) = 1.8 (br).

^{19}F NMR (483 MHz, $CDCl_3$) δ (ppm) = -132.4 (d, *J* = 10.1 Hz, 8F), -162.9 (t, *J* = 20.5 Hz, 4F), -166.6 (t, *J* = 18.1 Hz, 8F).

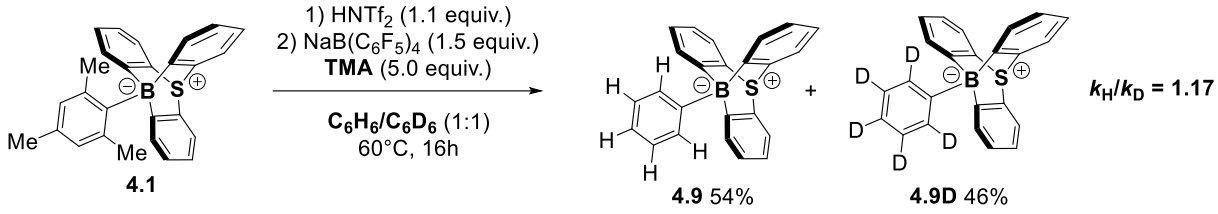
HRMS (MALDI$^+$) (*m/z*): calc. for [$C_{28}H_{27}BNNaS^+$] : 420.1957, [M^+] : 420.1946

IR (neat, ATR): $\tilde{\nu}$ / cm^{-1} = 2951, 2865, 1648, 1511, 1452, 1370, 1275, 1079, 978, 878, 750.

M.p. : 81-82 °C

IV.4 Kinetic isotope effect

IV.4.1 Isotope effect with benzene as substrate and TMA as Brønsted base.



In glovebox, $HNTf_2$ (24 mg, 0.084 mmol, 1.1 equiv.) was added to a suspension of 10-mesityl-9-sulfonium-10-boratriptycene-ate complex **4.1** (30 mg, 0.077 mmol, 1.0 equiv.) in benzene (1.50 ml) and benzene-d_6 (1.49 ml). The reaction mixture was stirred 5 min and $NaB(C_6F_5)_4$ (84 mg, 0.12 mmol, 1.5 equiv.). After stirring for further 5 min, *N*,*N*,3,5-tetramethylaniline (65 µl, 0.38 mmol, 5.0 equiv.) was added, the Schlenk tube was sealed with a glass stopper and put out of the glovebox. The mixture was stirred and warmed in an oil bath at 60°C. After 16h, the crude was evaporated to dryness and purified via flash chromatography. The k_H/k_D ratio is calculated using the signals of the triptycene scaffold as internal standard and the signals integrations from the exocyclic ring were compared to the fully hydrogenated product.

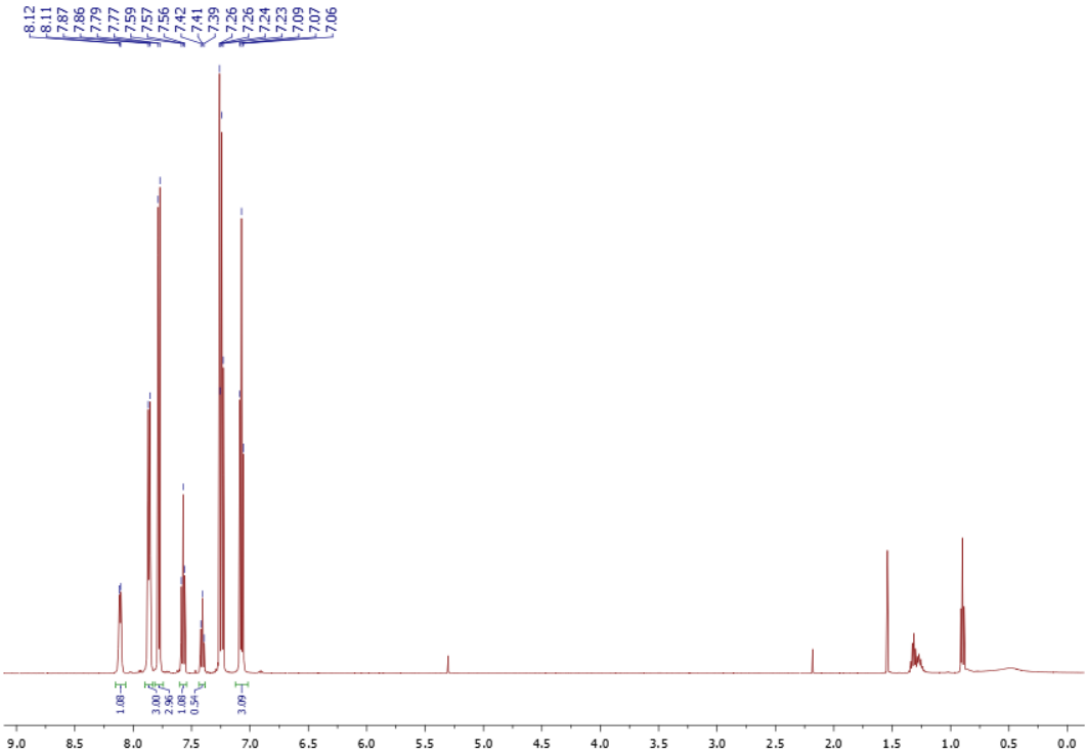
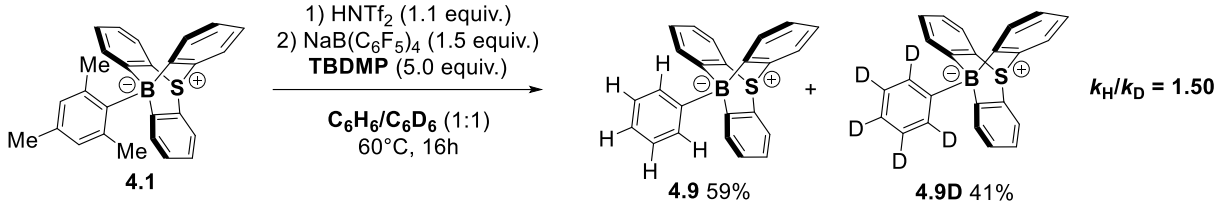


Figure SIV.1. ^{1}H NMR (500 MHz, 25°C, $CDCl_3$) of competition Csp^2–H borylation reaction between benzene and benzene-d_6 as substrate and TMA as base.

IV.4.2 Isotope effect with benzene as substrate and TBDMP as Brønsted base.



In glovebox, $HNTf_2$ (24 mg, 0.084 mmol, 1.1 equiv.) was added to a suspension of 10-mesityl-9-sulfonium-10-boratriptycene-ate complex (30 mg, 0.077 mmol, 1.0 equiv.) in benzene (1.50 ml) and benzene-d_6 (1.49 ml). The reaction mixture was stirred 5 min and $NaB(C_6F_5)_4$ (84 mg, 0.12 mmol, 1.5 equiv.). After stirring for further 5 min, TBDMP (78 mg, 0.38 mmol, 5.0 equiv.) was added, the Schlenk tube was sealed with a glass stopper and put out of the glovebox. The mixture was stirred and warmed in an oil bath at 60°C. After 16h, the crude was evaporated to dryness and purified via flash

chromatography. The k_H/k_D ratio is calculated using the signals of the triptycene scaffold as internal standard.

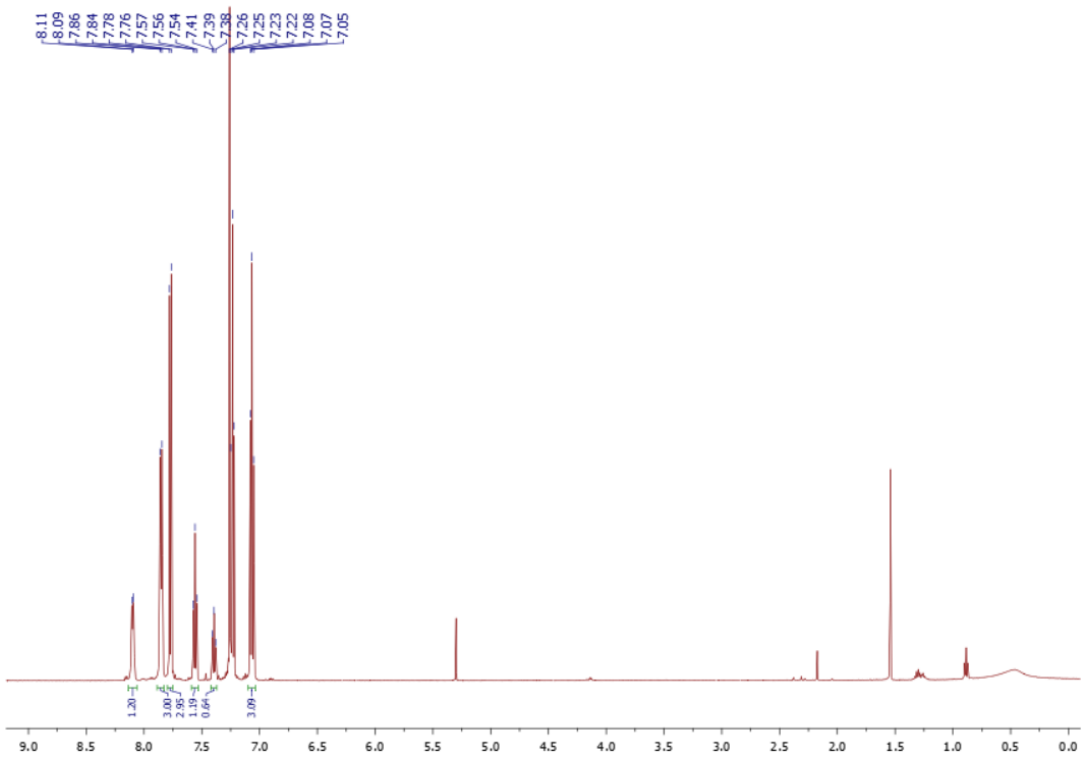
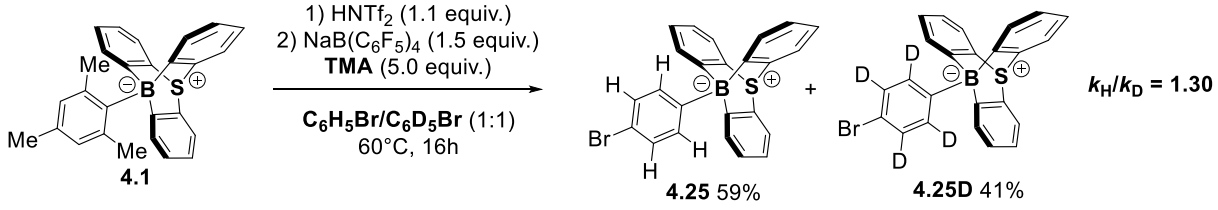


Figure SIV.2. ^{1}H NMR (500 MHz, 25°C, $CDCl_3$) of competition Csp^2–H borylation reaction between benzene and benzene-d_6 as substrate and TBDMP as base.

IV.4.3 Isotope effect with bromobenzene as substrate and TMA as Brønsted base.



In glovebox, $HNTf_2$ (24 mg, 0.084 mmol, 1.1 equiv.) was added to a suspension of 10-mesityl-9-sulfonium-10-boratriptycene-ate complex (30 mg, 0.077 mmol, 1.0 equiv.) in bromobenzene (1.50 ml) and bromobenzene-d_5 (1.50 ml). The reaction mixture was stirred 5 min and $NaB(C_6F_5)_4$ (84 mg, 0.12 mmol, 1.5 equiv.). After stirring for further 5

min, *N*,*N*,3,5-tetramethylaniline (65 µl, 0.38 mmol, 5.0 equiv.) was added, the Schlenk tube was sealed with a glass stopper and put out of the glovebox. The mixture was stirred and warmed in an oil bath at 60°C. After 16h, the crude was evaporated to dryness and purified via flash chromatography. The k_H/k_D ratio is calculated using the signals of the triptycene scaffold as internal standard.

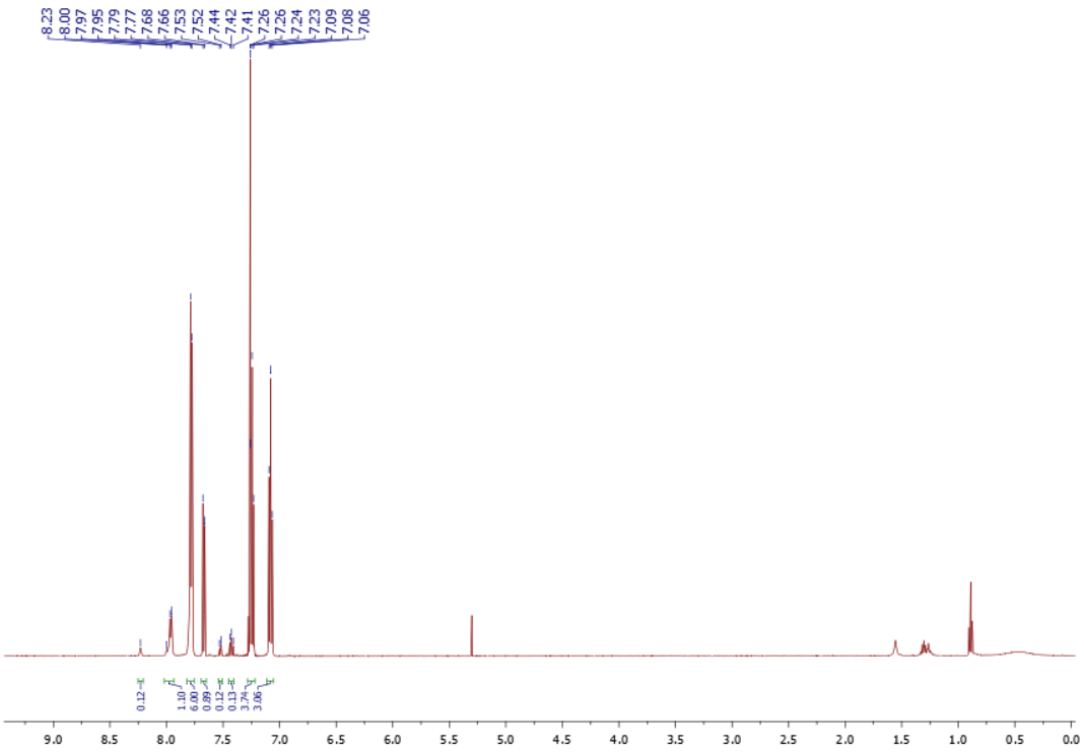
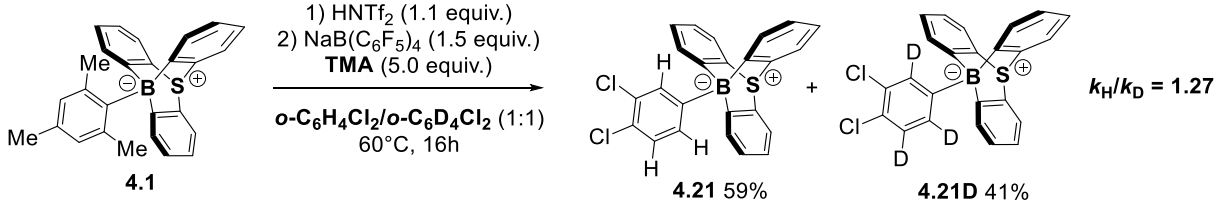


Figure SIV.3. ^{1}H NMR (500 MHz, 25°C, $CDCl_3$) of competition Csp^2–H borylation reaction between bromobenzene and bromobenzene-d_5 as substrate and TMA as base.

IV.4.4 Isotope effect with 1,2-dichlorobenzene as substrate and TMA as Brønsted base.



In glovebox, $HNTf_2$ (18 mg, 0.056 mmol, 1.1 equiv.) was added to a suspension of 10-mesityl-9-sulfonium-10-boratriptycene-ate complex (20 mg, 0.051 mmol, 1.0 equiv.) in

1,2-dichlorobenzene (1.00 ml) and 1,2-dichlorobenzene-d_4 (1.00 ml). The reaction mixture was stirred 5 min and $NaB(C_6F_5)_4$ (56 mg, 0.077 mmol, 1.5 equiv.). After stirring for further 5 min, *N*,*N*,3,5-tetramethylaniline (43 µl, 0.25 mmol, 5.0 equiv.) was added, the Schlenk tube was sealed with a glass stopper and put out of the glovebox. The mixture was stirred and warmed in an oil bath at 60°C. After 16h, the crude was evaporated to dryness and purified via flash chromatography. The k_H/k_D ratio is calculated using the signals of the triptycene scaffold as internal standard.

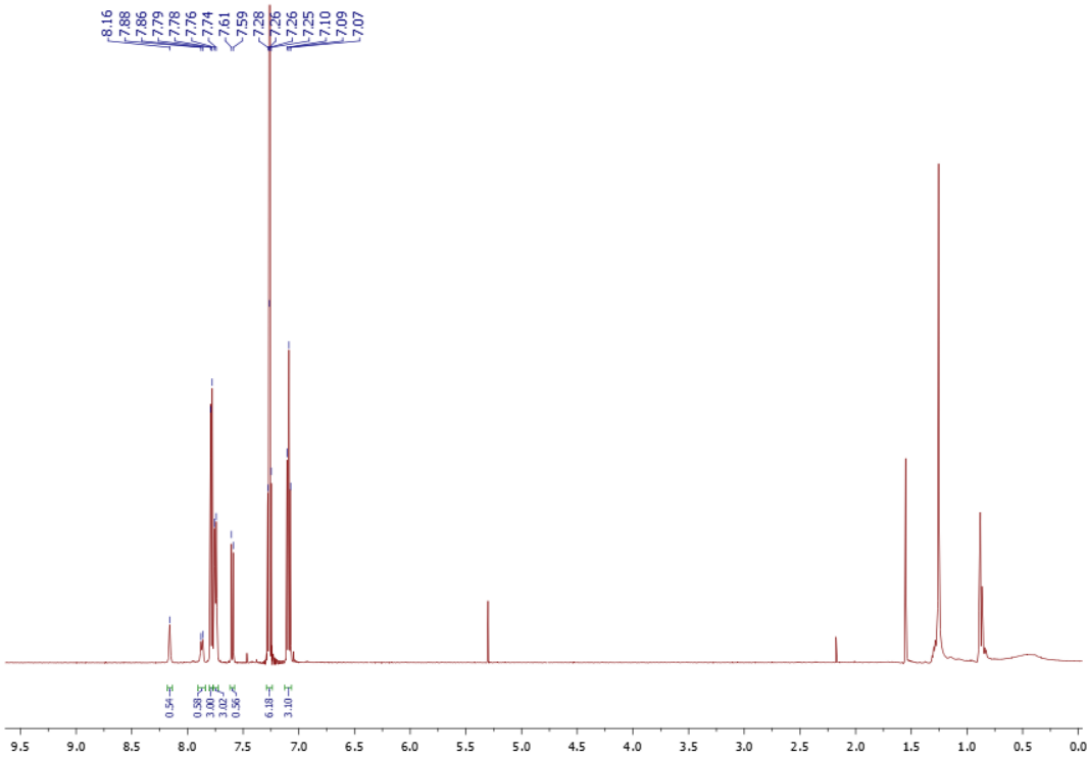
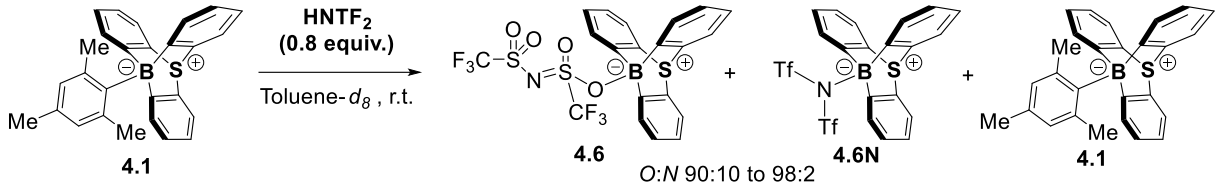


Figure SIV.4. ^1H NMR (500 MHz, 25°C, $CDCl_3$) of competition Csp^2–H borylation reaction between 1,2-dichlorobenzene and 1,2-dichlorobenzene-d_4 as substrate and TMA as base.

IV.5 Determination of the active species

IV.5.1 Protodeborylation with 0.8 equivalents of triflimidic acid



In glovebox, $HNTf_2$ (5.8 mg, 0.021 mmol, 0.80 equiv.) was added to a suspension of 10-mesityl-9-sulfonium-10-boratriptycene-ate complex **4.1** (10 mg, 0.026 mmol, 1.0 equiv.) in toluene-d_8 (0.7 ml) in a 2 ml vial. The reaction mixture was stirred 5min then transferred into a NMR tube equipped with a J. Young valve. ^{1}H, ^{11}B, ^{19}F NMR spectra were recorded after 5 min, 16h and 40h. The ^{19}F NMR analysis showed the progressive isomerization of the *N*-isomer into *O*-isomer, the thermodynamic product.

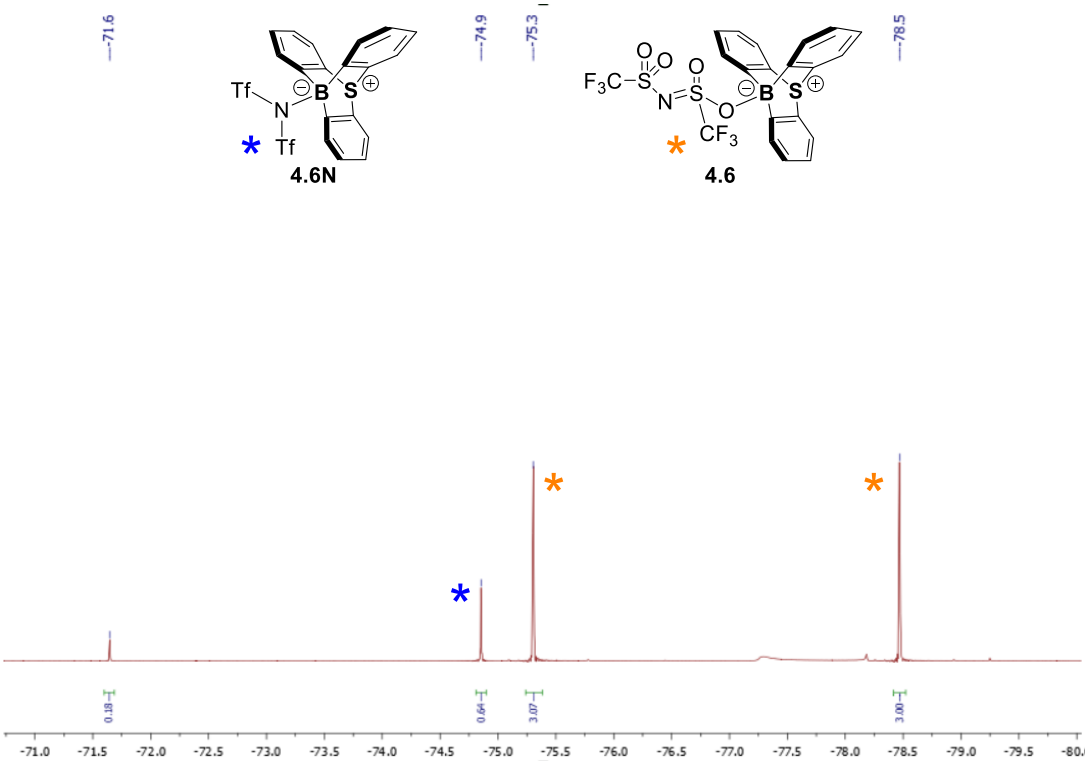


Figure SIV.5. ^{19}F NMR (470 MHz, 25°C, toluene-d_8) after 5 min of protodeborylation of 10-mesityl-9-sulfonium-10-boratriptycene-ate complex **4.1** with 0.8 equivalents of $HNTf_2$.

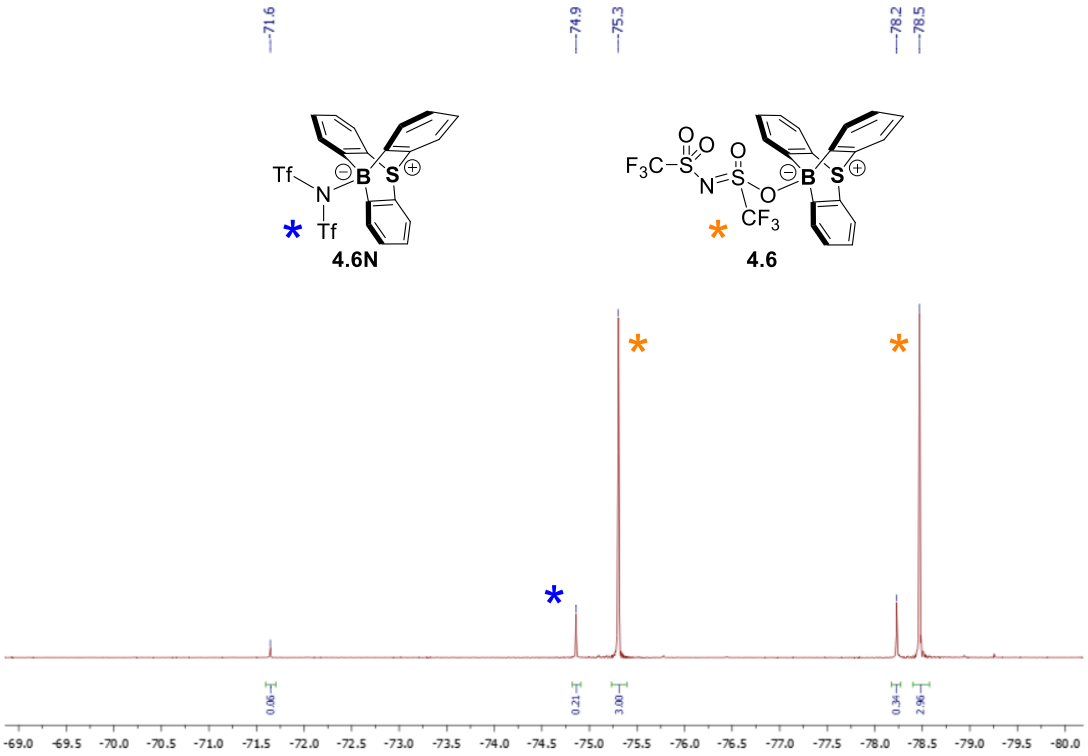


Figure SIV.6. ^{19}F NMR (470 MHz, 25°C, toluene-d_8) after 16h of protodeborylation of 10-mesityl-9-sulfonium-10-boratriptycene-ate complex **4.1** with 0.8 equivalents of $HNTf_2$.

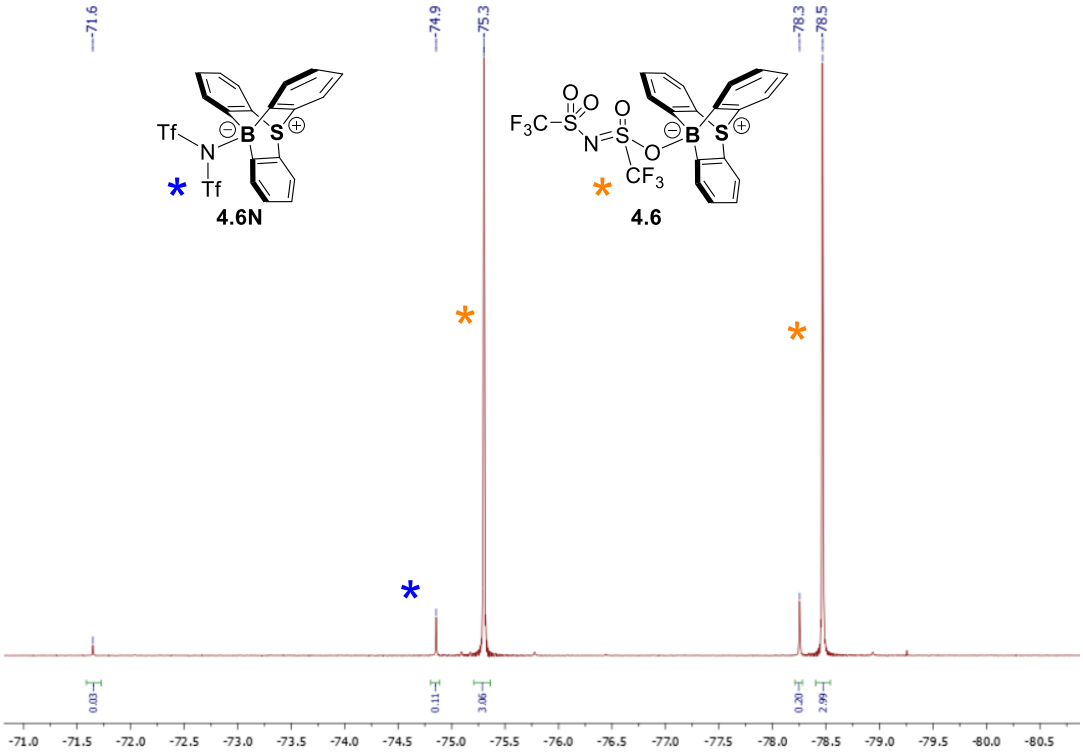


Figure SIV.7. ^{19}F NMR (470 MHz, 25°C, toluene-d_8) after 40h of protodeborylation of 10-mesityl-9-sulfonium-10-boratriptycene-ate complex **4.1** with 0.8 equivalents of $HNTf_2$.

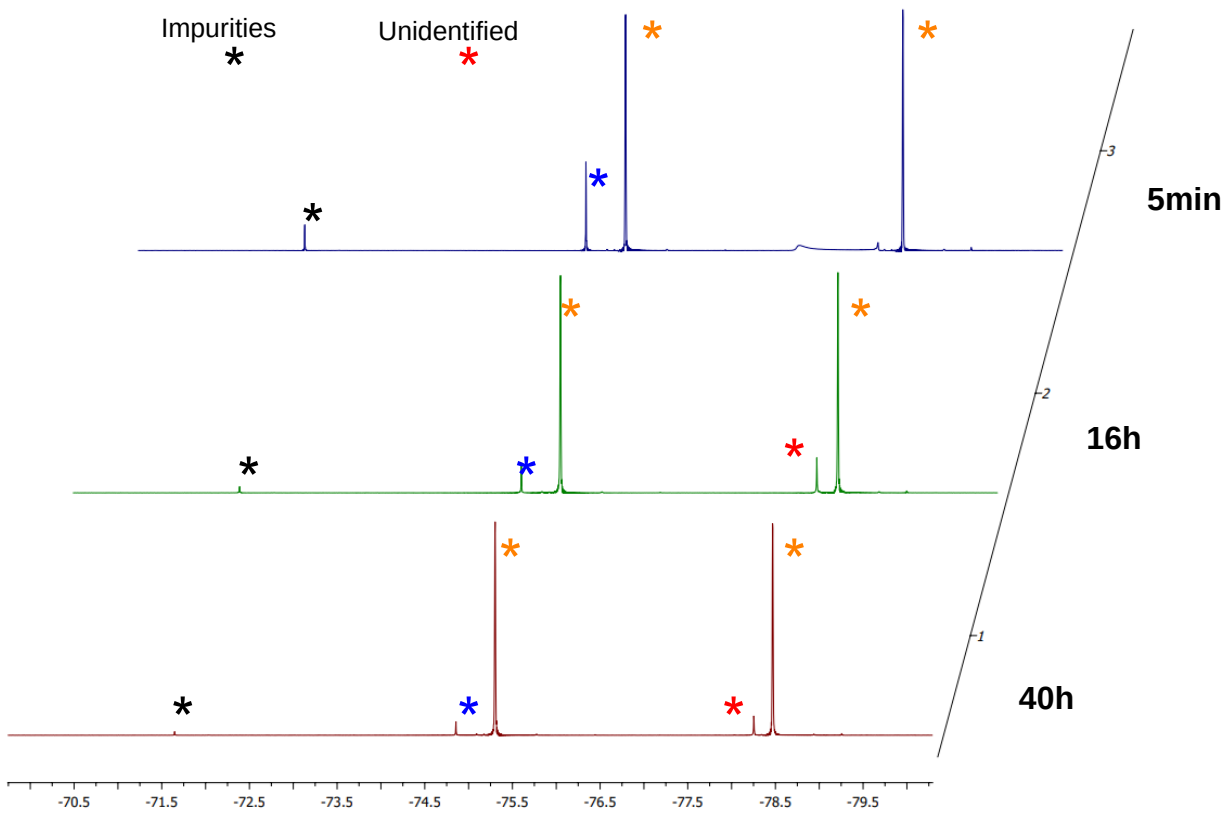
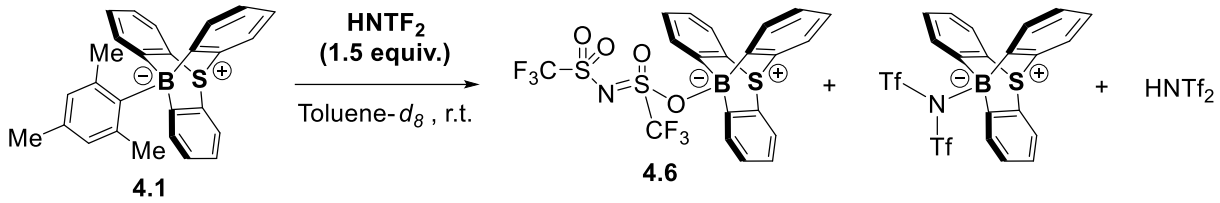


Figure SIV.8. Combined ^{19}F NMR (470 MHz, 25°C, toluene-d_8) of protodeborylation of 10-mesityl-9-sulfonium-10-boratriptycene-ate complex **4.1** with 0.8 equivalents of $HNTf_2$.

IV.5.2 Protodeborylation with 1.5 equivalents of triflimidic acid



In glovebox, $HNTf_2$ (11 mg, 0.038 mmol, 1.5 equiv.) was added to a suspension of 10-mesityl-9-sulfonium-10-boratriptycene-ate complex **4.1** (10 mg, 0.026 mmol, 1.0 equiv.) in toluene-d_8 (0.7 ml) in a 2 ml vial. The reaction mixture was stirred 5min then transferred into a NMR tube equipped with a J. Young valve. ^{1}H, ^{11}B, ^{19}F NMR spectra were recorded after 5 min, 16h and 40h. The ^{19}F NMR analysis showed the progressive

isomerization of the *N*-isomer into *O*-isomer, the thermodynamic product, even though the isomerization seems to be slower than with a default of $HNTf_2$.

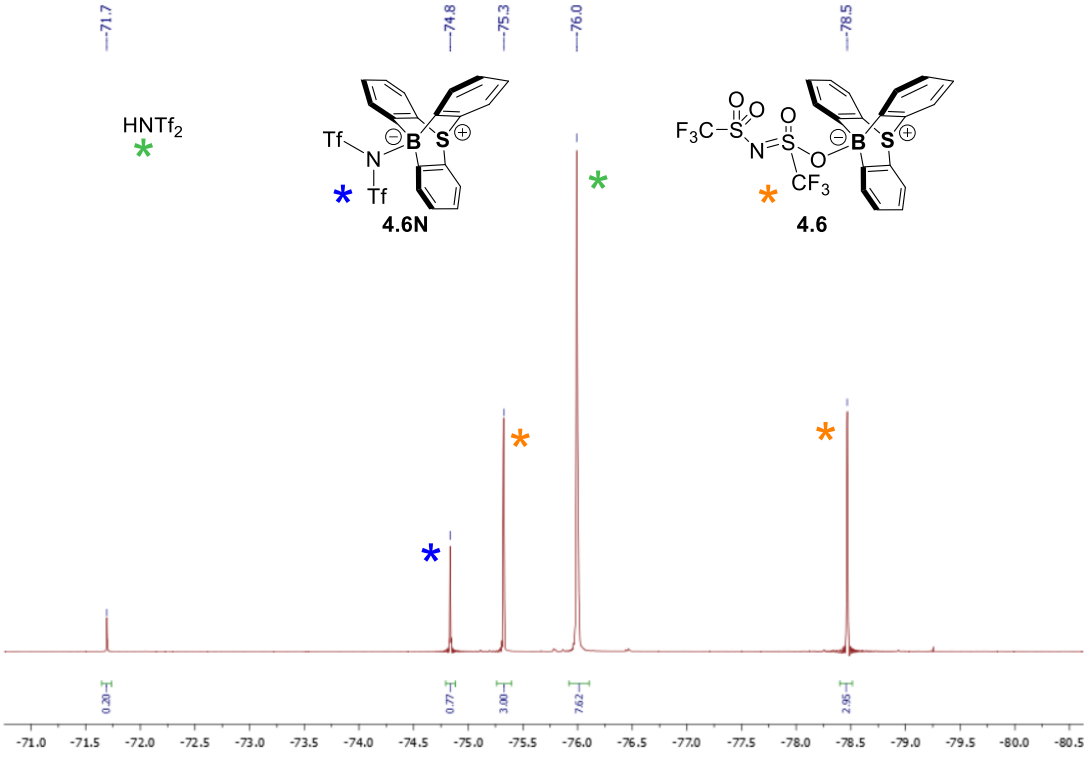


Figure SIV.9. ^{19}F NMR (470 MHz, 25°C, toluene-d_8) after 5min of protodeborylation of 10-mesityl-9-sulfonium-10-boratriptycene-ate complex **4.1** with 1.5 equivalents of $HNTf_2$.

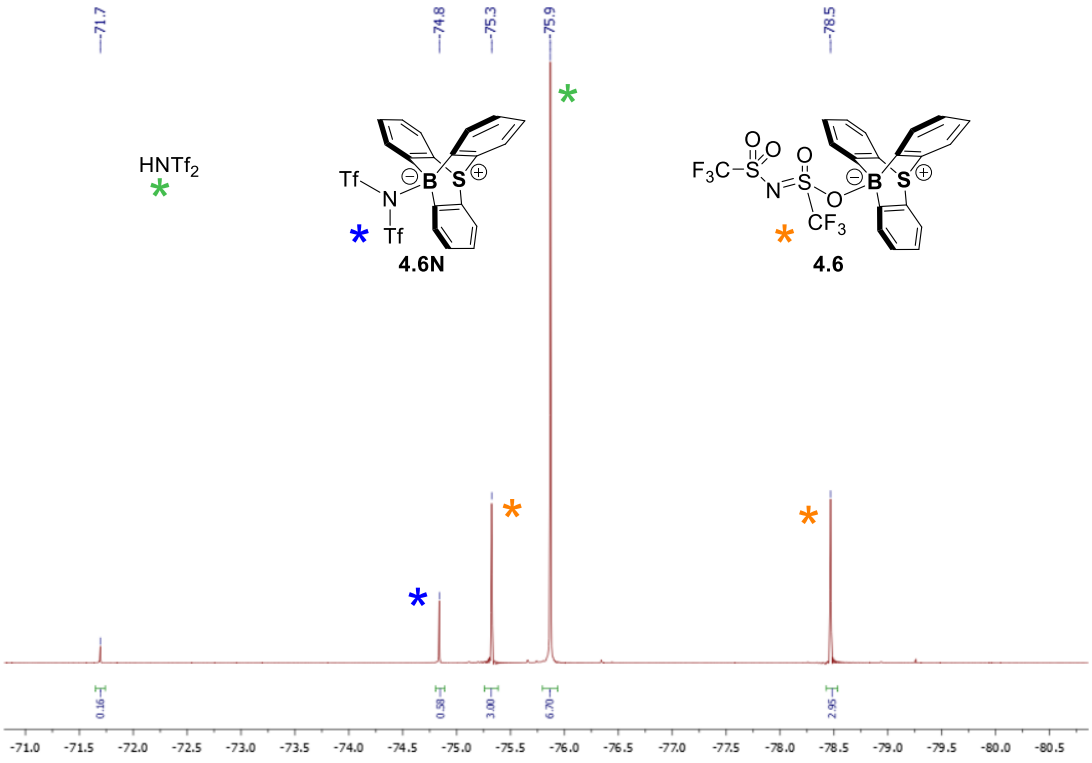


Figure SIV.10. ^{19}F NMR (470 MHz, 25°C, toluene-d_8) after 16h of protodeborylation of 10-mesityl-9-sulfonium-10-boratriptycene-ate complex **4.1** with 1.5 equivalents of $HNTf_2$.

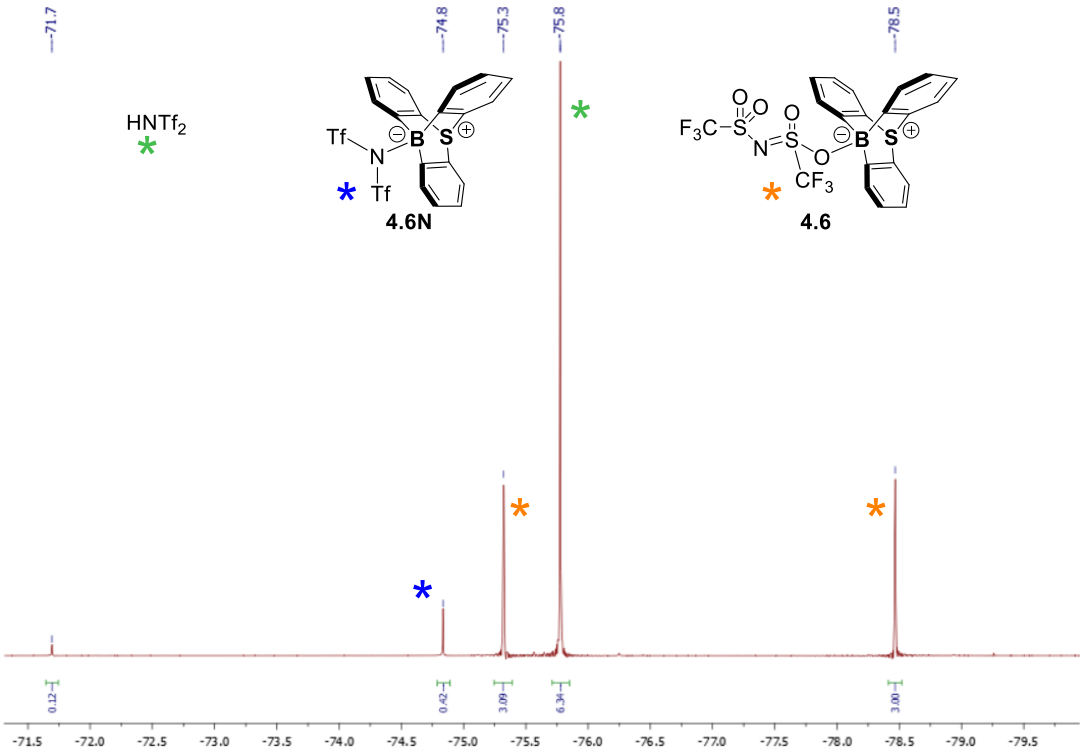


Figure SIV.11. ^{19}F NMR (470 MHz, 25°C, toluene-d_8) after 40h of protodeborylation of 10-mesityl-9-sulfonium-10-boratriptycene-ate complex **4.1** with 1.5 equivalents of $HNTf_2$.

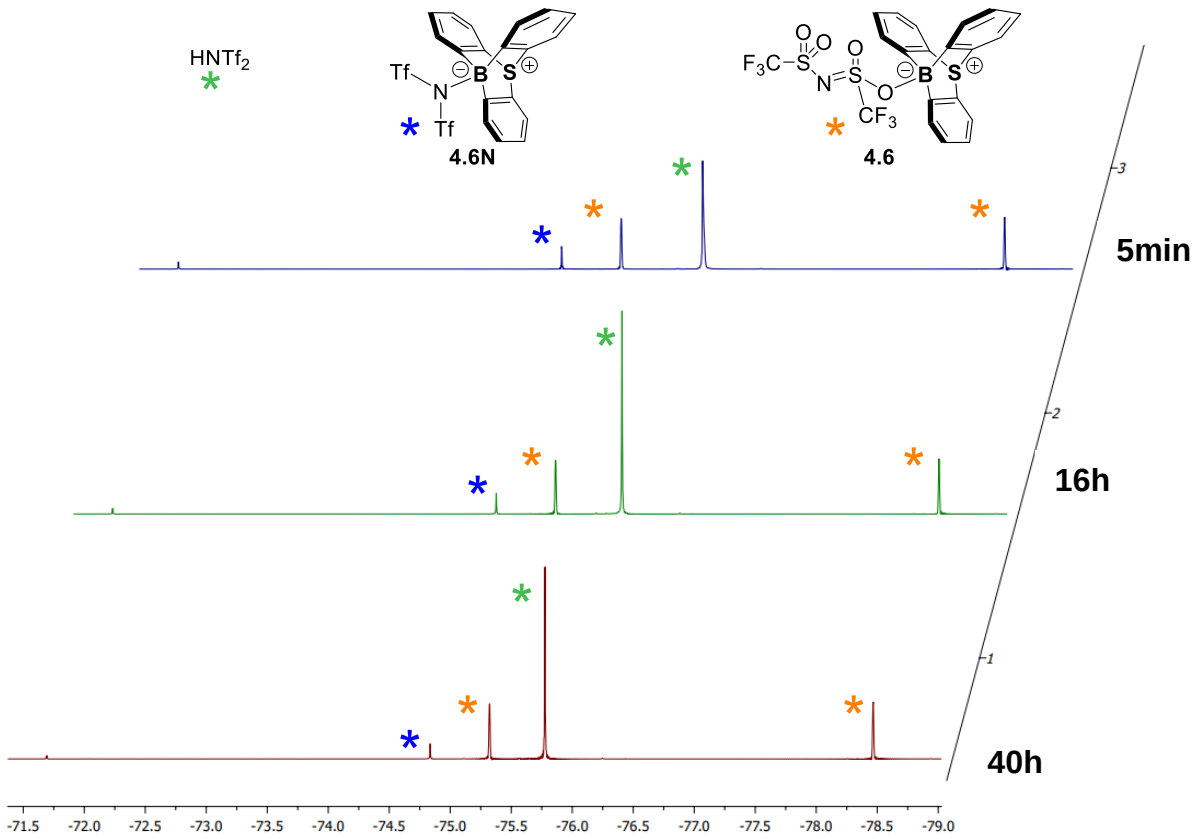
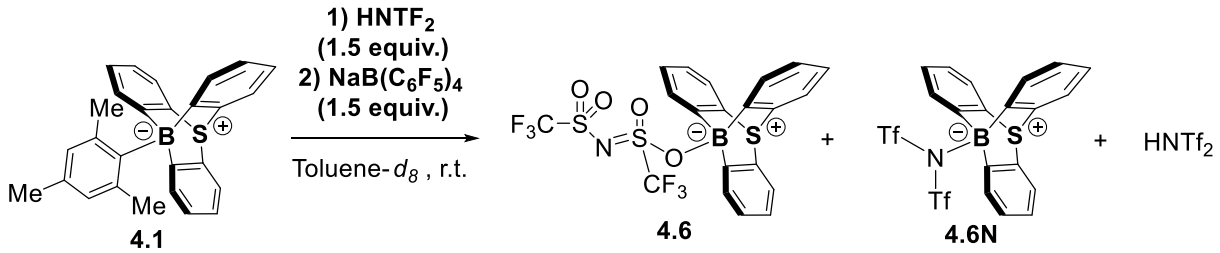


Figure SIV.12. Combined ^{19}F NMR (470 MHz, 25°C, toluene-d_8) of protodeborylation of 10-mesityl-9-sulfonium-10-boratriptycene-ate complex **4.1** with 1.5 equivalents of $HNTf_2$.

IV.5.3 Protodeborylation with 1.5 equivalents of triflimidic acid and $NaB(C_6F_5)_4$



In glovebox, $HNTf_2$ (11 mg, 0.038 mmol, 1.5 equiv.) was added to a suspension of 10-mesityl-9-sulfonium-10-boratriptycene-ate complex **4.1** (10 mg, 0.026 mmol, 1.0 equiv.) in toluene-d_8 (0.7 ml) in a 2 ml vial. The reaction mixture was stirred 5min and $NaB(C_6F_5)_4$ (28 mg, 0.038 mmol, 1.5 equiv.) was added. The mixture was then transferred into a NMR tube equipped with a J. Young valve. ^1H, ^{11}B, ^{19}F NMR specta

were recorded after 5 min, 16h and 40h. The ^{19}F NMR analysis showed the progressive isomerization of the *O*-isomer into *N*-isomer, which present the opposite isomerization compared to the isomerization observed in absence of $NaB(C_6F_5)_4$.

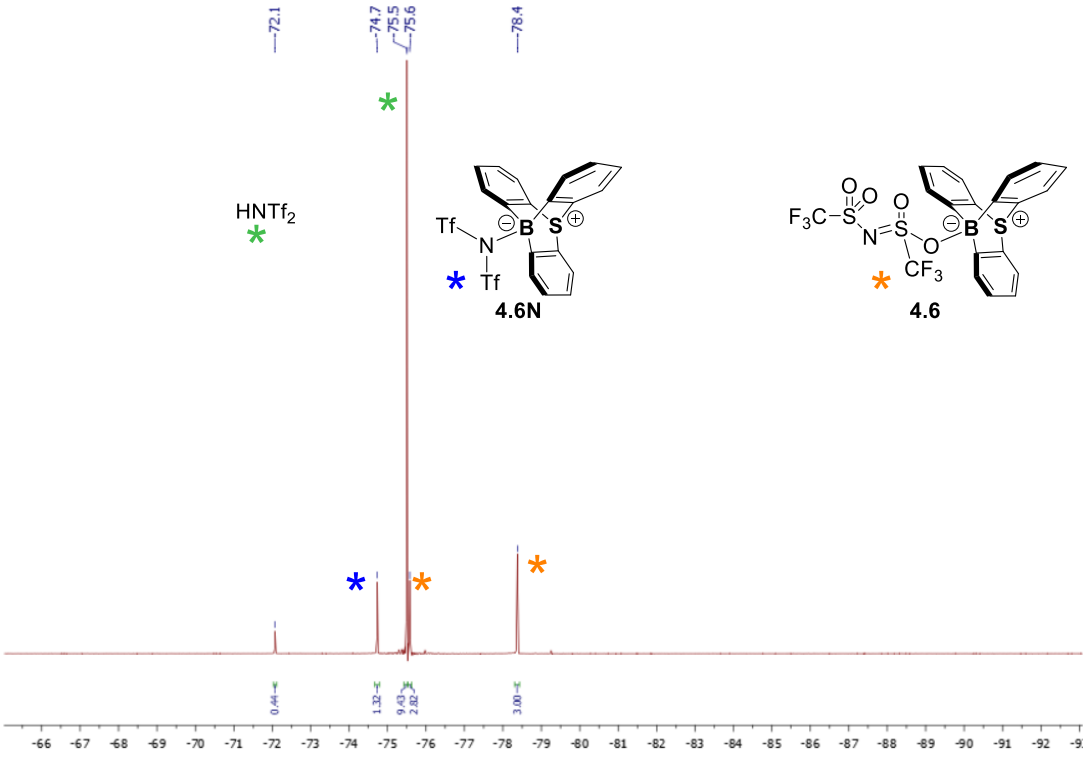


Figure SIV.13. ^{19}F NMR (470 MHz, 25°C, toluene-d_8) after 5 min of protodeborylation of 10-mesityl-9-sulfonium-10-boratriptycene-ate complex **4.1** with 1.5 equivalents of $HNTf_2$ and $NaB(C_6F_5)_4$.

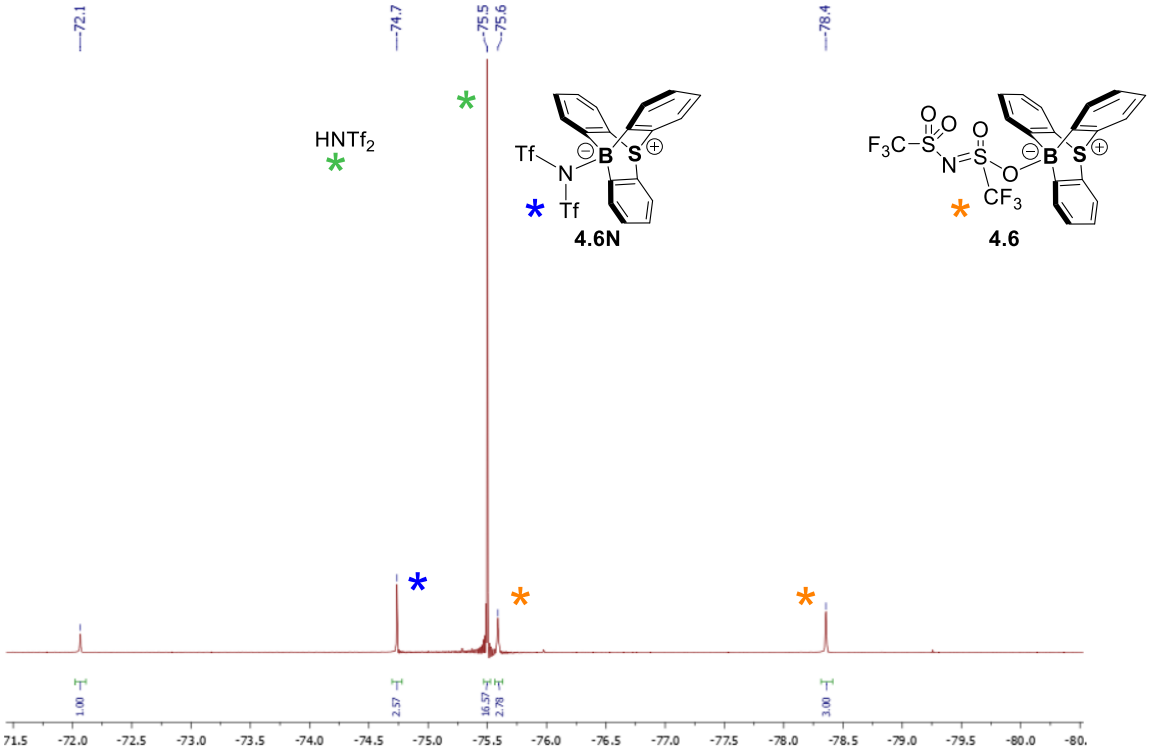


Figure SIV.14. ^{19}F NMR (470 MHz, 25°C, toluene-d_8) after 16h of protodeborylation of 10-mesityl-9-sulfonium-10-boratriptycene-ate complex **4.1** with 1.5 equivalents of $HNTf_2$ and $NaB(C_6F_5)_4$.

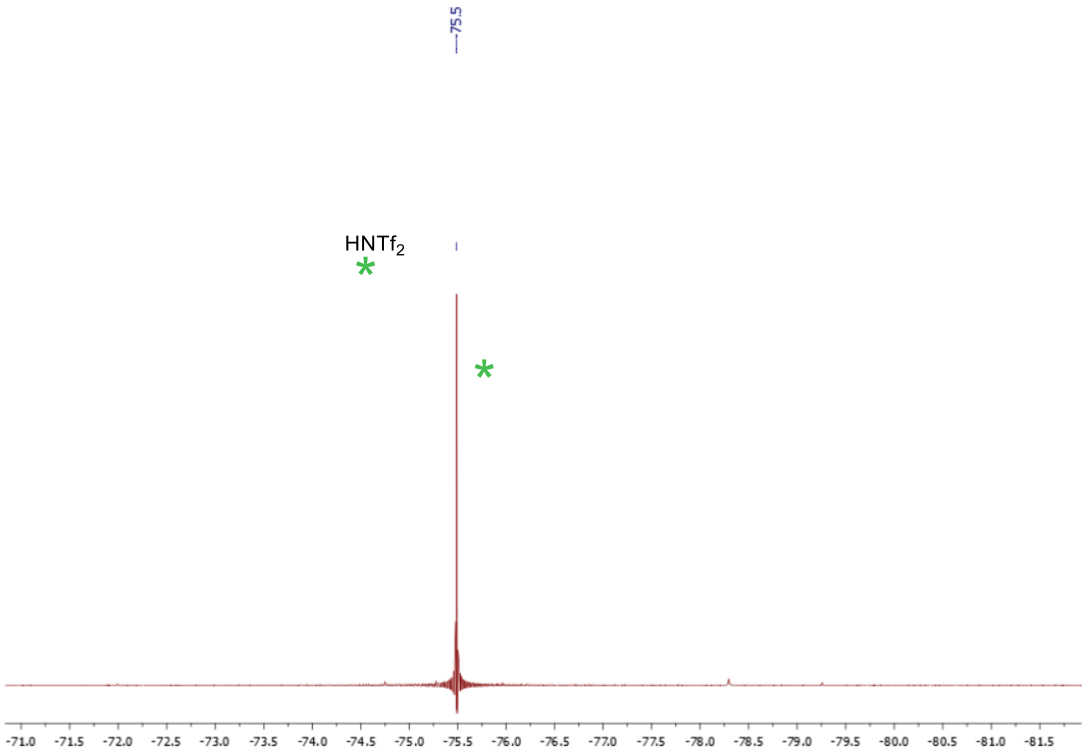


Figure SIV.15. ^{19}F NMR (470 MHz, 25°C, toluene-d_8) after 40h of protodeborylation of 10-mesityl-9-sulfonium-10-boratriptycene-ate complex **4.1** with 1.5 equivalents of $HNTf_2$ and $NaB(C_6F_5)_4$.

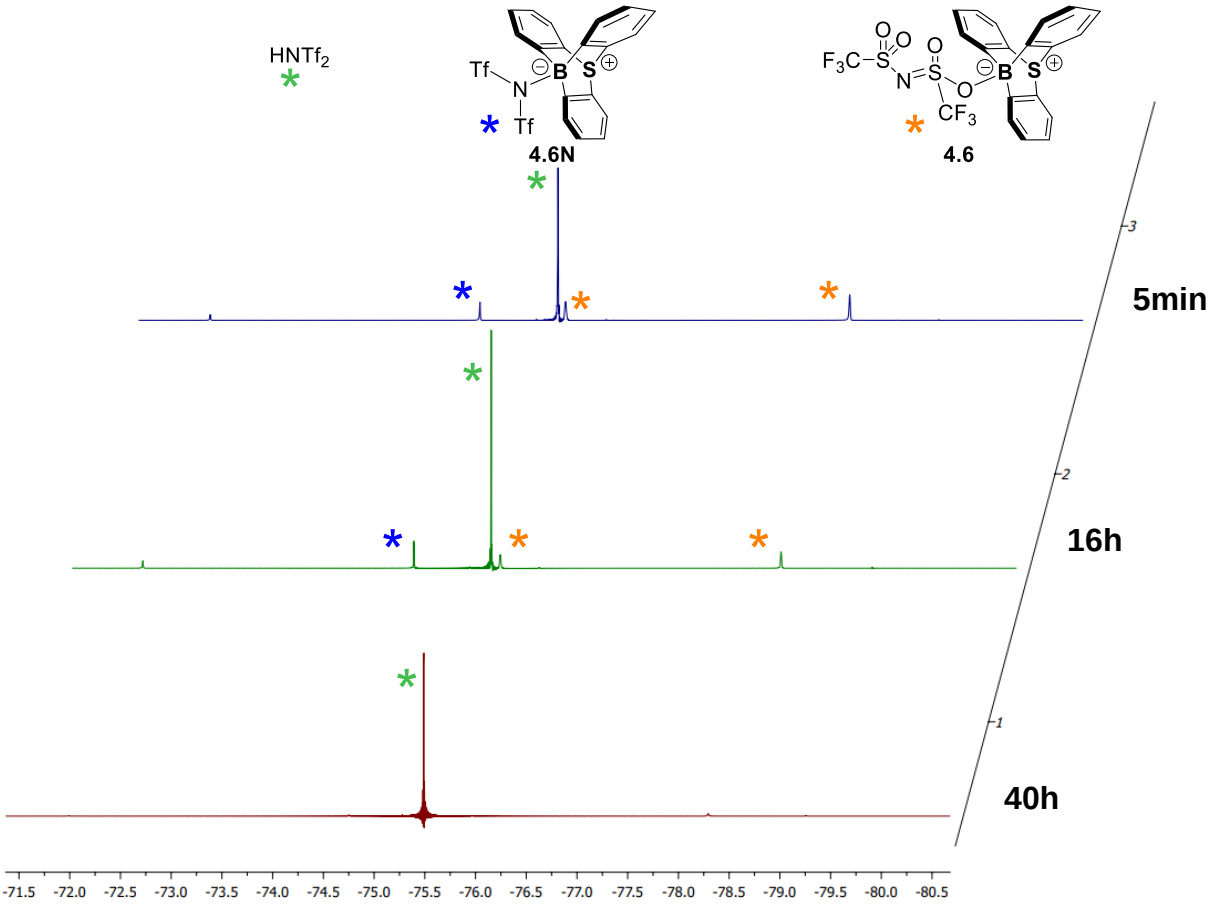
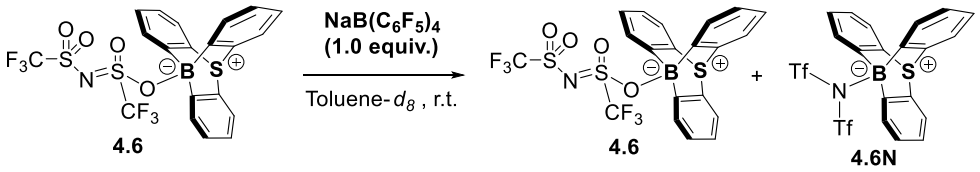


Figure SIV.16. Combined ^{19}F NMR (470 MHz, 25°C, toluene-d_8) of protodeborylation of 10-mesityl-9-sulfonium-10-boratriptycene-ate complex **4.1** with 1.5 equivalents of $HNTf_2$ and $NaB(C_6F_5)_4$.

IV.5.4 Addition of 1.0 equivalent of $NaB(C_6F_5)_4$ over 10-triflimidate-9-sulfonium-10-boratriptycene-ate complex **4.6** *O*-isomer.



In glovebox, $NaB(C_6F_5)_4$ (13 mg, 0.018 mmol, 1.0 equiv.) was added to a solution of 10-triflimidate-9-sulfonium-10-boratriptycene-ate complex **4.6** (10 mg, 0.018 mmol, 1.0 equiv.) in toluene-d_8 (0.7 ml) in a 2 ml vial. The mixture was then transferred into a NMR tube equipped with a J. Young valve. ^{1}H, ^{11}B, ^{19}F NMR specta were recorded after 5 min and 16h. ^{19}F NMR analysis showed the isomerization of the *O*-isomer into the *N*-isomer in presence of $NaB(C_6F_5)_4$.

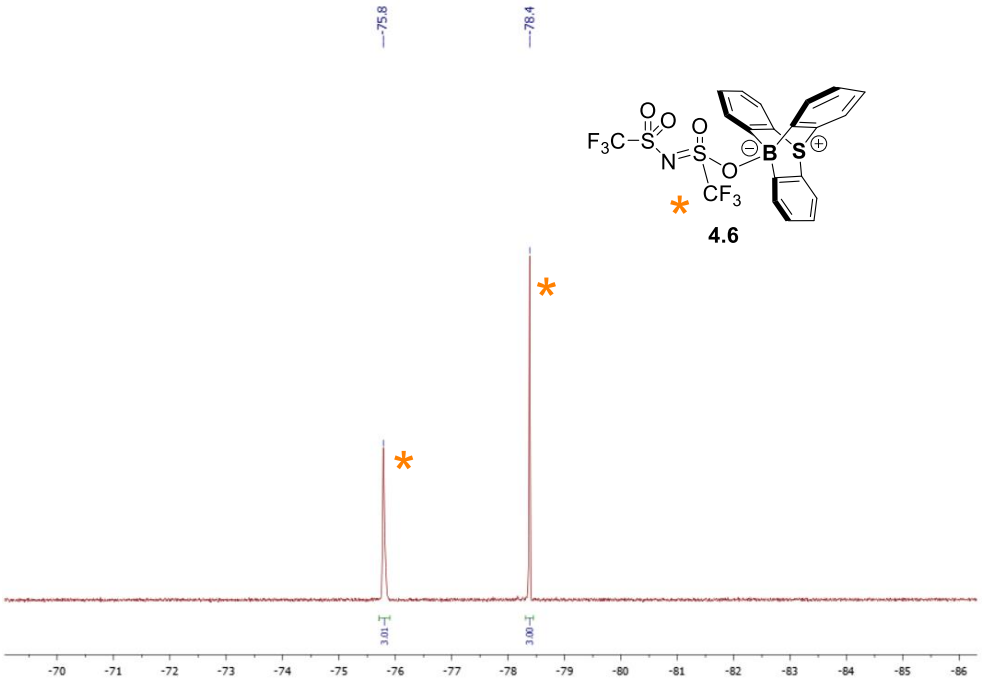


Figure SIV.17. ^{19}F NMR (470 MHz, 25°C, toluene-d_8) after 5min of addition of $NaB(C_6F_5)_4$ over 10-triflimidate-9-sulfonium-10-boratriptycene-ate complex **4.6**.

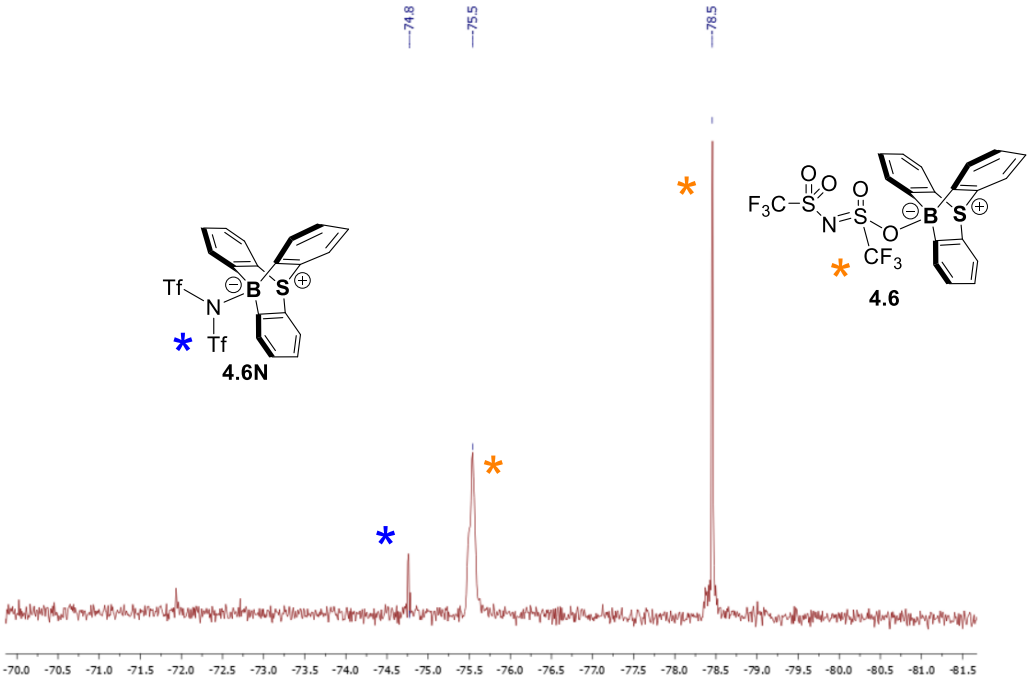
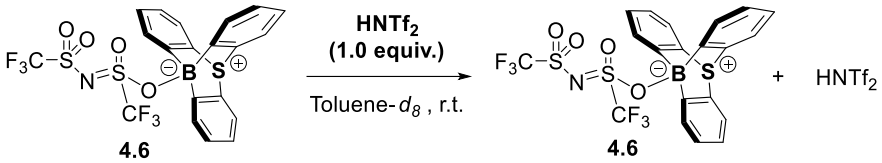


Figure SIV.18. ^{19}F NMR (470 MHz, 25°C, toluene-d_8) after 16h of addition of $NaB(C_6F_5)_4$ over 10-triflimidate-9-sulfonium-10-boratriptycene-ate complex **4.6**.

IV.5.5 Addition of 0.1 equivalent of $HNTf_2$ over 10-triflimidate-9-sulfonium-10-boratriptycene-ate complex **4.6** *O*-isomer.



In glovebox, $HNTf_2$ (5 mg, 0.018 mmol, 1.0 equiv.) was added to a solution of 10-triflimidate-9-sulfonium-10-boratriptycene-ate complex **4.6** (10 mg, 0.018 mmol, 1.0 equiv.) in toluene-d_8 (0.7 ml) in a 2 ml vial. The mixture was then transferred into a NMR tube equipped with a J. Young valve. ^{1}H, ^{11}B, ^{19}F NMR specta were recorded after 5 min and 16h, showing absence of isomerization.

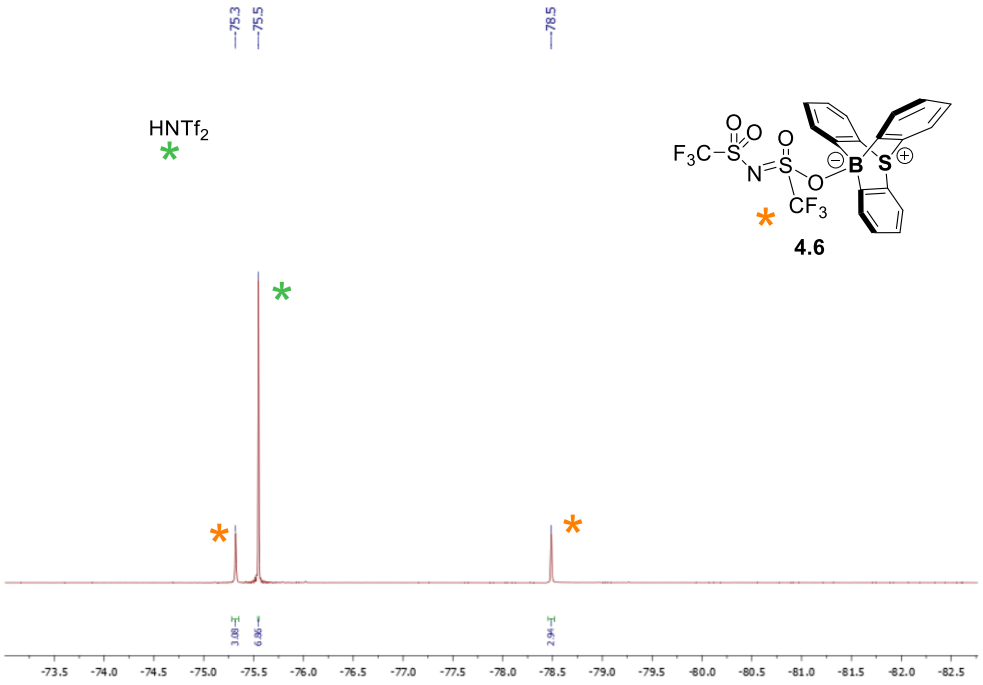
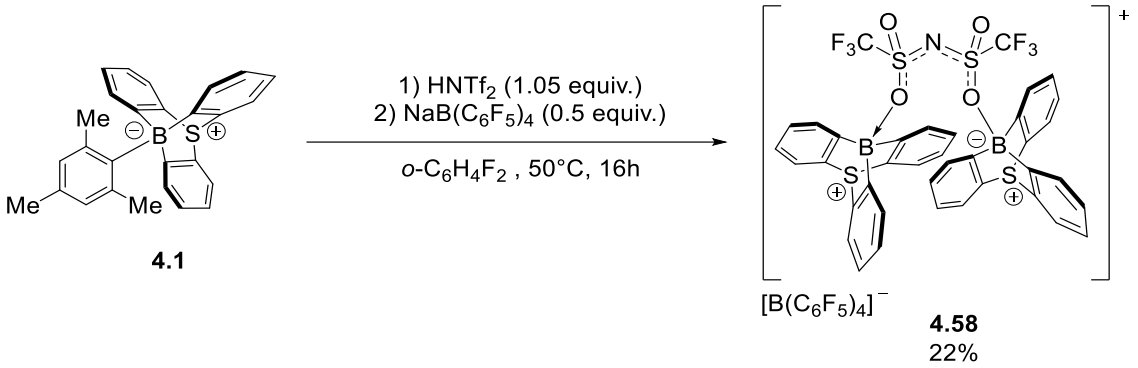


Figure SIV.19. ^{19}F NMR (470 MHz, 25°C, toluene-d_8) after 5min and 16h of addition of $HNTf_2$ over 10-triflimidate-9-sulfonium-10-boratriptycene-ate complex **4.6**. The spectra were strictly identical after 5min and 16h.

IV.6. Synthesis of tetrakis(pentafluorophenyl)borate bis(10-trifluoromethylsulfonyl-9-sulfonium-10-boratriptycene)iminium



In a glovebox, triflimidic acid (76 mg, 0.27 mmol, 1.05 equiv.) is added to a suspension of 10-mesityl-9-sulfonium-10-boratriptycene-ate complex **4.1** (100 mg, 0.26 mmol, 1.0 equiv.) in 1,2-difluorobenzene. After stirring for 5 min, sodium tetrakis(pentafluorophenyl)borate (93 mg, 0.13 mmol, 0.5 equiv.) is added and the reaction mixture is stirred out of the glovebox at 50°C. After 16h, the reaction mixture is evaporated to dryness and the crude is purified by flash chromatography (50:50 *n*-hexane/CH_2Cl_2 then pure CH_2Cl_2) affording the desired tetrakis(pentafluorophenyl)borate bis(10-trifluoromethylsulfonyl-9-sulfonium-10-boratriptycene)iminium **4.58** (42 mg, 0.028 mmol, 22% yield) as a white powder. The flash chromatography has to be performed as quick as possible due to slow decomposition of the product on the silica gel and in presence of CH_2Cl_2 or $CHCl_3$. The product could be stored under ambient conditions in a capped vial. However, long term storage in a glovebox is preferable.

TLC: R_f = 0.1 (*n*-hexane/CH_2Cl_2 50:50)

^{1}H NMR (500 MHz, $CDCl_3$) δ (ppm) = Major isomer : 7.70 (d, *J* = 7.7 Hz, 6H), 7.53 (dd, *J* = 7.4, 1.0 Hz, 6H), 7.01 (td, *J* = 7.6, 1.2 Hz, 6H), 6.70 (td, *J* = 7.4, 0.8 Hz, 6H). Minor isomer : 7.74 (d, *J* = 7.7 Hz, 6H), 7.61 (d, *J* = 7.8 Hz, 6H), 7.06 (td, *J* = 7.6, 1.2 Hz, 6H), 6.82 (td, *J* = 7.4, 0.8 Hz, 6H).

^{13}C NMR (126 MHz, $CDCl_3$) δ (ppm) = 150.4 (CB), 131.1 (CH), 130.5 (Cq), 129.3 (CH), 128.3 (CH), 126.6 (CH).

^{11}B NMR (160 MHz, $CDCl_3$) δ (ppm) = 11.7 (br), -17.6 (s)

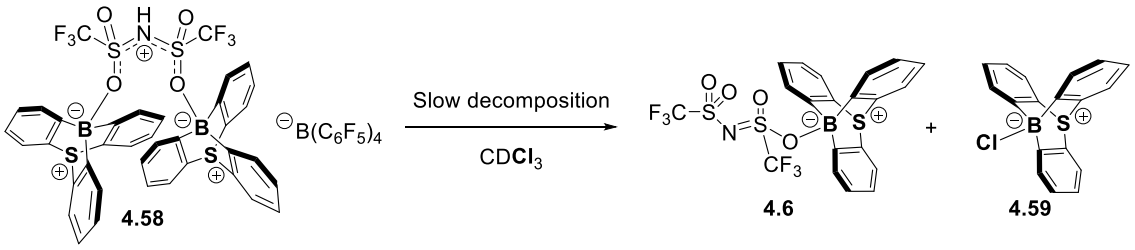
^{19}F NMR (483 MHz, $CDCl_3$) δ (ppm) = -71.6 (s, 1.24 F), -73.9 (s, 4.87 F), -132.4 (s, 8F), -163.1 (t, *J* = 20.6 Hz, 4F), -166.7 (t, 18.0 Hz, 8F).

HRMS (MALDI$^-$) (*m/z*): Could not be determined due to decomposition during injection.

IR (neat, ATR): $\tilde{\nu}$ / cm^{-1} = 3060, 1647, 1510, 1465, 1359, 1231, 1142, 1084, 974, 832, 752.

M.p. (C_6H_5F): 179 °C (dec)

IV.7. Slow chloride abstraction from $CDCl_3$ with tetrakis(pentafluorophenyl)borate bis(10-trifluoromethylsulfonyl-9-sulfonium-10-boratriptycene)iminium.



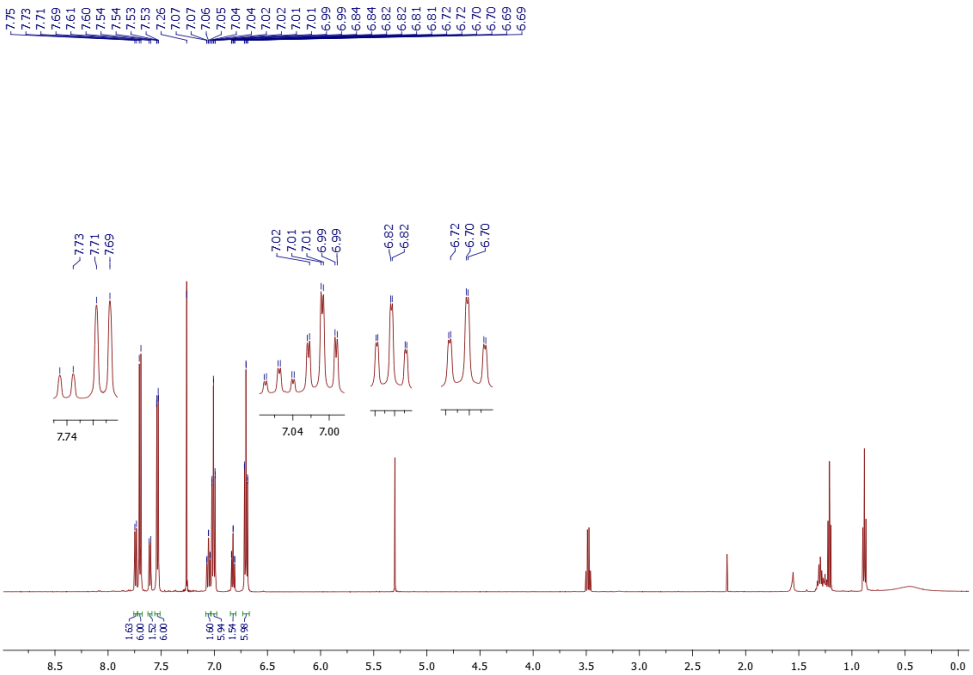


Figure SIV.20. ^{1}H NMR (500 MHz, 25°C, $CDCl_3$) of **4.58** after 5min

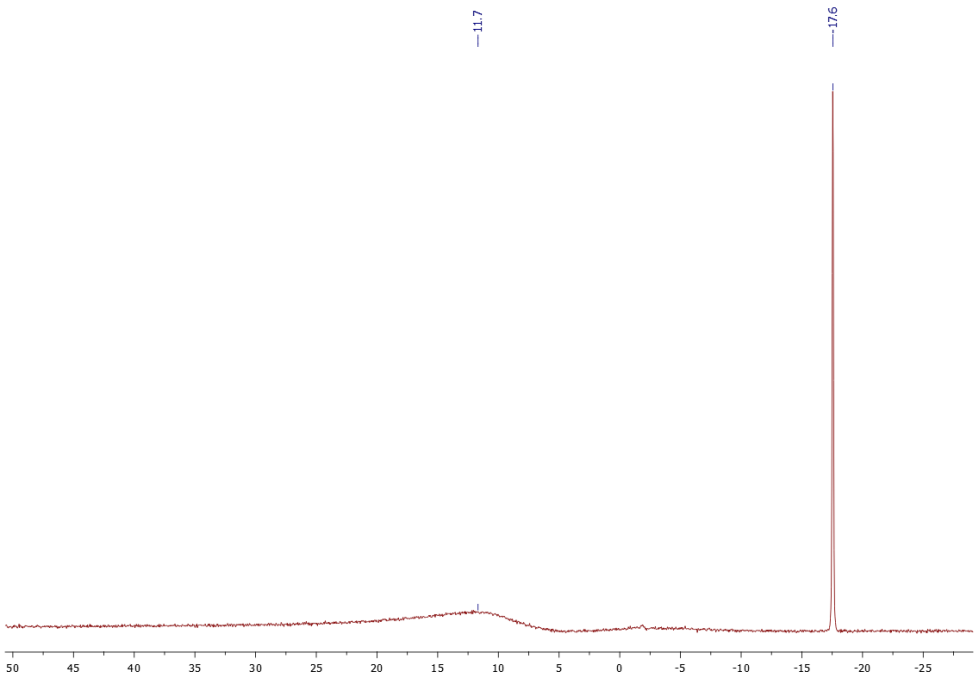


Figure SIV.21. ^{11}B NMR (160 MHz, 25°C, $CDCl_3$) of **4.58** after 5min

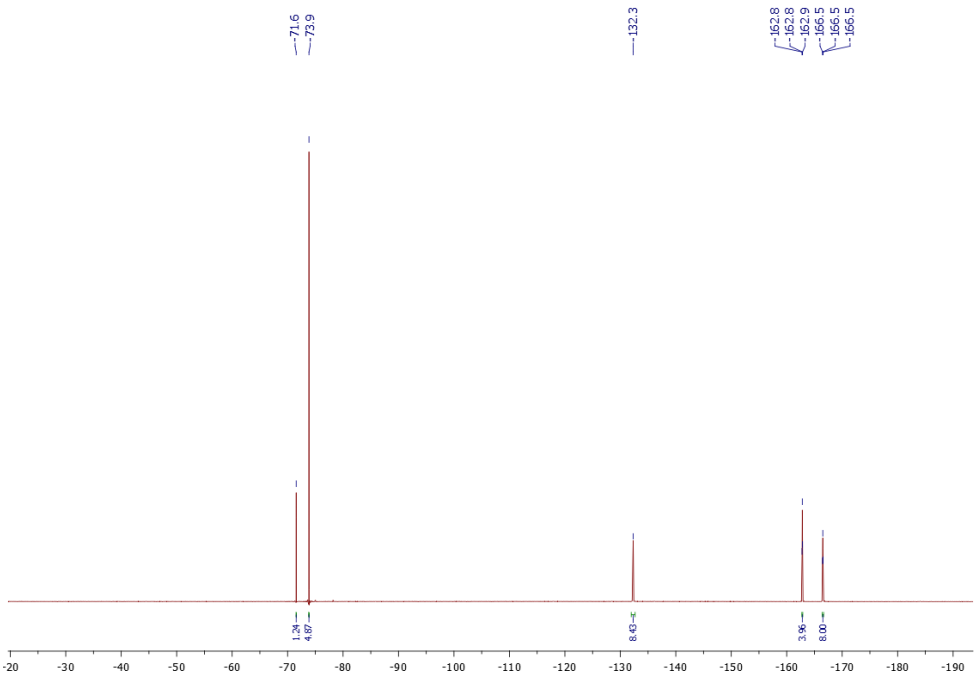


Figure SIV.22. ^{19}F NMR (470 MHz, 25°C, $CDCl_3$) of **4.58** after 5min

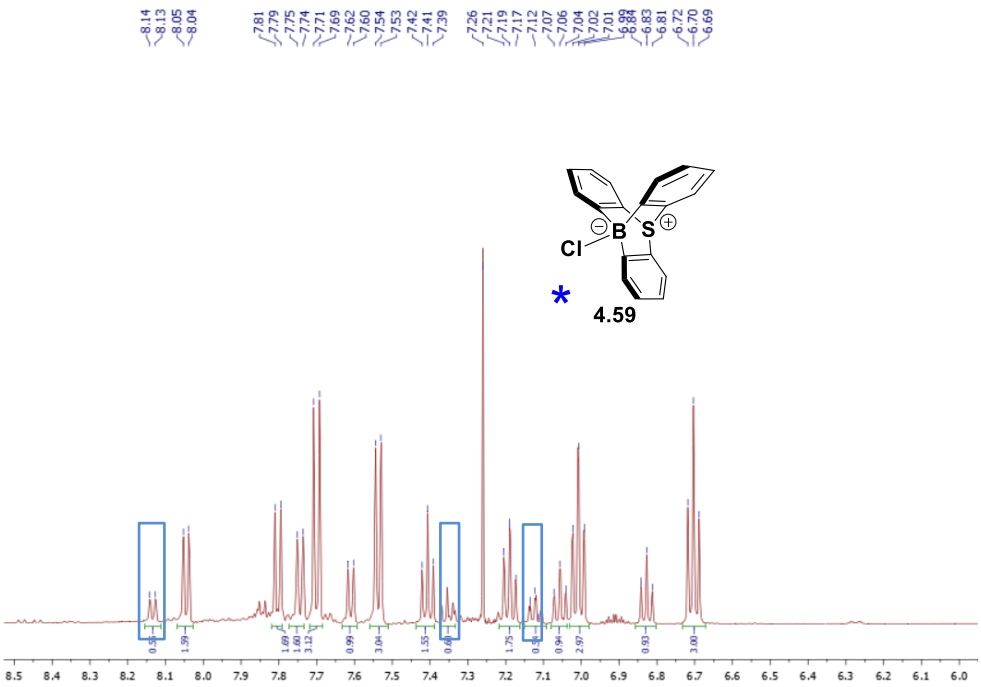


Figure SIV.23. ^{1}H NMR (500 MHz, 25°C, $CDCl_3$) of **4.58** after 16h

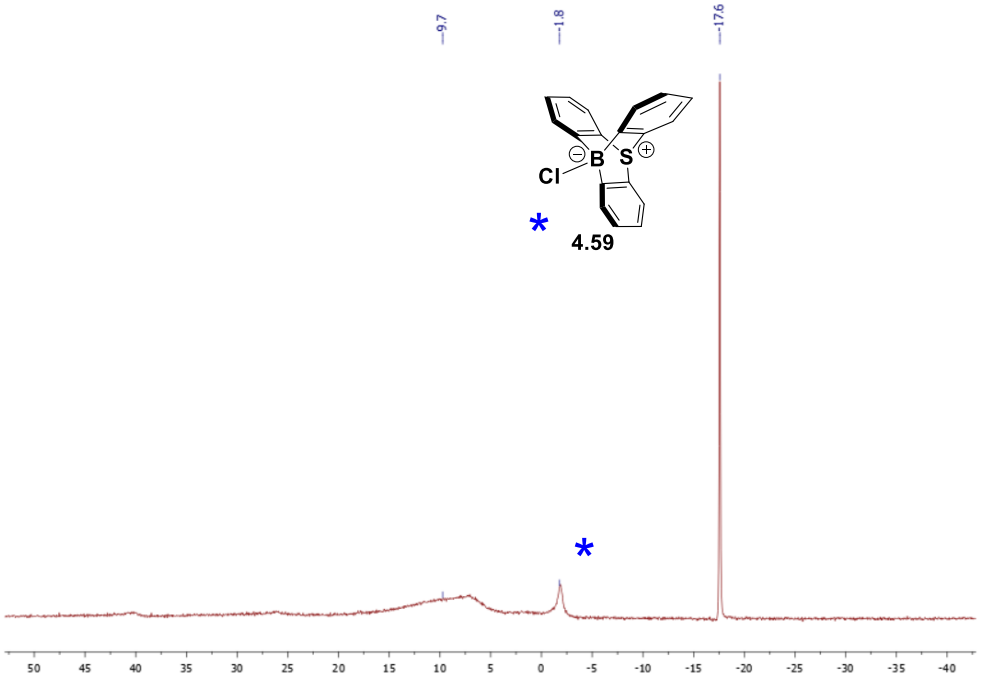


Figure SIV.24. ^{11}B NMR (160 MHz, 25°C, $CDCl_3$) of **4.58** after 16h

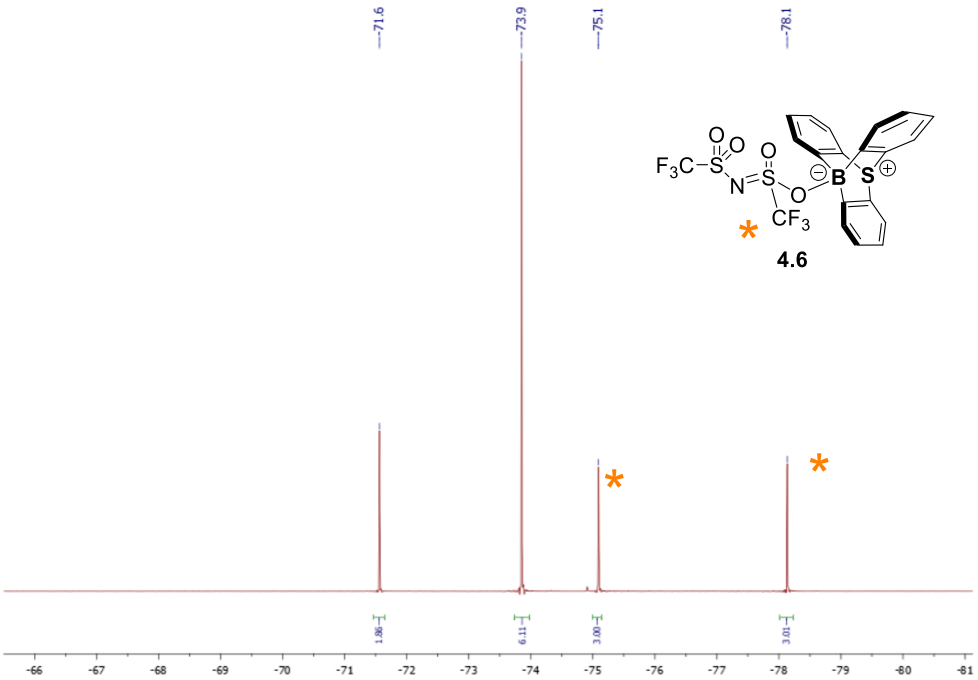
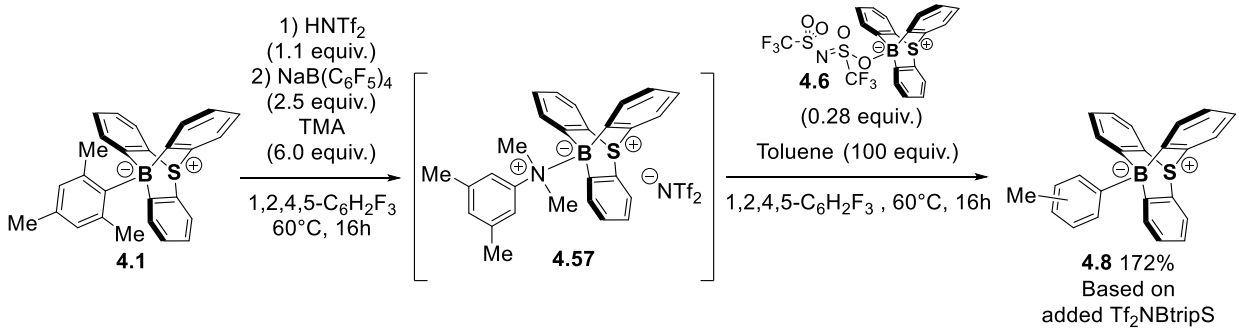


Figure SIV.25. ^{19}F NMR (470 MHz, 25°C, $CDCl_3$) of **4.58** after 16h

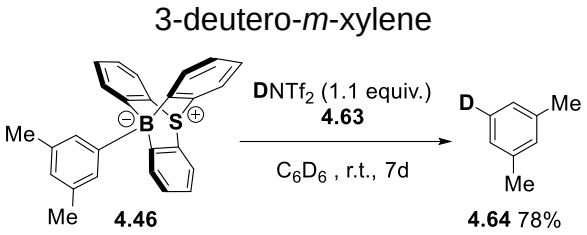
IV.8. Demonstration of the 10-(*N*,*N*,3,5-tetramethylaniline)-9-sulfonium-10-boratriptycene Lewis adduct reversibility.



Under glovebox, $HNTf_2$ (16 mg, 0.056 mmol, 1.1 equiv.) was added to a suspension of 10-mesityl-9-sulfonium-10-boratriptycene-ate complex **4.1** (20 mg, 0.051 mmol, 1.0 equiv.) in 1,2,4,5-tetrafluorobenzene (2.0 ml). The mixture was stirred for 5 min then $NaB(C_6F_5)_4$ (93 mg, 0.13 mmol, 2.5 equiv.) was added. After stirring for further 5min, *N*,*N*,3,5-tetramethylaniline (50 µl, 0.31 mmol, 6.0 equiv.) was added, the Schlenk tube was sealed with a glass stopper and stirred and warmed at 60°C in an oil bath out of

the glovebox. After 16h, 10-triflimidate-9-sulfonium-10-boratriptycene-ate complex (7.9 mg, 0.014 mmol, 0.28 equiv.) and toluene (0.54 ml, 5.1 mmol, 100 equiv.) was added under gentle stream of Ar. The Schlenk tube was sealed again with a glass stopper, stirred and warmed for further 16h at 60°C. The crude was evaporated to dryness and purification by flash chromatography afforded pure 10-tolyl-9-sulfonium-10-boratriptycene-ate complex (8.9 mg, 0.025 mmol, 172% based on **4.6**).

IV.9. Deuteration



In a glovebox, $DNTf_2$ **4.63** (3.8 mg, 0.012 mmol, 1.1 equiv.) was added to a suspension of 10-(3,5-dimethylphenyl)-9-sulfonium-10-boratriptycene)ate complex **4.46** (5.0 mg, 0.011 mmol, 1.0 equiv.) in benzene-d_6 (0.6 ml). The mixture was transferred in a NMR tube equipped with a J. Young stopper. After 7 days, the reaction mixture was analyzed by ^{1}H NMR. The yield is determined using the signals from the triptycene scaffold as internal standard. It might be of interest to perform GC-MS analysis for better characterization and yield determination.

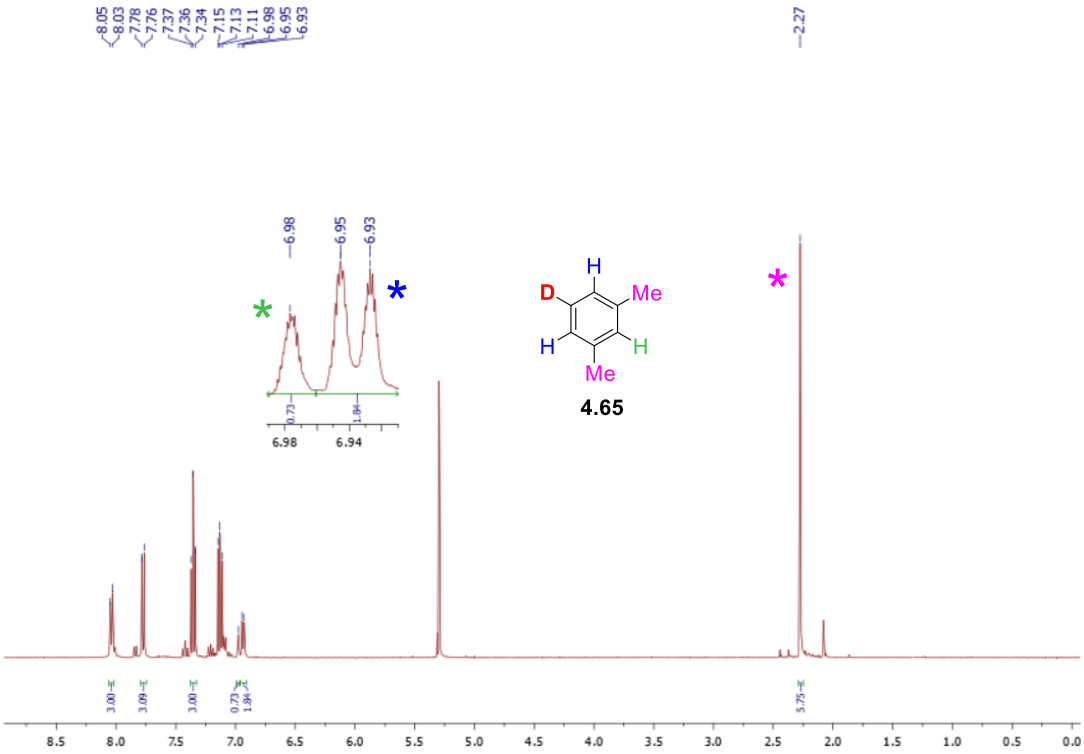
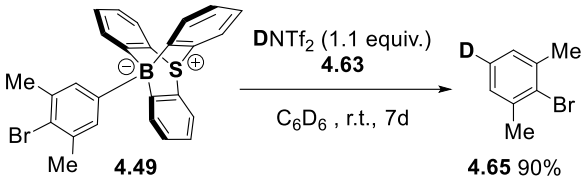
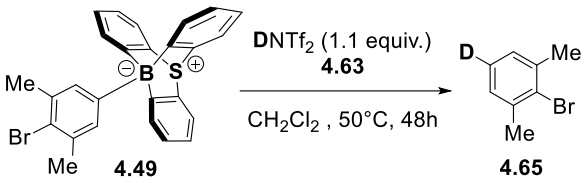


Figure SIV.26. ^{1}H NMR (500 MHz, 25°C, benzene-d_6) of deuteration of **4.46**

4-deutero-2,6-dimethyl-bromobenzene



In a glovebox, $DNTf_2$ **4.63** (3.4 mg, 0.012 mmol, 1.1 equiv.) was added to a suspension of 10-(4-bromo-3,5-dimethylphenyl)-9-sulfonium-10-boratriptycene)ate complex **4.49** (5.0 mg, 0.011 mmol, 1.0 equiv.) in benzene-d_6 (0.6 ml). The mixture was transferred in a NMR tube equipped with a J. Young stopper. After 7 days, the reaction mixture was analyzed by ^{1}H NMR.



To confirm the selectivity of the reaction, the reaction was reproduced in CH_2Cl_2 and the crude was analyzed by ^{2}D NMR.

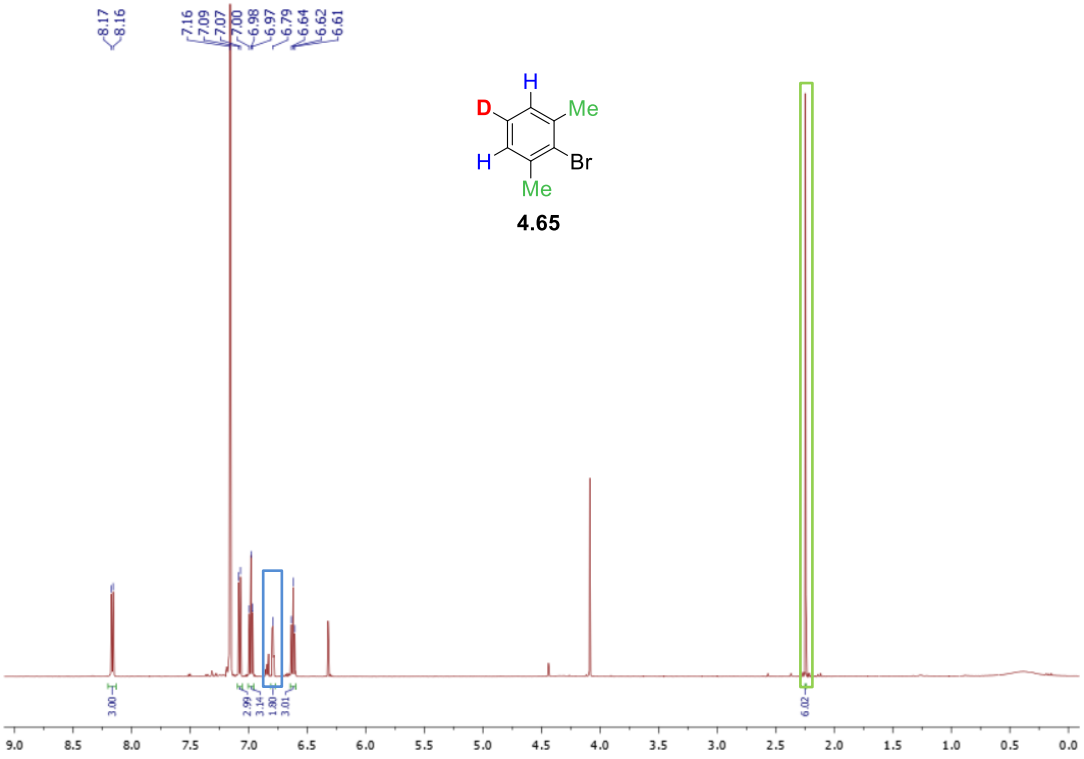


Figure SIV.27. ^{1}H NMR (500 MHz, 25°C, benzene-d_6) of deuteration of **4.49**

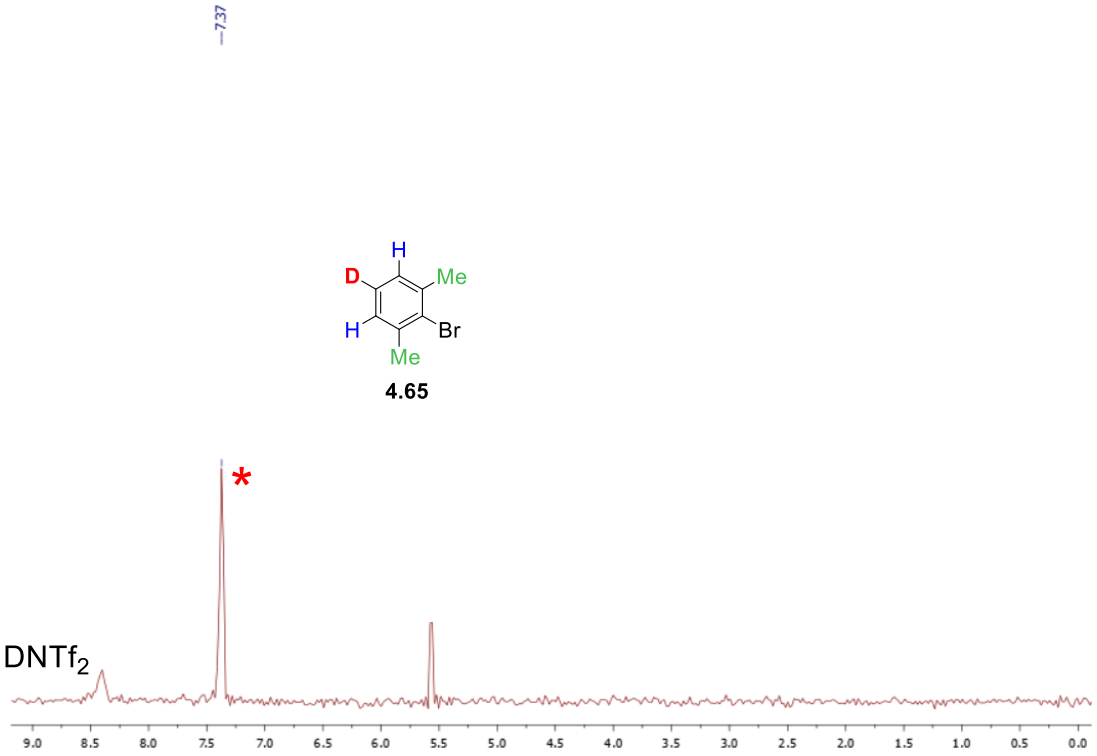
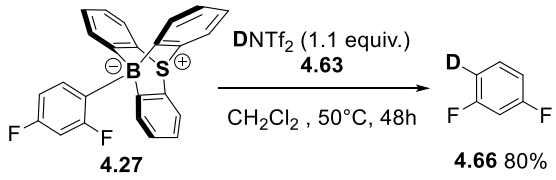


Figure SIV.28. ^{2}D NMR (77 MHz, 25°C, CH_2Cl_2) of deuteration of **4.49**

1,3-difluoro-6-deuterobenzene



In a glovebox, $DNTf_2$ **4.63** (4.0 mg, 0.014 mmol, 1.1 equiv.) was added to a suspension of 10-(2,4-difluorophenyl)-9-sulfonium-10-boratriptycene)ate complex **4.66** (5.0 mg, 0.013 mmol, 1.0 equiv.) in CH_2Cl_2 (0.6 ml). The mixture was transferred in a NMR tube equipped with a J. Young stopper. The reaction was warmed at 50°C for 48h then analyzed by ^{2}D NMR. Acetonitrile-d_3 was used as internal standard for the determination of the yield.

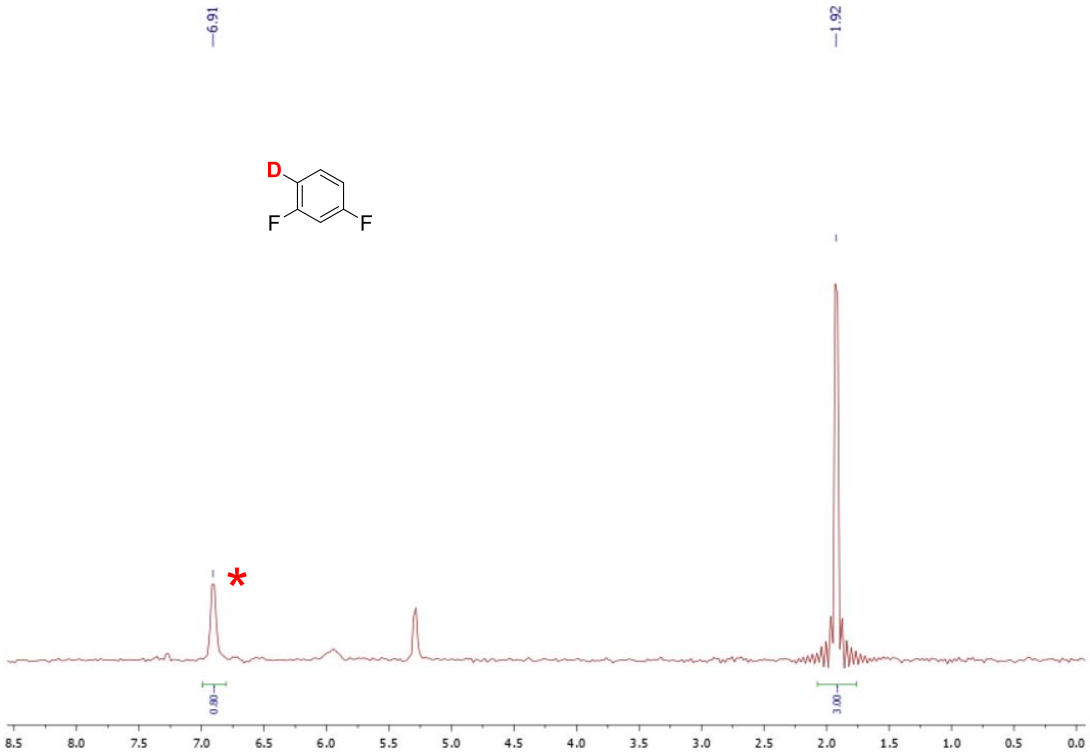
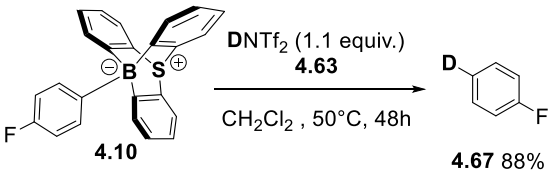


Figure SIV.29. ^{2}D NMR (77 MHz, 25°C, CH_2Cl_2) of deuteration of **4.27**

4-deutero-fluorobenzene



In a glovebox, $DNTf_2$ **4.63** (4.2 mg, 0.015 mmol, 1.1 equiv.) was added to a suspension of 10-(4-fluorophenyl)-9-sulfonium-10-boratriptycene)ate complex **4.10** (5.0 mg, 0.014 mmol, 1.0 equiv.) in CH_2Cl_2 (0.6 ml). The mixture was transferred in a NMR tube equipped with a J. Young stopper. The reaction was warmed at 50°C for 48h then analyzed by ^{2}D NMR. Acetonitrile-d_3 was used as internal standard for the determination of the yield.

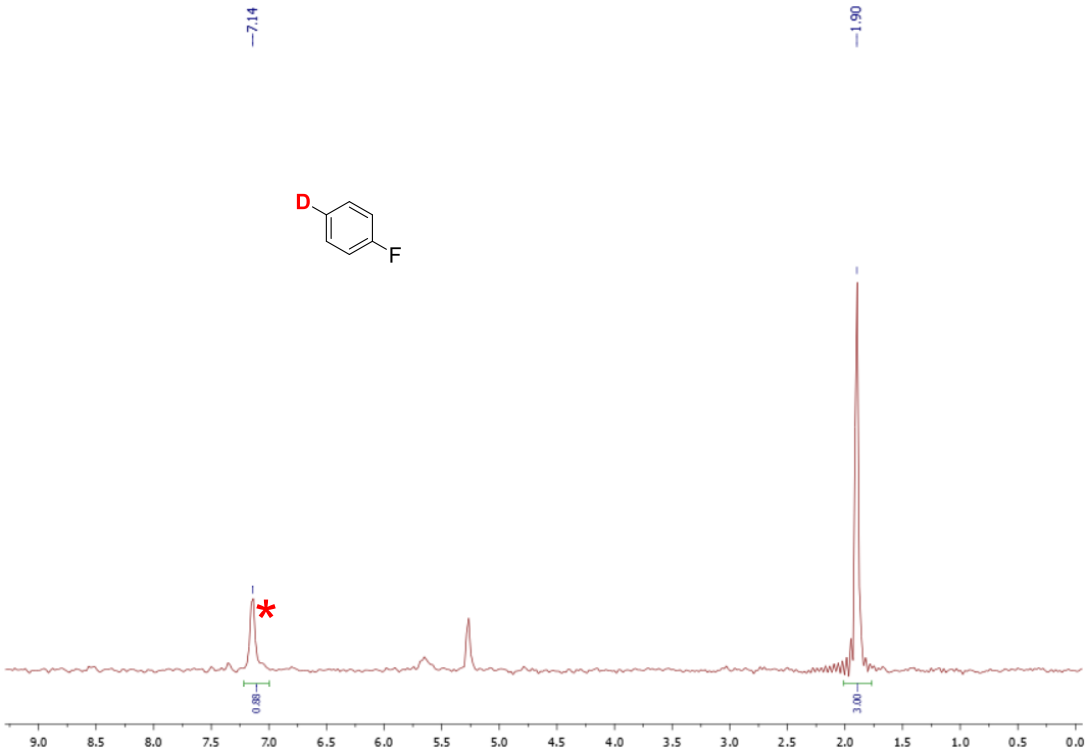
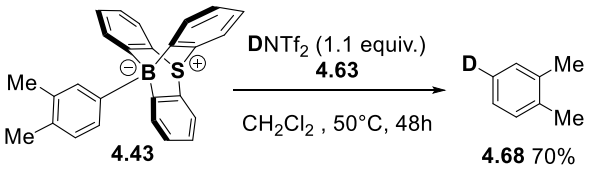


Figure SIV.30. ^{2}D NMR (77 MHz, 25°C, CH_2Cl_2) of deuteration of **4.10**

3-deutero-*o*-xylene



In a glovebox, $DNTf_2$ **4.63** (4.2 mg, 0.015 mmol, 1.1 equiv.) was added to a suspension of 10-(3,4-dimethylphenyl)-9-sulfonium-10-boratriptycene)ate complex **4.43** (5.0 mg, 0.013 mmol, 1.0 equiv.) in CH_2Cl_2 (0.6 ml). The mixture was transferred in a NMR tube equipped with a J. Young stopper. The reaction was warmed at 50°C for 48h then analyzed by ^{2}D NMR. Acetonitrile-d_3 was used as internal standard for the determination of the yield.

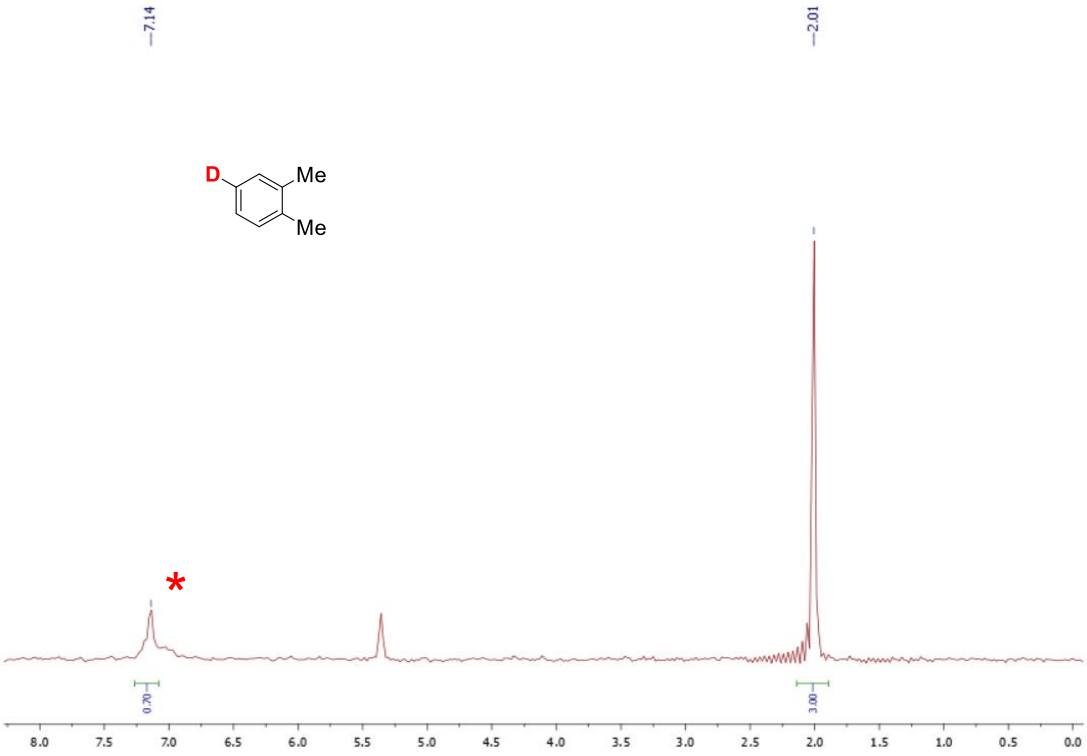
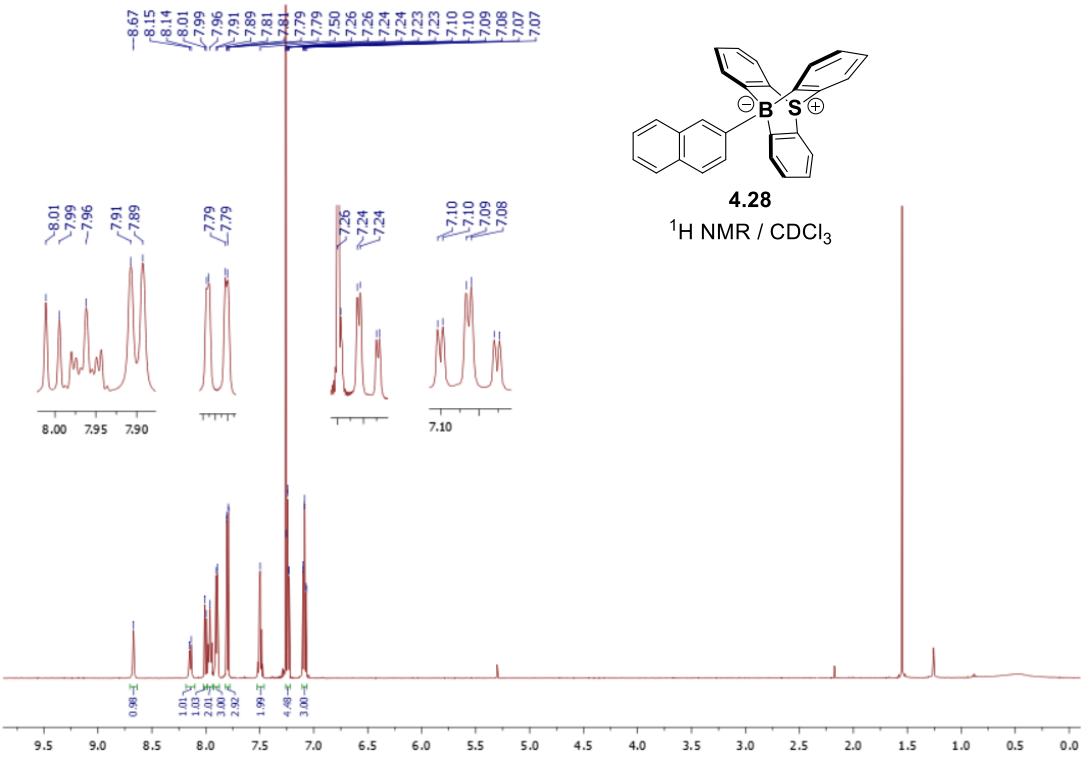
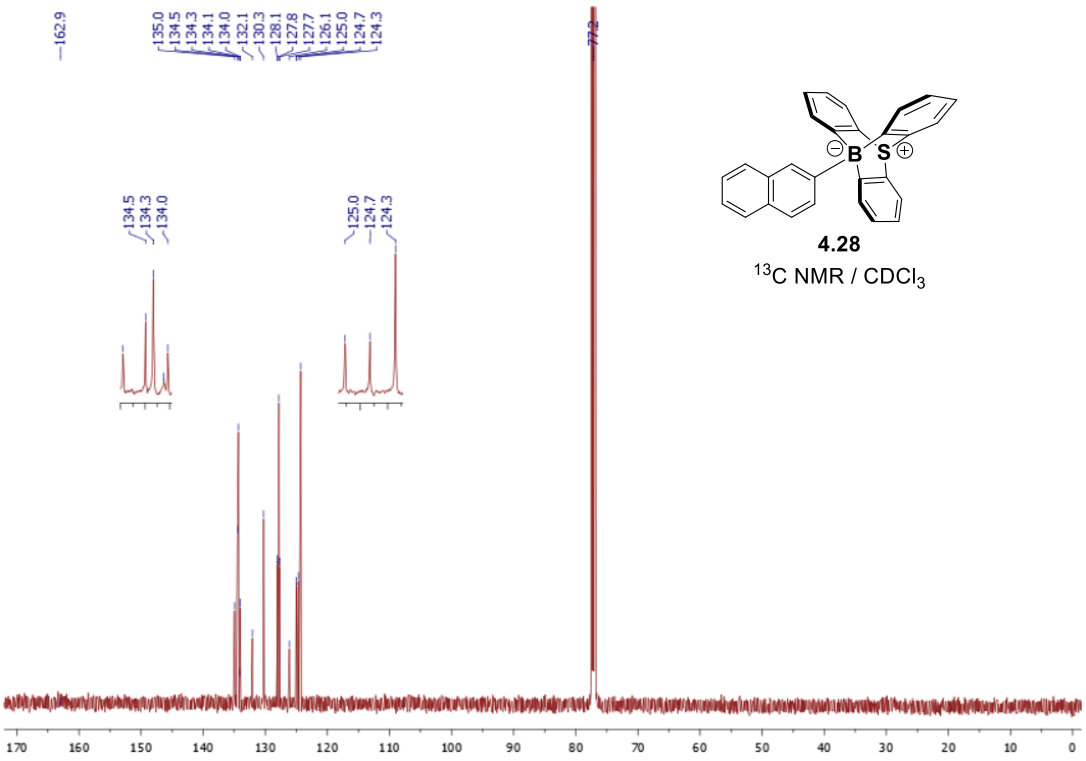


Figure SIV.31. ^{2}D NMR (77 MHz, 25°C, CH_2Cl_2) of deuteration of **4.43**

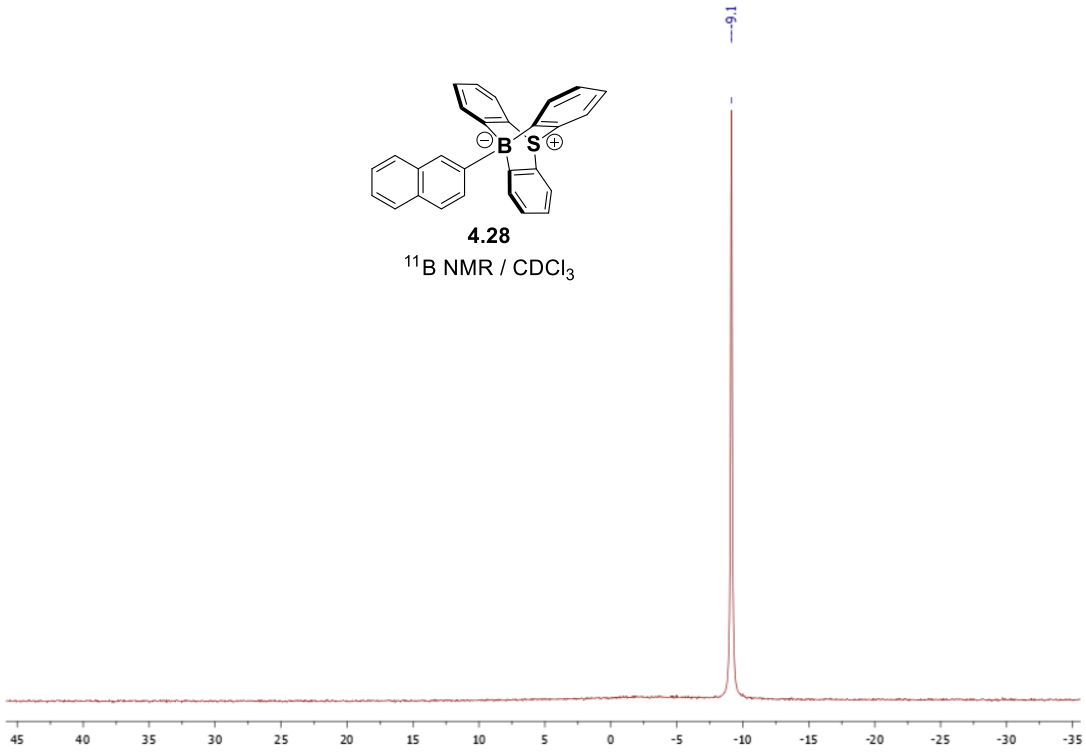
IV.10. NMR spectra of synthesized compounds



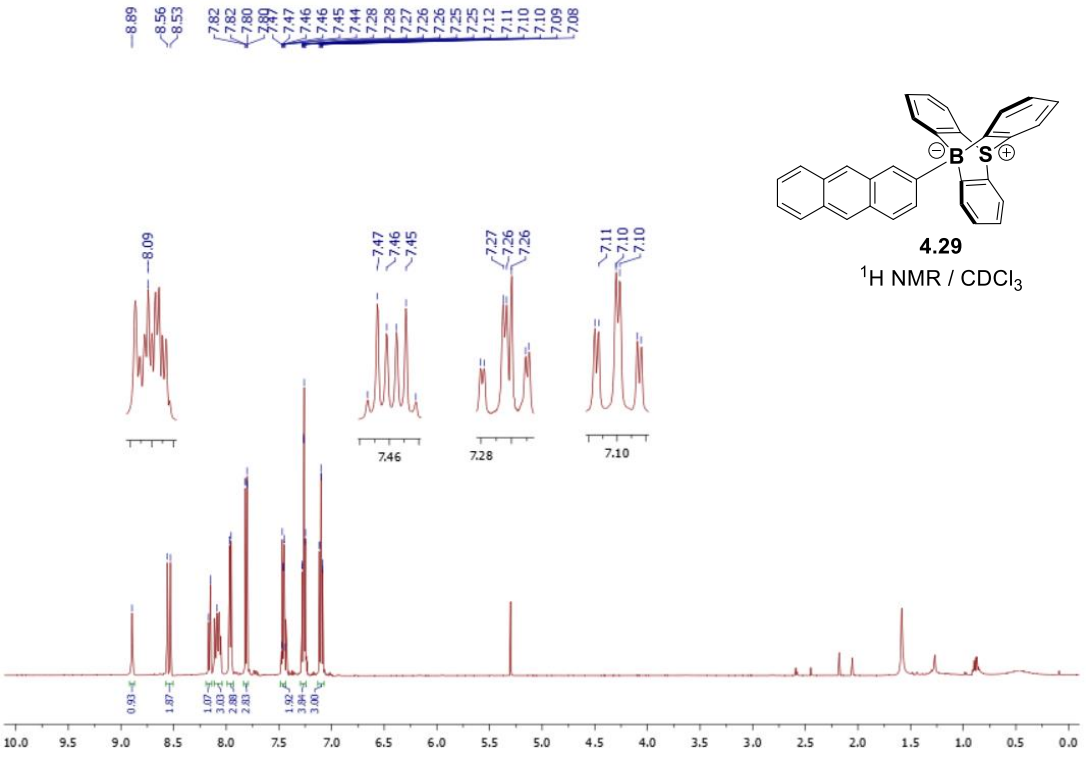
^{1}H NMR (500 MHz, 25°C, $CDCl_3$) of **4.28**



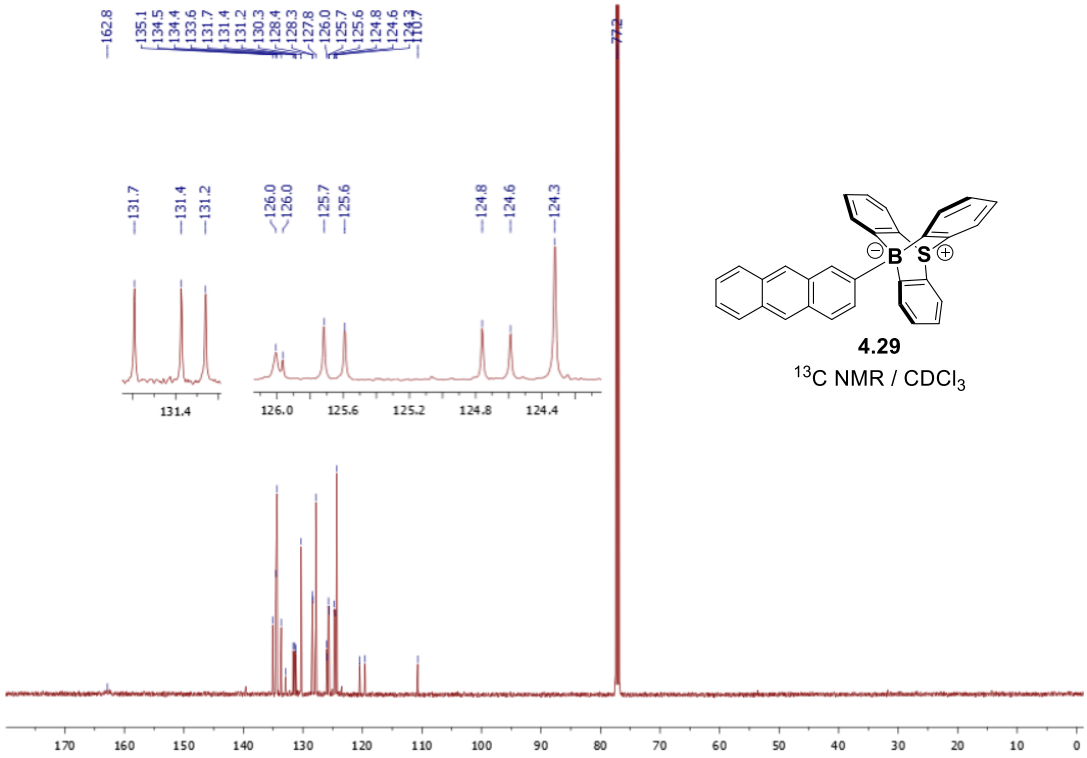
^{13}C NMR (126 MHz, 25°C, $CDCl_3$) of **4.28**



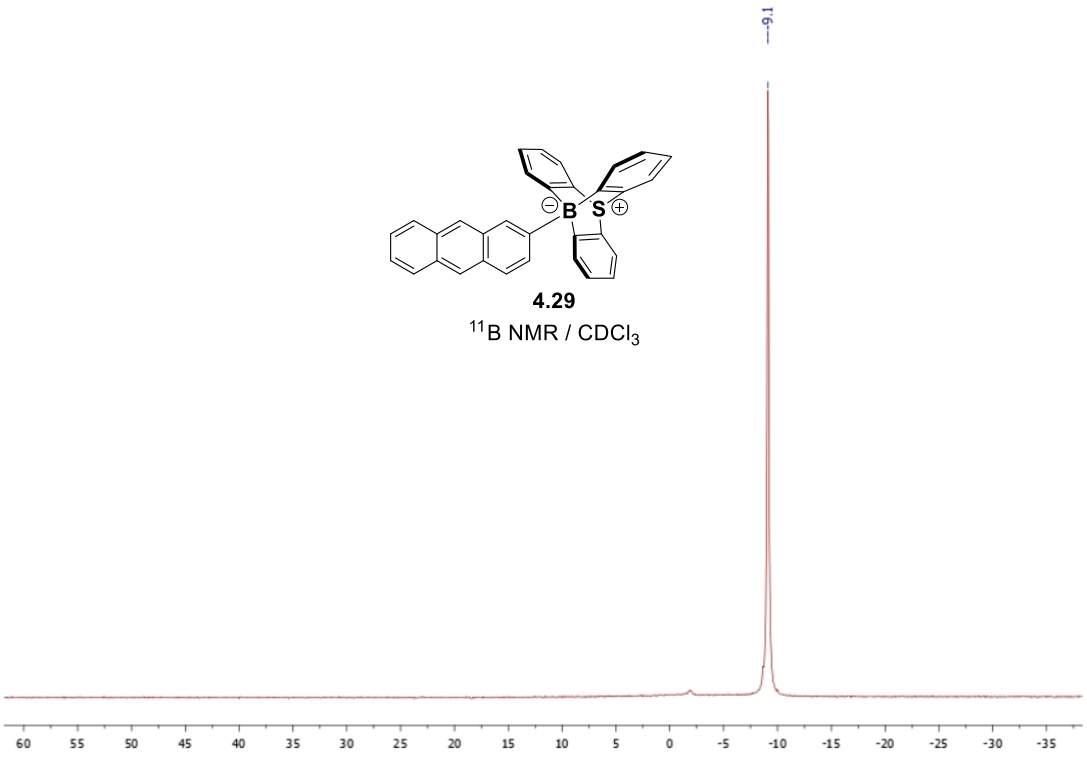
^{11}B NMR (160 MHz, 25°C, $CDCl_3$) of **4.28**



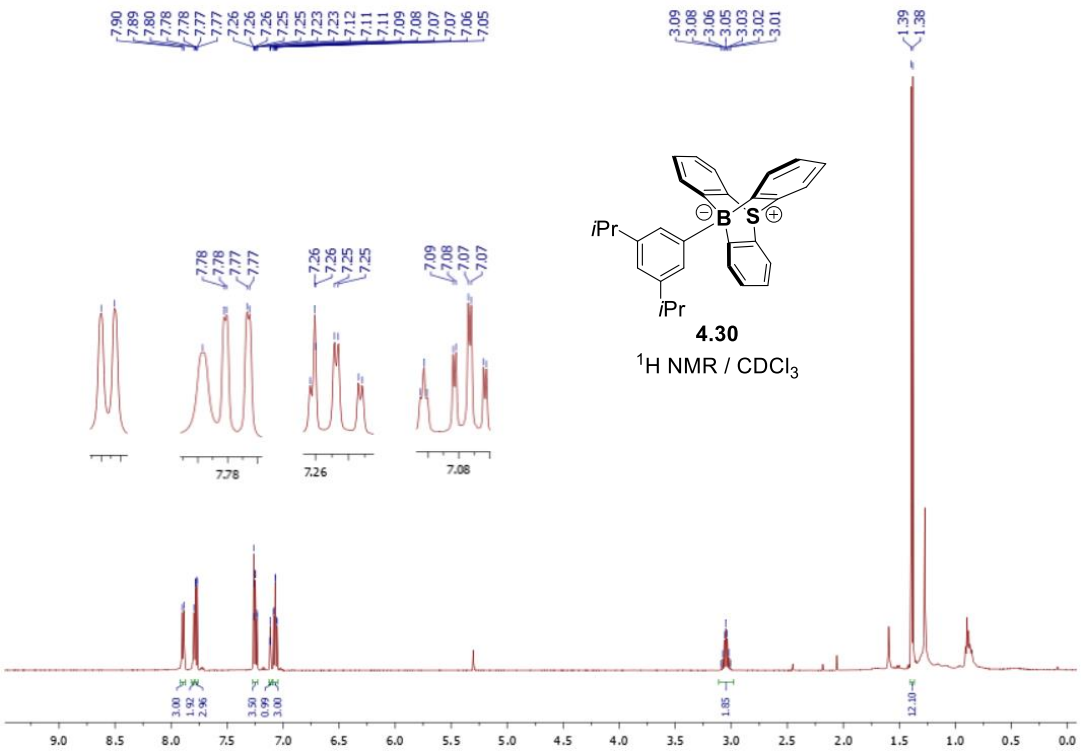
^{1}H NMR (500 MHz, 25°C, $CDCl_3$) of **4.29**



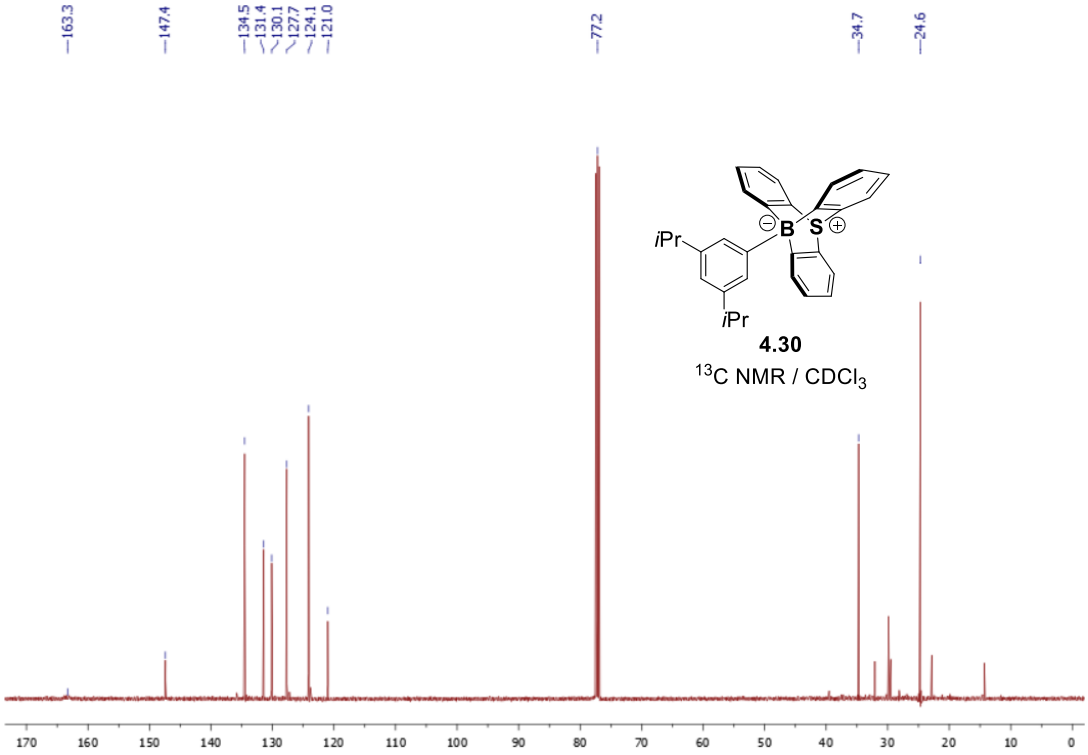
^{13}C NMR (126 MHz, 25°C, $CDCl_3$) of **4.29**



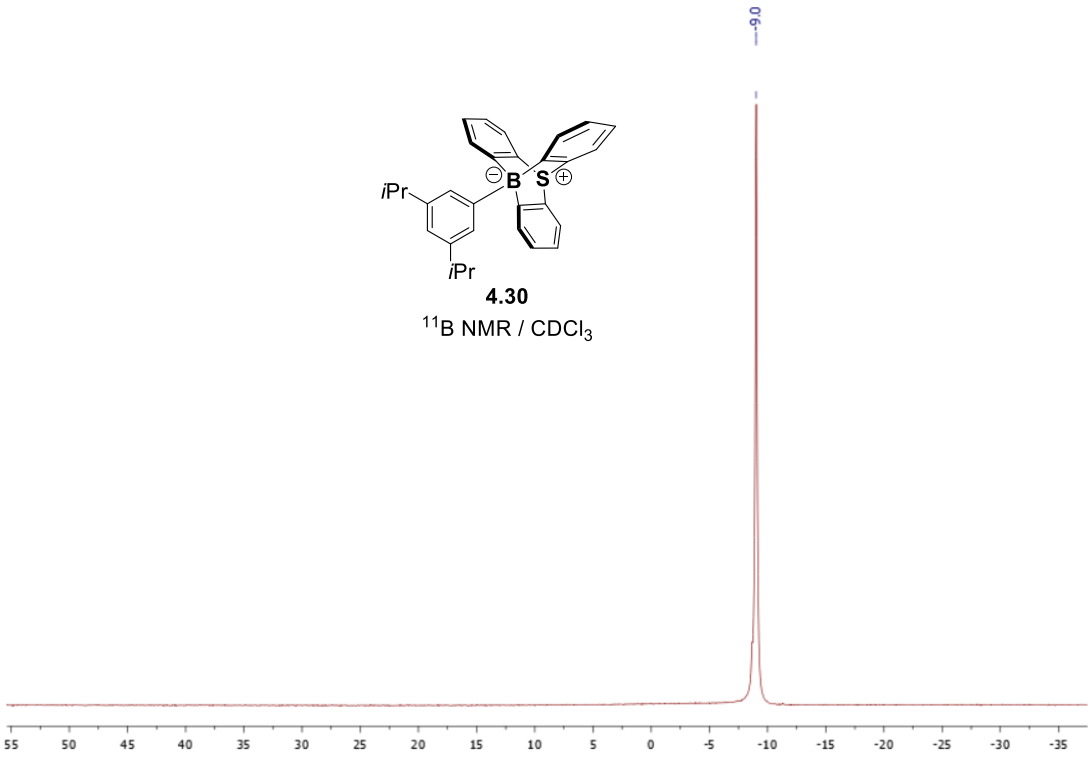
^{11}B NMR (160 MHz, 25°C, $CDCl_3$) of **4.29**



^{1}H NMR (500 MHz, 25°C, $CDCl_3$) of **4.30**



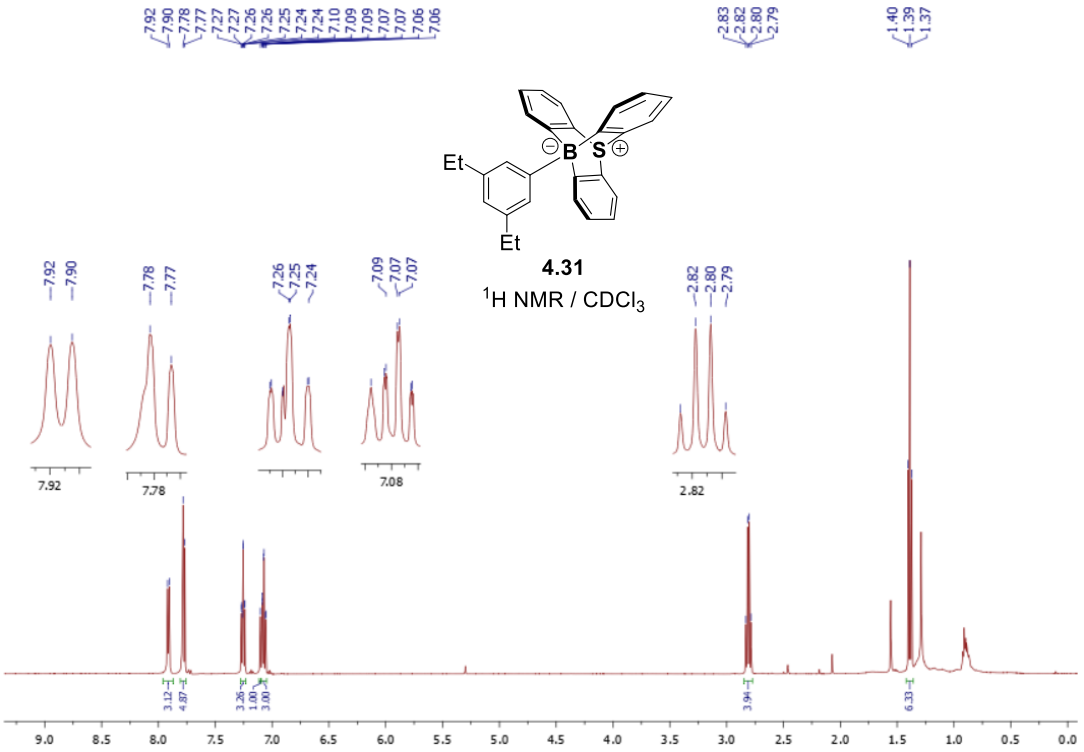
^{13}C NMR (126 MHz, 25°C, $CDCl_3$) of **4.30**



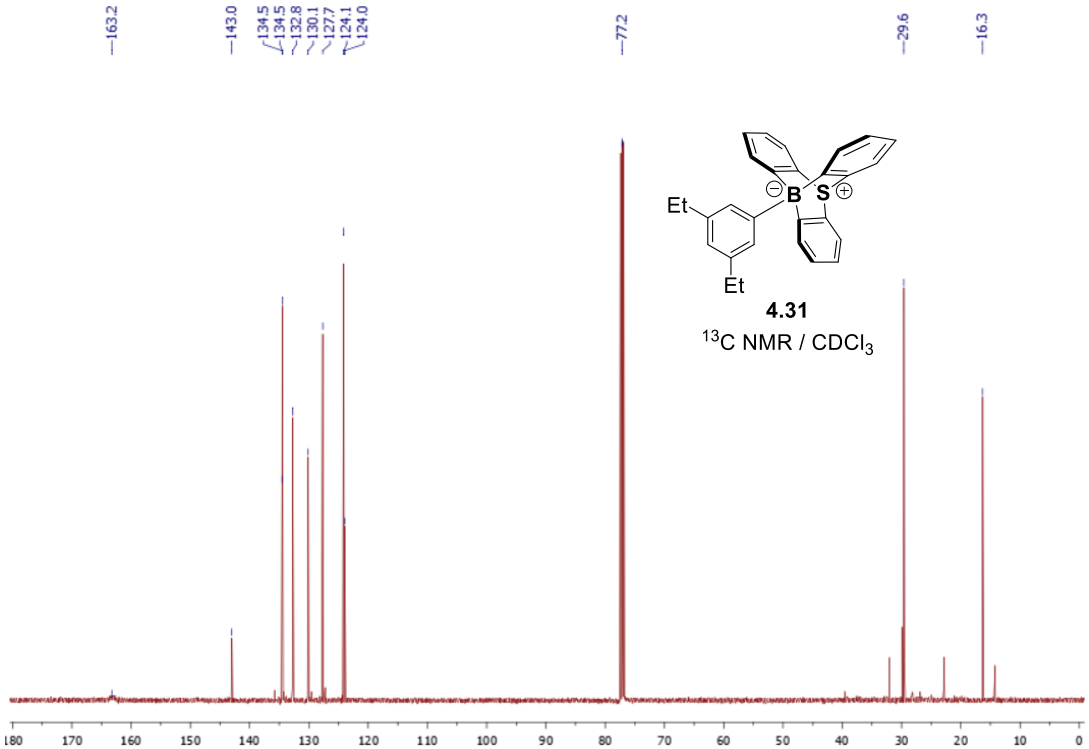
4.30

^{11}B NMR / $CDCl_3$

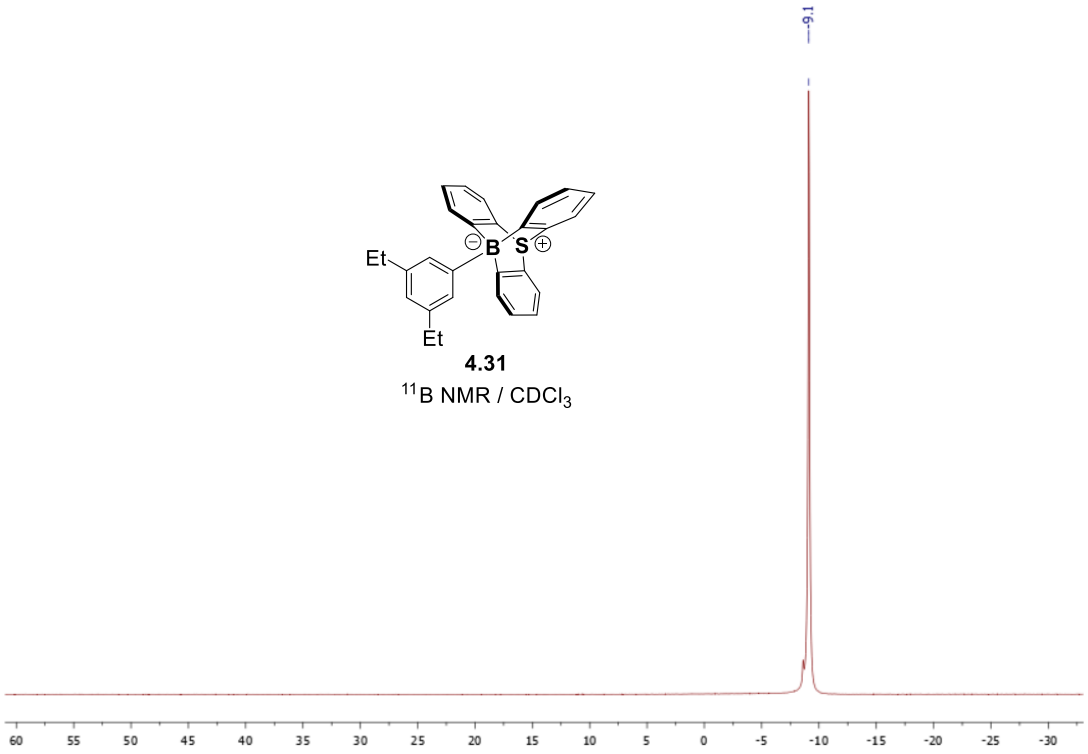
^{11}B NMR (160 MHz, 25°C, $CDCl_3$) of **4.30**



^{1}H NMR (500 MHz, 25°C, $CDCl_3$) of **4.31**



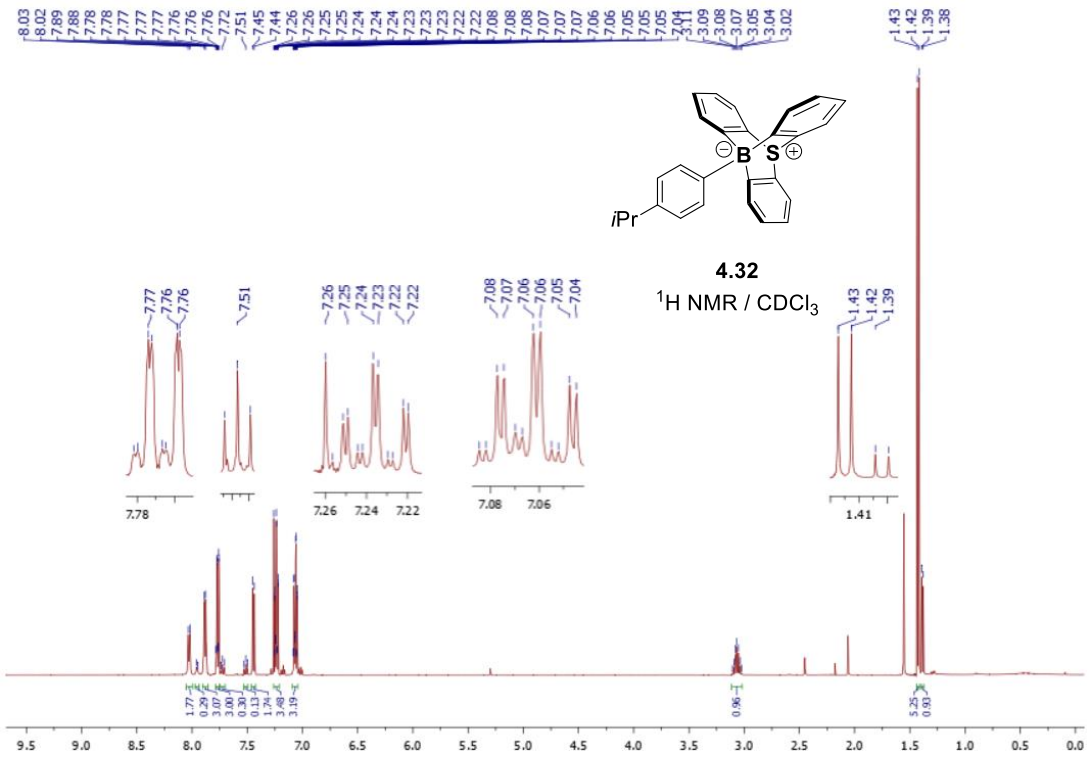
^{13}C NMR (126 MHz, 25°C, $CDCl_3$) of **4.31**



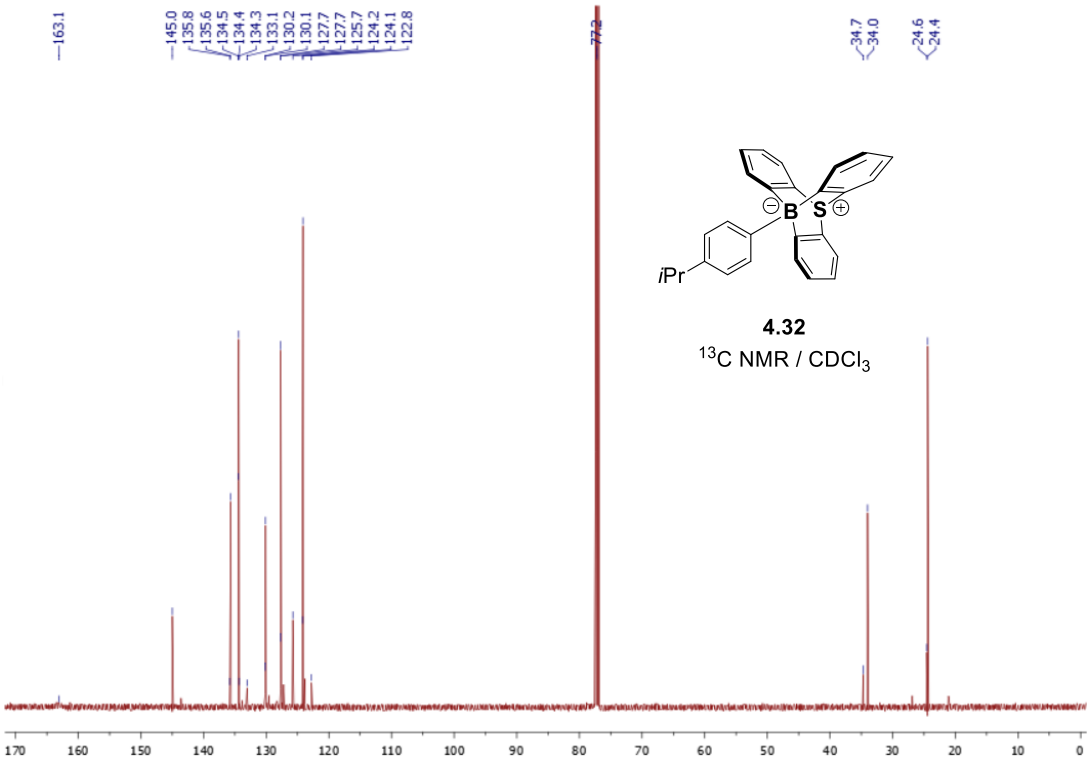
4.31

^{11}B NMR / $CDCl_3$

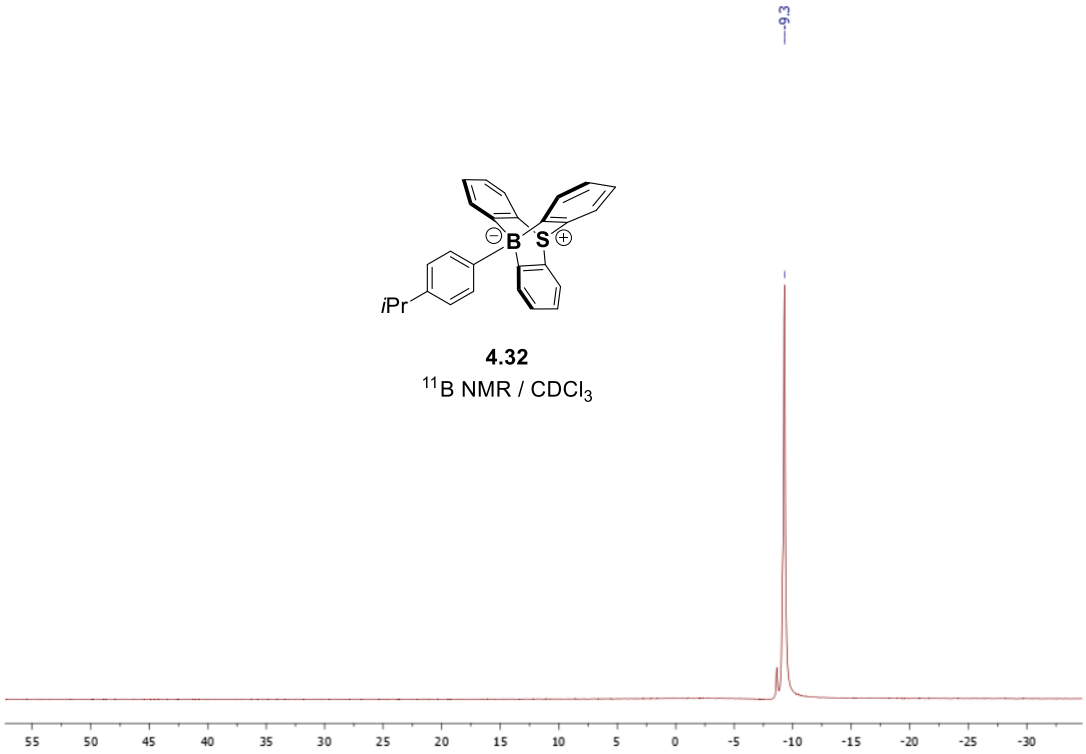
^{11}B NMR (160 MHz, 25°C, $CDCl_3$) of **4.31**



^{1}H NMR (500 MHz, 25°C, $CDCl_3$) of **4.32**



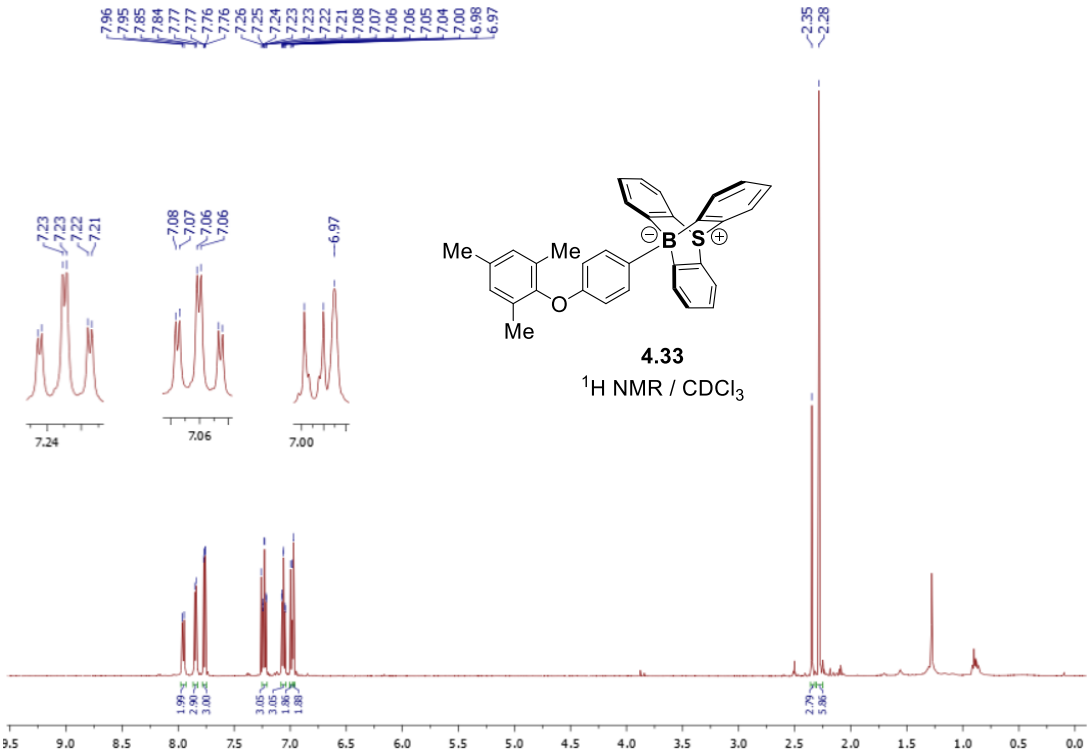
^{13}C NMR (126 MHz, 25°C, $CDCl_3$) of **4.32**



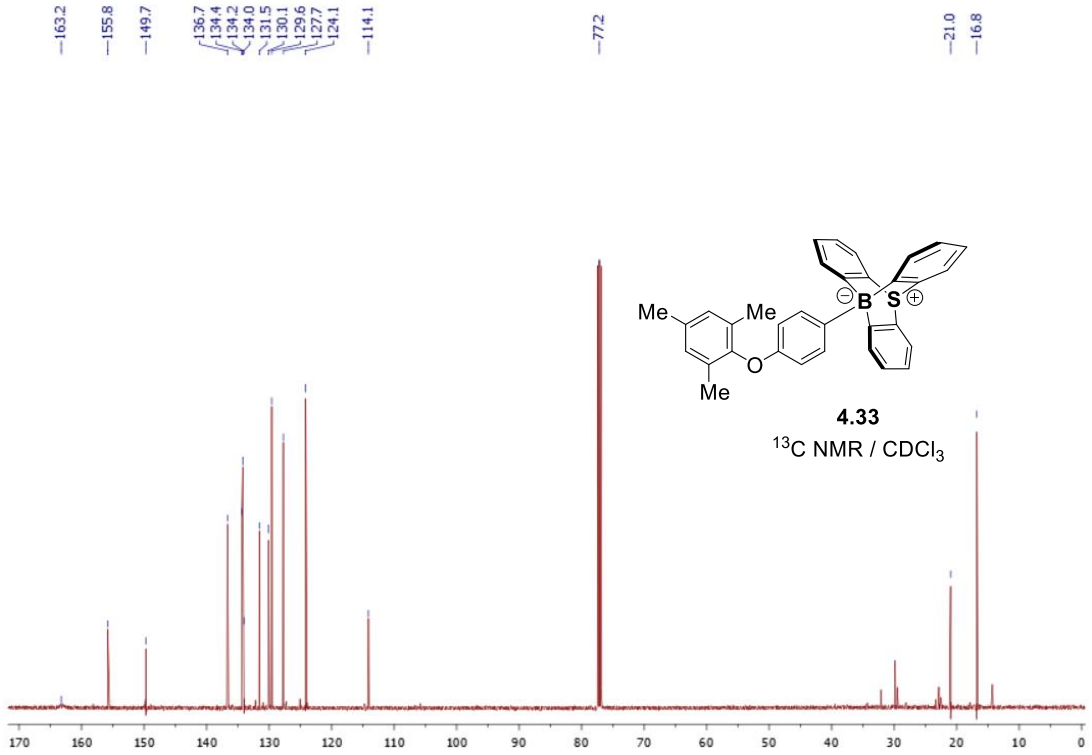
4.32

^{11}B NMR / $CDCl_3$

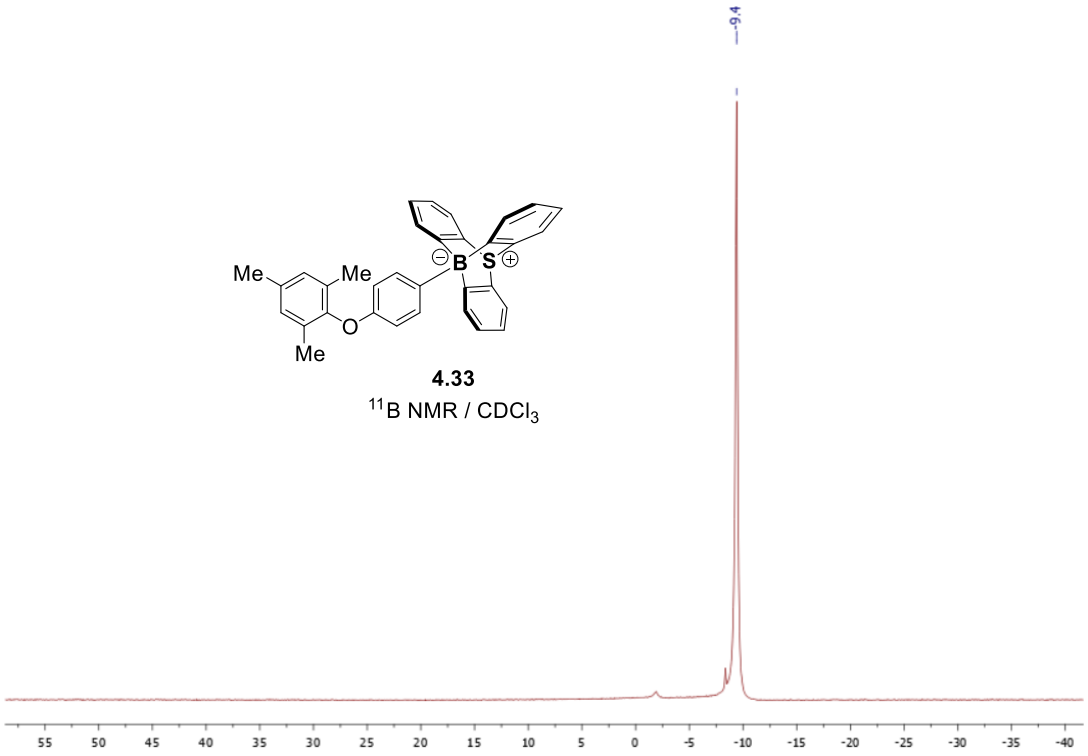
^{11}B NMR (160 MHz, 25°C, $CDCl_3$) of **4.32**



^{1}H NMR (500 MHz, 25°C, $CDCl_3$) of **4.33**



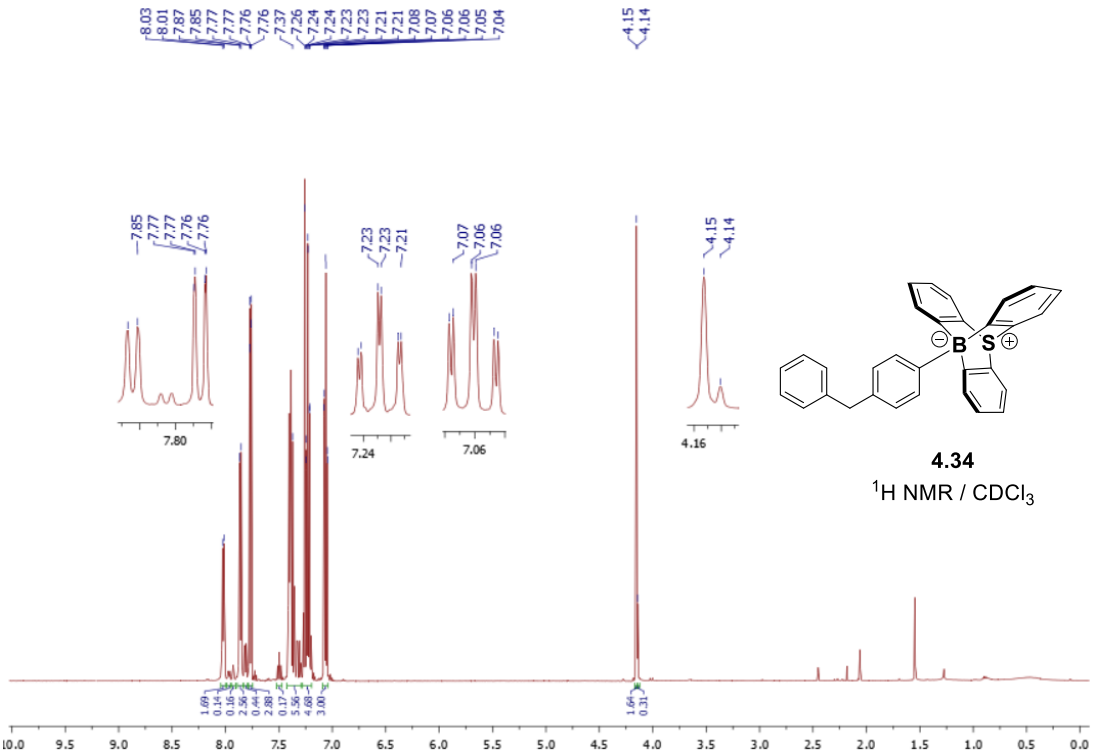
^{13}C NMR (126 MHz, 25°C, $CDCl_3$) of **4.33**



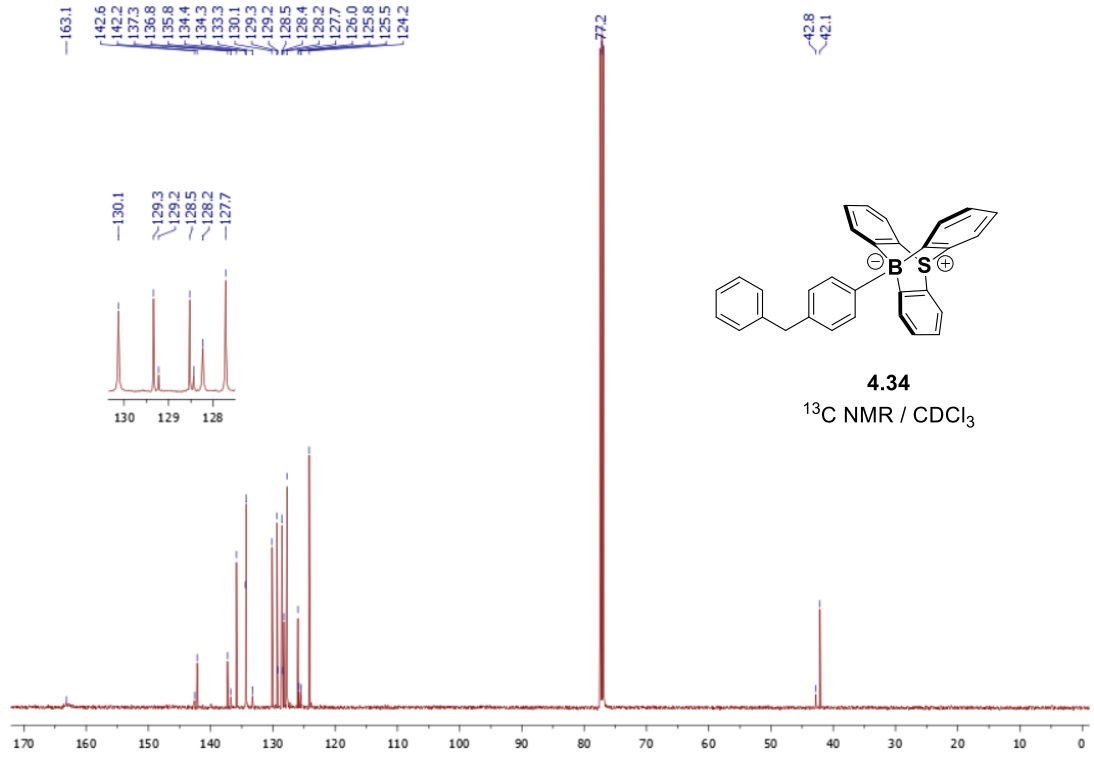
4.33

^{11}B NMR / $CDCl_3$

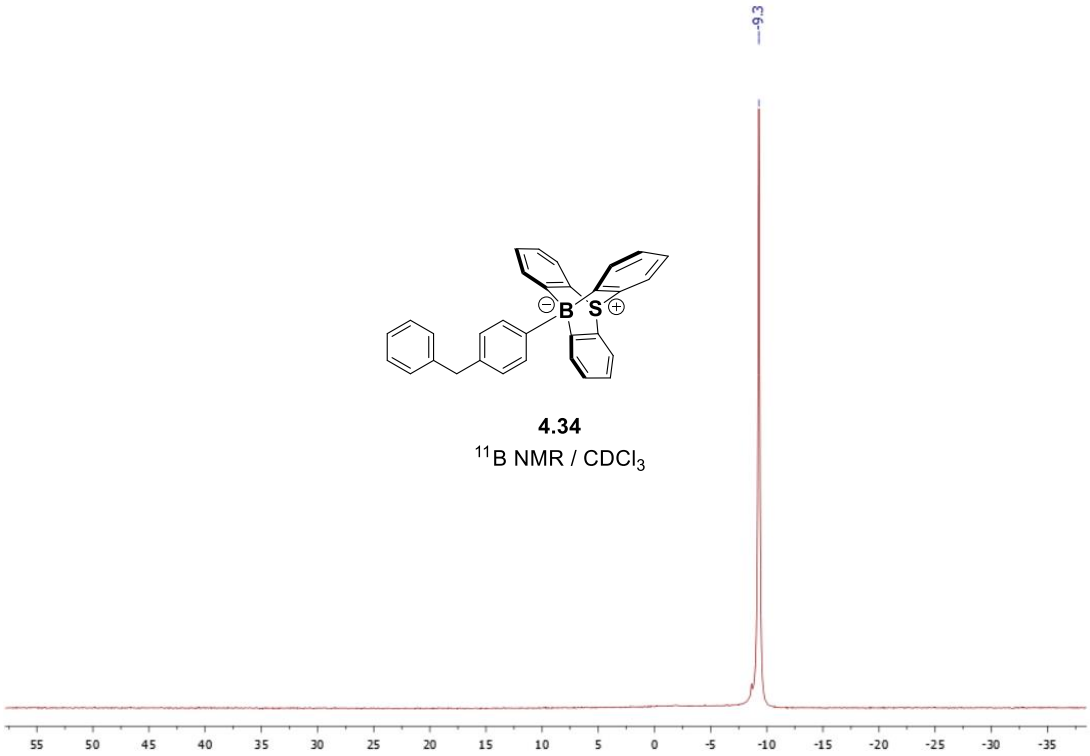
^{11}B NMR (160 MHz, 25°C, $CDCl_3$) of **4.33**



^{1}H NMR (500 MHz, 25°C, $CDCl_3$) of **4.34**



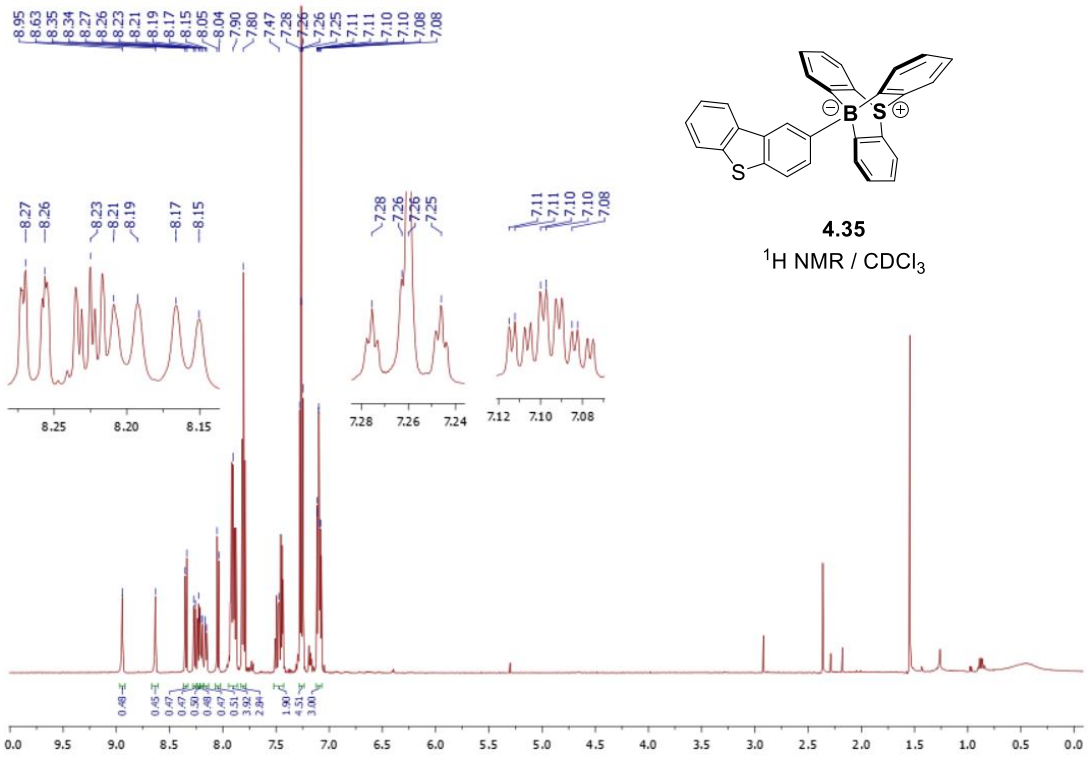
^{13}C NMR (126 MHz, 25°C, $CDCl_3$) of **4.34**



4.34

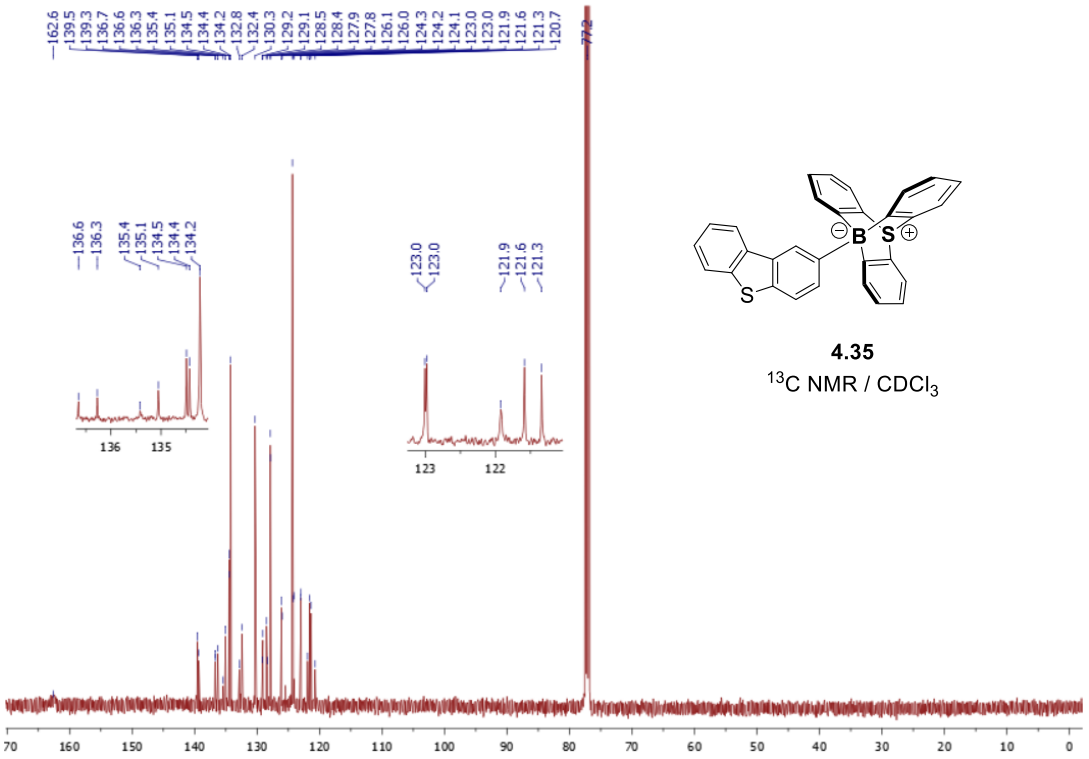
^{11}B NMR / $CDCl_3$

^{11}B NMR (160 MHz, 25°C, $CDCl_3$) of **4.34**



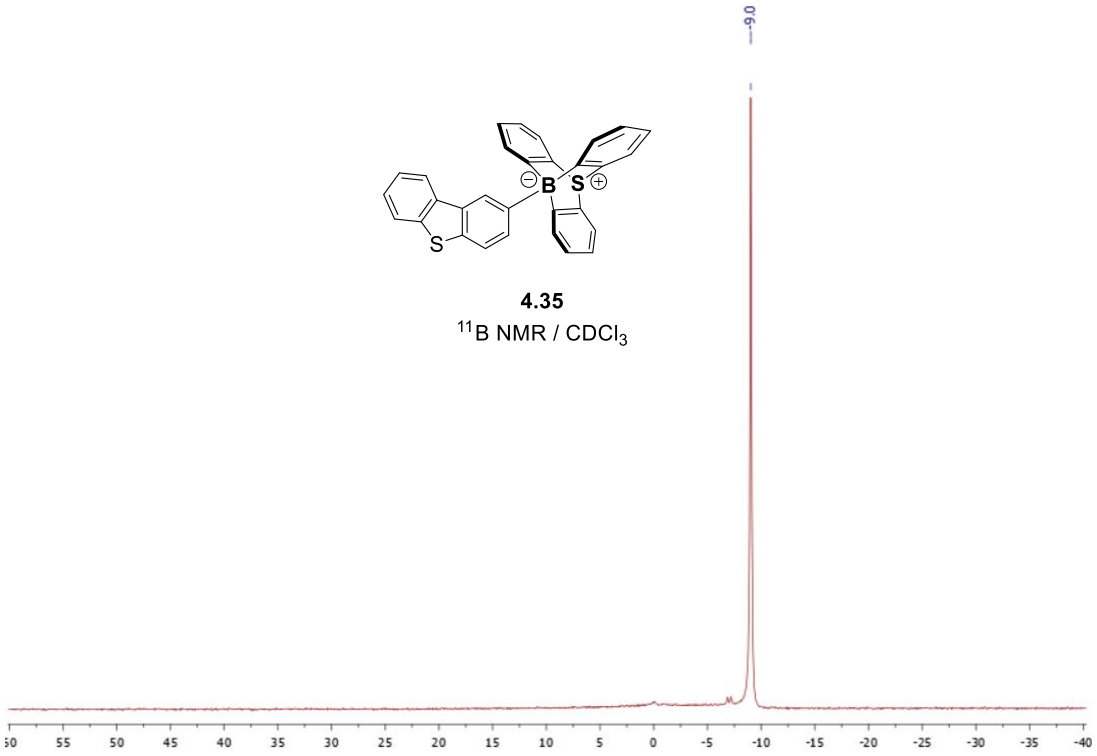
4.35
^{1}H NMR / $CDCl_3$

^{1}H NMR (500 MHz, 25°C, $CDCl_3$) of **4.35**



4.35
^{13}C NMR / $CDCl_3$

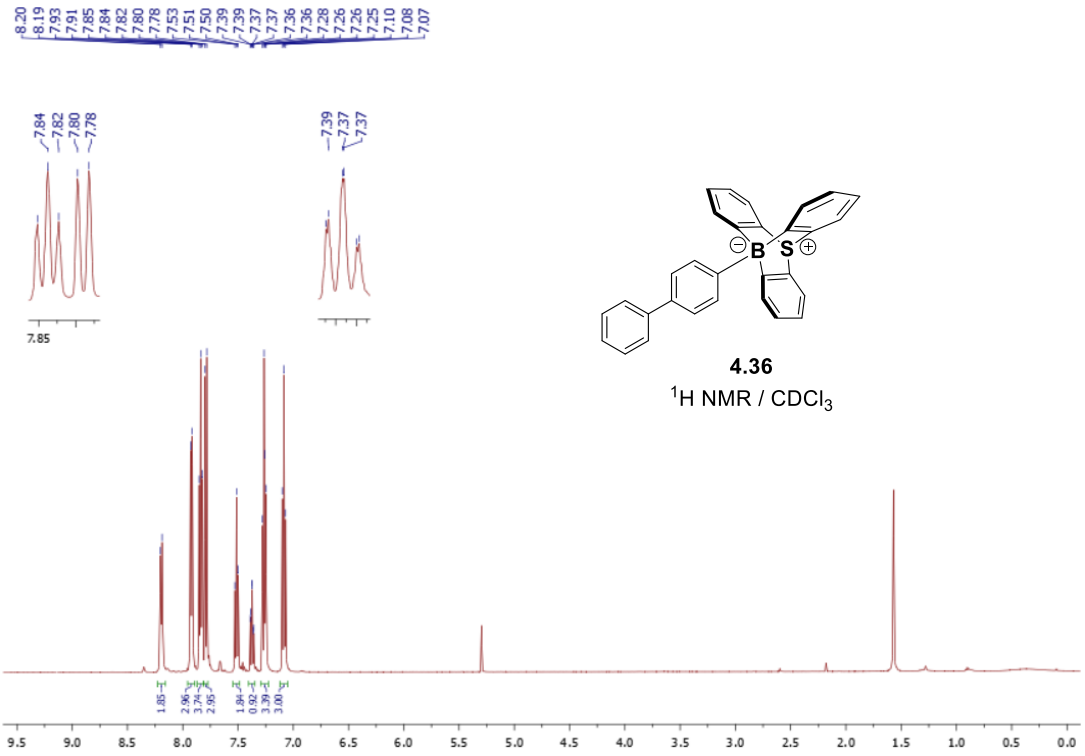
^{13}C NMR (126 MHz, 25°C, $CDCl_3$) of **4.35**



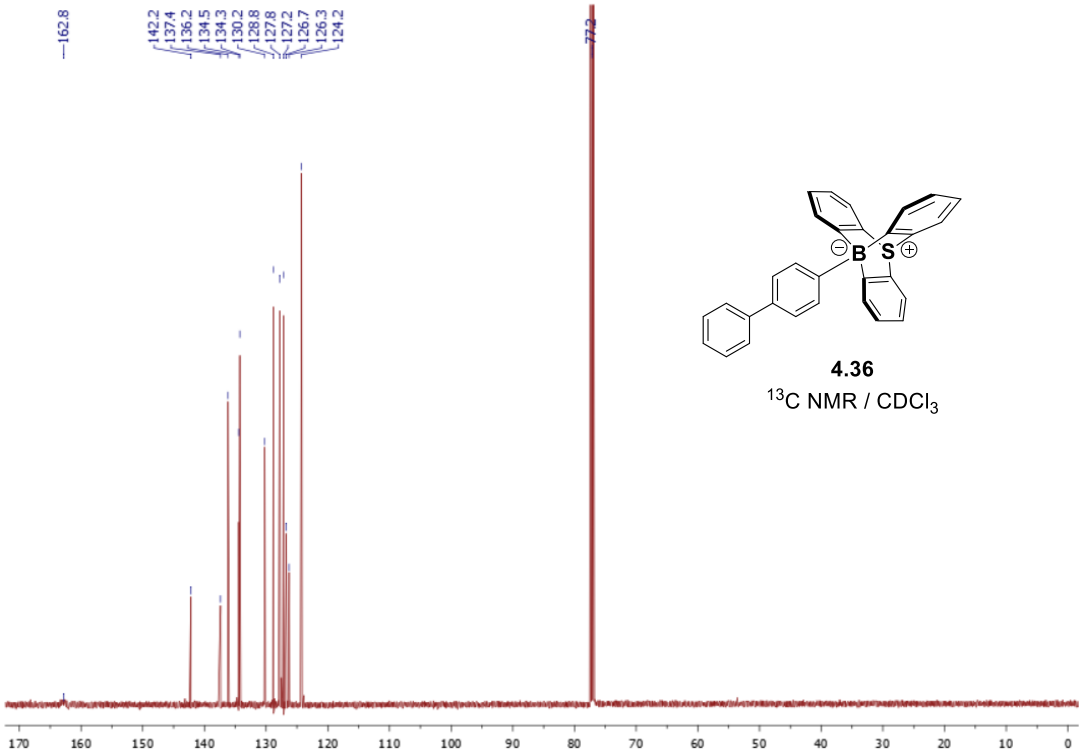
4.35

^{11}B NMR / $CDCl_3$

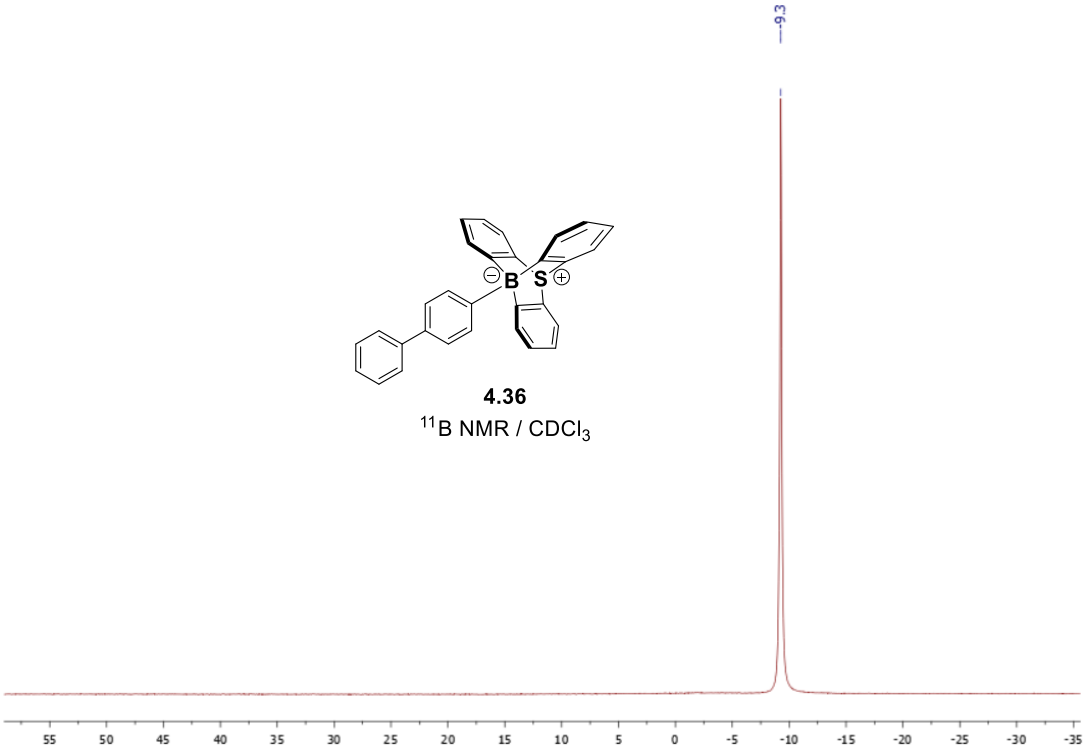
^{11}B NMR (160 MHz, 25°C, $CDCl_3$) of **4.35**



^{1}H NMR (500 MHz, 25°C, $CDCl_3$) of **4.36**



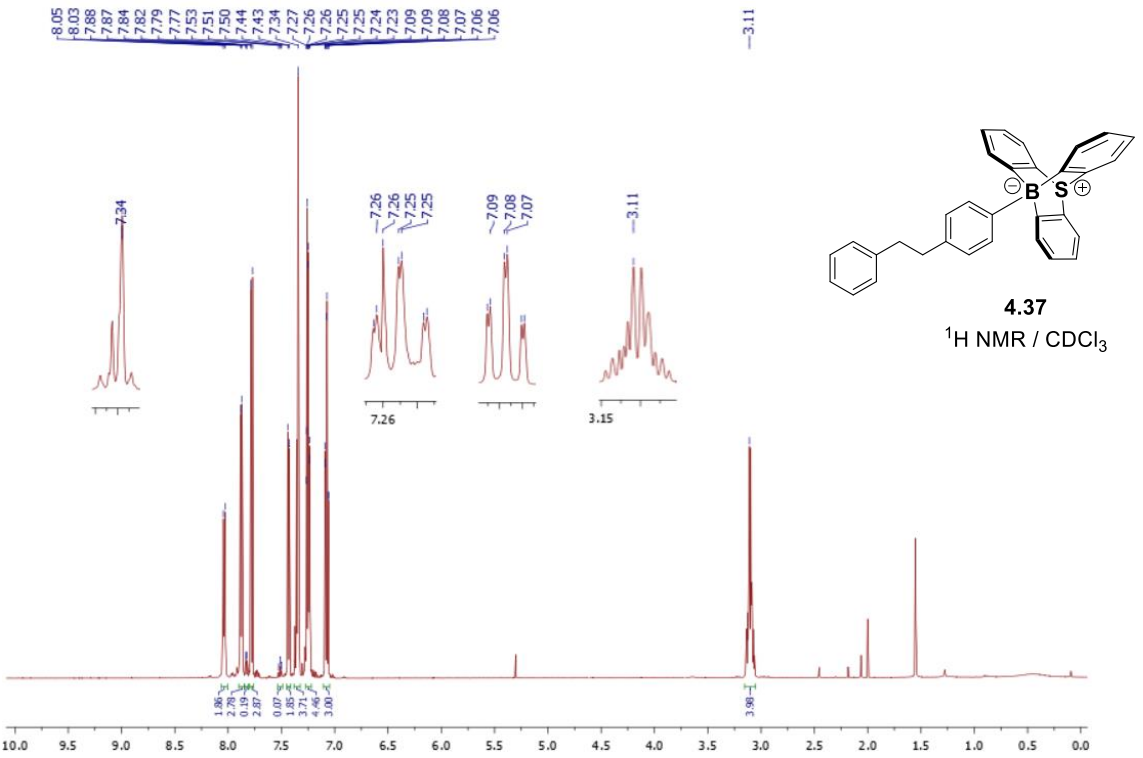
^{13}C NMR (126 MHz, 25°C, $CDCl_3$) of **4.36**



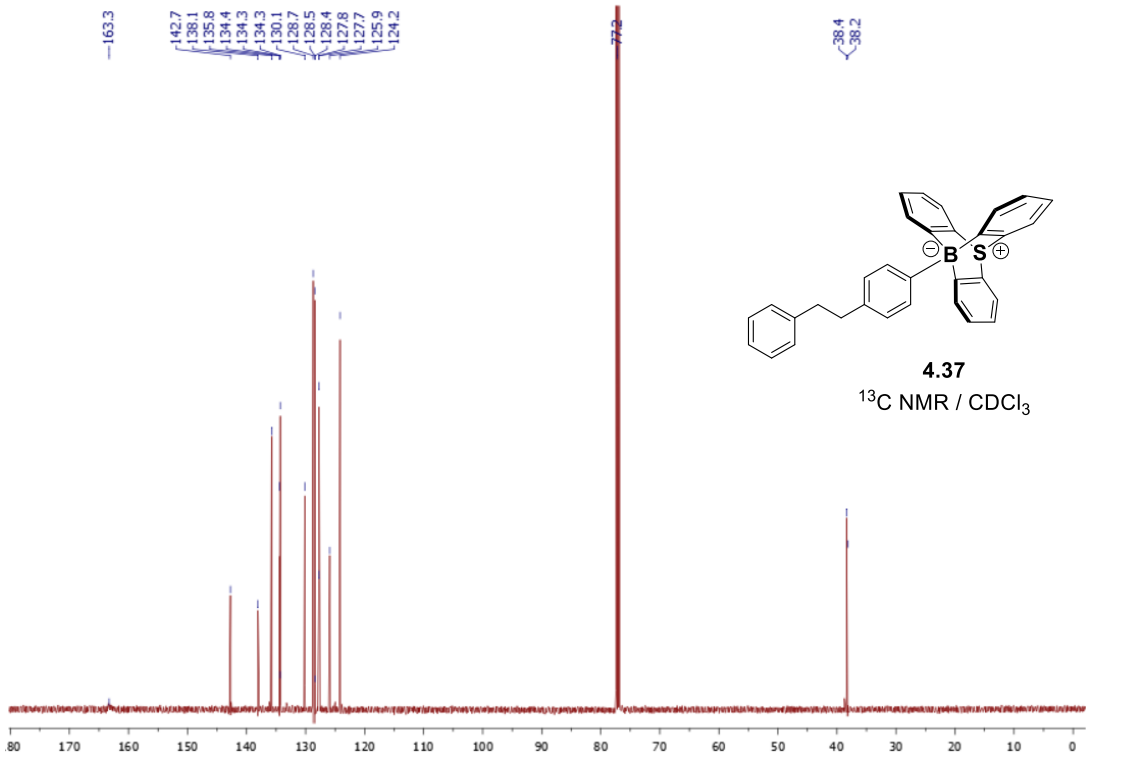
4.36

^{11}B NMR / $CDCl_3$

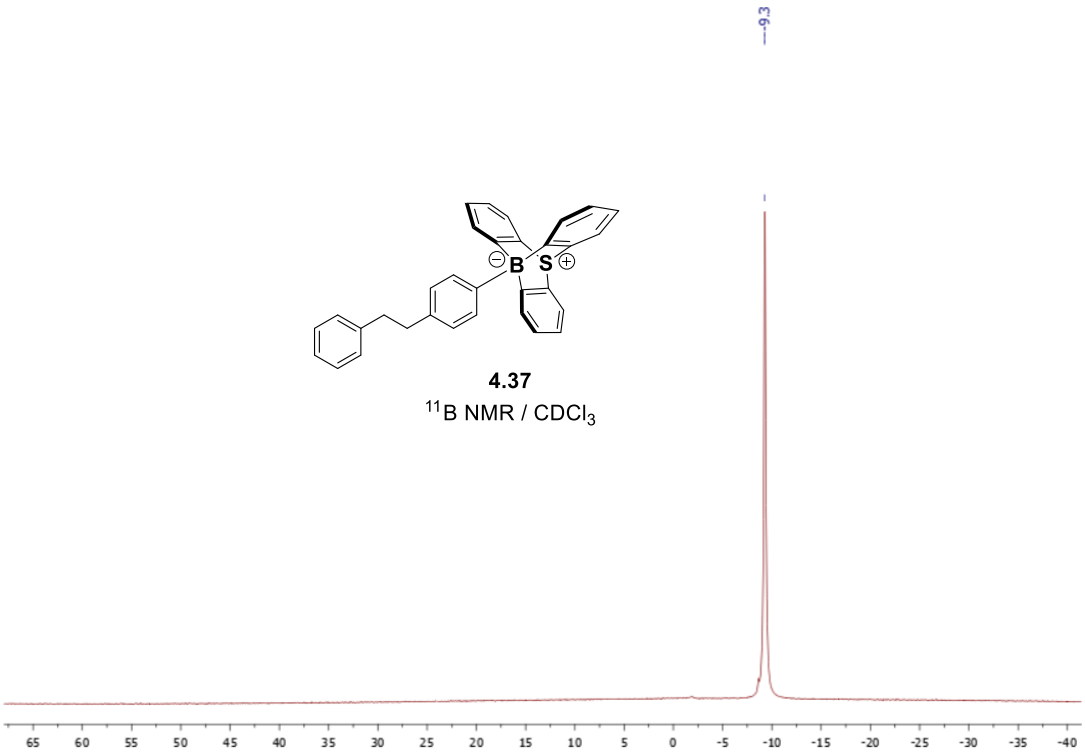
^{11}B NMR (160 MHz, 25°C, $CDCl_3$) of **4.36**



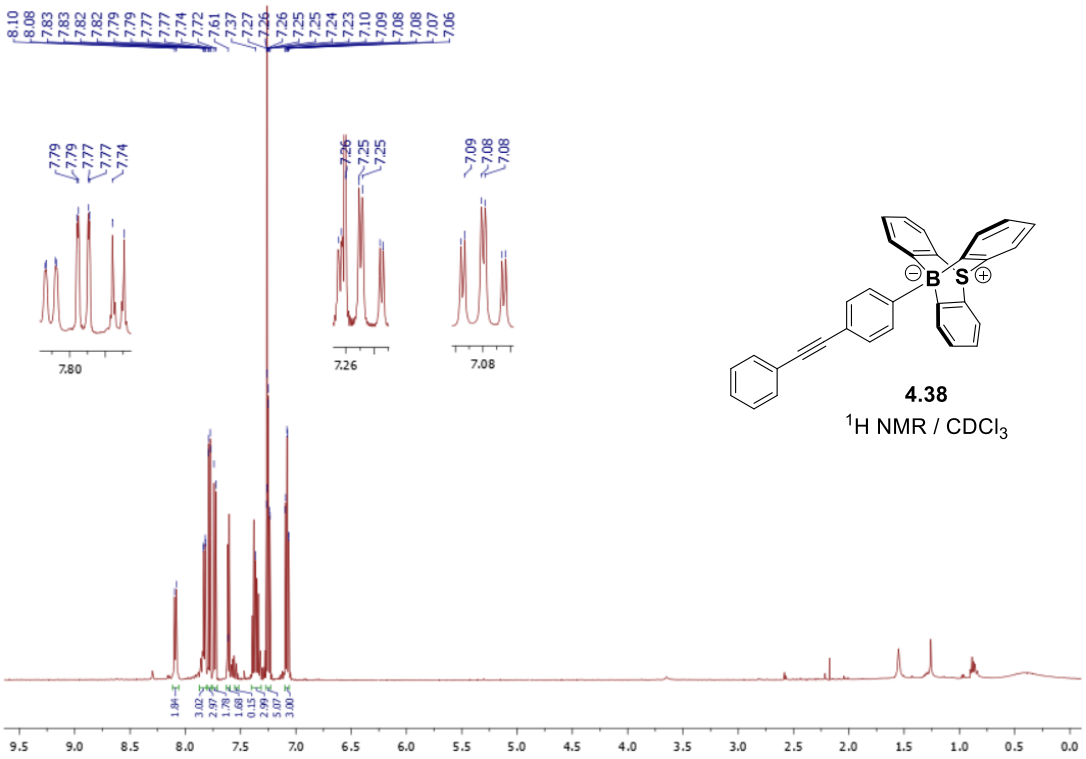
^{1}H NMR (500 MHz, 25°C, $CDCl_3$) of **4.37**



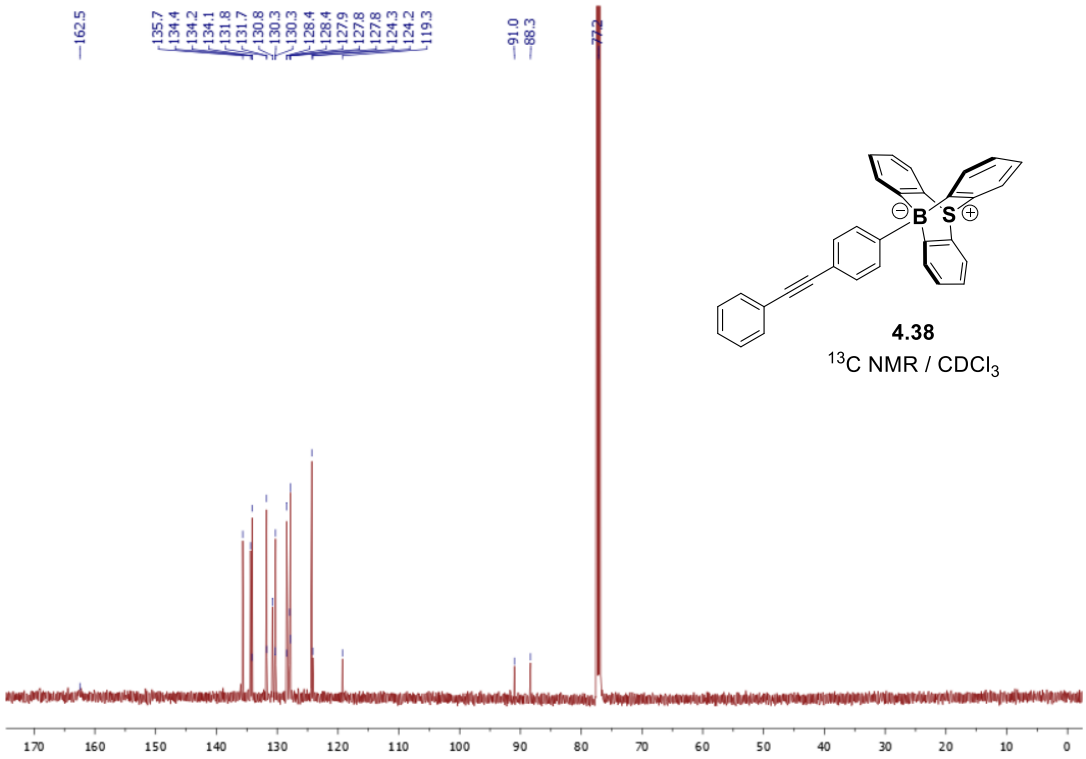
^{13}C NMR (126 MHz, 25°C, $CDCl_3$) of **4.37**



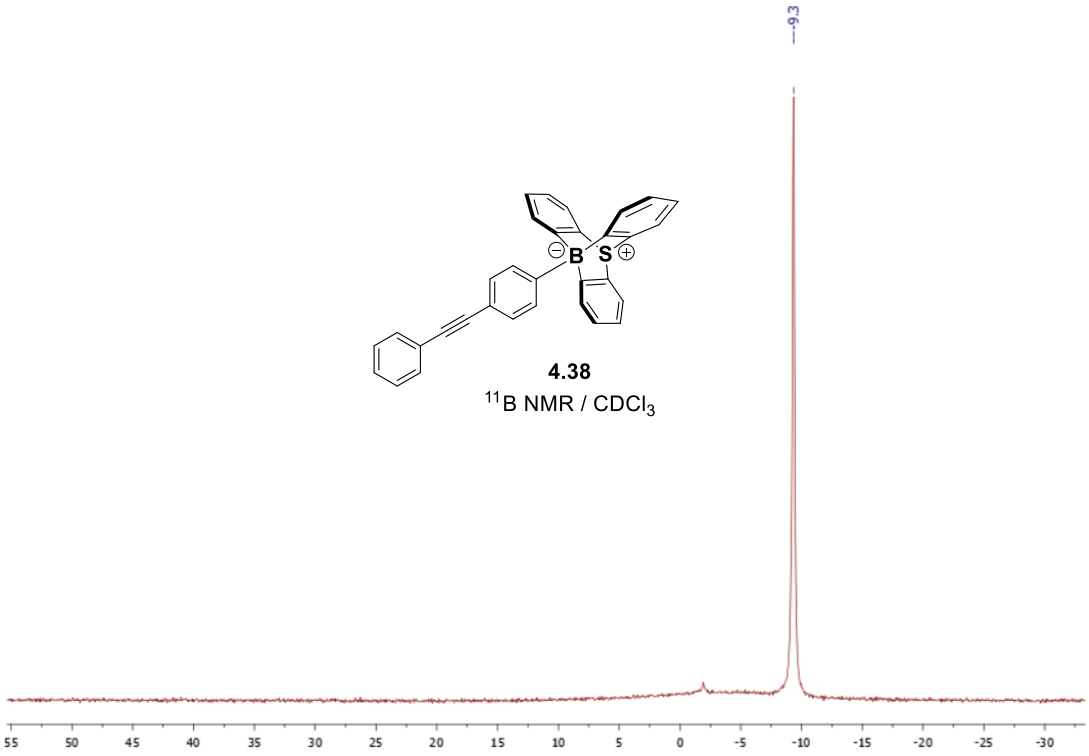
^{11}B NMR (160 MHz, 25°C, $CDCl_3$) of **4.37**



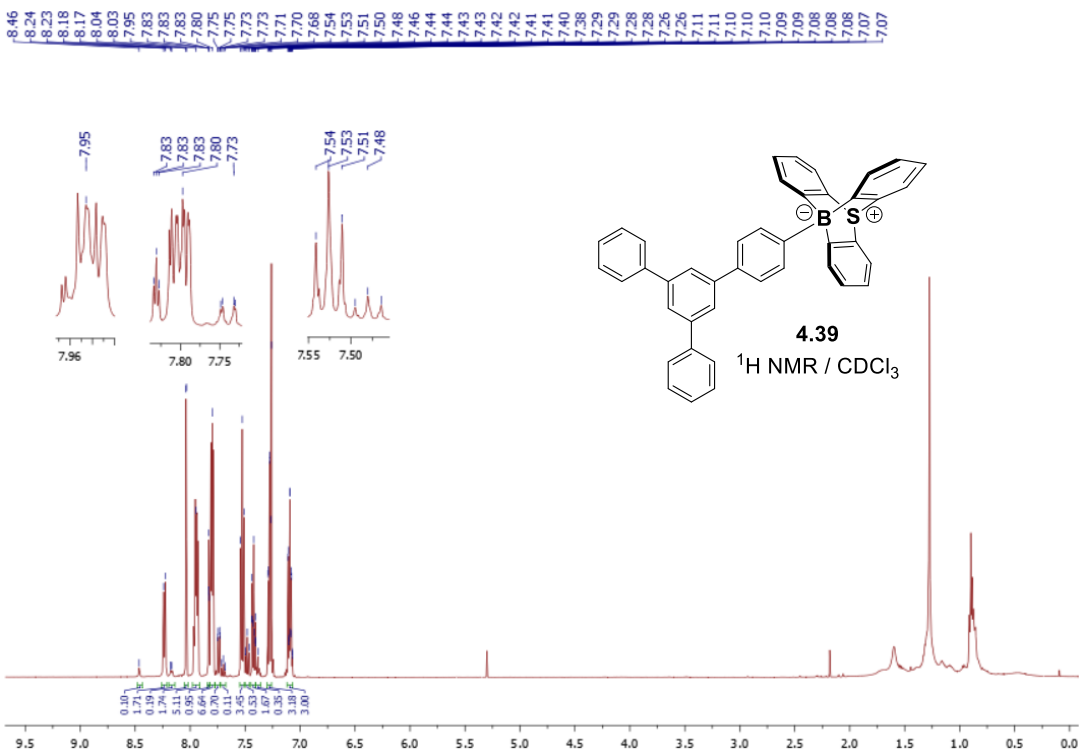
^{1}H NMR (500 MHz, 25°C, $CDCl_3$) of **4.38**



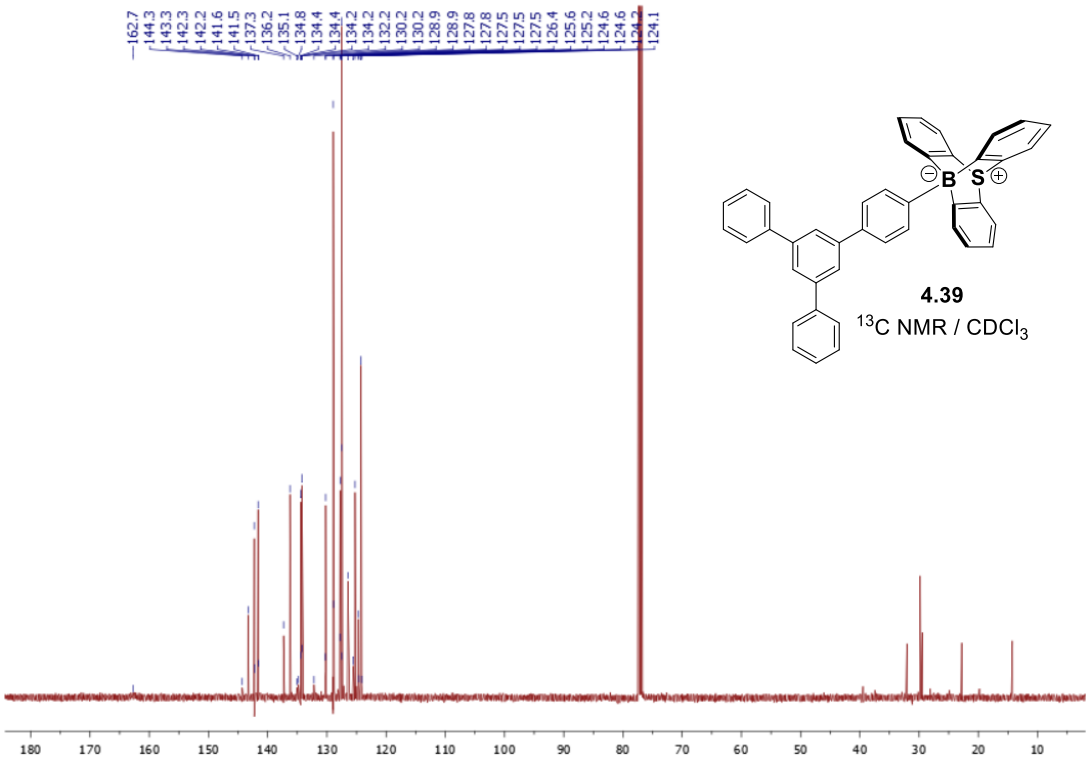
^{13}C NMR (126 MHz, 25°C, $CDCl_3$) of **4.38**



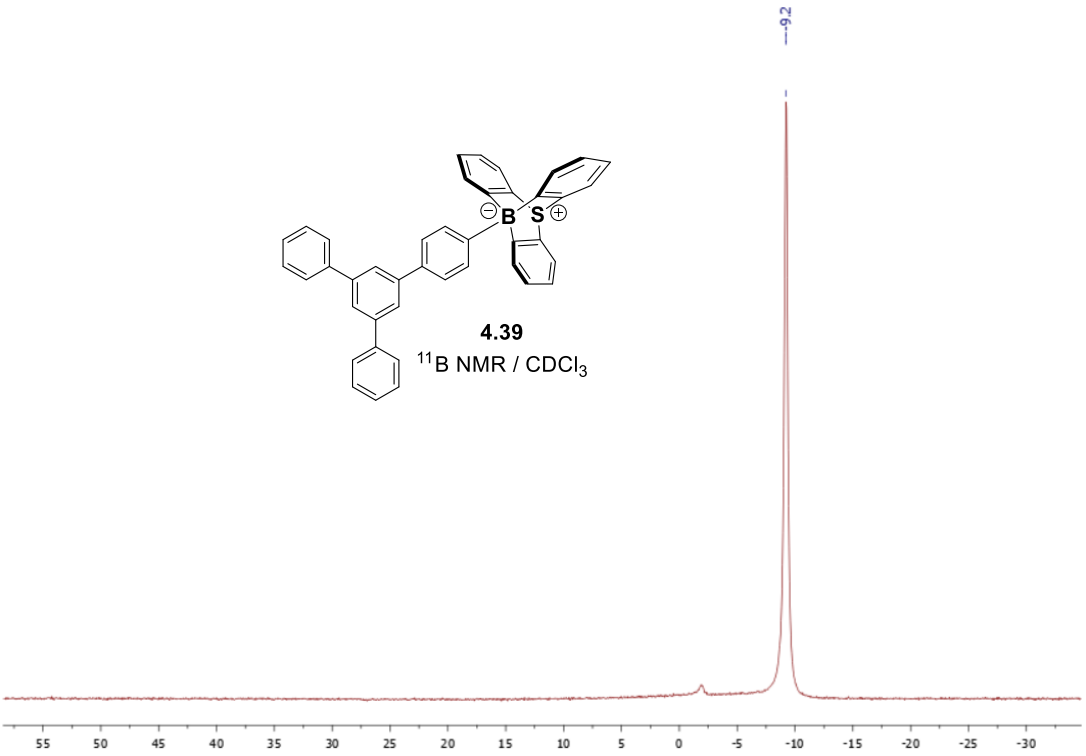
^{11}B NMR (160 MHz, 25°C, $CDCl_3$) of **4.38**



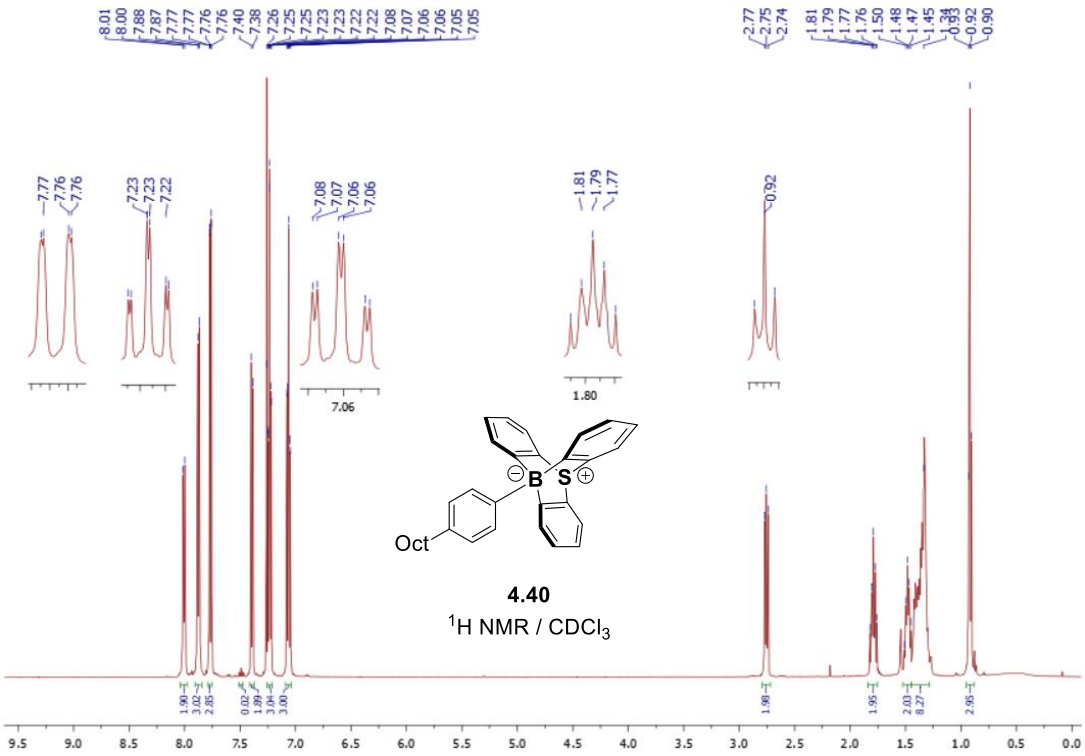
^{1}H NMR (500 MHz, 25°C, $CDCl_3$) of **4.39**



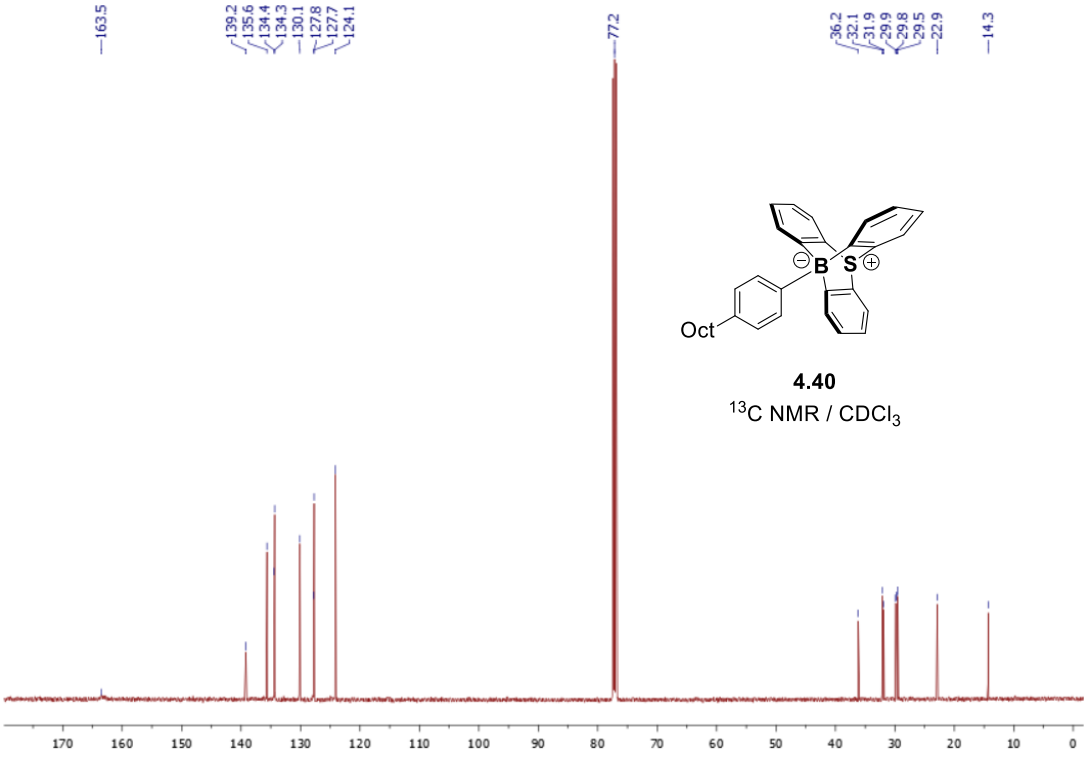
^{13}C NMR (126 MHz, 25°C, $CDCl_3$) of **4.39**



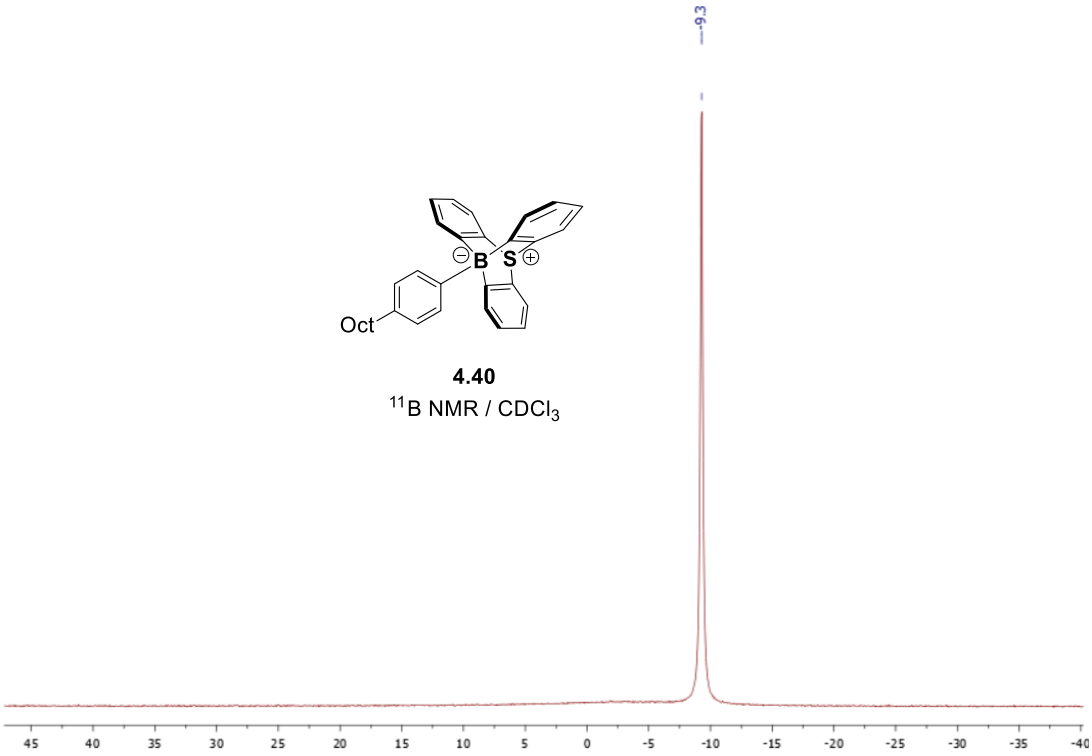
^{11}B NMR (160 MHz, 25°C, $CDCl_3$) of **4.39**



^{1}H NMR (500 MHz, 25°C, $CDCl_3$) of **4.40**



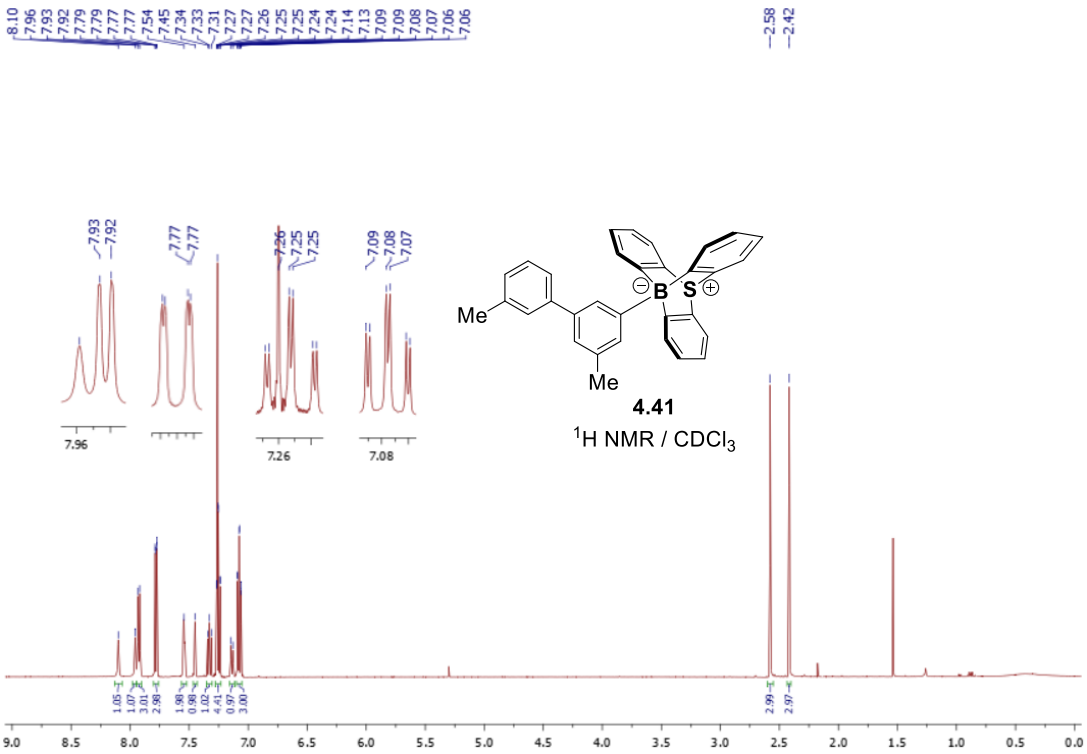
^{13}C NMR (126 MHz, 25°C, $CDCl_3$) of **4.40**



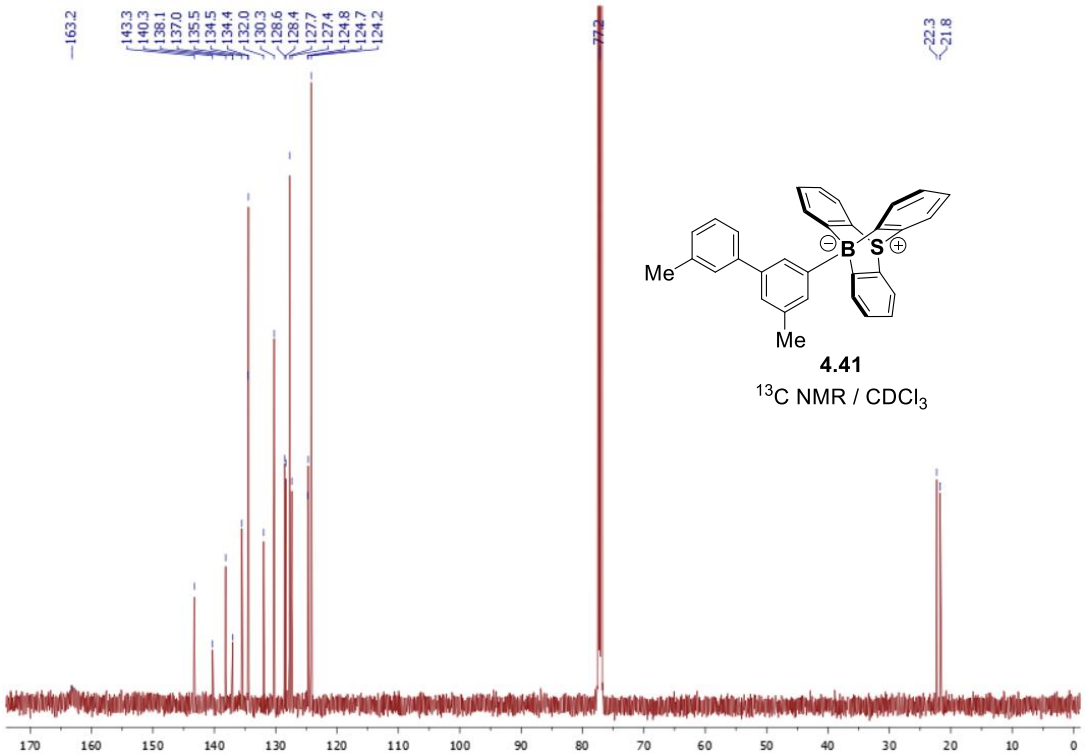
4.40

^{11}B NMR / $CDCl_3$

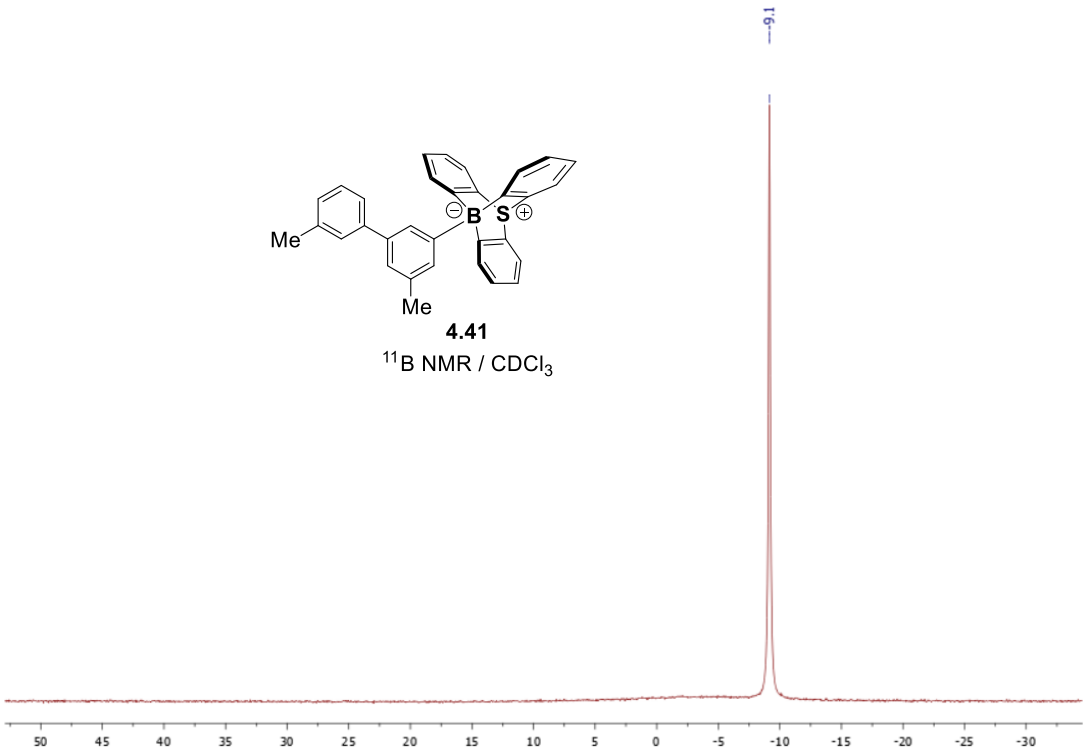
^{11}B NMR (160 MHz, 25°C, $CDCl_3$) of **4.40**



^{1}H NMR (500 MHz, 25°C, $CDCl_3$) of **4.41**



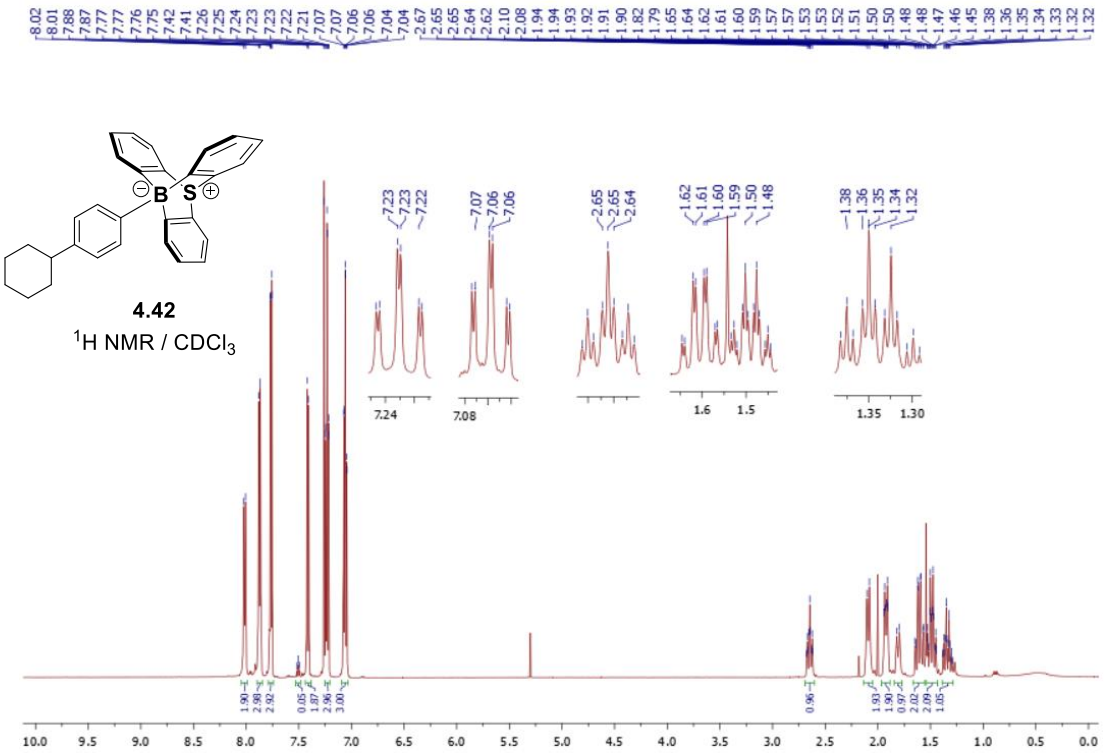
^{13}C NMR (126 MHz, 25°C, $CDCl_3$) of **4.41**



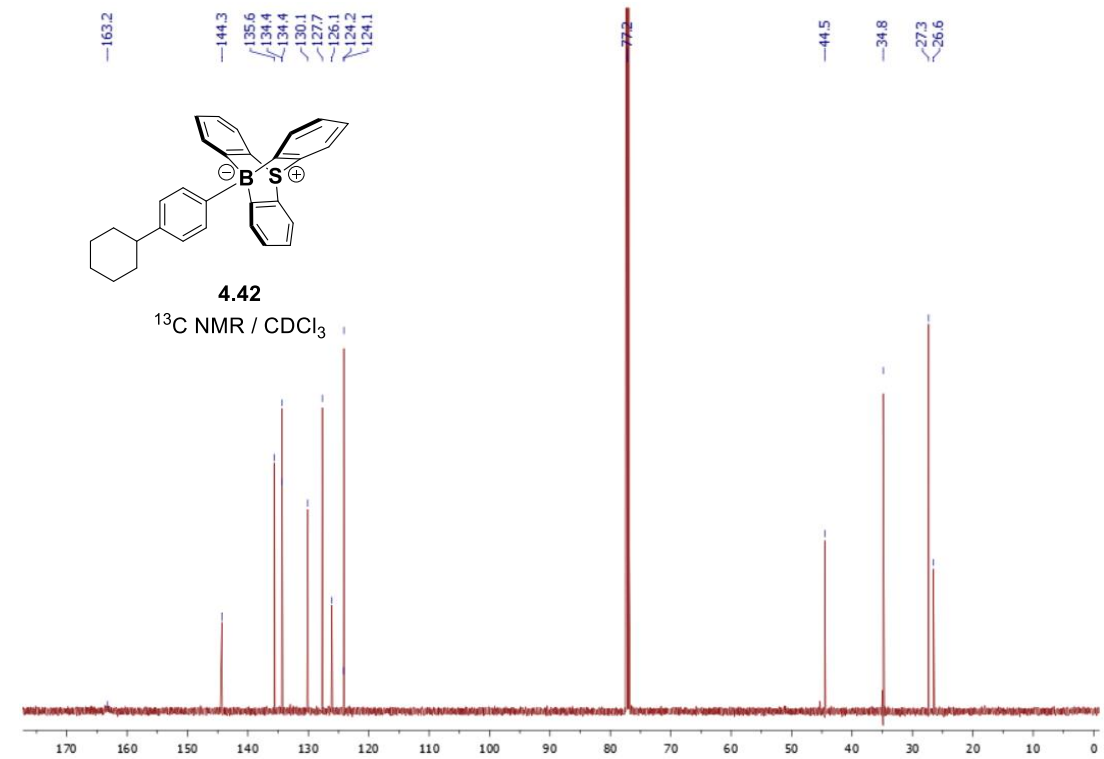
4.41

^{11}B NMR / $CDCl_3$

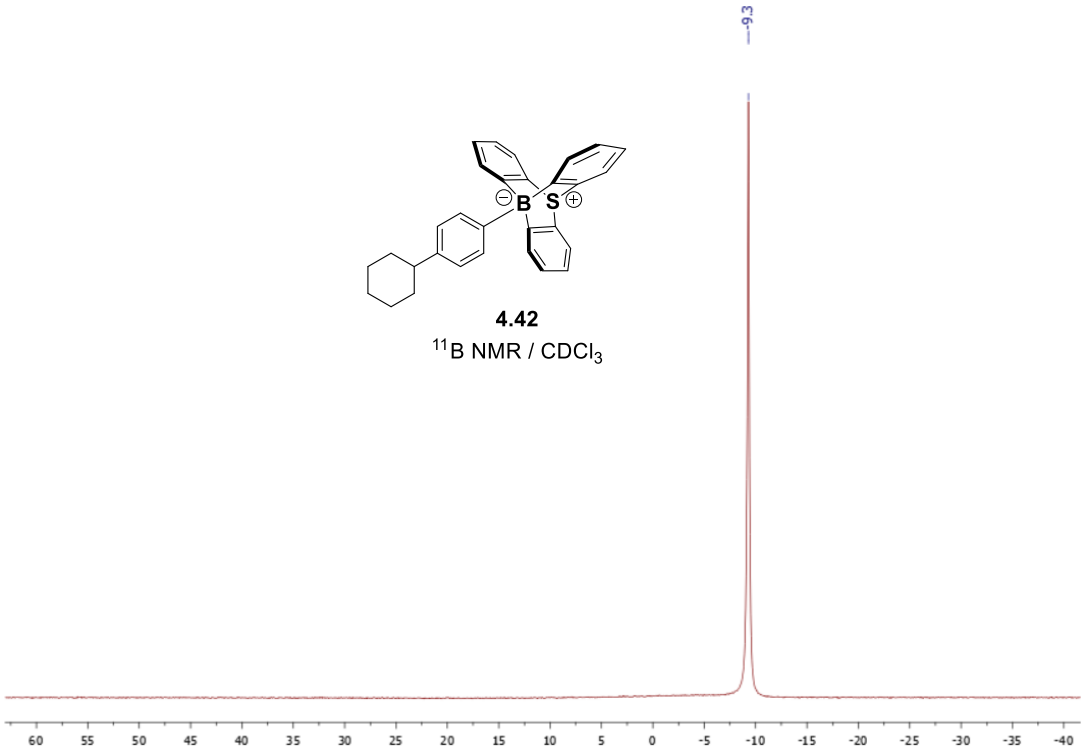
^{11}B NMR (160 MHz, 25°C, $CDCl_3$) of **4.41**



^{1}H NMR (500 MHz, 25°C, $CDCl_3$) of **4.42**



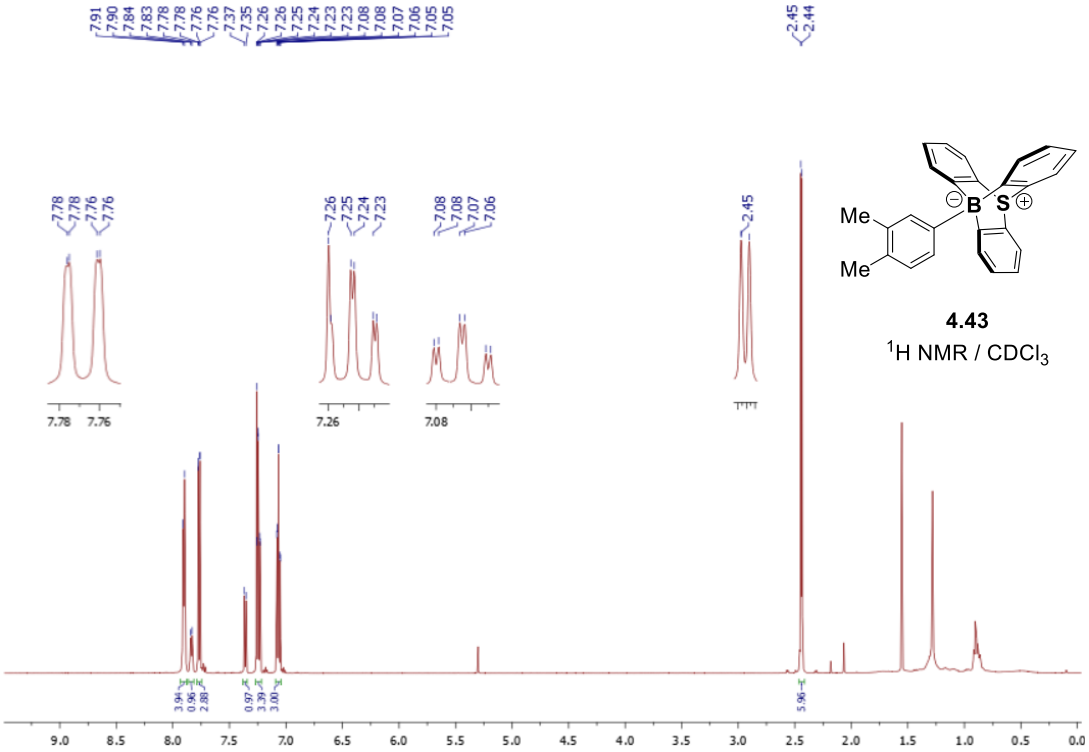
^{13}C NMR (126 MHz, 25°C, $CDCl_3$) of **4.42**



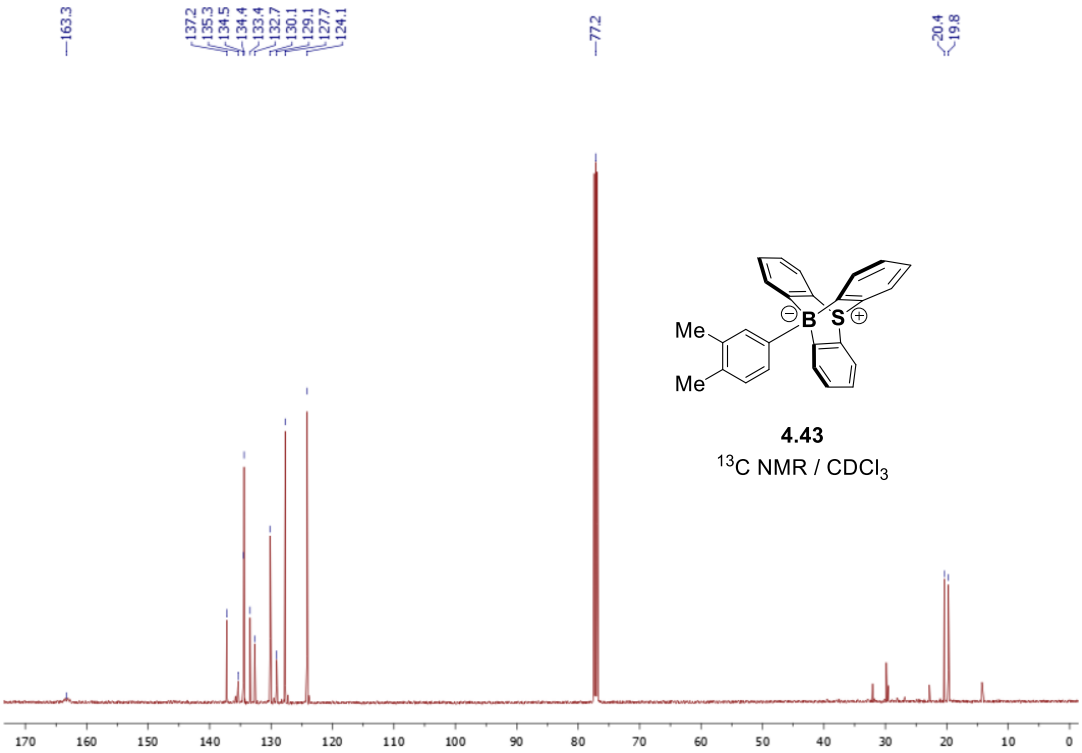
4.42

^{11}B NMR / $CDCl_3$

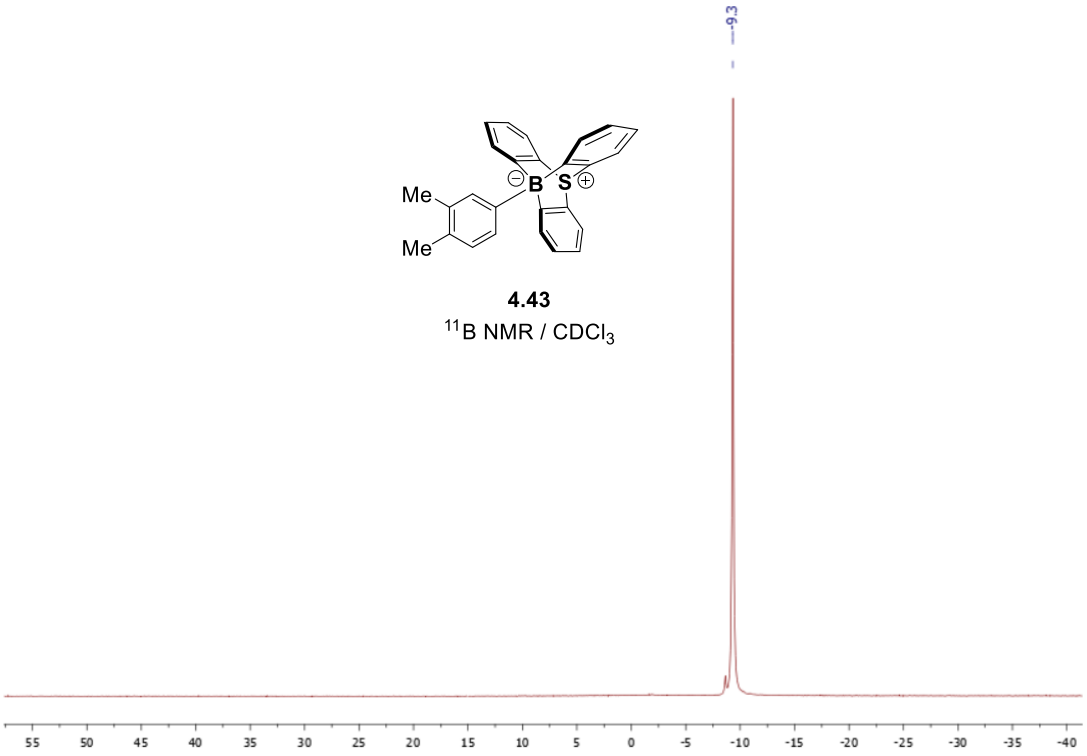
^{11}B NMR (160 MHz, 25°C, $CDCl_3$) of **4.42**



^{1}H NMR (500 MHz, 25°C, $CDCl_3$) of **4.43**



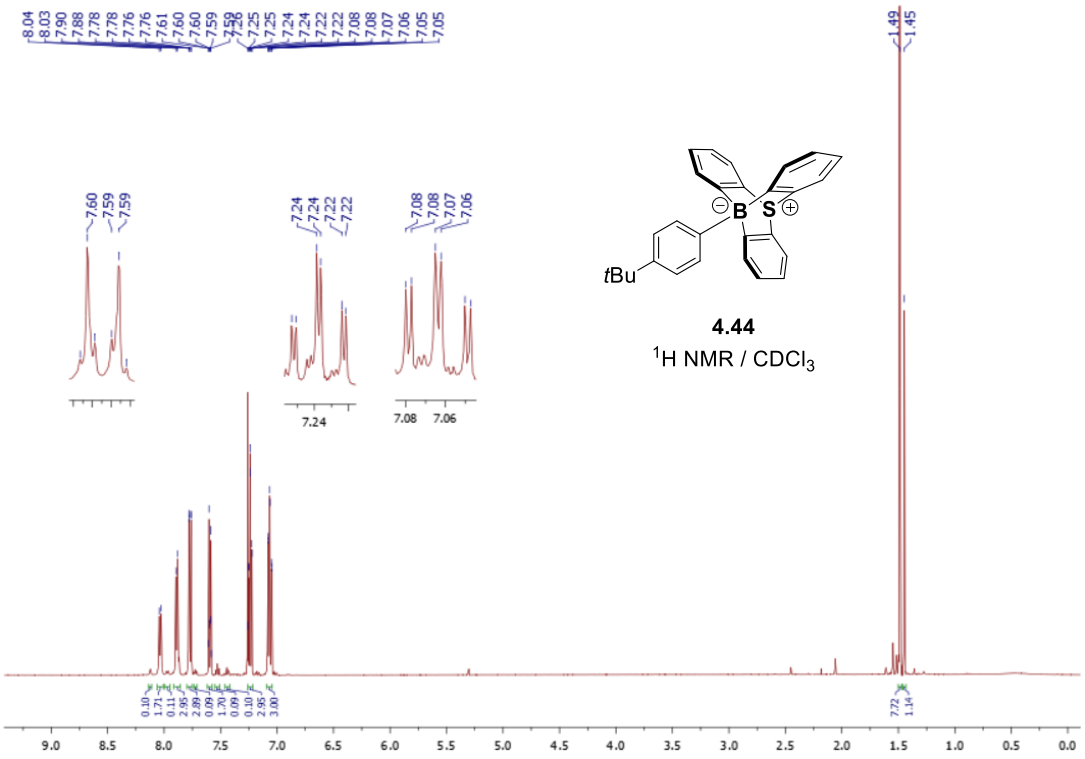
^{13}C NMR (126 MHz, 25°C, $CDCl_3$) of **4.43**



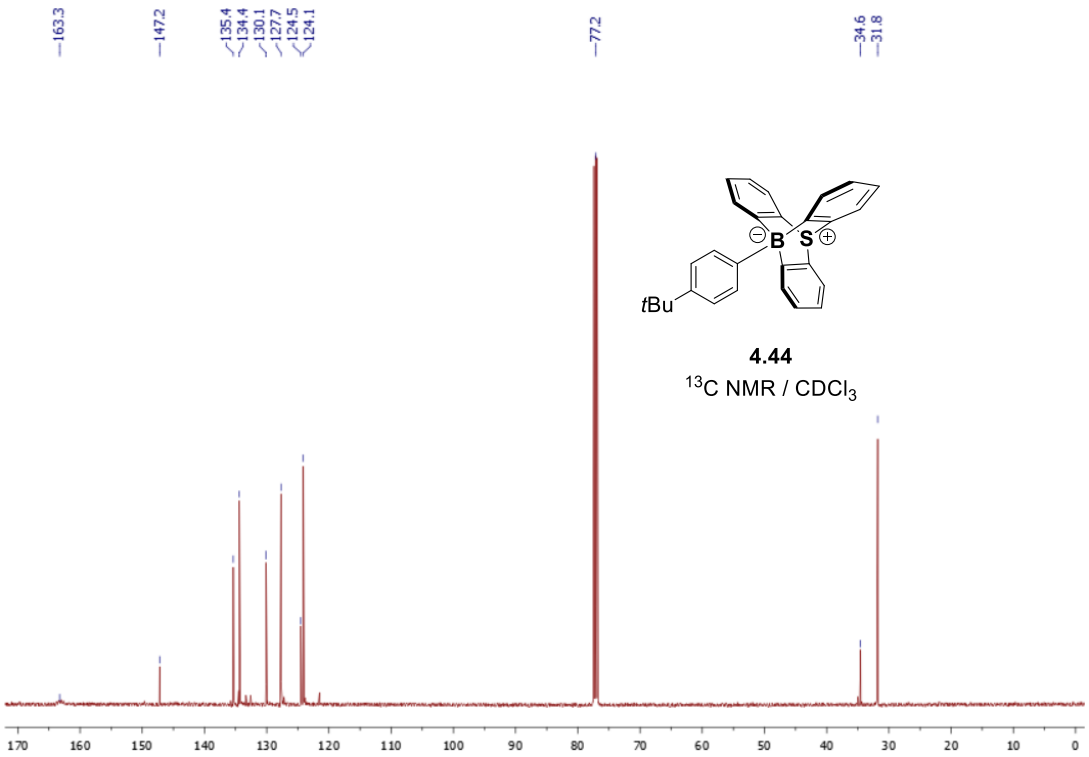
4.43

^{11}B NMR / $CDCl_3$

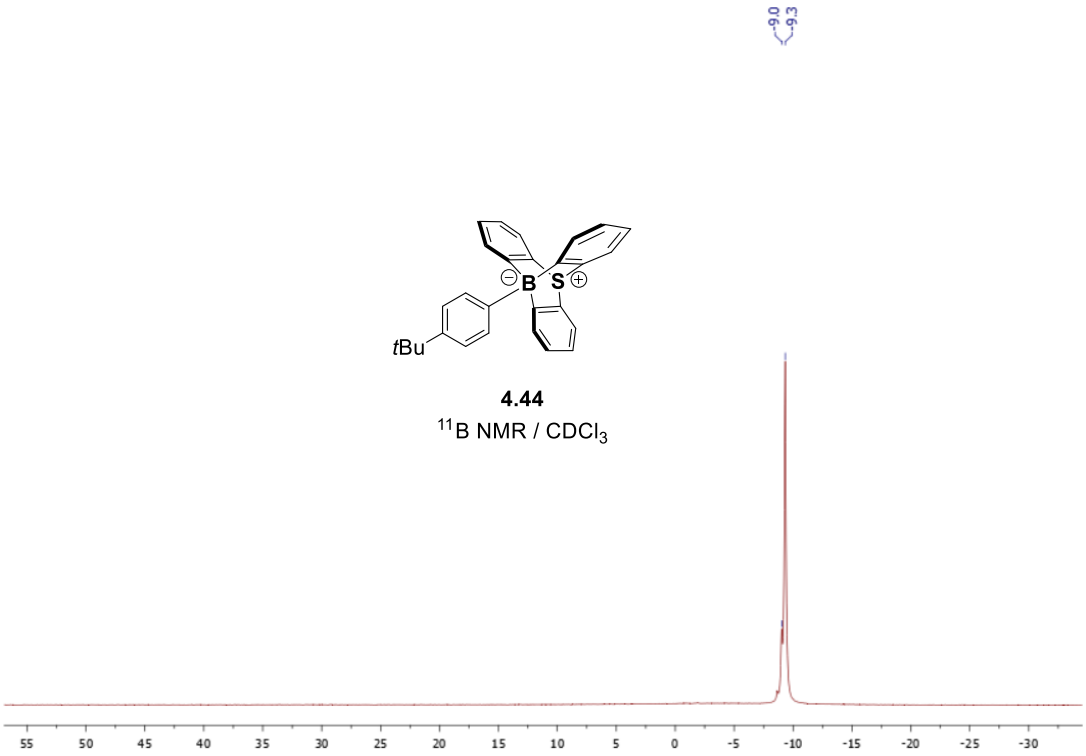
^{11}B NMR (160 MHz, 25°C, $CDCl_3$) of **4.43**



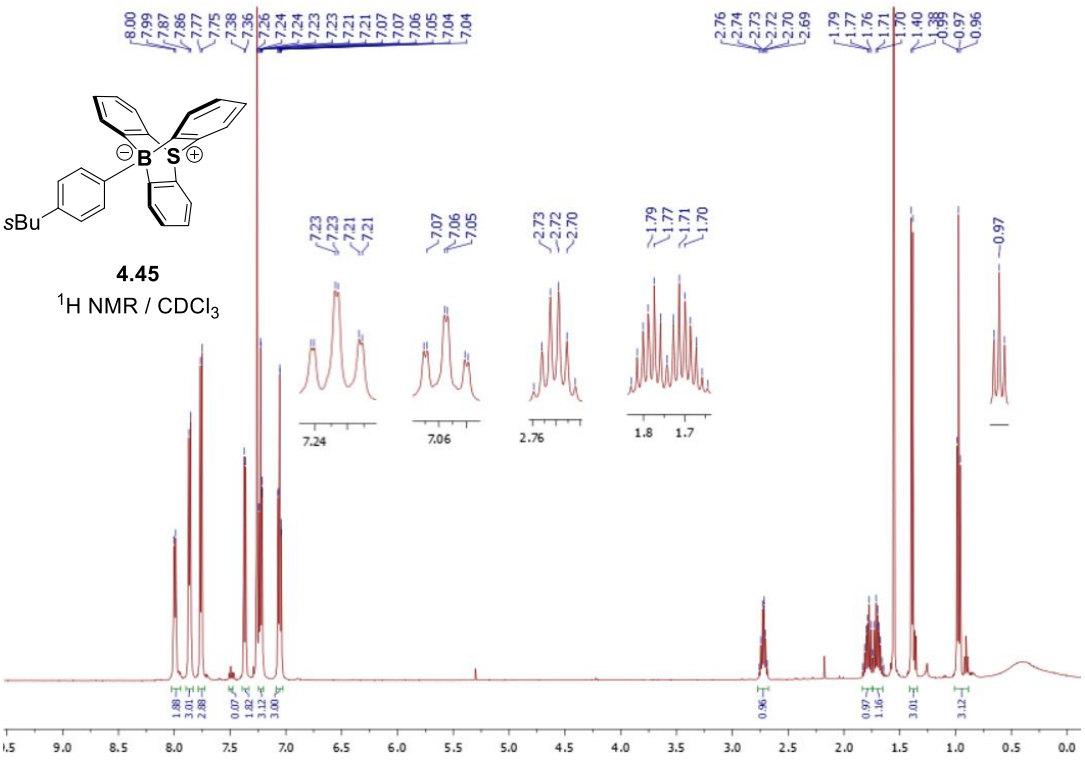
^{1}H NMR (500 MHz, 25°C, $CDCl_3$) of **4.44**



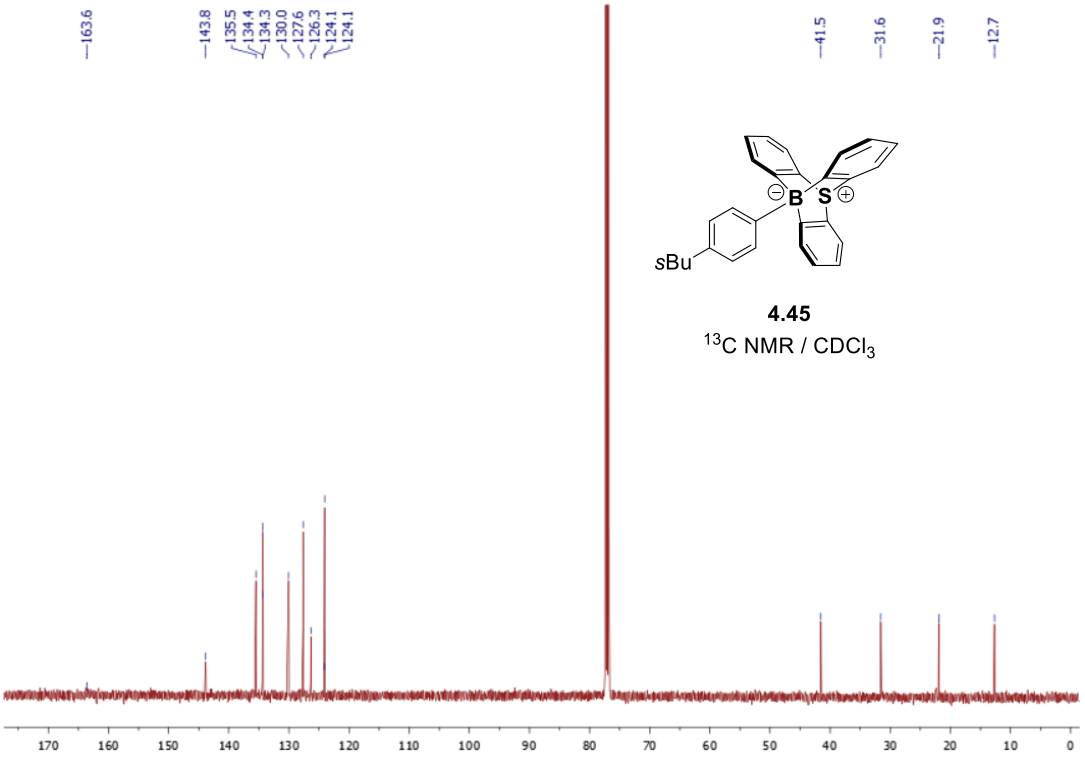
^{13}C NMR (126 MHz, 25°C, $CDCl_3$) of **4.44**



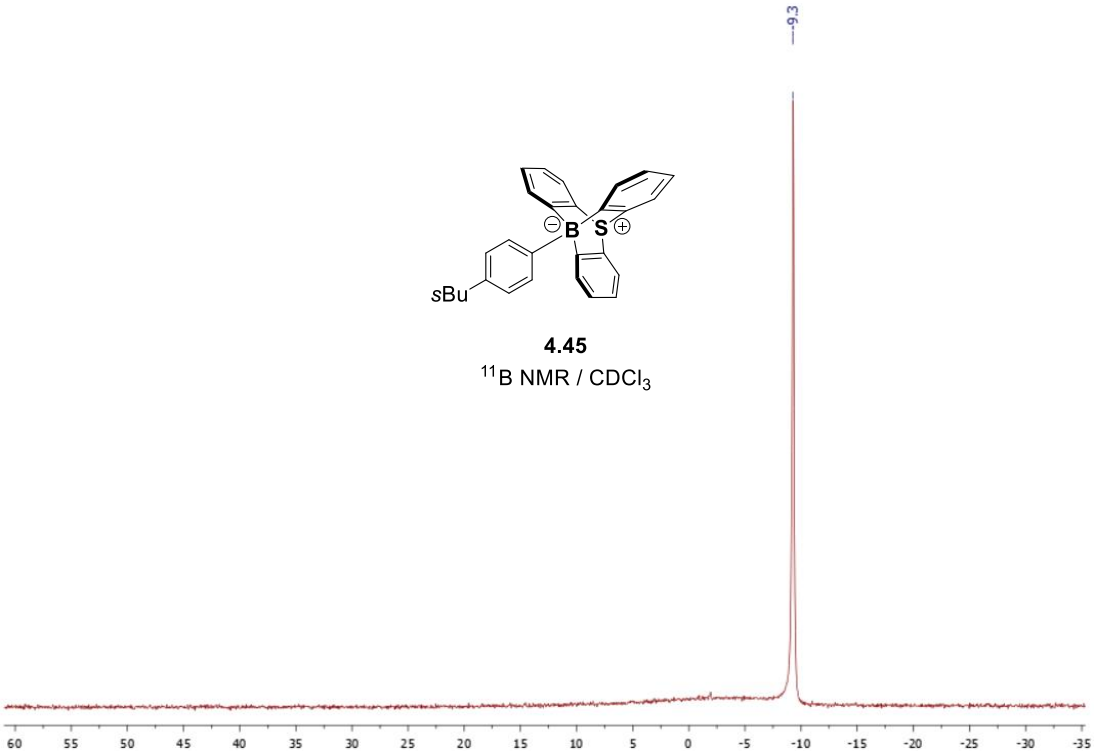
^{11}B NMR (160 MHz, 25°C, $CDCl_3$) of **4.44**



^{1}H NMR (500 MHz, 25°C, $CDCl_3$) of **4.45**



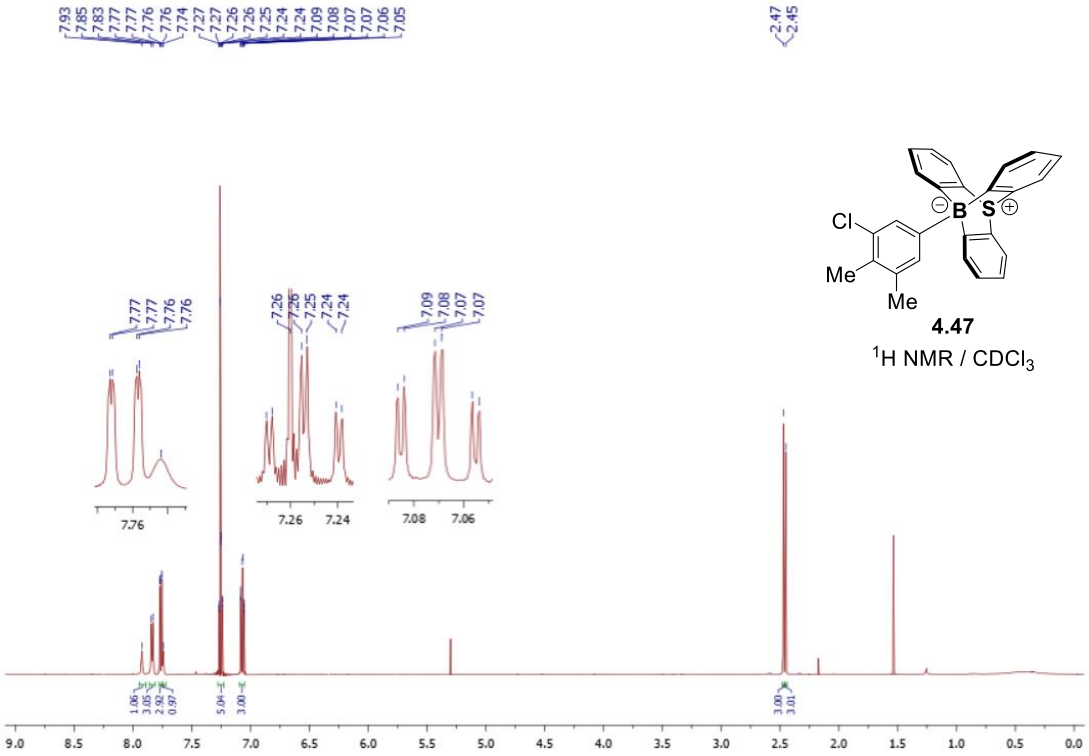
^{13}C NMR (126 MHz, 25°C, $CDCl_3$) of **4.45**



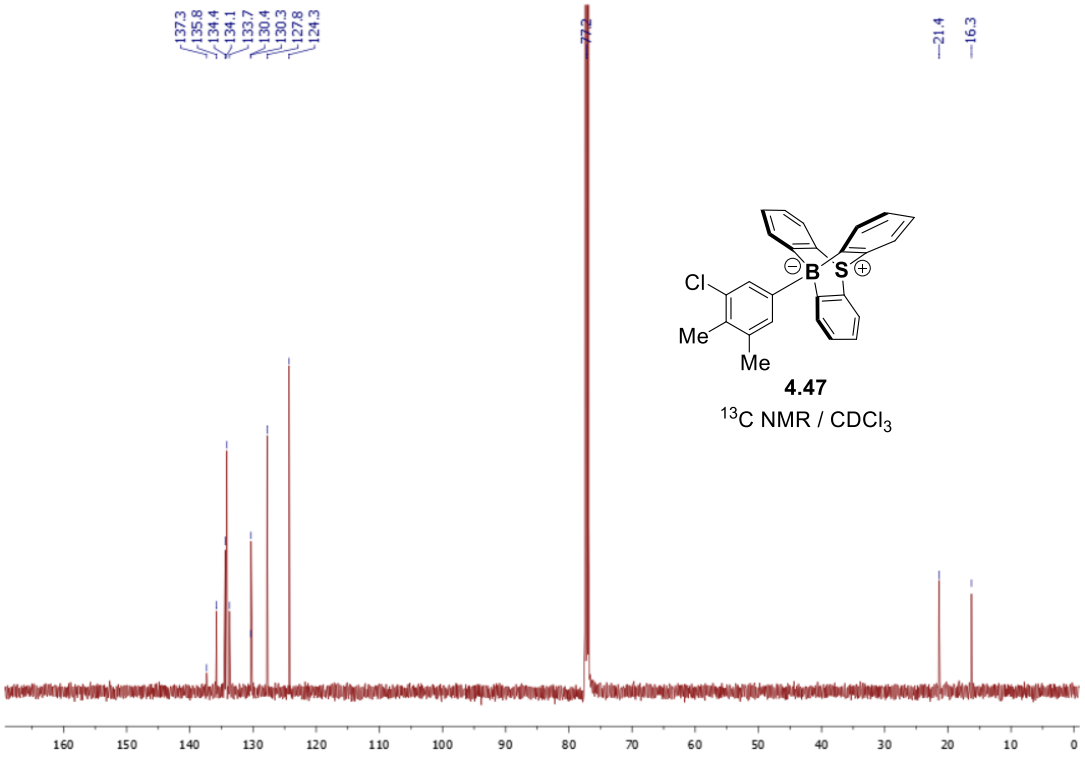
4.45

^{11}B NMR / $CDCl_3$

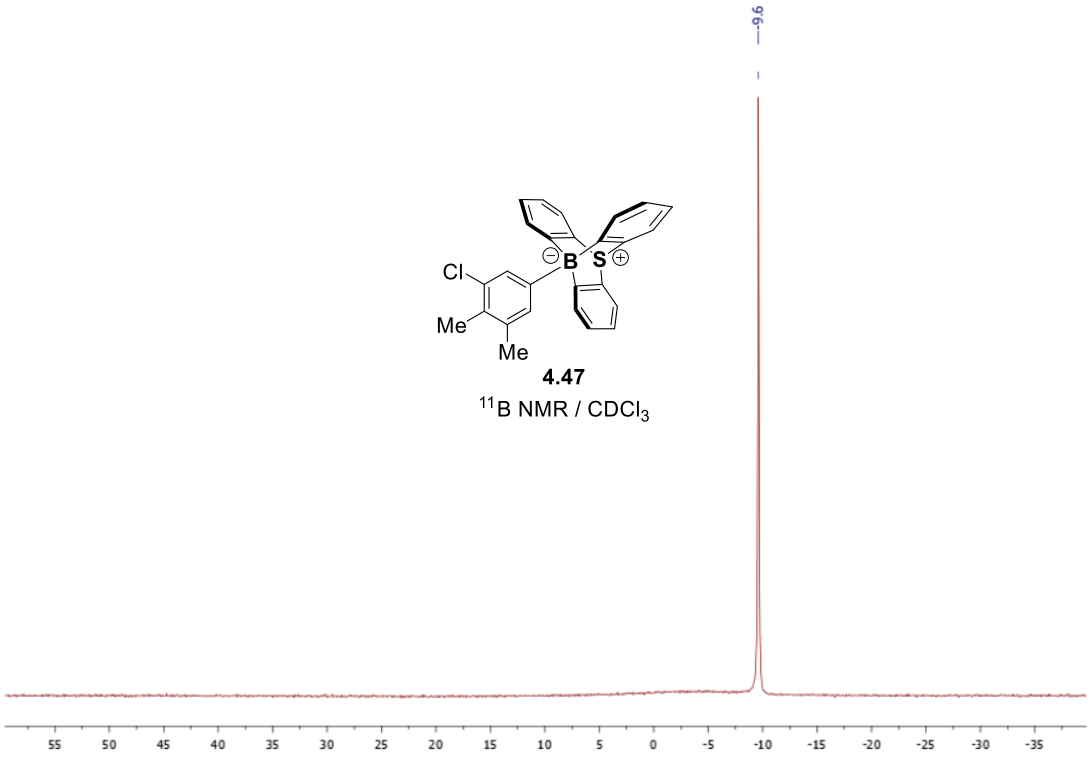
^{11}B NMR (160 MHz, 25°C, $CDCl_3$) of **4.45**



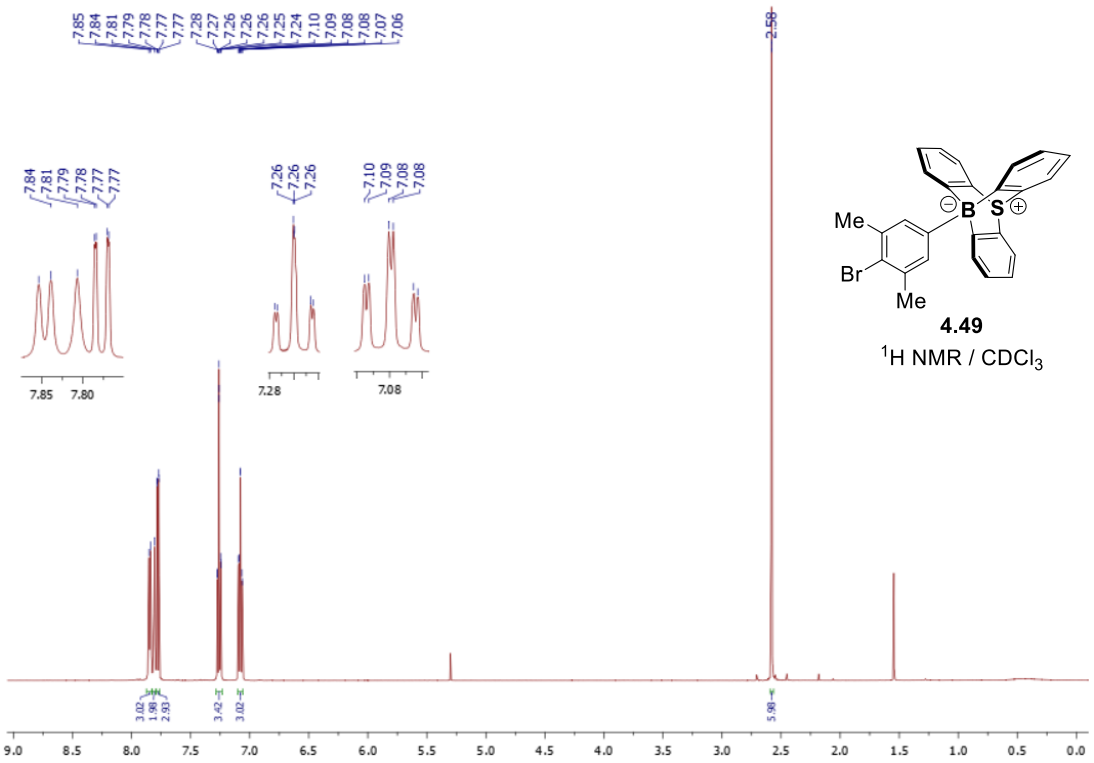
^{1}H NMR (500 MHz, 25°C, $CDCl_3$) of **4.47**



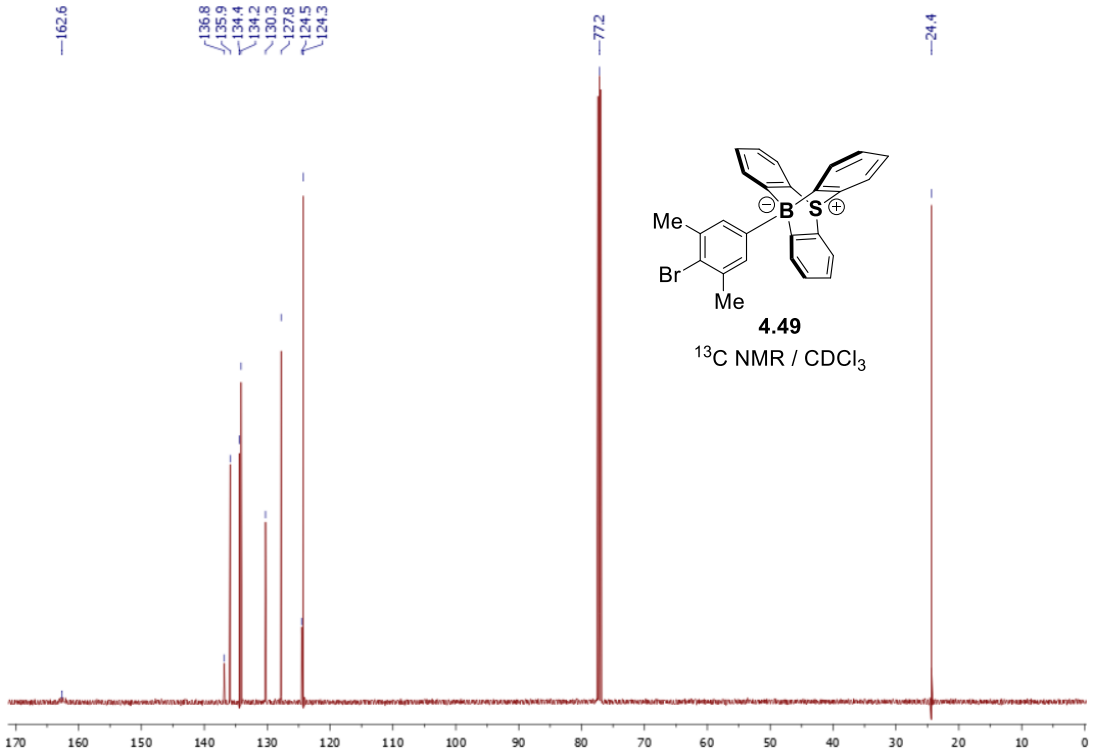
^{13}C NMR (126 MHz, 25°C, $CDCl_3$) of **4.47**



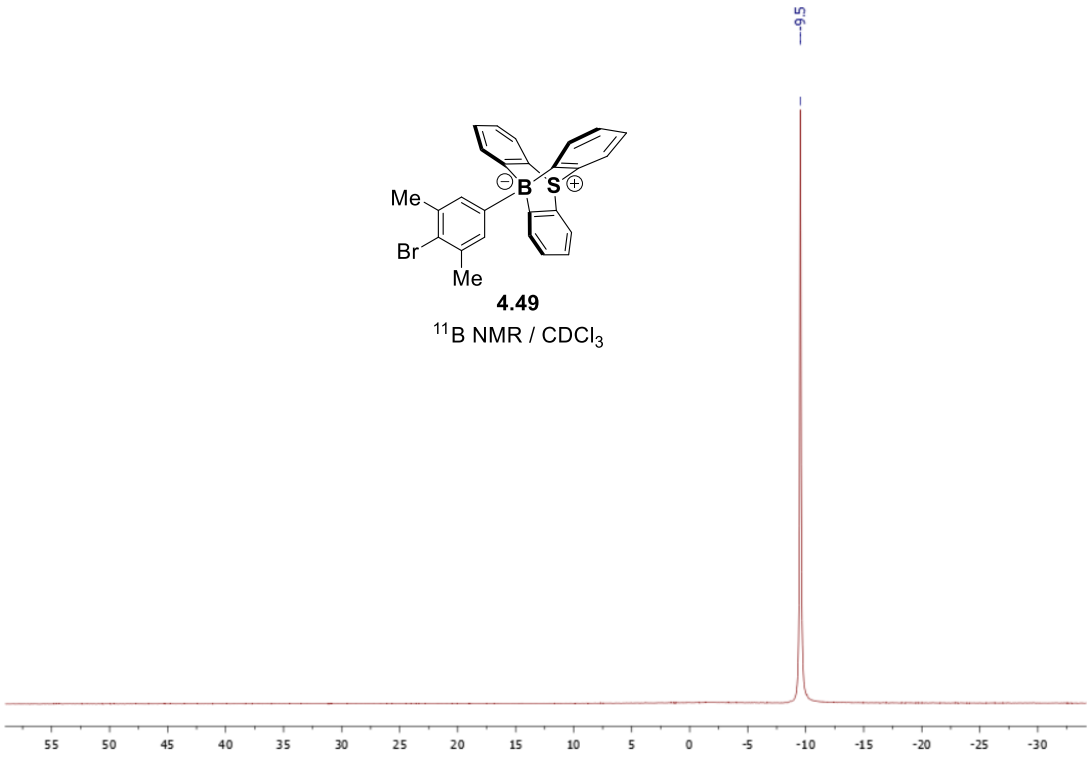
^{11}B NMR (160 MHz, 25°C, $CDCl_3$) of **4.47**



^{1}H NMR (500 MHz, 25°C, $CDCl_3$) of **4.49**



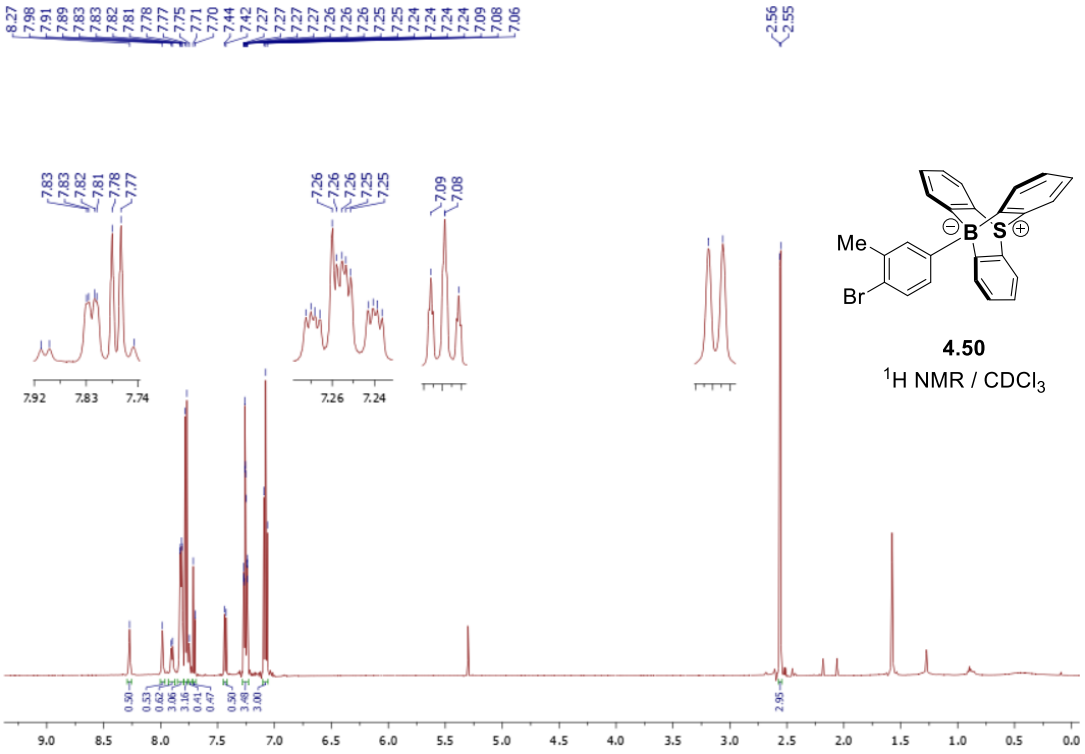
^{13}C NMR (126 MHz, 25°C, $CDCl_3$) of **4.49**



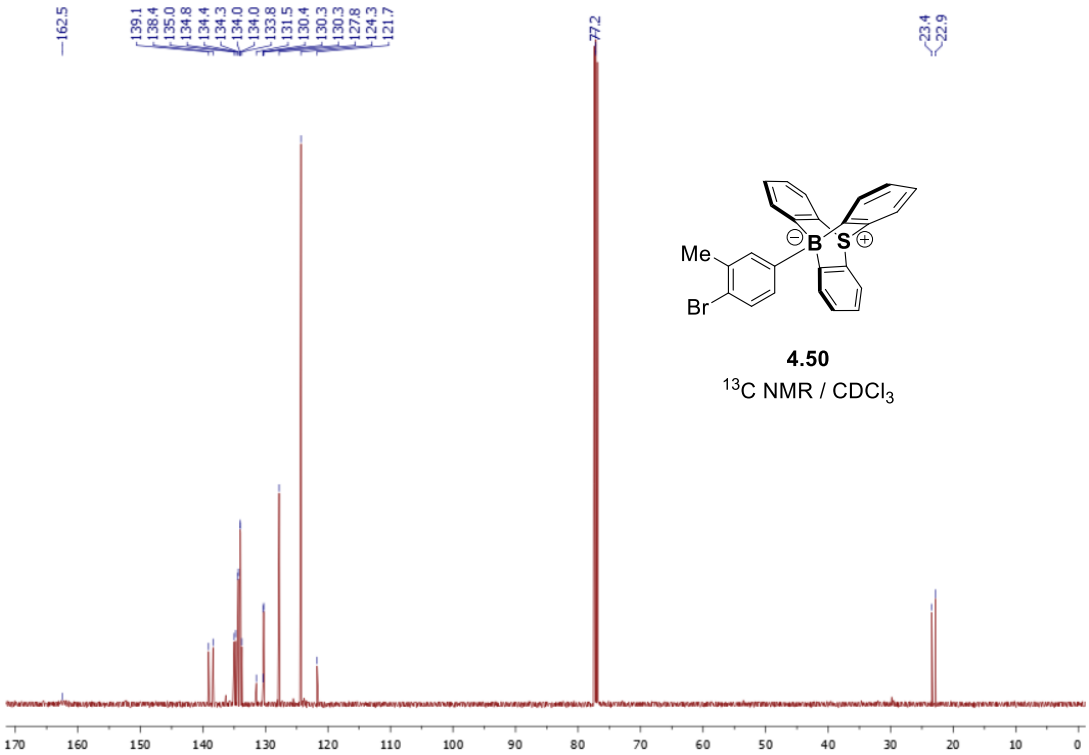
4.49

^{11}B NMR / $CDCl_3$

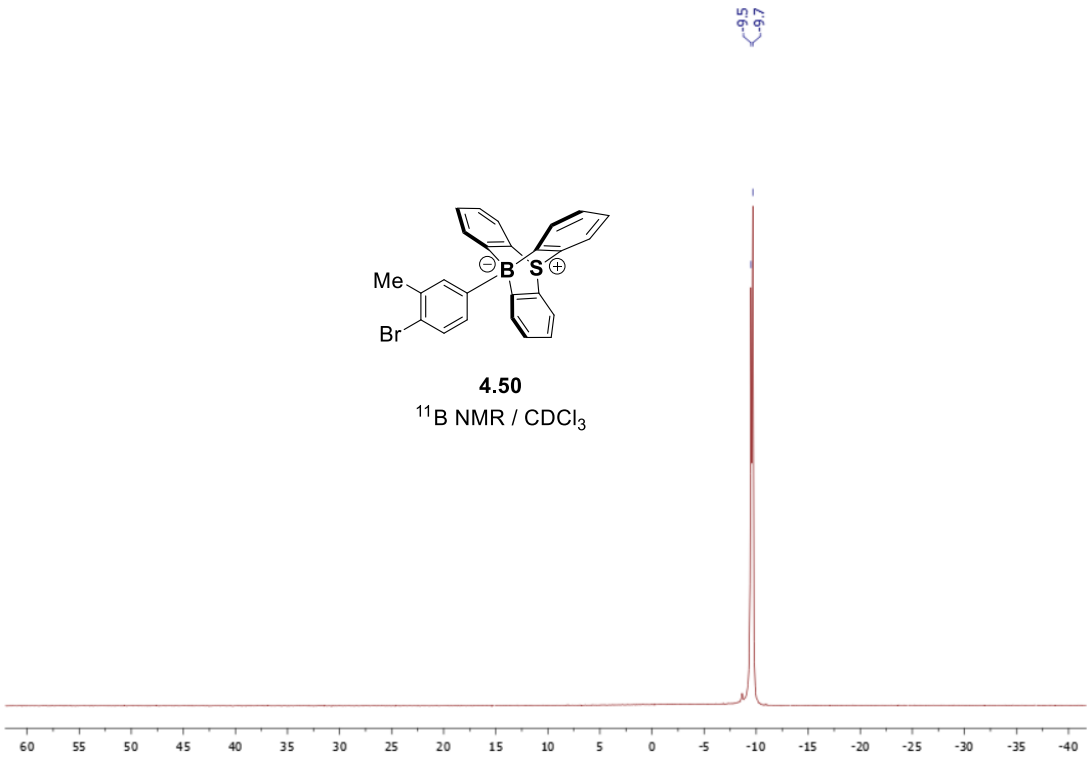
^{11}B NMR (160 MHz, 25°C, $CDCl_3$) of **4.49**



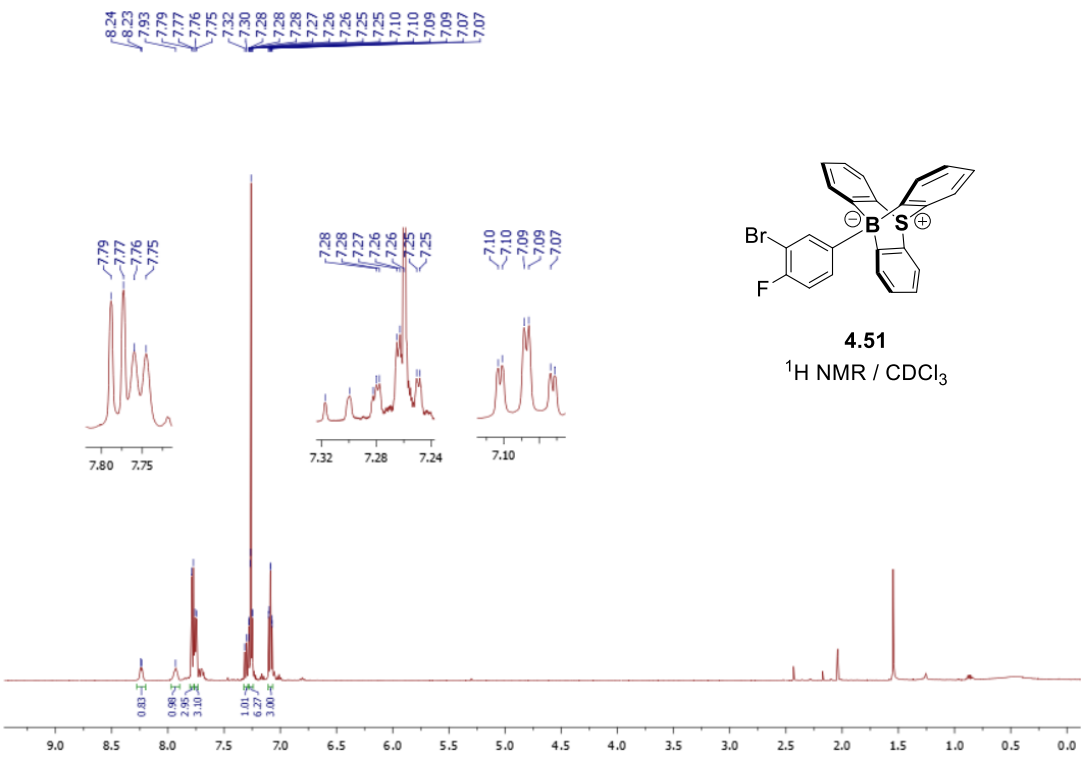
^{1}H NMR (500 MHz, 25°C, $CDCl_3$) of **4.50**



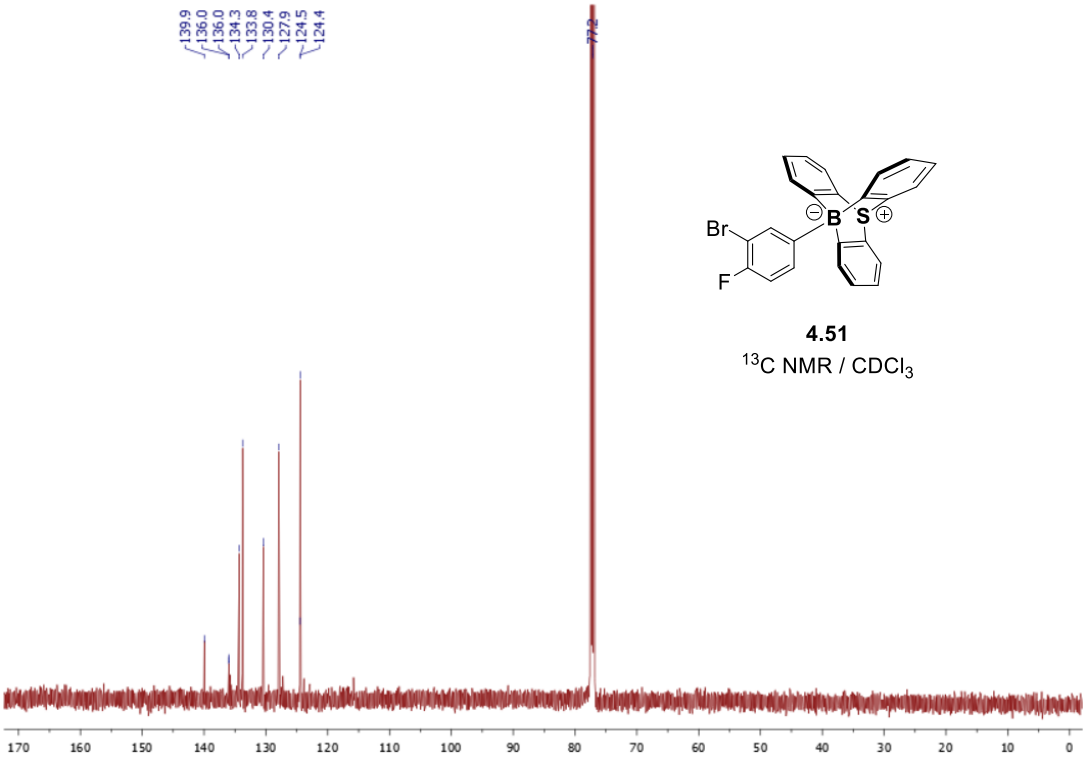
^{13}C NMR (126 MHz, 25°C, $CDCl_3$) of **4.50**



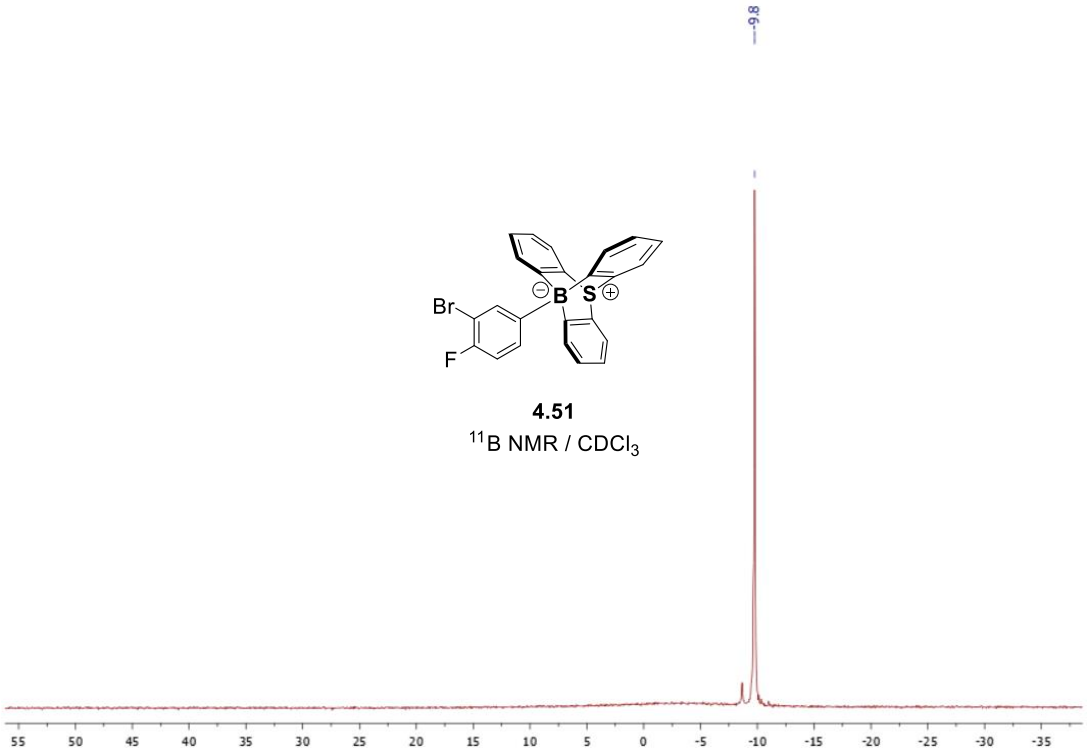
^{11}B NMR (160 MHz, 25°C, $CDCl_3$) of **4.50**



^{1}H NMR (500 MHz, 25°C, $CDCl_3$) of **4.51**



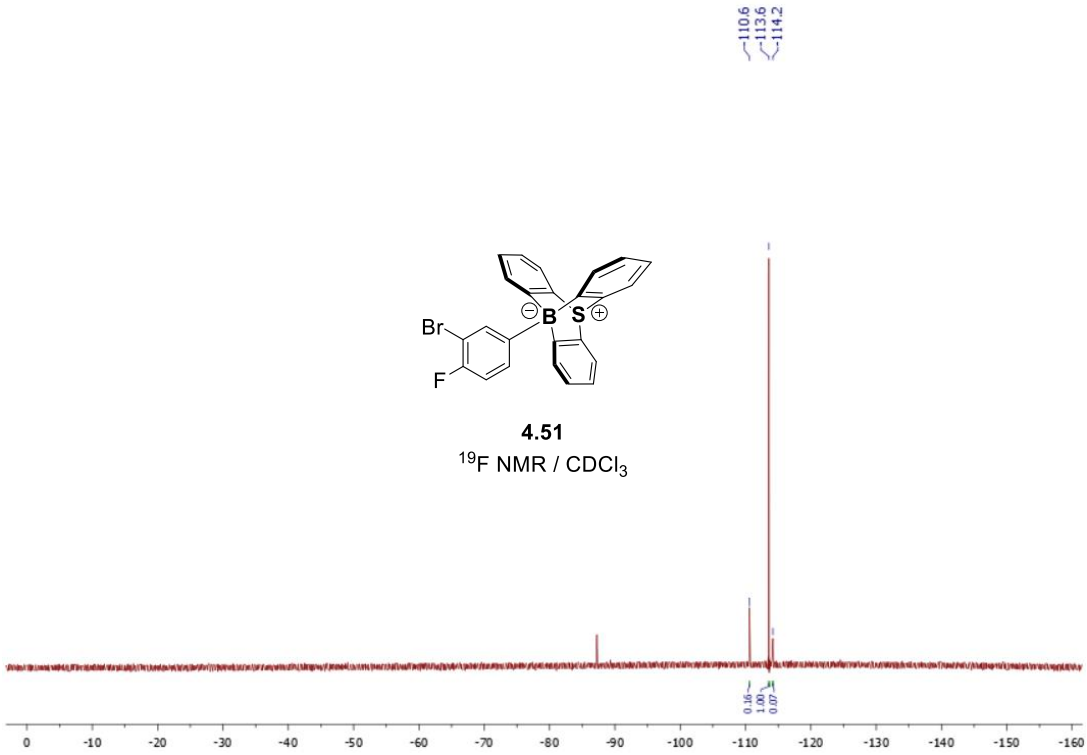
^{13}C NMR (126 MHz, 25°C, $CDCl_3$) of **4.51**



4.51

^{11}B NMR / $CDCl_3$

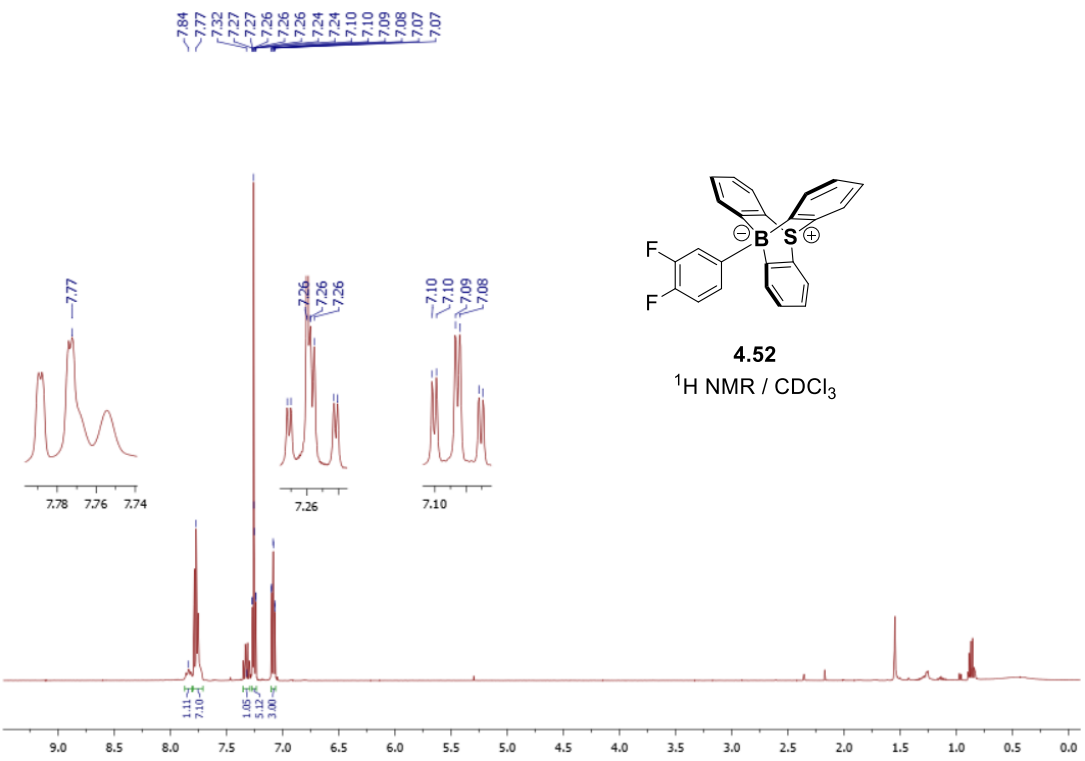
^{11}B NMR (160 MHz, 25°C, $CDCl_3$) of **4.51**



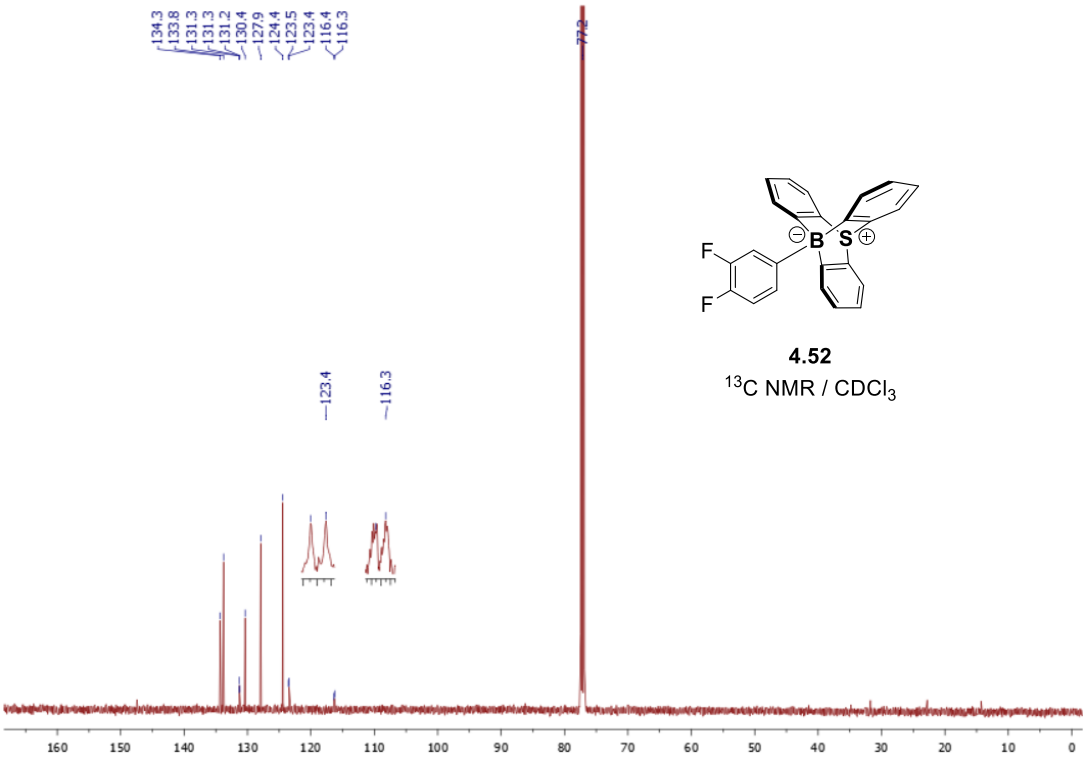
4.51

^{19}F NMR / $CDCl_3$

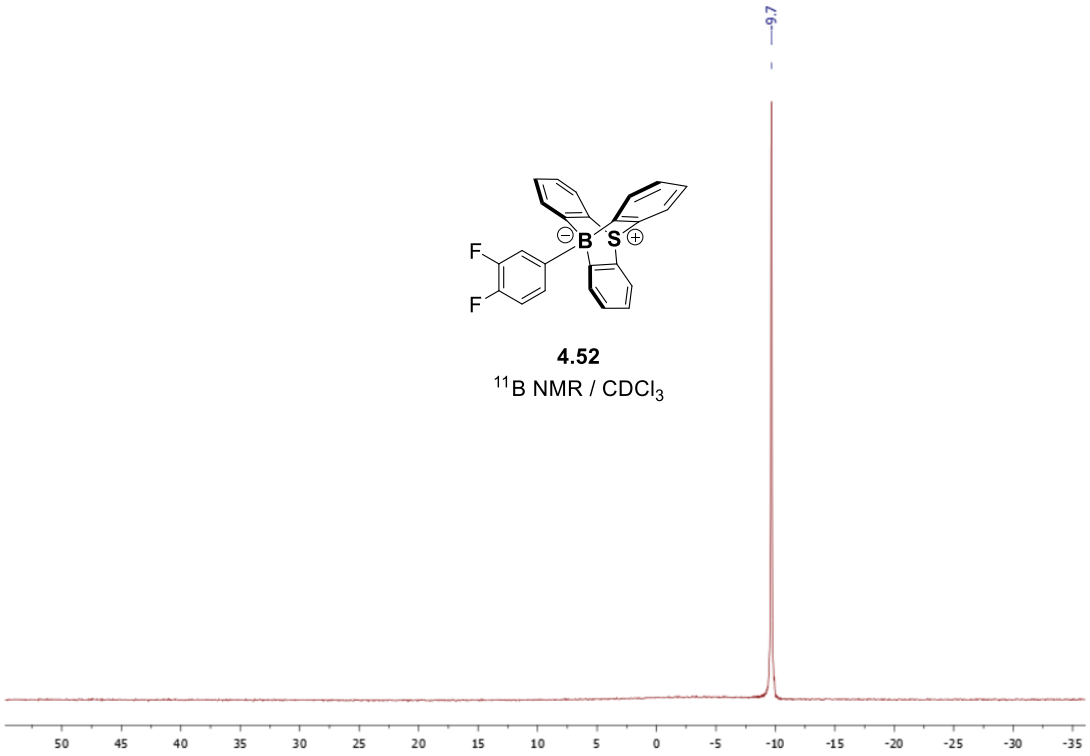
^{19}F NMR (470 MHz, 25°C, $CDCl_3$) of **4.51**



^{1}H NMR (500 MHz, 25°C, $CDCl_3$) of **4.52**



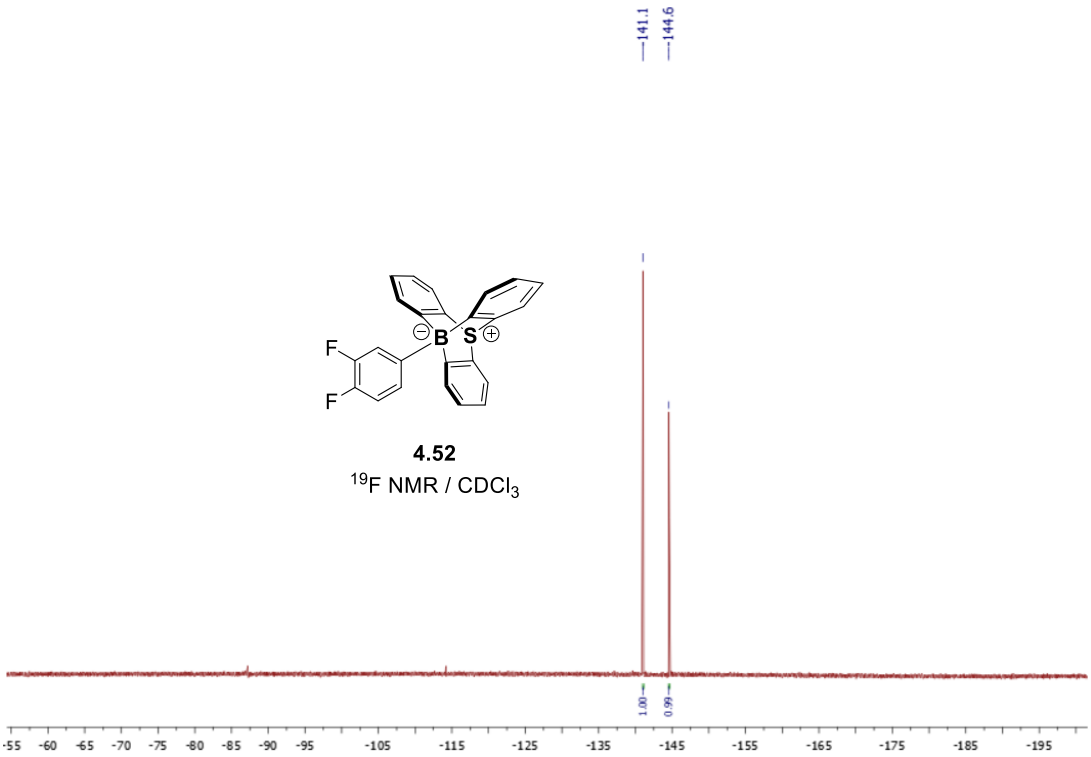
^{13}C NMR (126 MHz, 25°C, $CDCl_3$) of **4.52**



4.52

^{11}B NMR / $CDCl_3$

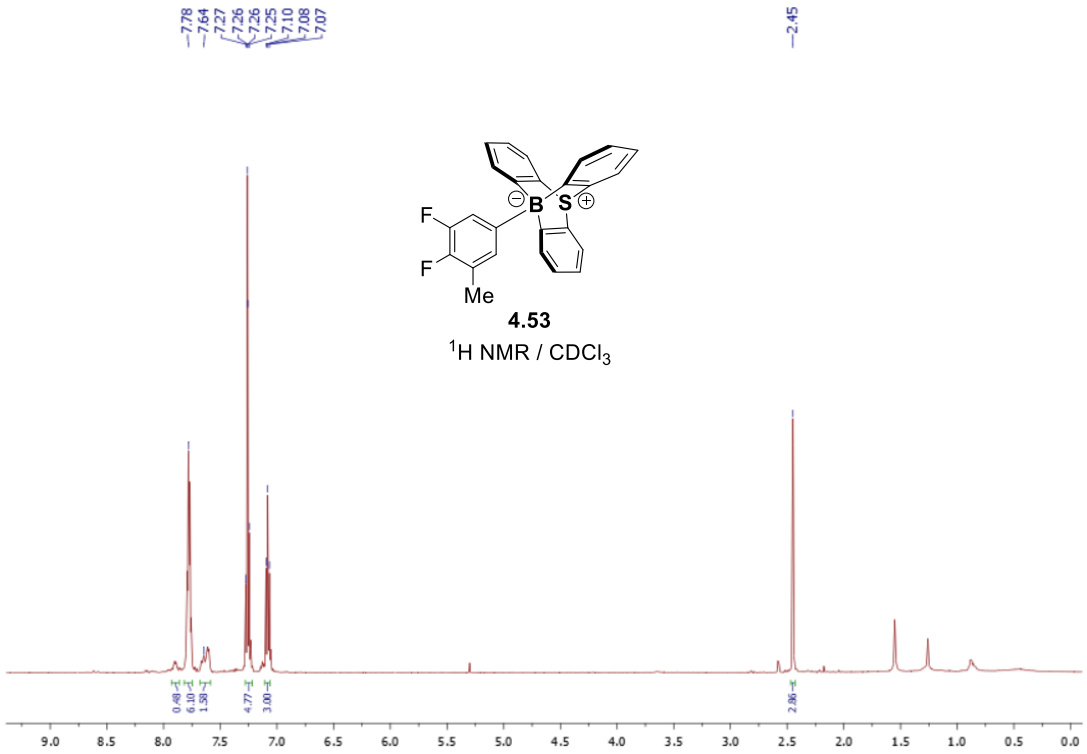
^{11}B NMR (160 MHz, 25°C, $CDCl_3$) of **4.52**



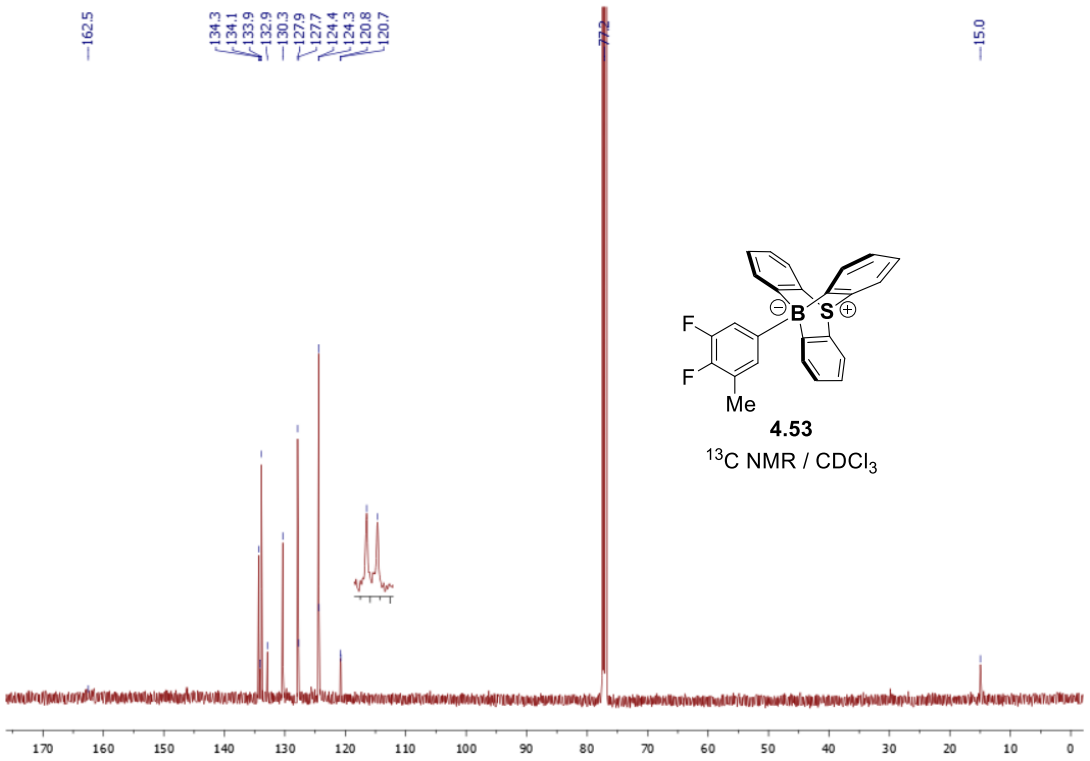
4.52

^{19}F NMR / $CDCl_3$

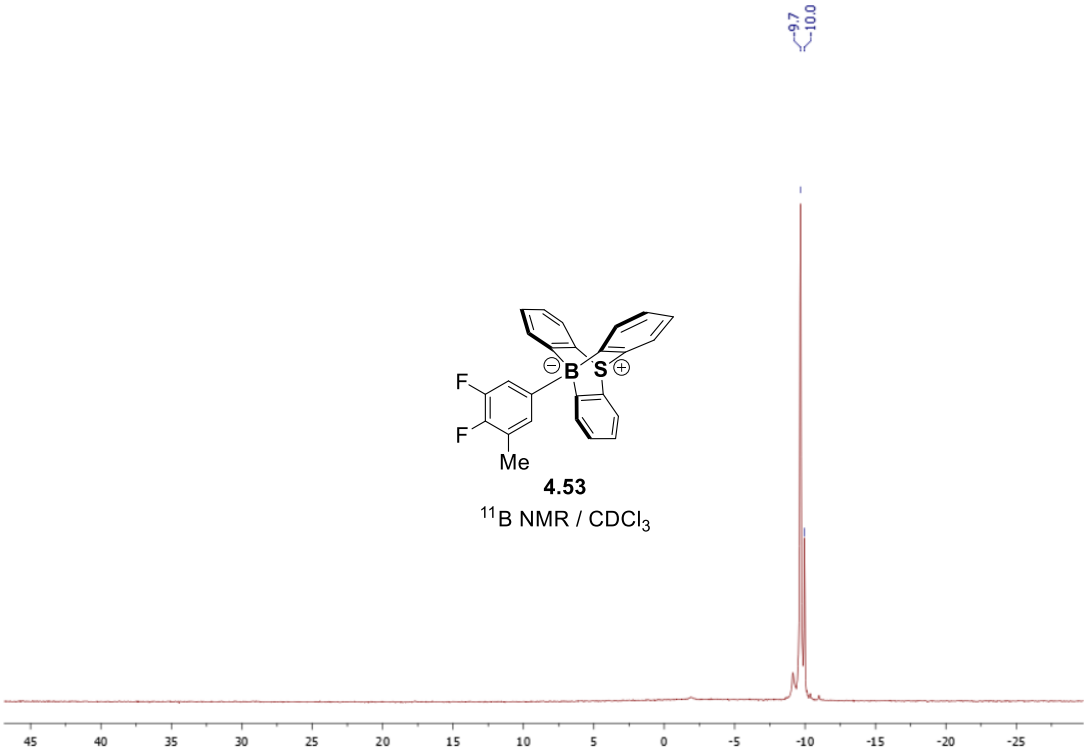
^{19}F NMR (470 MHz, 25°C, $CDCl_3$) of **4.52**



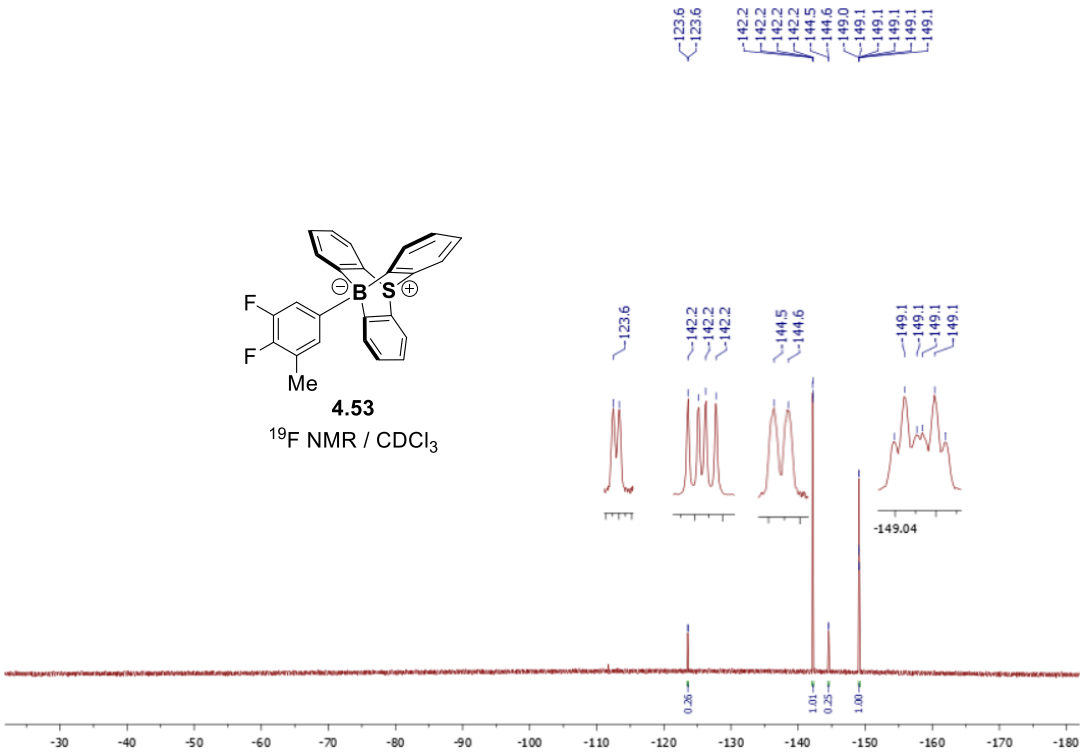
^{1}H NMR (500 MHz, 25°C, $CDCl_3$) of **4.53**



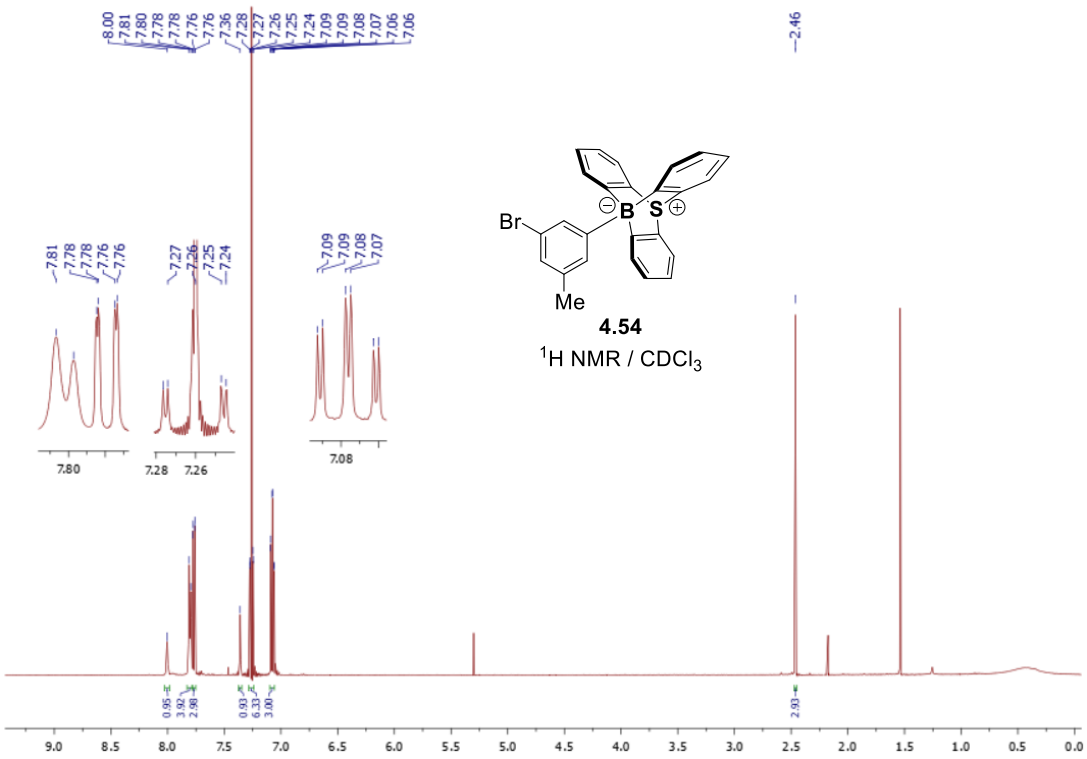
^{13}C NMR (126 MHz, 25°C, $CDCl_3$) of **4.53**



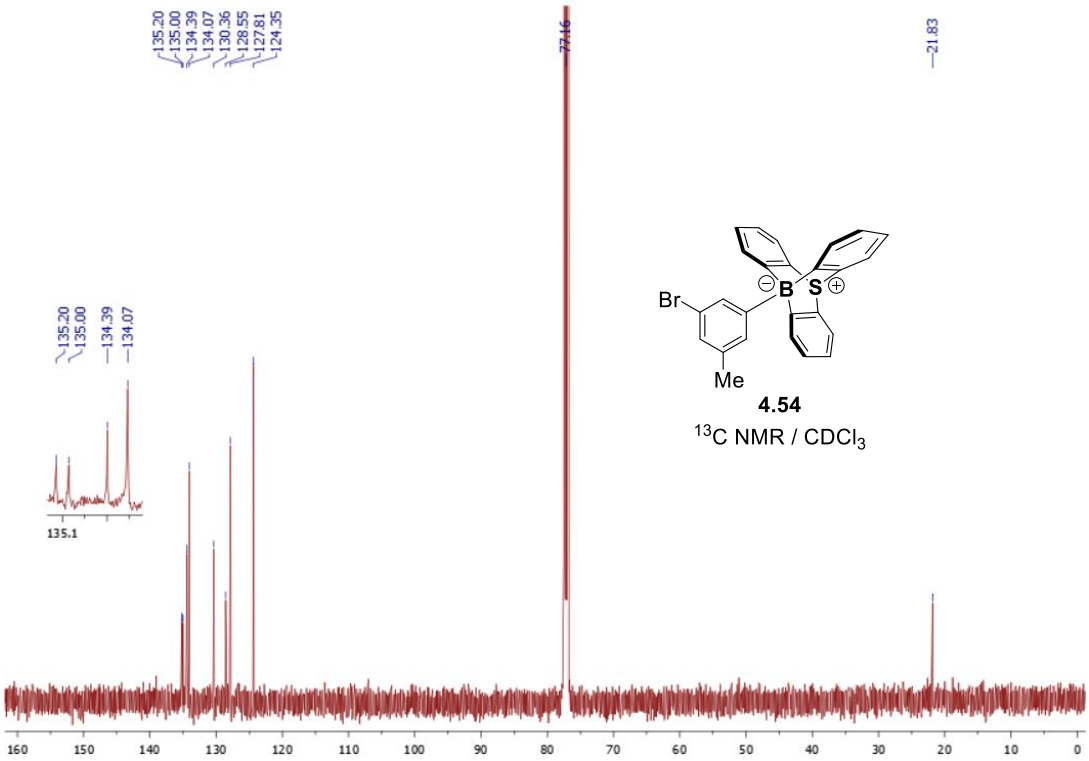
^{11}B NMR (160 MHz, 25°C, $CDCl_3$) of **4.53**



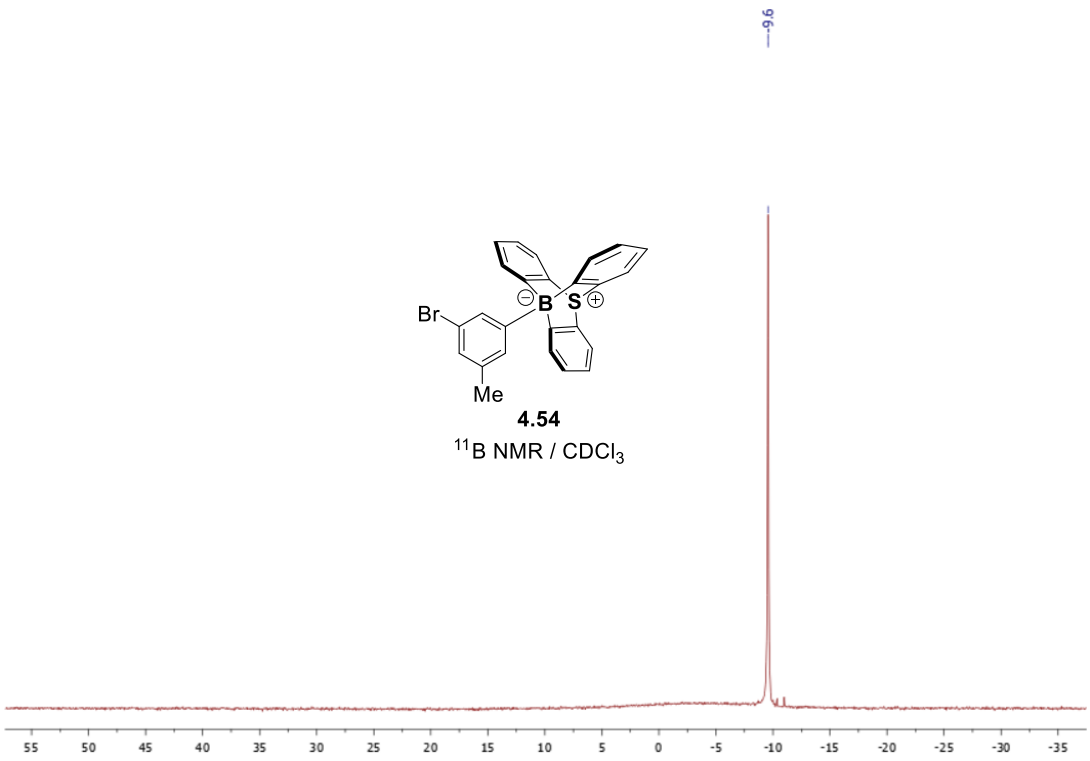
^{19}F NMR (470 MHz, 25°C, $CDCl_3$) of **4.53**



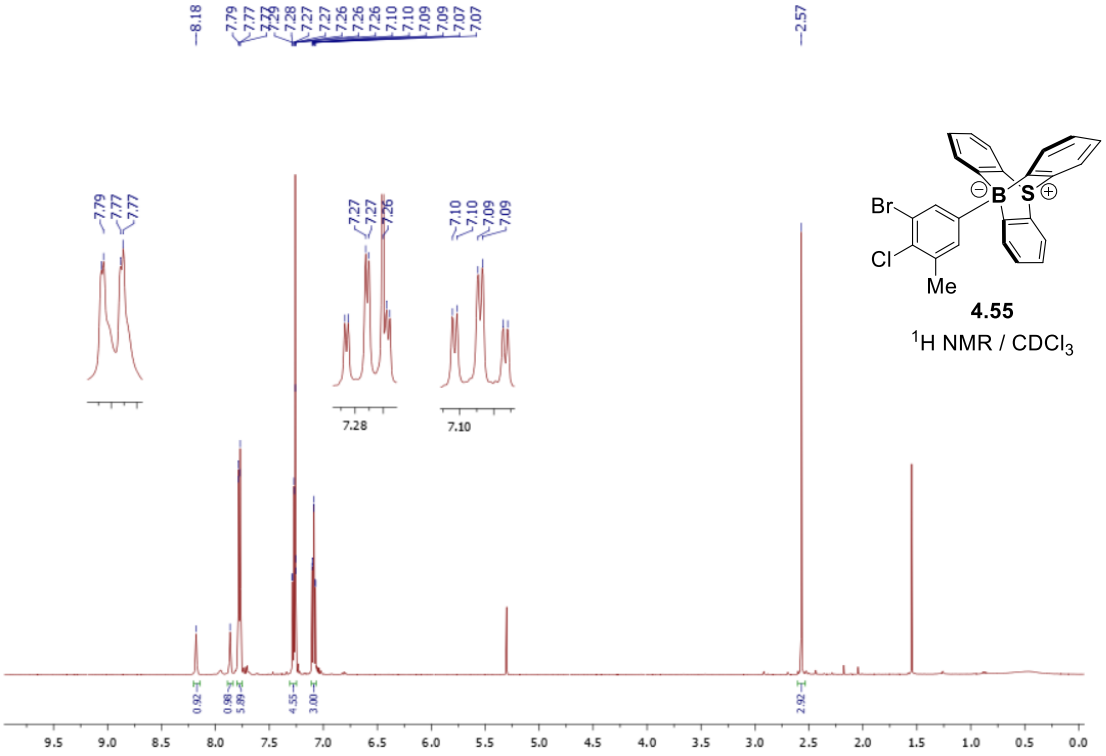
^{1}H NMR (500 MHz, 25°C, $CDCl_3$) of **4.54**



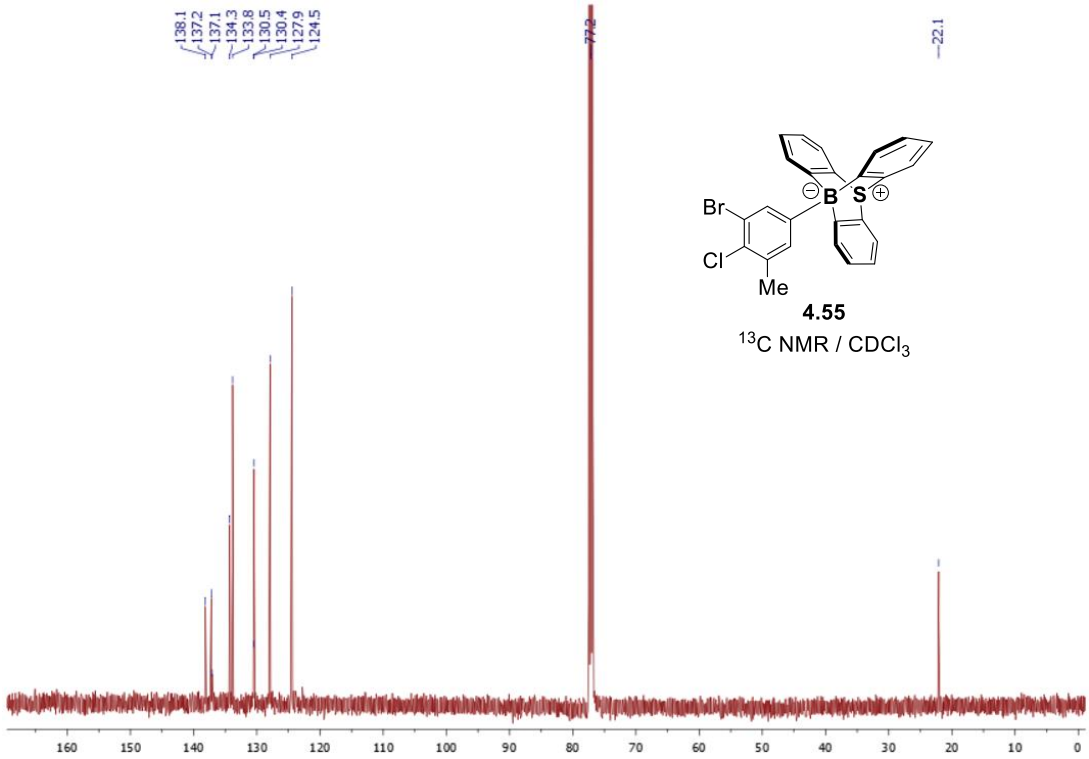
^{13}C NMR (126 MHz, 25°C, $CDCl_3$) of **4.54**



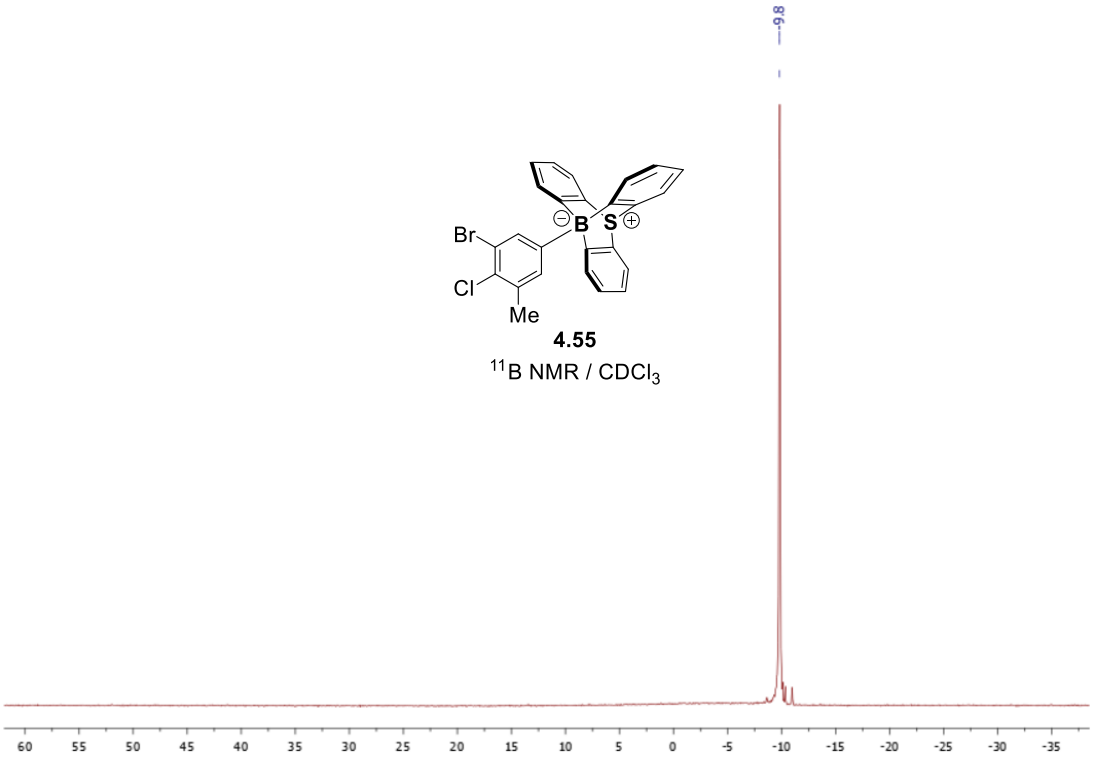
^{11}B NMR (160 MHz, 25°C, $CDCl_3$) of **4.54**



^{1}H NMR (500 MHz, 25°C, $CDCl_3$) of **4.55**



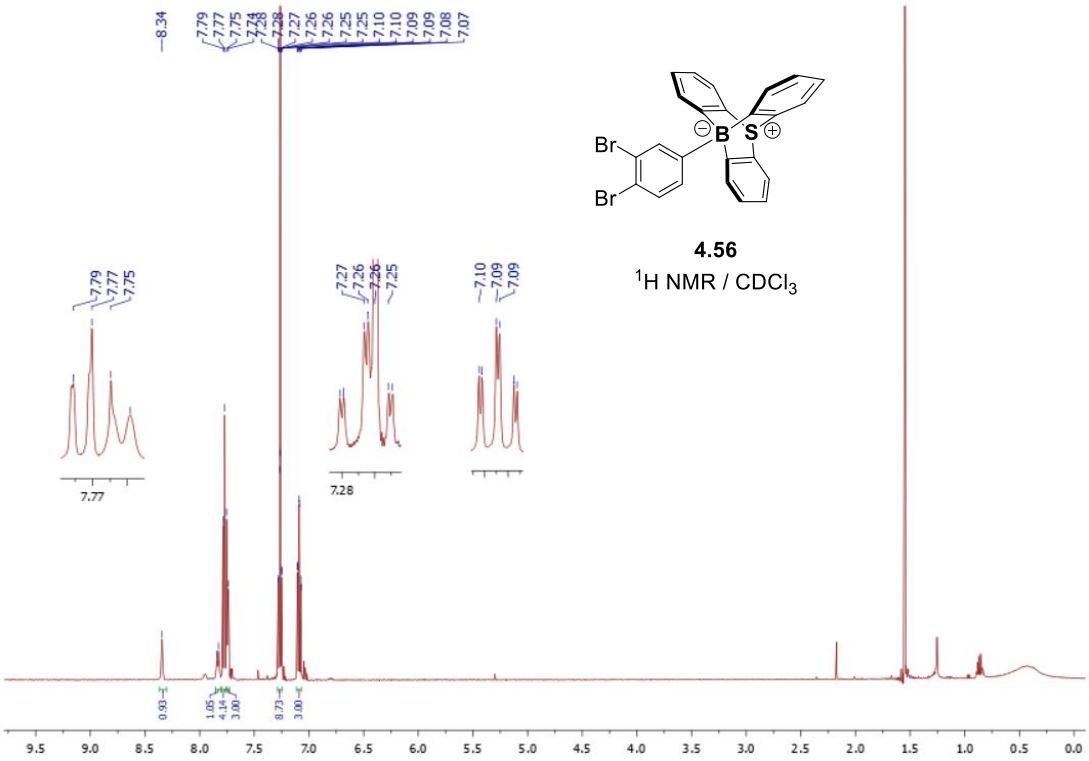
^{13}C NMR (126 MHz, 25°C, $CDCl_3$) of **4.55**



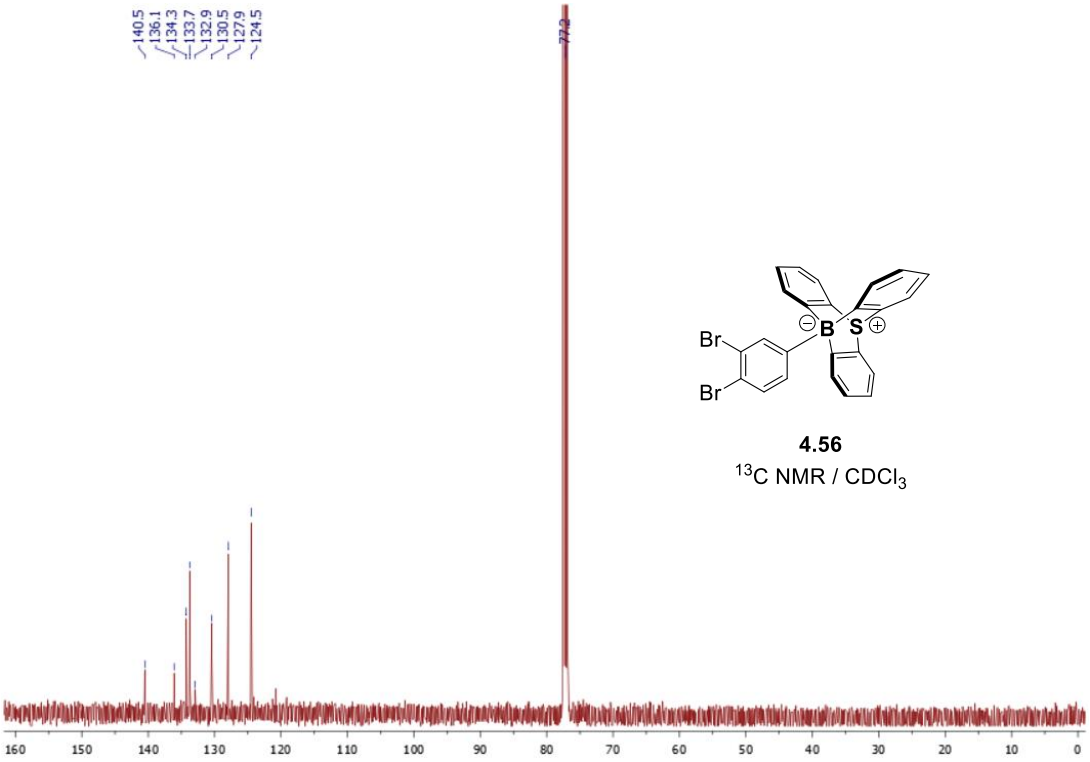
4.55

^{11}B NMR / $CDCl_3$

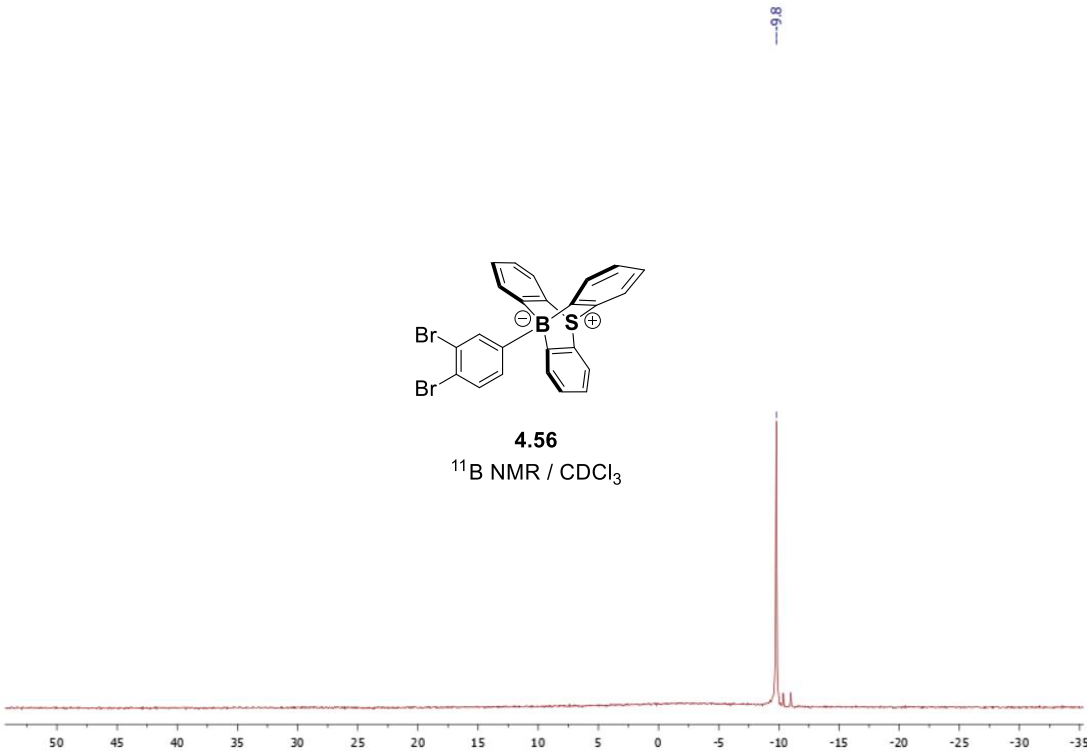
^{11}B NMR (160 MHz, 25°C, $CDCl_3$) of **4.55**



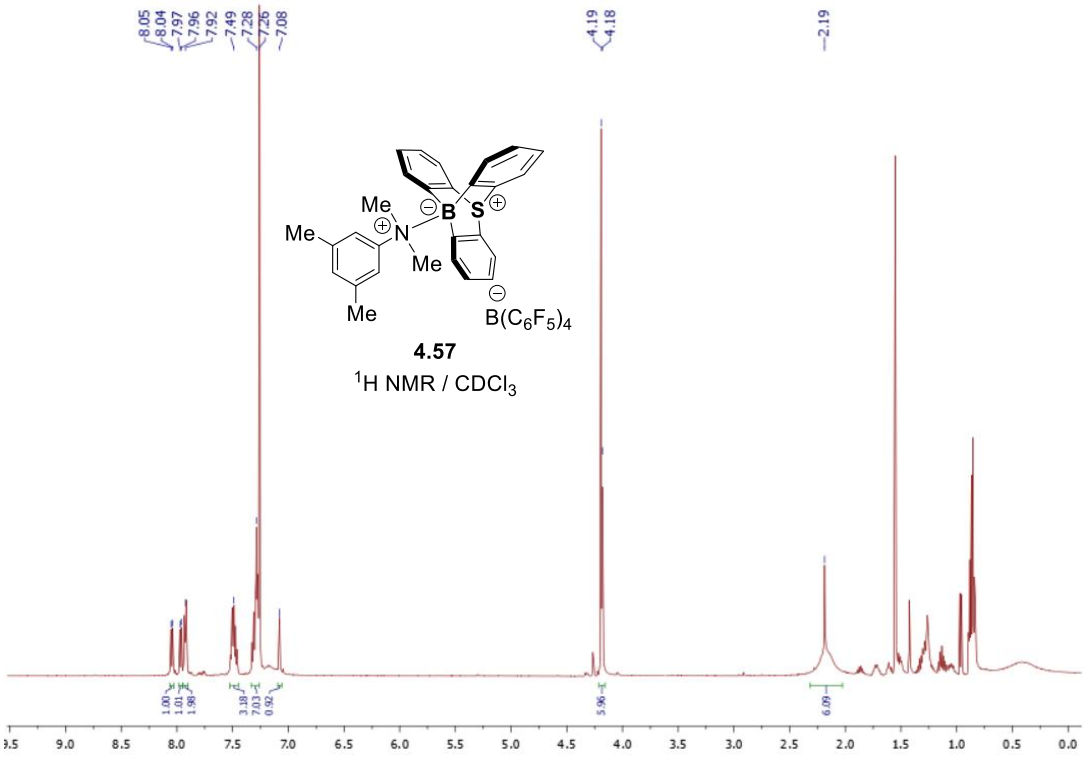
^{1}H NMR (500 MHz, 25°C, $CDCl_3$) of **4.56**



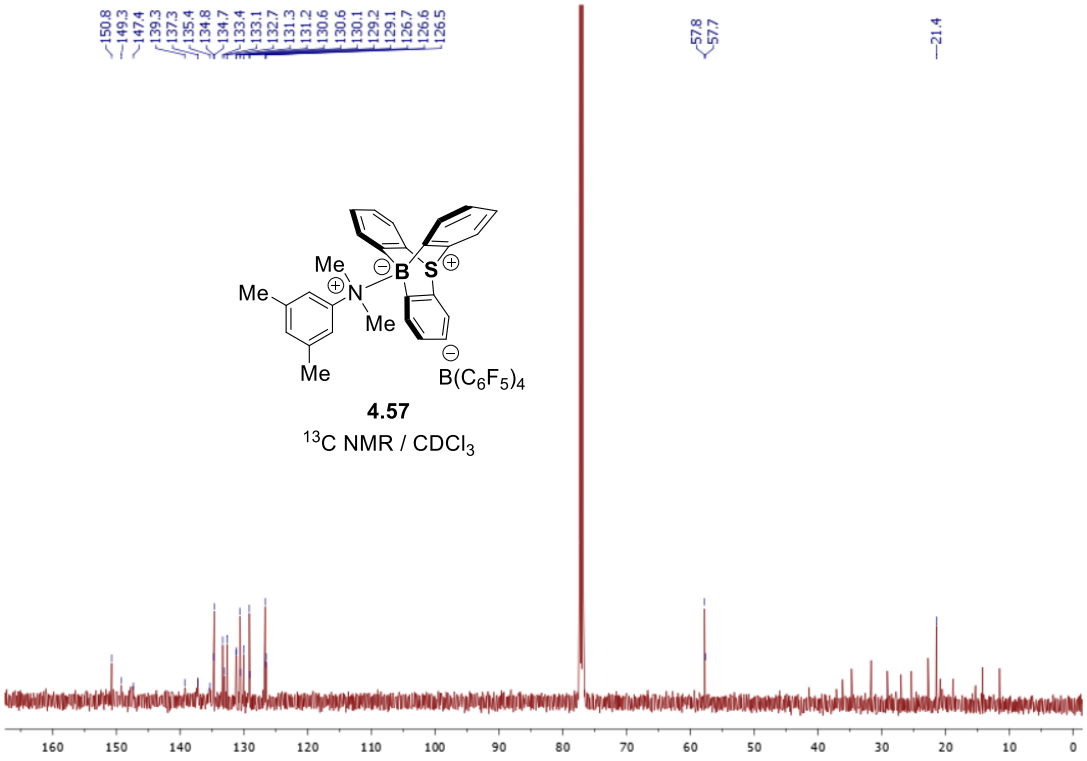
^{13}C NMR (126 MHz, 25°C, $CDCl_3$) of **4.56**



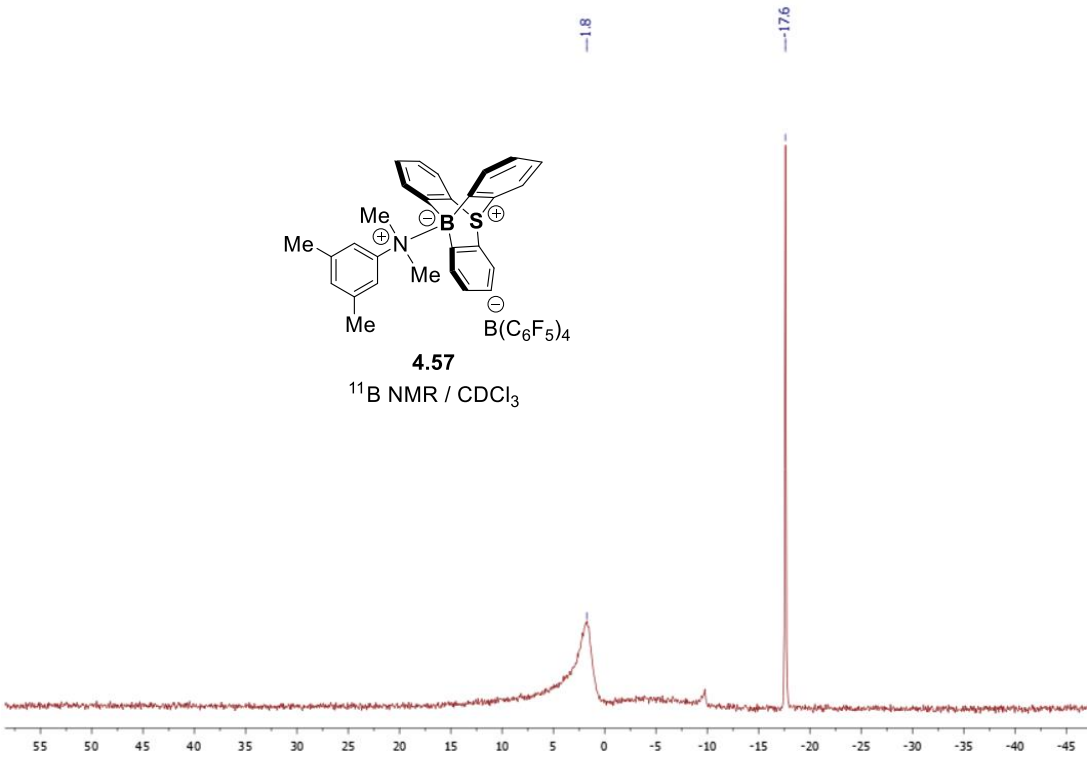
^{11}B NMR (160 MHz, 25°C, $CDCl_3$) of **4.56**



^{1}H NMR (500 MHz, 25°C, $CDCl_3$) of **4.57**



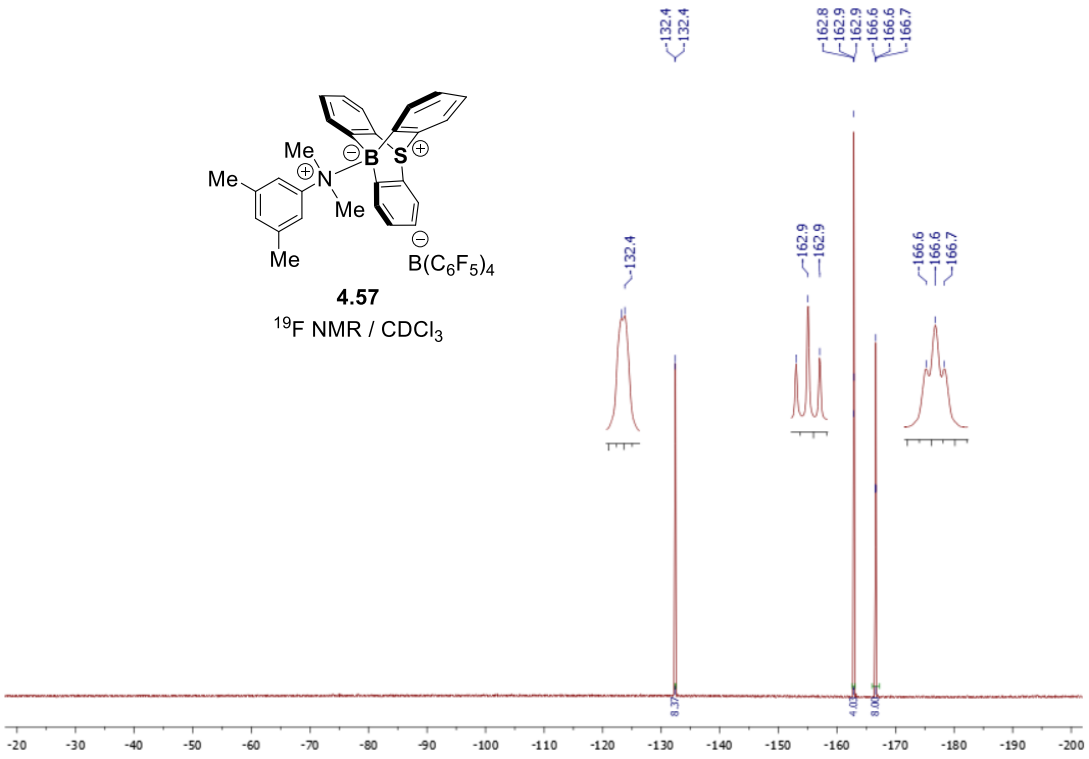
^{13}C NMR (126 MHz, 25°C, $CDCl_3$) of **4.57**



4.57

^{11}B NMR / $CDCl_3$

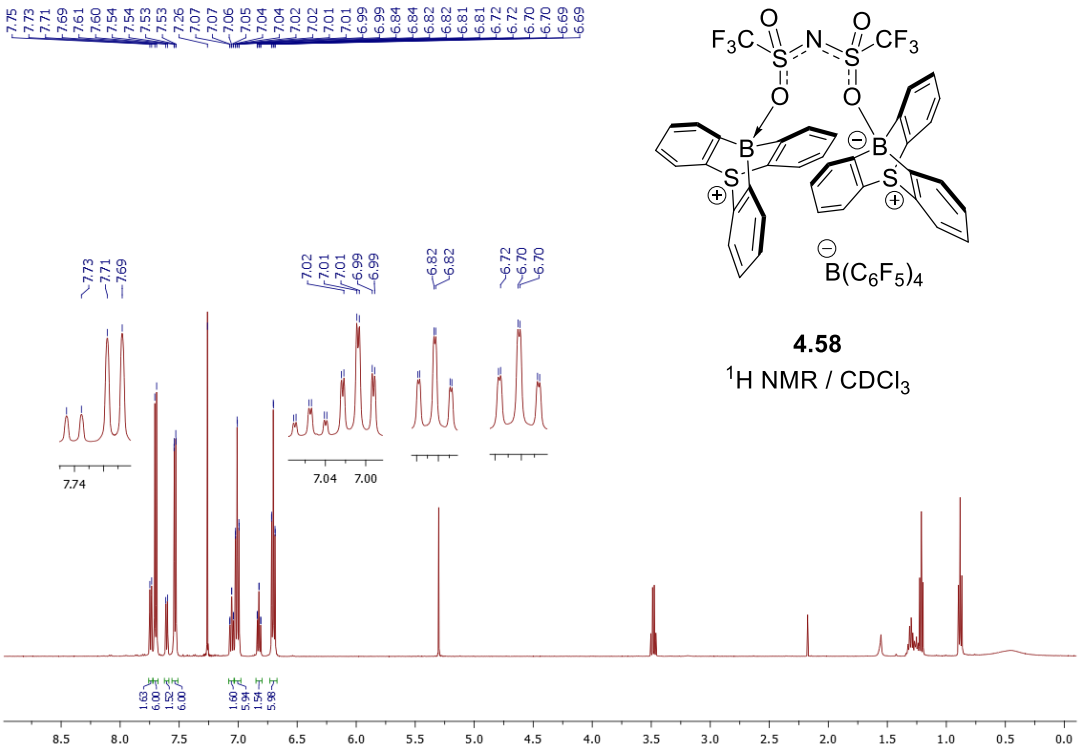
^{11}B NMR (160 MHz, 25°C, $CDCl_3$) of **4.57**



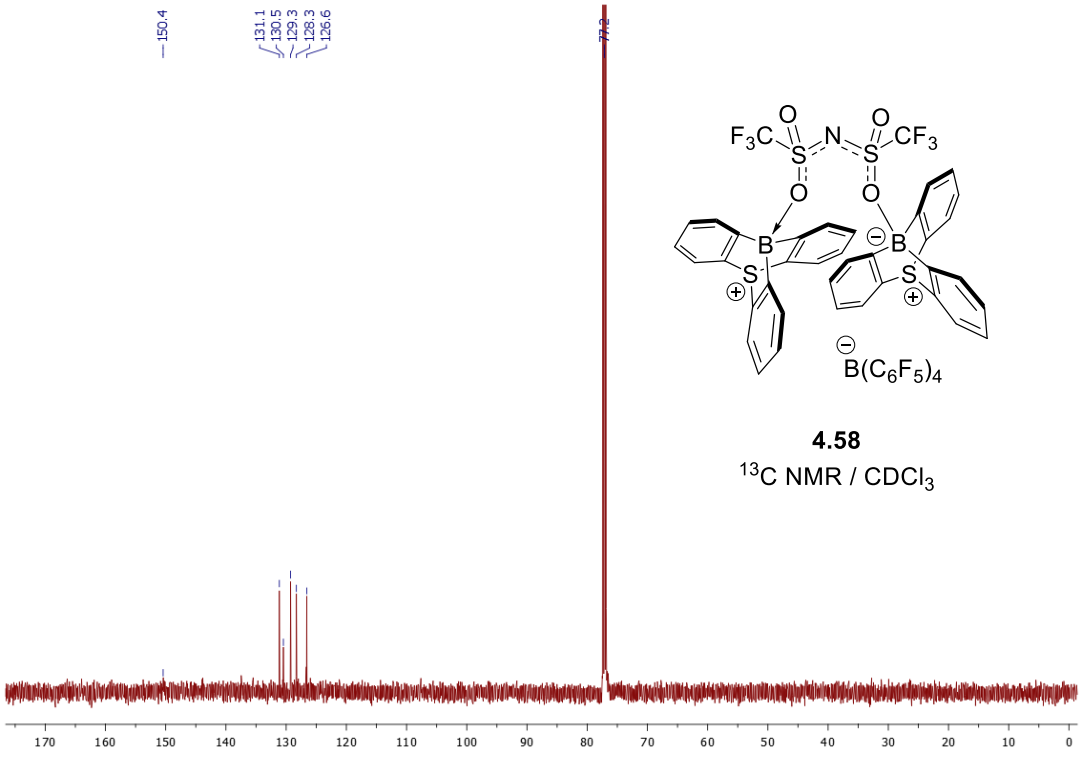
4.57

^{19}F NMR / $CDCl_3$

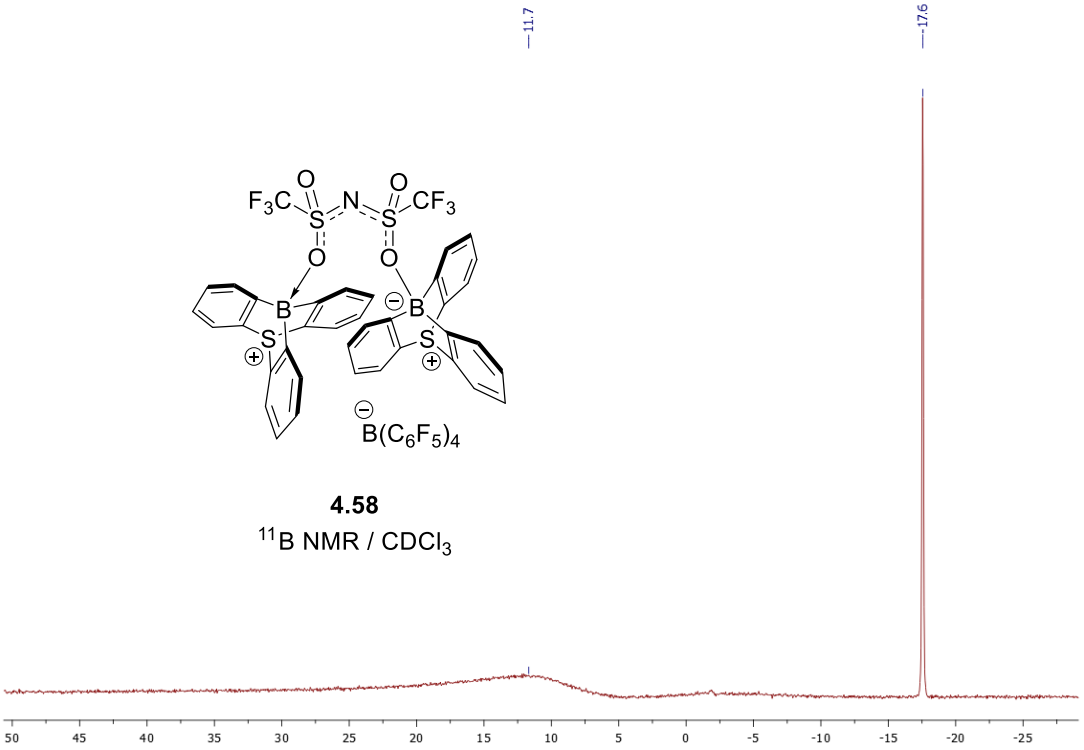
^{19}F NMR (470 MHz, 25°C, $CDCl_3$) of **4.57**



^{1}H NMR (500 MHz, 25°C, $CDCl_3$) of **4.58**



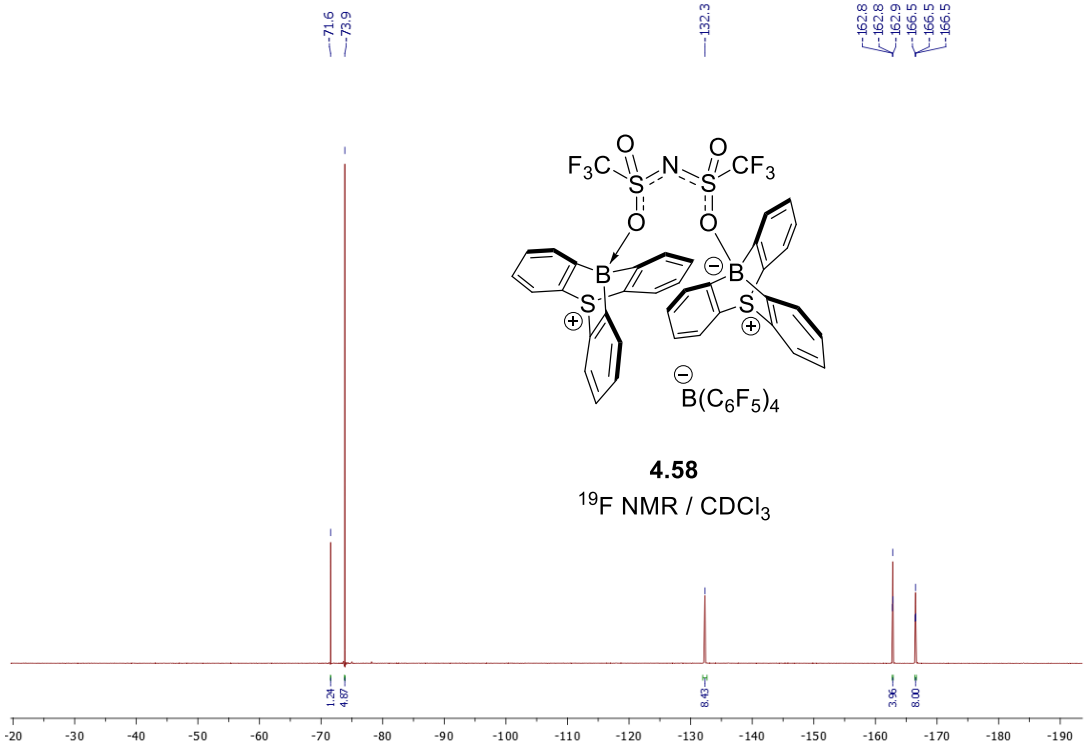
^{13}C NMR (126 MHz, 25°C, $CDCl_3$) of **4.58**



4.58

^{11}B NMR / $CDCl_3$

^{11}B NMR (160 MHz, 25°C, $CDCl_3$) of **4.58**



4.58

^{19}F NMR / $CDCl_3$

^{19}F NMR (470 MHz, 25°C, $CDCl_3$) of **4.58**

IV.11 Quantum chemical calculations

Full geometry optimizations and vibrational frequency calculations were performed, using the Gaussian16 package,[S3] at the M06-2X/6-311G(d) level of theory. For each investigated compound, all vibrational frequencies are real, demonstrating that these structures are minima on the potential energy surface. Solvent effects for benzene (C_6H_6) were considered using the Polarizable Continuum Model put into Integral Equation Formalism by Tomasi and coworkers (IEFPCM).[S4] The natural atomic orbital and natural bond orbital analysis was performed using the Gaussian NBO 3.1 program at the M06-2X/6-311G(d) level of theory.[S5]

IV.12. References

[S4.1] A. Osi, D. Mahaut, N. Tumanov, L. Fusaro, J. Wouters, B. Champagne, A. Chardon, G. Berionni, *Angew. Chem. Int. Ed.* **2022**, 61, e202112342.

[S4.2] R. T. Gallagher, S. Basu, D. R. Stuart, *Adv. Synth. Catal.* **2020**, 362, 320.

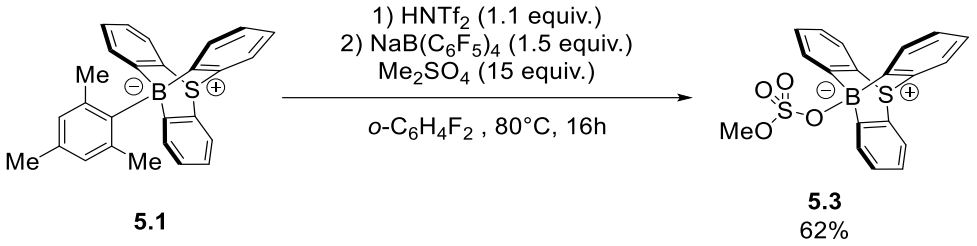
[S4.3] M. J. Frisch, G. W. Trucks, H. B. Schlegel, G. E. Scuseria, M. A. Robb, J. R. Cheeseman, G. Scalmani, V. Barone, G. A. Petersson, H. Nakatsuji, X. Li, M. Caricato, A. V. Marenich, J. Bloino, B. G. Janesko, R. Gomperts, B. Mennucci, H. P. Hratchian, J. V. Ortiz, A. F. Izmaylov, J. L. Sonnenberg, D. Williams-Young, F. Ding, F.Lipparini, F. Egidi, J. Goings, B. Peng, A. Petrone, T. Henderson, D. Ranasinghe, V. G. Zakrzewski, J. Gao, N. Rega, G. Zheng, W. Liang, M. Hada, M. Ehara, K. Toyota, R. Fukuda, J. Hasegawa, M. Ishida, T. Nakajima, Y. Honda, O. Kitao, H. Nakai, T. Vreven, K. Throssell, J. A. Montgomery, J. E. Peralta, Jr., F. Ogliaro, M. J. Bearpark, J. J. Heyd, E. N. Brothers, K. N. Kudin, V. N. Staroverov, T. A. Keith, R. Kobayashi, J. Normand, K. Raghavachari, A. P. Rendell, J. C. Burant, S. S. Iyengar, J. Tomasi, M. Cossi, J. M. Millam, M. Klene, C. Adamo, R. Cammi, J. W. Ochterski, R. L. Martin, K. Morokuma, O. Farkas, J. B. Foresman, D. J. Fox, *Gaussian 16 Rev, A.03* (Gaussian Inc., 2016).

[S4.4] J. Tomasi, B. Mennucci, R. Cammi, *Chem. Rev.* **2005**, *105* (8), 2999.

[S4.5] E. D. Glendening, A. E. Reed, J. E. Carpenter, F. Weinhold, *NBO Version 3.1*, (Gaussian Inc., 2003).

V.1. Preparation of starting materials.

(9-Sulfonium-10-boratriptycene)-10-methylsulfate **5.3**



Under glovebox conditions in a Schlenk tube, $HNTf_2$ (80 mg, 0.28 mmol, 1.1 equiv.) was added to a suspension of 10-mesityl-9-sulfonium-10-boratritpycene-ate complex **5.1** (100 mg, 0.25, 1.0 equiv.) in 1,2-difluorobenzene (2.0 ml). The reaction was stirred for 5min then $NaB(C_6F_5)_4$ (278 mg, 0.38 mmol, 1.5 equiv.) and stirred for further 2 min. Me_2SO_4 (0.36 ml, 3.8 mmol, 15 equiv.) was then added, the Schlenk tube was sealed with a glass stopper and stirred at 80°C out of the glovebox. **/!\ Care should be taken using Me_2SO_4 out of the glovebox due to high toxicity /!**. After 16h, the crude was evaporated to dryness and purified via flash column chromatography (50:50 *n*-hexane/CH_2Cl_2 then 100% CH_2Cl_2). After evaporation, the resulting brown product was washed with small amount of MeOH affording pure (9-sulfonium-10-boratriptycene)-10-methylsulfate **5.3** (61 mg, 0.16 mmol, 62% yield) as white powder. Single crystals suitable for X-ray diffraction analysis were obtained by a slow evaporation of a saturated solution of **5.3** in CH_2Cl_2.

TLC: R_f = 0.8 (CH_2Cl_2)

^{1}H NMR (500 MHz, $CDCl_3$) δ (ppm) = 8.21 (d, *J* = 7.0 Hz, 3H), 7.74 (d, *J* = 7.7 Hz, 3H), 7.37 (t, *J* = 7.4 Hz, 3H), 7.12 (t, *J* = 7.6 Hz, 3H), 4.27 (s, 3H).

^{13}C NMR (126 MHz, $CDCl_3$) δ (ppm) = 155.9 (CB), 131.6 (Cq), 131.5 (CH), 131.1 (CH), 127.5 (CH), 125.2 (CH), 57.6 (CH_3).

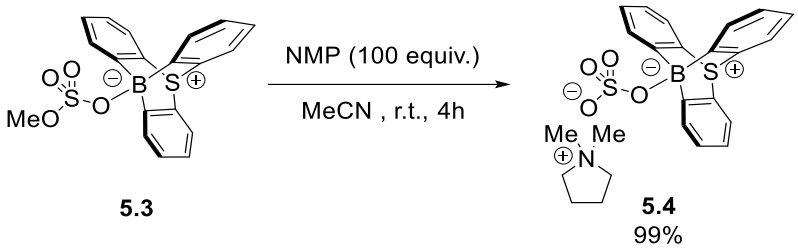
^{11}B NMR (160 MHz, acetone-d_6) δ (ppm) = 1.8 (br)

HRMS (MALDI$^+$) (*m/z*): calc. for [$C_{19}H_{15}BO_4NaS_2^+$] : 405.0403, [M^+] : 405.0400

IR (neat, ATR): $\tilde{\nu}$ / cm^{-1} = 3047, 2956, 1434, 1349, 1196, 1147, 1043, 1016, 989, 908, 782.

M.p. : 277.7-284.8°C

N,N-Dimethylpyrolidinium (9-sulfonium-10-boratriptycene)-10-sulfate **5.4**



5.3 **5.4** 99%

To a solution of (9-sulfonium-10-boratriptycene)-10-methylsulfate **5.3** (50 mg, 0.13 mmol, 1.0 equiv.) in MeCN (5 ml) was added *N*-methylpyrolidine (NMP) (1.3 ml, 13 mmol, 100 equiv.). The reaction mixture was stirred at room temperature for 4h then evaporated and further dried at 50°C overnight affording pure *N,N*-dimethylpyrolidinium (9-sulfonium-10-boratriptycene)-10-sulfate **5.4** (61 mg, 0.13 mmol, 99% yield) as a highly hygroscopic white powder. The hygroscopic solid was then immediately transferred and stored in a glovebox.

Single crystals suitable for X-ray diffraction analysis were obtained by a slow evaporation of a saturated solution of **5.4** in MeCN in the glovebox.

^{1}H NMR (500 MHz, CD_3CN) δ (ppm) = 8.41 (dd, *J* = 7.3, 1.2 Hz, 3H), 7.80 (dd, *J* = 7.7, 3.0 Hz, 3H), 7.31 (td, *J* = 7.3, 1.1 Hz, 3H), 7.08 (td, *J* = 7.5, 1.5 Hz, 3H), 3.43-3.36 (m, 4H), 3.02 (s, 6H), 2.14-2.07 (m, 4H).

^{13}C NMR (126 MHz, CD_3CN) δ (ppm) = 161.6 (CB), 133.9 (CH), 133.0 (Cq), 130.6 (CH), 128.6 (CH), 125.1 (CH), 66.6 (CH_2), 52.5 (CH_3), 22.6 (CH_2).

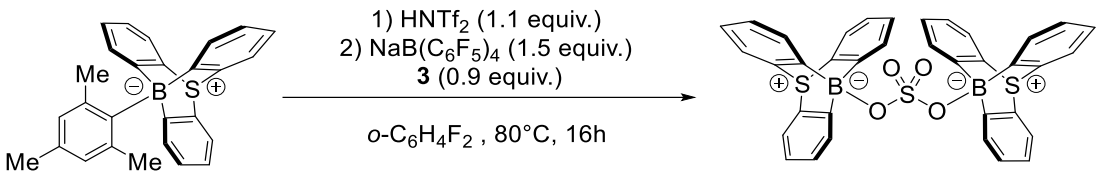
^{11}B NMR (160 MHz, CD_3CN) δ (ppm) = -1.0 (s)

HRMS (MALDI$^-$) (*m/z*): calc. for [$C_{18}H_{12}BO_4S_2^-$] : 367.0270, [M^-] : 367.0273

IR (neat, ATR): $\tilde{\nu}$ / cm^{-1} = 3388, 3011, 1636, 1515, 1465, 1429, 1362, 1303, 1187, 1151, 1088, 1043, 989,935, 912, 872.

M.p. (C_6H_5F): 195-197 °C (dec)

Bis(9-sulfonium-10-boratriptycene)-10-sulfate **5.6**



5.1 **5.6** 31%

Under glovebox conditions in a Schlenk tube, $HNTf_2$ (16 mg, 0.056 mmol, 1.1 equiv.) was added to a suspension of 10-mesityl-9-sulfonium-10-boratritpycene-ate complex **5.1** (20 mg, 0.051, 1.0 equiv.) in 1,2-difluorobenzene (2.0 ml). The reaction was stirred for 5min then $NaB(C_6F_5)_4$ (56 mg, 0.076 mmol, 1.5 equiv.) and stirred for further 2 min. (9-Sulfonium-10-boratriptycene)-10-methylsulfate **5.3** (18 mg, 0.046 mmol, 0.90 equiv.) was then added, the Schlenk tube was sealed with a glass stopper and stirred at 80°C out of the glovebox. After 16h, the crude was evaporated to dryness and purified via flash chromatography (50:50 *n*-hexane/CH_2Cl_2 then CH_2Cl_2). After evaporation, the resulting brown product was washed with small amount of MeOH affording pure bis(9-sulfonium-10-boratriptycene)-10-sulfate **5.6** (10 mg, 0.016 mmol, 31% yield) as a white powder.

Single crystals suitable for X-ray diffraction analysis were obtained by a slow evaporation of a saturated solution of **5.6** in CH_2Cl_2/MeOH.

TLC: R_f = 0.8 (CH_2Cl_2)

^{1}H NMR (500 MHz, $CDCl_3$) δ (ppm) = 8.71 (dd, *J* = 7.4, 1.1 Hz, 6H), 7.76 (d, *J* = 7.3 Hz, 6H), 7.41 (td, *J* = 7.4, 1.0 Hz, 6H), 7.12 (td, *J* = 7.5, 1.4 Hz, 6H).

^{13}C NMR (126 MHz, $CDCl_3$) δ (ppm) = 157.6 (CB), 132.6 (CH), 131.8 (Cq), 130.9 (CH), 127.3 (CH), 124.8 (CH).

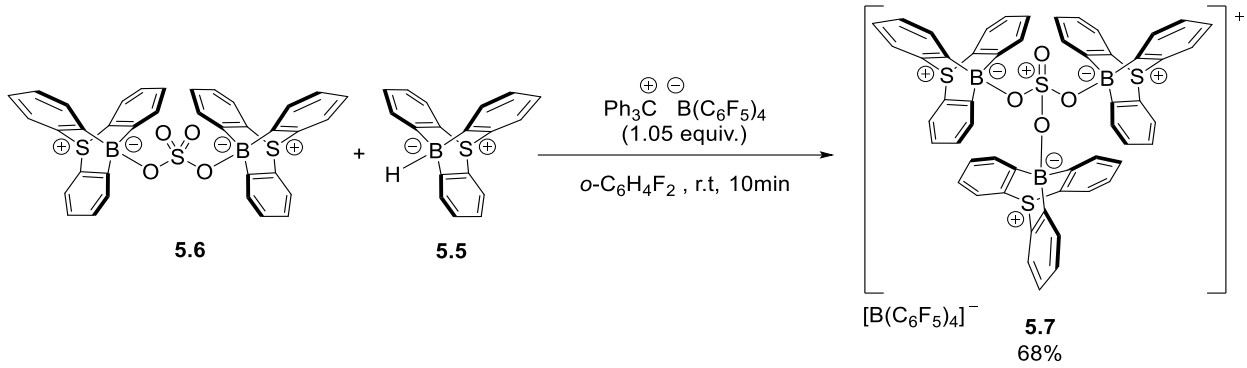
^{11}B NMR (160 MHz, acetone-d_6) δ (ppm) = 1.6 (br)

HRMS (MALDI$^+$) (*m/z*): calc. for [$C_{36}H_{24}B_2O_4NaS_3^+$] : 661.0921, [$M^+$] : 661.0925

IR (neat, ATR): $\tilde{\nu}$ / cm^{-1} = 3052, 1421, 1317, 1304, 1268, 1183, 1142, 1043, 1016, 962, 760.

M.p. : >300°C

Tetrakis(pentafluorophenyl)borate tris(10-oxo-9-sulfonium-10-boratriptycene)sulfoxonium **5.7**



Under glovebox conditions, tritylium tetrakis(pentafluorophenyl)borate (15 mg, 0.016 mmol, 1.05 equiv.) was added to a suspension of bis(9-sulfonium-10-boratriptycene)-10-sulfate **5.6** (10 mg, 0.016 mmol, 1.0 equiv.) and 10-hydrido-9-sulfonium-10-boratriptycene-ate complex **5.5** (4.2 mg, 0.016 mmol, 1.0 equiv.) in 1,2-difluorobenzene (1.5 ml). The reaction mixture was stirred for 10 min at room temperature the evaporated to dryness out of the glovebox. The crude was washed with *n*-hexane and C_6H_6 then dried under dynamic vacuum affording pure tetrakis(pentafluorophenyl)borate tris(10-oxo-9-sulfonium-10-boratriptycene)sulfoxonium **5.7** (17 mg, 0.011 mmol, 68% yield) as a white powder.

Single crystals suitable for X-ray diffraction analysis were obtained by a slow evaporation of a saturated solution of **5.7** in CH_2Cl_2/MeOH.

^{1}H NMR (500 MHz, $CDCl_3$) δ (ppm) = 8.32 (d, *J* = 7.4 Hz, 9H), 7.83 (d, *J* = 7.7 Hz, 9H), 7.11 (t, *J* = 7.5 Hz, 9H), 7.03 (t, *J* = 7.4 Hz, 9H).

^{13}C NMR (126 MHz, $CDCl_3$) δ (ppm) = 153.5 (CB), 131.3 (Cq), 131.2 (CH), 131.0 (CH), 128.2 (CH), 126.0 (CH).

^{11}B NMR (160 MHz, acetone-d_6) δ (ppm) = 8.4 (br)

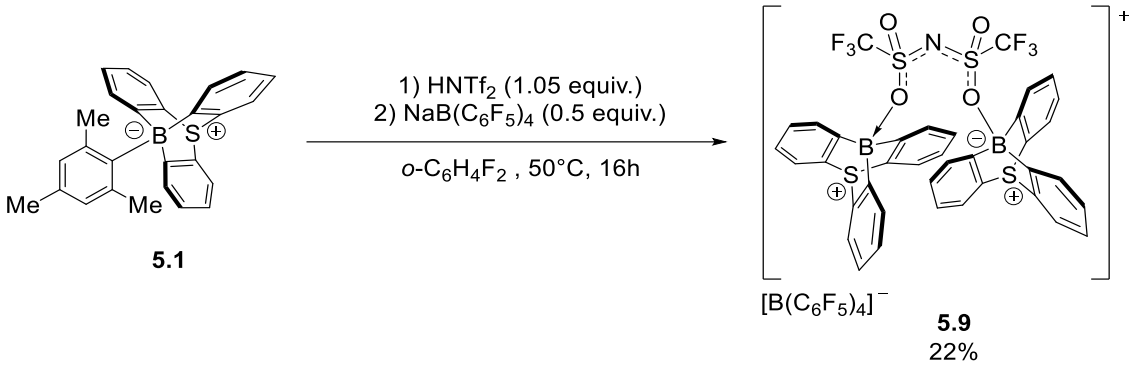
^{19}F NMR (483 MHz, $CDCl_3$) δ (ppm) = -132.4 (s, 8F), -163.1 (t, *J* = 20.6 Hz, 4F), -166.7 (t, 18.0 Hz, 8F).

HRMS (MALDI^{+}) (*m/z*): calc. for [$C_{54}H_{36}B_3O_4S_4^{+}$] : 909.1776, [$M^{+}$] : 909.1793

IR (neat, ATR): $\tilde{\nu}$ / cm^{-1} = 3056, 2921, 2854, 1726, 1641, 1515, 1461, 1434, 1375, 1317, 1272, 1142, 1075, 980, 868, 755.

M.p. : 258.4-260.3°C (dec)

Tetrakis(pentafluorophenyl)borate bis(10-trifluoromethylsulfonyl-9-sulfonium-10-boratriptycene)imminium **5.9**



In a glovebox, triflimidic acid (76 mg, 0.27 mmol, 1.05 equiv.) is added to a suspension of 10-mesityl-9-sulfonium-10-boratriptycene-ate complex **5.1** (100 mg, 0.26 mmol, 1.0 equiv.) in 1,2-difluorobenzene. After stirring for 5 min, sodium tetrakis(pentafluorophenyl)borate (93 mg, 0.13 mmol, 0.5 equiv.) is added and the reaction mixture is stirred out of the glovebox at 50°C. After 16h, the reaction mixture is evaporated to dryness and the crude is purified by flash chromatography (50:50 *n*-hexane/CH_2Cl_2 then pure CH_2Cl_2) affording the desired tetrakis(pentafluorophenyl)borate bis(10-trifluoromethylsulfonyl-9-sulfonium-10-boratriptycene)iminium **5.9** (42 mg, 0.028 mmol, 22% yield) as a white powder. The flash chromatography has to be performed as quick as possible due to slow decomposition of the product on the silica gel and in presence of CH_2Cl_2 or $CHCl_3$. The product could be stored under ambient conditions in a capped vial. However, long term storage in a glovebox is preferable.

Crystals suitable for X-ray diffraction analysis were obtained by slow evaporation of a saturated solution of **5.9** in CH_2Cl_2/*n*-hexane.

TLC: R_f = 0.1 (*n*-hexane/CH_2Cl_2 50:50)

^{1}H NMR (500 MHz, $CDCl_3$) δ (ppm) = Major isomer : 7.70 (d, *J* = 7.7 Hz, 6H), 7.53 (dd, *J* = 7.4, 1.0 Hz, 6H), 7.01 (td, *J* = 7.6, 1.2 Hz, 6H), 6.70 (td, *J* = 7.4, 0.8 Hz, 6H). Minor

isomer : 7.74 (d, *J* = 7.7 Hz, 6H), 7.61 (d, *J* = 7.8 Hz, 6H), 7.06 (td, *J* = 7.6, 1.2 Hz, 6H), 6.82 (td, *J* = 7.4, 0.8 Hz, 6H).

^{13}C NMR (126 MHz, $CDCl_3$) δ (ppm) = 150.4 (CB), 131.1 (CH), 130.5 (Cq), 129.3 (CH), 128.3 (CH), 126.6 (CH).

^{11}B NMR (160 MHz, $CDCl_3$) δ (ppm) = 11.7 (br), -17.6 (s)

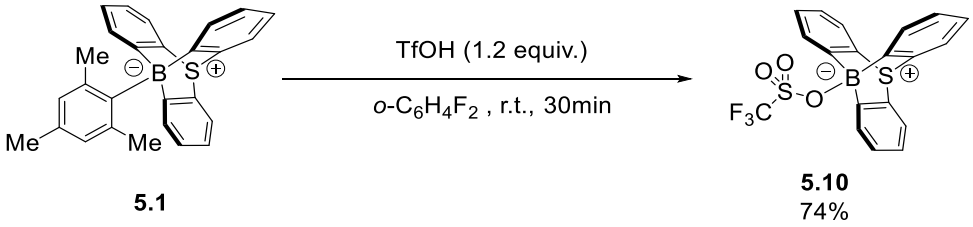
^{19}F NMR (483 MHz, $CDCl_3$) δ (ppm) = -71.6 (s, 1.24 F), -73.9 (s, 4.87 F), -132.4 (s, 8F), -163.1 (t, *J* = 20.6 Hz, 4F), -166.7 (t, 18.0 Hz, 8F).

HRMS (MALDI$^-$) (*m/z*): Could not be determined due to decomposition during injection.

IR (neat, ATR): $\tilde{\nu}$ / cm^{-1} = 3060, 1647, 1510, 1465, 1359, 1231, 1142, 1084, 974, 832, 752.

M.p. (C_6H_5F): 179.2 (dec)

10-Triflate-9-sulfonium-10-boratriptycene-ate complex **5.10**



5.1 **5.10** 74%

Triflic acid (27 µl, 0.31 mmol, 1.2 equiv.) was added to a suspension of 10-mesityl-9-sulfonium-10-boratriptycene-ate complex **5.1** (100 mg, 0.26 mmol, 1.0 equiv.) in 1,2-difluorobenzene (3 ml). After 30 min at room temperature, the reaction mixture was evaporated to dryness and purified by flash chromatography (60:40 *n*-hexane/CH_2Cl_2) affording pure 10-triflate-9-sulfonium-10-boratriptycene-ate complex **5.10** (80 mg, 0.19 mmol, 74% yield) as a white powder.

Single crystals suitable for X-ray diffraction analysis were obtained by a slow evaporation of a saturated solution of **5.10** in CH_2Cl_2.

TLC: R_f = 0.5 (*n*-hexane/CH_2Cl_2 50:50)

^{1}H NMR (500 MHz, $CDCl_3$) δ (ppm) = 8.16 (dd, *J* = 7.4, 0.3 Hz, 3H), 7.77 (dd, *J* = 7.7, 0.4 Hz, 3H), 7.40 (td, *J* = 7.4, 1.0 Hz, 3H), 7.15 (td, *J* = 7.6, 1.2 Hz, 3H).

^{13}C NMR (126 MHz, $CDCl_3$) δ (ppm) = 154.6 (CB), 131.4 (CH), 131.3 (Cq), 131.2 (CH), 237.6 (CH), 125.5 (CH).

^{11}B NMR (160 MHz, $CDCl_3$) δ (ppm) = 3.6 (br)

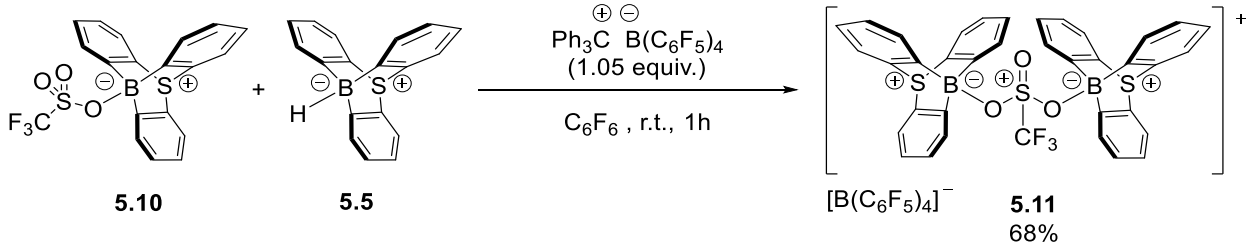
^{19}F NMR (483 MHz, $CDCl_3$) δ (ppm) = -76.1 (s)

HRMS (MALDI$^+$) (*m/z*): calc. for [$C_{19}H_{12}BO_3F_3NaS_2^+$] : 443.0171, [$M^+$] : 443.0174

IR (neat, ATR): $\tilde{\nu}$ / cm^{-1} = 3047, 1461, 1421, 1346, 1245, 1205, 1139, 1042, 1002, 874, 751.

M.p. : 234.3-235.4°C

Tetrakis(pentafluorophenyl)borate bis(10-oxy-9-sulfonium-10-boratriptycene)trifluoromethyloxosulfonium **5.11**



5.10 **5.5** **5.11** 68%

In a glovebox, tritylium tetrakis(pentafluorophenyl)borate (23 mg, 0.025 mmol, 1.05 equiv.) is added to a suspension of 10-triflate-9-sulfonium-10-boratriptycene-ate complex **5.10** (10 mg, 0.024 mmol, 1.0 equiv.) and 10-hydrido-9-sulfonium-10-boratriptycene-ate complex **5** (6.5 mg, 0.024 mmol, 1.0 equiv.) in hexafluorobenzene (1.5 – 2.0 ml). After stirring for 1h, the yellow suspension is filtered and washed several times with hexane affording pure tetrakis(pentafluorophenyl)borate bis(10-oxy-9-sulfonium-10-boratriptycene)trifluoromethyloxosulfonium **5.11** (22 mg, 0.016 mmol, 68% yield) as yellow powder. In some case, the reaction mixture forms a red oily precipitate which, after addition of a few drops of hexane, reforms a yellow precipitate which is filtered and washed with hexane providing the desired product. A purification by flash chromatography can also be performed in pure CH_2Cl_2, however a drastic yield drop is observed due to decomposition on the silica gel and in presence of CH_2Cl_2. The product could be stored under ambient conditions in a capped vial. However, long term

storage in a glovebox is preferable. Crystals suitable for X-ray diffraction analysis were obtained by cooling a saturated solution of **5.11** in HC_6F_5/*n*-hexane.

^{1}H NMR (500 MHz, $CDCl_3$) δ (ppm) = 7.95 (d, *J* = 7.3 Hz, 6H), 7.85 (d, *J* = 7.7 Hz, 6H), 7.19 (td, *J* = 7.7, 1.2 Hz, 6H), 7.13 (td, *J* = 7.4, 0.9 Hz, 6H).

^{13}C NMR Could not be measured due to acquisition time incompatible with any solvent.

^{11}B NMR (160 MHz, $CDCl_3$) δ (ppm) = 12.3 (br), -17,6 (s)

^{19}F NMR (483 MHz, $CDCl_3$) δ (ppm) = -71.7 (s, 3H), -132.4 (s, 8F), -163.1 (t, *J* = 20.6 Hz, 4F), -166.7 (t, *J* =18.0 Hz, 8F).

HRMS (MALDI$^-$) (*m/z*): Could not be determined due to decomposition during injection.

IR (neat, ATR): $\tilde{\nu}$ / cm^{-1} = 3060, 1634, 1585, 1505, 1457, 1364, 1301, 1275, 1244, 1142, 1089, 1031, 978, 765.

M.p. : 148.8°C (dec)

V.2. Protocols and NMR monitoring of selected reactions:

Decomposition of **5.11** in $CDCl_3$:

Tetrakis (pentafluorophenyl) borate bis(10-oxy-9-sulfonium-10-boratriptycene) trifluoromethyloxosulfonium **5.11** (5.0 mg, 3.6 µmol, 1.0 equiv.) was dissolved in $CDCl_3$ (0.7 ml) in a J-Young NMR tube. After standing at room temperature for 16h, the reaction was subjected to ^{1}H and ^{11}B NMR spectroscopy. Both analysis showed the absence of cationic complex **5.11** and the appearance of chloroborane **5.12** (Fig S1-S2, red stars) as well as ate-complex **5.10** (Fig S1-S2, blues stars) which have found to be partially decomposed due to the concomitant formation of $[CDCl_2]^+[B(C_6F_5)_4]^-$.

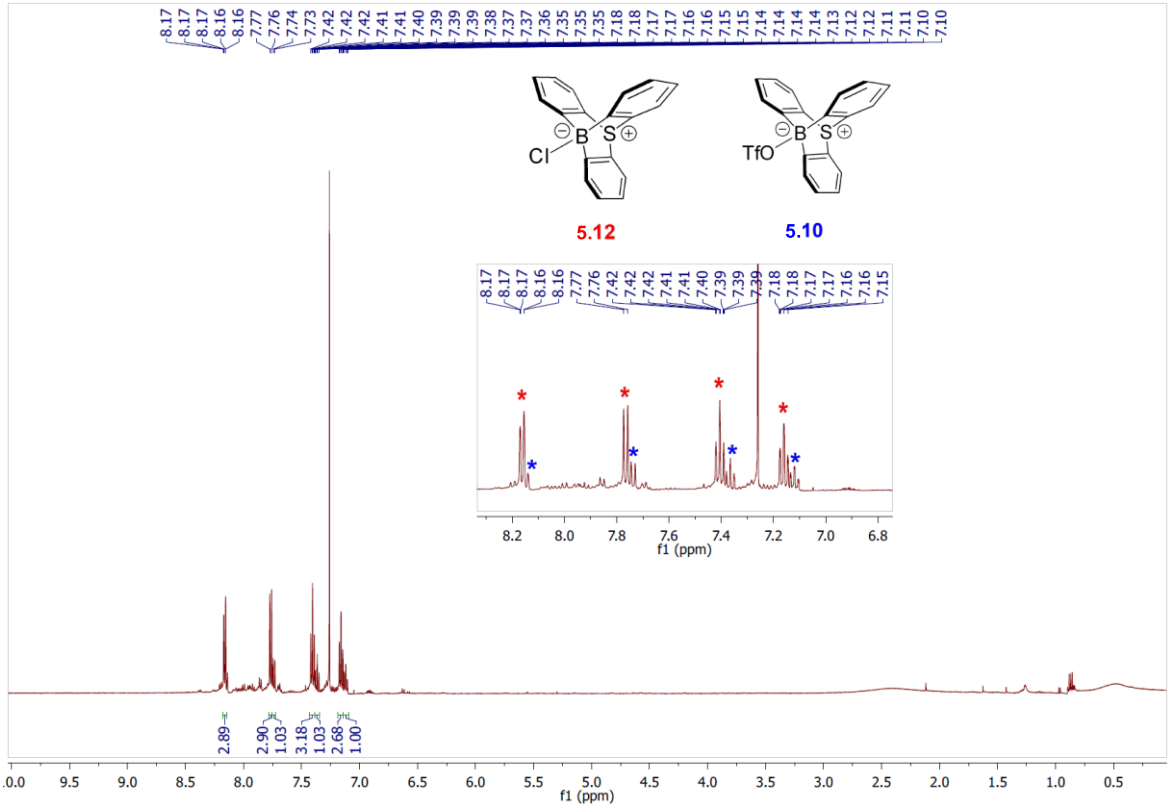


Fig. SV.1. ^{1}H NMR spectra (500 MHz, 25 °C, $CDCl_3$) for the reaction of **5.11** with $CDCl_3$.

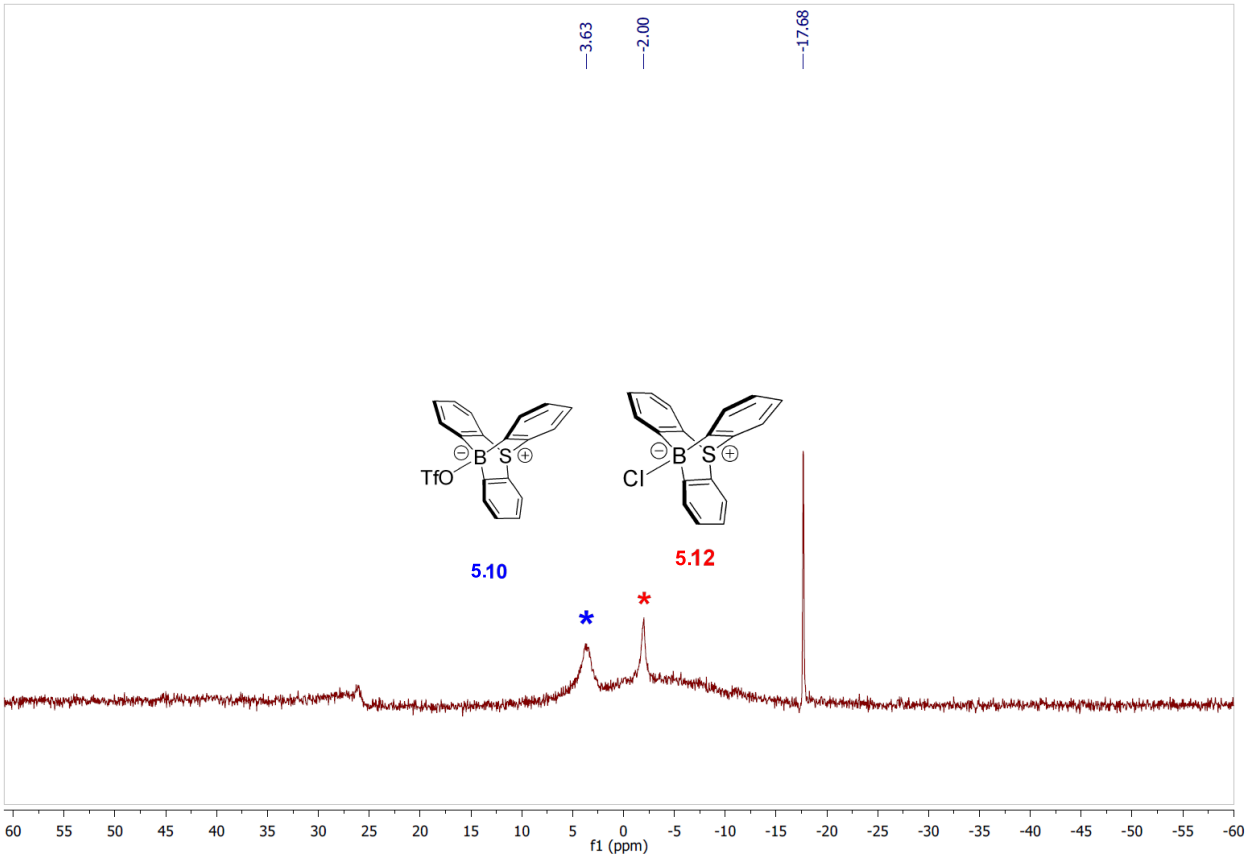
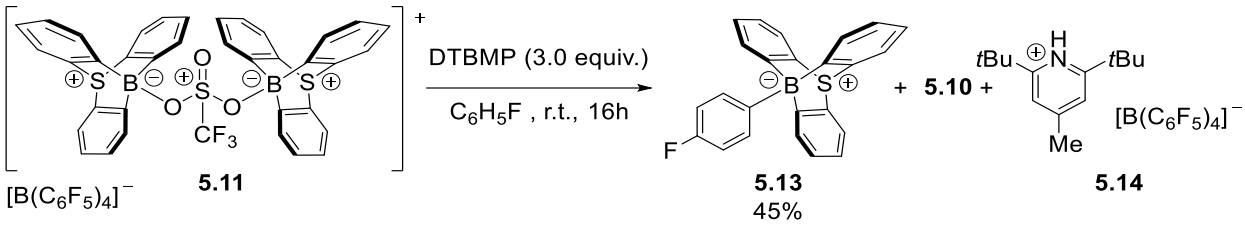


Fig. SV.2. ^{11}B NMR spectra (160 MHz, 25 °C, $CDCl_3$) for the reaction of **5.11** with $CDCl_3$.

Csp^2-H borylation of C_6H_5F:



Tetrakis (pentafluorophenyl) borate bis(10-oxy-9-sulfonium-10-boratriptycene) trifluoromethyloxosulfonium **5.11** (5.0 mg, 3.6 µmol, 1.0 equiv.) and 2,6-di*ter*butyl-4-methyl-pyridine (TBDMP) (2.8 mg, 11 µmol, 3.0 equiv.) were mixed with fluorobenzene (0.5 ml). After stirring at room temperature for 16h, the reaction mixture was evaporated to dryness. The crude was then dissolved in $CDCl_3$ and analyzed by NMR (Fig S3). Integration of the signal corresponding to known 10-(4-fluorophenyl)-9-sulfonium-10-boratriptycene-ate complex **5.13** with respect to the signal corresponding to tetrakis(pentalfuorophenyl)borate ion provides 45% yield.

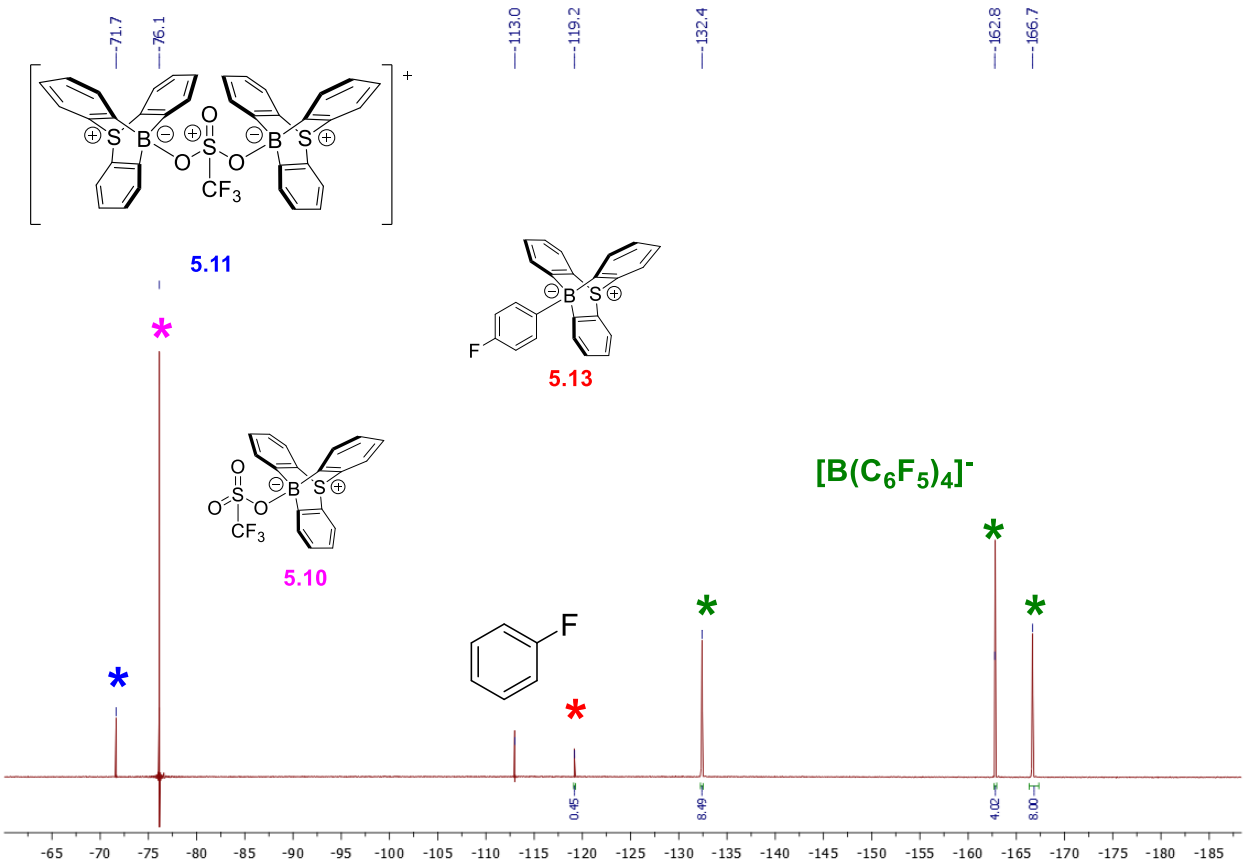
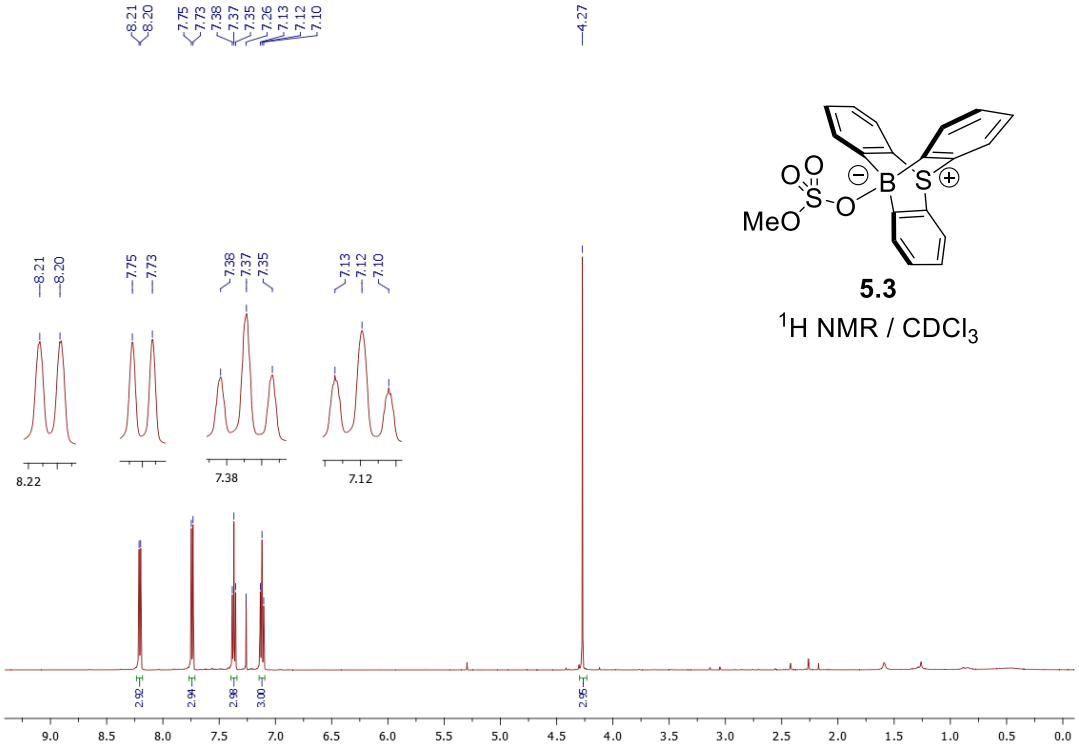


Fig. SV.3. ^{19}F NMR spectra (483 MHz, 25 °C, $CDCl_3$) for the reaction of **5.11** with fluorobenzene.

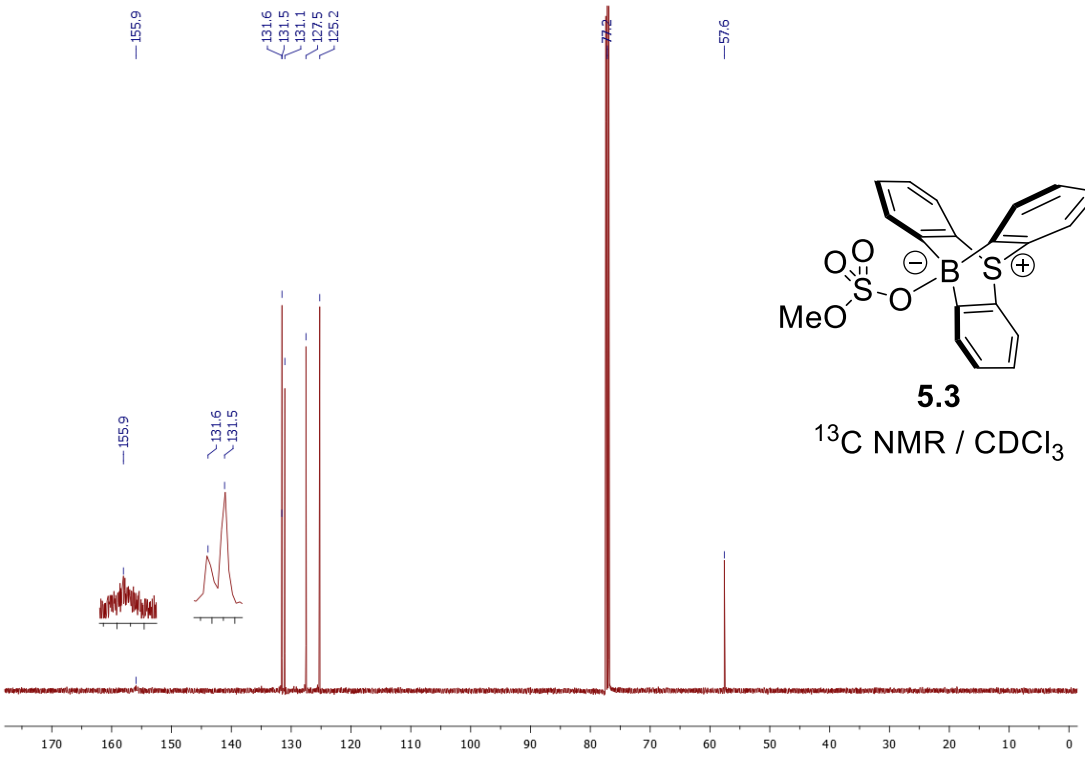
V.3. NMR spectra of synthesized compounds



5.3

^{1}H NMR / $CDCl_3$

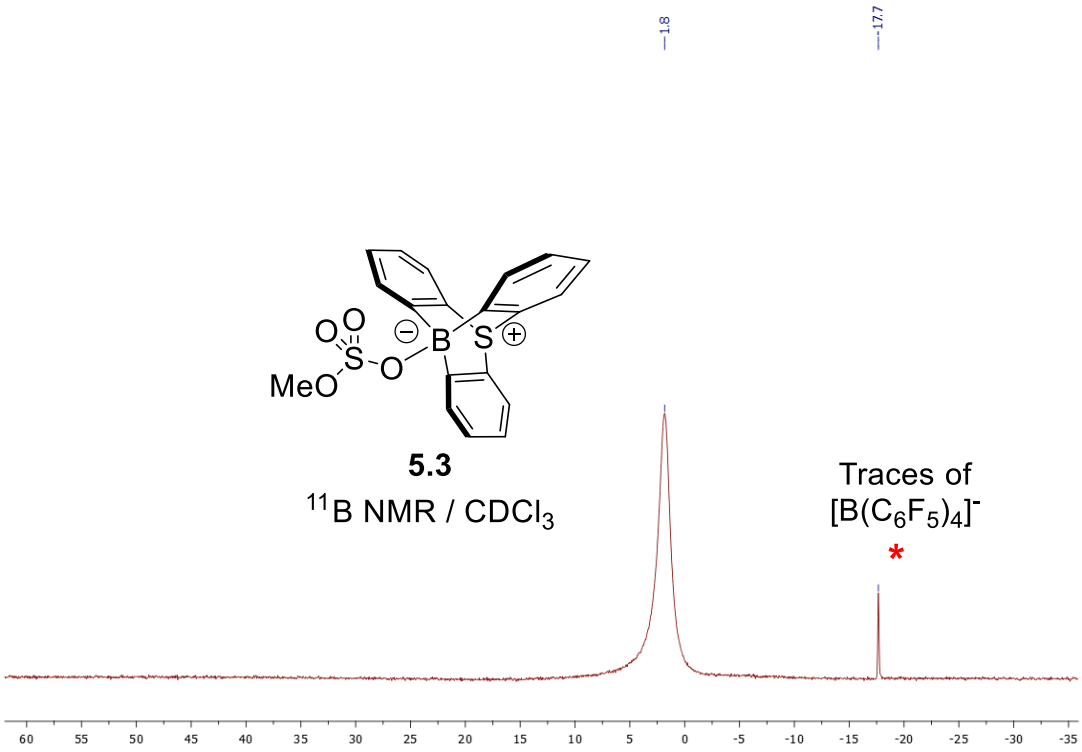
^{1}H NMR (500 MHz, 25°C, $CDCl_3$) of **5.3**



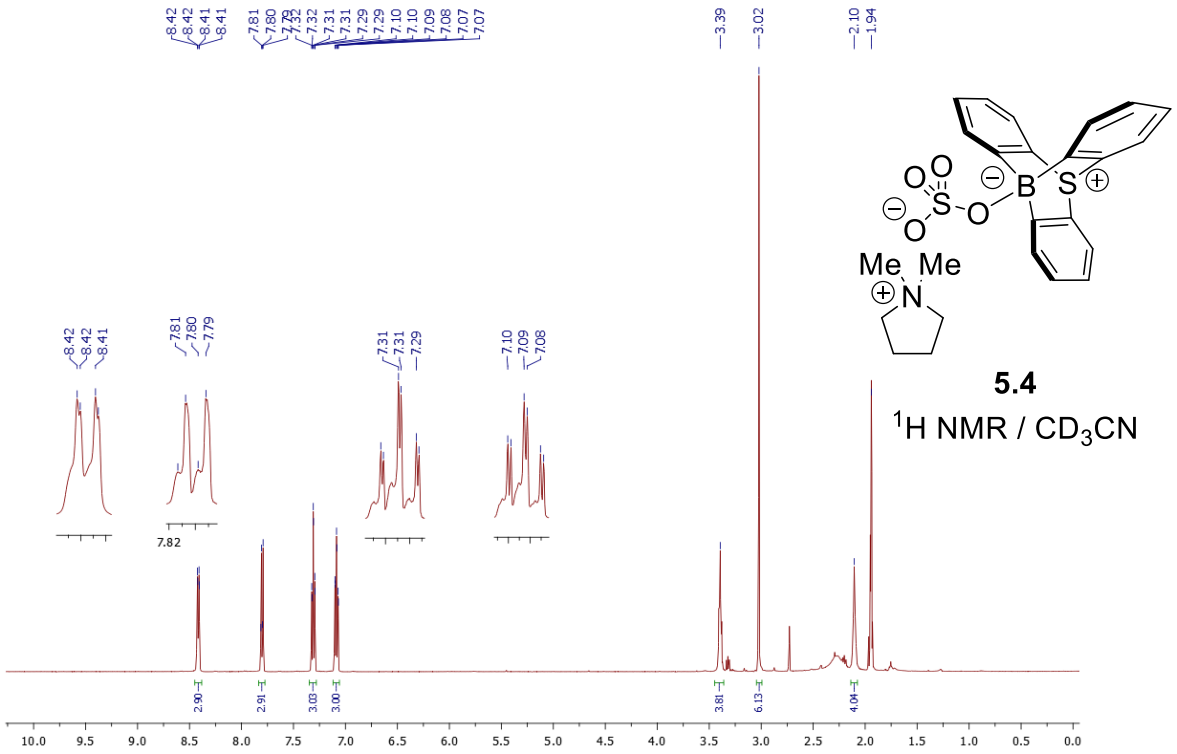
5.3

^{13}C NMR / $CDCl_3$

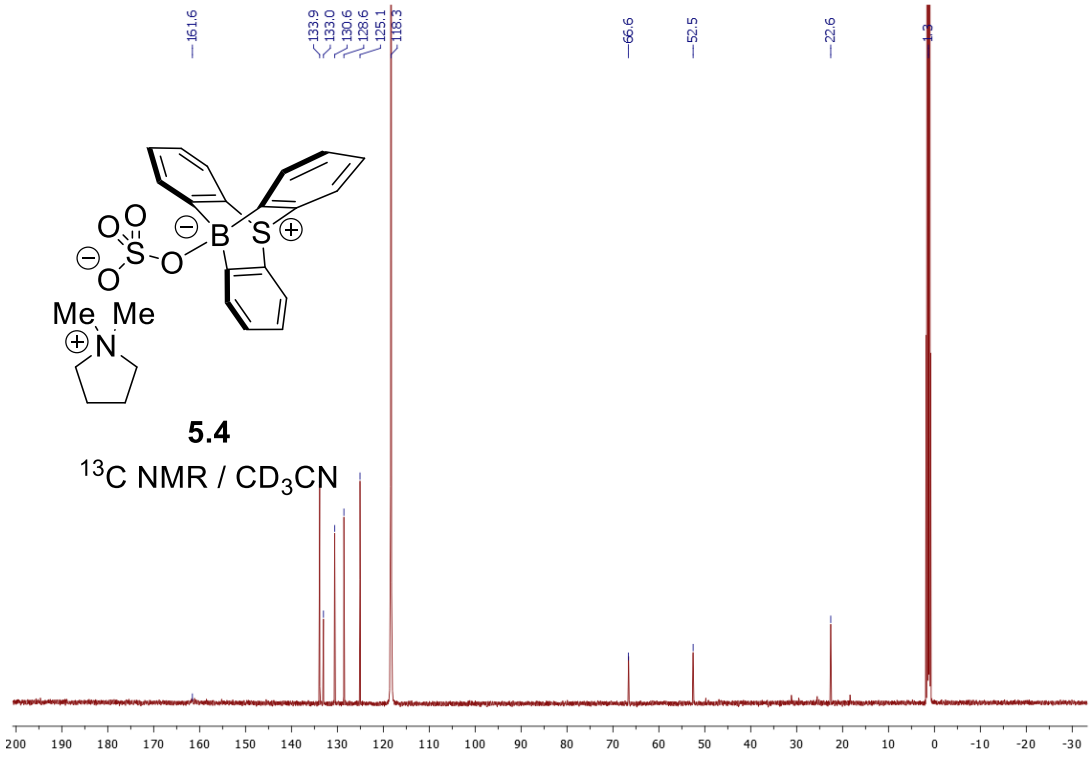
^{13}C NMR (126 MHz, 25°C, $CDCl_3$) of **5.3**



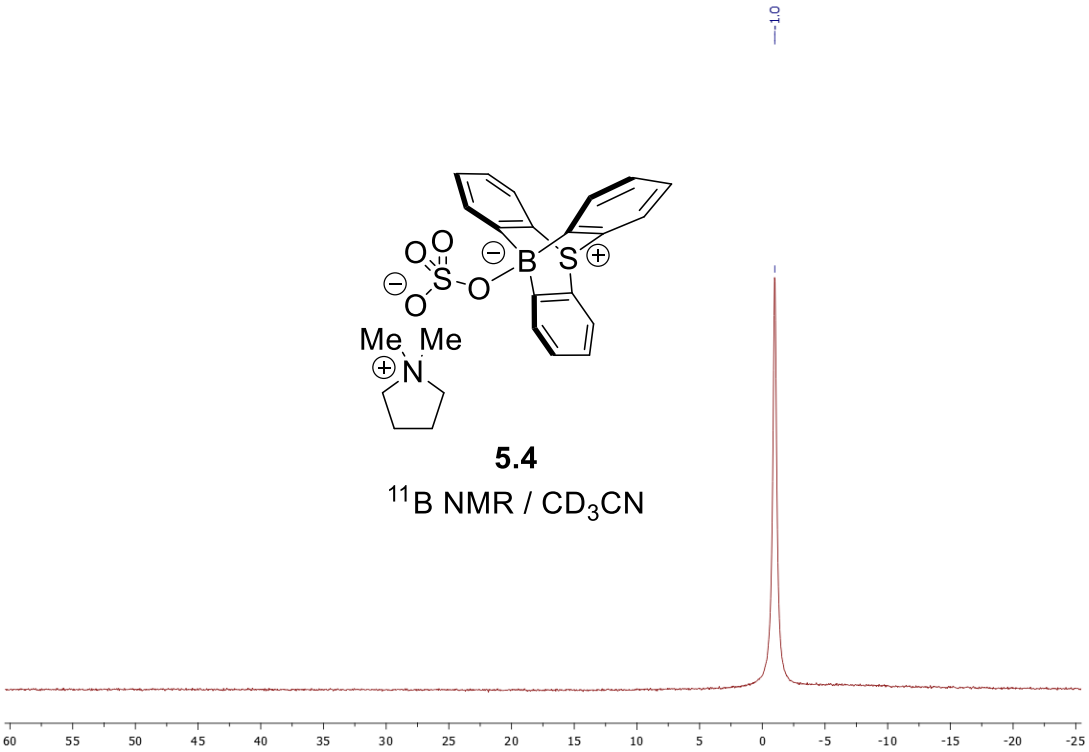
^{11}B NMR (160 MHz, 25°C, $CDCl_3$) of **5.3**



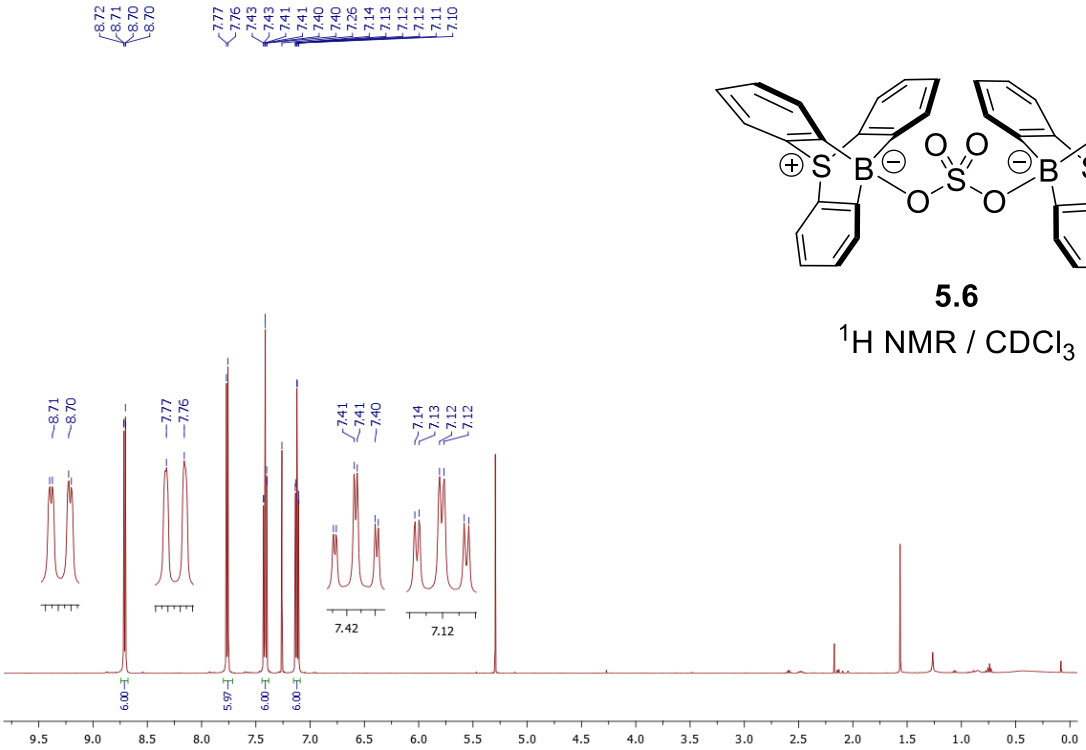
^{1}H NMR (500 MHz, 25°C, CD_3CN) of **5.4**



^{13}C NMR (126 MHz, 25°C, CD_3CN) of **5.4**



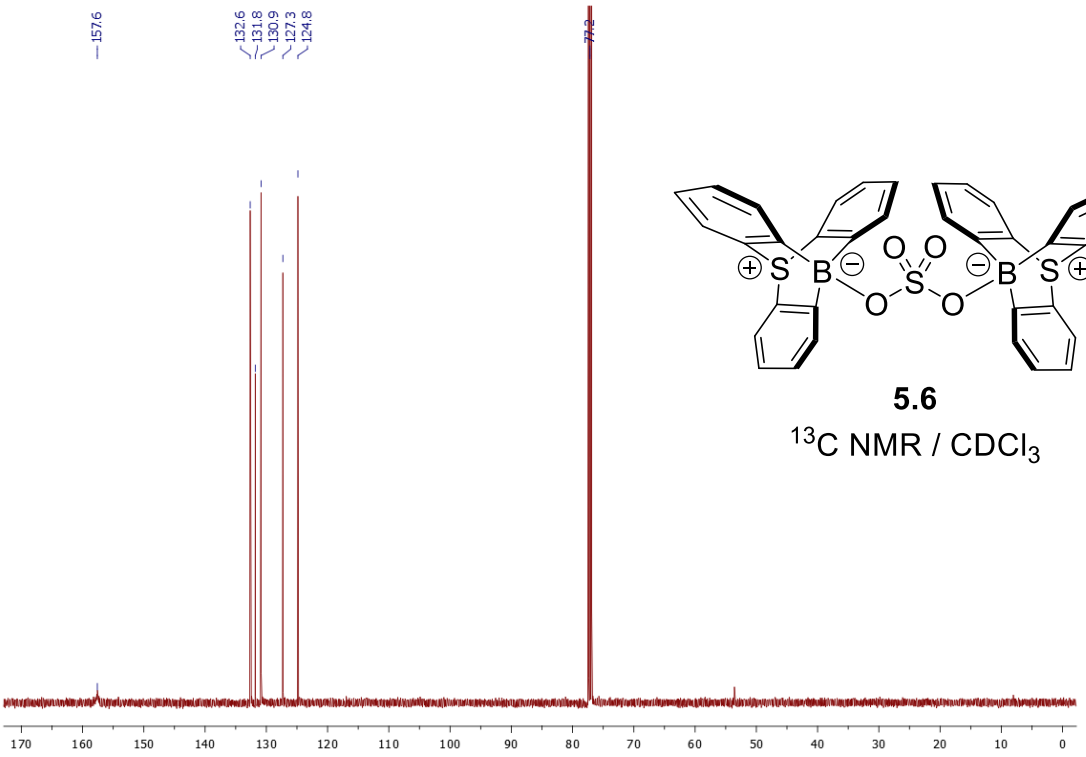
^{11}B NMR (160 MHz, 25°C, CD_3CN) of **5.4**



5.6

^{1}H NMR / $CDCl_3$

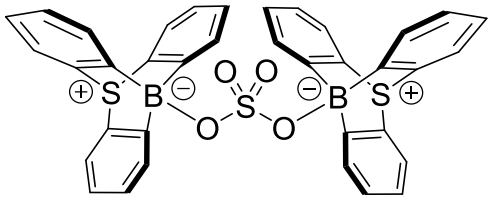
^{1}H NMR (500 MHz, 25°C, $CDCl_3$) of **5.6**



5.6

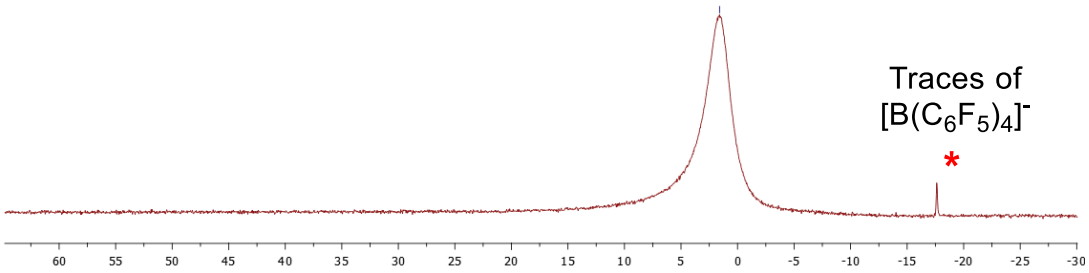
^{13}C NMR / $CDCl_3$

^{13}C NMR (126 MHz, 25°C, $CDCl_3$) of **5.6**

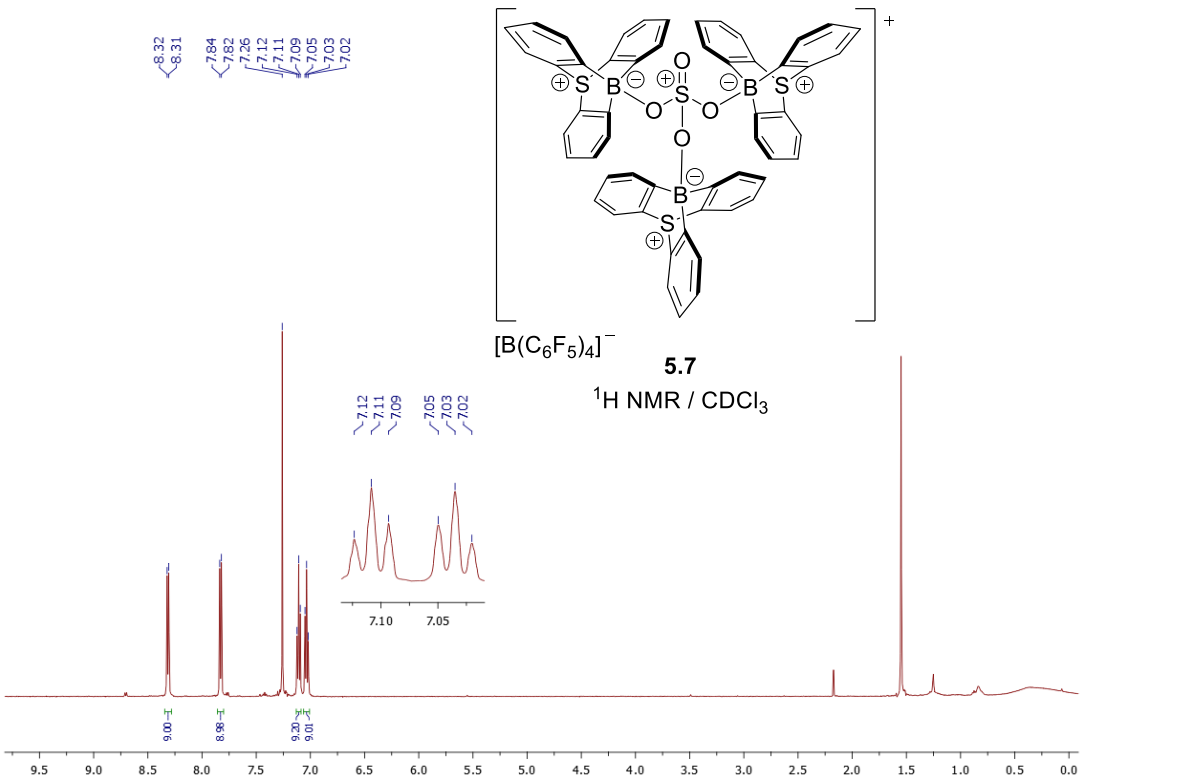


5.6

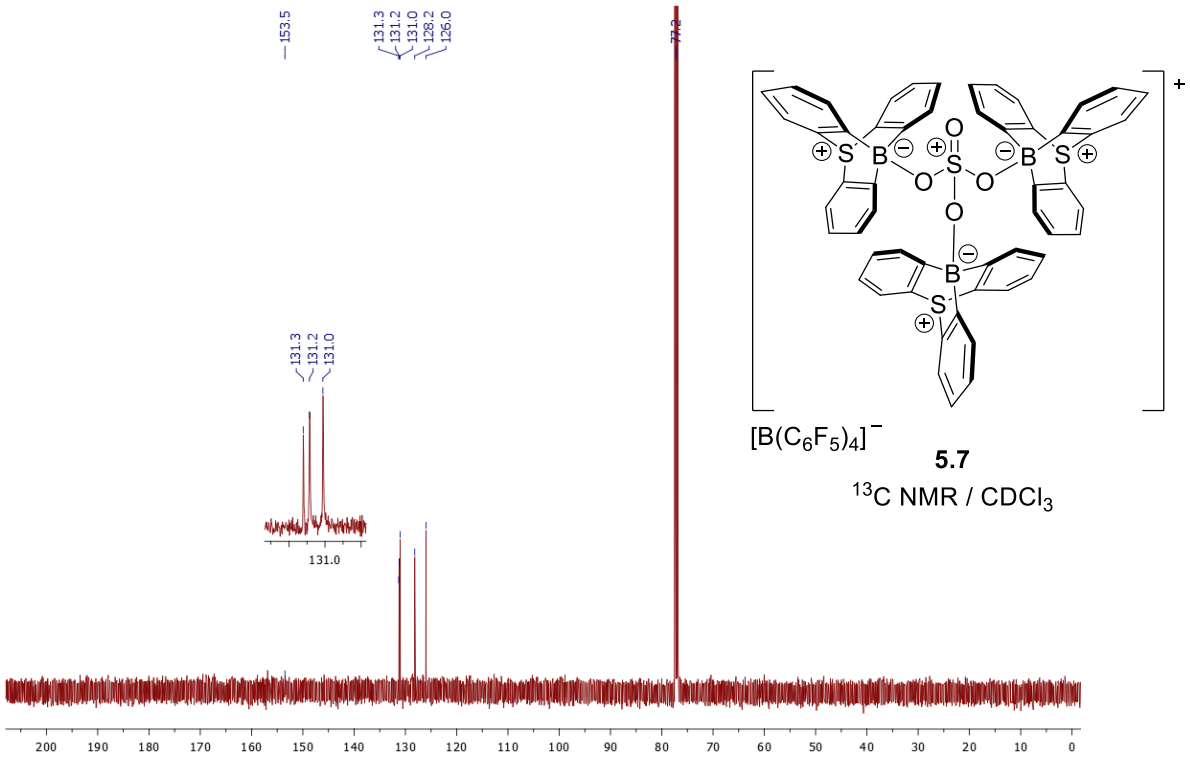
^{11}B NMR / $CDCl_3$



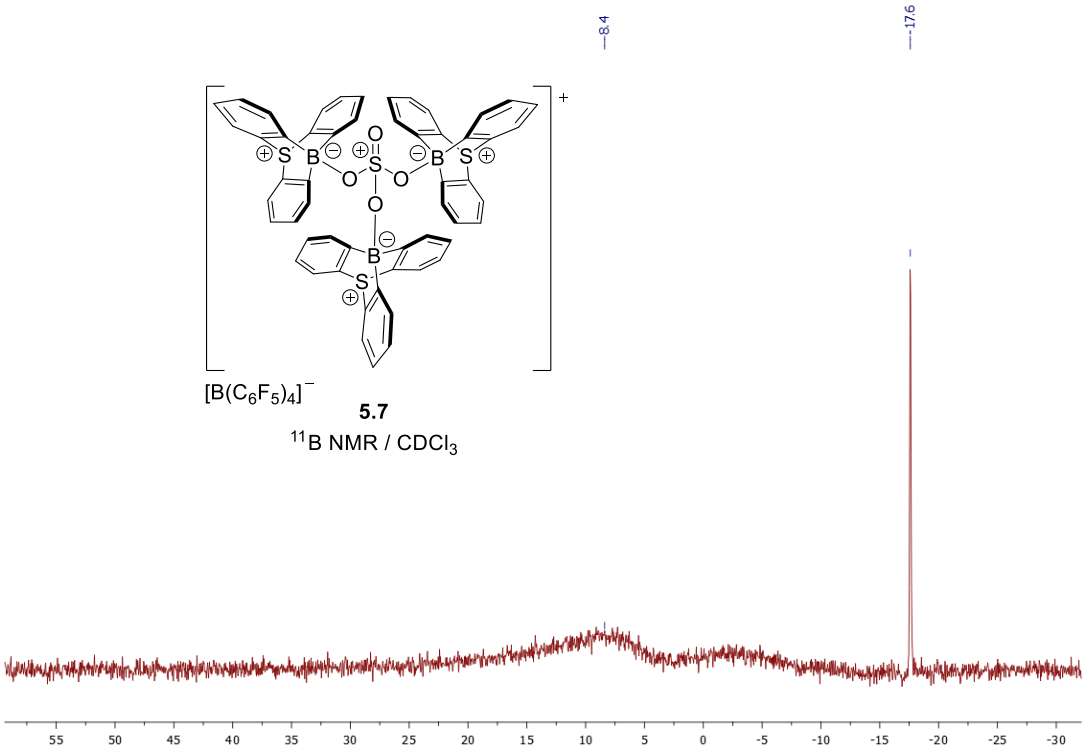
^{11}B NMR (160 MHz, 25°C, $CDCl_3$) of **5.6**



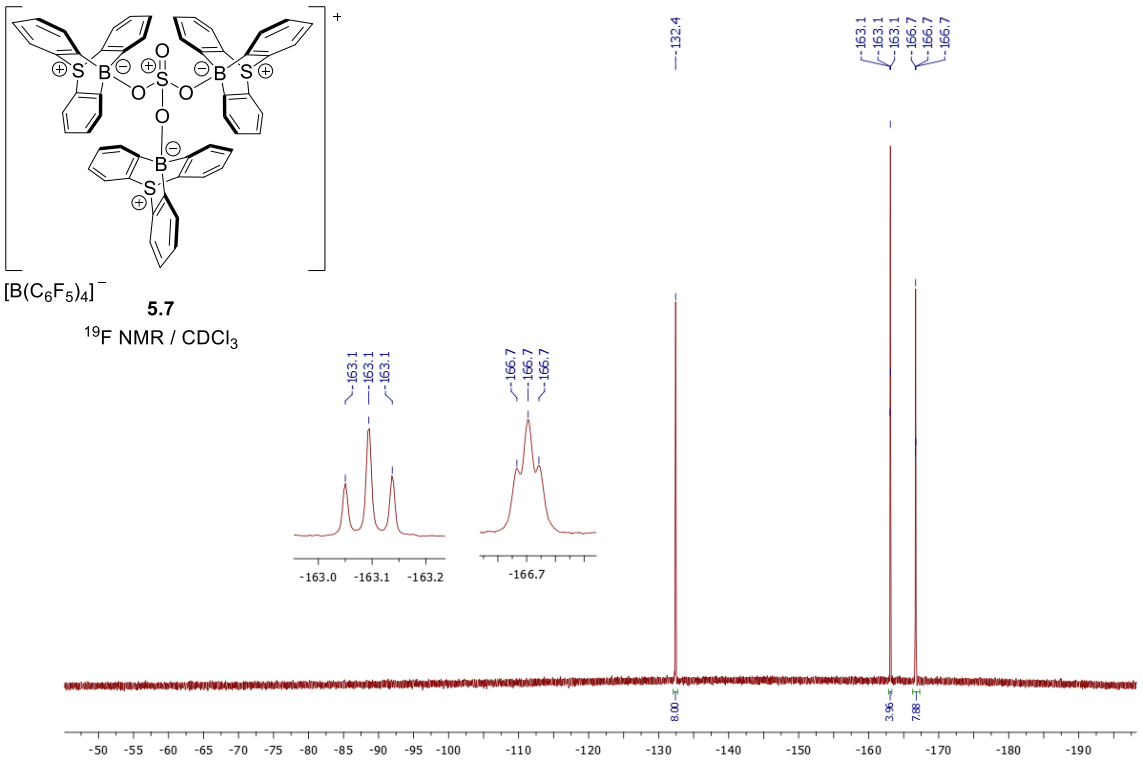
^{1}H NMR (500 MHz, 25°C, $CDCl_3$) of **5.7**



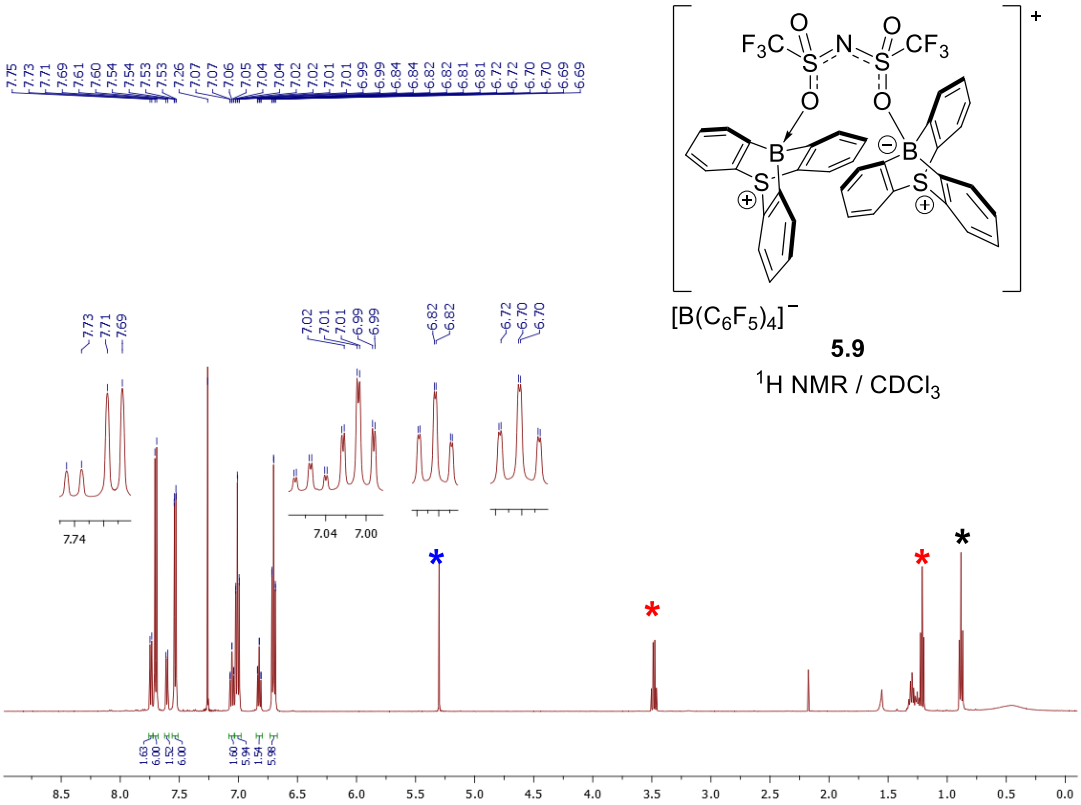
^{13}C NMR (126 MHz, 25°C, $CDCl_3$) of **5.7**



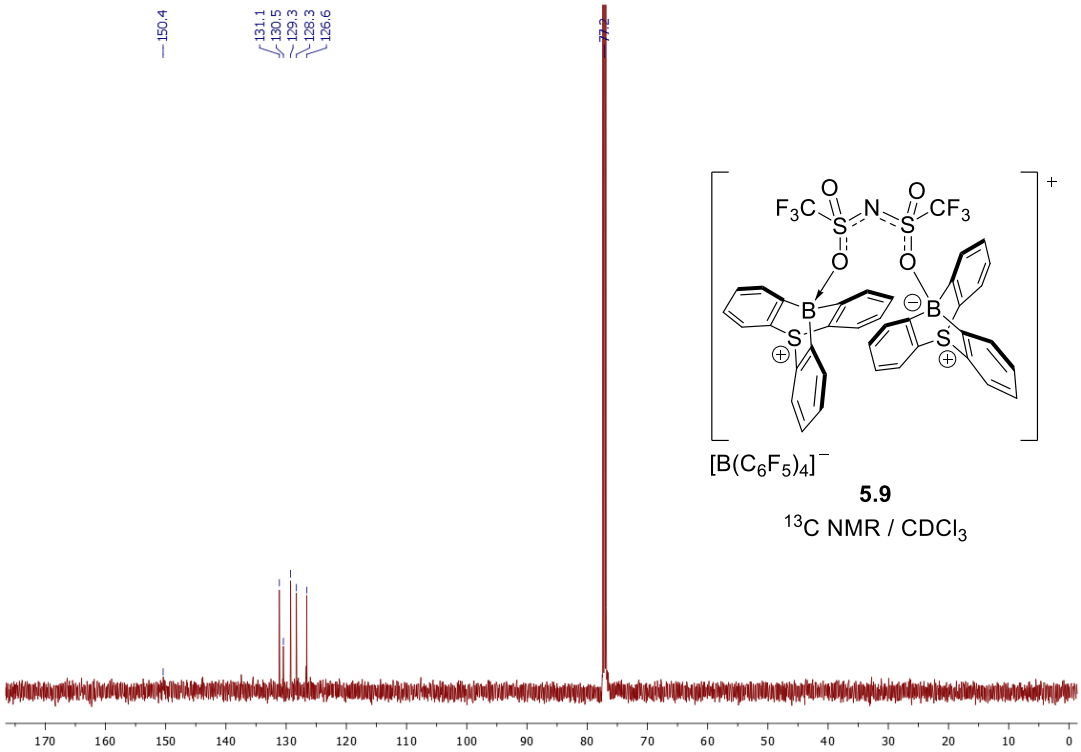
^{11}B NMR (160 MHz, 25°C, $CDCl_3$) of **5.7**



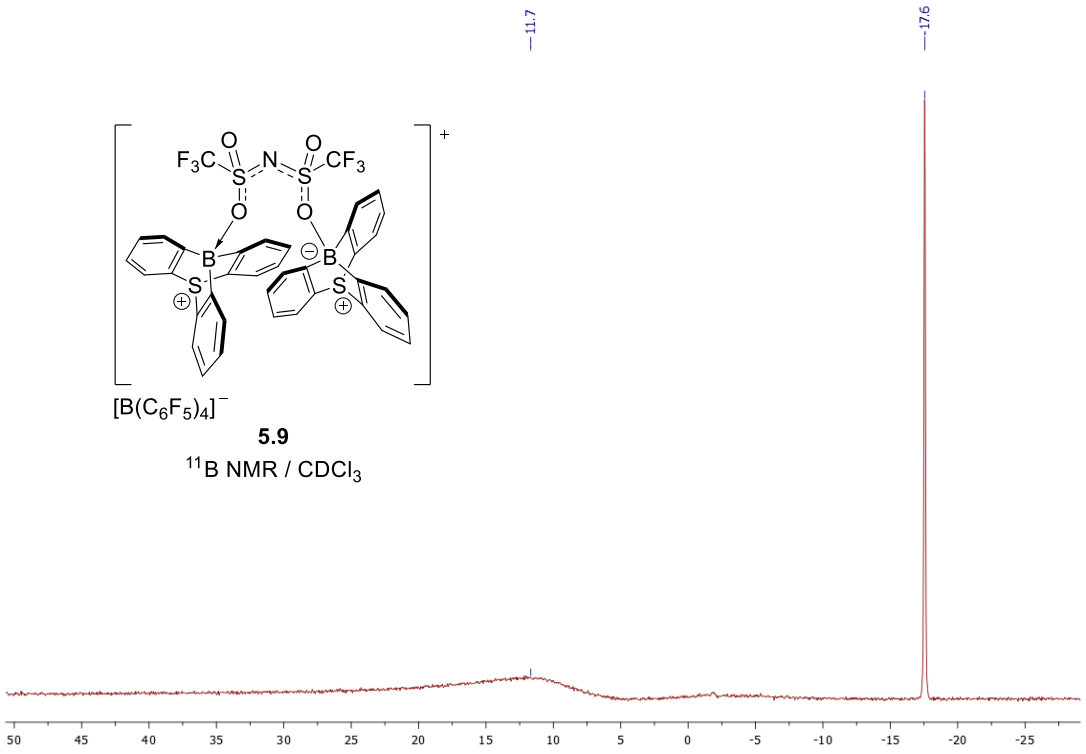
^{19}F NMR (470 MHz, 25°C, $CDCl_3$) of **5.7**



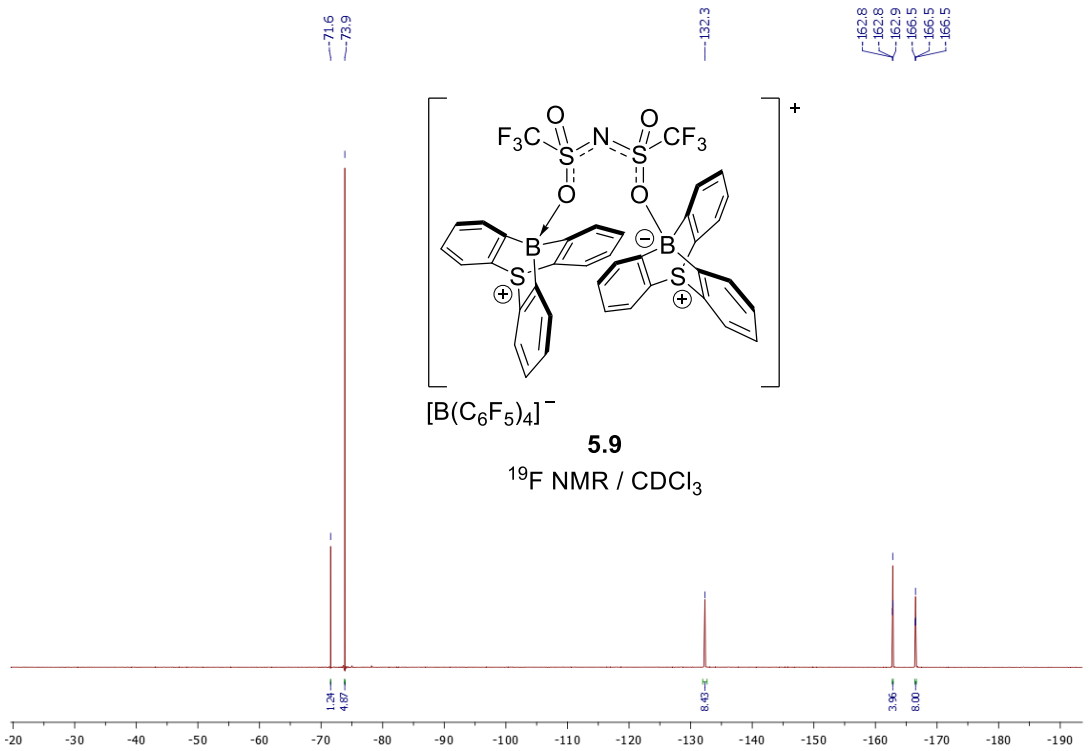
^{1}H NMR (500 MHz, 25°C, $CDCl_3$) of **5.9**, * residual CH_2Cl_2, * residual ethanol and * residual *n*-hexane.



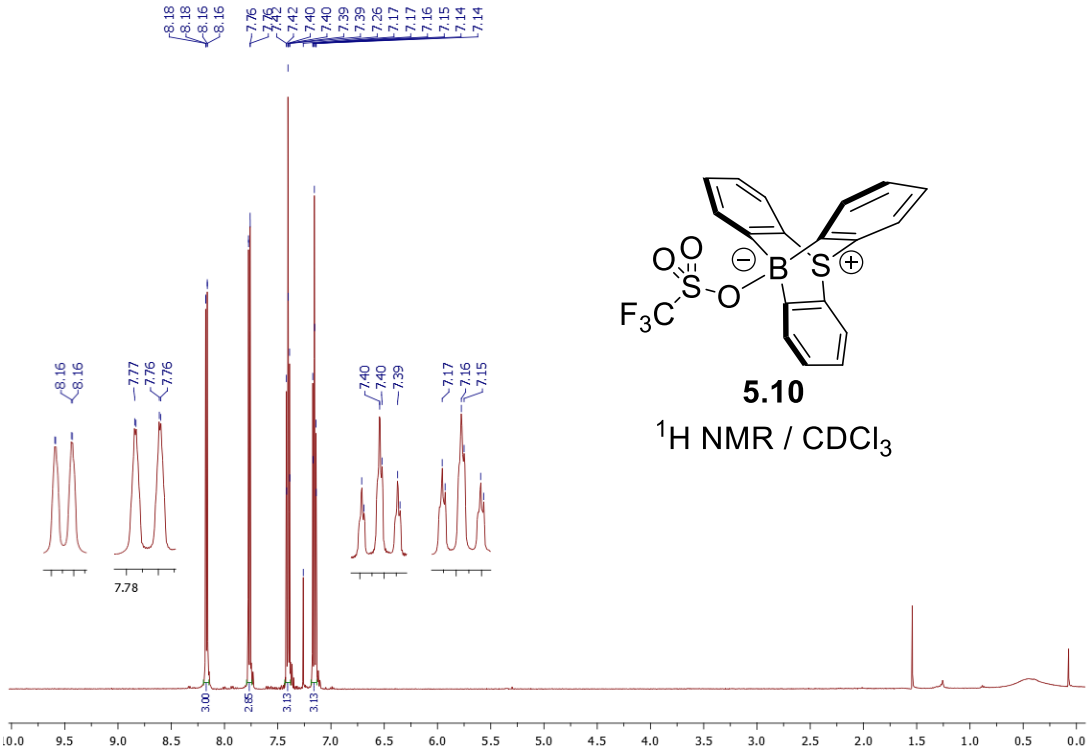
^{13}B NMR (126 MHz, 25°C, $CDCl_3$) of **5.9**



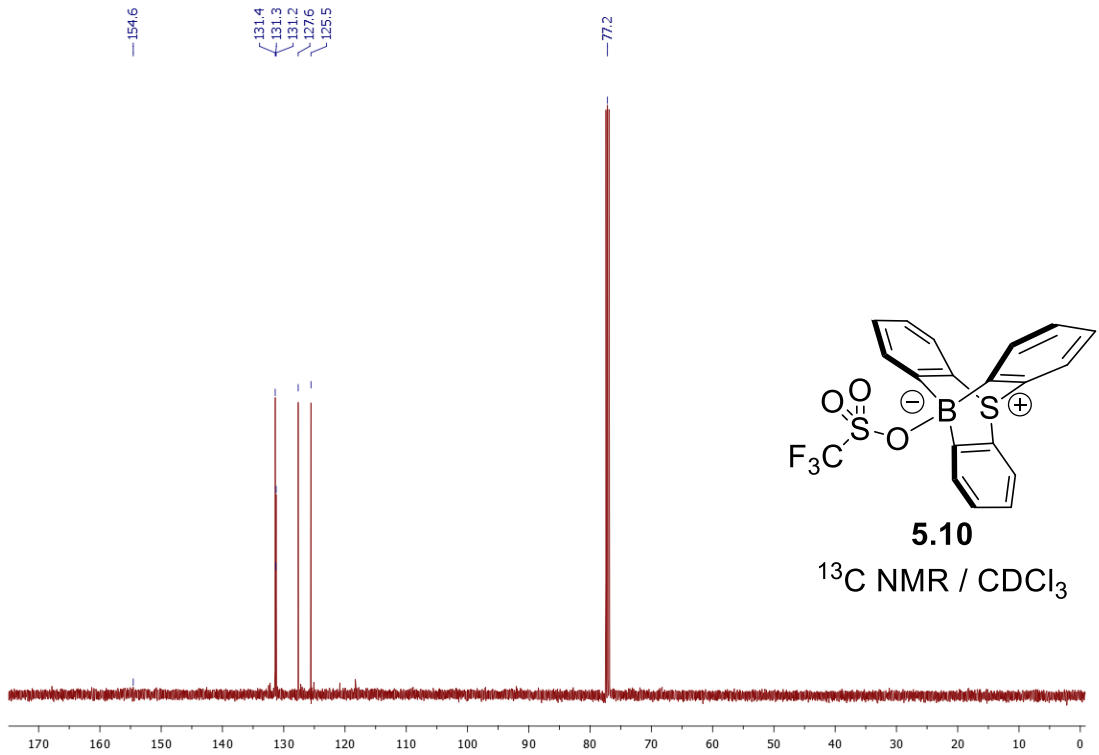
^{11}B NMR (160 MHz, 25°C, $CDCl_3$) of **5.9**



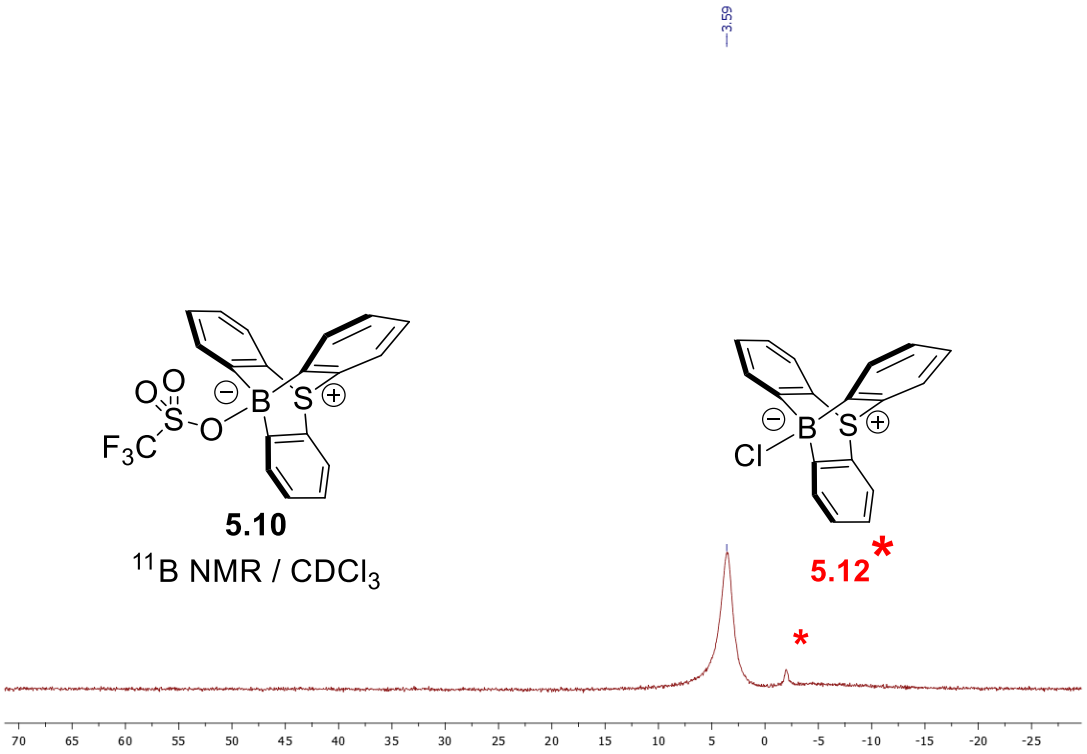
^{19}F NMR (470 MHz, 25°C, $CDCl_3$) of **5.9**



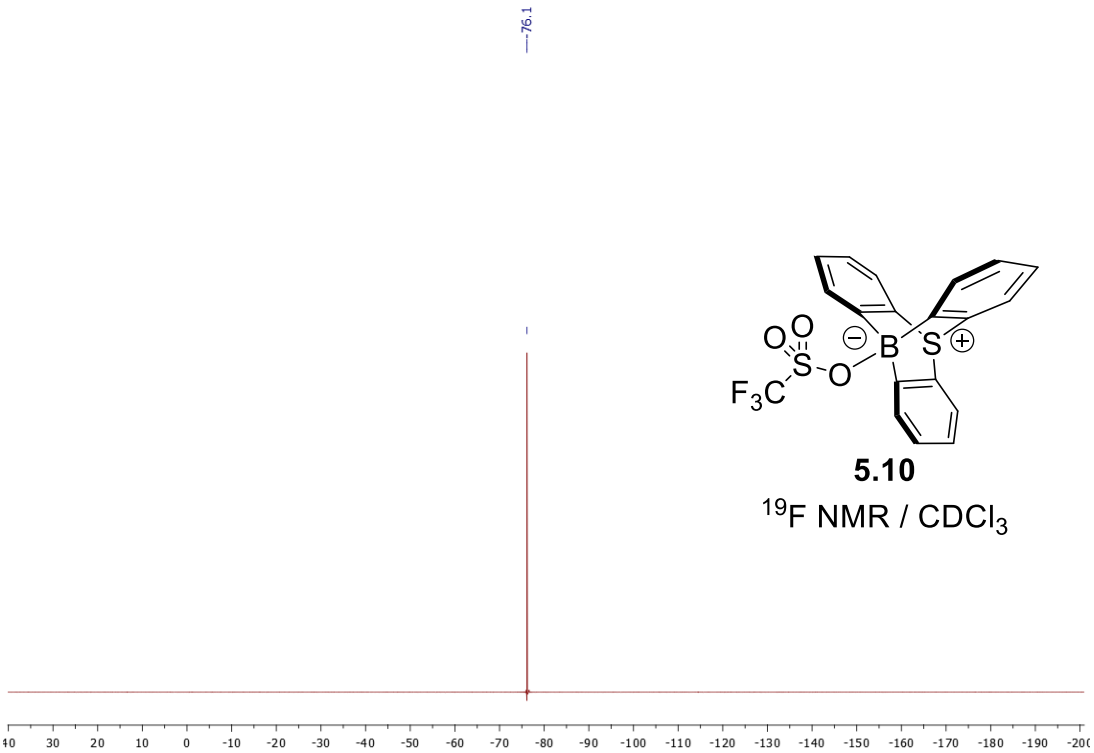
^{1}H NMR (500 MHz, 25°C, $CDCl_3$) of **5.10**



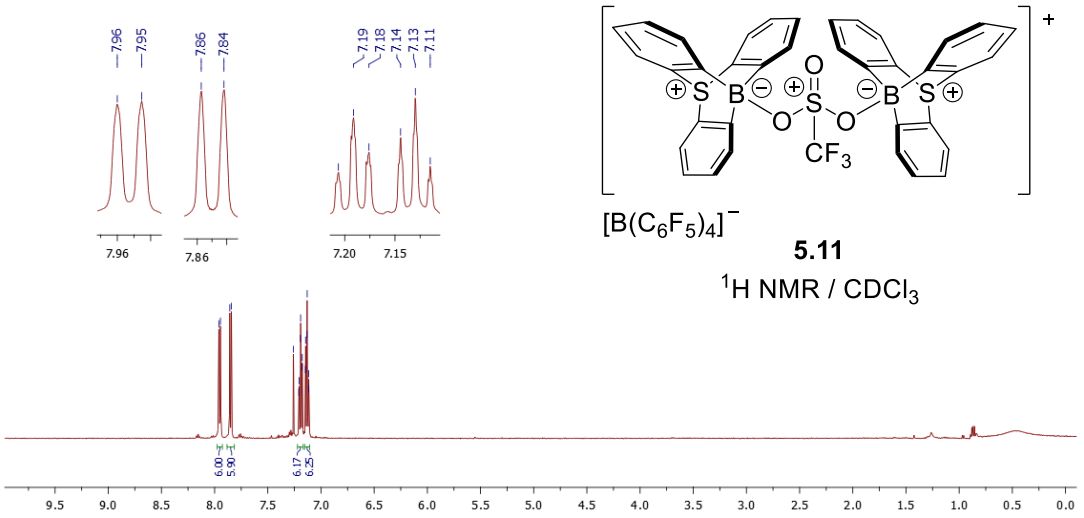
^{13}C NMR (126 MHz, 25°C, $CDCl_3$) of **5.10**



^{11}B NMR (160 MHz, 25°C, $CDCl_3$) of **5.10**



^{19}F NMR (470 MHz, 25°C, $CDCl_3$) of **5.10**

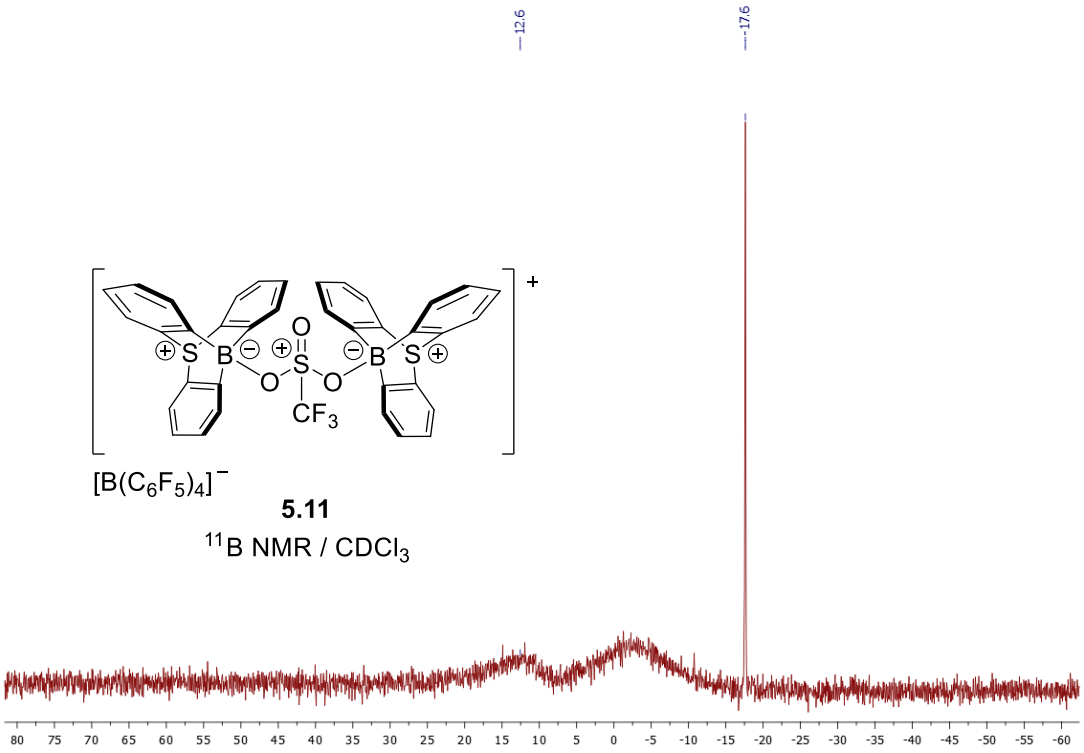


$[B(C_6F_5)_4]^-$

5.11

^{1}H NMR / $CDCl_3$

^{1}H NMR (500 MHz, 25°C, $CDCl_3$) of **5.11**

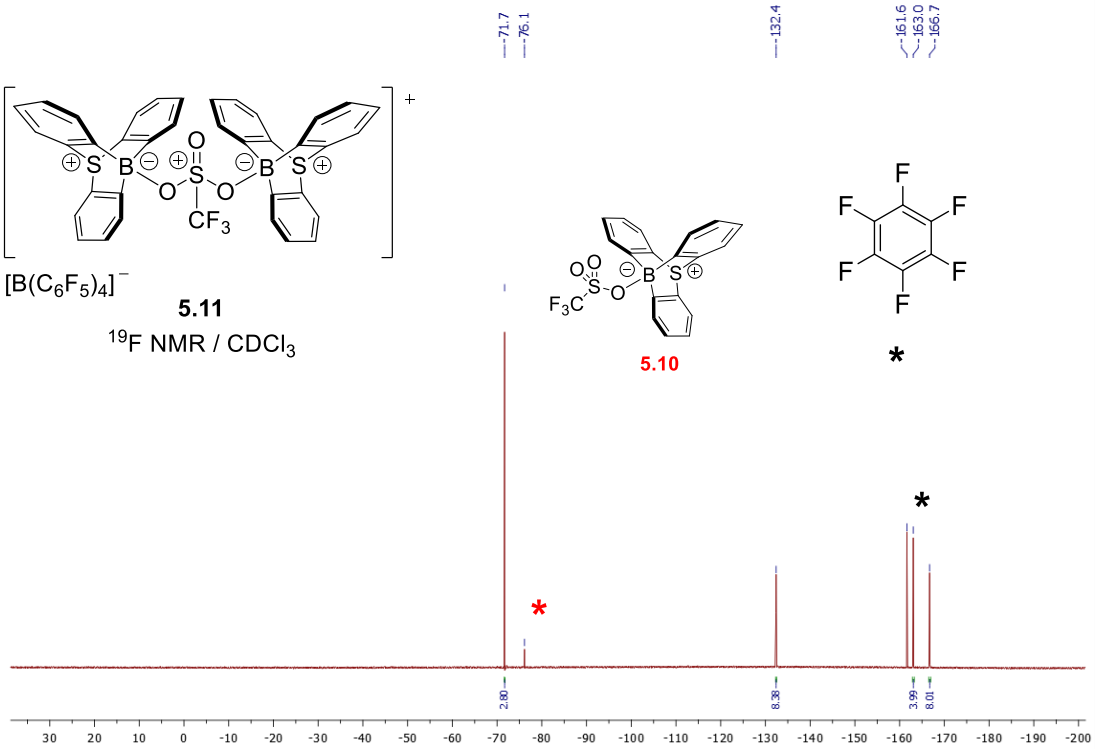


$[B(C_6F_5)_4]^-$

5.11

^{11}B NMR / $CDCl_3$

^{11}B NMR (160 MHz, 25°C, $CDCl_3$) of **5.11**



^{19}B NMR (470 MHz, 25°C, $CDCl_3$) of **5.11**

V.4. Crystallographic parameters

The crystal structures were determined from single-crystal X-ray diffraction data collected using an Oxford Diffraction Gemini Ultra R diffractometer (Cu Kα radiation with multilayer mirror or Mo Kα radiation with graphite monochromator). The data were integrated using the CrysAlisPro software.[S2] The structures were solved by the dual-space algorithm implemented in SHELXT,[S3] and refined by full-matrix least squares on $|F|^2$ using SHELXL-2018/3,[S4] the shelXLe,[S5] and Olex2 software.[S6] Non-hydrogen atoms were refined anisotropically; and hydrogen atoms in most of the cases were located from the difference Fourier map but placed on calculated positions in riding mode with equivalent isotropic temperature factors fixed at 1.2 times U_{eq} of the parent atoms (1.5 times U_{eq} for methyl groups).

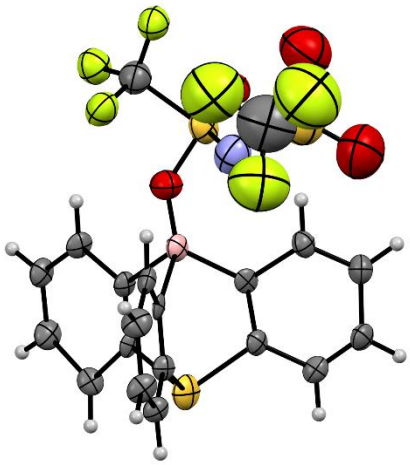


Figure SV.4. Molecular structure of triflimide-9-sulfonium-10-boratriptycene **5.8**. Large thermal factor for the second triflyl moiety result from large vibration of this linear chain during the crystallization process. Despite numerous attempts, better resolution could not be reached.

Table SV.1. Crystal data and structure refinement for compounds **5.3**, **5.4**, **5.6**, **5.7**, **5.9-5.11**.

	5.3	**5.4**	**5.6**	**5.7**
Chemical formula	$C_{19}H_{15}BO_4S_2$	$C_{18}H_{12}BO_4S_2^-\cdot 2(C_6H_{13}ClN^+)\cdot Cl^-\cdot 1.5(H_2O)$	$C_{36}H_{24}B_2O_4S_3\cdot 0.275(CH_4O)$	$C_{54}H_{36}B_3O_4S_4^+\cdot C_{24}BF_{20}^-$
M_r	382.24	698.93	647.17	1588.55
Crystal system, space group	Monoclinic, $P2_1/n$	Monoclinic, $P2_1/c$	Orthorhombic, *Pbca*	Monoclinic, $I2/a$
Temperature (K)	100	295	295	295
a, *b*, *c* (Å)	12.7954 (2), 10.6397 (2), 13.1167 (2)	19.1751 (11), 9.9544 (4), 18.0757 (8)	10.9638 (3), 16.7851 (6), 34.5599 (13)	14.2569 (8), 28.9774 (16), 35.5805 (18)
α, β, γ (°)	90, 98.1201 (16), 90	90, 103.806 (5), 90	90, 90, 90	90, 96.312 (5), 90
V (Å^3)	1767.81 (6)	3350.6 (3)	6360.0 (4)	14610.2 (14)
Z	4	4	8	8
Radiation type	Mo *K*α	Cu *K*α		
μ (mm^{-1})	0.32	3.99	2.46	2.10
Crystal size (mm)	0.62 × 0.47 × 0.22	0.24 × 0.13 × 0.05	0.11 × 0.08 × 0.01	0.19 × 0.13 × 0.02
Absorption correction	Analytical			Gaussian
T_{min}, T_{max}	0.866, 0.950	0.540, 0.832	0.830, 0.969	0.731, 0.960

No. of measured, independent and observed [$I > 2\sigma(I)$] reflections	34962, 9005, 7852	10246, 1996, 1690	12855, 3048, 2265	7833, 7833, 5077
R_{int}	0.025	0.037	0.076	0.037
θ_{max} (°)	37.6	40.1	48.5	40.3
$(\sin\theta/\lambda)_{max}$ (Å^{-1})	0.859	0.418	0.485	0.420
$R[F^2 > 2\sigma(F^2)]$, $wR(F^2)$, S	0.032, 0.091, 1.04	0.056, 0.149, 1.09	0.044, 0.108, 1.03	0.036, 0.076, 0.91
No. of reflections	9005	1996	3048	7833
No. of parameters	296	436	427	1011
No. of restraints	0	118	16	15
H-atom treatment	all H-atom parameters refined		mixed	
$\Delta\rho_{max}$, $\Delta\rho_{min}$ (e·Å^{-3})	0.56, -0.35	0.47, -0.29	0.16, -0.31	0.25, -0.22
CCDC deposition number	2231811	2231812	2231813	2231814

	5.9	**5.10**	**5.11**
Chemical formula	$C_{38}H_{24}B_2F_6NO_4S_4^+ \cdot C_{24}BF_{20}^-$	$C_{19}H_{12}BF_3O_3S_2 \cdot 0.5(C_{10}H_8)$	$C_{37}H_{24}B_2F_3O_3S_3^+ \cdot C_{24}BF_{20}^-$
M_r	1501.49	484.30	1370.41
Crystal system, space group	Triclinic, $P\bar{1}$	Triclinic, $P\bar{1}$	Monoclinic, $C2/c$
Temperature (K)	295	100	100
a, b, c (Å)	10.8756 (3), 16.0788 (7), 17.8559 (6)	10.5834 (5), 11.2499 (5), 11.6588 (5)	20.4619 (15), 17.1882 (13), 17.2961 (11)
α, β, γ (°)	87.689 (3), 82.773 (3), 79.671 (3)	62.209 (4), 65.001 (4), 64.437 (4)	90, 113.274 (8), 90
V (Å^3)	3046.91 (19)	1064.31 (10)	5588.1 (8)
Z	2	2	4
Radiation type	Cu $K\alpha$	Mo $K\alpha$	Cu $K\alpha$
μ (mm^{-1})	2.62	0.30	2.36
Crystal size (mm)	0.18 × 0.12 × 0.04	0.87 × 0.60 × 0.44	0.23 × 0.19 × 0.06
Absorption correction			
T_{min}, T_{max}	0.866, 0.950	0.540, 0.832	0.830, 0.969
No. of measured, independent and observed [$I > 2\sigma(I)$] reflections	34962, 9005, 7852	10246, 1996, 1690	12855, 3048, 2265
R_{int}	0.025	0.037	0.076

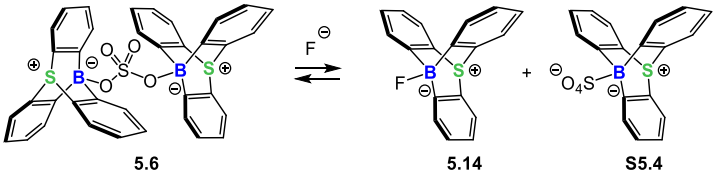
θ_{max} (°)	37.6	40.1	48.5
$(\sin\theta/\lambda)_{max}$ (Å^{-1})	0.859	0.418	0.485
$R[F^2 > 2\sigma(F^2)]$, $wR(F^2)$, S	0.032, 0.091, 1.04	0.056, 0.149, 1.09	0.044, 0.108, 1.03
No. of reflections	9005	1996	3048
No. of parameters	296	436	427
No. of restraints	0	118	16
H-atom treatment	H-atom parameters refined		mixed
$\Delta\rho_{max}$, $\Delta\rho_{min}$ (e·Å^{-3})	0.56, -0.35	0.47, -0.29	0.16, -0.31
CCDC deposition number	2231815	2231816	2231815

V.5. Quantum chemical calculations

Full geometry optimizations and vibrational frequency calculations were performed, using the Gaussian16 package,[S7] at the M06-2X/6-311G(d) level of theory. For each investigated compound, all vibrational frequencies are real, demonstrating that these structures are minima on the potential energy surface. Solvent effects for benzene (C_6H_6) were considered using the Polarizable Continuum Model put into Integral Equation Formalism by Tomasi and coworkers (IEFPCM).[S8] The natural atomic orbital and natural bond orbital analysis was performed using the Gaussian NBO 3.1 program at the M06-2X/6-311G(d) level of theory.[S9]

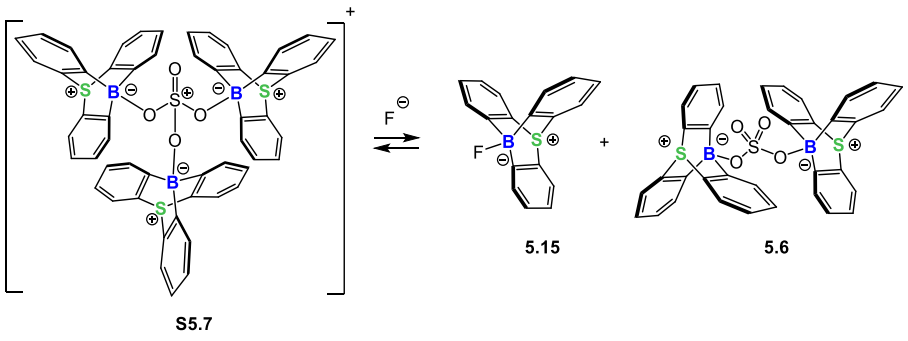
Fluoride anion affinity (FIA) were computed using *non-isodesmic* reactions according to the following equations and tables.

Table SV.2. Association enthalpy of fluoride anion $[F]^-$ with **5.6** at the M06-2X/6-311G(d) level of theory in the gas phase in kJ.mol^{-1}



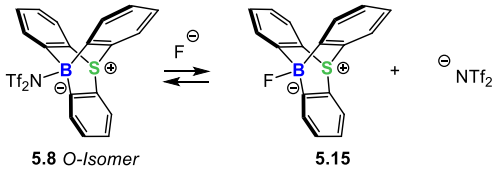
Complexation with F^-	ΔH^0
5.6	-17.1

Table SV.3. Association enthalpy of fluoride anion $[F]^-$ with **S5.7** at the M06-2X/6-311G(d) level of theory in the gas phase in kJ.mol^{-1}



Complexation with F^-	ΔH^0
S5.7	-334.2

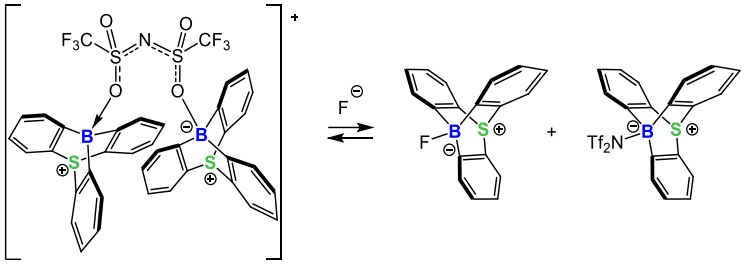
Table SV.4. Association enthalpy of fluoride anion $[F]^-$ with **5.8** at the M06-2X/6-311G(d) level of theory in the gas phase in kJ.mol^{-1}



5.8 *O-Isomer* **5.15**

Complexation with F^-	ΔH^0
5.8	-156.0

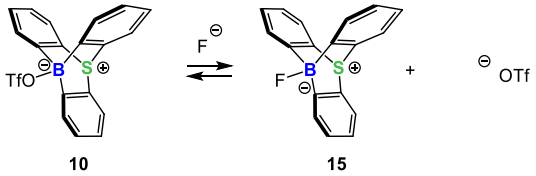
Table SV.5. Association enthalpy of fluoride anion $[F]^-$ with **S5.9a** at the M06-2X/6-311G(d) level of theory in the gas phase in $kJ.mol^{-1}$



S5.9a **5.15** **5.8** *O-isomer*

Complexation with F^-	ΔH^0
5.9a	-371

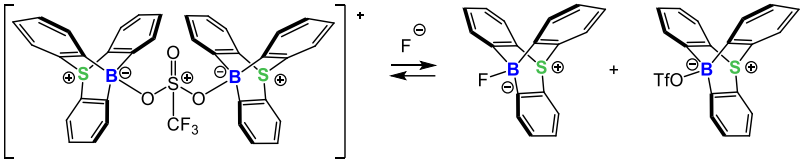
Table SV.6. Association enthalpy of fluoride anion $[F]^-$ with **5.10** at the M06-2X/6-311G(d) level of theory in the gas phase in $kJ.mol^{-1}$



10 **15**

Complexation with F^-	ΔH^0
5.10	-66.9

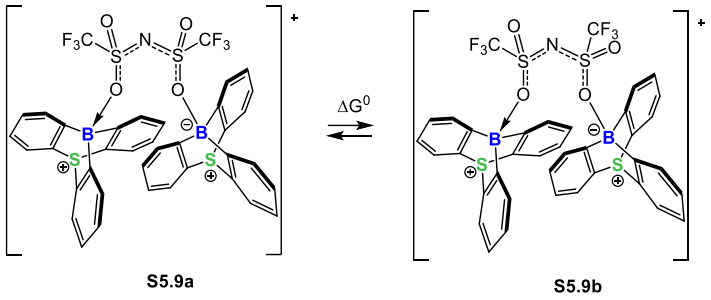
Table SV.7. Association enthalpy of fluoride anion $[F]^-$ with **S5.11** at the M06-2X/6-311G(d) level of theory in the gas phase in $kJ.mol^{-1}$



S5.11 **5.15** **5.10**

Complexation with F^-	ΔH^0
S5.11	-418.7

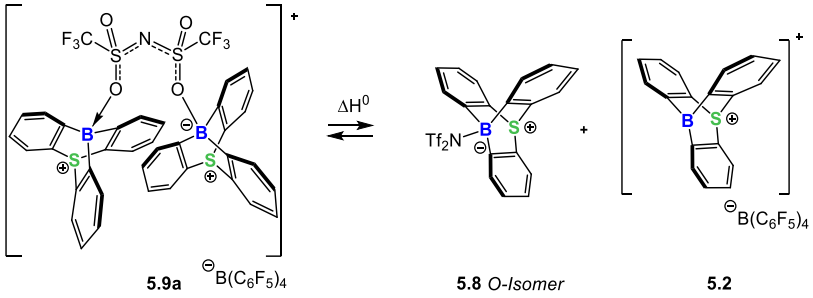
Table SV.8. Equilibrium between **5.9a**-*cisoid* and **5.9b**-*transoid* form of **5.9** at the M06-2X/6-311G(d) level of theory in kJ.mol^{-1}, iefpcm=C_6H_6.



S5.9a S5.9b

ΔG^0
2.1

Table SV.9. Single B-O bond dissociation enthalpy in **5.9a** to form **5.8** and **5.2** at the M06-2X/6-311G(d) level of theory in kJ.mol^{-1}, iefpcm=C_6H_6.



5.9a $^{\ominus}B(C_6F_5)_4$ **5.8** *O-Isomer* **5.2**

Dissociation enthalpy	ΔH^0
5.9a	186

V.6. References

[S5.1] A. Osi, D. Mahaut, N.Tumanov, L. Fusaro, J. Wouters, B. Champagne, A. Chardon, G. Berionni, *Angew. Chem. Int. Ed.* **2022**, *61*, e202112342; *Angew. Chem.* **2022**, *134*, e202112342.

[S5.2] Rigaku Oxford Diffraction. *CrysAlis PRO*, (Rigaku Oxford Diffraction., 2018).

[S5.3] G. M. Sheldrick, *Acta Crystallogr. Sect. A Found. Adv,* **2015**, *71*, 3.

[S5.4] G. M. Sheldrick, *Acta Crystallogr. Sect. C Struct. Chem,* **2015**, *71*, 3.

[S5.5] C. B. Hübschle, G. M. Sheldrick, B. Dittrich, *J. Appl. Crystallogr,* **2011**, *44*, 1281.

[S5.6] O. V. Dolomanov, L. J. Bourhis, R. J. Gildea, J. A. K. Howard, H. Puschmann, *J. Appl.Crystallogr,* **2009**, *42*, 339.

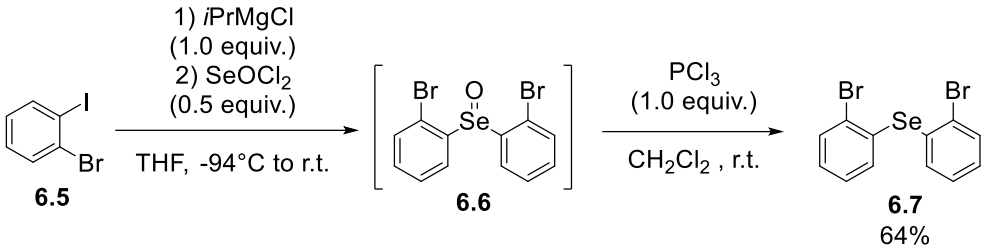
[S5.7] M. J. Frisch, G. W. Trucks, H. B. Schlegel, G. E. Scuseria, M. A. Robb, J. R. Cheeseman, G. Scalmani, V. Barone, G. A. Petersson, H. Nakatsuji, X. Li, M. Caricato, A. V. Marenich, J. Bloino, B. G. Janesko, R. Gomperts, B. Mennucci, H. P. Hratchian, J. V. Ortiz, A. F. Izmaylov, J. L. Sonnenberg, D. Williams-Young, F. Ding, F.Lipparini, F. Egidi, J. Goings, B. Peng, A. Petrone, T. Henderson, D. Ranasinghe, V. G. Zakrzewski, J. Gao, N. Rega, G. Zheng, W. Liang, M. Hada, M. Ehara, K. Toyota, R. Fukuda, J. Hasegawa, M. Ishida, T. Nakajima, Y. Honda, O. Kitao, H. Nakai, T. Vreven, K. Throssell, J. A. Montgomery, J. E. Peralta, Jr., F. Ogliaro, M. J. Bearpark, J. J. Heyd, E. N. Brothers, K. N. Kudin, V. N. Staroverov, T. A. Keith, R. Kobayashi, J. Normand, K. Raghavachari, A. P. Rendell, J. C. Burant, S. S. Iyengar, J. Tomasi, M. Cossi, J. M. Millam, M. Klene, C. Adamo, R. Cammi, J. W. Ochterski, R. L. Martin, K. Morokuma, O. Farkas, J. B. Foresman, D. J. Fox, *Gaussian 16 Rev, A.03* (Gaussian Inc., 2016).

[S5.8] J. Tomasi, B. Mennucci, R. Cammi, *Chem. Rev.* **2005**, *105* (8), 2999.

[S5.9] E. D. Glendening, A. E. Reed, J. E. Carpenter, F. Weinhold, *NBO Version 3.1*, (Gaussian Inc., 2003).

VI.1. Preparation of starting materials.

Bis(2-bromophenyl)selenide **6.7**



6.5 **6.6** **6.7** 64%

Under Ar atmosphere, a solution of *i*PrMgCl (2.0 M in THF, 30.0 ml, 60 mmol, 2.0 equiv.) was added slowly (1ml/min) to a solution of 1-iodo-2-bromobenzene **6.5** (7.7 ml, 60 mmol, 2.0 equiv.) in THF (200 ml) at -94°C (acetone/N_2 bath). The reaction mixture was stirred at -94°C for 1h30 and $SeOCl_2$ (2.05 ml, 30 mmol, 1.0 equiv.) was added dropwise. The mixture was stirred at -94°C for 1h then slowly allowed to warm up for 30 min. The reaction mixture was quenched with saturated NH_4Cl and the aqueous phase was extracted with Et_2O (3 × 50 ml). The combined organic layers were dried with $MgSO_4$ filtered and concentrated under reduced pressure. The crude was poured into hexane and the precipitate was filtrated affording crude bis(2-bromophenyl)selenoxide **6.6** as yellow solid which was used in the next step without further purification. PCl_3 (2.7 ml, 30 mmol, 1.0 equiv) was then added slowly to a solution of crude bis(2-bromophenyl)selenoxide **6.6** in CH_2Cl_2 (100 ml) at 0°C. The reaction was stirred 15 min at room temperature then filtered through a silica gel plug, washed with CH_2Cl_2 and concentrated under reduced pressure. The crude was purified via flash chromatography (hexane, R_f = 0.6) affording pure bis(2-bromophenyl)selenide **6.7** (7.5 g, 0.19 mmol, 64% yield over two steps) as pale yellow solid.

^{1}H NMR (500 MHz, $CDCl_3$): δ (ppm) =

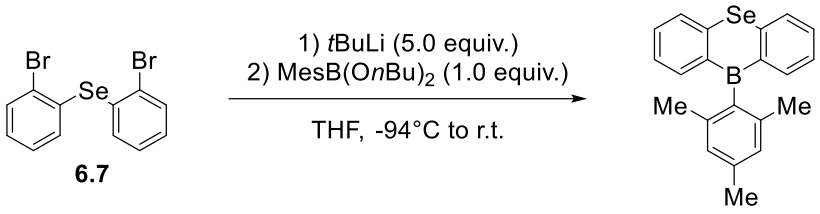
^{13}C NMR (126 MHz, $CDCl_3$): δ (ppm) = 134.4, 133.5, 133.4, 129.3, 128.4, 127.1.

HRMS (MALDI$^-$): *m/z* $[M]^+$ calcd for C12H8Br2Se: 389.8158; found: 389.8164.

IR (neat) cm^{-1}: 1564, 1438, 1420, 1245, 1092, 1007, 760, 724.

mp : 78.6 – 81.3 °C

10-Mesityl-10***H***-9-selena-boraanthracene **6.8**



Under Ar atmosphere, a solution of *t*BuLi (1.9 M in pentane, 5.9 ml, 11 mmol, 2.2 equiv.) was added dropwise to a solution of 2-bromomesitylene (0.86 ml, 5.5 mmol, 1.1 equiv.) in THF (15ml) at -94°C (acetone/N_2 bath). The reaction mixture was stirred at this temperature for 30 min then allowed to warm at room temperature for 30 min. The reaction mixture was cooled at -94°C again, B(O*n*Bu)$_3$ (1.5 ml, 5.5 mmol, 1.1 equiv.) was added dropwise and the reaction mixture was subsequently allowed to warm at room temperature and stirred for 16h, forming crude MesB(O*n*Bu)$_2$. Then, a solution of *t*BuLi (1.9 M in pentane, 13.5 ml, 26 mmol, 5.0 equiv.) was added slowly to a solution of bis(2-bromophenyl)selenide **6.7** (2.0 g, 5.1 mmol, 1.0 equiv.) in THF (20ml) at -94°C. The reaction mixture was stirred 30 min at -94°C then allowed to warm at room temperature for 30 min. The crude MesB(O*n*Bu)$_2$ was added and the reaction mixture was stirred 16h at room temperature. The reaction was quenched with saturated NH_4Cl, the aquous phase was extracted with Et_2O (3 × 20 ml), the combined organic phases were dried with $MgSO_4$ and concentrated under reduced pressure. The crude was poured into *i*PrOH, the precipitate was filtered and washed with *i*PrOH affording pure 10-mesityl-10***H***-9-selena-boraanthracene **6.8** (280 mg, 0.78 mmol, 15% yield) as yellow powder. Single crystals suitable for X-ray diffraction analysis were obtained by slow evaporation of a saturated CH_2Cl_2 solution.

^{1}H NMR (500 MHz, $CDCl_3$): δ (ppm) = 7.88 (dd, *J* = 7.7, 1.6 Hz, 2H), 7.83 (dd, *J* = 8.0, 1.0 Hz, 2H), 7.54 (td, *J* = 7.9, 1.6 Hz, 2H), 7.28 (td, *J* = 7.4, 1.1 Hz, 2H), 6.93 (s, 2H), 2.40 (s, 3H), 1.92 (s, 6H).

^{13}C NMR (126 MHz, $CDCl_3$): δ (ppm) = 144.5 (Cq), 141.4, 138.5 (Cq), 136.7 (Cq), 132.2, 127.4, 127.0, 125.3, 22.8 (CH_3), 21.3 (CH_3).

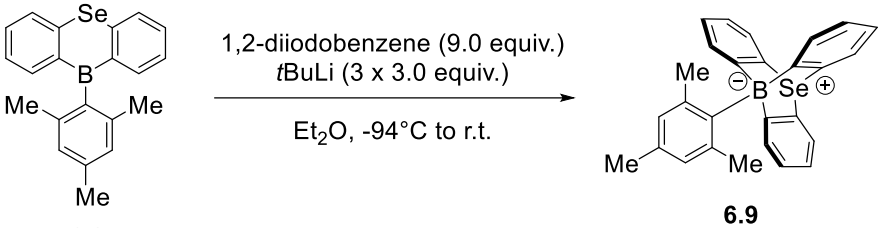
^{11}B NMR (160 MHz, $CDCl_3$): δ (ppm) = 60.7

HRMS (MALDI$^-$): *m*/*z* $[M]^+$ calcd for $C_{21}H_{19}BSe$: 362.0745; found: 362.0736.

IR (neat) cm^{-1}: 2966, 2903, 1604, 1578, 1551, 1452, 1416, 1294, 1258, 1223, 1160, 1106, 1036, 867, 773, 733.

mp: 175.7 – 178.0 °C

10-Mesityl-9-selenenium-10-boratriptycene-ate complex **6.9**



6.8 **6.9** 68%

Under Ar atmosphere, a solution of *t*BuLi (1.9 M in pentane, 0.81 ml, 1.5 mmol, 3.0 equiv.) was added dropwise to a solution of 10-mesityl-10***H***-9-selena-boraanthracene **6.8** (200 mg, 0.55 mmol, 1.0 equiv.) and 1,2-diiodobenzene (0.66 ml, 5.0 mmol, 9.0 equiv.) in Et_2O (15ml) at -94°C. The reaction was subsequently allowed to warm at room temperature. After 9h, the reaction was cooled again at -94°C and a solution of *t*BuLi (1.9 M in pentane, 0.81 ml, 1.5 mmol, 3.0 equiv.) was added dropwise. The reaction was subsequently allowed to warm at room temperature. After another 9h, the reaction was cooled again at -94°C and a solution of *t*BuLi (1.9 M in pentane, 0.81 ml, 1.5 mmol, 3.0 equiv.) was added dropwise for the third time. The reaction was subsequently allowed to warm at room temperature and stirred for another 9h. The crude was then evaporated to dryness, diluted with CH_2Cl_2 (30 ml) and water (30 ml). The aqueous phase was extracted with CH_2Cl_2 (3 × 20 ml). The combined organic layers were washed with brine, dried with $MgSO_4$ then concentrated under reduced pressure. The crude was poured into Et_2O, the precipitate was filtered and thoroughly washed with Et_2O and hexane, affording 10-mesityl-9-selenenium-10-boratriptycene-ate complex **6.9** (164 mg, 0.37 mmol, 68 % yield.) as a pale yellow powder. Single

crystals suitable for X-ray diffraction analysis were obtained by slow evaporation of a saturated CH_2Cl_2 solution.

^{1}H NMR (500 MHz, $CDCl_3$): δ (ppm) = 7.73 (d, *J* = 7.1 Hz, 3H), 7.68 (dd, *J* = 7.6, 1.0 Hz, 3H), 7.17 (td, *J* = 7.3, 1.2 Hz, 3H), 7.05 (s, 2H), 6.98 (td, *J* = 7.4, 1.5 Hz, 3H), 2.44 (s, 3H), 2.00 (s, 6H).

^{13}C NMR (126 MHz, $CDCl_3$): δ (ppm) = 143.7 (Cq), 137.2 (Cq), 136.7, 133.7 (Cq), 129.6, 128.3, 127.6, 124.1, 27.1 (CH_3), 21.1 (CH_3).

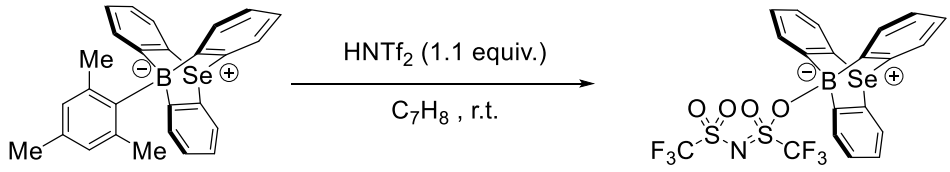
^{11}B NMR (160 MHz, $CDCl_3$): δ (ppm) = -6.9

HRMS (MALDI$^-$): *m*/*z* $[M+DCTB]^+$ calcd for $C_{44}H_{41}BN_2Se$: 688.2528; found: 688.2544.

IR (neat) cm^{-1}: 3042, 2989, 2917, 1600, 1425, 1371, 1294, 1254, 1146, 998, 854, 746, 611.

mp: 265.3 – 268.0

10-Triflimidate-9-selenenium-10-boratriptycene-ate complex **6.10**



6.9 **6.10** 52%

Under glovebox conditions, triflimidic acid (14 mg, 0.050 mmol, 1.1 equiv.) was added to a suspension of 10-mesityl-9-selenenium-10-boratriptycene-ate complex **6.9** (20mg, 0.046 mmol, 1.0 equiv.) in toluene (2.0 ml) at room temperature. The reaction was stirred for 10 minutes then put out of the glovebox, evaporated to dryness then purified by flash chromatography (70:30 Hexane/DCM, R_f : 0.5 in 50:50 Hexane/DCM) affording 10-triflimidate-9-selenenium-10-boratriptycene-ate complex **6.10** (14 mg, 0.024 mmol, 52% yield) as white powder. Single crystals suitable for X-ray diffraction analysis were obtained by slow evaporation of a saturated CH_2Cl_2 solution.

^{1}H NMR (500 MHz, $CDCl_3$): δ (ppm) = 8.11 (dd, *J* = 7.4, 0.8 Hz, 3H), 7.77 (d, *J* = 7.8 Hz, 3H), 7.44 (td, *J* = 7.4, 0.9 Hz, 3H), 7.17 (td, *J* = 7.6, 1.4 Hz, 3H).

^{13}C NMR (126 MHz, $CDCl_3$): δ (ppm) = 148.9 (C-B), 133.1 (Cq), 131.5, 131.4, 128.2, 126.2.

^{11}B NMR (160 MHz, $CDCl_3$): δ (ppm) = 8.8

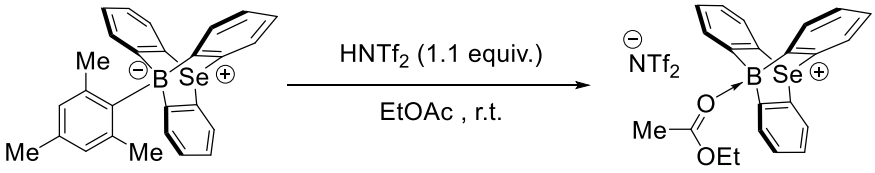
^{19}F NMR (483 MHz, $CDCl_3$): δ (ppm) = -74.9, -78.2

HRMS (MALDI$^-$): *m*/*z* : could not be determined due to decomposition during injection.

IR (neat) cm^{-1}: 3074, 1967, 1427, 1365, 1328, 1184, 1130, 1101, 1044, 833, 792, 743.

mp: 243.2 – 245.6 °C

Triflimidate-9-selenenium-10-boratriptycene-ethyl acetate Lewis adduct **6.11**



6.9 **6.11** 71%

Under glovebox conditions, triflimidic acid (14 mg, 0.050 mmol, 1.1 equiv.) was added to a suspension of 10-mesityl-9-selenenium-10-boratriptycene-ate complex **6.9** (20mg, 0.046 mmol, 1.0 equiv.) in EtOAc (2.0ml) at room temperature. The reaction was stirred for 10 minutes then put out of the glovebox and evaporated to dryness. The solid was washed with cold CH_2Cl_2 and dried under dynamic vacuum affording triflimidate-9-selenenium-10-boratriptycene-ethyl acetate Lewis adduct **6.11** (23 mg, 0.033 mmol, 71% yield) as white solid. Traces of 10-triflimidate-9-selenenium-10-boratriptycene-ate complex **6.10** remained impossible to remove. Single crystals suitable for X-ray diffraction analysis were obtained by slow evaporation of a saturated CH_2Cl_2 solution.

^{1}H NMR (500 MHz, CD_2Cl_2): δ (ppm) = 7.96 (d, *J* = 7.8 Hz, 3H), 7.59 (d, *J* = 7.3 Hz, 3H), 7.48 (t, *J* = 7.4 Hz, 3H), 7.28 (t, *J* = 7.6 Hz, 3H), 5.21 (br, 2H), 2.78 (br, 3H), 1.77 (br, 3H).

^{13}C NMR (126 MHz, CD_2Cl_2): δ (ppm) = 187.9 (C=O), 134.4 (Cq), 131.5, 129.9, 128.8, 127.0, 60.7 (CH_2), 21.2 (CH_3), 14.4 (CH_3).

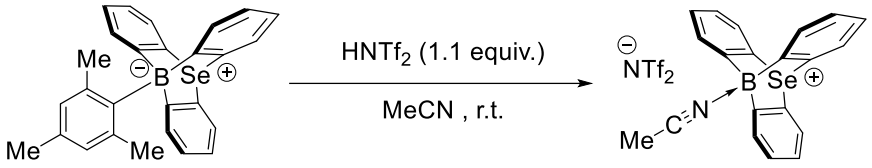
^{11}B NMR (160 MHz, CD_2Cl_2): δ (ppm) = 5.0

^{19}F NMR (483 MHz, CD_2Cl_2): δ (ppm) = -79.4

IR (neat) cm^{-1}: 1592, 1555, 1473, 1448, 1415, 1332, 1196, 1147, 1056, 871, 825, 751.

mp: 208.4 – 212.3 (decomposition)

Triflimidate-9-selenenium-10-boratriptycene-acetonitrile Lewis adduct **6.12**



6.9 **6.12** 82%

Under glovebox conditions, triflimidic acid (14 mg, 0.050 mmol, 1.1 equiv.) was added to a suspension of 10-mesityl-9-selenenium-10-boratriptycene-ate complex **6.9** (20mg, 0.046 mmol, 1.0 equiv.) in MeCN (2.0 ml) at room temperature. The reaction was stirred for 10 minutes then put out of the glovebox and evaporated to dryness. The solid was washed with cold CH_2Cl_2 and dried under dynamic vacuum affording triflimidate-9-selenenium-10-boratriptycene-acetonitrile Lewis adduct **6.12** (24 mg, 0.038 mmol, 82% yield) as white solid. Single crystals suitable for X-ray diffraction analysis were obtained by slow evaporation of a saturated CH_2Cl_2 solution.

^{1}H NMR (500 MHz, CD_2Cl_2): δ (ppm) = 7.91 (dd, *J* = 7.7, 0.5 Hz, 3H), 7.86 (dd, *J* = 7.4, 1.3 Hz, 3H), 7.50 (td, *J* = 7.4, 1.0 Hz, 3H), 7.28 (td, *J* = 7.6, 1.4 Hz, 3H).

^{13}C NMR (126 MHz, CD_2Cl_2): δ (ppm) = 136.4 (Cq), 133.8, 132.3, 131.4, 129.2, 6.4. The carbon directly linked to the boron atom could not be seen as well as the carbon linked to the nitrogen atom.

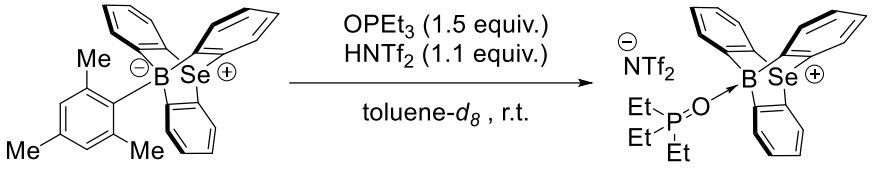
^{11}B NMR (160 MHz, CD_2Cl_2): δ (ppm) = -2.4

^{19}F NMR (483 MHz, CD_2Cl_2): δ (ppm) = -77.4

IR (neat) cm^{-1}: 2373, 1740, 1586, 1449, 1423, 1339, 1186, 1146, 1049, 882, 829, 741.

mp: 207.1 – 211.2 (decomposition)

VI.2. Generation of Gutmann-Beckett Lewis adduct **6.13**



6.9 **6.13**

Under glovebox conditions, triflimidic acid (7.0 mg, 0.025 mmol, 1.1 equiv.) was added to a solution of $OPEt_3$ (4.8 mg, 0.035 mmol, 1.5 equiv.) in toluene-d_8 (0.7 ml). After 2 min, 10-mesityl-9-selenenium-10-boratriptycene-ate complex **6.9** was added and the turbid mixture was stirred until being homogeneous. The ^{31}P NMR analysis show a signal at 80.5 ppm for the Lewis adduct **6.13** which corresponds to an acceptor number (AN) of 87. A broad signal at 74.8 ppm correspond to an excess of protonated $OPEt_3$.

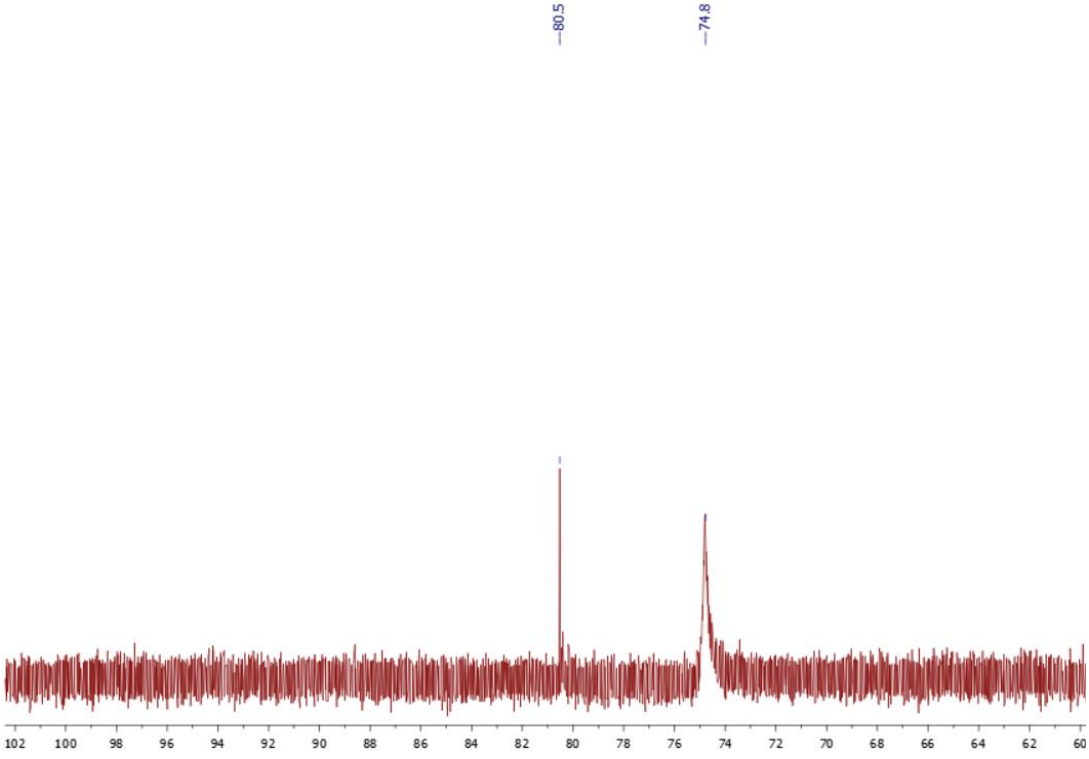


Fig. SVI.1 ^{31}P NMR spectra (202 MHz, 25°C, toluene-d_8) for the reaction of **6.4** with $OPEt_3$.[S1]

VI.3. Quantum chemical calculations

Full geometry optimizations and vibrational frequency calculations were performed, using the Gaussian09 package, at the M06-2X/6-311G(d) level of theory. A tight convergence threshold on the residual forces of the atoms ($1.5x10^{-5}$ Hartree/Bohr or Hartree/radian) was used for geometry optimizations. For each investigated compound, all vibrational frequencies are real, demonstrating that these structures are minima on the potential energy surface. For each investigated compound, all vibrational frequencies are real, demonstrating that these structures are minima on the potential energy surface. Hydride Ion Affinities (HIA) were computed according to the scheme of Krosing,[S2] *via* isodesmic reactions, using respectively $FSiMe_3 \rightarrow SiMe_3^+ + F^-$ (ΔH^0 = 958kJ mol^{-1}) and $HSiMe_3 \rightarrow SiMe_3^+ + H^-$ (ΔH^0 = 959 kJ mol^{-1}) evaluated at the G3 level as anchor points. Consequently, the initial M06-2X/6-311G(d) FIA and HIA values were corrected by -119.1 kJ.mol^{-1} and -32.3 kJ.mol^{-1} respectively.

VI.4. Crystallographic parameters

The crystal structures were determined from single-crystal X-ray diffraction data collected using an Oxford Diffraction Gemini Ultra R diffractometer (Cu Kα radiation with multilayer mirror or Mo Kα radiation with graphite monochromator). The data were integrated using the CrysAlisPro software.[S3] The structures were solved by the dual-space algorithm implemented in SHELXT,[S4] and refined by full-matrix least squares on $|F|^2$ using SHELXL-2018/3,[5] the shelXLe,[S6] and Olex2 software.[S7] Non-hydrogen atoms were refined anisotropically; and hydrogen atoms in most of the cases were located from the difference Fourier map but placed on calculated positions in riding mode with equivalent isotropic temperature factors fixed at 1.2 times U_{eq} of the parent atoms (1.5 times U_{eq} for methyl groups). In case of nt1013_AROS_BSe_MeCN_rod, the bis(trifluoromethanesulfonyl)imide is disordered by inversion center.

Table VI.1 Experimental details

	6.8	**6.8**	**6.9**	**6.11**	**6.12**
Chemical formula	$C_{21}H_{19}BSe$	$C_{21}H_{19}BSe$	$C_{27}H_{23}BSe$	$C_{22}H_{20}BO_2Se^+$ $C_2F_6NO_4S^-$	$C_{20}H_{15}BNSe^+$ $C_2F_6NO_4S^-$
M_r	361.13	361.13	437.22	686.30	639.25
Crystal system, space group	Orthorombic, *Pbca*	Orthorombic, *Pbca*	Monoclinic, $P2_1/n$	Triclinic, $P\bar{1}$	Monoclinic, $P2_1/m$
Temperature (K)	295	150	295	295	295
a, *b*, *c* (Å)	8.0924(3), 15.1058(13), 29.0748(11)	8.05222(17), 14.8240(4), 29.0905(6)	9.0393(3), 18.1827(6), 12.5483(5)	8.6057(3), 13.6101(5), 13.7813(3)	8.3386(5) 14.2444(7) 11.5380(8)
α, β, γ (°)	90, 90, 90	90, 90, 90	90, 93.362(3), 90	63.393(3) 74.271(3) 76.889(3)	90, 109.391(7), 90
V (Å^3)	3554.2(4)	3472.41(13)	2058.88(12)	1378.68(8)	1292.72(14)
Z	8	8	4	2	2
μ (mm^{-1})	2.11	2.16	1.83	1.60	1.69
Crystal size (mm)	0.83 × 0.73 × 0.20	0.61 × 0.35 × 0.21	0.99 × 0.78 × 0.05	0.64 × 0.49 × 0.28	0.73 × 0.17 × 0.10
T_{min}, T_{max}	0.211, 1.000	0.429, 0.780	0.064, 1.000	0.405, 1.000	0.657, 1.000
No. of measured, independent and observed [$I > 2\sigma(I)$] reflections	10462, 3133, 2241	29933, 4478, 3499	37447, 6013, 4791	19096, 19096 12869	7580, 3474, 2583
R_{int}	0.025	0.030	0.040	0.047	0.020
$(\sin\theta/\lambda)_{max}$ (Å^{-1})	0.595	0.676	0.704	0.763	676
$R[F^2 > 2\sigma(F^2)]$, $wR(F^2)$, S	0.046, 0.125, 1.03	0.036, 0.092, 1.03	0.032, 0.084, 1.02	0.036, 0.095, 0.98	0.047, 0.132, 1.03
No. of reflections	3133	4478	6013	19096	3474
No. of parameters	212	211	266	373	257
No. of restraints	0	10	0	0	124
$\Delta\rho_{max}$, $\Delta\rho_{min}$ (e Å^{-3})	0.45, -0.69	0.57, -0.75	0.33, -0.30	0.40, -0.38	0.49, -0.36
CCDC deposition number	2156118	2156119	2156120	2156121	2156122

VI.5. References

[S6.1] Holthausen, M. H.; Hiranandani, R. R.; Shephan, D. W. *Chem. Sci*. **2015**, 6, 2016.

[S6.2] (a) Böhrer, H.; Trapp, N.; Himmel, D.; Schleep, M.; Krossing, I. *Dalton Trans*. **2008**, *44*, 7489-7499. (b) Greb, L. *Chem. Eur. J.* **2018**, 24, 17881.

[S6.3] Rigaku Oxford Diffraction. CrysAlisPro Software system. Rigaku Corporation, Wroclaw, Poland, **2020**.

[S6.4] Sheldrick, G. M. *Acta Crystallogr. Sect. A Found. Adv.* **2015**, *71*, 3.

[S6.5] Sheldrick, G. M. *Acta Crystallogr. Sect. C Struct. Chem.* **2015**, *71*, 3.

[S6.6] Hübschle, C. B.; Sheldrick, G. M.; Dittrich, B. *J. Appl. Crystallogr.* **2011**, *44*, 1281.

[S6.7] Dolomanov, O. V.; Bourhis, L. J.; Gildea, R. J.; Howard, J. A. K.; Puschmann, H. *J. Appl.Crystallogr.* **2009**, *42*, 339.